The effect of therapeutic ultrasound on wound repair with emphasis on fibroblast activity.

Hart, Geoffrey

The effect of therapeutic ultrasound on dermal wound repair with emphasis on fibroblast activity.

A thesis submitted to the University of London for the
Degree of Doctor of Philosophy in Anatomy

Jeffrey Hart

Tissue Repair Research Unit
Division of Anatomy and Cell Biology
United Medical and Dental Schools
of Guy's and St. Thomas's
Hospitals
Guy's Hospital Campus
London
SE1 9RT

Abstract

Treatment of wounds with therapeutic ultrasound has been shown to induce physiological changes which result in the stimulation of tissue repair. Such stimulation has been demonstrated under both clinical and experimental conditions. Although ultrasound is employed to help resolve a multitude of clinical conditions, which suggests efficacy and clinical acceptance, the specific physiological mechanisms by which ultrasound produces these effects remain elusive. This thesis describes *in vivo* and *in vitro* studies examining the effect of therapeutic levels of ultrasound on certain aspects of mammalian cutaneous repair.

The effect of 3 MHz therapeutic ultrasound, pulsed 2ms on, 8ms off, at spatially and temporally averaged intensities ($I^{(SATA)}$) of 0.1 and 0.5 W/cm^2 on the rate of contraction of full thickness excised rat flank skin wounds was examined. It was found that ultrasound increased the rate of wound contraction leading to a significantly smaller scar.

In vitro studies were carried out to determine the ability of ultrasound to interact with various components of the repair process thought to be central to the wound contraction process. The fibroblast is thought to generate the forces necessary to facilitate wound contraction. *In vitro* studies reported here appear to suggest that therapeutic ultrasound does not directly promote fibroblast proliferation or fibroblast-mediated matrix contraction. The recruitment of fibroblasts into the wound site is thought to depend on a variety of substances, including several growth factors, which promote fibroblast proliferation and migration. It is known that platelet α-granules are stores for some of these substances and it is thought that platelet degranulation at the wound site is the initial source of fibroblast mobilisation factors. *In vitro* studies reported here appear to suggest that therapeutic ultrasound may interact with platelets thereby encouraging their degranulation and the concomitant release of factors that may encourage fibroblast activity within the wound site. Later in the repair process macrophage-derived substances are thought to take over this fibroblast activating role. *In vitro* studies carried out here suggest that therapeutic ultrasound can interact with macrophage-like cells (U937s) and in doing so modulate the elaboration of fibro-proliferative and fibro-contractile substances.

Acknowledgement

I am grateful to all the members of the Tissue Repair Research Unit, both past and present, for encouraging me "in their own special way" to complete this work - it has been an education! I would like to express my sincere gratitude to Dr Mary Dyson for her instruction and for displaying undying optimism and patience throughout. I would like to thank Dr Martin Sherriff for his expert advice on statistical analysis.

I would like to thank my parents for their unfailing support, direction and foresight.

Finally, and most importantly, I thank my wife for her understanding, patience and generosity, especially during my "Ph.D period", and my sons Thomas and Edward for giving me insight into what is, and what is not, important in life.

Preface

This thesis is divided into 14 chapters. Chapters 1 and 2 are introductory chapters which describe the basic principles of cutaneous wound repair and ultrasound physics, respectively. Chapter 3 deals with the mechanisms by which therapeutic levels of ultrasound are thought to interact with biological materials. Chapter 4 describes the clinical and laboratory-based literature regarding the effect of therapeutic levels of ultrasound on wound repair. This thesis contains both *in vivo* and *in vitro* studies into the effect of ultrasound on wound repair; chapter 5 describes the materials, methods and models employed in *vitro* studies, together with experiments designed to examine, and optimise, the sensitivity of the *in vitro* models employed. Chapter 6 describes the techniques employed and the results obtained during the characterisation of the ultrasound dose to which biological materials were exposed in this thesis. Ultrasonic dosimetry is essential if the findings made in this study are to be related to the findings of other workers.

Chapters 7 through 11 are experimental chapters. Chapter 7 describes a study carried out to investigate the effect of treatment with therapeutic ultrasound on the contraction of full thickness flank skin wounds in the rat. Having observed that therapeutic ultrasound could promote wound contraction *in vivo*, further studies were performed in an attempt to elucidate the responsive biological target(s) involved in this response. Chapters 8 and 9 consider the ability of ultrasound to interact directly with human fibroblasts *in vitro* to promote their proliferation and their ability to contract collagen lattices. Chapter 10 describes a study into the ability of therapeutic ultrasound to indirectly modify human fibroblast proliferation and/or fibroblast-mediated lattice contraction by first interacting with platelets. Chapter 11 describes a similar study in which the ability of ultrasound to modulate pro-proliferative and/or pro-contractile substance release from macrophages was examined.

Chapter 12 summarises the experimental findings of this thesis and chapter 13 describes conclusions that may be drawn from those findings. The final chapter in this thesis, chapter 14, describes certain avenues of important future work that may be followed. Towards the end of this thesis are the appendices which include: reagent and culture media recipes, detailed experimental protocols, small supplementary experiments and the results of statistical analyses. The thesis concludes with a list of referenced literature.

Contents

List of figures

List of tables

List of Appendices

List of abbreviations in text

ATP	Adenosine triphosphate
bFGF	Basic fibroblast growth factor
β-TG	β-Thromboglobulin
cFn	Cellular fibronectin
c.w.	Continuous wave
DGEA	Aspartic acid-Glycine-Glutamic acid-Alanine (amino acid sequence)
ECM	Extracellular matrix
EGF	Epidermal growth factor
EILVD	Glutamic acid-Isoleucine-Leucine-Aspartic acid-Valine (amino acid sequence)
ERA	Effective radiating area
ERD	Effective radiating diameter
FAF	Fibroblast activating factor
FCS	Fetal calf serum
FITC	Fluorescein isothiocyanate
FPCL	Fibroblast populated collagen lattice
GAG	Glycosaminoglycan
GM-CSA	Granulocyte macrophage - colony stimulating activity
Hz	Hertz
HA	Hyaluronic acid
IGF-1	Insulin-like growth factor-1
IL-1	Interleukin-1
kHz	KiloHertz
LDCF-F	Lymphocyte-derived chemotactic factor for fibroblasts
MDGF	Macrophage-derived growth factor
mg/μg	Milligrams/micrograms
MHz	MegaHertz
MPa	MegaPascal
mRNA	Messenger ribonucleic acid
ms	millisecond
mW/cm^2	milliWatts per square cm
p	Passage
PAF	Platelet activating factor
PBM	Peripheral blood monocytes
PBS	Phosphate buffered saline
PD-ECGF	Platelet-derived endothelial cell growth factor
PDGF	Platelet-derived growth factor
PF4	Platelet factor 4
pFn	Plasma fibronectin
PGE_2	Prostaglandin E_2
PMA	4 β-phorbol 12-myristate 13-acetate
PRP	Platelet rich plasma
PVDF	Polyvinylidene difluoride
PWB	Platelet washing buffer
PZT	Lead zirconate titanate
RGD	Arginine-Glycine-Aspartic acid (amino acid sequence)
RGDS	Arginine-Glycine-Aspartic acid-Serine (amino acid sequence)
SMC	Smooth muscle cell
TGF-α	Transforming growth factor-α
TGF-β	Transforming growth factor-β
TNF-α	Tumour necrosis factor-α
TRITC	Tetramethylrhodamine iosthiocyanate
W/cm^2	Watts per square cm
λ(nm)	Wavelength (nanometers)

Chapter 1. Cutaneous wound repair

Introduction

Many attempts have been made to define the process of wound healing. It has been described consisely by Walter and Israel (1987) as "the body's replacement of destroyed tissue by living tissue". This replacement includes both regeneration, the complete re-establishment of the original tissue, and repair, the replacement of the original tissue with functionally inferior scar tissue. This definition encompasses the field of adult cutaneous repair, as the epidermis heals by regeneration, whereas, the dermis heals by repair.

Acute tissue injury initiates a dynamic and orderly but complex series of cellular and biochemical interactions that leads to the formation of new tissue and the eventual repair of the wound. The cellular components of the repair process include blood cells such as platelets, polymorphonuclear leucocytes, mast cells, monocytes and T lymphocytes as well as connective tissue cells such as fibroblasts and endothelial cells. The cells migrate to the site of tissue damage in a precise sequence thought to be determined primarily by a wide variety of soluble factors that are released at the site of injury from a wide variety of sources such as tissue breakdown, blood coagulation and cells. Once they arrive, each cell type has specific functions to perform in order to facilitate the process of repair.

As an aid to comprehension, the process of repair is classically and arbitrarily described as a scheme of temporally overlapping events, termed phases of repair. The three phases of wound repair, as described by Clark (1990), are:

1. inflammation
2. new tissue formation
3. matrix formation and remodelling.

Following injury, and in the absence of any retarding phenomena, cutaneous wounds are visualised as proceeding through the above phases of repair, with the ultimate generation of scar tissue.

This chapter will describe the cellular and extracellular activities associated with each of the three phases, as mentioned above. Cutaneous repair phenomena directly associated with the work undertaken in completion of this thesis will be described in a more extensive fashion. Subsequent sections will describe wound contraction and the theories put forward to explain this phenomenon.

1.1 Inflammation

Inflammation is a vascular and cellular response which defends the body against alien substances, disposes of dead and dying tissue, and which generates an environment conducive to the generation and propagation of granulation tissue. The process of inflammation can be temporally divided into early and late phases (Clark, 1988b).

1.1.1 Early inflammation

The early phase of inflammation is characterised by clot formation within damaged vessels which effects haemostasis, and within the wound void which provides a provisional matrix for cell migration into the wound space. Blood vessel disruption leads to the extravasation of blood constituents and results in platelet aggregation and blood coagulation. Platelet adhesion and aggregation, stimulated by locally generated thrombin and exposed fibrillar collagens, initially leads to the generation of a haemostatic plug. The initial adhesion of platelets leads to the release of various substances, including ADP and thrombin, that are responsible for stimulating the recruitment of additional platelets. Several adhesive proteins including fibrinogen, fibronectin, thrombospondin and von Willebrand factor are also released from platelet α-granules; these proteins promote further platelet aggregation and adhesion to sub-endothelial fibrillar collagen matrix (Terkeltaub and Ginsberg, 1988).

Coagulation of extravasated blood at the wound site is thought to be the result of both the intrinsic and extrinsic blood clotting pathways, and the action of activated platelets (figure 1.1). The inciting event in each route of clotting is the expression of a surface, a consequence of injury, that promotes adsorption and activation of specific coagulation coenzymes (Dvorak *et al.* 1988). Factor XII (Hageman factor) is activated (to XIIa) by adsorption onto fibrillar collagen, exposed during injury, which activates the intrinsic coagulation cascade. Tissue factor, released during tissue damage, activates factor VII; active factor VII (VIIa) induces activation of the extrinsic coagulation cascade. Platelets and endothelial cells activated by low levels of thrombin (Stern *et al.* 1988), and platelets activated by contact with fibrillar collagen, express surface membrane coagulation factors shared by the intrinsic and common coagulation pathways, and thereby assist in the coagulation process. The overall effect of these different coagulation mechanisms is to convert the plasma protein fibrinogen into an insoluble network of fibrin, which stabilises the initial haemostatic platelet plugs within the damaged vessels and provides a provisional

Figure 1.1 Coagulation pathways initiated by tissue injury

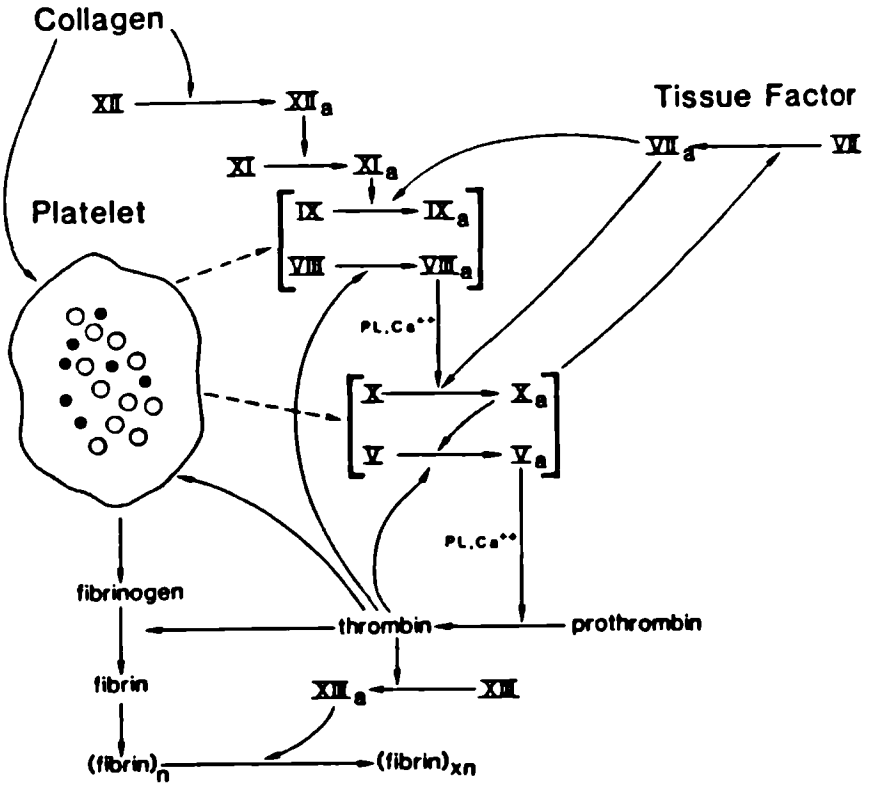

(after Clark, 1990)

Figure 1.1 Injury exposes blood constituents to fibrillar collagen and tissue factor. Factor XII (Hageman factor) is activated to XIIa on the surface of fibrillar collagen, initiating the *intrinsic clotting cascade* by activating XI (to XIa). Tissue factor released during tissue damage activates factor VII; active factor VII (VIIa) induces activation of the *extrinsic clotting cascade*. Platelets activated by low levels of thrombin, or by contact with fibrillar collagen, express surface membrane coagulation factors shared by both the intrinsic and extrinsic coagulation pathways, and thereby assist the coagulation process.

matrix within the wound void. Clotting via the intrinsic coagulation pathway leads to the generation of bradykinin (Proud and Kaplan, 1988) and to the initiation of the classical complement cascade (Ghebrehiwet *et al.* 1981) which leads to the generation of the complement derived anaphylatoxins C5a and C3a. Both bradykinin and the anaphylatoxins increase the permeability of undamaged vessels adjacent to the injured area, resulting in the release of plasma proteins (including fibrinogen) and the generation of an extravascular clot. The mechanism by which bradykinin increases vessel permeability is thought to involve an induction of prostaglandin production (Terragno *et al.* 1972).

The anaphylatoxins increase blood vessel permeability both directly, by inducing a rapid interaction between neutrophils and microvascular endothelium (Wedmore and Williams, 1981; Issekutz, 1981) which results in vascular damage by hydrogen peroxide production; and indirectly, by stimulating the release of the vasoactive mediators histamine and leukotriene C4 and D4 from mast cells (Williams, 1988). The anaphylatoxins are also thought to attract neutrophils (Snyderman *et al.* 1970) and monocytes (Marder *et al.* 1985) to the site of injury; the latter develop into macrophages, which characterise the late inflammatory phase.

In addition to their activities associated with clotting, activated platelets also release a plethora of biologically active substances. Such substances released from activated platelets may contribute to the inflammatory process by:

(a) modulating vascular tone and permeability e.g. serotonin (dePrada *et al.* 1981), thromboxanes and prostaglandins (Goetzl, 1981).

(b) attracting inflammatory cells, such as neutrophils and monocytes, to the site of injury, e.g. platelet-derived growth factor PDGF (Deuel and Huang, 1984); platelet factor-4 PF4 (Deuel *et al.* 1981).

(c) initiating subsequent phases of repair by stimulating the migration, proliferation and the synthesis of extracellular matrix components by connective tissue cells e.g. PF4, (Senior *et al.* 1983), PDGF (Huang *et al.* 1988), transforming growth factor-beta TGF-β (Assoian, 1988), epidermal growth factor EGF (Banks, 1988), basic fibroblast growth factor bFGF (Fox, 1988), and platelet-derived endothelial cell growth factor (Pierce *et al.* 1991; Miyazono and Heldin, 1989).

Neutrophils are classically considered to be the first leucocytes to populate an area of inflammation and injury; however, it has been suggested that monocytes, the precursors of macrophages, begin to invade the wound at much the same time (Turk

et al. 1976). Both cell types are attracted to the site of injury by an array of chemotactic factors generated during the physical process of wounding and as a consequence of the initial response to injury (table 1.1).

Table 1.1 Identified leucocyte attractants

Attractant	Source	Reference
C5a#	Complement cascade	Hugli and Morgan, 1984
Kallikrein#	Intrinsic clotting pathway	Gallin and Kaplan, 1974
Fibrinopeptides#	Fibrin clot formation	Senior *et al.* 1986
Fibrin degradation products#	Plasmin degradation of fibrin	McKenzie *et al.* 1975
Formylmethionyl peptides#	Contaminating bacteria	Freer *et al.* 1980
Leukotriene B_4#	Activated neutrophils	Ford-Hutchinson, 1981
Platelet activating factor (PAF)#	Platelets, neutrophils, monocytes and endothelial cells	Hanahan, 1986
TNF-α#	Activated monocytes	Ming *et al.* 1987
PDGF#	Platelets and activated macrophages	Deuel and Huang, 1984 Deuel *et al.* 1982
PF4#	Platelets	Deuel *et al.* 1981
PD-ECGF*	Platelets	Pierce *et al.* 1991
TGF-β*	Platelets and activated macrophages/T lymphocytes	Wahl *et al.* 1987
Thrombin*	Clotting cascade	Bar-Shavit *et al.* 1983
Elastin fragments*	Wound site debridement	Senior *et al.* 1980
Fibronectin fragments*	Wound site debridement	Clark *et al.* 1988
Collagen fragments*	Wound site debridement	Postlethwaite and Kang, 1976

Key: # = Chemoattractive to both neutrophils and monocytes
* = Chemoattractive to monocytes alone

In addition to providing the stimulus for directed migration of neutrophils, chemotactic factors have been shown to induce an upregulation in the expression of the $\beta 2$ integrin family of receptors on the surface of neutrophils (Tonnenson *et al.* 1988). These dimeric complexes mediate the adherence of neutrophils to blood vessel endothelium and thereby facilitate diapedesis of leucocytes between adjacent endothelial cells. Activation of the neutrophil by chemoattractants stimulates the release of elastase and collagenase enzymes (Janoff, 1985; Hibbs *et al.* 1985), which are thought to facilitate cellular penetration of blood vessel basement membranes. As neutrophils traverse the endothelium, they respond to a concentration gradient of chemotactic signals (table 1.1) by cellular polarization and migration toward the source of that gradient. As the neutrophils reach the source of the chemoattractant, the gradient is no longer apparent and their directed motion ceases (Wahl, 1989).

The main function of neutrophils within the wound site is thought to be to rid the site of foreign particles, especially contaminating bacteria, as experimentally induced neutropenia has been shown to have no effect on wound healing in guinea pigs in the absence of gross infection (Simpson and Ross, 1972). The environment of the inflammatory site stimulates neutrophil degranulation, a consequence of which is the secretion of toxic reactive oxygen intermediates (ROI). The release of O_2^-, H_2O_2 and other toxic oxygen species complements their phagocytic capacity to destroy contaminating bacteria (Wahl, 1989); however, the release of these ROI can also cause significant damage to surrounding tissues (Halliwell, 1987). Neutrophil infiltration is observed to cease, and neutrophil numbers to fall, within a few days after injury in the absence of significant ongoing bacterial infection. Effete neutrophils are phagocytosed by tissue macrophages (Haslett and Henson, 1988). This fall in neutrophil number is regarded as the end of the early inflammatory phase of repair (Clark, 1988b).

1.1.2 Late inflammation

Irrespective of whether the neutrophil infiltrate resolves or persists, monocyte infiltration continues, a process presumably dependent on selective monocyte chemoattractants (table 1.1) which include fragments of extracellular matrix components (Schiffmann and Gallin, 1979) including collagen (Postlethwaite and Kang, 1976), elastin (Senior *et al.* 1980) and fibronectin (Clark *et al.* 1988); thrombin (Bar-Shavit *et al.* 1983) and transforming growth factor-β (TGF-β) (Wahl *et al.* 1987)

also act as chemoattractants. After injury, the number of blood monocytes in general circulation has been observed to increase two to threefold (van Furth *et al.* 1973; van Waarde *et al.* 1976). This is thought to be caused by a macrophage product called "factor inducing monopoiesis" (FIM), which is produced at the site of inflammation (Sluiter *et al.* 1983). Thus infiltrating macrophages may augment the number of monocytes entering the wound site in a positive feedback manner. During the waning stages of inflammation, this feedback loop is thought to be terminated by another soluble factor called monocyte production inhibitor (MPI) (van Waarde *et al.* 1978).

After migrating from the vasculature into the wound site, monocytes rapidly differentiate into activated inflammatory macrophages (Riches, 1988). The mechanisms responsible for driving the differentiation of monocytes into activated inflammatory macrophages are unclear, however, certain environmental stimuli including: the presence of insolubilized fibronectin (Hosein *et al.* 1985), low oxygen tension (Hunt, 1987), the presence of certain chemotactic stimuli (Ho *et al.* 1987), the presence of interferons and of bacterial lipopolysaccharides, have all been implicated in this process (Riches, 1988).

Wound macrophages, like neutrophils, take part in bacterial clearance and also scavenge dead and damaged tissue from within the wound site (Newman *et al.* 1982). Macrophages not only phagocytose bacteria and scavenge tissue debris, but also generate chemotactic factors which recruit additional inflammatory cells and release enzymes which augment tissue degradation (Tsukamoto *et al.* 1981). In addition to their role in tissue debridement, wound macrophages are thought to elaborate growth and regulatory factors critical to the coordination of granulation tissue formation. Evidence for this latter role comes from the pioneering work of Leibovich and Ross in 1975, who demonstrated that the induction of monocytopenia, through a combination of hydrocortisone to eliminate circulating macrophage precursors and anti-macrophage serum to eliminate resident macrophages, severely inhibited the repair of guinea pig wounds. Under these conditions, fibroblast and endothelial cell recruitment and proliferation, capillary generation and matrix biosynthesis were all adversely affected. Furthermore, the removal of damaged tissue was markedly reduced with the accumulation of large amounts of fibrin.

Subsequent studies by Leibovich and Ross (1976) reported that peritoneal macrophages cultured *in vitro* secreted growth factor activity, called macrophage-derived growth factor (MDGF), which stimulated the proliferation of guinea pig

wound fibroblasts. MDGF, secreted by activated macrophages, has also been shown to stimulate the proliferation of smooth muscle cells (Greenburg and Hunt 1978; Glenn and Ross, 1981; Martin *et al.* 1981), arterial endothelial cells (Greenburg and Hunt, 1978; Martin *et al.* 1981) and mouse keratinocytes (Ristow, 1986). It has since been realised that MDGF activity is a combination of several well characterised growth factors (Raines and Ross, 1989). The factors macrophages are known to secrete include platelet-derived growth factor (PDGF) (Shimokado *et al.* 1985; Martinet *et al.* 1986), basic fibroblast growth factor (bFGF) (Baird *et al.* 1985), transforming growth factor-β (TGF-β) (Assoian *et al.* 1987), insulin-like growth factor-1 (IGF-1) (Rom *et al.* 1989), tumour necrosis factor-α (TNF-α) (Kreigler *et al.* 1988), the epidermal growth factor-related transforming growth factor-α (TGF-α) (Madtes *et al.* 1988), interleukin-1 (IL-1) (Postlethwaite *et al.* 1983) and fibroblast-activating factor (FAF) (Dohlman *et al.* 1984). The production of many of these factors, including TGF-α, TGF-β, PDGF A-chain and insulin-like growth factor 1 (IGF-1), have been demonstrated in wound macrophages by mRNA phenotyping (Rappolee *et al.* 1988). The functions of these and other substances in the initiation and propagation of granulation tissue will be discussed in subsequent sections of this chapter.

1.2 New tissue formation

The inflammatory response provoked by tissue injury is rapidly followed by the phase of new tissue formation often referred to as the proliferative or fibroplastic phase. During cutaneous wound repair, new tissue formation is manifest by

1. Re-epithelialization
2. Granulation tissue formation.

1.2.1 Re-epithelialization

Re-epithelialization is the reconstitution of the cells of the epidermis into an organised, keratinised stratified squamous epithelium that covers the wound defect and provides the barrier properties of the skin. The process of re-epithelialization begins some time before the initiation of granulation tissue formation, usually commencing within a few hours after injury (Stenn and Depalma, 1988). Re-epithelialization is brought about by the migration of epidermal cells from the free edge of the wound towards the centre of the surface separating viable from non-viable tissue.

In response to wounding, epidermal cells at the wound margin have been observed to undergo a cellular metamorphosis that involves the retraction of intracellular tonofilaments, dissolution of intercellular attachments (specifically desmosomes) and basement membrane attachments (hemidesmosomes) (Krawczyk and Wilgram, 1973), cellular flattening, the formation of peripheral actin filaments (Gabbiani *et al.* 1978) and the projection of pseudopodia (Odland and Ross, 1968). The free edge generated during wounding, in tandem with these cellular changes, give the epidermal cells of the wound margin somewhere to migrate and the cellular machinery to expedite that migration. Because of the proliferative capacity of cells of the *stratum basale*, it was initially assumed that wounds were re-epithelialized by cells originating from this layer of the epidermis. However, it has been demonstrated that epidermal cells at the wound margin have a unique phenotype, termed the phenotype of regenerative maturation (Mansbridge and Knapp, 1987), in which they display certain phenotypical characteristics common to cells of both the *stratum basale* and the *stratum granulosum*.

The signals for epidermal cell phenotype switching are effectively unknown. However the observations that low extracellular calcium concentrations impart keratinocytes with the phenotype of regenerative maturation, whereas normal calcium concentrations drive terminal differentiation *in vitro* (Hennings *et al.* 1980), and that a calcium chelating protein called SPARC (Holland *et al.* 1987) is absent from normal epithelium but present during re-epithelialization, suggests that calcium may be involved in this switching (Clark, 1990).

These modified epidermal cells form a multilayered tongue-like structure at the wound margin that migrates beneath the eschar, and in doing so dissects viable tissue from desiccated non-viable tissue (Clark, 1990) a process thought to involve the elaboration of hydrolases including collagenase by the migrating cells (Harris and Krane, 1974). As the epidermis migrates over the wound surface the basement membrane is regenerated (Woodley and Briggaman, 1988). The stimuli for epidermal migration are not well understood; however, it has been suggested that the driving force for epidermal cell movement may involve contact guidance by matrix components of the clot, chemotactic factors generated during clotting and platelet degranulation, the loss of nearest neighbour cells (Heinmark and Schwartz, 1988), or a combination of all of these stimuli (Clark, 1990). While re-epithelialization is a well documented phenomenon, mechanistically much has yet to be determined.

In vitro studies have demonstrated that when epithelial explants are cultured on a basement membrane-like substratum (i.e composed of laminin, heparan sulphate, proteoglycans and collagen types IV and V) few of the explants spread out, but explants in contact with non-basement membrane proteins, collagens type I and III or fibronectin, exhibit significant migration (Woodley *et al.* 1985). This suggests that loss of the basement membrane during wounding, and its replacement by a provisional matrix of fibrin and fibronectin, generated during clotting, may be a major stimulus for epidermal cell migration over the wound (Clark *et al.* 1983; Fujikawa, 1981). The observation that migrating epithelial cells generate fibronectin (Clark *et al.* 1983), has led to the suggestion that the initial stimulus for migration is probably plasma-derived fibronectin, and further migration is promoted by the synthesis of fibronectin by the migrating cells themselves (Clark *et al.* 1983). Transforming growth factor-β (TGF-β), which has been observed to encourage epithelial cell migration *in vivo* (Yang and Moses, 1990), has been proposed as a critical signal in epithelial cell migration (Clark, 1990). This proposal stems from the observations that TGF-β has been shown to stimulate a 6-fold increase in fibronectin synthesis in cultured keratinocytes (Wilkner *et al.* 1988), to stimulate keratinocytes motility apparently through stimulation of fibronectin deposition (Nickoloff *et al.* 1988), and is thought to induce fibronectin receptor expression in keratinocytes (Toda *et al.* 1987). Thus TGF-β may facilitate epidermal migration through the induction of matrix fibronectin production and cell surface fibronectin receptor expression.

Epidermal migration over the wound surface is known not to depend on cell proliferation (Winter, 1972), in fact, it has been suggested that TGF-β, which is a potent inhibitor of keratinocyte proliferation *in vitro* (Shipley *et al.* 1986), may be actively engaged in inhibiting cellular proliferation of the epidermal tongue (Clark, 1990). The migrating epidermal tongue is thought to be supplied with additional cells by epidermal cell proliferation at or near the wound margin (Winter, 1972). The stimuli for epithelial cell proliferation have not been delineated, but several growth factors, such as epidermal growth factor, transforming growth factor-α and fibroblast growth factor, have been suggested as possible candidates (Clark, 1990). Such growth factors may arise as a consequence of platelet degranulation or macrophage activation and act to promote proliferation in a paracrine manner, or, may be synthesized by epidermal cells themselves and promote proliferation in a autocrine fashion (Coffey *et al.* 1987). Once the migrating edges have united, migration ceases

and epidermal cells rapidly reassume their normal phenotype and attach to each other by desmosomes, to the basement membrane via hemidesmosomes, and thereby reconstitute the epidermis. A more comprehensive review of re-epithelialization has been written by Stenn and DePalma (1988).

1.2.2 Granulation tissue formation

The process of granulation tissue formation, which is partially dependent on cellular interactions initiated during the inflammatory phase, is an early step towards replacing the dermal component, lost during injury, with scar tissue. It is characterised by the accumulation of macrophages, the colonisation of the wound space by fibroblasts (which involves both fibroblast proliferation and migration), the deposition of a loose connective tissue matrix (composed of fibronectin, hyaluronic acid and collagen types I and III), and neovascularisation. Fibroblast proliferation, migration and the synthesis and elaboration of collagenous and non-collagenous matrix are collectively referred to as fibroplasia (Clark, 1990).

It is thought that the processes of fibroplasia and angiogenesis are stimulated in part by a number of growth and chemotactic factors released by platelets and macrophages during inflammation (Huang *et al.* 1988), and by the fibroblasts and endothelial cells themselves, to which they respond in an autocrine fashion (Sporn and Roberts, 1986). Fibroblasts respond to these stimuli by proliferation, migration, matrix deposition, and wound contraction. The matrix generated by fibroblasts provides a substrate on which macrophages (Ciano *et al.* 1986), new blood vessels (Madri and Pratt, 1988) and fibroblasts (McCarthy *et al.* 1988) can migrate into the wound. Endothelial cells of vessels within the undamaged wound periphery respond to these growth and chemotactic signals by degradation of their basement membranes, directed migration, proliferation and capillary formation. Neovascularization is necessary to satisfy the metabolic demands of fibroplasia and re-epithelialization.

1.2.2.1 Neovascularization

Neovascularization of wounds occurs simultaneously with fibroplasia by the sprouting of capillary buds from blood vessels adjacent to the wound; these buds subsequently extend into the wound site. Granulation tissue, while only transient, is metabolically very active and consequently requires a profuse blood supply. New capillary

formation (angiogenesis) is an extremely complex process that depends on endothelial phenotype alteration, migration, proliferation, and synthesis of an appropriate extracellular matrix (Madri and Pratt, 1988). This section will briefly review the process of wound neovascularisation; more comprehensive reviews of the process include those of Madri and Pratt (1988) and Zetter (1988).

Angiogenesis in the adult occurs as a sprouting process in which new capillaries bud from pre-existing small venules (Findlay, 1986; Furcht, 1986; Zetter, 1988), and can be summarised as follows. One of the first events that can be observed in angiogenesis involves the disruption of the basement membrane on the side of the venule facing the angiogenic stimulus. It is thought that the basement membrane is degraded by enzymes from the endothelial cells themselves, as high concentrations of collagenases and plasminogen activator are secreted by capillary endothelial cells stimulated *in vitro* by angiogenic substances (Gross *et al.* 1983). After the basement membrane has been opened the second essential event in the angiogenic process is the directed migration of the endothelial cells from pre-existing vessels toward the site of the angiogenic stimulus (Ausprunk and Folkman, 1977). The migrating cells align with each other in a bipolar configuration to form a sprout. The vessel sprouts elongate and undergo a process of canalization (tube formation) formed by a curvature that develops in the capillary endothelial cell. Once a sprout has formed, endothelial cells in its mid section undergo mitosis. The leading cells at the tip of the sprout continue to migrate but usually do not divide (Ausprunk and Folkman, 1977; Burger and Klintworth, 1981). Individual sprouts then join, or anastomose, with each other to form a loop. These loops elongate and may become the origin of additional sprouts. The loops and sprouts continue to converge on the source of angiogenic activity. Blood flow begins slowly shortly after loops have formed. Since the junctions between endothelial cells are initially loose and there are gaps in the endothelial lining these immature capillaries are fragile and very permeable (Hashimoto and Prewitt 1987). The final stage of capillary development is the development of a mature capillary bed in which the capillaries are surrounded by basement membrane components (Ausprunk *et al.* 1981), and in some cases by a layer of perivascular cells called pericytes (Hashimoto and Prewitt 1987)

The angiogenic stimuli responsible for wound neovascularization are unknown, however, numerous stimuli (reviewed by Folkman and Klagsbrun, 1987; Madri and Pratt, 1988; Zetter, 1988) have been reported that promote endothelial cell growth

in vitro and/or angiogenesis *in situ* (using the chick chorioallantoic membrane and the corneal angiogenesis assays), several of which are known to be found in healing wounds. The process of wound neovascularization is thought to result from the actions of various angiogenic stimuli, generated during injury or as a consequence of the initiation of the repair process (Zetter, 1988; Clark, 1990). Vascular and cellular damage during tissue injury leads to the release of proteolytic enzymes into the interstitium, enzymatic degradation of components of the extracellular matrix is thought to release matrix fragments which have both direct and indirect angiogenic effects. Fragments of fibronectin have been shown to be directly chemotactic for endothelial cells *in vitro* (Bowersox and Sorgente, 1982), and fragments of fibronectin, elastin and collagen have been shown to be chemotactic for monocyte-macrophages (Postlethwaite and Kang, 1976; Senior *et al.* 1980; Clark *et al.* 1988). Activated macrophages are known to release potent angiogenic stimuli (Polverini *et al.* 1977) including: fibroblast growth factor (FGF) (Baird *et al.* 1985), E-series prostaglandins (Ziche *et al.* 1982; Form and Auerbach, 1983), tumour necrosis factor-α (Frater-Schroder *et al.* 1987; Leibovitch *et al.* 1987) and angiotropin (Hockel *et al.* 1987). Macrophage activation and the elaboration of angiogenic agents is thought to be modulated in part by the relatively hypoxic environment of the wound (Knighton *et al.* 1983). Various platelet-derived substances, generated during platelet degranulation, are also thought to promote the angiogenic response. Platelet-derived endothelial cell growth factor (PD-ECGF) has been shown to directly promote both endothelial cell migration (Ishikawa *et al.* 1989) and proliferation (Miyazono and Heldin, 1989) *in vitro*, and has been shown to promote angiogenesis *in vivo* (Ishikawa *et al.* 1989). PD-ECGF is also thought to be indirectly angiogenic due to its chemotactic attraction for monocytes (Pierce *et al.* 1991), which may augment its direct angiogenic effects. Transforming growth factor-β (TGF-β) has also been shown to both directly influence endothelial cell migration *in vivo* (Yang and Moses, 1990) and, like PD-ECGF, promote monocyte-macrophage chemotaxis (Wahl *et al.* 1987) and can thus be considered to be directly and indirectly angiogenic.

Other platelet-derived substances are thought to be indirectly angiogenic as a result of their chemotactic attraction for monocyte-macrophages. Such substances include: platelet activating factor (PAF) (Hanahan, 1986), platelet-derived growth factor (Deuel and Huang, 1984), and platelet factor 4 (Deuel *et al.* 1981). Platelets also produce an enzyme (Oosta *et al.* 1982), that may function to release heparin

from the basement membrane of endothelial cells, a substance also released by mast cells during degranulation that is known stimulate endothelial cell migration *in vitro* (Azizkhan *et al.* 1980). Also, as basement membrane heparin is thought to be a storage site for FGF (Vlodavsky *et al.* 1987; Baird and Ling, 1987), degradation of this storage depot may result in solubilisation of this potent angiogenic agent. Although neutrophils are recruited into the wound site in the early phase of inflammation (p 21) there is currently no evidence for the role of specific neutrophil products in the direct stimulation of angiogenesis. However, neutrophils are known to elaborate substances chemotactic for monocyte-macrophages, including leuktriene B_4 (Ford-Hutchinson, 1981) and PAF (Hanahan, 1986), and may consequently be involved indirectly in the process of angiogenesis.

The mechanisms that limit the process of wound angiogenesis are not clear. Orlidge and D'Amore (1987) showed that pericytes act to inhibit the growth of adjacent endothelial cells and thus may be responsible for a down regulation in the angiogenic response. Other events associated with later stages of repair may also act as a brake to the angiogenic process. Such events include: (1) the cessation of chemotactic/mitogenic factor generation, as the inflammatory response wanes, (2) the production of heparin-like molecules by endothelial cells, which may serve to capture, store and inactivate FGF molecules (Zetter, 1988), and, (3) a return to a normal, non-macrophage-activating, oxygen tension; thus reducing angiogenic factor production by these cells (Knighton *et al.* 1983).

Granulation tissue has a lavish blood supply, however, as the wound matures and the granulation tissue is remodelled into a relatively acellular scar, a regression in the capillary network occurs. The mechanism underlying capillary regression is effectively unknown, but is thought to be a continuation of the angiogenesis "braking" system described above, i.e. a result of the loss of angiogenic stimuli. Capillary regression is characterized by a swelling of mitochondria within the endothelial cells of regressing vessels, platelet adherence to the degenerating endothelial cells, vascular stasis and endothelial cell necrosis, and finally, ingestion of effete endothelial cells by macrophages (Ausprunk *et al.* 1978; Folkman, 1982).

1.2.2.2 Fibroplasia

The recruitment of fibroblasts to the wound site and the ensuing synthesis and elaboration of collagenous and non-collagenous matrix is often referred to as

fibroplasia. The colonisation of the wound site by fibroblasts, essential for granulation tissue formation, is thought to involve both fibroblast migration and proliferation. The origin of wound fibroblasts has been the centre of debate for a long time (Skalli and Gabbiani, 1988). Initially it was thought that leucocytes became transformed into fibroblasts during the process of repair (Cohnheim, 1867), however, it has since been proven that leucocytes do not have the capacity to transform in such a manner, and that granulation tissue fibroblasts arise from local connective tissue. The question still remains as to whether granulation tissue fibroblasts can arise from any mesenchymally-derived cell present in dermis and subcutaneous tissue such as fibrocytes, pericytes and smooth muscle cells (Crocker *et al.* 1970). The work of Bouissou *et al.* (1988) suggests that granulation tissue fibroblasts originate from resting fibrocytes, rather than smooth muscle cells, in the wound margins, a view generally supported by actin isoform and intermediate filament cytoskeletal analysis (Schurch *et al.* 1984; Skalli and Gabbiani, 1988). However, α-actin which is apparently specific to smooth muscle cells, has been found to be transiently expressed by granulation tissue fibroblasts (Darby *et al.* 1990).

1.2.2.2.1 Fibroblast migration

It is thought that the migration of fibroblasts into the wound site is achieved by various mechanisms under the control of a complex array of stimuli. The stimulus for directional movement can be a soluble attractant gradient (chemotaxis), an adhesion gradient (haptotaxis) or associated with the three dimensional arrangement of extracellular matrix fibrils within the tissue (contact guidance).

A variety of substances found in healing wounds have been shown to promote the migration of fibroblasts *in vitro*, and thus may contribute to the colonisation of wounds by fibroblasts *in vivo*.

A. Chemotaxis

Chemotaxis has been defined as the directed migration of cells in response to a concentration gradient of soluble attractant (McCarthy *et al.* 1988). A multitude of agents known to be present during cutaneous repair have been shown to be chemotactic for fibroblasts. Such substances include complement metabolites, growth factors generated during platelet degranulation and synthesized by activated

macrophages and lymphocytes, and matrix fragments generated during wound debridement (table 1.2).

B. Cell adhesion and haptotaxis of fibroblasts migrating into wounds

Haptotaxis has been defined as the directed migration of cells along an adhesion gradient (McCarthy *et al.* 1988). It is now appreciated that certain components of the extracellular matrix can promote the migration of cells directly, while other components may impede it (McCarthy *et al.* 1988). When the dermis is wounded, the composition of the extracellular matrix changes drastically (Repesh *et al.* 1982). As a result of the vascular response to injury, a transudate of plasma escapes into the extravascular space and coagulates within the lesion forming a clot. The fibrin within the clot is decorated with fibronectin originating from plasma (Kurkinen *et al.* 1980). As the wound matures and granulation tissue is formed, the composition of the extracellular matrix changes. Fibroblast infiltration into the wound coincides with an increase in fibroblast-derived fibronectin, collagen type III fibres and hyaluronic acid (Repesh *et al.* 1982). As granulation tissue resolves, collagen type I fibrils begin to predominate, and the wound undergoes remodelling. The adhesive non-collagenous proteins, primarily fibronectin, of the extracellular matrix are of primary importance when considering the migration of connective tissue cells into the wound.

Fibronectin has multiple ligand-binding activities which can be simplified as matrix-binding activities and cell-binding activities. Different binding activities are localised in different domains of the fibronectin molecule.

Matrix-binding activities:	binding to collagen types I-IV, fibrin, thrombospondin, chondroitin sulphate, dermatan sulphate, heparin, heparan sulphate, hyaluronic acid
Cell-binding activities:	binding to fibroblasts, macrophages and vascular endothelial cells

The adhesion of cells to the extracellular matrix is essential to cell motility. Cells must adhere sufficiently to the substrate to generate the traction force required for cell motility yet not be so adherent that they are incapable of breaking adhesions and translocating (McCarthy *et al.* 1988). Cell adhesion to fibronectin is primarily thought to involve integrin recognition of the tetrapeptide arginyl-glycyl-aspartyl-

serine (RGDS using the single-letter amino acid code) sequences within fibronectin (Yamada and Kennedy, 1984). However, the binding of cells to fibronectin has also been shown to involve the interaction of cell membrane-associated proteoglycans with heparin binding domains within fibronectin (Lark *et al.* 1985; McCarthy *et al.* 1986). There is also some evidence that glycosaminoglycans (Schwartz and Juliano, 1985) and glycolipids (gangliosides) (Speigel *et al.* 1984) are involved in cellular adhesion to fibronectin.

Two types of adhesion structures, close contacts and focal contacts, have been observed on attached cells *in vitro* (Izzard and Lochner, 1980). Close contacts, which are thought to represent relatively weak cellular adhesion, are characterized by a distance of 20-30 nm between cell membrane and substrate, whereas focal contacts represent stronger adhesion and are characterised by a distance of 10-15 nm between cell membrane and substrate. Since the number of focal adhesions increases the motility rate decreases, it is probable that the close contacts may be involved in facilitating cell movement (Kolega *et al.* 1982). When cell binding to fibronectin is restricted to either the RGDS domain, or the heparin binding (proteoglycan) domain, only the weak close contacts form. However, when cell binding to both adhesive domains is permitted, using whole fibronectin, both close and the stronger focal contacts form (Lark *et al.* 1985), thus indicating that strong adhesion to fibronectin is facilitated by the collective influence of several distinct, weaker, interactions. Close contacts are thought to supply the cell with sufficient adhesion to facilitate traction (i.e to allow grip) without being too adhesive and thus preventing translocation. By regulating the level of adhesion to fibronectin the cell may be able to regulate its capacity to migrate.

The binding of cell membrane-associated heparan sulphate proteoglycan to fibronectin, via the heparin binding domain, is thought to partially facilitate cell-fibronectin adhesion. It has been demonstrated that hyaluronic acid and chondroitin sulphate weaken this binding (Culp *et al.* 1979; Brennan *et al.* 1983). Thus an interplay between different proteoglycans and hyaluronic acid at cell-matrix attachment sites may be involved in determining the state of cell adhesion. It has been suggested that chondroitin sulphate directly competes with heparan sulphate for heparin binding sites on the fibronectin molecule, thus the differential synthesis and elaboration of proteoglycans by fibroblasts could dictate the level of their adhesion, and thereby dictate their capacity to respond to migratory stimuli (McCarthy *et al.*

Table 1.2 Chemoattractants for fibroblasts

Chemoattractant	Source	References stating chemotaxis
C5a derivative (not C5a itself)	Complement cascade	Postlethwaite *et al.* 1979
Platelet-derived growth factor (PDGF)	Platelet α-granule release (Kaplan *et al.* 1986; Assoian and Sporn, 1986) and wound macrophages (Martinet *et al.* 1986; Rappolee *et al.* 1988)	Seppa *et al.* 1982; Deuel and Huang, 1984
Platelet factor 4 (PF4)	Released from platelets (Terkeltaub and Ginsberg, 1988)	Senior *et al.* 1983
β-thromboglobulin	Released from platelets (Terkeltaub and Ginsberg, 1988)	Senior *et al.* 1983
Transforming growth factor-β (TGF-β)	Released from platelet α-granules (Ross *et al.* 1986), wound macrophages (Rappolee *et al.* 1988), activated lymphocytes (Kehrl *et al.* 1986)	Postlethwaite *et al.* 1987; Yang and Moses, 1990
Platelet-derived endothelial cell growth factor (PDECGF)	Released from platelets (Ishikawa *et al.* 1989)	Pierce *et al.* 1991
basic Fibroblast growth factor (bFGF)	Released from platelets, activated macrophages and keratinocytes (Newman and Marcone, 1991)	Buckley-Sturrock *et al.* 1989
Epidermal growth factor (EGF)	Released from platelets, activated macrophages and keratinocytes (Newman and Marcone, 1991)	Davidson *et al.* 1988
Fibronectin and collagen type I and III fragments	Generated by macrophages during debridement	Tsukamoto *et al.* 1981; Postlethwaite *et al.* 1981
Arachidonic acid metabolites	Produced by macrophages	Mensing and Czarnetozki, 1984
Lymphocyte-derived chemotactic factor for fibroblasts (LDCF-F)	Produced by activated lymphocytes	Postlethwaite *et al.* 1976

1988). This may explain the high levels of hyaluronic acid found during granulation tissue formation, a time when fibroblasts are actively migrating into the wound. McCarthy *et al.* (1985) demonstrated that fibronectin gradients, set up in a Boyden chamber, haptotactically influence cell motility. Further work by McCarthy *et al.* suggests that the fibronectin cell motility domain (which is also thought to facilitate cell adhesion) is distinct from the RGDS cell adhesion domain (McCarthy *et al.* 1986).

C. Contact guidance during fibroblast migration into wounds

Contact guidance refers to the tendancy of cells to align along and thereafter migrate along discontinuities in substrata to which they are attached. The orientation of the filamentous components of the wound extracellular matrix changes as the wound progresses through repair. The clot (primarily fibrin and fibronectin) and newly deposited collagen at the wound periphery has a random fibrillar pattern. As fibroblasts migrate into the wound there is a progressive change from this random fibrillar pattern to a more orderly array of fibrils running parallel to the wound surface (Repesh *et al.* 1982). This ordered array is thought to be a consequence of centripetal fibroblast migration, towards the centre of the wound, within the early matrix. It is suggested that during this centripetal migration, fibroblasts advance, remove the random fibronectin fibrils, and leave ordered fibronectin fibrils in their wake (Sas *et al.* 1985). This modification of the early fibrous matrix is thought to influence the entry of further cells into the wound site. As fibroblasts migrate into such orientated matrices they are observed to align parallel to the orientation of the matrix fibres (Bryant, 1977; Repesh *et al.* 1982). In this way contact guidance forces exerted by the fibres contribute directly to sustaining the influx of fibroblasts into the wound site.

D. Penetration of the matrix

In addition to the stimuli for directional movement, fibroblasts and other migratory cells must have free space into which they can migrate. Fibroblast and macrophage migration into the wound site involves the penetration of the extracellular matrix (ECM). Such cellular penetration is thought to be facilitated by various mechanisms. Fibroblasts and macrophages are known to elaborate a variety of enzymes (plasmin, plasminogen activator, and collagenase) capable of digesting the matrix (Reich *et al.*

1976). Fibroblasts also clear a route by phagocytosis of the ECM, a process potentiated by fibronectin (Saba and Jaffe, 1980). The hydration of hyaluronic acid, produced by fibroblasts, may also be involved in opening up spaces within the matrix of the healing wound (Toole, 1981). In addition to the mechanical expansion of hyaluronic acid, it may also function to stabilise chemotactic gradients by holding free water in place (McCarthy *et al.* 1988)

1.2.2.2.2 Fibroblast proliferation

As previously mentioned the recruitment of fibroblasts into the wound site involves both migration and proliferation. A variety of substances found in healing wounds have been shown to promote the proliferation of fibroblasts *in vitro*, and thus may contribute to the colonisation of wounds by fibroblasts *in vivo*.

Proliferation is thought to be influenced by many agents, the most critical of which are thought to be peptide growth factors (Wong and Wahl, 1989). Table 1.3 lists the growth factors thought to be responsible for fibroblast proliferation during wound repair. Growth factors can be divided into two distinct classes which are complementary, as neither class of factor alone will cause proliferation. Prior to the initiation of growth, fibroblasts apparently require two signals, a competence signal and a progression signal (Pledger *et al.* 1977). Competence factors do not stimulate DNA synthesis but activate quiescent cells in the G_0 phase of the mitotic cycle, enabling them to become responsive to the action of progression factors. Progression factors cause cells to progress from G_1 to the S phase and causes initiation of DNA synthesis (Scher *et al.* 1979). Factors such as PDGF and bFGF impart competence signals (Scher *et al.* 1979), whereas factors such as EGF act as progression factors (Wong and Wahl, 1989). Some of the factors that stimulate fibroblast proliferation have not yet been classified as either competence or progression signals. Among these are IL-1 and TGF-β. It is uncertain whether IL-1 acts to increase cell surface receptors for other growth factors such as EGF and PDGF (Wong and Wahl, 1989). TGF-β may stimulate fibroblast proliferation through the stimulation of PDGF or IL-1 production by fibroblasts to which they respond in an autocrine manner (Loef *et al.* 1986). From table 1.3 it would appear that there is a great deal of overlap, and consequently redundancy, in the mitogenic capabilities of growth factors released during wound repair. This apparent redundancy may be explained by the fact that many of the observations of growth factor mitogenicity reported in table 1.3 were

made *in vitro* under two dimensional (planar) culture conditions, environmental conditions rarely encountered *in vivo*. It is possible that the three dimensional environment experienced by cells within wound tissue regulates their ability to respond to mitogenic stimuli. Alternatively, this array of mitogenic factors may be necessary to induce proliferation under the assortment of environmental conditions experienced by the fibroblast during the repair process. Supporting evidence for the role of one growth factor, PDGF, in wound fibroblast proliferation comes from *in vivo* observations of peak levels of this growth factor at times of peak fibroblast proliferation (Grotendorst *et al.* 1988).

With the exception of the relatively recently discovered PD-ECGF (Ishikawa *et al.* 1989), activated macrophages have been shown to be able to produce all of the currently accepted fibroblast growth factors; thus further supporting the view that the macrophage and its activities are central to the process of wound repair.

1.3 Matrix formation and remodelling

While matrix formation and remodelling is generally described as the third phase in the repair process, it begins at about the same time as the new tissue formation phase. However, matrix remodelling continues for many months if not years after granulation tissue has resolved, which explains its position in the temporal sequence of wound repair (Clark, 1990). During matrix remodelling, granulation tissue is gradually replaced by scar tissue, a less cellular and less vascular connective tissue. Even under optimal conditions the scar is an imperfect substitute for the dermis, since it has lower breaking strength, serves as a diffusional barrier to nutrients and oxygen and often results in deformation and reduction of function of the original tissue (Shosan, 1981; Chvapil and Koopman, 1984).

The deposition of the extracellular matrix (ECM) within the wound site follows a fixed temporal and spatial scheme, with the composition and structure of the ECM progressively changing from the time at which it is first deposited. Spatially, ECM is first deposited at the wound margins as part of the initial granulation tissue and later more centrally as the granulation tissue fills the wound space. Consequently, the composition and structure of granulation tissue ECM at a given site within the wound depends on the time elapsed since injury and the location of that site with regard to its distance from the wound margin.

Table 1.3 Factors mitogenic for fibroblasts

Mitogen	Source	References stating mitogenicity
Platelet-derived growth factor (PDGF)	Released from platelet α-granules (Kaplan *et al.* 1979; Assoian and Sporn, 1986), wound macrophages (Martinet *et al.* 1986; Rappolee *et al.* 1988) and fibroblasts (Paulsson *et al.* 1987)	Autocrine mitogenic effect (Ross *et al.* 1986), paracrine mitogenic effect (Paulsson *et al.* 1987)
Transforming growth factor-β (TGF-β)	Released from platelet α-granules (Ross *et al.* 1986), activated wound macrophages (Grotendorst *et al.* 1988; Rappolee *et al.* 1988), activated lymphocytes (Kehrl *et al.* 1986), and keratinocytes (Nicolas *et al.* 1988)	Mitogenic effect reported (Moses *et al.* 1985), however effect may be indirect due to induction of IL-1 and/or PDGF (Wahl *et al.* 1987; Loef *et al.* 1986)
PD-ECGF[#]	Released from platelets during degranulation (Ishikawa *et al.* 1989)	Pierce *et al.* 1991
basic fibroblast growth factor (bFGF)	Released from platelets, generated by activated wound macrophages (Rappolee *et al.* 1988) and keratinocytes (Newman and Marcone, 1991)	Gospodarowicz *et al.* 1987; Raines and Ross, 1989
Transforming growth factor-α (TGF-α)	Released from platelet α-granules (Terkeltaub and Ginsberg, 1988), generated by activated wound macrophages (Rappolee *et al.* 1988) and keratinocytes (Coffey *et al.* 1987; Newman and Marcone, 1991; Nicolas *et al.* 1991)	DeLarco and Todaro, 1978
Insulin-like growth factor-1 (IGF-1)	Produced by activated wound macrophages (Rappolee *et al.* 1988; Nagoaka *et al.* 1990)	Conover *et al.* 1985/1986; Froesch *et al.* 1985; Vetter *et al.* 1986
Fibroblast activating factor (FAF)	Produced by activated macrophages (Dohlman *et al.* 1984) and activated T lymphocytes (Wahl *et al.* 1985)	Turck *et al.* 1989; Demeter *et al.* 1991; Wahl *et al.* 1985
Interleukin-1 (IL-1)	Produced by activated macrophages	Schmidt *et al.* 1982; Libby *et al.* 1985; Wahl *et al.* 1987
Tumour necrosis factor-α (TNF-α)	Produced by activated macrophages, mast cells and T lymphocytes (Wong and Goeddel, 1989), keratinocytes (Nicolas *et al.* 1991)	Sugarman *et al.* 1985; Vilcek *et al.* 1988.

[#] = Platelet-derived endothelial cell growth factor

The temporal scheme by which the different ECM components are deposited is thought to be associated with their function within the wound. The clot formed as a consequence of vascular injury is primarily fibrin decorated with plasma fibronectin. As the wound matures and granulation tissue is formed, the composition of the extracellular matrix changes. Initially the extracellular matrix is primarily composed of hyaluronic acid and fibronectin supplemented with limited levels of collagens types I, III and V, all primarily synthesized by fibroblasts. The high levels of the non-sulphated glycosaminoglycan hyaluronic acid endow this early matrix with a low impedance for cellular ingrowth. Fibronectin is thought to provide both chemotactic and haptotactic stimuli for cellular migration, and also to act as a substrate for that migration. Fibronectin appears to act as a nidus for collagen fibrillogenesis and subsequently to transmit the forces of contraction from fibroblasts to the collagenous matrix. The early deposition of collagen types I, III and V is thought to provide the wound with nascent tensile strength. As the matrix matures: (1) hyaluronic acid and fibronectin effectively disappear, (2) type I collagen becomes the predominant ECM component - thus increasing the tensile strength of the wound, and, (3) proteoglycans are deposited - increasing the wounds resilience to deformation. The individual extracellular matrix components will now be discussed in more detail.

1.3.1 Hyaluronic acid (HA)

HA is a glycosaminoglycan (GAG). HA is primarily found during the first few days after injury, after which time HA levels fall (Balaz and Holmgren 1950; Bently, 1967; Dorner, 1967; Anseth 1961). It was initially suggested by Balaz and Holmgren (1950) that HA plays a critical role in fibroblast proliferation, a suggestion supported by the observation that HA appears at times of mitosis and cell movement during organ generation (Toole, 1972).

Two, not necessarily exclusive, theoretical explanations have been proposed to explain the role of HA in cell motility. (1) HA may control the adhesion and detachment of the cell membrane from the extracellular matrix (Lark *et al.* 1985; Rollins and Culp, 1979), and, (2) HA, which can become highly hydrated, could cause tissue swelling, thus creating additional space between the matrix and/or cells and thereby allow the recruitment of additional cells into these areas (Toole, 1981). HA may also be important for fibroblast proliferation. Several workers have reported that HA synthesis is elevated in subconfluent fibroblasts (Tomida *et al.* 1974) and

following growth factor induced proliferation (Lembach, 1976). As granulation tissue matures, HA is progressively lost by the action of fibroblast-derived hyaluronidase (Ruggiero *et al.* 1987). The sulphated GAGs that replace HA are associated with a protein core (Hascall and Hascall, 1981) and are termed proteoglycans. Little work has been directed at defining the stimuli responsible for HA and proteoglycan synthesis by fibroblasts; IL-1 and TGF-β have, however, been implicated (Whiteside *et al.* 1985; Postlethwaite and Kang, 1988).

1.3.2 Fibronectin

The adhesive glycoprotein fibronectin is thought to fulfil many roles in the repair of cutaneous wounds. Fibronectin has been shown to act as a chemotactic factor for monocytes (Clark *et al.* 1988a) and as a non-specific opsonin of tissue debris (Brown, 1986), as a haptotactic substrate and chemotactic factor for cell movement (fibroblasts McCarthy *et al.* 1988, epithelial cells (Nickoloff *et al.* 1988) during new tissue formation, and as a scaffold for new matrix deposition (Clark, 1988a). In all these situations cell binding is crucial (p 33). Fibronectin is a component of the fibrin clot (Kurkinen *et al.* 1980), its association with fibrin within the clot is thought to regulate monocyte-macrophage invasion of the wound space (Ciano *et al.* 1986). Fibronectin also augments the attachment of fibroblasts to fibrin thereby facilitating their early ingrowth into the fibrin clot at the wound site (Grinnell *et al.* 1980). Fibronectin is often found in areas of the wound bed where active migration and proliferation are occurring for example around ingrowing fibroblasts, underneath the migrating epidermis, and within the walls of new blood vessels; thus suggesting that it provides a provisional matrix for cell translocation (Clark, 1990). It has also been speculated that a template of fibrillar, extracellular fibronectin is essential for collagen deposition (McDonald *et al.* 1982; Clark, 1988a). Such speculation derives from the spatial and temporal distribution of fibrillar fibronectin and collagen during granulation tissue formation (Kurkinen *et al.* 1980; Holund *et al.* 1982; Viljanto *et al.* 1981), and the observation that the pattern of collagen deposition follows that previously portrayed by fibronectin (Clarke, 1988a). Fibronectin is also a component of the fibronexus (Singer, 1979), the linkage structure between myofibroblasts and collagen, which is thought to transmit cellular contraction forces to the wound margin, via collagen, and thereby affect wound contraction (p 49). The factors within wounds that regulate production of fibronectin by fibroblasts are effectively unknown.

However, the peptide growth factors EGF and TGF-β (known to be released from platelet α-granules during degranulation and by activated macrophages) and IL-1 (released primarily by activated macrophages) have been shown to increase fibronectin synthesis *in vitro* (Chen *et al.* 1977; Krane *et al.* 1985; Ignotz and Massague, 1986; Ignotz *et al.* 1987) and consequently may involved in fibronectin synthesis during cutaneous repair *in vivo.*

1.3.3 Proteoglycans (Chondroitin-4-sulphate, Dermatan sulphate, Heparan sulphate)
Chondroitin-4-sulphate and dermatan sulphate levels increase during granulation tissue formation as hyaluronic acid levels decrease (Bently, 1967). Little is known about proteoglycan function *in vivo* except that these substances contribute significantly to tissue resilience (Hascall and Hascall, 1981).

Other proteoglycan functions have been suggested:

1. Regulation of cell motility.
2. Regulation of cell growth
3. Regulation of collagen synthesis

1. Regulation of cell motility
The state of cell adhesion-deadhesion to surfaces is critical to the process of cell motility. It has been proposed that an interaction of cell surface heparan sulphate proteoglycan with fibronectin mediates the bonding of cells to substrate, while accumulation of hyaluronic acid is known to weaken this bond (Culp *et al.* 1979). By regulating cell surface heparan sulphate and hyaluronic acid levels the cell is able to regulate adhesion and thus motility.

2. Regulation of cell growth
Cell shape and substratum anchorage are critical to the process of cell division. As proteoglycans are involved with the regulation of cellular adhesion, modulations of that adhesion would also be expected to influence proliferation (Letourneau *et al.* 1980). Evidence for this regulatory role have come from observations of reduced sulphated proteoglycan synthesis, in tandem with elevated hyaluronic acid synthesis, during active proliferation (Underhill and Keller, 1976), and, the observation that cells actively shed heparan sulphate prior to division (Kraemer and Tobey, 1972).

Further, it has been suggested that heparan sulphate may regulate cell proliferation within the wound by binding growth factors (Klagsbrun and Shing, 1985; Raines and Ross, 1985).

3. Regulation of collagen synthesis

It has been suggested, from various lines of evidence, that proteoglycans may regulate collagen synthesis (Wood, 1960; Armitage and Chapman, 1971; Kischer and Shetlar, 1974; McPherson and Piez, 1988). As chondroitin-4-sulphate is present in significant amounts in granulation tissue (Kischer and Shetlar, 1974), but not in mature scar (Shetler *et al.* 1972) it is suggested that it may be involved in the initial generation of the collagenous matrix and subsequent matrix remodelling.

1.3.4 Collagen

Collagen is a generic term encompassing a family of at least 12 triple chain glycoproteins found in the extracellular matrix (McPherson and Piez, 1988). At least three classes of collagen occur in connective tissue: (1) fibrillar collagens (types I, III and V), which have uninterrupted triple helices; (2) basement membrane collagen (type IV), which has an interrupted triple helix and forms a mesh work in the *lamina densa*; and, (3) other interstitial collagens with interrupted helices (types VI, VII and VIII). The chief characteristic of the fibrillar collagens (I, III and V) is the ability of their monomers to polymerise both side by side and end to end into long fibrillar aggregates or bundles (Trelstad and Silver, 1981). These fibrillar bundles are the major structural collagens in all connective tissues (Clark, 1990).

Studies of collagen deposition during wound repair have primarily focused on the two most characterised and abundant collagen types, i.e. fibrillar collagens type I and type III. Normal skin contains approximately 80-90% type I and 10-20% type III (Epstein, 1974; Miller, 1976). Various laboratories have observed a transient increase in the relative levels of type III collagen relative to type I collagen, during the first few days after wounding; levels subsequently rapidly return to that of normal skin (Bailey *et al.* 1975; Clore *et al.* 1979; Gay *et al.* 1978). As fetal skin has a higher ratio of type III to I collagen (Epstein, 1974), these observations have led to the suggestion that skin fibroblasts may transiently assume fetal fibroblast characteristics in response to tissue injury (McPherson and Piez, 1988). It is thought that the same fibroblast population produces both types I and III collagen; the mechanism of

switching is unclear, but is thought to involve the actions of prostaglandin E_2 and IL-1 (Agelli *et al.* 1987; Steinman *et al.* 1982).

More recent studies have reported that fibrillar type V collagen increases during granulation tissue development in parallel with tissue vascularity, an observation that led to the suggestion of an association between capillary endothelial cells and type V collagen (Hering *et al.* 1983). The observation that collagen type V is abundant in hypertrophic scars (Ehrlich and White, 1981), which are known to have a lavish capillary network, may further support this association.

The factors that regulate collagen deposition within the wound are not fully understood; however certain peptide growth factors, which have been shown to stimulate collagen synthesis by fibroblasts *in vitro*, are thought to encourage collagen production during wound healing. Both TNF-α and IL-1, which are secreted by activated macrophages, have been shown to promote collagen synthesis by fibroblasts (Beutler and Cerami, 1986; Krane *et al.* 1985). This upregulation of collagen synthesis is apparently controlled at the level of mRNA (Krane *et al.* 1985; Agelli *et al.* 1987). Whether this is due to an increased transcription of the collagen gene or increased stability of the mRNA molecule itself is not clear. TGF-β, elaborated by platelets and macrophages, is also thought to mediate collagen synthesis directly. When injected subcutaneously into newborn mice, rapid fibrosis consistent with rapid increases in the production of collagen are observed (Roberts *et al.* 1986). *In vitro* studies have shown that, like IL-1, TGF-β stimulates the amount of collagen protein and mRNA produced per fibroblast (Ignotz and Massague, 1986; Ignotz *et al.* 1987). In addition to stimulating collagen synthesis, TGF-β also causes an increase in the incorporation of newly synthesized collagen into the extracellular matrix (Ignotz and Massague, 1986; Roberts *et al.* 1986). While the above discussion relates to the stimulation of synthesis of fibrillar types I and III collagen, Narayan and Page (1983) reported that PDGF, which is released by platelets and secreted by activated macrophages, stimulates the synthesis and matrix incorporation of fibrillar type V collagen. Certain other factors may play an indirect role in stimulating collagen synthesis by stimulating the recruitment of fibroblasts into the wound site. Tables 1.2 and 1.3 (p35 and p39) list many of the factors thought to be responsible for stimulating the colonisation of wound sites by fibroblasts.

Mechanisms are thought to exist that downregulate the production of matrix proteins, and thereby prevent uncontrolled deposition of matrix components within

the wound site. Though such mechanisms have yet to be fully elucidated, the following may bring about this regulation. While IL-1 has been shown to stimulate collagen mRNA transcription by fibroblasts (see above), it has also been shown to induce fibroblasts to synthesize prostaglandin E_2 (PGE_2), and PGE_2 is known to cause a down regulation in the synthesis of collagen types I and III (Wong and Wahl, 1991). Also interferon-γ, released by activated T-lymphocytes, has been shown to specifically suppress collagen synthesis in human fibroblasts with little or no suppression in overall protein synthesis (Duncan and Berman, 1985; Jiminez *et al.* 1983).

The early formation of collagen types I, III and V fibrils are thought to furnish the wound with nascent tensile strength. As the matrix matures during the ensuing few weeks after injury, these fibrils progressively aggregate into larger fibrillar bundles and gradually provide the wound with increasing rigidity and tensile strength (Heughan and Hunt, 1975; Trelstad and Silver, 1981). The rate at which wounds gain tensile strength is slow. Levenson *et al.* (1965) studied the gain in tensile strength of incisional rat skin wounds, and reported that such wounds had only gained between 20 and 25% of their final strength three weeks after injury. Scar tissue is mechanically weaker than normal unwounded skin. Levenson *et al.* 1965 reported that by 9 weeks post wounding, after which time little improvement in tensile strength is observed, wound tissue was 20 to 30% weaker than unwounded rat skin.

The way in which wounds progressively gain tensile strength is thought to be dependent not only on the rate of collagen deposition, but also on collagen remodelling with the gradual formation of larger collagen bundles (Kirscher and Shetlar, 1974) and an alteration of inter-molecular cross-links (Bailey *et al.* 1975). Collagen remodelling during the formation of a scar is thought to be dependent on both continued synthesis and collagen degradation (Clark, 1990). The rate of collagen degradation changes as wound healing proceeds, starting relatively slowly during the early stages and becoming progressively more rapid as wound maturation occurs (Zeitz *et al.* 1978). The degradation of fibrillar collagen types I and III during remodelling is thought to be undertaken by specific collagenases synthesised by fibroblasts (Mignatti *et al.* 1988), whereas, fibrillar type V collagen degradation may involve the release of a specific collagenase from macrophages (Hibbs *et al.* 1985). The secretion of collagenase is not a constitutive property of fibroblasts, but is thought to be induced by various growth factors secreted primarily by macrophages

(Riches, 1988) and possibly epithelial cells (Johnson-Wint, 1980). A variety of growth factors have been shown to stimulate collagenase production by fibroblasts *in vitro*, including: IL-1 (Postlethwaite *et al.* 1983; Huybrechts-Godin *et al.* 1985), TNF-α (Dayer *et al.* 1985), EGF (Chua *et al.* 1985), PDGF (Deuel and Huang, 1984; Bauer *et al.* 1985), and IGF-1 (Conover *et al.* 1985/1986). However, the physiological role of these mediators in collagen turnover during the wound repair process remains to be defined (Mignatti *et al.* 1988).

Growth factors may also regulate the level of new matrix degradation. TGF-β not only directly stimulates collagen synthesis (see above), but also has the ability to inhibit proteolytic degradation of newly synthesized matrix proteins including collagen (Sporn *et al.* 1987). In this regard TGF-β has been shown to both induce fibroblasts to produce protease inhibitors (Laiho *et al.* 1986; Docherty *et al.* 1985) and secrete reduced levels of the proteases themselves (Laiho *et al.* 1986; Chiang and Nilsen-Hamilton, 1986; Matrisian *et al.* 1986).

1.4 Wound contraction

Wound contraction is the process by which the surface area of excisional wounds is decreased by the inward movement of the wound margins (Snowden *et al.* 1984). It may also be defined as the process by which the size of a full thickness open wound is diminished, and is characterised by the centripetal movement of the whole thickness of surrounding skin (Peacock, 1984).

In many loose-skinned mammals contraction is the major process by which surface wounds are healed; it seldom leads to deformity or loss of function unless it occurs over a joint and scar tissue is fixed to the underlying tissue. In humans however, contraction rarely goes to completion except in very small wounds, and may result in significant deformity and loss of function, the extent of which depends on the size and location of the wound. Humans have lost local dermal mobility in many areas. In man, skin is more or less firmly attached to relatively inelastic and immobile fascia, which in turn is attached to major musculature, bone or other underlying structures. Many mammals such as rats possess a well developed layer of cutaneous striated muscle, the *panniculus carnosus*, of which only vestigial remnants remain in human beings. This muscle and the lack of substantial attachment of integument to underlying structures permit contraction to occur to its fullest extent without interfering with the mechanical function of underlying structures. The same process

occurs in human beings, but in contrast to many other mammals it can lead to constriction, distortion or immobilisation in some locations owing to tension developed through attachment of the integument to underlying structures. Thus excessive contraction is often seen as a serious complication to healing.

Although initially wound contraction was thought to be caused by forces generated by newly deposited collagen fibres (Billingham and Russell, 1956) in 1956 Abercrombie and colleagues showed that this movement was the result of forces generated by cells residing in the central granulation tissue. It appears that wound contraction is a dynamic process where cells organise their surrounding connective tissue matrix. Historically, many theories have been proposed but few have survived the test of time.

1.4.1 Theories of wound contraction

Five major theories regarding the mechanism of wound contraction have been put forward:

1. The Push Theory: the wound margins may be pushed in by extension of the surrounding skin.
2. The Growth and Push Theory: the wound margins may grow and push themselves inwards by pushing on the surrounding skin.
3. The Sphincter Theory: contractile material at the wound edge may act as a sphincter.
4. The Picture Frame Theory: active cells within the margin of the wound may migrate inwards, pulling on the material within the margins of the defect.
5. The Pull Theory: material within the defect may exert tension and pull the margins of the defect inwards.

Reviewed by van Winkle 1967

Theories 1 and 2 were abandoned after the demonstration that excision of the wound bed led to re-expansion of the wound (Cuthbertson, 1959), suggesting that tension had been created within the wound bed and that no growth of the wound margins had occurred. Theory 3 was abandoned when it was observed that rectangular wounds do not contract into a circular shape, a prerequisite for the purse string effect of sphincter action (Peacock, 1984).

Theory 4, the picture frame theory was first advanced by Grillo *et al.* (1958);

supporting evidence for this theory came from the observation that when the wound margin is removed wounds retract (Watts *et al.* 1958). Critics of this theory have argued that contraction was inhibited due to a physical separation of granulation from the surrounding skin thus removing the mechanism of force transduction from granulation tissue to wound margins (van Winkle, 1967).

The remaining theory, the Pull Theory, which proposes that "material" within the wound defect exerts a tension and pulls the margin of the defect inwards. Supporting evidence for this theory comes from the observation of wound expansion following the complete excision of granulation tissue within the wound (Abercrombie *et al.* 1954; Watts *et al.* 1958; Cuthbertson, 1959) and the centripetal movement of marks tattooed onto the surface of granulation tissue within splinted wounds (Charlton *et al.* 1961). Snowden and Cliff (1985) demonstrated that explanted granulation tissue contracts *in vitro*, and that the tension generated by such explants is associated with total cellularity, thus supporting both the pull theory and the role of cellular components of the granulation tissue in contraction. The cell-derived force of wound contraction has been ascribed to the fibroblasts, which unlike macrophages and the endothelial cells of capillaries, are mainly orientated along the radial lines of contraction within wounds (Welch *et al.* 1990).

Two main theories have been proposed to explain how fibroblasts may generate, and transmit, the force necessary to facilitate wound contraction.

1. The cell contraction - myofibroblast theory (Gabbiani *et al.* 1971).
2. The cell traction - fibroblast theory (Ehrlich and Rajaratnam, 1990).

Both theories agree that wound contraction is an active cellular phenomenon that depends on the activity of viable fibroblasts; however, the two theories propose different mechanisms by which such cells generate the contractile force necessary to facilitate this process. The myofibroblast theory suggests that the contraction force is derived from a muscle-like cellular contraction; whereas, the fibroblast theory suggests a tank tread-like traction activity by the cell on the matrix.

The two theories of wound contraction are described below. The *in vivo* and *in vitro* evidence in support of a given theory follows its description. Fibroblast-mediated contraction of fibroblast-populated collagen lattices [FPCLs] (p160), a widely accepted *in vitro* model of the process of wound contraction, has been

differentially employed to provide support for both theories; its application will be discussed.

1.4.1.1 The cell contraction - myofibroblast theory

While examining wound granulation tissue, Gabbiani *et al.* (1971) observed significant numbers of cells, termed myofibroblasts, that displayed morphological characteristics of both fibroblasts and smooth muscle cells (SMCs). The presence of significant numbers of these cells, morphologically similar to smooth muscle cells (i.e. contractile cells), within actively contracting granulation tissue encouraged Gabbiani *et al.* to suggest a role for these apparently contractile cells in the process of wound contraction.

The morphological characteristics of myofibroblasts include:

1. Large bundles of actin microfilaments (40-80 Å) running parallel to the long axis of the cell, which display electron dense areas where filaments attach to the cell membrane, both similarly observed in SMCs.
2. Deformed/indented nuclei. SMC nuclei become folded and twisted during active contraction.
3. Numerous intercellular junctions including desmosomes and gap junctions, and structures resembling the basal lamina of SMC.

   (Gabbiani *et al.* 1971; 1972; 1978)
4. A co-linear assembly of intracellular microfilaments and extracellular fibronectin (and types I and III collagen) termed "the fibronexus".

   (Singer, 1979; Singer *et al.* 1984; Tomasek *et al.* 1987; Tomasek and Haaksma, 1991).

The cell contraction - myofibroblast theory suggests that movement of microfilament (actin) bundles (also termed stress fibres), contracts the myofibroblast in a muscle-like fashion. As the myofibroblast displays many cell:cell and cell:matrix (fibronexus) contacts, this cellular contraction pulls collagen fibrils towards the body of the myofibroblast, and holds them until they are stabilized into position (Rudolph, 1980). This gathering of collagen fibres towards the myofibroblast cell "body" leads to the shrinkage of granulation tissue. As the extracellular matrix of the wound is continuous with the undamaged wound margin, this granulation tissue shrinkage pulls on the wound margin and leads to wound contraction. This theory proposes that the

coordinated contraction (cellular shortening) of many myofibroblasts, synchronised with the help of gap junctions, generates the force necessary for wound contraction (Skalli and Gabbiani, 1988).

Evidence which appears to support the cell contraction - myofibroblast theory

1. Cells with myofibroblastic characteristics, primarily actin microfilament bundles, are present within actively contracting granulation tissue (Gabbiani *et al.* 1971). It has been reported that after active contraction has ceased the myofibroblast population declines (Rudolph *et al.* 1977; McGrath and Hundahl, 1982).
2. Wound contraction is known to be inhibited by the application of skin grafts, full-thickness grafts being more inhibitory than split-thickness grafts. It has been demonstrated that myofibroblasts make only a fleeting appearance in contraction-inhibited grafted wounds, whereas in ungrafted contracting wounds they remain for much longer (Rudolph, 1979); their presence suggests an active role.
3. Strips of granuloma tissue, rich in myofibroblasts, can be induced to contract by stimuli known to induce smooth muscle cell contraction. This suggests that myofibroblasts are not only morphologically but functionally similar to smooth muscle cells, thus supporting the role of the smooth muscle-like cell, the myofibroblast, in wound contraction (Majno *et al.* 1971, Garcia-Valdecasas *et al.* 1981).
4. Microfilament bundles (stress fibres) dissected out of living cells or studied within permeabilized cells can contract upon the addition of ATP (Isenberg *et al.* 1976; Kreis and Birchmeier, 1980), thus suggesting that a cell containing such bundles contains the machinery for cellular contraction and consequently wound contraction.

Evidence from FPCL contraction *in vitro.*

1. Attached FPCL, i.e. those adherent to the surface on which the collagen polymerised, do not undergo a reduction in surface area; they do, however, reduce in volume due to dorso-ventral contraction (Guidry and Grinnell, 1985). Various workers have reported that fibroblasts within such contracting attached FPCL develop characteristics morphologically similar to myofibroblasts in tissues undergoing contraction (Skalli and Gabbiani, 1988; Schultz and Tomasek, 1990). Tomasek *et al.* (1992) demonstrated that normal human palmar aponeurosis fibroblasts cultured for 5 days in attached collagen lattices developed abundant actin microfilaments orientated parallel to the long axis of the cell. They also demonstrated

that bundles of microfilaments formed close associations with extracellular filaments, which showed intense anti-fibronectin labelling, resembling the fibronexuses described by Singer (1979). Fibroblasts from other sources have also been reported to acquire certain of these myofibroblastic characteristics when cultured in attached collagen lattices, including fibronexus-like fibronectin fibrils on, and microfilament bundles within, human foreskin fibroblasts (Mochitate *et al.* 1991), and microfilament bundles within rabbit synovial fibroblasts (Unemori and Werb, 1986) and porcine periodontal ligament fibroblasts (Farsi and Aubin, 1984). The presence of myofibroblastic cells within these contracting attached lattices suggests a role for the myofibroblast in collagen lattice contraction and presumably in wound contraction. It should, however, be noted that other workers studying similar attached lattices have been unable to observe microfilament bundles, the principal characteristic of myofibroblasts (Grinnell and Lamke, 1984).

2. Release of attached lattices, by "rimming", some time after polymerisation, results in a rapid, symmetric contraction of the collagen lattice (Dodd *et al.* 1982; Unemori and Werb, 1986; Mochitate *et al.* 1991; Tomasek *et al.* 1992). Rapid contraction occurs within the first 10 minutes after release of the lattice from the substratum, with greater than 70% of this contraction occurring within the first 2 minutes (Tomasek *et al.* 1992). Rapid contraction results in a shortening of the elongated fibroblasts and a compaction of stress fibres with their subsequent disappearance from the cell (Dodd *et al.* 1982; Unemori and Werb, 1986; Mochitate *et al.* 1991; Tomasek *et al.* 1992). This rapid collagen lattice contraction is thought to be primarily dependent upon active fibroblast contraction, as disruption of the actin cytoskeleton of the cell with cytocholasin D, just prior to release, inhibits it (Dodd *et al.* 1982; Tomasek *et al.* 1992). Such results suggest that the fibroblast-derived force, necessary for both lattice contraction and wound contraction, can be generated by cellular contraction of the actin component of the cytoskeleton i.e. stress fibre contraction. Such rapid contraction has been observed in rabbit skin wounds following the removal of a wound splint (Abercrombie *et al.* 1960), an observation that tends to support the myofibroblast theory of wound contraction.

3. Studies using free floating FPCL, which are released from their attachment to the petri dish soon after polymerisation, have reported the transient expression of certain myofibroblastic characteristics, specifically gap junctions, during active lattice contraction (Bellows *et al.* 1982).

1.4.1.2 The cell traction - fibroblast theory

The traction theory proposes that fibroblasts bring about a closer approximation of matrix fibrils by exerting "traction forces" (analogous to the traction of wheels on tarmac) on extracellular matrix fibres to which they are attached. This theory proposes that fibroblasts neither shorten in length, nor do they act in a co-ordinated multicellular manner (as proposed by the myofibroblast theory); but, rather that a composite force, made up of traction forces of many individual fibroblasts, is responsible for matrix contraction. Such traction forces are shearing forces tangential to the cell surface generated during cell elongation and spreading (Stopak and Harris, 1982).

The traction theory is based on observations and proposals made by Harris *et al.* (1981) and Stopak and Harris (1982). From observing fibroblasts and the forces they generate while cultured on distortable sheets of silicone rubber and in collagen lattices, they proposed that the phenomenon seen as fibroblast migration in two dimensional culture conditions, actually serves quite a different and previously unsuspected function in the body, namely the remodelling of extracellular matrix fibres, an activity critical to wound repair. As individual fibroblasts elongate and spread on distortable silicone sheets they cause that surface to wrinkle (Harris *et al.* 1981). This wrinkling is thought to represent a "gathering effect" of the fibroblast on the elastic surface. According to this theory, the composite effect of many fibroblasts gathering collagen fibrils within the wound, is thought bring about wound contraction. The traction theory of connective tissue remodelling has since been championed in the field of wound repair by Ehrlich (Ehrlich, 1988a/b; Ehrlich and Rajaratnam 1990).

Evidence which appears to support the cell traction - fibroblast theory

There are several lines of evidence to suggest that wound contraction is brought about by means other than coordinated cellular contraction.

1. Significant contraction (25%) has been shown to occur in full-thickness pig skin wounds prior to the appearance of cells with myofibroblastic characteristics (McGrath and Hundahl, 1982), thus suggesting that wound contraction can proceed without such cells being present.

2. Rat wounds have been observed to contract to 60% of their original size by 7 days post wounding, although during this time less than 15% of fibroblasts had

myofibroblastic characteristics. At 21 days when active contraction has all but ceased peak levels of myofibroblastic cells were observed (Rudolph, 1979). These observations suggesting that the myofibroblastic phenotype may be a consequence of contraction rather than the cause.

3. Darby *et al.* (1990) reported that full thickness rat skin wounds contract by approximately 40% prior to the appearance of myofibroblastic cells.

4. Very few fibroblasts displaying myofibroblastic characteristics are present in burn wounds at 7 days post-wounding, by which time such wounds had contracted by 40% (Ehrlich and Hembry, 1984).

5. Myofibroblasts are not readily identifiable in healing rat wounds before 7 days when closure is 50% complete (Majno *et al.* 1971).

5. Skin wounds in the mutant Tight Skinned Mouse (TSM) are slow to contract, taking approximately 6 weeks to full closure rather than the normal 3 weeks. Wound closure in the TSM is characterised by a three week delay, prior to the onset of contraction, then a 3 week period of contraction. During the pre-contractile phase large numbers of myofibroblasts were found; however, after the onset of, and during, active contraction fewer myofibroblasts were found (Hembry *et al.* 1986), thus suggesting that myofibroblasts may not be actively involved in wound contraction.

6. Myofibroblasts are apparent in frostbite injury, where there is little if any contraction (Li *et al*, 1980).

7. Whereas it has been reported that strips of granuloma tissue contract in response to agent known to stimulate SMC contraction, wound granulation tissue does not respond in a similar fashion (Majno *et al.* 1971), thus questioning the role of these smooth muscle-like cells, myofibroblasts, in wound contraction.

Evidence from FPCL contraction *in vitro.*

1. Fibroblasts within actively contracting collagen lattices have also been observed to gather together collagen fibrils as they elongate and spread (Bell *et al.* 1979; Harris *et al.* 1981).

2. It has been reported that fibroblasts contracting collagen lattices actually elongate in the direction of the contractile force they exert rather than shorten as would be expected of a contractile cell (Bell *et al.* 1979; Stopak and Harris, 1982).

3. It has been reported that during active contraction of FPCL, few cells displaying actin bundles (stress fibres) are present, however, upon cessation of lattice

contraction many cells displaying prominent stress fibres are apparent (Bellows *et al.* 1982; Ehrlich, 1988a; Tomasek *et al.* 1992). This implies that fibroblasts rather than myofibroblasts bring about matrix compaction of this wound contraction model.

4. Cells with myofibroblastic characteristics are more apparent at the lattice periphery than in more central areas of contracting FPCL (Bellows *et al.* 1982; Stopak and Harris, 1982; Ehrlich, 1988a). When the contraction of myofibroblast-enriched lattices, prepared by removing the central (myofibroblast deficient) area of the lattice, was compared with that of whole lattices, the rate of lattice contraction was unaffected by myofibroblast enrichment (Ehrlich 1988a). Additionally, contraction of the central area, removed during this attempt at myofibroblast enrichment, was unaffected by removal of the myofibroblast-rich perimeter (Ehrlich, 1988a). These observations suggest that there is no requirement for myofibroblastic cells in lattice contraction.

5. When contraction was studied in similar-sized wedges cut from FPCLs that either included or excluded the myofibroblast-rich lattice perimeter, contraction was seen to be slowest in those areas rich in myofibroblasts (Ehrlich and Rajaratnam, 1990).

6. It has also been observed that cells in more central areas of FPCL have fewer, if any, intercellular connections than those in the lattice perimeter (Ehrlich, 1988a). This observation taken together with the observation that central areas of FPCL contract equally as well as, if not more rapidly than, more peripheral areas, suggests that fibroblasts compact the collagen matrix by working as individual units, rather than, as the myofibroblast theory suggests, as a mass of interconnecting/inter-communicating cells (Ehrlich, 1988a).

7. When the rate of FPCL contraction in lattices seeded with fibroblasts cultured from normal skin (no myofibroblasts) was compared with that of lattices seeded with fibroblasts cultured from hypertrophic scar (rich in myofibroblasts), the source of cells was found to have no influence on the rate of lattice contraction (Ehrlich, 1984). This appears to question the idea that a contraction-specialised cell (i.e. the myofibroblast) resides in actively contracting tissue.

8. Rungger-Brandle & Gabbiani (1983) suggested that the morphological attributes of myofibroblasts, specifically their prominent stress fibres, made these cells the most logical choice for the production of contractile forces, especially as stress fibres in permeabilised cells can be made to contract by adding ATP. However, Ehrlich and Rajaratnam (1990) demonstrated that both myofibroblasts (with actin filament

bundles or stress fibres) and fibroblasts (with fine filamentous actin) permeabilised with glycerol could contract equally well in response to ATP. Cellular contraction appears to have no requirement for stress fibre bundles. Additionally, when ATP is applied to fibroblasts in collagen lattices at levels known to stimulate cellular contraction in monolayer, neither a stimulation in cellular contraction nor in lattice contraction is observed (Ehrlich and Rajaratnam, 1990). Microscopical examination of ATP treated lattice fibroblasts revealed ruptured intracellular actin filaments thus questioning the ability of stress fibre-based cellular contraction to bring about wound contraction.

These *in vitro* observations suggest that the presence of microfilament bundles (or stress fibres), and by inference myofibroblasts, is not necessary for cell-mediated wound contraction. Wound contraction would appear to proceed in the presence of fibroblasts alone. It has recently been proposed that the myofibroblastic phenotype, which displays many stress fibres, rather than being responsible for contraction, is in fact a highly motile form of the fibroblast thought to facilitate migration from the wound site after conclusion of active contraction (Ehrlich, 1992 personal communication). This however contradicts the widely held belief that the presence of stress fibres is normally associated with tight adhesion to the underlying substrate (Willingham *et al.* 1977; Herman *et al.* 1981). Fibroblasts migrating out of a primary tissue explant generally lack stress fibres in the first few days of culture when they are migrating rapidly; with time migration slows down and the stress fibres become more prominent (Couchman and Rees, 1979).

In vitro evidence from FPCL studies

Evidence given in support of the cell contraction - myofibroblast theory invariably comes from FPCL studies carried out on fibroblast seeded collagen lattices that remain attached to the plastic culture dish in which the lattice was polymerised; such lattices are termed "attached lattices" and unless released do not decrease in surface area, though their volume (i.e. depth) has been shown to slowly reduce as a consequence of fibroblast activity (Guidry and Grinnell, 1985). In contrast, evidence given in support of the cell traction - fibroblast theory invariably comes from studies using "rimmed" lattices that float beneath the surface of exuded culture medium, termed "free floating collagen lattices". The surface area of such floating lattices is seen to diminish with time. Which of these methods of use of the FPCL assay is

more like the *in vivo* situation, and consequently more closely parallels wound contraction, is a matter of opinion. It has, however, been suggested that during contraction attached FPCLs develop into an active "tissue" resembling granulation tissue, whereas floating FPCLs develop into a resting tissue that resembles the dermis (Mochitate *et al.* 1991). The granulation tissue of a full thickness excisional skin wound is attached at its periphery to "normal" dermis, the major component of which is type I collagen. This "normal" tissue at the wound margin is neither rigidly fixed, nor is it completely free to move; it exerts a reactive force in response to the inward pull of the granulation tissue. Thus an isometric tension would be expected to be generated within the wound, associated with the contractile force of the granulation tissue and the reaction by the wound margin. It thus would appear that neither free floating lattices, which experience no opposing or reactive force, nor, attached lattices, which experience an insuperable opposing force, accurately parallel the *in vivo* situation. Such observations may question the relevance of this model, as it is currently employed, to study the mechanisms underlying the process of wound contraction.

The rapid recoil following the release of attached FPCL, described by several authors including Tomasek *et al.* (1992) and Dodd *et al.* (1982) in support of the cell contraction - myofibroblast theory, may also be explained in terms of cell traction. It is possible that cyto-tractile activities of fibroblasts put the collagen matrix and consequently matrix-attached cells under tension leading to the formation of stress fibres, and that these traction induced stress fibres act as a tension store. The rapid contraction, observed after rimming attached lattices, may thus be an indirect effect of cellular traction, due to the generation of stress fibres as a consequence of frustrated cell locomotion (Ehrlich and Rajaratnam, 1990).

1.4.1.3 Summary

There are currently two theories of cell-mediated wound contraction, the cell contraction - myofibroblast theory and the cell traction - fibroblast theory. The former suggests that myofibroblasts, cells with characteristics of both fibroblasts and smooth muscle cells, undergo contraction in a muscle-like fashion, while attached to each other and the extracellular matrix, and thereby bring about contraction. The latter suggests that fibroblasts compact the extracellular matrix by a traction-like matrix gathering process and thereby facilitate contraction. The two theories of

contraction are not necessarily mutually exclusive. It is possible that wound contraction is brought about by fibroblasts actively engaging in both tractile and contractile activities either simultaneously or sequentially. From the observations of Majno *et al.* (1971); Rudolph, (1979); McGrath and Hundahl, (1982); Ehrlich and Hembry, (1984) and Darby *et al.* (1990) contraction is known to proceed initially without myofibroblastic cells. However, these cells become more prevalent as the wound contraction process continues. It is possible that the wound matrix is initially remodelled by the process of fibroblast traction which is subsequently superseded by the contractile activity of myofibroblastic cells. Regardless of the mechanism by which the forces necessary for wound contraction are generated, current evidence suggests that contraction is a cell-mediated event and that the cells involved are of fibroblastic lineage.

Chapter 2. Ultrasound

2.1 Basic physics of mechanical vibrations

Ultrasonic energy travels through a medium in the form of a wave. Mechanical or acoustic waves arise when particles, composing a medium, are supplied with energy and are driven to vibrate. These particles then transfer some of this energy to adjacent particles causing them to vibrate and so pass on the energy in the form of a wave. Mechanical waves thus require a conducting medium. The human ear can detect a wide range of airborne sounds, but is unable to detect extremely low notes (infrasound), or extremely high notes (ultrasound). Ultrasound is usually defined as having a frequency above 20 kHz. All mechanical vibrations whether they are ultrasound, audible sound or infrasound, and irrespective of whether they are propagating through solids, liquids or gases, have certain common physical properties. In this chapter these properties are described.

2.1.1 The surface wave analogy

The pattern of circular ripples produced on the surface of a still pond by throwing in a small stone is a useful analogy for the wave properties of sound (figure 2.1). These expanding ripples consist of a series of alternating peaks and troughs which at any one point in time resemble the pattern seen in figure 2.2. If wave propagation is frozen any given point in time, the diagonal RS of figure 2.1 would have an appearance resembling figure 2.2. The regular repeating unit that describes the wave is termed the wavelength (λ) and is defined as the distance from any measurable point to the next similar point after it has completed one full cycle of positive and negative displacement (e.g. from crest to crest). The amplitude of a wave is the maximum excursion of the wave above (or below) its original undisturbed value. A large wave from a large stone has a greater amplitude than a small wave from a small stone. Amplitude is thus a measure of the power of a wave.

It is not necessary to freeze time to get the same pattern as that illustrated in figure 2.2. If one imagines a float, located at point P (figure 2.1), close to the site of impact of a stone, when waves pass the float it will be lifted during the peak and dropped during the trough relative to its original position, but remain in essentially the same position relative to the source of the wave. The displacement of the float from its original position is displayed as a function of time (figure 2.3). The regular

Figure 2.1. Graphical representation of the expanding series of waves propagating away from a point source (S). The solid circles represent the wave peaks while the broken circles represent the wave troughs (refer to text).

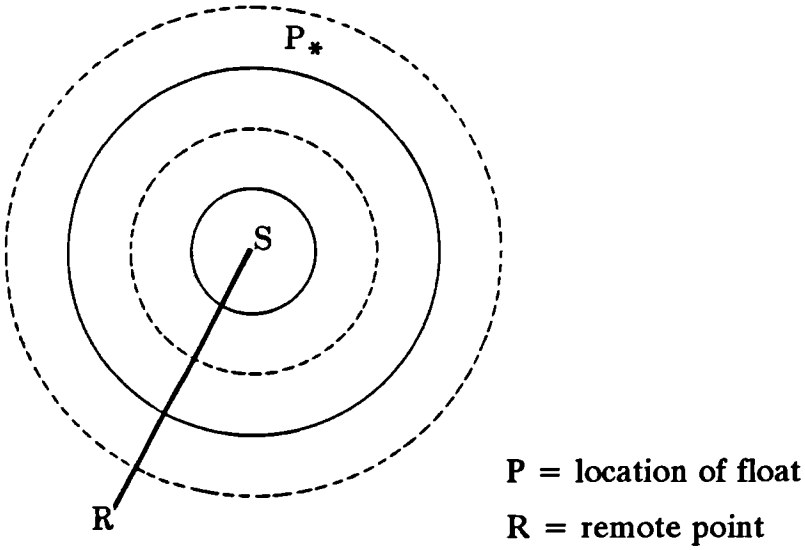

Figure 2.2. Sectional view, along the line RS, of the wave pattern in figure 2.1. Showing the wavelength (λ), the wave amplitude (A) and the distance from the wave source.

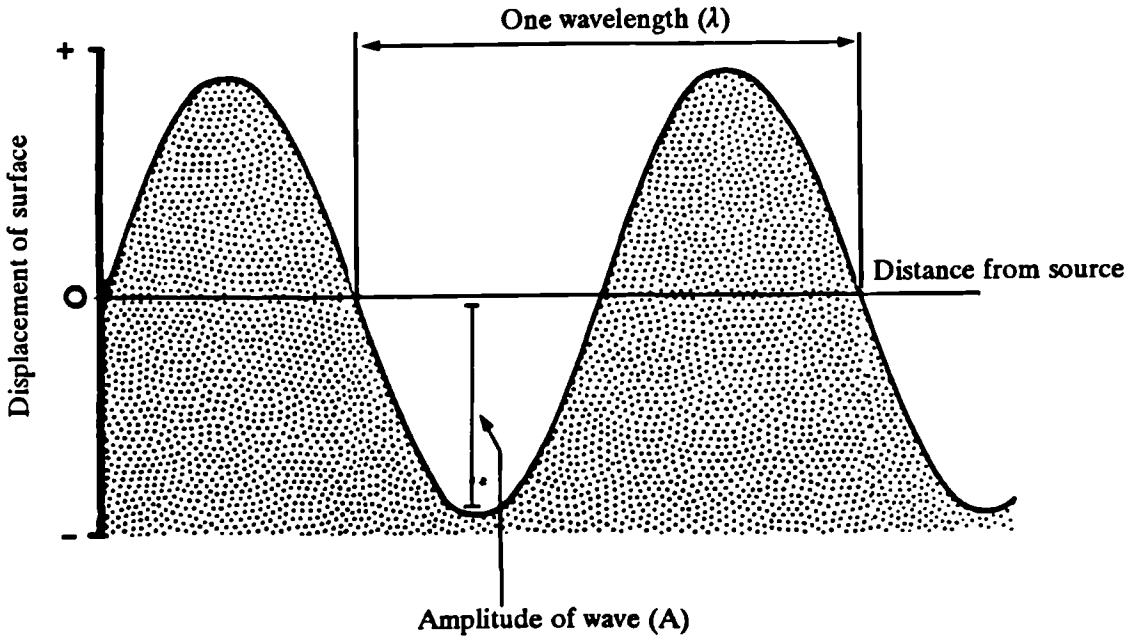

Figure 2.3. Diagrammatic representation of the displacement of a particle in the path of a ultrasonic wave as a function of time.

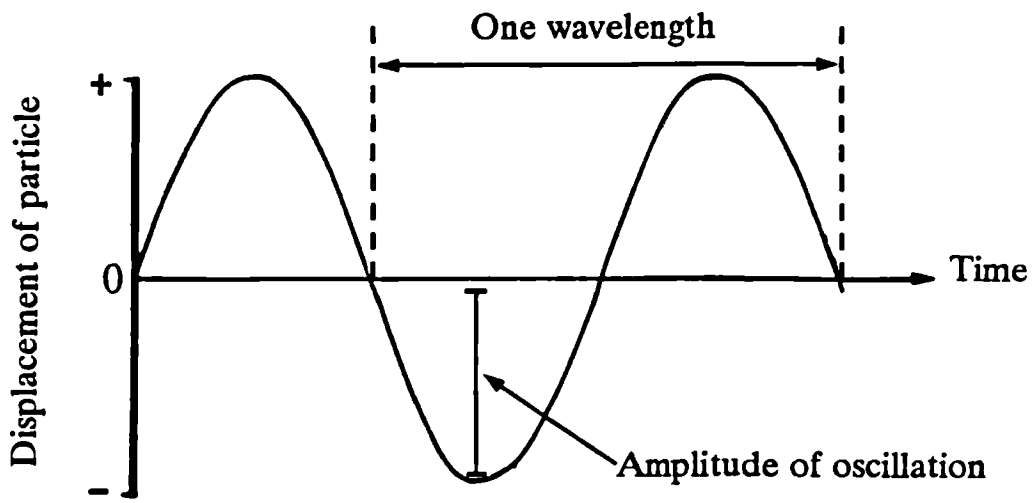

(After Williams, 1983)

movement of a body, as described for this float, about a mean point is an example of simple harmonic motion (SHM), which is described by a sine curve. Thus, particles (in this case molecules of the water surface) oscillate with SHM, remaining in essentially the same position relative to the source (S) while the wave may cover large distances. Wave progression occurs through energy transfer; no net movement of the medium occurs. The advancing wave is effectively the energy put in by the disturbance causing particles to oscillate with SHM. Particles transfer their energy, by colliding with, or rubbing against, neighbouring particles. This energy transfer drives neighbouring particles to oscillate. This repeating process of particle oscillation followed by energy transfer is commonly termed wave propagation.

2.1.2 Physical properties of mechanical waves

Waves flow away from their source. The whole curve in figure 2.3 is effectively moving forward with a velocity (v), which is measured by the distance which any particular part of the curve travels in unit time. The velocity of wave propagation is highly dependent upon the efficiency of energy transfer from a given vibrating particle to its neighbour. Energy transfer, and thus velocity of propagation, is fundamentally dependent upon the physical properties of the conducting media. Such physical properties include both the size and number of particles present per unit volume (i.e. density, ρ) and the magnitude of the complex inter-molecular interactions of the conducting medium (Table 2.1). The relationship between wave velocity and medium density (for a typical solid or liquid) is described by this equation:

$$v = \sqrt{\frac{K}{\rho}}$$

Where:

K is the Young's modulus of a solid rod or the bulk modulus of elasticity of a liquid

When liquids are heated significant expansion occurs; the same mass occupies a greater volume, which leads to a decrease in density. This decrease in density facilitates more rapid propagation of sound waves. Thus the velocity of mechanical

waves in a liquid usually increases with increasing temperature. For example, the velocity of sound in water rises from about 1400 ms^{-1} at 0°C to about 1550 ms^{-1} at 60°C. As can be seen in Table 2.1 the velocity of ultrasound in soft tissues is approximately 1500 ms^{-1}.

Table 2.1. Velocity and characteristic impedance of sound in biological and other materials.

Material	Velocity ($m\ sec^{-1}$)	Density ($g\ ml^{-1}$)	Acoustic impedance* ($kg\ m^{-2}\ sec^{-1}$)
Air	333.5	1.29×10^{-3}	429
Water (20°C)	1480	1.00	1.52×10^{6}
Water (37°C)	1520	1.00	1.52×10^{6}
Blood	1555	1.06	1.62×10^{6}
Fat	1460-1470	0.92	1.35×10^{6}
Muscle	1545-1630	1.07	$1.65\text{-}1.74 \times 10^{6}$
Kidney	1560	1.04	1.62×10^{6}
Liver	1540-1585	1.06	$1.63\text{-}1.68 \times 10^{6}$
Bone	2710-4000	1.38-1.81	$3.75\text{-}7.38 \times 10^{6}$

(* - see p71) (Adapted from Wells, 1977)

The number of wavelengths which pass any given point per unit time is termed the frequency (f) of that source. Once generated, this frequency remains constant irrespective of the propagating medium. The particles which propagate this wave also vibrate with this frequency.

The velocity (v), frequency (f) and the wavelength (λ) are interrelated as described by this equation:

$$v = \frac{f}{\lambda}$$

Since the frequency remains constant, but the velocity changes as the wave travels from one medium to another, it follows from the above equation that the wavelength must also change.

When observing the pattern of expanding ripples on a pond it can be seen that as the wave moves further away from the source its amplitude progressively decreases. The perimeter of each circular wave gradually increases and so the initial input of energy has to be spread over an ever increasing area. Absorption is another contributing factor to the loss of energy content from the wave. The transfer of energy between particles is never 100% efficient and so some energy is lost at each transfer; this energy appears as heat which elevates the temperature of the conducting medium.

The wave produced by a small source (termed a point source) is initially a circle having a small radius. As the wave travels away from the source its radius of curvature increases until any small portion of the wave front appears flat. This flat wave front, which continues to move away from the source, is called a plane progressive wave.

Interference is a fundamental property of all waves. If any two or more waves arrive together at the same point in space, they will merge together to form a new wave which is the algebraic sum of the amplitudes of each individual wave. If two waves of the same frequency, amplitude and phase, interfere, a wave of twice the original amplitude but of the same frequency results. If two similar waves which are 180° out of phase interfere their amplitudes cancel each other out.

2.1.3 Transverse and Longitudinal (compressional) waves

The basic physics of mechanical waves have so far been described in terms of surface waves. Though useful, this analogy has several limitations. In surface waves the particles oscillate in the vertical plane as the wave propagates in the horizontal plane. Such waves are termed transverse waves (figure 2.4 (B)) and are usually restricted to solids; materials having strong three-dimensional intermolecular coupling forces. Liquid-borne surface waves, though useful as an analogy, are a special case. Energy is propagated and transferred by a cyclical flow of water just beneath the surface of the liquid. Anything which interferes with this cyclical flow of water beneath the surface will effect energy propagation and hence velocity of this wave. Thus, liquid-borne surface waves are unusual in that propagation velocity is dependent upon the depth of the liquid. This is clearly demonstrated as oceanic waves approach a beach. As the sea becomes shallower the wave's propagation velocity decreases and consequently its wavelength decreases.

Figure 2.4. A graphical illustration of the direction of the particles of a medium relative to the direction of wave propagation for compressional (or longitudinal) and transverse (or shear) waves.

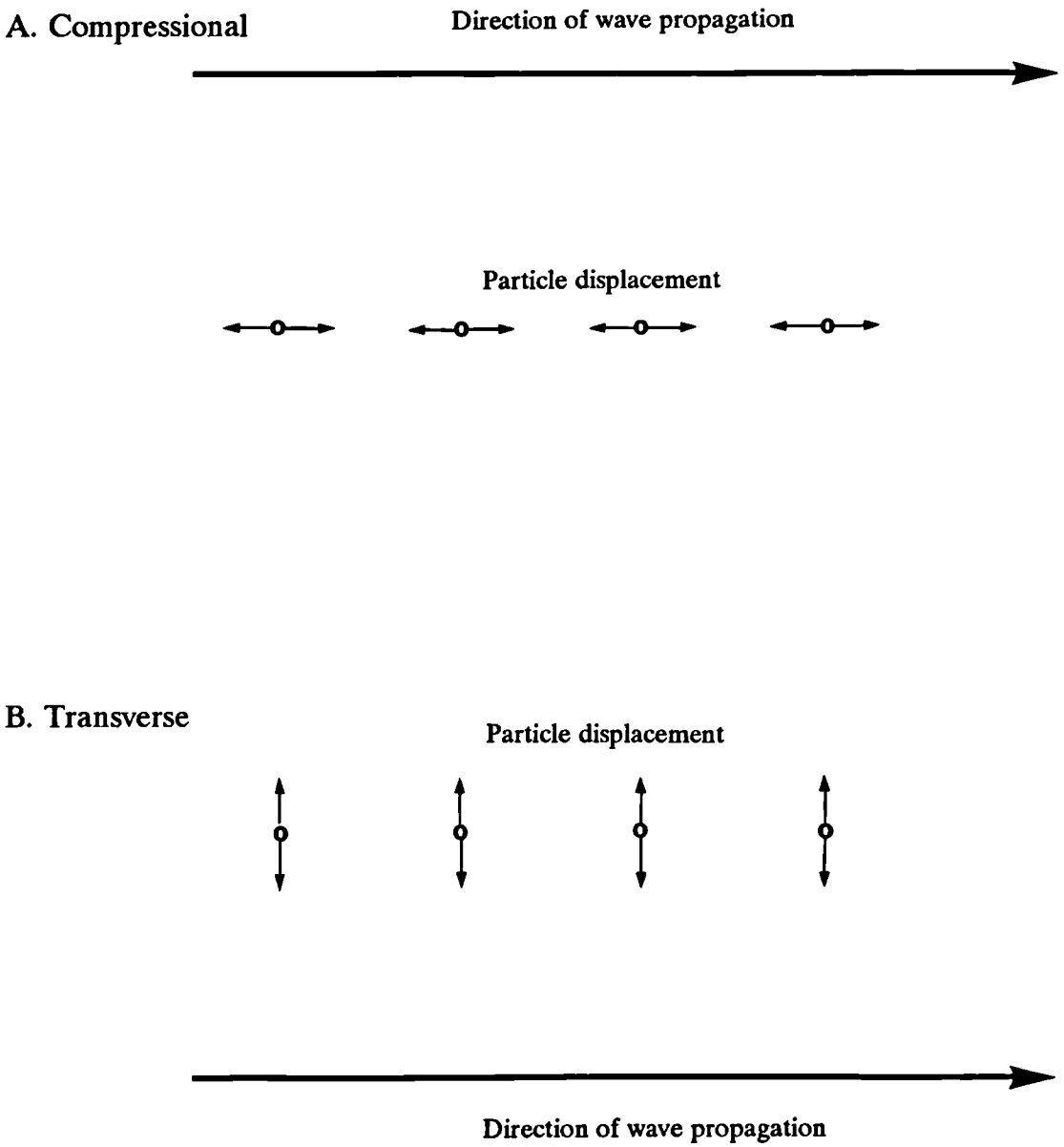

The other class of mechanical wave, which includes both audible sound and ultrasound, differ from transverse waves in that the direction of particle vibration is the same as the direction of wave propagation. Such waves are termed longitudinal or compressional waves (figure 2.4 (A)).

When a compressional wave propagates as a plane progressive wave, all the particles of the medium which lie in a plane parallel to the advancing wave front are displaced together. It is convenient to think of the propagating medium as being composed of multiple layers (i.e. planes of particles) arranged parallel to the wave front. At any given point in time some of these layers will be displaced in the direction of the propagating medium while others will have returned to their original position or overshot it and be displaced in the opposite direction (figure 2.5 (A)). As explained in the surface wave analogy each layer of the conducting medium should be oscillating with simple harmonic motion. So the displacement at any given point in time can be found from a sine curve. Figure 2.5 (B) shows the displacement of each layer from its original position at time t. Certain layers are passing through their undisturbed position and are thus demonstrating zero displacement. Taking positive displacement to be a movement to the left of zero and negative displacement to be to the right. It can be seen that layers on either side of the layers of zero displacement are either moving towards them or away from them. If moving towards them the medium at that point is compressed and therefore the pressure at that point must be increased. Conversely, if adjacent layers are moving away from zero displacement layers then the pressure at that point must be decreased. Points of zero particle displacement are points of maximum or minimum pressure.

As the displacement follows a sine wave (figure 2.5 (C)), and displacement generates pressure, it follows that pressure follows the same sine wave (figure 2.5 (D)). The mid points between maximum and minimum pressure (i.e. zero pressure) are also points of maximal displacement; which correspond to the point in SHM where the particle has stopped moving. Thus, the displacement of the layers and instantaneous pressure produced within a medium by a mechanical wave are both described by a sine wave having the same frequency, but the maximum of one curve corresponds to zero in the other. That is to say the two curves are a quarter of a cycle out of phase with each other. For a mechanical wave propagating through a liquid medium it is more convenient to measure pressure than particle displacement.

Figure 2.5. Graphical representation of the displacement of layers of a medium by a compressional wave and the effect of this displacement on the distribution of pressure within that medium.

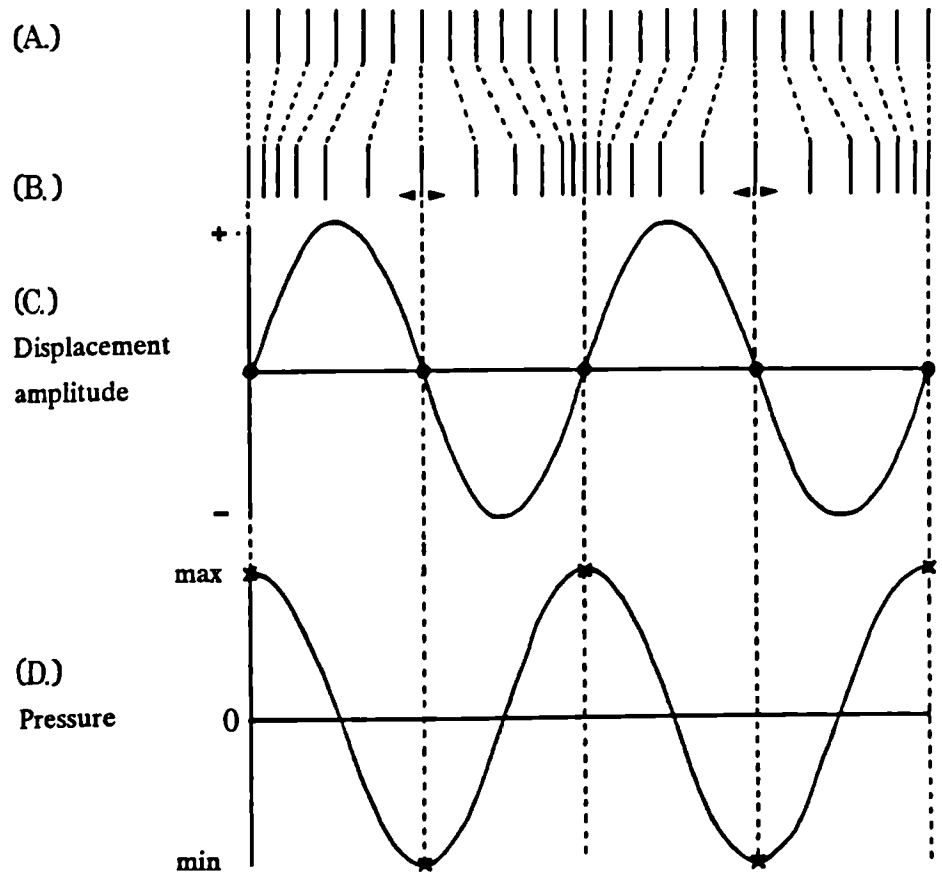

(After Williams, 1983)

In any given solid medium transverse or shear waves travel much more slowly than compressional waves. For a solid the velocity of transverse waves (Vt) is given by:

$$Vt = \sqrt{\frac{G}{\rho}}$$

Where: G is the shear modulus of elasticity

ρ is the density of the material (Williams, 1983)

In general, the velocity of transverse waves in a given medium is half the velocity of compressional waves in that same medium.

Under certain circumstances some of the energy of a compressional wave can be transformed into transverse waves, this phenomenon is termed mode conversion. For example, it is thought to occur when ultrasound is obliquely incident upon a strong reflector such as at soft tissue - hard tissue (bone) interfaces. As transverse waves do not propagate well in aqueous media they are readily absorbed by the soft tissue and their energy appears as heat. It has been suggested that the sensation of pain experienced when the hand is placed in the path of moderately high intensity therapeutic ultrasound is due to temperature rises within the periosteum (nutritive and sensory outer coating of bone) due to the absorption of transverse waves.

2.1.4 Reflection and refraction

Whenever a mechanical wave encounters a boundary between two dissimilar media both reflection and refraction of that wave occurs. A simple way of explaining these phenomena is to apply Huygen's principle, which states that every point along a wave is itself a point source and emits either a circular wave (in two dimensions) or a spherical wave (in three dimensions). The line obtained by joining up all the wave fronts from each of these numerous point sources indicates the next shape and position of that wave front (figure 2.6). The reflection and refraction of a plane wave front is shown in figure 2.7. The same information is displayed as a ray diagram (figure 2.8), where a ray represents a line drawn at right angles to each wave front.

Figure 2.6 An illustration of Huygen's principle - any wave front is regarded as a large number of point sources each generating a spherical wave. Interference between each of the generated waves reforms a new wave front, which is parallel to the source.

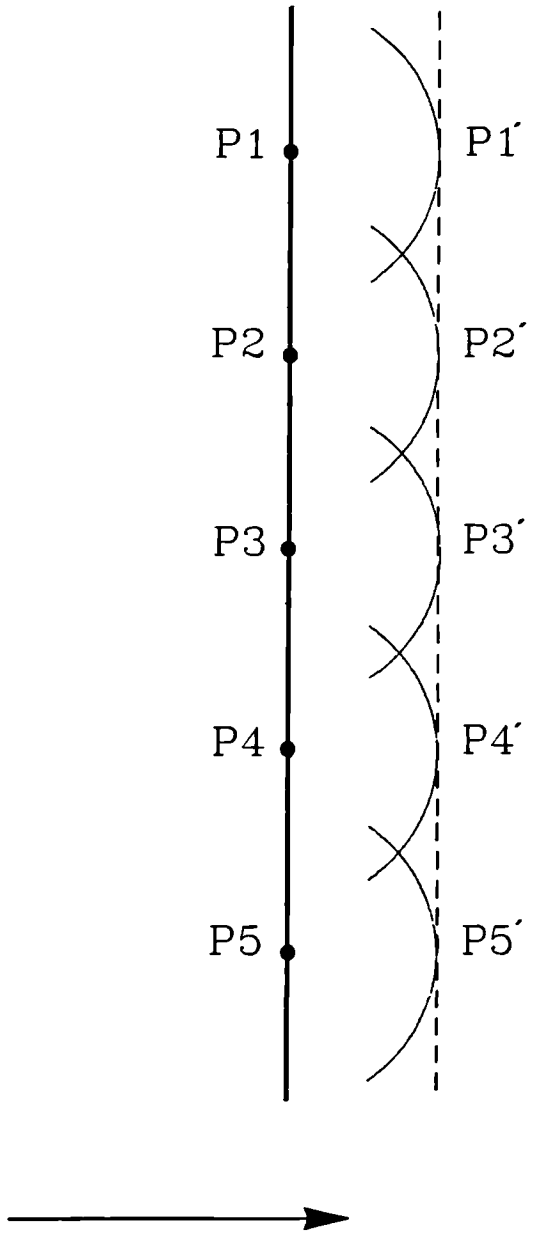

Figure 2.7 A schematic illustration of reflection and refraction occurring at the interface between two media. The refracted wave is deflected because the velocity of the wave in medium 2 is different to that in medium 1.

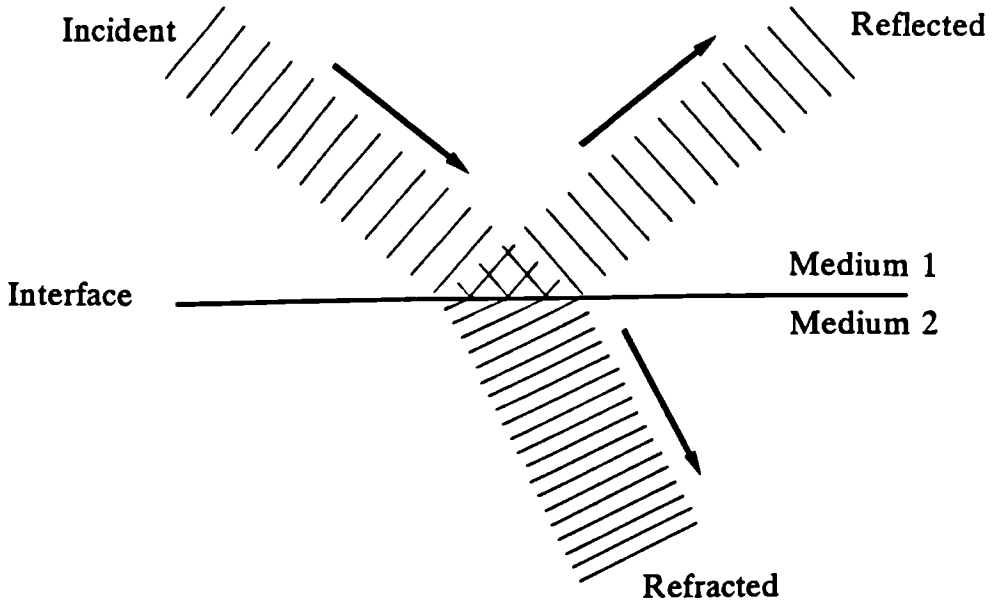

Figure 2.8. Showing the same information presented in figure 2.7 except that the individual wave fronts have been replaced by rays (i, r and r' represent the angles of incidence, reflection and refraction).

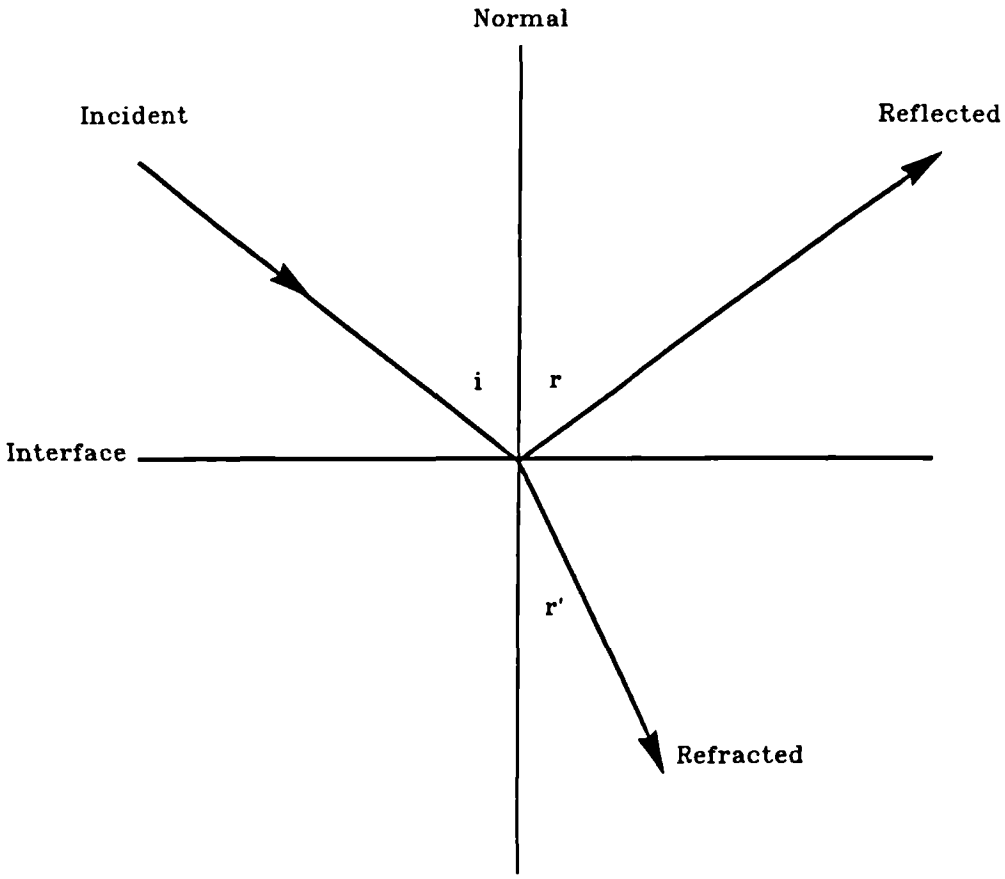

The angle of incidence (i) can be seen to equal the angle of reflection (r), whereas the angle of incidence and the angle of refraction (r') are related by Snell's Law:

$$\frac{\sin i}{\sin r'} = \frac{v1}{v2}$$

Where: v1 is the velocity of the incident wave in medium 1.
v2 is the velocity of the refracted wave in medium 2.

2.1.5 Acoustic impedance

The parameter that determines how much of the incident wave is reflected or refracted at any given interface between two media is acoustic impedance. Acoustic impedance (Z) is defined as the product of the density of a material (ρ) and the velocity (v) of sound within it:

$$Z = \rho v$$

Referring to figures 2.7 and 2.8, let Z1 be the acoustic impedance of medium 1 and Z2 be the acoustic impedance of medium 2. If Z1 equals Z2 there will be no reflection at the interface (if the velocities are also the same there will be no refraction at the interface). However, if Z1 does not equal Z2 then some of the wave will be reflected and some will be refracted. The larger the difference between Z1 and Z2 then the greater the proportion of the incident energy will be reflected. The relationship of partitioning between reflection and refraction is complicated by the angle of incidence. The simplest situation is where the incident wave approaches the interface at right angles to it. The reflected wave would then retrace its own path and the transmitted portion of the wave would carry on in a straight line without refraction, though its velocity, and thus its wavelength, may be different. For normal incidence the equations which relate to this partitioning of incident energy (Ii) into the reflected (Ir) or transmitted (It) portions are as follows:

$$\frac{Ir}{Ii} = \left[\frac{(Z_2-Z_1)}{(Z_2+Z_1)}\right]^2$$

and

$$\frac{It}{Ii} = \frac{4Z_2Z_1}{(Z_2+Z_1)^2}$$

Where I is the intensity of the wave (transmitted power per unit area).
(Table 2.1 (p62) gives acoustic impedance values for some common biological and other materials).

2.1.6 Standing waves

A plane wave of normal incidence which is reflected back along its own path interferes with that portion of itself which has not yet reached the reflector to form a standing wave. On reflection waves undergo a half wavelength phase change. Figure 2.9 demonstrates what happens when a plane travelling wave strikes a flat perfect reflector.

Figure 2.9(1) shows that when an incident wave meets the reflector at the instant of zero displacement it is reflected (with a half wavelength phase shift) so that both waves are exactly in phase. The amplitudes of both waves add together to give a resultant wave whose amplitude, at any given point, is twice that of the incident wave - constructive interference.

Figure 2.9(2) shows the same wave incident one quarter of a wavelength later. That same wave is now striking the reflector at a displacement maximum. The reflected wave at the point of reflection (due to phase change) will be at a displacement minimum and will therefore cancel out the incident wave giving a resultant zero displacement at every point - destructive interference.

Figure 2.9(3) shows the wave incident a further quarter of a wavelength later, at a point of zero displacement so that the incident and reflected waves interfere constructively giving a wave whose amplitude is twice that of the incident wave. However, since this wave is half a wavelength out of phase with the first reflected wave (figure 2.9(1)), the displacement at any point is in the opposite direction to that shown in figure 2.9(1). A quarter wavelength later, the wave meets the reflector at a displacement maximum (as in figure 2.9(2)) and destructive interference again occurs.

Standing wave fields, demonstrating constructive interference, can be described as a regularly repeating pattern of points where the displacement of particles is always zero - termed displacement nodes (N), and points where the displacement

Figure 2.9 A diagrammatic representation of the formation of a standing wave.

(after Williams, 1983)

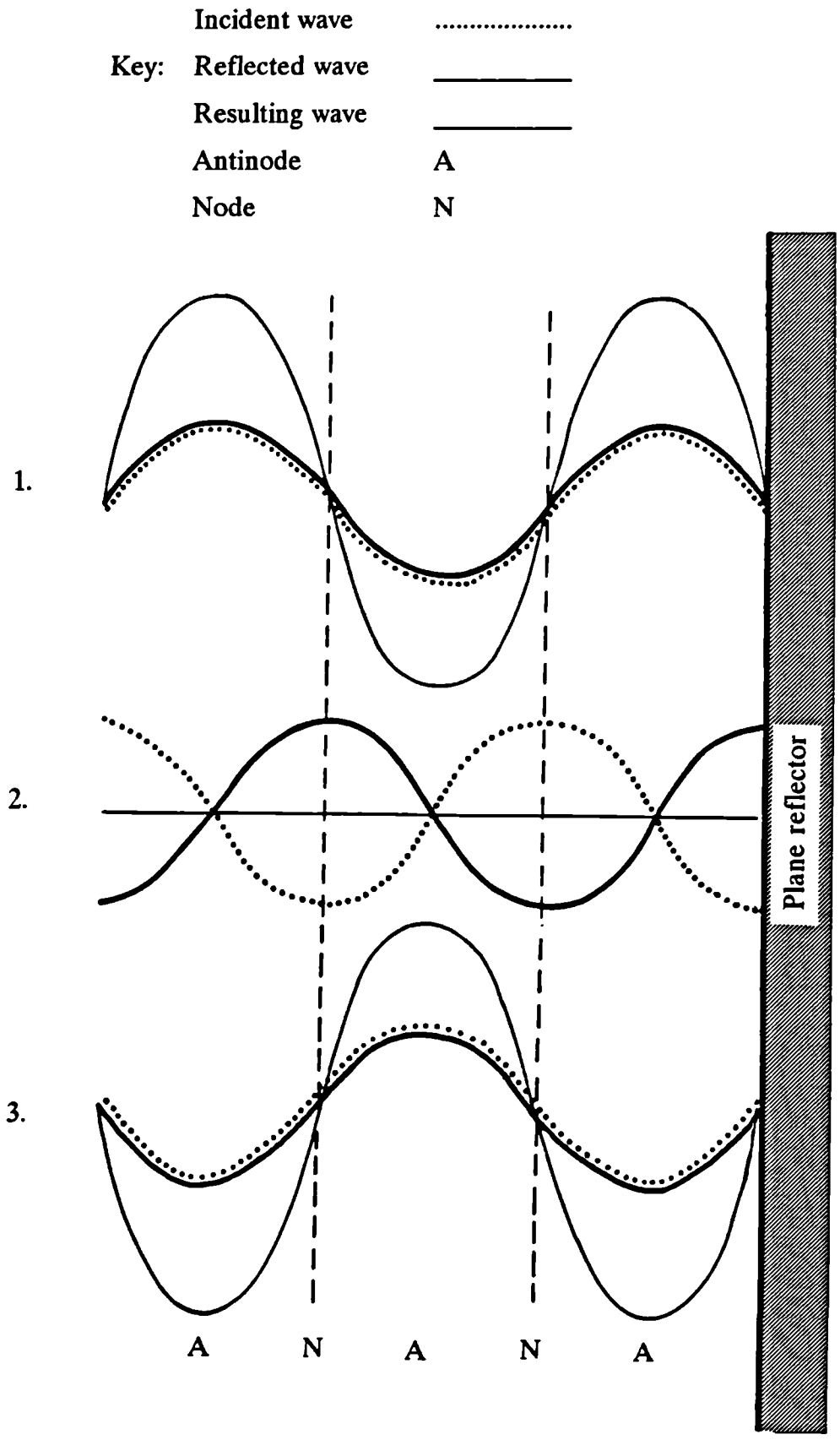

varies from positive to negative at the same frequency as the incident wave, but at twice its amplitude - termed displacement antinodes (A), figure 2.9(3). Nodes and antinodes are separated by a distance equal to one quarter of a wavelength. Under the conditions described above, all the energy contained in the incident wave (except for that lost by absorption) is returned in the reflected wave. That is to say there is no net flow of energy through the medium supporting the standing wave. This does not mean, however, that the standing wave field has no energy. The standing wave phenomenon concentrates and effectively amplifies the ultrasonic energy applied to a system, which may lead to potentially hazardous ultrasonic exposure of biological tissues (Williams, 1983).

If any other sinusoidally varying parameter of the wave is examined, under standing wave conditions, it can be seen that we get the same result. The pressure generated by a compressional wave is a quarter of a wavelength out of phase with particle displacement (figure 2.5 (D)). Therefore the pressure measured in a standing wave field would have the same alternating pattern but would be displaced by a quarter of a wavelength from the displacement pattern, so that the displacement node would be located at a pressure antinode and the displacement antinode at a pressure node.

Partial standing waves occur when the reflector is less than 100% efficient. In such a situation the standing wave would be superimposed on the plane progressive wave field, and the maximum displacements or pressures would be less than twice that of the incident wave. In practice, standing waves seldom occur in the absence of travelling waves, and thus the minimum displacement and hence minimum pressure amplitudes have some finite value.

2.1.7 Resonance

Resonance occurs when the input of energy to a system is in phase with the natural frequency of oscillation of that system. If energy is supplied in phase then the amplitude of the oscillating system is maintained or increased. If the same energy is supplied in a random manner then destructive interference occurs and the amplitude decreases. To improve the efficiency of any device which is required to transmit, generate or receive a single frequency of mechanical vibration it is usual to manufacture such a device so that it is in resonance at that frequency.

2.1.8 Power density - intensity

The amount of energy contained in a wave as it passes a given point is normally expressed in terms of the intensity at that point. Intensity is defined as the rate of flow of energy through an imaginary plane, one centimetre or one metre squared, orientated at right angles to the direction of wave motion. The units of intensity are thus watts/m^2 (Wm^{-2}), more commonly expressed as Wcm^{-2} or even as $mWcm^{-2}$. The intensity (I) of a plane progressive wave is related to the maximum pressure amplitude (Po) produced within the conducting medium by the equation:

$$I = \frac{Po^2}{2\rho c}$$

Where ρ is the density of that medium and c is the velocity of the wave in it. ρc is the acoustic impedance.

This equation may be rewritten:

$$I = \frac{PoUo}{2}$$

or

$$I = \frac{\rho c Uo^2}{2}$$

(Williams, 1983)

Where Uo is the maximum velocity of the oscillating particles of the medium as the wave passes. If there is no absorption or scattering, the intensity of a plane progressive wave remains constant.

2.1.9 Mechanical waves of different frequencies

Figure 2.10 shows a frequency spectrum for mechanical waves where a logarithmic scale has been chosen. The spectrum consists of three overlapping regions. The central region encompasses the audible spectrum from about 20-30 Hz up to about 16000 Hz, these frequencies approximating to the upper and lower frequency limits of the human ear. The region below about 20 Hz is termed infrasound whilst frequencies above 16 kHz are termed ultrasound.

Air becomes a progressively less efficient propagating medium for mechanical vibration as its frequency increases above 20 kHz. The main reason for this is that for a given power input, the maximum displacement amplitude of the gas molecules decreases with increasing frequency until the amplitude of displacement is less than

Figure 2.10. The acoustic spectrum, showing the source or application throughout the range of mechanical wave frequencies.

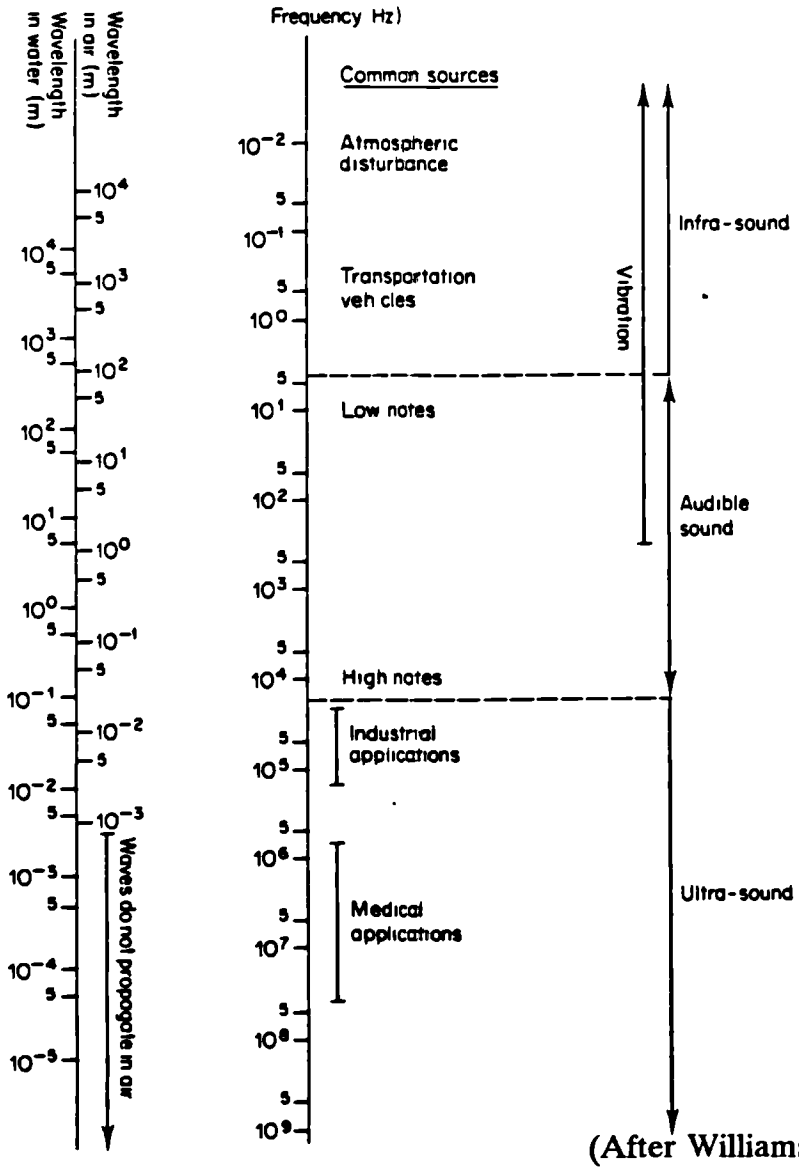

(After Williams, 1983)

the average distance (mean path) between molecules. Thus most of the gas molecules close to the source of vibration will be unable to collide with neighbouring molecules and thus pass on energy and facilitate wave propagation.

As propagation of mechanical waves within a given medium is dependent upon the transmission of energy from one particle to another, the upper frequency at which waves will propagate is also determined by the inertia of particles which make up that medium. The inertia of a body is a measure of its tendency to resist motion when subjected to a small transient force. For a given power input the displacement amplitude decreases with increasing frequency. Eventually the particle is unable to respond as the applied force is not sufficient to overcome its inertia and thus remains stationary. The wave therefore does not propagate.

2.2 Generation of therapeutic ultrasound

In the previous section the basic physics and properties of mechanical waves were described. This section deals more specifically the generation of ultrasonic wave forms associated with the therapeutic application of ultrasound. Ultrasonic waves are defined as mechanical waves having frequencies above the limit of detection of the human ear, i.e. greater than 16 - 20 kHz. Therapeutic applications of ultrasound are normally restricted to the use frequencies between 0.5 - 3 MHz (Dyson, 1990) generated by piezoelectric transducers.

2.2.1 Piezoelectric transducers

A transducer is a device for converting energy from one form into another, in this case a conversion of electrical energy into ultrasonic energy. Piezoelectric transducers rely on the capacity of certain crystals to generate an electric charge when they are subjected to pressure or distortion. This effect, known as the piezoelectric effect, was first described by Pierre and Jacques Curie in 1880 (Williams, 1983). The converse effect is true, i.e. when a voltage is applied to a piezoelectric material it undergoes mechanical deformation. The phenomenon is due to electric charges bound within the crystal lattice of the material. It is the interaction between this bound electric field and the applied electric field that leads to the mechanical deformational changes (Cady, 1964).

If a disc is cut from a piezoelectric material and electrodes appropriately applied by coating with a film of a metallic conductor (e.g. gold, silver or aluminium),

when a voltage is applied across the two electrode surfaces the crystal undergoes a mechanical deformation. This change in shape can be reversed if the field is reversed, i.e. a change in the polarisation of the voltage applied across the electrodes results in a corresponding change in the direction of distortion of the crystal. Thus, the application of an a.c. voltage across the crystal results in an oscillating change in shape. The application of an a.c. voltage having an ultrasonic frequency would therefore result in the crystal oscillating at the same frequency.

As the amplitudes of oscillation of the piezoelectric crystals are very small the phenomenon of resonance is employed to maximise output. The thickness of the piezoelectric disc determines the resonant frequency of the sinusoidal voltage to be applied across the disc in order to produce ultrasound. This can be explained as follows:

A state of resonance arises when the surfaces of a piezoelectric disc are separated by a distance equal to an odd number of half wavelengths; here all waves constructively interfere leading to summation of displacement and hence ultrasonic output. To manufacture a transducer which is resonant at a particular frequency, the wavelength is first calculated from the velocity of sound in that material and the desired frequency. The crystal is then cut to be half (or a multiple of half) of the calculated wavelength in thickness. The frequency of the electrical signal is then swept around the expected resonant frequency until the crystal oscillates with maximum displacement amplitude for any given input power.

This resonant frequency is called the fundamental resonant frequency of the transducer. This is dependent on transducer thickness. If the driving frequency is progressively raised above this value, the ultrasonic output decreases as you move away from resonance and approaches zero when the driving frequency corresponds to 1 wavelength within the transducer. As the driving frequency is further increased the ultrasonic output also increases until another resonant state is attained at a frequency 3 times that of the fundamental frequency. This frequency corresponds to 1.5 wavelengths within the transducer, and is termed the third harmonic frequency. Yet another resonant condition occurs at the fifth harmonic when the driving frequency is 5 times the fundamental frequency and corresponds to 2.5 wavelengths within the transducer.

The piezoelectric effect is restricted to crystals which lack electrical symmetry e.g. quartz, tourmaline, lithium sulphate, cadmium sulphide. Piezoelectric materials

can be fabricated from barium titanate and lead zirconate titanate (PZT) (Jaffe *et al.* 1955). These materials are mixed with various chemicals, cast to the desired shape and dimensions and then heated above the materials Curie temperature (typically 300 - 600°C) while exposed to a polarising 2000 V/mm d.c. voltage. The Curie temperature is that temperature above which the molecules of the material are free to move in response to an applied force. If a piezoelectric material is heated above its Curie temperature and allowed to cool in the absence of a d.c. field it will lose its piezoelectric properties.

Initially, quartz crystals were used for the generation of therapeutic ultrasound by the reverse piezo-electric effect. Quartz has now generally been replaced by barium titanate and PZT. The last two materials have the advantage that, because of their ferro-electric properties, only a small voltage is required to drive the crystal to oscillate. This obviates the requirement for a bulky sound head transformer common to quartz transducers, which require a high (several kV) driving voltage. PZT is preferable to barium titanate because it retains its marked piezo-electric properties up to much higher temperatures and is less sensitive to mechanical shock. Polyvinylidene difluoride (PVDF), a plastic with piezoelectric properties, has been introduced more recently. The piezoelectric property is conferred on this plastic by applying a large voltage (about 10^8 V/m) across the polymer (de Reggi *et al.* 1981). PVDF has an acoustic impedance which is much closer to that of water than other piezoelectric transducer materials and as such is more efficient at delivering the ultrasound to the biological target.

2.2.2 Transducer construction

Piezoelectric transducers designed to supply therapeutic levels of ultrasound consist of a single circular piezoelectric disc, the dimensions of which favour resonance at the particular frequency of interest. The piezoelectric element has electrodes on the inner and outer (relative to the treatment face) surfaces. The inner face of this disc is air backed leading to an impedance mismatch which encourages the reflection of the generated ultrasonic energy. This reflected energy leaves the applicator head by the outer face of the transducer, which is bonded to the applicator casing with an adhesive of similar impedance to the piezoelectric disc. This adhesive also functions as an electrical insulator. As the piezoelectric element also vibrates in its lateral plane it is necessary to isolate it from the casing material, by a layer of acoustic

insulation, to reduce possible operator exposure hazards by side wall irradiation on protracted use. The front face of therapeutic transducers is usually metallic; this protects the more delicate piezoelectric element within and encourages a more even acoustic field distribution.

2.3 The structure of ultrasonic fields

If the wavelength of sound is larger than the dimensions of the source which produced it, then the sound will spread in all directions (i.e. as a spherical wave) away from the source, like the ripples in a pond caused by a small stone. This is true for audible sound which has a typical frequency of 1 kHz and a velocity in air of about 340 m/s, and consequently a wavelength of about 34 cm. In the resulting acoustic field the intensity (I) at any point (x) is given by the following equation:

$$Ix = \frac{Io}{d^2}$$

where: Io is the emitted intensity by the source
d is the distance of point x from the source

If the wavelength of sound is smaller than the dimensions of the source a different set of conditions apply. The wavelength of 1 MHz ultrasound, which travels through water or body tissues at a velocity of 1540 m/s, is approximately 1.5 mm. Ultrasonic sources, in therapy equipment, range from 10 to 25 mm in diameter, and as such are of the order of 10 times larger than the wavelength of sound they are emitting. Under such conditions the sonic energy does not spread as a spherical wave; rather, it is contained within a cylindrical beam of approximately the same diameter as the transducer and travels in the form of a plane progressive wave.

However, the intensity of that wave is not the same at all points within the beam. This is because individual wave fronts from different parts of the source have to travel different distances to reach a given point. Waves fronts, originating from different points, that arrive in phase with one another interfere constructively to produce sites of high ultrasonic intensity. However, wave fronts that arrive a half wavelength out of phase with each other destructively interfere and produce sites of zero intensity. The resulting interference pattern, called a diffraction pattern, can be divided into two regions (figure 2.11). The region close to the source (transducer) is

called the near field (or Fresnel zone) whilst the other region is known as the far field (or Fraunhofer zone). The boundary between these regions occurs at a distance d from the source; this can be found by employing the following equation:

$$d = \frac{a^2}{\lambda}$$

where: a is the radius of a circular source

λ is the wavelength in that medium.

At the point d the cylindrical beam begins to diverge. If the rays which depict the diverging waves are extrapolated back to their source they meet at the centre of a circular generator. The angle of divergence, θ, of the beam in the far field is given by:

$$\sin \theta = \frac{0.61\lambda}{a}$$

where: λ is the wavelength of sound in that medium

a is the radius of a circular source.

This pattern is generated within biological tissues whenever high frequency ultrasound is used; it is thus of great importance that it be examined in full.

If a pressure sensitive detector, whose dimensions are smaller than a wavelength, is placed at the centre of a large circular transducer and slowly moved away from it at right angles to its transmitting surface (i.e. along its central axis), the detector output will show a repeating sequence of peaks and troughs similar to that in figure 2.12 (1). The peaks are those points where individual waves have arrived approximately in phase and have constructively interfered to give pressure maxima. The troughs are those points where almost half of the waves have arrived half a wavelength out of phase with the remainder and have thus destructively interfered. Complete constructive or destructive interference is virtually impossible to achieve so the pressure maxima and minima never reach zero.

Close to the transducer, in the near field, the peaks are sharp and close together. They become broader and wider apart with increasing distance from the transducer until the last peak, normally higher and broader than the rest and called the last axial maximum. This peak (at C in figure 2.12) is at the point, d, which marks the boundary between the Fresnel and Fraunhofer zones. The area around point d

Figure 2.11. A diagrammatic representation of the cylindrical (Fresnel) and diverging (Fraunhofer) portions of the ultrasonic beam produced by ultrasound transducers.

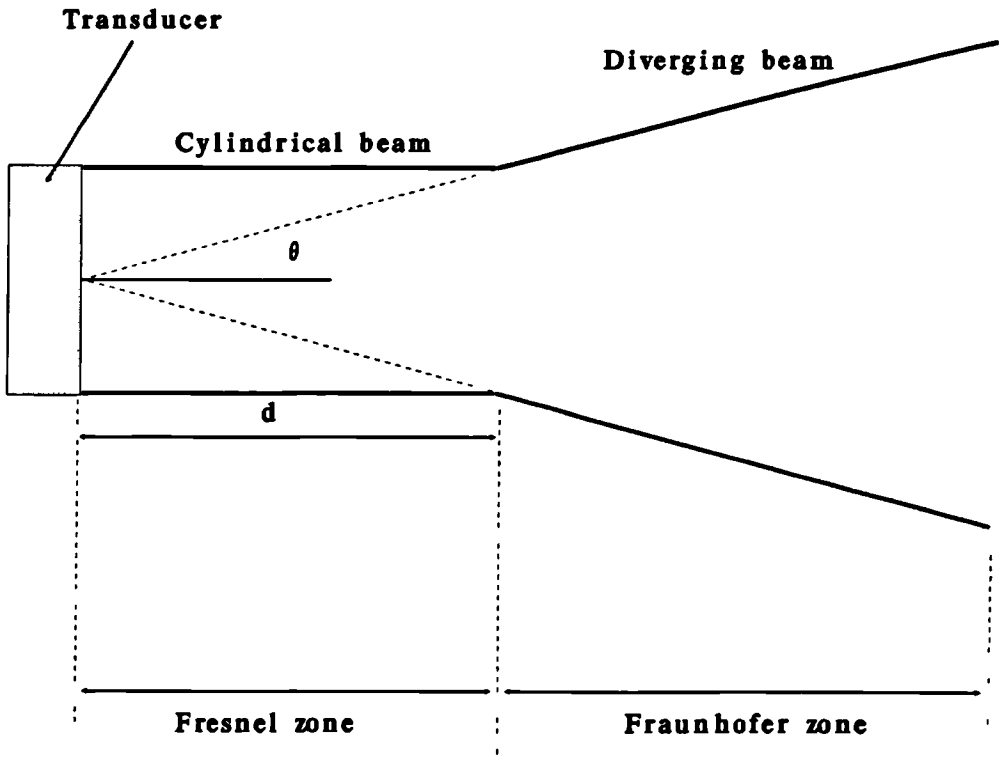

d = distance from source after which beam diverges

θ = angle of divergence

Figure 2.12. Diagrammatic representation of the distribution of acoustic pressure within an ultrasonic beam: (1) along the central axis of the transducer, (2) across the beam axis, at various axial locations, and, (3) in the form of 'ring patterns', which demonstrate the symmetrical distribution of pressure within the beam.

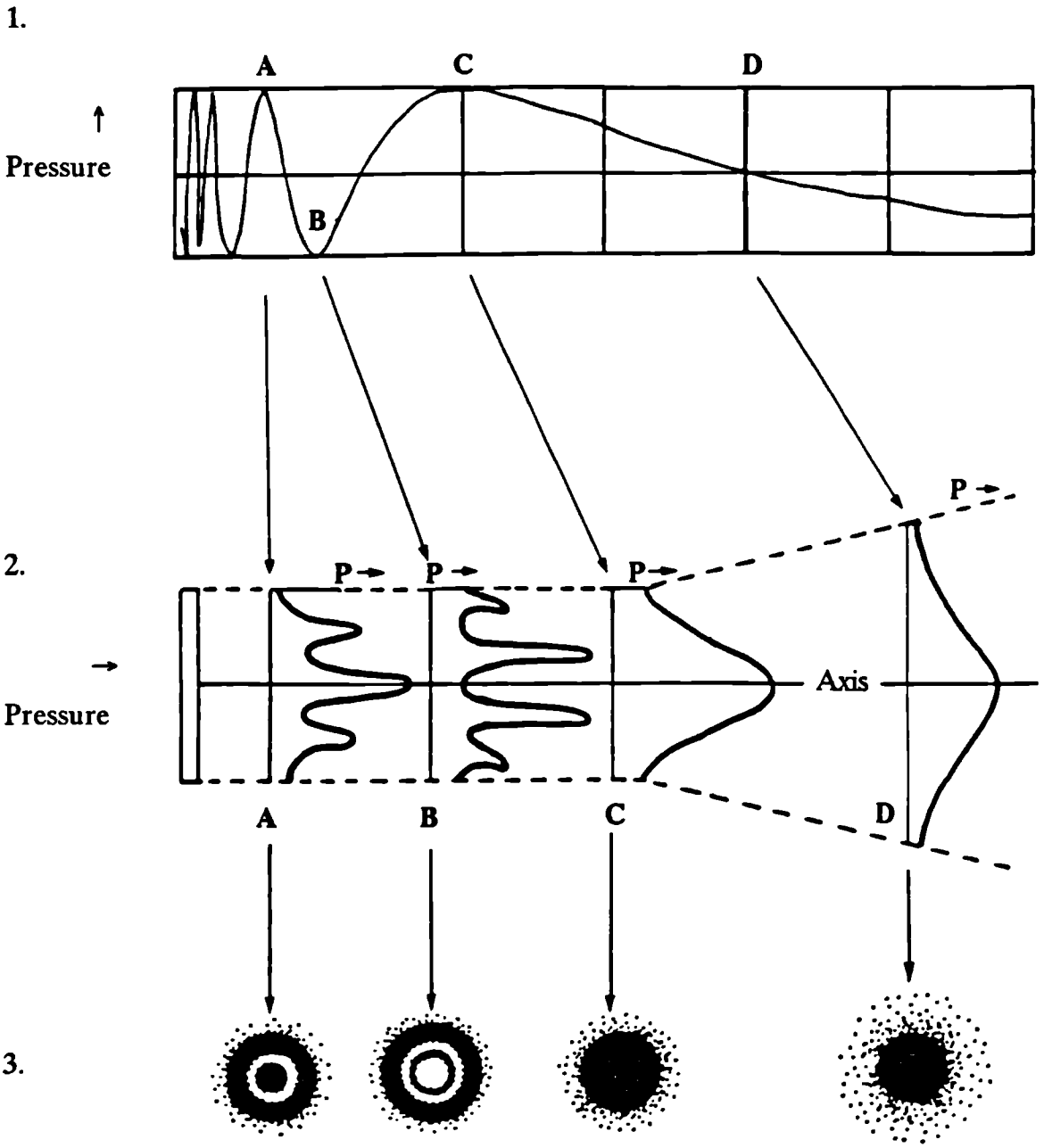

is usually the most uniform high intensity region within the ultrasonic beam.

The variation in pressure is more complicated transversely, as is revealed if the detector is swept across the face of the transducer, at right angles to the beam axis. As can be seen from figure (2.12 (2)) the trace that cuts the axis at point A, an axial maximum, has a central peak and two or more side lobes separated by troughs. However, the trace that cuts the axis at point B, an axial minimum, has a central trough and two or more peaks which occupy the positions of the troughs in scan A. This situation is repeated at each axial minimum and maximum in the near field. The amount of energy in the side lobes decreases with distance from the transducer until only a single axial peak is found in the scan of the last axial maximum (scan through point C of figure 2.12 (2)). Beyond this point the far field is entered and the height of the peak decreases as its base broadens with divergence of the beam (scan through point D in figure 2.12 (2)).

The acoustic field generated by a circular source, as in therapeutic ultrasound transducers, has circular symmetry. The three dimensional distribution of intensity can be visualised if the two dimensional map in figure 2.12 (2) is spun about its long axis. Sections through this three dimensional map show so called "ring patterns"; which can be obtained if some material sensitive to some parameter of the acoustic field is placed in a plane parallel to the transducer face. Figure 2.12 (3) shows the ring patterns expected at the four points A - D previously described.

2.4 Ultrasonic dosimetry

The previous section demonstrated that because of interference phenomena the ultrasonic intensity, measured as pressure, varied from point to point within the beam, especially within the near field. Such inhomogeneity emphasises the requirement for full quantitative and qualitative description of these fields so that we can relate biological effects to specific ultrasonic characteristics. If, as in ultrasound therapy, the beam is continually moved evenly and repeatedly through the treatment area, then that area receives a time-averaged dose which is a function of the amount of ultrasonic energy emitted by the transducer and the duration of the treatment. It is therefore essential that we are able to measure the quantity of ultrasound emitted and have some idea of its distribution in both time (if pulsed) and space. In order to attempt to reproduce experimental bioeffects, in both the experimental and the clinical arena, it is essential that experimentalists and clinicians are supplied with

clear, and unequivocal, information regarding exposure conditions necessary to observe a given bioeffect.

The numerous techniques in common use for ultrasonic dosimetry may be divided into two groups, those which measure total ultrasonic power emitted by the transducer and those which describe the distribution and variation of this power within the field. The most common approach to ultrasonic dosimetry is to measure the total amount of radiated energy by one technique and divide this by the effective radiating area (ERA) of the beam, obtained by some other technique. Such an approach would give us the *spatially averaged intensity* (I^a), normally quoted in terms of watts per square centimetre (W/cm^2), over the whole beam. The dosimetry methods employed in this thesis, to measure the total amount of radiated energy and its distribution in time and space, are described in chapter 6. Rather than simply supplying information regarding the average intensity applied to a given biological target, some authors prefer to quote the most extreme "hot spot" intensity, here defined as the *spatial peak intensity* (I^p), experienced by a biological target within the ultrasonic field. When one is examining the effect of ultrasound on biological targets exposed within the near field (as in this thesis) the spatial peak intensity is usually located in the centre of the beam, co-axial with the centre of the transducer face. Due to the highly variable pressure distribution within the near field the spatial peak intensity (I^p), within a lateral cross section of an ultrasonic beam, may be several times the spatial average intensity (I^a) at the same site.

When applied in pulsed mode, ultrasonic intensity can be described in four ways. The most commonly employed method of quantifying the output of pulsed ultrasound is by averaging the intensity over time (including off time when the transducer is not emitting) and effective radiating area, this is known as the *spatial averaged temporal averaged intensity* ($I^{(SATA)}$). The second method is to quote the temporally averaged intensity at the most intense hot spot of the ultrasonic field, which is equivalent to the spatial peak intensity of continuous ultrasound. This is known as the *spatial peak temporal average intensity* ($I^{(SPTA)}$). The remaining two ways of quantifying intensity in the pulsed mode are calculated from the $I^{(SATA)}$ and $I^{(SPTA)}$ values while taking into account transducer on time only. These give values of the average and peak intensities within each pulse and are known as *spatial average temporal peak intensity* ($I^{(SATP)}$) and *spatial peak temporal peak intensity* ($I^{(SPTP)}$). The term temporal peak is often replace with *pulsed averaged* (PA) when ultrasound is

delivered as long (ms) pulses and thus become $I^{(SAPA)}$ and $I^{(SPPA)}$ respectively.
For example:
Suppose that a therapeutic transducer is driven in continuous mode so that its spatially averaged intensity is 1 W/cm^2. Its spatial peak intensity could be somewhere between 2 & 6 W/cm^2 (say 4 W/cm^2). If the generator is now switched to pulsed mode so that the pulse off time is four times longer than the pulse on time (i.e., a duty cycle of 1:4), then the $I^{(SATA)}$ and $I^{(SPTA)}$ would drop to 0.2 W/cm^2 and 0.8 W/cm^2 respectively, whereas the $I^{(SAPA)}$ and $I^{(SPPA)}$ values would remain at 1 and 4 W/cm^2 respectively.

In addition to these peak and averaged intensity measurements, complete characterisation of an ultrasonic field should include measurement of the intensity distribution across the beam, perpendicular to the beam axis (lateral beam plots) at a site which corresponds to the location of the biological target under study. There are other dosimetric parameters which need to be known and quoted when any biological effect of ultrasound is being examined. Certain ultrasound bioeffects appear to be dependant upon frequency. Young and Dyson (1990) demonstrated that ultrasound at a frequency of 0.75 MHz encouraged wound angiogenesis to a greater extent than 3 MHz, all other parameters being fixed. In addition to frequency, the following should also be stated: mode of exposure (continuous or pulsed), description of the modulation envelope (pulsed), pulse and pause time - termed the *mark:space ratio*, exposure duration, the number of exposures given and the time between exposures. The amount of heat generated as a consequence of exposure should also be stated.

2.5 Detection and measurement of ultrasound

Ultrasound output can be measured in a number of ways. The most common methods used are:

1. Radiation force methods
2. Piezoelectric hydrophone methods
3. Calorimetric (absorption) methods
4. Optical methods

2.5.1 Radiation force methods

Any medium or object placed in the path of an ultrasonic beam is subject to a steady

force called the radiation pressure force which tends to push that material in the direction of wave propagation. This pressure is distinct from the oscillating particle pressure (described earlier in section 2.4) and is not fully understood. If an ultrasonic beam strikes a totally absorbing target, at room temperature, the force generated by the beam is approximately 68 mg for each watt of ultrasound. The measurement of radiation force is the most commonly used technique for measuring total power produced by a transducer. The total ultrasonic power of the therapy device employed in this study was measured using a custom engineered radiation force balance (chapter 6, p190).

2.5.2 Piezoelectric hydrophone methods

A hydrophone is a small piezoelectric ultrasound transducer which is used as a receiving element. The piezoelectric element in hydrophones produces a voltage response to ambient pressure. The element dimensions are small compared with the dimensions of a wavelength, which allows the hydrophone to measure point pressures produced irrespective of pressures at neighbouring points. They have resonant frequencies much greater than the source being investigated to reduce the likelihood of a state of resonance occurring (e.g. it is appropriate to use a hydrophone of resonant frequency 20 MHz to study the output of transducers producing a 1 or 3 MHz field). Hydrophones are usually used to investigate relative intensity distribution within ultrasonic fields, (i.e. for beam plots, see chapter 6). They can also be used to measure absolute intensity, for example at hot spots such at the last axial maximum; for this the hydrophones have to be calibrated in terms of acoustic intensity. A polyvinylidene difluoride (PVDF) piezoelectric hydrophone was used to obtain beam plots of the therapy transducers used in this study. The method used to generate beam plots is describe in chapter 6.

2.5.3 Calorimetric (absorption) methods

When a beam of ultrasound travels through a medium, part of the energy of the beam is absorbed and converted to heat which is manifested as a temperature rise in that medium. From the temperature rise of a given volume of liquid of known absorption coefficient at the frequency and temperature of interest (e.g. castor oil), the power dissipated from the transducer can be calculated. The temperature rise within the absorbing volume is normally measured using highly sensitive

thermocouples.

As well as this measurement of total power, thermocouples or thermistors can be used as point intensity detectors in both absorbent and non-absorbent media. In absorbent materials, e.g. biological tissue, local absorption of ultrasonic energy gives rise to a temperature rise. From this temperature rise, knowing the absorption coefficient of that tissue, at the frequency and experimental temperature under study, the ultrasonic intensity at that site can be calculated. In non-absorbent materials thermocouples or thermistors contained within a small volume of absorbing material are used. As the absorbent material absorbs energy it heats up. This increase in temperature is monitored by the encapsulated calorimeter and again can be related to ultrasonic intensity at a given point. Field plots of the distribution of intensity within a sound field can be obtained by using many of these calorimeters distributed throughout the ultrasonic beam or by moving the calorimeter across the beam.

2.5.4 Optical methods

The molecules of the medium through which a sound beam is propagating are alternately compressed and then pulled apart. This results in small local variations in the medium density which in turn leads to variation in refractive index. A beam of light which is passing through a sound beam is deflected by an amount which is proportional to the intensity of the acoustic field. Schlieren systems utilise this property to produce a visual display of the shape of the ultrasonic beam passing through an optically transparent medium such as water. Optical techniques are generally used for qualitative assessment of the extent and uniformity of ultrasonic fields.

This section covered briefly the most common detection and measuring methods used by investigators in the field of ultrasonic bioeffects. These, and other less common methods, have been more extensively described by Wells (1977).

2.6 Attenuation of ultrasound

The intensity of a wave of ultrasound travelling through a medium is found to decrease as a function of distance. This attenuation is thought to be due to a number of mechanisms including beam divergence, scattering, absorption, diffraction and reflection (Wells, 1977). Of these it is thought that scattering and absorption are most important.

2.6.1 Divergence

As explained earlier (p84), beam divergence refers to the deviation from a parallel beam so that the energy per unit area is reduced. The role played by this phenomenon is greater at lower frequencies.

2.6.2 Scattering

Scattering refers to the random reflection of incident ultrasound by small (relative to wavelength) obstacles placed in its path. As previously explained (section 2.1.5), when an ultrasound beam encounters an interface between two substances of differing acoustic impedances part of the energy is reflected. If the size of the reflector is large relative to the wavelength of sound and the dimensions of the beam then it is called a specular reflector and a plane wave is reflected as a plane wave. If, however, the dimensions of the reflector are smaller than a wavelength then the reflector acts as a point source and radiates a spherical wave. Biological material is far from homogenous; different tissues vary widely in the composition and architecture of their cellular and acellular components and as such exhibit differing acoustic impedances. They thus contain a range of surfaces whose dimensions vary from that of a specular reflector through to cell nuclei, which are approximately one thousandth of the wavelength of 1 MHz ultrasound. Provided that they are of different acoustic impedance to their surroundings, these small reflectors scatter or re-radiate the ultrasonic energy in all directions; the energy no longer moves in the original direction of propagation and so attenuation of the beam occurs (figure 2.13).

2.6.3 Absorption

Ultrasound attenuation by absorption occurs when the ordered vibrational energy of the wave is converted into other forms of energy such as heat. The mechanisms by which absorption occurs include those due to viscous loss (termed classical mechanisms) and those due to the relaxation process.

2.6.3.1 Viscous Loss

Ultrasound travels through a medium by driving the particles of that medium to vibrate. Energy transfer between neighbouring particles then facilitates its propagation. The mechanism of absorption by viscous loss is based on the fact that the viscosity of the medium tends to oppose the vibrational motion of the particles,

Figure 2.13 A diagrammatic representation of the scattering patterns produced by small particles of a reflector in the path of an acoustic beam.

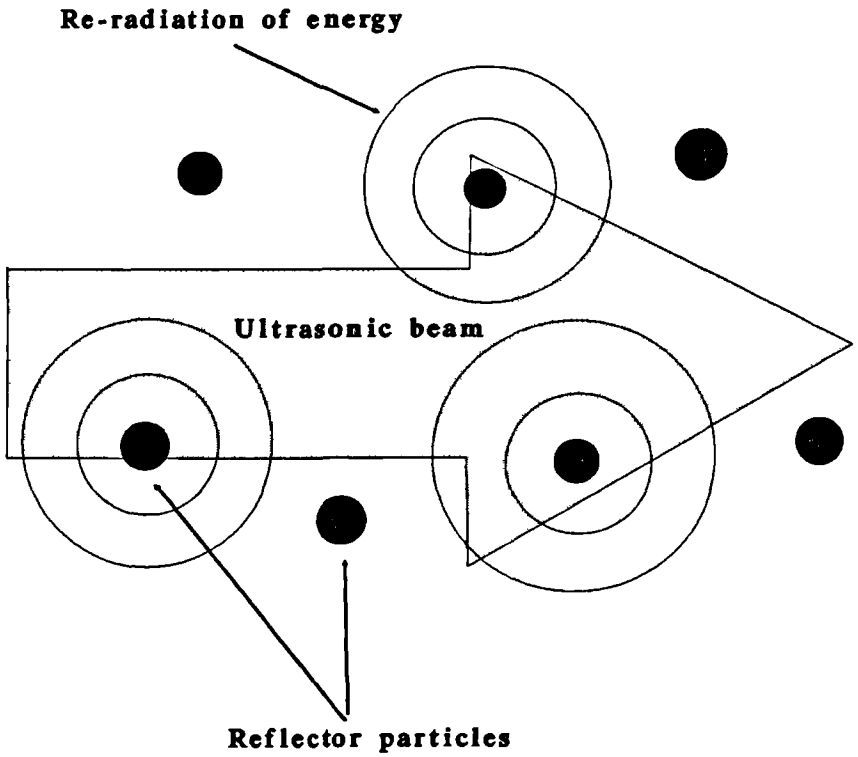

and some of this energy is converted into heat. Absorption is thus dependent upon the viscosity of the propagating medium. Absorption due to viscous loss increases non-linearly with increasing frequency. At frequencies used in biomedical research, viscous loss does not account for much ultrasonic absorption (Wells, 1977).

2.6.3.2 Relaxation

Another mechanism by which absorption can occur arises because energy can exist in a system in various forms, such as molecular vibrational energy, lattice vibrational energy, translational energy, and so on. When an ultrasonic wave propagates through this system there is an increase in energy in one or more of these forms during the compressive part of the cycle. If none of this energy flows to another form, then it would be immediately returned to vibrational energy of the wave during the decompressive part of the cycle and there would be no net absorption. However, some energy always flows into another form during the compressional half cycle (Wells, 1969). During the decompressional half cycle the majority of the energy will be immediately returned in the form of vibrational energy. However, the energy which had flowed to one or more of the other energy forms takes a characteristic period of time to return as vibrational energy. Thus some energy is returned out of phase with the original propagating wave which results in absorption.

Furthermore, some energy does not return to the vibrational form but remains in one of the other forms and is thus effectively absorbed. The magnitude of relaxational absorption is determined by the time constant of the relaxation process. At low frequencies, the phase delay in energy transfer is negligible, and the absorption is small. The absorption increases with frequency, up to a maximum value when the shared energy is anti-phase; above this frequency the absorption falls because there is less time available for the energy to flow from one form to another. Typically, maximum absorption due to relaxation occurs at frequencies around 2 to 5 MHz (Wells, 1969). Relaxation processes are generally the most important contributors to ultrasonic absorption in biological tissues at these frequencies.

Chapter 3. Interaction of ultrasound with biological materials

Introduction

The mechanisms of interaction of ultrasound with biological materials can be divided into two groups, thermal and non-thermal.

1. Thermal
2. Non-thermal
   (a). Acoustic cavitation
   (b). Acoustic micro-streaming
   (c). Radiation Force

A given bioeffect may result from the action of one, or the interaction of several, of the mechanisms listed above.

3.1 Thermal

Biological materials do not transmit ultrasonic energy with 100% efficiency. As an ultrasonic beam travels through tissue the energy contained within it decreases with distance traversed. This energy loss from the beam, termed attenuation, results from the absorption or scattering of energy by the material. The energy absorbed by the material primarily appears as heat and causes an increase in temperature of that material. The amount of absorption, and thus the amount of heat generated, within a material is dependent upon: 1. absorption characteristics of that material, 2. the characteristics of ultrasound (such as frequency) and, 3. the amount of ultrasonic energy passing through it.

1. Characteristics

The absorption of ultrasonic energy, and thus the amount of heat generated, is greater in tissues having high absorption coefficients. Tissues with high protein (or mineral) content such as muscle (or bone) have higher absorption coefficients than tissues with high fat or water content. For example the intensity of a beam of 3 MHz ultrasound is 50% attenuated by about 16mm of fat but only about 3mm of muscle (table 3.1). Structures having high absorption coefficients such as superficial cortical bone, joint menisci, fibrotic muscle, tendon sheaths and major nerve roots are therefore preferentially heated (Lehman and Guy, 1972). Ultrasound will largely pass through fatty layers and selectively heat underlying muscular tissues (ter Haar and

Table 3.1 The half value depth for 1 and 3 MHz ultrasound in various media

Medium	Penetration depth (mm)	
	1 MHz	3 MHz
Water	11500.0	3833.0
Adipose tissue	50.0	16.5
Skeletal muscle (fibres coaxial with beam)	24.6	8.0
Skin	11.1	4.0
Skeletal muscle (fibres normal to beam)	9.0	3.0
Tendon	6.2	2.0
Cartilage	6.0	2.0
Air	2.5	0.8
Compact bone	2.1	-

(after Hoogland, 1986)

Hopewell, 1982). For bone, which has an even higher absorption coefficient than muscle, the rate of heating is even higher, possibly explaining the benefit of ultrasonic therapy in selectively heating joints such as in the treatment of epicondylitis (Binder *et al.* 1985). When an ultrasonic wave travelling through muscle is incident upon bony structures, because of impedance mismatch, nearly 30% of the incident energy is reflected. This reflected wave returns through the muscle traversed on its incident journey. Energy is again removed during this return journey and deposited as additional heat. In addition to reflection, mode conversion is also thought to occur at such muscle/bone interfaces. Briefly, part the of the incident compressional wave is converted into a transverse wave; as soft tissues have a limited ability to conduct transverse waves they are rapidly absorbed and converted into heat. The majority of the transverse wave energy is deposited within a few millimetres of the muscle/bone interface. This area close to the bone, which is richly endowed with blood vessels and nerve endings, includes the periosteum. The heat deposited within the periosteum raises its temperature and, if it exceeds a certain value, is interpreted as pain. Consequently, the application of therapeutic ultrasound at anatomical sites where bone is close to the surface of the skin will lead to the sensation of pain at lower intensities than sites that have a thick layer of absorbent muscle (Williams, 1983).

The temperature rise within a tissue depends upon the transport of heat away

by blood flow. Tissues differ widely in their degree of vascularity, and the rate of blood flow through any given tissue can vary in response to physiological need at any given time. It should be noted that as soon as a temperature rise is produced within most tissues, *in vivo*, it initiates physiological responses that result in the dilation of blood vessels and an increase in blood flow, which increases the rate that heat is lost (Williams, 1983). Overheating, and consequently thermal damage, can occur in tissues of impaired vascularity at ultrasonic intensities unable to produce significant temperature rises in similar healthy, well vascularised, tissue (Dyson, 1990).

2. Ultrasonic frequency

For a given tissue the absorption of ultrasonic energy, and thus the amount of heat generated in that tissue, will increase with increasing frequency. For example 1 MHz ultrasound has lost half of its initial intensity after passing through 48mm of fat and about 9mm of muscle, while 3 MHz ultrasound can pass through only about 16mm of fat or about 3mm of muscle before it has lost half its energy (table 3.1). The loss of ultrasonic intensity from the beam is paralleled by a gain in temperature by the tissue. Thus by controlling the frequency of ultrasound applied, with a knowledge of the composition of the tissue under treatment, the therapist has some control over the depth at which heating occurs.

3. Ultrasonic intensity applied

For a given tissue, exposed to a given frequency of ultrasound for a fixed amount of time, the amount of heat generated in that tissue will increase with increasing ultrasonic intensity.

It is possible to estimate the order of temperature rise (ΔT) that may be expected after irradiation with an intensity I after a time t, in the absence of any cooling mechanism, such as blood flow, from the equation:

$$\Delta T = \frac{2\alpha_a I t}{\rho C_a}$$

(ter Haar, 1990)

Where:

α_a is the absorption coefficient of the tissue (typically 0.03 Np cm at 1 MHz)

ρ is the tissue density (approximately 1 g/cc)

C_m is the specific heat per unit mass of the tissue (4.2 Joules/g)

From the equation it can be seen that temperature change is directly related to ultrasonic intensity. According to the typical values indicated, temperature increases of the order of 0.014°C/second (0.8°C/minute) would be expected for an ultrasonic intensity of 1.0 W/cm^2 ($I^{(a)}$). These estimates may be more applicable to poorly vascularised tissues such as cutaneous scars or tendons, but will probably over-estimate the actual heating observed in highly vascularised tissue such as muscle or granulation tissue. It has been stated that the temperature rise caused by a given time-averaged intensity, applied for a given amount of time, will be the same regardless of whether ultrasound is applied in pulsed or continuous mode (Williams, 1990) i.e. continuous 1 MHz ultrasound applied at an intensity of 0.5 W/cm^2 ($I^{(a)}$) for 5 minutes will cause the same temperature rise as 5 minutes of 1 MHz pulsed (2ms on, 8 ms off) ultrasound at an intensity of 2.5 W/cm^2 $I^{(SAPA)}$. However, the process of pulsing ultrasound may reduce the likelihood of cavitation (p96) (Williams, 1990).

Regulated exposure to heat, regardless of the means of its generation, can have various beneficial effects. Increase in the extensibility of collagenous tissue, blood flow, pain relief and the resolution of inflammation, and decrease in muscle spasm and joint stiffness have all been observed in tissues maintained for between 5 - 30 minutes at temperatures between 40 - 45°C (Lehman and Delateur, 1982). It has been suggested that the main advantage of using ultrasound rather than a non-acoustic method to raise tissue temperature is that ultrasound allows protein-rich tissues to be heated preferentially. Highly collagenous (i.e. proteinaceous) scar tissue, joint capsules, and tendons lying deep within the body can therefore be heated to within the therapeutically effective range without producing damaging temperature elevations within the less collagenous skin and subcutaneous adipose tissue lying superficial to them.

The thermal mechanism is thought to be the major mechanism by which ultrasound exerts its therapeutic effects in the treatment of musculo-skeletal disorders (Summer and Patrick, 1964), where intensities of the order of 0.5 - 3.0 W/cm^2 ($I^{(a)}$/$I^{(SATA)}$) are employed. However, this mechanism is thought to be implicated to a lesser degree in the stimulation of tissue repair (Dyson *et al.* 1968), where beneficial therapeutic effects can be achieved without a significant elevation in temperature. Such studies have employed intensities of the order of 0.1 - 0.2 W/cm^2 ($I^{(SATA)}$).

More comprehensive reviews of the biological effects of ultrasound attributed to heat have been compiled by Wells (1977), Fry (1979) and Williams (1983).

3.2 Non thermal

If an ultrasonic bioeffect is observed in the absence of physiologically significant heating or cannot be mimicked by heating to the temperature attained during ultrasonic exposure then the observed bioeffect was probably not caused by a thermal mechanism i.e. a non thermal mechanism was involved. Such bioeffects can be demonstrated when the average ultrasonic intensity is low, or the system is cooled, so that little or no temperature rise occurs.

Bioeffects of therapeutic ultrasound that appear to result from non-thermal mechanisms include: the stimulation of tissue repair (Dyson *et al.* 1968) and more specifically soft tissue repair (Paul *et al.* 1960; Dyson *et al.* 1976) stimulation of blood flow in chronically ischaemic tissues (Hogan *et al.* 1982), stimulation of protein synthesis by fibroblasts (Webster *et al.* 1978) and of bone repair (Dyson and Brookes, 1983).

3.2.1 Acoustic Cavitation

The theories and physics of acoustic cavitation are extremely complex. This section should be viewed as a gross simplification of the physics with a bias towards possible biological interactions. Acoustic cavitation is the term applied to describe the oscillatory activity of gas or vapour-filled bubbles which are powered by and thus extract energy from the incident acoustic field (Williams, 1983). Some of the energy (about 10%) is re-radiated as an acoustic wave but the remainder is transformed into other forms and may appear as heat (resulting in the production of free radicals) or as shock waves or hydrodynamic shear fields which can disrupt biological tissue.
These bubbles grow by a process termed rectified diffusion, from tiny in-homogeneities within conducting media, called micronuclei, under the influence of ultrasonic fields. The occurrence of any form of cavitational activity is highly dependent on the number and availability of these micronuclei.

Rectified diffusion may be explained as follows:
When bubbles contract, in response to ambient pressure increase, the partial pressure of the gas within the bubble increases. This encourages gas to diffuse out of the

bubble. Conversely when the bubble expands, gas is encouraged to diffuse into the bubble. Since the rate of diffusion is dependent upon the surface area for diffusion less gas will leave the bubble when it is contracting (smaller surface area) than will enter it when it is expanding (larger surface area) this mechanism of rectified diffusion is termed the *"area effect"*. In addition to this mechanism, another mechanism termed the *"shell effect"* is also thought to facilitate rectified diffusion. This second mechanism is due to the fact that as the bubble expands it compresses vapour around the outside of the bubble, thus increasing the concentration gradient across the skin of the bubble. As the rate of diffusion into the bubble depends on this gradient, inward diffusion is greater when the vapour is compressed i.e. when the bubble is in its expanded state. The process of rectified diffusions thus results in a net diffusion of gas into the bubble which results in bubble growth. This process of rectified diffusion competes with the normal diffusion of gas out of the bubble which is due to the normal tendency of small bubbles to shrink in response to surface tension.

A more complete physics-based description of the theory of rectified diffusion is given by Crum (1984).

The cavitational behaviour of these bubbles once formed depends upon the ultrasonic field they experience. Two extremes of cavitation activity have been identified, the gentle oscillation of gas filled bubbles in low intensity sound fields termed stable cavitation, and the violent and destructive behaviour of short-lived vapour-filled bubbles in high intensity sound fields termed transient cavitation (Flynn, 1964). Stable and transient cavitation should not be thought of as separate entities but rather extremes of a continuum. This is illustrated by the fact that a bubble exhibiting the characteristics of stable cavitation changes its behaviour as intensity increases until it exhibits characteristics associated with transient cavitation at high acoustic intensities (Williams, 1983).

3.2.1.1 Stable cavitation

Stable cavitation is thought of as being non-violent. It refers to the motion of a bubble gently oscillating in phase with the pressure variations induced by the acoustic wave (Nyborg, 1977). Thus, the bubble contracts by a given amount as the acoustic pressure at that site reaches a maximum and expands by almost the same amount when acoustic pressure reaches its minimum value. With stable cavitation, bubbles

grow in response to the pressure fluctuations of the sound field, over a period of several wave cycles, from micronuclei present in the sonicated medium, by rectified diffusion. Throughout the period of bubble growth, the sound field leads to a pulsating motion of the bubble.

The biological activity associated with stable cavitation is based upon the generation of microscopic streaming fields around oscillating bubbles called acoustic micro-streaming. Large hydrodynamic shear stresses occur within the acoustic streaming flow generated near solid or gaseous bodies oscillating at an ultrasonic frequency while immersed in a liquid (Nyborg, 1965). This microstreaming flow includes a small closed inner circulation and an outer circulation which may extend over distances many times larger than the dimensions of the oscillating source. The greatest shear stresses occur within the inner (boundary layer) flow, and objects in suspension, such as cells, are only subject to large shear stresses for a short time (milliseconds) as they are carried past the oscillating surface by the outer eddy of the micro-streaming flow (Williams and Miller, 1980). However, in tissues cells which are not free to move can be exposed to these stresses throughout the period of irradiation, unless the ultrasound applicator is kept in motion.

The amplitude of bubble oscillation, and thus cavitational activity, is dependent upon bubble size. Cavitational activity associated with a growing microbubble increases with increasing size of the oscillating bubble until it reaches resonant size, at which point further increase in size of the bubble will result in a decrease in the magnitude of cavitational activity. The resonant size for a bubble at an ultrasonic frequency of 1 MHz is approximately 7μm in diameter (Williams, 1983).

3.2.1.2 Transient Cavitation

Transient cavitation is the phenomenon whereby a bubble grows very rapidly during that portion of the wave cycle when the pressure falls to a low value, then collapses during the next part of the wave cycle when the pressure increases. The whole process from formation of the bubble to its collapse is thought to occupy less than one wave period. It occurs most readily at low ultrasonic frequencies (15 - 40 kHz) and high ultrasonic intensities (Williams, 1983).

Transient cavitation is a violent but microscopic phenomenon generating shock waves and very high temperatures within bubbles. Noltingk and Neppiras (1950) deduced that the temperature rise within a collapsing bubble could exceed several

thousand °C. Such high temperatures lead to the pyrolytic breakdown of water vapour leading to the production of highly reactive H and OH free radicals (Coakley and Nyborg, 1978). Such free radicals are short lived, but, after interaction with undissociated water or gas molecules, may generate longer lived secondary species such as H_20_2 (Del Duca *et al.* 1958). It is well documented that the presence of free radicals, particularly hydroxyl radicals, can result in adverse biological effects (Ward, 1981), such as cell death and DNA strand breaks resulting in chromosomal aberrations (Sasaki and Matsubara, 1972).

There is, however, despite many studies, no evidence of chromosomal defects produced by clinical ultrasound (Duck and Whish, 1986; Miller, 1985a; Miller *et al.* 1991). Further, there is , as yet, no evidence that ultrasound causes free radical production within the cell itself. It is generally thought that the cells in such close proximity to a collapsing bubble would be destroyed by shock waves before their DNA could be altered. Not allowing for this, the free radicals would have a cell membrane and various cytoplasmic constituents to traverse en route to the nucleus, and would thus have ample opportunity to regain their less reactive status.

However, it has been demonstrated that free radicals can develop in the extracellular fluid around cells (Crum *et al.* 1987). As the reaction length of a free radical under such conditions is of the order of between 15 and 90 Å (Ward *et al.* 1985) any free radical-cell interaction would occur at or near the cell membrane. Studies have shown that therapeutic ultrasound can cause damage to endothelial cells when standing waves are generated (Dyson *et al.* 1974), and increase the ion transport through biological membranes (Mortimer, 1981). However, it is not clear what role, if any, free radicals play in these particular phenomena. It is generally accepted that transient cavitation is an unlikely event using ultrasound at therapeutic levels, especially if standing wave formation is avoided.

3.2.1.3 The study of acoustic cavitation

The phenomenon of cavitation is highly unpredictable which makes its physical and biological effects difficult to study. The unpredictability in its occurrence stems from the fact that far more energy is required to generate bubbles than is required to drive pre-existing bubbles to oscillate. As explained earlier cavitation is dependent upon the presence of micronuclei; it is also dependent upon many other variables including ultrasonic intensity (its temporal and spatial distribution), frequency and the

availability of dissolved gases.

This has led many investigators to examine *in vitro* model systems in which the cavitational activity of stabilised bubbles, of resonant size, are driven to oscillate. Miller *et al.* (1978) developed such a system, based on a Nucleopore® membrane, to examine the cavitation derived micro-streaming effects of megaHertz frequency ultrasound. Miller *et al.* (1978) demonstrated that stable gas bubbles can produce significant biological changes at extremely low acoustic intensities in the megahertz range. Fresh human platelets were shown to aggregate *in vitro*, in the presence of such stable gas bubbles, at continuous wave (c.w.) intensities as low as 32 - 64 mW/cm^2 ($I^{(a)}$) using 1 MHz ultrasound (Miller *et al.* 1978) and, subsequently, at c.w. intensities as low as 16 - 32 mW/cm^2 ($I^{(a)}$) using 2.1 MHz ultrasound (Miller, 1979a). Rupture has also been demonstrated in platelets following exposure to similar acoustic parameters in the presence of stabilised gas bubbles (Miller *et al.* 1979b). More recently Williams and Miller (1980) demonstrated that human erythrocytes could be ruptured when exposed to 1.6 MHz ultrasound at intensities as low as 20 - 30 mW/cm^2 in the presence of resonant sized gas bubbles.

Thus stable gas bubbles of the correct size may be driven to oscillate by extremely low intensities of therapeutic ultrasound at megaHertz (therapy) frequencies. The hydrodynamic shear forces within the acoustic micro-streaming fields generated by these oscillating bubbles are more than large enough to disrupt cells *in vitro* (Williams, 1983). Whether such cavitational activity is responsible for the many *in vivo* bioeffects associated with low level, apparently non-thermal, ultrasonic exposure depends upon the presence of nucleation sites and the subsequent growth and development of cavities is currently unknown.

3.2.1.4 Cavitational activity *in vitro*

Much of the wealth of information on cavitationally-induced bioeffects comes from *in vitro* experiments. This is because the energy absorbed by cells in suspension *in vitro* can easily flow away into the suspending medium, and as such, cells in suspension are less likely to be influenced by temperature rise (Williams, 1985). It has been suggested that some form of cavitation mechanism is involved in most if not all of the reported *in vitro* ultrasonic bioeffects (Miller, 1985b) as many of the bioeffects demonstrated to date *in vitro* can be suppressed by elevating ambient pressure (Ciaravino *et al.* 1981; Webster *et al.* 1978; Mortimer and Dyson, 1988).

Many workers have attempted to quantitate the "threshold" conditions required for cavitation to occur *in vitro*. Unfortunately there are many cavitation detection techniques, of varying sensitivities, each with its own following of experimentalists. This has lead to the publication of markedly different values for the "threshold" conditions for its occurrence. It was pointed out by Iernetti (1971) that the reported threshold acoustic pressure amplitudes for bubble formation using 1 MHz ultrasound ranged from 1.75 to 240 atmospheres (0.175 - 24 MPa). There is thus no "safe" threshold pressure amplitude below which cavitation is always absent.

Many of the factors which influence this "threshold" have been mentioned earlier in this section; they include the number and size of micronuclei, the presence of foreign surfaces for the attachment and stabilisation of bubbles, the content of dissolved gas, the treatment of the sample (eg mixing/stirring) and the frequency, intensity and pulsing regime of the ultrasonic beam. In general, the intensity "threshold" for the occurrence of cavitation increases with frequency in the megahertz range. One explanation for this is that as the frequency increases there is progressively less time for gas molecules to diffuse into the micronucleus during the negative pressure portion of the cycle, so bubbles are less likely to develop. Many therapeutic ultrasound generators can deliver pulsed as well as continuous wave ultrasound. The effect of pulsing ultrasound on cavitation varies with the pulsing scheme. Hill (1972) stated that if the same amount of acoustic energy is delivered in the form of extremely short but intense pulses, separated by relatively long intervals (as in diagnostic ultrasound), the long off-time would facilitate dissolution of bubbles developed during the pulse. This dissolution can be encouraged by increasing the ambient pressure of the system. In contrast, it has been stated that multiple millisecond pulses (similar to the pulsing regimes of therapy devices) encourages the likelihood of transient cavitation within a medium (Ciaravino, 1981).

The rate at which a given bubble will develop is dependent upon the instantaneous value of the acoustic pressure amplitude of a pulsed beam and its duration rather than the time averaged intensity at that site. It has been demonstrated that the level of lysis of a stirred erythrocyte suspension was greater when the same spatially and temporally averaged intensity was delivered in the form of 2 millisecond pulses (from a commercially available therapeutic device) than when delivered in continuous mode. The level of erythrocyte lysis increased as the length of the pulses became shorter i.e with increasing pulse peak intensity (Williams, 1983).

In vitro studies of cells in suspension invariably employ some form of vessel to hold the sample under test. The walls of such vessels may contain microscopic gas-filled cracks or hydrophobic sites which will encourage the growth of small gas bubbles under the appropriate acoustic conditions. Micronuclei may also be introduced into an experimental system by pippetting, stirring, shaking or rotating cell suspensions in an attempt to ensure they are homogenous. Williams (1982) demonstrated increasing cavitationally-induced red blood cell lysis as the speed of a magnetic stirrer was increased when the system was exposed to 0.75 MHz continuous ultrasound at an intensity of 1 W/cm^2 (within the therapeutic range). Williams also investigated other methods of agitation on the level of red blood cell lysis including shaking and percussive impact on the exposure vessel and found elevated cavitationally induced red blood cell lysis with increasing mechanical disturbance (Williams, 1982). These effects were so dramatic that the author pointed out that it was pointless carrying out *in vitro* studies without considering pre-treatment of the sample and the effects of any agitation technique on the nucleation properties of that suspension.

The geometry of the *in vitro* exposure system also has a profound effect on the subsequent growth and development of bubbles during exposure. Any interface at right angles to the path of a plane acoustic beam will reflect part of the incident beam forming a partial standing wave field. The increased pressures produced by standing wave fields can lead to highly active cavitational phenomenon, possibly transient cavitation with concomitant heat generation and free radical release as demonstrated in biological fluids such as plasma and amniotic fluid (Crum *et al.* 1987). Iernetti (1971) studying cavitation in gassy distilled water, demonstrated that the threshold ultrasonic intensity at which cavitation occurred decreased as the volume of the sample increased. This probably reflects the greater probability of finding nuclei in a greater volume of liquid.

In view of the above considerations it is not surprising that there is no single "threshold" value for the occurrence of cavitation. The cavitation-based lysis of erythrocytes *in vitro* is a fine example. Using 1 MHz continuous wave ultrasound the threshold intensity required to lyse a suspension of unstirred erythrocytes is about 1.5 W/cm^2, but, when gently stirred this drops to about 0.6 W/cm^2. The threshold intensity drops even lower to 0.2 W/cm^2 when resonant sized gas bubbles are introduced into the exposure system (Williams and Miller, 1980).

3.2.1.5 Cavitational activity *in vivo*

Many workers have previously suggested that nucleation sites for bubbles do not exist *in vivo*, for example in freshly drawn cat blood (Harvey, 1951). However, it has been suggested that micronuclei must occur *in vivo* in mammalian tissues as these are the nucleation sites from which bubbles grow during decompression (Fulton, 1951). It has been proposed that micronuclei are continuously formed as a result of local mechanical tensions. It has been observed that animals at complete rest, experiencing mild decompressional conditions, form visible bubbles; whereas, if muscular contraction occurs bubbles occur in profusion (Fulton, 1951). There is more recent evidence to support this proposal; Chater and Williams (1982) could not get mammalian blood to cavitate *in vivo* at MHz frequencies and yet Gramiak and Shah (1971) could readily detect microscopic gas bubbles in the chambers of a beating human heart; where it is suggested that a combination of rapid flow and sudden pressure changes favour nucleation.

Martin *et al.* (1981), working on mice, demonstrated transient cavitation associated damage *in vivo* following application of therapeutic levels of ultrasound to surgically exposed liver tissue coupled with saline. The ultrasound was applied at frequencies between 0.88 and 3.0 MHz in continuous mode and the intensities used were between 1 and 7 W/cm^2. However, it was suggested that the initiating cavitational events occurred within the saline or at the liver/fluid interface, rather than within the liver itself. Also skin blisters, with an appearance that suggested they were formed as a result of a transient cavitation event, have been produced following a 25 minute exposure to 0.8 MHz ultrasound at an intensity of 1.33 W/cm^2 (Wittenzeller, 1976); however, it has been suggested that the impedance mismatch between the coupling medium and the skin may have given rise to cavitational events at this interface rather than within the skin (Williams, 1983).

Until recently, there appeared to be conclusive *in vivo* evidence for the existence of gaseous nuclei, and the occurrence of cavitation within tissues insonated with therapeutic levels of ultrasound (ter Haar and Daniels, 1981; ter Haar *et al.* 1982). These authors exposed the legs of anaesthetized guinea pigs to 0.75 MHz continuous wave ultrasound at intensities of 0.08 to 0.68 W/cm^2 ($I^{(a)}$) and observed the production of gas bubbles associated with tissue interfaces. At 0.68 W/cm^2 many bubbles were present within muscles throughout the leg; whereas, 0.08 W/cm^2 appeared to be the threshold intensity for stable bubble generation *in vivo*. However

the accuracy of this work, specifically the cavitation detection method used, has recently been challenged (Watmough *et al.* 1991).

Other workers have reported much higher threshold intensities, well beyond the therapeutic range, for the occurrence of cavitation *in vivo*. Sommer and Pounds (1982) reported that the threshold for cavitation in porcine tissue was 75 +/- 8 W/cm^2 ($I^{(a)}$) at a frequency of 0.37 MHz. They defined the onset of cavitation using the presence of bubble subharmonics as a detection mechanism. Lee and Frizzel (1988) found the threshold of cavitation in mouse neonates to be between 53 and 74 W/cm^2 ($I^{(a)}$) at a frequency of 1 MHz. They used a biological endpoint, namely cavitationally-induced hind limb paralysis of neonates, as their assessment mechanism. Frizzel *et al.* (1983) used the same biological endpoint method to show the cavitation threshold intensity requirement to be approximately 60 W/cm^2 ($I^{(a)}$) for 3 MHz ultrasound.

Williams (1981a) showed that the diverse changes in platelet function and the blood coagulation system he observed *in vitro* (see section 3.2.1.4, p100) appeared to be initiated by some form of cavitational activity within the blood or plasma. When he attempted to reproduce these effects *in vivo*, in a volunteer, by insonating (with 0.75 MHz ultrasound at an intensity of between 0.25 and 0.34 W/cm^2, $I^{(a)}$, for between 30 and 45 seconds) an antecubital vein upstream of a sampling cannula no effect was observed. A similar result was observed in rabbits by Chater and Williams (1982) who were again unable to detect platelet damage or erythrocyte lysis using 30 - 40 second exposures of 0.75 MHz ultrasound at intensities up to 17 W/cm^2 ($I^{(a)}$). Contradictory results were presented by Wong and Watmough (1981) who found that 1 - 2 W/cm^2 ($I^{(a)}$) of 0.75 MHz ultrasound directed into the beating hearts of anaesthetized rats (applied through the diaphragm) resulted in cavitation-based erythrocyte lysis. It was initially suggested that the turbulence and large pressure changes experienced within the beating heart enhanced the nucleation characteristics of the blood and in doing so lowered the threshold intensity for generating ultrasonic cavitation *in vivo* (Williams, 1983). However, it was subsequently shown by Williams *et al.* (1986) that this erythrocyte lysis resulted from a thermal ultrasonic effect. Damage to endothelial cells in the chick embryo and to the uterus of the mouse have been reported (Dyson *et al.* 1974; ter Haar *et al.* 1979) in standing wave fields, the mechanism of this damage is unknown but appear not to be typical of heating (Sacks *et al.* 1981), and it has been suggested that hydrodynamic shear stress-induced changes induced in cells located adjacent to vibrating bubbles trapped in the standing wave field could be involved

(Dyson 1993, personal communication).

In general mammalian tissues *in vivo* contain fewer micronuclei than solutions *in vitro*; it has been stated (Williams, 1983) that this is probably because all fluids entering or leaving living tissues must be filtered through cell membranes. Thus quiescent biological fluids and tissues appear to be remarkably resistant to bubble formation during decompression (Harvey, 1951) or to ultrasonically-induced cavitation at intensities similar to and greater than those commonly employed in physiotherapy (Williams *et al.* 1981; Chater and Williams, 1982).

In summary, there is no conclusive evidence available to date that demonstrates beyond doubt that therapeutic intensities, and frequencies, of ultrasound are able to induce bubble growth and oscillation (stable cavitation) *in vivo* in the absence of standing wave fields. That is not to say such events do not occur *in vivo*; rather, attempts and techniques employed so far have been unable to detect them. Less complex biological systems *in vitro* suggest that if such events did occur *in vivo* they could modify cell function and possibly even lead to localised tissue damage. As yet undetectable cavitational events *in vivo* may explain many of the observed ultrasound bioeffects shown to occur in the absence of any physiologically significant temperature rise (Dyson *et al.* 1970, Dyson *et al.* 1976; Dyson, 1981; Dyson and Smalley, 1983; Young and Dyson, 1990a,c).

3.2.2 Acoustic Microstreaming

Large hydrodynamic shear stresses occur within the acoustic streaming flow generated near solid, or gaseous, bodies (see stable cavitation above) oscillating at an ultrasonic frequency while immersed in a liquid (Nyborg, 1965). Several workers have suggested that these shear forces are responsible for cell rupture and damage (Williams, 1972; ter Haar *et al.* 1979). Others have suggested that microstreaming and its associated stresses are responsible for altering the surface charge of cells (Repacholi, 1970; Repacholi *et al.* 1971; Taylor and Newman, 1972). It has also been suggested that this microstreaming around cellular and/or extracellular biological entities may modulate cell function, possibly by affecting the integrity of the cell membrane (Dyson, 1985). Microstreaming may also influence cell function by modifying the local environment around cells such as by altering metabolite gradients surrounding cells (Young, 1988).

3.2.3 Radiation Force

Any structure, large or small, suspended in a liquid and exposed to ultrasound is acted on by a net radiation force. In a plane progressive wave (section 2.1.2., p61) the force is in the direction of wave propagation and is proportional to the intensity of the beam. This forms the basis of dosimetric total power measurements made using sound balances (sections 2.5.1., p87 and 6.1.1., p189). In a standing wave field (described in section 2.1.6, p72) the direction of the force on an object depends upon the properties of that object. Most free cells in suspension move to pressure minima (nodes) whereas, gas bubbles in suspension move towards pressure maxima (antinodes). Cells in suspension are thus encouraged to form bands. This is thought to explain the banding phenomenon described by Dyson *et al.* (1974) who demonstrated the banding of blood in small blood vessels of chick embryos exposed to standing wave fields. This banding proved to be reversible but was sometimes accompanied by endothelial damage. Standing wave occurrence should be avoided as it is also associated with elevated likelihood of transient cavitation and concomitant free radical/thermal damage to biological tissues.

Chapter 4. Physiological effects of therapeutic ultrasound

4.1 Introduction

The previous chapter described the major physical mechanisms thought to be responsible for the bioeffects observed when therapeutic levels of ultrasound are employed experimentally and clinically. Therapeutic ultrasound is used to treat both acute and chronic injuries; there is experimental and clinical evidence that it can, in certain circumstances, produce physiological changes which result in reduced swelling, facilitated healing, improved musculoskeletal mobility and the relief of pain (Kitchen and Partridge, 1990). This chapter will review the literature relevant to modulation of soft tissue repair by therapeutic ultrasound. As this thesis relates to studies carried out to examine the interaction of therapeutic ultrasound with wound healing processes of the skin, emphasis has been placed upon literature relating to cutaneous repair.

The nature of many wound healing studies including clinical trials, case reports and some experimental studies carried out *in vivo*, is such that observations of ultrasonic bioeffects are often made some time after initial injury and treatment. As such they are often reported in terms of eventual outcome, rather than in terms of the immediate response or responding biological target. Treatment often occurs during the inflammatory phase (soon after injury), whereas the effect of treatment is often not assessed until much later, perhaps during the subsequent granulation tissue production or matrix synthesis and remodelling phases of repair. Such studies are essential, often supplying the impetus for further experimental and clinical work, though their value is limited in that they do little to advance understanding of the effect of ultrasound at the cellular or molecular level. These studies will be discussed in terms of the observed biological effects, rather than in terms of the possible biological target.

Other studies set out to explain the mechanisms of interaction in terms of responding biological targets. These studies often involve studying the ability of ultrasound to modulate specific cellular activities *in vitro*, and some may appear to require unacceptable extrapolation with regard to their clinical relevance. These studies will be described in terms of the wound healing phase to which the cellular activity under study is normally associated.

4.2. Cutaneous repair.

Although little is known about the direct effect of ultrasound on the repair of the epidermis, progress has been made in describing and understanding its effects on the repair of the underlying soft connective tissue that constitutes the dermis. Though a time-scale compartmentalisation of wound repair phenomena risks over simplification and inaccuracy, such a dissection of information is useful as an aid to understanding the complexities of the repair process. For this reason, tissue response to injury and its modulation by therapeutic ultrasound is divided up into three overlapping phases:

1. Inflammation
2. New tissue formation
3. Matrix formation and remodelling

The process of cutaneous repair has previously been described in chapter 1. In the following sections, each phase of repair will be briefly described, together with the appropriate ultrasound bioeffects literature.

4.2.1. Inflammation

Blood vessel disruption during tissue injury leads to the extravasation of blood constituents. The resulting processes of platelet aggregation and blood coagulation at the site of injury initiate the early inflammatory phase of wound repair. Clot formation within damaged vessels affects haemostasis, and within the surrounding connective tissue provides a provisional matrix for cell migration into the wound space. Mediators released as a consequence of blood coagulation, complement pathways, matrix damage, cell activation or death, induce the recruitment of inflammatory leucocytes and increase the permeability of undamaged vessels at the wound periphery resulting in additional leakage of plasma proteins. Neutrophils, which arrive in the early inflammatory phase, attempt to clear the area of foreign particles, especially bacteria. If effective, no further influx of neutrophils occurs and the effete neutrophils are phagocytosed by macrophages. As the neutrophil infiltrate resolves and macrophage accumulation continues, an arbitrary division can be drawn between the early and late inflammatory phases. Peripheral blood monocytes continue to infiltrate the wound site in response to specific monocyte chemoattractants. Monocytes once within the wound site are progressively activated and display the phenotype of macrophages. Macrophages are thought to elaborate a wealth of biologically active substances many of which are involved with the

recruitment of further inflammatory cells. Growth factors and other substances are also released by macrophages and are thought to be essential for the initiation and propagation of granulation tissue.

4.2.1.1 The effect of ultrasound on inflammation

The effect of ultrasound on activities associated with the process of inflammation will be described under the following sub-headings:

A. The effect of ultrasound on early inflammation - platelets

B. The anti-inflammatory action of ultrasound

C. The effect of ultrasound on the resolution of inflammation - oedema

D. The effect of ultrasound on late inflammation

A. The effect of ultrasound on early inflammation - platelets

Studies examining the effects of ultrasound on platelet activity have been conducted less in anticipation of beneficial therapeutic interaction than from concern over the possible hazards of bringing about a haemostatic reaction inadvertently during the clinical use of this modality. It has been reported that *in vitro* insonation (c.w., 1 MHz) of anti-coagulated whole blood for 5 minutes at an intensity as low as 65 mW/cm^2 ($I^{(a)}$) caused a time-dependent decrease in recalcification time (ie., the time taken for macroscopic fibrin strand formation when enough calcium ions are added to overcome the effects of the anticoagulant) (Williams *et al.* 1976a). Williams *et al.* (1976b) later demonstrated that this effect was due to limited ultrasound-derived platelet damage of a sub-population of platelets leading to the release of platelet factor 3. They found that thrombi, produced by the recalcification of insonated and sham-insonated human platelet rich plasma (PRP), where morphologically dissimilar. Platelet thrombi from insonated samples contained some debris of disrupted platelets and the remaining intact platelets were abnormal in that (a) they were more vacuolated, (b) they formed a larger number of smaller aggregates and (c).their clot retraction mechanism was impaired. It was found that these morphological changes could be duplicated by incubating similar PRP samples with small amounts of platelet debris from homogenised platelets.

Williams *et al.* (1978) examined the release of β-thromboglobulin (β-Tg) from platelets in anti-coagulated whole blood insonated with 0.75 MHz continuous ultrasound. They demonstrated an intensity-dependent increase in β-Tg release above

an intensity of 0.8 W/cm^2 ($I^{(a)}$). When the platelets were insonated in a mixture of EDTA and theophylline (which inhibits the normal release mechanism of platelets and leaves them functionally inert) the level of β-Tg released was reduced by 70%. The remaining 30% indicates that ultrasound causes some β-Tg release by other than physiological means. It was suggested that ultrasound in some way mechanically disrupts a certain percentage of possibly more susceptible platelets, which in turn facilitates the degranulation of further platelets by normal physiological mechanisms. This mechanical disruption argument was supported by the observation of corresponding increases of free haemoglobin from insonated erythrocytes (Williams *et al.* 1978).

In addition to platelet degranulation Chater and Williams (1977) found that under certain *in vitro* ultrasonic irradiation conditions it was possible to initiate aggregation of platelets and that the magnitude of this effect decreased with increasing frequency at a constant intensity of 2.0 W/cm^2 ($I^{(a)}$). Such an observation suggests that the phenomenon of cavitation, which is less probable with increasing frequency, may be involved in platelet disruption *in vitro*.

Such studies have lead to concern being expressed over the ability of therapeutic ultrasound to cause intravascular blockage by inducing platelet aggregation and degranulation *in vivo*. Contradictory observations have been made. *In vivo* studies by Zarod and Williams (1977) demonstrated the presence of occasional small aggregates of platelets trapped within capillaries of the guinea pig pinna, following ultrasound treatment (1:1 pulsed 0.75 and 3 MHz ultrasound at an intensity of 1.0 W/cm^2, $I^{(SATA)}$) of the central ear artery. However, subsequent studies demonstrated excessive (i.e. damaging) temperature elevations under the experimental conditions employed and it was suggested that the platelet aggregates observed resulted from thermal damage to the endothelium rather than a direct interaction with platelets (Williams, 1985). Furthermore *in vivo* studies on adult human volunteers using continuous wave 0.75 MHz ultrasound at an intensity of 0.34 W/cm^2 ($I^{(a)}$) for 30 seconds (Williams *et al.* 1981) and in rabbits again using continuous wave 0.75 MHz ultrasound at intensities of up to 17 W/cm^2 ($I^{(a)}$) (Chater and Williams, 1982) were unable to demonstrate any platelet activation or vascular damage following insonation of blood vessels with therapeutic ultrasound.

Thus, while there is a significant body of experimental evidence that suggests that therapeutic ultrasound can modulate platelet activity *in vitro*, apparently by

limited cavitational damage, it would appear that therapeutic ultrasound cannot similarly modulate or damage platelets *in vivo*, provided that excessive temperature elevations are avoided.

It is difficult to relate the above *in vivo* studies where uninjured vasculature is insonated, to the application of ultrasound to sites of traumatised vascular endothelium as found in wounds, as in the latter situation platelet aggregation would be initiated by the exposure to subendothelial matrix components prior to ultrasound treatment. It is possible that ultrasound, when applied to acutely traumatised tissue, may modulate additional platelet activity at the wound site, possibly encouraging wound repair by stimulating the release of growth factors and other stimulatory agents, rather than acting as the inciting event.

B. The anti-inflammatory action of ultrasound

For many years clinicians have claimed that ultrasound may be a potent anti-inflammatory agent (Reid, 1981 cited by Snow and Johnson, 1988). Support for these opinions are based more on clinical impressions rather than on scientific evidence (Snow and Johnson, 1988). Earlier placebo-controlled clinical trials were unable to demonstrate any clear cut difference in inflammation between insonated and sham-insonated individuals (Mueller *et al.* 1954; Roman, 1960; Flax, 1964). In a more recent experimental study on Wistar rats, which compared the effect of pulsed ultrasound (1.5 MHz, pulsed 1:1, intensities 0.5 - 2.0 W/cm^2 $I^{(SAPA)}$) with a nonsteroidal anti-inflammatory drug (flurbiprofen) on the acute inflammatory response to subcutaneously implanted (bacteria-laden) irritant sponges, no anti-inflammatory action was observed (Goddard *et al.* 1983).

El Hag *et al.* (1985), in a clinical trial of 33 patients, found that pulsed therapeutic ultrasound (3 MHz, pulsed 1:4, intensity 0.5 $I^{(SAPA)}$) could reduce swelling almost as effectively as 10 mg of steroidal anti-inflammatory dexamethazone. However, in more recent placebo controlled work, they demonstrated anti-inflammatory activity following sham-insonation, and it was therefore suggested that the anti-inflammatory action of ultrasound may be placebo-based (Hashish *et al.* 1986). In a later placebo-controlled double blind clinical trial Hashish *et al.* (1988) examined the contribution of placebo and massaging effects of pulsed ultrasound therapy (3 MHz, pulsed 1:4, intensity 0.5 W/cm^2 $I^{(SAPA)}$) following bilateral surgical extraction of lower third molars. The results of this study demonstrated that the anti-

inflammatory effects of ultrasound therapy were placebo-mediated via sham treatment rather than massage action. Other studies have been unable to demonstrate an anti-inflammatory effect of therapeutic ultrasound. Snow and Johnson (1988), reported no difference when they compared the anti-inflammatory action of insonation (0.75 MHz, pulsed 1:4, intensity 1 W/cm^2 $I^{(SAPA)}$) with sham-insonation on inflammation of the abdomen induced by ultraviolet radiation, in 20 adult volunteers. On examination of their results, it would appear that they demonstrated a trend towards more rapid resolution of inflammation following insonation though this was apparently ignored by the authors. To date there is no conclusive evidence that supports the concept that therapeutic ultrasound can act in an anti-inflammatory manner.

C. The effect of ultrasound on the resolution of inflammation - oedema

In 1985, 79% of NHS physiotherapy departments and 68% of private practitioners reported that they used therapeutic ultrasound to reduce "local oedema" (ter Haar *et al.* 1987). As physiotherapists are generally unlikely to see patients during the early part of the inflammatory phase of repair, i.e. during the onset of oedema, it can be assumed that clinicians employ the modality in an attempt to diminish swelling rather than to prevent its occurrence. Several more specific clinical reports have indicated that therapeutic ultrasound can encourage oedema resolution; such reports include some uncontrolled clinical observations made by Ferguson (1981) using pulsed 1 MHz ultrasound at an intensity of 0.5 W/cm^2 (presumably $I^{(SAPA)}$, as not stated) and Oakley (1982) using continuous 3 MHz ultrasound at an intensity of 0.125 W/cm^2 ($I^{(a)}$) who both reported greatly reduced swelling as a result of treatment in cases of acute physical trauma. The lack of appropriate controls and dosimetry does, however, limit the value of such observations.

There is a significant body of laboratory-based work that supports the idea that therapeutic ultrasound is capable of encouraging oedema resolution. Fyfe and Chahl (1985) demonstrated that a single application of pulsed therapeutic ultrasound (0.75/1.5/3.0 MHz, pulsed 1:1/1:4, intensity 0.5 W/cm^2 $I^{(SAPA)}$) had a significant effect on sites of silver nitrate-induced oedema in the rat. They observed that over the first 24 hours, oedema was elevated above control levels; after this time insonated sites demonstrated significantly less oedema. A similar observation was made by Hustler *et al.* (1978) studying the effect of continuous ultrasound (0.75 MHz, intensity 0.61

W/cm^2 $I^{(a)}$) on the resolution of bruising and oedema in guinea pig pinnae. After making standard injuries, they observed that in some experimental animals more extensive oedema resulted in ears treated with ultrasound than in ears that were sham-treated, but the subsequent oedema and bruise regression rates were greater in insonated ears than in control ears. Such work appears to indicate that ultrasound both (1) encourages the development of oedema and (2) supports the above clinical findings in that it appears to favour its subsequent resolution. This has led to the suggestion that ultrasound acts in a "pro-inflammatory" manner, accelerating the process of inflammation and its resolution, rather than suppressing inflammation by acting in an anti-inflammatory manner (Dyson, 1990).

As the earliest changes in vascular permeability following injury are thought to be brought about by histamine and the major source of histamine in man is the mast cell, it is possible that the enhanced oedema results from ultrasound mediated mast cell degranulation at the wound site. There are several reports in support of this hypothesis. Straburzynski (1964) was able to demonstrate a significant elevation in the blood histamine level, and a corresponding depletion of mast cells in the skin and the lungs, following application of 0.8 MHz ultrasound (no other dosimetry given) to the thorax of 107 guinea pigs. More recently, Fyfe and Chahl (1984) demonstrated that a single treatment of therapeutic ultrasound (0.75/1.5/3.0 MHz, pulsed 1:4, intensity 0.5 W/cm^2 $I^{(SAPA)}$), to unwounded rat ankles *in vivo* led to a small but significant increase in vascular permeability, as demonstrated by dye leakage, which could be abolished by prior treatment with a combination of a histamine H_1-receptor antagonist and a serotonin antagonist. Further, on histological examination significantly more degranulated mast cells were observed in ultrasound-exposed tissues than in similar sham-exposed tissues. Additional *in vitro* evidence came from Hashish (1986) who similarly demonstrated that pulsed ultrasound at therapeutic levels (3 MHz, pulsed 1:4; intensities of 0.1, 0.5 and 1.5 W/cm^2 $I^{(SAPA)}$) could stimulate degranulation in rat peritoneal mast cell preparations.

The mechanism by which non-cytolytic mast cell degranulation occurs is thought to be triggered by raised intracellular calcium ions within the cell (Yurt, 1981). As it has been demonstrated that therapeutic levels of pulsed ultrasound (1 MHz, pulsed 1:4, 0.5 - 1.0 W/cm^2 $I^{(SAPA)}$) can increase the uptake of calcium ions by fibroblasts *in vitro,* apparently as a result of reversible cell membrane perturbation (Mummery 1978; Mortimer and Dyson, 1988), it has been suggested that this

modulation of calcium flux may be the mechanism by which ultrasound alters mast cell activity (Dyson, 1985) and consequently early inflammation.

D. The effect of ultrasound on late inflammation

Few studies have specifically examined the effect of ultrasound on the cellular activities associated with late inflammation, fewer still have specifically employed therapeutic parameters of ultrasound.

Saad and Williams (1982), working on the rat, reported that the application of therapeutic ultrasound (1.65 MHz continuous, approximate intensity 1.0 - 1.5 W/cm^2 $I^{(a)}$) to the umbilical area of the abdomen, led to a decrease in the clearance of colloidal particles by the reticuloendothelial system. This suggests an effect on the mononuclear phagocyte system, which, if it occurred in wounds, could effect the course of inflammation and hence subsequent repair processes. However, Saad and Williams (1986) demonstrated that injection of *in vitro* insonated (1.65 MHz continuous, intensity 1.6 W/cm^2 $I^{(a)}$) lymphocytes similarly reduced colloid clearance. They also showed that these *in vitro* insonated lymphocytes demonstrated reduced electrophoretic mobility, thought to be associated with changes in surface glycoprotein. As it is known that such altered lymphocytes are sequestered by macrophages prior to "glycoprotein repair" (Ford *et al.* 1976), it was proposed that the reduced ability to clear blood-borne colloids was a consequence of over-loading the reticuloendothelial system with damaged lymphocytes.

As previously stated, macrophages not only phagocytose damaged tissue, but also elaborate various bioactive substances, including growth factors, that appear crucial to the later granulation tissue production phase of repair. These substances stimulate fibroblasts and endothelial cells to form a collagen-rich, well vascularised tissue, called granulation tissue, at the wound site. The effect of ultrasound on the interaction between inflammatory phase cells and proliferative phase cells has been examined *in vitro*. Work on the interaction of therapeutic ultrasound with the promonocyte "macrophage-like" cell line U937, suggested that pulsed therapeutic ultrasound (0.75 & 3.0 MHz, pulsed 1:4, intensity 2.5 W/cm^2 $I^{(SAPA)}$) could both encourage the synthesis, and release, of "factors" mitogenic to 3T3 fibroblasts (Young and Dyson, 1990b). If the synthesis, and elaboration, of such factors is similarly up-regulated in macrophages *in vivo* this may, in part, explain the improvement in wound repair noted in the clinical and experimental use of this modality.

There is evidence that T lymphocytes play a significant role in the process of wound repair (Barbul, 1988). While there is at present no evidence to suggest a similar role for the B lymphocyte population, the close functional associations and interrelationships between T and B lymphocytes encourages further investigation of this possibility. Desai *et al.* (1989) were unable to observe any effect of a 15 minute *in utero* insonation, with therapeutic intensities (1.0 and 3.0 W/cm^2 $I^{(a)}$) of 1 MHz continuous ultrasound, on the proliferation and differentiation of both T lymphocytes and B lymphocytes during murine fetal development. Further, they were unable to detect changes in the proportion of polymorphonuclear leucocytes, lymphocytes, or monocytes 5-10 days after birth as a result of fetal exposure to ultrasound. This work suggests that therapeutic levels of ultrasound appear not to interact, in any significant manner, with the process of leucopoiesis; this, however, does not preclude significant interactions with peripheral leucocytes actively engaged with the process of wound repair. Further work is necessary to investigate the effect of therapeutic ultrasound on the activity of T lymphocytes during the wound repair process.

Experimental evidence *in vivo* has further supported the idea that ultrasound can accelerate the resolution of the inflammatory phase. Young and Dyson (1990a) demonstrated that by five days post wounding ultrasound-treated (0.75 & 3.0 MHz, pulsed 1:4, intensity 0.5 W/cm^2 $I^{(SAPA)}$) excisional wounds in the rat contained fewer 'inflammatory' cells (neutrophils and macrophages) and more mature granulation tissue than sham-insonated control wounds. This suggests that insonated wounds were more "advanced" than similar sham-insonated control wounds. Such an observation could be explained in terms of the ultrasonic exposure encouraging the rate of one, or more, of the leucocytic activities associated with the late inflammatory phase, thus shortening the duration of this phase. Alternatively, it may be explained in terms of a more rapid resolution of the former early inflammatory phase in response to ultrasound, thus facilitating a more rapid progression to the late inflammatory phase.

4.2.2. The new tissue formation phase of wound repair

The formation of new tissue occurs next in this simplified scheme of wound repair. New tissue formation during cutaneous repair involves re-epithelialisation and granulation tissue formation. Re-epithelialisation is the reconstruction of the epidermis into an organised stratified squamous keratinised epithelium that covers the wound defect and provides the barrier properties of the skin. The process of

granulation tissue formation includes the further accumulation of macrophages, colonisation of the wound space by fibroblasts (which involves both proliferation and migration), deposition of loose extracellular matrix (containing fibronectin, hyaluronic acid and collagen), and angiogenesis. As fibroblasts proliferate and migrate into the wound space, they have been reported to undergo an alteration in phenotype, which permits cell motility and concomitant deposition of the aforementioned loose extracellular matrix (fibroplasia). In addition these cells align themselves and their newly deposited matrix along the radial axes of the wound, form cell-cell and cell-matrix associations, and are thereby able to generate a force within the tissue that results in wound contraction. The generation of a rich vasculature (angiogenesis) occurs simultaneously with the process of fibroplasia and is essential to meet the high metabolic demands encountered during the formation of new tissue within a wound site.

4.2.2.1 The effect of ultrasound on new tissue formation.

This section will initially describe the clinical literature regarding the effect of ultrasound on the repair of soft tissue lesions, specifically work examining its effect on impaired or chronic wound healing states such as venous ulcers and pressure sores. Later in this section non-clinical studies which may help to explain clinical observations will be described. Such studies included those relating to the effect of ultrasound on cell proliferation, cell migration, wound contraction and angiogenesis. As the direct effect of ultrasound on the process of re-epithelialisation has not been investigated, these non-clinical studies will centre around the process granulation tissue formation. The literature regarding the effect of ultrasound on the synthesis and deposition of extracellular matrix components found in granulation tissue and scar tissue will be dealt with later in this chapter (section 4.2.3.1).

Clinical literature

Adequately controlled clinical trials, reporting the change of an objectively measurable parameter, in response to therapeutic ultrasound are rare. Dyson *et al.* (1976) examined the effect of treatment with 3 MHz pulsed (2:8) ultrasound, at an intensity of 0.2 W/cm^2 ($I^{(SAPA)}$), on the healing of varicose ulcers. In a single-blind study involving 25 patients, they found that ultrasonic therapy significantly encouraged healing, as assessed by measuring the reduction in ulcer area, when

compared with similar sham-exposed ulcers. Roche and West (1984), in a similar venous ulcer trial that employed the same ultrasonic treatment and assessment parameters, this time with a sample of 26 patients, also observed a more rapid reduction in ulcer size in ultrasound treated than in sham-treated control ulcers.
In a more recent clinical trial Callam *et al.* (1987) carried out a twelve week, 108 patient, study of the effect of weekly ultrasound therapy on the healing of chronic leg ulcers of mixed aetiology (including: venous only, venous and arterial, venous and diabetic). They employed 1 MHz pulsed ultrasound at an intensity of 0.5 W/cm^2 (presumably $I^{(SAPA)}$, though not stated) and found that the proportion of ulcers healed after 12 weeks was 20% greater in the standard treatment plus ultrasound group, than in the group that received standard treatment alone. Unfortunately, as with many clinical studies in the field of ultrasound bioeffects, this study was not placebo-controlled and as such should be viewed with caution. The most recent trial studying the effect of therapeutic ultrasound (pulsed 1:9, 1 MHz ultrasound at an intensity of 0.5 W/cm^2, presumably $I^{(SAPA)}$, as not stated) on venous ulcer healing did not demonstrate any statistically significant difference between ultrasound-treated and similar sham-treated wounds (Lundeberg *et al.* 1990). They did, however, report a trend that suggested that ultrasound was more effective than placebo treatment. Interestingly, they stated that their experimental design, particularly their sample size (n = 44), was such that an improvement of less than 30% could not be detected.

As with the literature on the effect of ultrasound on venous ulcer healing, the literature relating to its effect on pressure sore resolution is limited, both in quantity and quality. Paul *et al.* (1960) made the clinical observation that therapeutic ultrasound was "*markedly effective in relieving congestion, cleansing necrotic areas and promoting healing with healthy, non-adherent skin approaching normal thickness*", following treatment of 23 sores on spinal cord injury patients, which were previously refractive to standard therapies. They employed 1 MHz ultrasound (presumably continuous) at intensities of 1.0 and 0.5 W/cm^2 (presumably $I^{(a)}$) for various exposure times depending upon area to be treated. A better designed study of pressure sore healing, in response to ultrasound, has been carried out more recently by McDiarmid *et al.* (1985). In a preliminary randomised double blind trial, employing 3 MHz pulsed (2:8) ultrasound at an intensity of 0.8 W/cm^2 ($I^{(SAPA)}$) for various exposure periods depending on area of treatment, it was found that there was a non-statistically significant trend towards improved healing in insonated sores when

compared with sham-insonated sores. McDiarmid *et al.* (1985) indicated that their study was carried out in an attempt to validate the clinical observations made by Paul *et al.* (1960). However, the ultrasonic parameters employed by the two groups were completely different. Interestingly, McDiarmid *et al.* (1985) reported that microbially-infected sores appeared significantly more responsive to ultrasound therapy than similar uninfected sores. This observation finds parallels in the work of Popisilova *et al.* (1984) who demonstrated that 4 week old experimental murine granulomata, generated by the subcutaneous implantation of *E. coli* inoculated viscose sponges, contained more than twice as much collagen following exposure to continuous wave therapeutic ultrasound (0.8 MHz, 1.5 W/cm^2, I$^{(a)}$) than similar non-insonated control granulomata.

Non-clinical literature

Research reports relating to the effect of therapeutic ultrasound on specific cellular activities of the granulation tissue formation will be described under the following headings:

A. The effect of ultrasound on cell proliferation *in vitro.*
B. The effect of ultrasound on cell proliferation *in vivo.*
C. The effect of ultrasound on other aspects of granulation tissue formation.

A. The effect of ultrasound on cell proliferation *in vitro*

During wound repair, fibroblast recruitment is essential for the subsequent elaboration, remodelling and contraction of the extracellular matrix; endothelial cell proliferation is crucial to meeting the metabolic demands of reparative tissue.

Unfortunately, there are only two published reports relating to the direct effect of therapeutic ultrasound on the proliferative capacity of untransformed fibroblasts (Loch *et al.* 1971; Webster, 1980), and none which relate to the *in vitro* proliferation of endothelial cells, transformed or otherwise. Ultrasound studies to date have invariably employed spontaneously transformed or transformation-induced cell lines, for example chinese hamster ovary fibroblasts (Armour and Corry, 1982), L5178Y lymphocytic cells (Clarke and Hill, 1969), C1300 neuroblastoma cells (Ross *et al.* 1983), Hela epithelial cells (Kaufmann *et al.* 1977) and Chinese hamster V79 cells (Ciaravino *et al.* 1981). As the proliferative capacity of such cells has already

been compromised, and consequently cannot be termed "normal", the use of such cells to attempt to reproduce the modulatory effects of ultrasound on cell proliferation, in normal tissues, *in vivo* should be contested.

Most studies which report the effect of ultrasound on proliferative capacity of mammalian cells *in vitro* have been conducted either in view of safety concerns of ultrasonic exposure (mostly diagnostic), or to examine the capacity of therapeutic ultrasound to selectively kill cells under hyperthermic conditions (cancer therapy). As such their experimental endpoints were usually cell death or loss of proliferative capacity and the ultrasonic doses applied are excessive when compared with normal therapeutic doses. Few studies have been conducted with the specific aim of examining the beneficial interaction of clinically relevant therapeutic regimes of ultrasound, with the process of wound repair, at the cellular level. The limited number of cell growth and survival studies which have included therapeutic levels of ultrasound have reported conflicting results.

The majority of studies have indicated that ultrasound at therapeutic levels in some way impairs the proliferative capacity of mammalian cells *in vitro*, and that this damage is related to ultrasonic intensity, the mode of ultrasound application (continuous or pulsed), and to the availability of gaseous nuclei at which cavitational activity may occur.

Loch *et al.* (1971) carried out an ultrasonic safety study which included therapeutic ultrasound parameters. They examined the effect of a 10 minute exposure of 1 MHz continuous wave ultrasound, at intensities of between 0.05 - 3.0 W/cm^2 ($I^{(a)}$), on the growth and proliferation of three mammalian cell lines exposed in monolayer (embryonic brain fibroblasts, HeLa epithelial cells and transformed amnion cells). They observed that intensities above 0.1 W/cm^2 led to damage and a reduced proliferative ability in all cell types studied. Kaufman *et al.* (1977) examined the effect of increasing intensities (from 0.3 - 30 W/cm^2 $I^{(a)}$) of a 5 minute 1 MHz continuous wave insonation on the viability and colony forming ability of HeLa and Chinese Hamster Ovary (CHO) cells *in vitro*. They found that viability and proliferative capacity was unaffected below approximately 1 W/cm^2 ($I^{(a)}$), but was then reduced progressively to an intensity of 10 W/cm^2 ($I^{(a)}$). The threshold for impairment was significantly higher than that found by Loch *et al.* (1971), though their exposure times and experimental design differed. In agreement with the work of Kaufmann *et al.* (1977), Ross *et al.* (1983) was unable to demonstrate any significant deleterious

effect on C1300 neuroblastoma cell division following insonation with 1 MHz continuous wave ultrasound when they employed intensities up to a maximum of 1 W/cm^2 ($I^{(a)}$). Similarly, Decat and Leonard (1984) were unable to demonstrate any effect, beneficial or deleterious, on the proliferation of phytohaemagglutinin-stimulated rabbit peripheral blood lymphocytes following exposure to 1 MHz continuous wave ultrasound at intensities of 0.5 or 1 W/cm^2 ($I^{(a)}$).

Other workers have demonstrated deleterious effects on cells and impairment of proliferation post-insonation using fixed intensities which represent the upper limit of the therapeutic range. Ciaravino and Miller (1978) reported a 15 - 20% reduction in V-79 chinese hamster cell proliferation exposed for more than 0.1 min to 1 MHz continuous wave ultrasound at an intensity of 3 W/cm^2 ($I^{(a)}$). Kaufman and Miller (1978) demonstrated impaired growth of V-79 cells post-sonication with 1.07 MHz continuous wave ultrasound at an intensity of 2.5 W/cm^2 ($I^{(p)}$). Fu *et al.* (1980), expanding on the work of Kaufman and Miller (1978), examined V-79 proliferation following insonation with continuous wave 1 MHz ultrasound at intensities of 0.25 to 30 W/cm^2 ($I^{(p)}$) during different phases of the cell cycle. They found that mitotically synchronised cells insonated during the M and S phases were more resistant to loss in reproductive integrity than cells in G_1 or G_2.

Evidence to implicate cavitation as a key agent in this ultrasound-derived *in vitro* cell damage includes the alleviation of such cell damage by: increasing ultrasonic frequency (Armour and Corry, 1982), increasing atmospheric pressure (Ciaravino *et al.* 1981b) and reducing culture medium gas content (Coakley *et al.* 1971); all the above are recognised methods of reducing the incidence of cavitation. Thus, Bleaney *et al.* (1972), under non-cavitating conditions, were unable to demonstrate any effect on the reproductive integrity of Chinese hamster lung cells following 1.5 MHz insonation at physiological temperatures. They employed intensities within, and well above, the therapeutic range using both pulsed (intensity max - 15.0 W/cm^2 $I^{(SAPA)}$) and continuous wave ultrasound (intensity max - 8.8 W/cm^2 $I^{(a)}$). Similarly, Webster (1980) insonating human foetal fibroblasts with 0.75 or 3 MHz pulsed ultrasound at intensities of 0.5 and 2 W/cm^2 ($I^{(SAPA)}$) was unable to demonstrate any effect on cell survival or proliferation.

Interestingly when cells are cultured in three dimensional arrangements (e.g. in spheroids) and exposed to therapeutic ultrasound, at parameters known to result in damage or impaired proliferation in cell suspensions, such damage and impairment

is significantly reduced (Sacks *et al.* 1981). The basis for this reduced response appears to be due to the physical protection of cells in spheroids. It is suggested that cells residing in comparable three dimensional structures *in vivo* would be similarly protected if cavitation was to occur (Sacks *et al.* 1981). As cavitation has yet to be conclusively observed during "therapeutic" insonation *in vivo* (Watmough *et al.* 1991), the relevance of *in vitro* test systems designed in such a way that they allow, or even encourage, cavitation must be questioned. Systems which actively discourage the onset, and perpetuation, of cavitation may be more relevant to the study of ultrasonic bioeffects associated with the therapeutic use of this modality *in vivo*.

DNA synthesis is a prerequisite to the division of cells. Several workers have examined the rate of DNA synthesis, measured by ^{3}H-thymidine incorporation, following exposure of mammalian cells to therapeutic ultrasound *in vitro*. Again conflicting results have been reported. Those reports that have demonstrated increased DNA synthesis in response to therapeutic levels of ultrasound are as follows. Elmer and Fleisher (1974), examining neonatal mouse tibial epiphyses in culture, reported an enhancement in DNA synthesis following exposure to 1 MHz continuous wave ultrasound at an intensity of 1.8 W/cm^2 ($I^{(a)}$). Repacholi *et al.* (1979), examining ^{3}H-thymidine incorporation in concanavalin A stimulated lymphocytes in response to 0.87 MHz continuous wave ultrasound, demonstrated an enhancement in DNA synthesis which was amplified as the intensity was increased from 0.5 to 1.1 W/cm^2 ($I^{(a)}$). Interestingly when the ultrasonic intensity was raised to 3 W/cm^2 (the maximum of the therapeutic range) or above, ^{3}H-thymidine uptake was suppressed. The authors associated this observation with lymphocytes being blocked in G_1. The low intensity work of Repacholi *et al.* (1979) has been validated by Kondo and Yoshii (1985) who reported enhanced DNA synthesis in mouse L cells following exposure to 1.2 MHz continuous wave ultrasound at intensities between 0.5 and 1.5 W/cm^2 $I^{(a)}$. However, Webster (1980) studying the effect of pulsed 0.75 and 3 Mhz ultrasound at pulse average intensities of 0.5 and 2.0 W/cm^2 ($I^{(SAPA)}$) was unable to demonstrate any effect on DNA synthesis in cultures of human foetal fibroblasts, which may suggest that the response to ultrasound may vary according to the cell type or the culture conditions employed.

The cell proliferation and DNA synthesis studies appear to contradict each other. Most proliferation studies indicate a reduction in proliferative capacity post insonation; whereas, most DNA synthesis studies suggest a stimulation in mitotic

activity. This may be explained as follows: many *in vitro* exposure systems encourage the likelihood of cavitation associated cell damage. If this cellular damage includes chromosomal damage it is possible that the observation of increased uptake of ^{3}H-thymidine may be associated with DNA repair rather than replication in preparation for cell division.

Therapeutic ultrasound is commonly used in clinical practice in both pulsed and continuous mode, at frequencies of between 1 and 3 MHz, and at spatially and temporally averaged intensities of up to 3 W/cm^2. There is, however, a dearth of experimental work examining the effect of ultrasound on mammalian cell proliferation/DNA synthesis at frequencies other than 1 MHz used in continuous mode and at relatively high ultrasonic intensities. As pulsed 3 MHz ultrasound, at low spatial and temporal averages, has been shown to encourage certain aspects of cutaneous repair both *in vivo* (e.g. Dyson *et al.* 1970; Webster *et al.* 1979; Dyson and Smalley, 1983; Young and Dyson, 1990a/c) and *in vitro* (e.g. Webster *et al.* 1978, Harvey *et al.* 1975; Young and Dyson, 1990b) further work, employing such apparently efficacious ultrasonic parameters, should be actively encouraged to redress this imbalance.

B. The effect of ultrasound on cell proliferation *in vivo*

Contradictory results have been reported by the few studies that have attempted to study cellular proliferation in response to therapeutic levels of ultrasound *in vivo*. Dyson *et al.* (1970), in a study of the effect of pulsed and continuous 3.5 MHz ultrasound on the repair of experimental rabbit ear wounds, demonstrated that ultrasound applied at certain intensities/pulsing regimes significantly enhanced the rate of cell proliferation, as measured by ^{3}H-thymidine uptake. They found that treatment with pulsed ultrasound (2:8) at intensities of 0.25, 0.5 and 1.0 W/cm^2 ($I^{(SAPA)}$) and continuous ultrasound at an intensity of 0.1 W/cm^2 ($I^{(a)}$), all stimulated cell proliferation; with the greatest increase observed after treatment with pulsed ultrasound at an intensity of 0.5 W/cm^2 ($I^{(SAPA)}$). This work finds support in the more recent work of Young and Dyson (1990a) who studied the effect of pulsed 0.75 and 3 MHz therapeutic ultrasound, at an intensity of 0.5 W/cm^2 $I^{(SAPA)}$, on the repair of full thickness excised wounds in the flank skin of adult Wistar rats. They demonstrated that by five days post wounding, there were significantly more fibroblasts in granulation tissue of ultrasound-treated wounds, than in granulation

tissue of similar sham-insonated control wounds. However, by seven days post-wounding there was no difference in cellularity between ultrasound-treated and similar-sham insonated wounds; this suggests that ultrasound-treated wounds attained maximal proliferative and/or migratory capacity more rapidly than sham-insonated wounds. In contrast, Miller *et al.* (1988) were unable to detect any change in the mitotic index of chinese hamster cheek pouch epithelia following insonation with 1.07 MHz continuous wave ultrasound at intensities of between 0.5 - 10.0 W/cm^2 ($I^{(a)}$).

This contradiction may be explained by examining the disposition of the cellular activities studied. It has been suggested that cells actively involved in reparative processes may be predisposed by the wound environment towards responding to therapeutic intervention with ultrasound. However, Kremkau and Witcofski (1974) studying the effect of ultrasound on hepatocyte proliferation during liver regeneration after partial hepatectomy, in which hepatocytes should be similarly predisposed, demonstrated a mitotic index reduction of between 20 and 60% following a 5 minute exposure to 1.9 MHz continuous ultrasound at an intensity of 60 mW/cm^2 ($I^{(a)}$). Similarly, Pospisilova and Rottova (1977) measuring the DNA content of experimental granulomas, a model for tissue repair that involves connective tissue proliferation, demonstrated that insonation with 0.8 MHz continuous ultrasound at an intensity of 1.0 W/cm^2 ($I^{(a)}$), led to a reduction in total DNA content.

As a consequence of this lack of agreement, the capacity of therapeutic ultrasound to modulate cell proliferation *in vivo* is still open to question. The different ultrasonic exposure conditions and cellular targets employed by different authors may explain the differing results obtained. Dyson *et al.* (1970) and Young and Dyson (1990a) employed 0.75 and/or 3 MHz pulsed ultrasound and enhanced proliferation, whereas the remaining authors were either unable to demonstrate any effect, or reported diminished proliferation, and used 1 MHz continuous ultrasound.

C. The effect of ultrasound on other aspects of the new tissue formation phase of repair

Cellular recruitment into the wound site involves both stimulated proliferation and migration. Mummery (1978) demonstrated that the motility of fibroblasts, on a two dimensional substrate, was increased following exposure to 3 MHz pulsed ultrasound

at intensities of between 0.5 and 2.0 W/cm^2 ($I^{(SAPA)}$). Ultrasound was found to reduce the number of changes in direction rather than increasing the velocity of individual cells. As migration of various cell types is central to the process of wound repair, stimulated cellular migration may in part explain many of the effects observed after clinical and non-clinical ultrasound application.

Fibroblast migration within the extracellular matrix has recently been proposed as a possible mechanism by which granulation tissue generates the force necessary for wound contraction (Ehrlich, 1988). This *in vitro* modulation in fibroblast movement may be, in part, responsible for the stimulatory effects of therapeutic ultrasound on wound repair observed *in vivo.* More specifically, this may explain the observations made by Dyson and Smalley (1983) who demonstrated that cryosurgical lesions made in the flank skin of adult Wistar rats and exposed to 3 MHz pulsed ultrasound, at an intensity of 0.5 W/cm^2 ($I^{(SAPA)}$), contracted more rapidly than similar sham-insonated control wounds. No temperature elevation consequent to ultrasonic exposure was observed and as such a thermal mechanism of interaction was deemed unlikely.

Granulation tissue contraction is thought by some to be effected by a population of phenotypically altered fibroblasts, often referred to as myofibroblasts, which demonstrate many morphological, pharmacological and immunological characteristics common to smooth muscle cells (SMC) (Gabbiani *et al.* 1971). It has been demonstrated that ultrasound can cause both the contraction of excised guinea pig uterine SMC preparations *in vitro* (Talbert *et al.* 1975) and increase the frequency of mouse uterine SMC contraction *in vivo* (ter Haar *et al.* 1978); in addition treatment with therapeutic ultrasound has also been shown to increase the contractility of cardiac muscle (Mortimer *et al.* 1984; Mortimer *et al.* 1986). The structural and functional similarities between myofibroblasts and SMCs, may provide an alternative explanation for the stimulation in wound contraction observed by Dyson and Smalley (1983). The excitation of smooth muscle cells· involves depolarisation of the plasma membrane followed by a transient flux of calcium ions activating an actin-myosin filament sliding system. Mummery (1978) and Mortimer & Dyson (1988) demonstrated that therapeutic levels of ultrasound could increase the uptake of calcium by fibroblasts *in vitro*, apparently as a result of a reversible perturbation of the cell membrane. This membrane perturbation, and the ensuing calcium flux, appear to result from cavitational activity within the exposure system,

as after pressurising the exposure system to 2.3 atmospheres, a method known to prevent cavitation, no change in fibroblast calcium uptake could be observed (Mortimer and Dyson, 1988). As it has yet to be conclusively proven that ultrasonic cavitation can occur *in vivo*, it is possible that some other non-cavitational and non-thermal mechanism of interaction may be capable of modulating intracellular calcium in fibroblasts within wounds, thus facilitating the more rapid wound contraction noted in cryosurgical lesions by Dyson and Smalley (1983).

As previously mentioned, the generation of a rich vasculature (angiogenesis) is essential to meet the high metabolic demands encountered during the formation of new tissue within a wound site. Young and Dyson (1990c) employed microfocal X-ray techniques to demonstrate that pulsed therapeutic ultrasound (both 0.75 and 3 MHz), applied soon after injury and employed at an intensity of 0.5 W/cm^2 ($I^{(SAPA)}$), could promote the process of angiogenesis in rat flank skin wounds. It was reported that by 5 days after injury there were approximately 30% more blood vessels in wounds treated with 0.75 MHz ultrasound, and 20% more blood vessels in those treated with 3 MHz ultrasound, compared with sham-insonated control wounds.

4.2.3 Matrix formation and remodelling

The third and final phase of wound repair is matrix formation and remodelling. This time scale compartmentalisation of wound repair, though useful, is artificial and over simplified. Matrix formation is not temporally exclusive of new tissue formation. In fact new tissue formation and matrix formation begin simultaneously. Matrix remodelling does, however, continue for months, if not years, after the dissolution of granulation tissue which explains its position in this scheme of repair.

The clot formed as a consequence of vascular injury is primarily fibrin supplemented with plasma fibronectin. With time and the recruitment of fibroblasts into the wound site this clot is replaced with a provisional matrix rich in fibronectin and hyaluronic acid and supplemented with collagen types I and III. Remodelling involves the relatively rapid elimination of most of the fibronectin and hyaluronic acid from the matrix and the slow accumulation of large fibrous bundles of type I collagen supplemented with proteoglycans that respectively provide the residual scar with increasing tensile strength and resilience to deformation.

4.2.3.1 The effect of ultrasound on matrix formation and remodelling

The effect of ultrasound on activities associated with the matrix formation and remodelling phase of repair will be described under the following sub-headings:

A. The effect of ultrasound on matrix synthesis *in vitro*

B. The effect of ultrasound on matrix synthesis *in vivo*

C. The effect of ultrasound on matrix remodelling.

A. The effect of ultrasound on matrix synthesis *in vitro*

The generation of a protein-rich extracellular matrix by fibroblasts during granulation tissue formation and its revision during the subsequent remodelling phase of repair are vital processes in the overall scheme of wound healing. There are few published reports relating to the effect of therapeutic ultrasound on the protein synthesis *in vitro*. Both increase and decreases in the rates of protein synthesis have been documented, sometimes in the same report, following exposure to ultrasound.

Repacholi (1981), studying protein synthesis in human lymphocytes, demonstrated a biphasic response to ultrasonic intensity. He demonstrated an increase in protein synthesis by activated lymphocytes which had been exposed to 0.87 MHz continuous ultrasound for 30 minutes at an intensity of 1.1 W/cm^2 ($I^{(a)}$); whereas, a similar exposure at the higher intensity of 4.0 W/cm^2 lead to an inhibition of protein synthesis. Elmer and Fleischer (1974) examined the effect of 1 MHz continuous ultrasound, at an intensity of 1.8 W/cm^2 ($I^{(a)}$), on the growth of cultured tibiae removed from new born mice. They found that insonated tibiae incorporated more radioactive proline than similar control tibiae, but this result did not prove to be statistically significant. Harvey *et al.* (1975) reported that treatment of human fibroblasts with 3 MHz pulsed ultrasound consistently led to greater stimulation of protein synthesis than continuous wave ultrasound. Continuous ultrasound at an intensity of 0.5 W/cm^2 ($I^{(a)}$) led to a 20% increase in protein synthesis, whereas, pulsed ultrasound, at an intensity of 0.5 W/cm^2 ($I^{(SAPA)}$), resulted in a 30% increase in protein synthesis above sham-insonated control fibroblasts. Interestingly, when fibroblasts were pretreated with cortisol, which acts as a membrane stabiliser, no increase in protein synthesis could be observed. This suggested that the cell membrane is involved with the modulation of protein synthesis by ultrasound.

Webster *et al.* (1978), again exposing human fibroblasts to 3 MHz ultrasound, this time only in pulse mode, at an intensity of 0.5 W/cm^2 ($I^{(SAPA)}$), also demonstrated an increase in protein synthesis. If their test system was pressurised to 2 atmospheres

the effect was no longer observed, suggesting that the effect may be attributable to cavitation. This taken together with the observed effect of cortisol by Harvey *et al.* (1975), suggests that cell membrane perturbation as a result of cavitational activity may be the mechanism by which ultrasound stimulates protein synthesis in this system. Later, Webster *et al.* (1980) demonstrated that collagen synthesis by human fibroblasts was up-regulated as a function of this enhanced general protein synthesis following exposure to pulsed, 3 MHz, ultrasound at an intensity of 0.5 W/cm^2 ($I^{(SAPA)}$). Edmonds and Ross (1988), in agreement with the work of Webster *et al.* (1978) and Harvey *et al.* (1975), demonstrated enhanced protein synthesis in murine C1300 neuroblastoma 2A cells following exposure to pulsed 1 MHz ultrasound (60 ms on, 60 ms off) at an intensity of 3.4 W/cm^2 ($I^{(SAPA)}$). Their results also suggested that enhancement in protein synthesis correlated closely with transient cavitational activity within their exposure system. As previously stated, cavitation has yet to be conclusively demonstrated during "therapeutic" insonation *in vivo* (Watmough *et al.* 1991); consequently the clinical relevance of these observations, that appear to implicate a major role for cavitation in the up-regulation of protein synthesis *in vitro*, must be viewed with caution.

B. The effect of ultrasound on matrix synthesis *in vivo*

Therapeutic ultrasound was first reported to stimulate protein synthesis *in vivo* by Belewa-Staikowa and Kraschkowa (1967). Protein synthesis in the liver, kidney and heart was studied after 1 MHz continuous wave ultrasound was applied to the abdomen of adult rats. They reported an ultrasonic intensity dependent biphasic response in all organs studied. An increase in protein synthesis was observed following exposure to intensities of 0.2 and 0.6 W/cm^2 ($I^{(a)}$). However, a decrease in protein synthesis was reported when they increased the intensity to 1 W/cm^2 ($I^{(a)}$). Other studies have been carried out that are more relevant to wound repair. Pospisilova *et al.* (1971), examined the effect of ultrasound (0.8 MHz, 1.5 W/cm^2 $I^{(a)}$) on the initial generation (first two weeks) of extracellular matrix components in experimental murine granulomata, induced by subcutaneous implantation of viscose-cellulose sponges. This is a widely accepted, though questionable, model of granulation tissue generation during cutaneous repair. They demonstrated that insonation led to a delay in granulation tissue maturation, as assessed by the replacement of glycosaminoglycans (measured by hexosamine levels) by collagen

(assessed by hydroxyproline levels) 8 and 12 days post implantation. They suggested that ultrasound interacts in such a manner as to lengthen the inflammatory process; and thus by implication, delays the normal process of "repair". This observation is in clear conflict with the work of Young and Dyson (1990) who reported a more rapid progression of wound repair in response to therapeutic ultrasound.

Later, Popisilova carried out a more comprehensive study into the effect of ultrasound on experimental granulation tissue generation and remodelling (Pospisilova, 1976). This study examined the effect of continuous ultrasound (0.8 MHz, 1 W/cm^2 I$^{(a)}$) on granulomata collagen, glycosaminoglycan (GAG) and glycoprotein levels, during both inflammation and granulation tissue formation. Granulomata were excised 7, 11, 15, 21, 25, 30 and 35 days post implantation. In inflammatory phase granulomata treated with ultrasound there was significantly more collagen, GAG and glycoprotein present. In "proliferative phase" granulomata there was significantly more collagen and glycoprotein, but significantly less GAGs present. This would suggest that ultrasound is facilitating more rapid, and perhaps more extensive, "repair"; by encouraging both earlier and more extensive collagen synthesis. This conflicts, somewhat, with their earlier data (Pospisilova *et al.* 1971) that suggested that ultrasound delayed granulation tissue maturation.

It has been reported that experimental granulomata generated by subcutaneous implantantion of viscose sponges inoculated with non-pathogenic bacteria (*E. coli*) produce significantly (three times) more collagen, as assessed by hydroxyproline three to four weeks after implantation, than similar uninocculated sponges. When such *E. coli* impregnated sponges are treated with continuous ultrasound (0.8 MHz, 1.5 W/cm^2, 5 minutes per day) for five days prior to sponge excision; protein synthesis is further enhanced such that insonated sponges contain eight times as much collagen as uninoculated sponges (Pospisilova *et al.* 1974). It was suggested by the authors that ultrasound prolongs cell proliferation at the "wound site", ensuring the presence of productive cells in the granulation tissue for a longer time. However, in view of the work Harvey *et al.* (1975) and Webster *et al.* (1978/1980) these observations may alternatively be explained in terms of more collagen being produced per cell rather than more collagen producing cells being present. In 1977, Pospisilova and Rottova substantiated earlier observations relating to the effect of ultrasound on granulomata protein synthesis. They again demonstrated that significantly more collagen was deposited in 21 day old

granulomata that received multiple applications of 0.8 MHz continuous ultrasound (intensity 1 W/cm^2 ($I^{(a)}$), treatment duration 5 minutes) than was synthesized and deposited in similar untreated controls.

Additional experimental evidence supporting that of Pospisilova *et al.* (1976) and Pospisilova and Rottova (1977) indicating that protein synthesis is/can be encouraged in response to ultrasonic therapy has been published. Webster (1979) studied protein synthesis during the repair of cryosurgical lesions made in the flank skin of rats, in response to the application of 3 MHz pulsed ultrasound at an intensity of 0.4 W/cm^2 ($I^{(SAPA)}$). Hydroxyproline assays clearly demonstrated that therapeutic ultrasound-treated wounds contained significantly more collagen than similar sham-insonated wounds by seven days after injury. Jackson *et al.* (1991) studied the effect of ultrasound therapy on the rates of repair of Achilles tendons in the rat. Following hypodermic needle puncture, tendons were either given a 4 minute exposure to continuous 1 MHz ultrasound at an intensity of 1.5 W/cm^2 ($I^{(a)}$), or given a similar sham-insonation, which was repeated each day for up to 5 days, after initial injury. Collagen synthesis was measured by incorporation of ^{3}H hydroxyproline at 3 and 5 days after injury. No difference in collagen synthesis was observed between insonated and sham-insonated tendons 3 days after injury. However, by 5 days after injury the ultrasound-treated tendons were synthesizing significantly more collagen than similar sham-insonated controls.

Other workers have been unable to demonstrate any effect of therapeutic levels of ultrasound on protein synthesis *in vivo*. Stevenson *et al.* (1986), studied the effect of therapeutic ultrasound (20 daily 5 minute applications of continuous 3 MHz ultrasound at an intensity of 0.75 W/cm^2 $I^{(a)}$) on tendon healing in the chicken. While they demonstrated that surgically damaged tendons treated with ultrasound made a more rapid functional recovery, they were unable to demonstrate any effect on collagen content, measured by hydroxyproline assay, within the repairing tissue.

C. The effect of ultrasound on the matrix remodelling

In the clinical and experimental application of ultrasound to sites of acute injury, wounds are normally treated within a few days, rather after a period of weeks or months following injury. As such, it is unlikely that the cellular activities predominantly associated with matrix remodelling will be direct targets of treatment. Rather, some cellular process(es) associated with the earlier, inflammatory or

granulation tissue formation, phases of repair may be modified by the applied ultrasound. It is assumed, therefore, that any change in the physical characteristics of the scar are as a result of ultrasonic modulation of one, or more, of the cellular processes associated with the preceding phases of repair.

Drastichova *et al.* (1973) reported that therapeutic levels of ultrasound (the only parameter reported was an "average" intensity of 1.5 W/cm^2) applied soon after wounding, significantly increased the ensuing gain in tensile strength of guinea pig scar tissue. More recently Dyson (1981) further added weight to this poorly reported observation by demonstrating that both the tensile strength and extensibility of rat scar tissue (Dyson, 1981) could be improved by the application of ultrasound. Dyson, (1981) studied bilateral cryosurgical lesions made in the flank skin of adult Wistar rats. Lesions that received 3 MHz pulsed ultrasound (2:8) at an intensity of 0.5 W/cm^2 ($I^{(SAPA)}$) had a greater breaking strength and were more extensible than similar sham insonated lesions when measured 1, 2 and 4 months after injury. It is likely that this improvement in tissue breaking strength is linked to the elevation in collagen synthesis observed in various ultrasound exposed wounds and wound models (Popisilova, 1976; Popisilova and Rottova, 1977; Harvey *et al.* 1975; Webster *et al.* 1979; Jackson *et al.* 1991). Scanning electron microscope studies have shown that ultrasound-treated cryosurgical lesions produce scars that have a finer and more regular lattice arrangement of collagen fibres than similar sham-insonated lesions (Dyson, 1981). Such an arrangement is more like that of uninjured skin, which may explain the greater extensibility of ultrasound treated scar tissue.

In contrast to the majority of publications suggesting that therapeutic ultrasound can encourage the rate, or "final" outcome, of the process of dermal repair, Shamberger *et al.* (1981) reported no improvement in the tensile strength of incisional rat skin wounds following treatment with 5 MHz ultrasound at therapeutic dosages. On examination of Shamberger's experimental protocol two significant points should be noted. Firstly, ultrasound was applied to the wound via a transducer arrangement that was rigidly fixed to the animal's skin. Such an arrangement prevents the movement of the applicator head, a practice advocated by Forster and Palanstanga (1981) which is known to be necessary (i), to prevent standing wave ultrasonic fields occurring within tissues (which can lead to potentially damaging ultrasonic exposures due to amplification); and (ii), to ensure that the applied ultrasound is not concentrated within small areas of the tissue receiving treatment.

The latter point relates to the non-uniform distribution of ultrasonic energy within ultrasonic fields that result from interference phenomena (see section 2.3). Secondly, both clinicians and basic scientists involved in the study of therapeutic ultrasound are gradually becoming aware of the benefits of treatment with ultrasound as soon after acute injury as is practicably possible. The literature appears to indicate that some component(s) of the inflammatory phase may be the responsive biological target(s) in the therapeutic application of ultrasound (Dyson, 1990). As Shamberger *et al.* (1981) was unable to apply ultrasound until the fourth post-operative day, due to experimental design, it is possible that many of the inflammatory components, with which ultrasound may react, were no longer present.

Chapter 5. *In vitro* techniques and methods

Introduction

This section details the cell lines and experimental models (bioassays) employed in the study of ultrasonic modulation of cellular activity *in vitro*. Model verification studies, carried out in an attempt to optimise the use of both the fibroblast proliferation assay and the fibroblast populated collagen lattice contraction assay, are also included.

This chapter includes the following:

(1). Human dermal fibroblast culture and characterisation.

(2). The U937 promonocyte cell line.

(3). The methylene blue fibroblast proliferation assay

(4). The fibroblast-populated collagen lattice contraction assay

5.1 Human dermal fibroblasts

5.1.1. Primary culture and sub-culture of human dermal fibroblasts

Human dermal fibroblasts were derived from a small elliptical skin biopsy taken from the flexor aspect of the distal third of the forearm of a 35 year old healthy male volunteer. Fibroblasts were cultured by the primary explant technique (Appendix 3, p337), originally developed by Harrison 1907, in which cells migrate out of fragments of tissue along the base of the tissue culture flask (figure 5.1). Cells were observed at the periphery of explanted skin by 5 days in culture. Confluency between the islands of explanted tissue was apparent by 10 days. Once confluence was achieved short trypsinization (Appendix 4, p338) was performed to select for fibroblasts and against the more adherent cell types such as epithelial cells. The cells recovered from the primary culture following short trypsinization were centrifuged at 80 x g, resuspended in fibroblast growth medium (Appendix 2B, p335), and seeded into a fresh culture flask. Once this secondary culture became confluent short trypsinization was again employed to select for fibroblasts. This secondary culture (termed passage 1, or p1) and subsequent cultures were passaged at near confluency with a sub-cultivation ratio of 1:3. At passage 2, fibroblasts in cultures derived from explanted skin were morphologically homogenous being multipolar in disperse culture and forming whorls of bipolar cells at near-confluency. No change in culture morphology was noted at any subsequent passage, prior to their use in proliferation and lattice

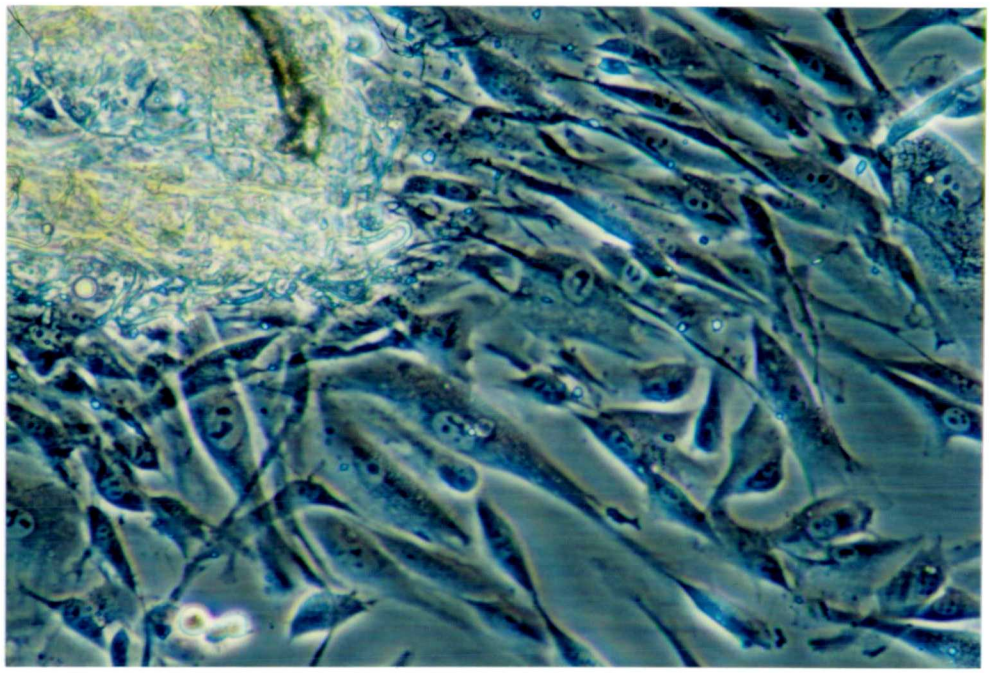

Figure 5.1. Primary growth from explanted human forearm skin (x 360)

contraction assays.

Fibroblasts were routinely cultured in 80 cm^2 tissue culture flasks (Nunclon®, Nunc, Denmark) in Ham's F10 medium buffered with 20 mM Hepes buffer (041-02390, Gibco, Scotland) and supplemented with 10% fetal calf serum and the antibiotics penicillin and streptomycin at 100 units/ml and 100 µg/ml respectively. Passage 4 (p4) fibroblasts were stored by freezing-down in liquid nitrogen ((Appendix 5A, p339). Two weeks prior to requiring fibroblasts for experimentation these p4 fibroblasts were recovered from the liquid nitrogen (Appendix 5B, p 339) and cultured as prior to freezing-down. Fibroblasts underwent a further two passages (to p6) prior to bioassay use.

5.1.2. Characterisation of human dermal fibroblasts

This section is concerned with demonstrating that the cells cultured from explanted human skin (as described above) were of a fibroblastic lineage rather than some other skin-derived cell lineage. Fortunately, for those interested in studying fibroblast activity *in vitro*, fibroblast growth from tissue explants is relatively prolific compared with the majority of the possible contaminating cell types. When tissue explants are cultured in serum-supplemented medium, certain factors contained in serum (many of them platelet-derived) have a strong mitogenic effect on fibroblasts, but tend to inhibit the growth of other cell types, such as epithelial cells, by inducing terminal differentiation (Freshney, 1987). While the cellular outgrowth from connective tissue explants may initially contain several cell lineages, continued culture in serum-supplemented medium preferentially encourages the growth of fibroblasts. Thus Murphy and Daniel (1987) reported that while primary cultures of explanted periodontal ligament initially contained 98% fibroblasts and 2% epithelial cells, 100% of the population were fibroblasts by the second passage.

In this thesis human dermal fibroblasts were cultured to, and used at, passage 6, thus reducing the possibility of cellular contamination, and allowing the generation of sufficient cell numbers for study. At passage 6, fibroblasts derived from explanted human forearm skin were morphologically homogenous under phase microscopy. Prior to confluency (figure 5.2a) they were multipolar with numerous lamellipodia (flattened cytoplasmic protrusions); when confluent (figure 5.2b), they assumed a spindle shaped morphology and were arranged in parallel arrays and whorls characteristic of human dermal fibroblasts (Freshney, 1987). The morphology of the

Figure 5.2 p6 human dermal fibroblast morphology under phase contrast

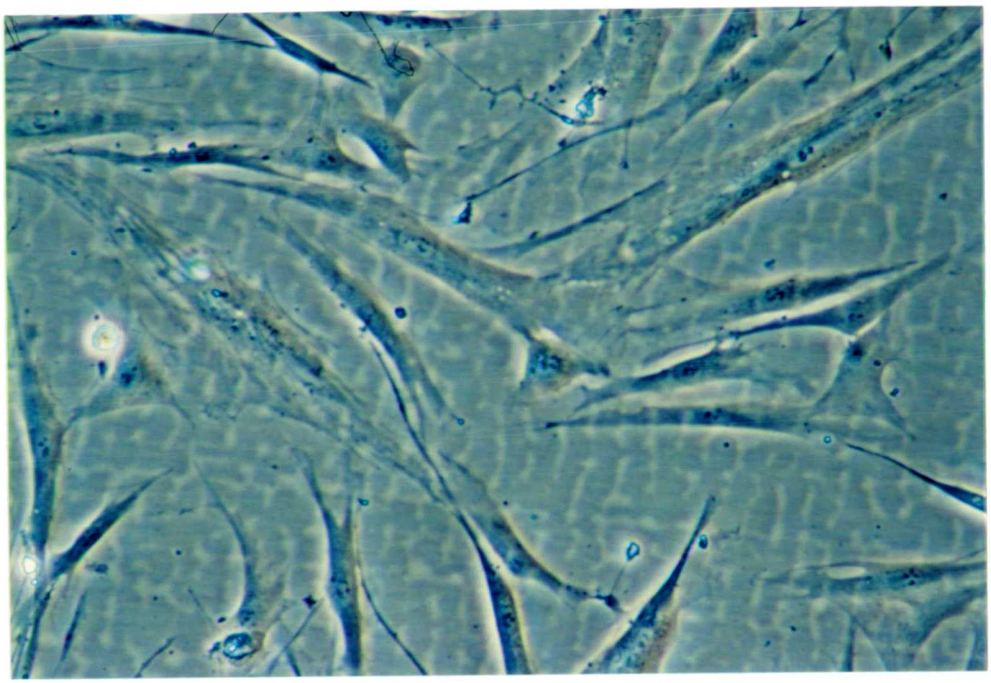

Figure 5.2a. Inverted phase micrograph (x 360) of subconfluent dermal fibroblasts

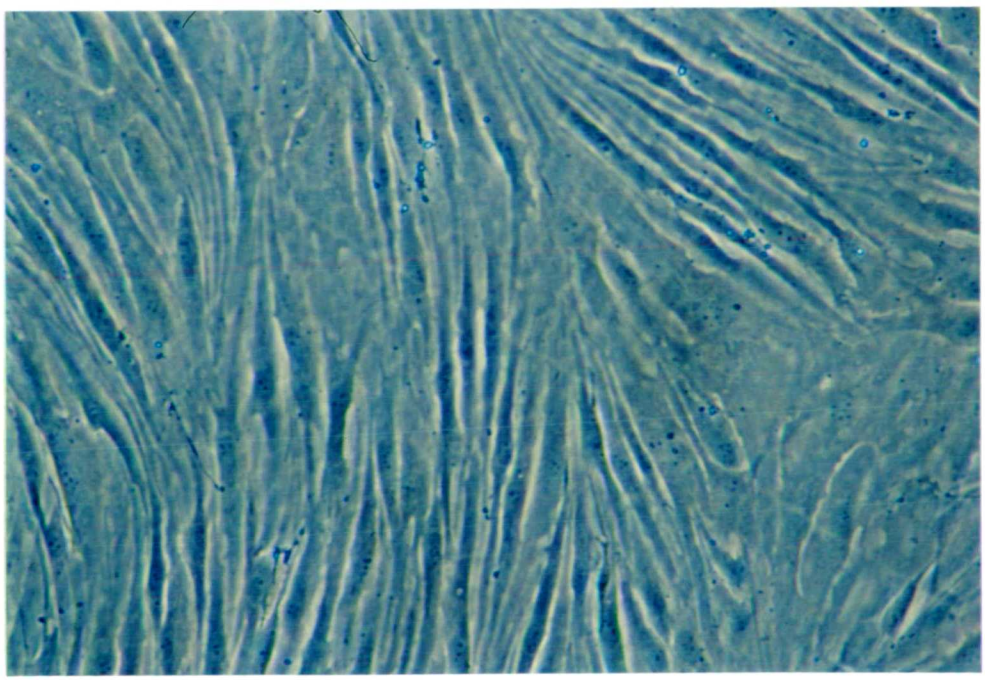

Figure 5.2b. Inverted phase micrograph (x 360) of confluent dermal fibroblasts.

human fibroblasts used in this thesis is consistent with that of the accepted human fibroblast morphology. The expression of characteristics specific to other cell lineages, known to contaminate primary fibroblast cultures, was investigated in order to confirm the identity of these presumptive p6 human dermal fibroblasts. This investigation took the form of immunocytochemical staining using indirect immunofluorescence techniques.

5.1.2.1. Contaminating cell types

The major cell types that may contaminate fibroblast cell lines are epithelial cells, endothelial cells and smooth muscle cells. Although macrophages and lymphocytes are present in biopsy material, in culture these cells are either weakly adherent or non-adherent to plastic tissue culture surfaces. As such they tend to be lost from the culture during medium replacement.

Epithelial cells tend to attach more firmly to tissue culture plastic, and are released less easily from this attachment by trypsin, than fibroblasts (Owens *et al.* 1974). Limited trypsinization (Appendix 4, p338) was initially performed to detach cells from the primary culture (around the explant) and subsequently during routine passage, in an attempt to reduce epithelial cell contamination. p6 human dermal fibroblasts were exposed to anti-cytokeratin antibodies in order to confirm the lack of epithelial cell contamination (p138). Cytokeratins are intermediate filaments expressed only in epithelial cells.

Endothelial cells appear to respond to trypsin in a similar manner to that observed in fibroblasts, and limited trypsinization does not preferentially select against them. Fortunately, endothelial cells have more stringent growth requirements than fibroblasts (Kumar *et al.* 1987) and tend to be easily overgrown by them. It has been widely reported that confluent cultures of endothelial cells have a cobblestone appearance (Kumar *et al.* 1987), clearly dissimilar to the whorl-like arrangement of bipolar fibroblasts at confluency noted above (figure 5.2b). p6 human dermal fibroblast cultures were stained with antibodies to Factor-VIII-related antigen, a universal marker for endothelial cells (Kumar *et al.* 1987), in order to confirm the lack of endothelial cell contamination (p139).

Smooth muscle cell (SMC) contamination represents more of a problem, as there is as yet no satisfactory method by which SMCs can be distinguished from fibroblasts. While the intermediate filament, desmin, is generally thought to be

restricted to muscle cells, several reports have demonstrated desmin within fibroblastic cells (Hansson *et al.* 1989; Skalli *et al.* 1986). Also, when SMCs are placed in culture, desmin disappears around the fifth passage (Skalli *et al.* 1986). It has, however, been reported that SMC may be differentiated from fibroblasts on the basis of cellular morphology (Freshney, 1987). Sub-confluent SMCs in culture are reported to be round cells, a shape they retain at confluency, giving cultures the cobblestone-like appearance of confluent endothelial cells. Such a morphology clearly differs from the initially multipolar sub-confluent and subsequently bipolar whorl-arranged fibroblasts. A distinction based purely on culture morphology cannot be totally conclusive, as cells in culture show an enormous capacity for morphological plasticity. That SMCs were present as cellular contaminants in p6 human dermal fibroblast cultures cannot be ruled out.

5.1.2.2. Immunohistochemical cell identification - background

A. Intermediate filaments

Intermediate filaments are rope-like polymers of fibrous polypeptides that are thought to play a structural or tension-bearing role in the cell. A variety of tissue specific/cell specific forms of intermediate filament are known; they differ in the type of polypeptide they contain. The different intermediate filaments and the cell type to which they are normally ascribed are: keratin filaments in epithelial cells, neurofilaments in nerve cells, glial filaments in astrocytes and Schwann cells, desmin filaments in muscle cells and vimentin filaments in mesenchymally derived-cells including fibroblasts (Alberts *et al.* 1989). A given cell type can contain more than one form of intermediate filament, for example glial cells contain both vimentin and glial filaments (Rungger-Brandle and Gabbiani, 1983). The intermediate filament profile of a cell tends to be retained at times when all other identifying criteria have been lost, such as during neoplastic growth (Gabbiani *et al.* 1981), and, as such is useful in the identification of cells of unknown origin.

p6 human dermal fibroblast cultures were stained with antibodies to vimentin (an intermediate filament marker of mesenchymal tissue-derived cells) and cytokeratins (intermediate filament markers of epithelial cells).

Vimentin: Vimentin is widely distributed in cells of mesenchymal origin including fibroblasts (Ngai *et al.* 1990), endothelial cells (Semich and Robenek, 1990), white

blood cells (Alberts *et al.* 1989), pigment cells (Rappersberger *et al.* 1990) and some muscle cells (Takase *et al.* 1988). Vimentin has also been shown to be present in some keratinocytes in culture (Rungger-Brandle and Gabbiani, 1983) but absent in sections of human skin (Rappersberger *et al.* 1990). The vimentin antibody employed in this characterisation was a mouse anti-swine monoclonal raised against purified vimentin from porcine eye lens (DAKO-vimentin, M725, DAKO Ltd, UK). The monoclonal is reported (1) not to cross react with any other intermediate filament, and, (2) to have a broad species reactivity.

Cytokeratins: Cytokeratins are found in epithelial and glial cells, both *in vivo* and *in vitro* (Rungger-Brandle and Gabbiani, 1983). It has also been reported that SMCs can contain cytokeratins (Turley *et al* 1988). Despite this latter report keratin expression has come to be regarded as the single most invariable characteristic of epithelial cells. There are at least 19 distinct forms of cytokeratin in human epithelia (Moll *et al.* 1982). These can be divided up into two subfamilies, acidic keratins and neutral or basic keratins, each subfamily coded for by a different set of genes. Keratin filaments are always heteropolymers formed from an equal number of subunits from each of these two subfamilies. Epithelial cells therefore express at least two keratins, the specific expression of keratins by epithelia depending on cellular location and the state of differentiation. While studying the labelling of a panel of 20 mouse-derived cytokeratin antibodies on human skin, Lane *et al.* (1985), observed that one antibody, namely LP34, labelled all epidermal cells with the exception of those comprising the inner hair root sheath; while another antibody, namely LE1, labelled the inner hair root sheath. LP34 and LE1, kind gifts to the laboratory from Dr P. Purkis (The London Hospital, London, UK), were employed to investigate epidermal cell contamination of p6 human dermal fibroblast cultures. A cloned cell line of simian virus 40 transformed human foreskin keratinocytes (SVK14), cultured in RPMI-1640 with 10% FCS, was used at passage 31 as a positive control for anti-cytokeratin labelling. Positive staining, with a polyclonal antibody to human cytokeratin, has previously been reported for this cell line (Taylor and Papadimitrou, 1982).

Secondary antibodies: The secondary antibody used to detect both anti-vimentin and anti-cytokeratin labelling was a sheep antibody to mouse IgG conjugated to fluorescein isothiocyanate (FITC) (Product number F-6257, Sigma, UK). Non-specific

labelling (independent of primary antibody) of this secondary antibody to both p6 human dermal fibroblasts and SVK14 keratinocytes was examined.

B. Factor-VIII-related antigen (von Willebrand factor)

Confluent monolayers of endothelial cells have a characteristic cobblestone appearance, clearly dissimilar to the whorl-like arrays of confluent fibroblasts. This cobblestone morphology cannot be totally relied upon to differentiate between fibroblasts and endothelial cells, as confluent endothelial monolayers undergo a phenomenon termed sprouting, in which confluent endothelial cells assume a fibroblast-like morphology (Kumar *et al.* 1987). Factor-VIII-related antigen is thought to be a universal marker for all endothelial cells with the exception of those of lymph node post-capillary venules (Kumar *et al.* 1987). Factor-VIII-related antigen has been shown to be localised within Wiebel-Palade bodies of endothelial cells (Warhol and Sweet, 1984). A rabbit polyclonal antibody to human Factor-VIII-related antigen (product number A082, DAKO Ltd, UK) was employed to assess endothelial contamination of p6 human dermal fibroblast cultures. Bovine aortic endothelial cells (p7), maintained in Modified Eagles Medium supplemented with 10% FCS, were used as a positive control for Factor-VIII-related antigen staining. The secondary antibody employed to detect anti-Factor-VIII-related antigen binding was a goat antibody to rabbit IgG, conjugated to tetramethylrhodamine isothiocyanate (TRITC) (product number T-5268, Sigma, UK). Non-specific labelling (independent of primary antibody) of this secondary antibody to both p6 human dermal fibroblasts and p7 bovine aortic endothelia was examined.

5.1.2.3. Immunohistochemical characterisation - methodology

The indirect immunofluorescence methods employed to characterise p6 human dermal fibroblasts are described in full in (Appendix 16, p352). Briefly, p6 human dermal fibroblasts, p31 SVK14 transformed keratinocytes, and p7 bovine aortic endothelial cells were cultured to confluence on glass coverslips. p6 human dermal fibroblasts underwent anti-vimentin, anti-cytokeratin (LP34 & LE1) and anti-Factor-VIII-related antigen inmmunofluorescent staining. p31 SVK14 transformed keratinocytes and p7 bovine aortic endothelial cells were stained for cytokeratin (LP34 & LE1) and Factor-VIII-related antigen respectively, and were used as positive staining controls. The sheep-anti-mouse FITC and goat-anti-rabbit TRITC

secondary antibodies were applied without prior addition of primary antibodies to demonstrate the level of non-specific binding of secondary antibodies. After staining the confluent cell monolayers were viewed under a fluorescence microscope (Olympus BH2, fitted 450-490 and 546 nm excitation filters). Monolayers demonstrating both positive and negative staining were photographed using Kodak Ektachrome P1600 film.

5.1.2.4. Results

From figures 5.3 - 5.5 (p142 to 144) the following points are apparent:

Vimentin labelling: As can be seen from figure 5.3a, p6 human dermal fibroblasts label positively for vimentin; the lack of labelling following the application of the secondary antibody alone (figure 5.3b) indicates that this labelling is due to the specific binding of anti-vimentin antibodies to cellular vimentin.

Cytokeratin labelling: As can be seen from figures 5.4a and 5.4b, p6 human dermal fibroblasts do not display positive staining for either LP34 or LE1. p31 SVK14 transformed keratinocytes are positive for both anti-cytokeratin antibodies (figures 5.4c & 5.4d). Non-specific labelling was not demonstrated in response to the application of the fluorescein-conjugated sheep anti-mouse secondary antibody to either p6 fibroblasts (figure 5.3b) or p31 SVK14 keratinocytes (figure 5.4e).

Factor-VIII-related antigen: As can be seen from figures 5.5a, p6 human dermal fibroblasts do not display positive staining for Factor-VIII-related antigen. p7 bovine aortic endothelial cells are positive for Factor-VIII-related antigen (figure 5.5c). Non-specific labelling was not demonstrated in response to the application of the rhodamine-conjugated goat anti-rabbit secondary antibody to either p6 fibroblasts (figure 5.5b) or p7 bovine aortic endothelial cells (figure 5.5d).

5.1.2.5. Discussion

The observation that p6 human dermal fibroblasts are vimentin positive confirms the mesenchymal origin of these cells. The lack of cytokeratin positive cells indicates that p6 human dermal fibroblast cultures were not contaminated with epithelial cells. On the basis of factor-VIII-related antigen staining there would appear to be no endothelial cell contamination.

5.1.2.6. Summary of p6 human dermal fibroblast characterisation

In summary, the p6 human dermal fibroblasts generated from human forearm skin were confirmed to be cells of the fibroblastic lineage. Evidence to confirm this includes: 1. The multipolarity of subconfluent cells and the whorl-like array of bipolar cells at confluency, 2. The labelling with vimentin, 3. The lack of labelling for cytokeratins, and, 4. The lack Factor-VIII-related antigen labelling.

Figure 5.3 Immunohistochemical localisation of vimentin intermediate filaments.

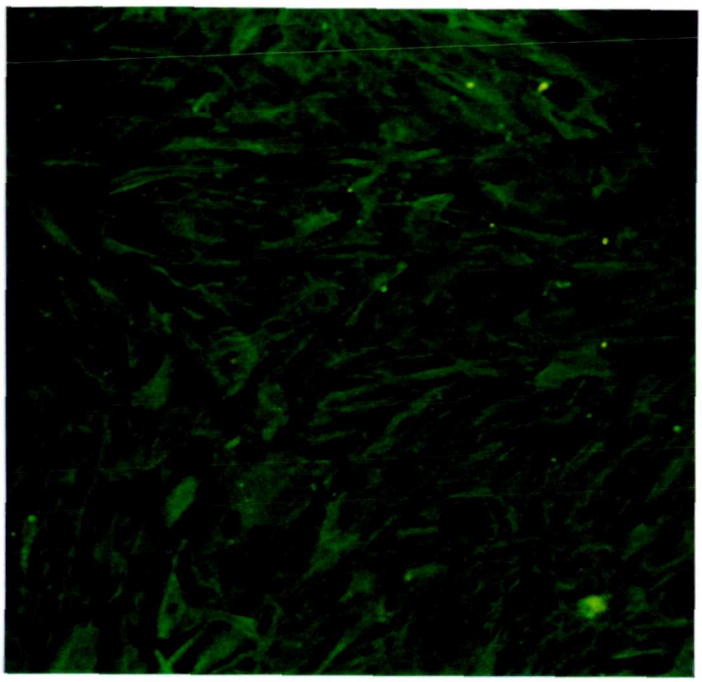

Figure 5.3a Positive staining of p6 fibroblasts incubated with mouse anti-swine vimentin, detected using FITC-conjugated sheep anti-mouse IgG (x 125).

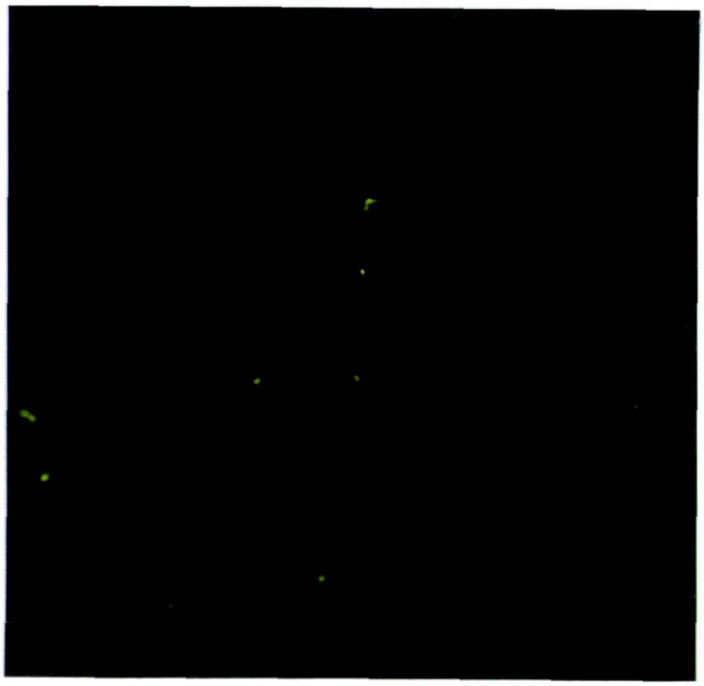

Figure 5.3b Lack of positive staining of p6 fibroblasts incubated with the secondary (primary detection) antibody, FITC-conjugated sheep anti-mouse IgG, alone (x125).

Figure 5.4 Immunohistochemical localisation of keratin intermediate filaments.

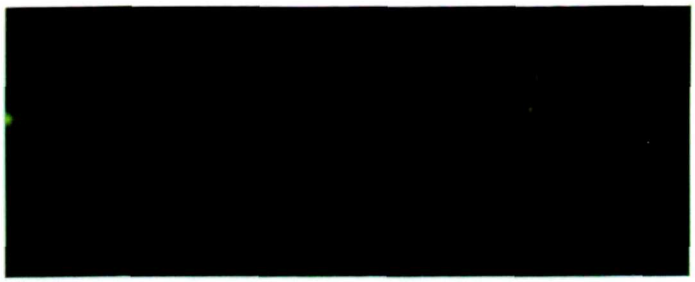

Figure 5.4a. p6 human dermal fibroblasts stained with the anti-cytokeratin antibody LP34 (x 125).

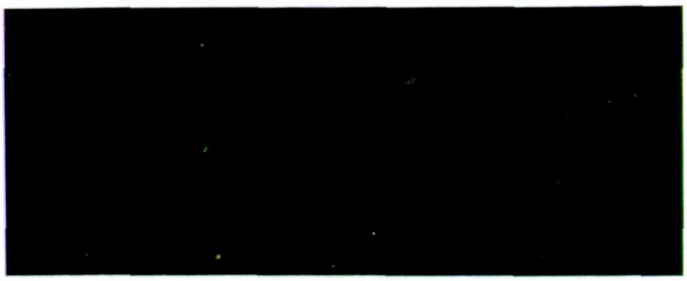

Figure 5.4b. p6 human dermal fibroblasts stained with the anti-cytokeratin antibody LE1 (x 125).

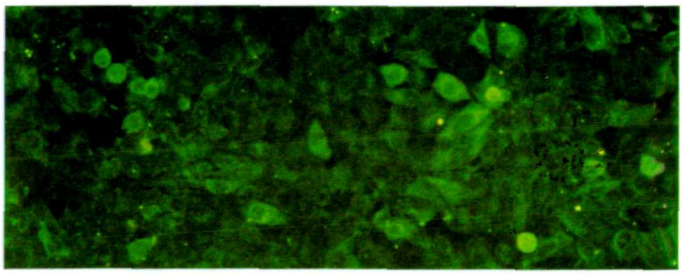

Figure 5.4c. p31 SVK14 keratinocytes stained with the anti-cytokeratin antibody LP34 (x 125).

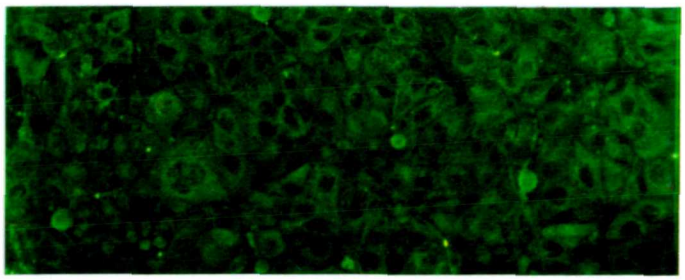

Figure 5.4d. p31 SVK14 keratinocytes stained with the anti-cytokeratin antibody LE1 (x 125).

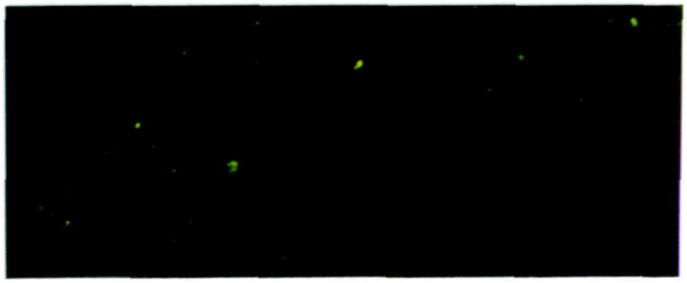

Figure 5.4e. p31 SVK14 keratinocytes stained with secondary (primary detection) antibody, FITC-conjugated sheep anti-mouse IgG, alone (x 125).

Figure 5.5 Immunohistochemical localisation of Factor-VIII-related antigen.

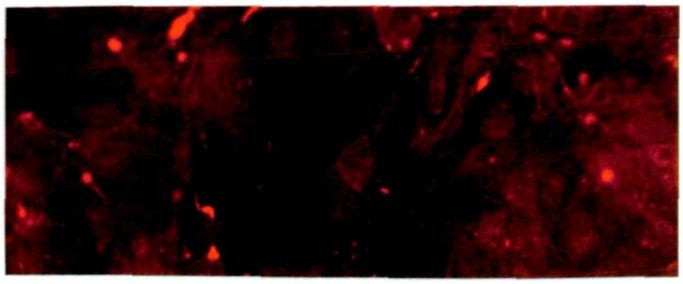

Figure 5.5a The lack of positive staining of p6 human dermal fibroblasts incubated with the Factor-VIII-related antigen, detected using TRITC-conjugated goat anti-rabbit IgG (x 125).

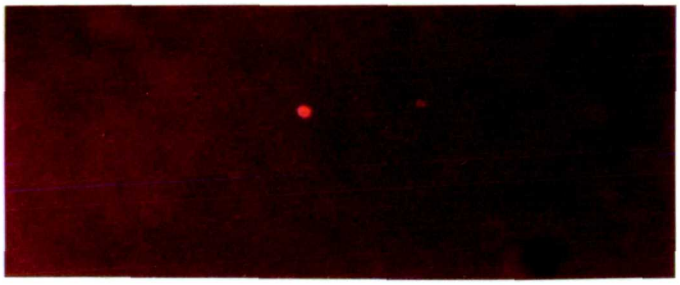

Figure 5.5b The lack of positive staining of p6 human dermal fibroblasts incubated with the secondary (primary detection) antibody, TRITC-conjugated goat anti-rabbit IgG, alone (x 125).

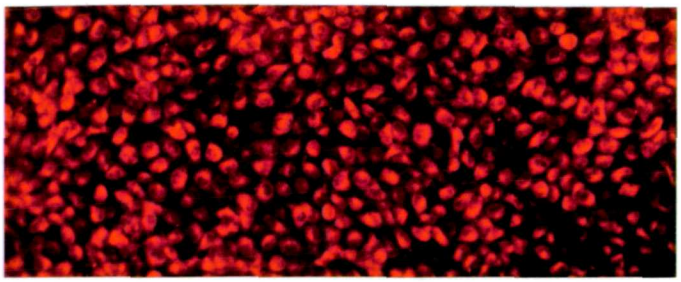

Figure 5.5c The positive staining of p7 bovine aortic endothelial cells incubated with the Factor-VIII-related antigen, detected using TRITC-conjugated goat anti-rabbit IgG (x 125).

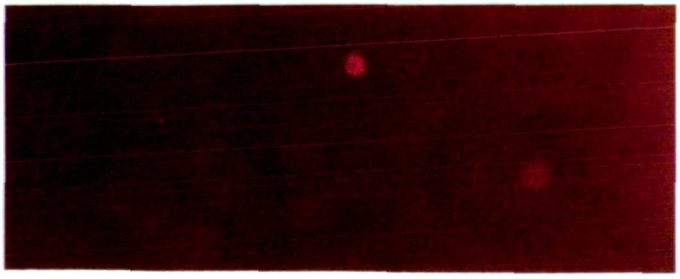

Figure 5.5d The lack of positive staining of p7 bovine aortic endothelial cells incubated with the secondary (primary detection) antibody, TRITC-conjugated goat anti-rabbit IgG, alone (x 125).

5.2. The U937 promonocyte cell line

5.2.1. Constitutive characteristics.

The U937 cell line originated from the pleural fluid of a 37 year old male patient with diffuse histiocytic lymphoma (Sundstrom and Nilsson, 1976). The U937 cell line has been shown to be a neoplastic cell of the monocyte lineage, sharing many morphological, histochemical and functional characteristics of monocyte-macrophages (Sundstrom and Nilsson, 1976; Harris and Ralph 1985; Lyons and Ashman, 1989). Some of the most notable monocyte-macrophage characteristics displayed by U937s include: (1) the surface expression of the leucocyte integrin CR3 (the receptor for complement component C3bi and the antigen recognised by the "macrophage specific" antibodies Mac-1, OKM1 and Mo1) which is thought to be an important receptor for particle phagocytosis and subsequent respiratory burst in mononuclear phagocytes (Beller *et al.* 1982), (2) the surface expression of the FCR1 immunoglobulin G receptor which is expressed specifically by monocytes and tissue macrophages (Anderson, 1982), (3) the release of lysozyme into culture medium, a monocyte specific characteristic (Ralph *et al.* 1976), (4) U937s, like monocytes, elaborate tumour necrosis factor in response to granulocyte macrophage-colony stimulating factor (Sabatini *et al.* 1990), (5) the cytochemical profile of monocytic lineage cells, including the presence of fluoride inhibitable esterase, alkaline and acid phosphatase, and β-glucuronidase activities (Sundstrom and Nilsson, 1976; Harris and Ralph, 1985).

The U937 is a morphologically monoblastic cell which shares many morphological, histochemical and functional characteristics of monocyte-macrophages. The U937 can be induced to differentiate further along the monocyte-macrophage lineage by exposure to both physiological agents (cytokines, retinoic acid, vitamin D derivatives) and non-physiological inducing agents (phorbol esters) (Lyons and Ashman, 1989). This induced differentiation involves phenotypic changes that resemble those observed during terminal differentiation of normal monocytic cells (Pedrinaci *et al.* 1990). Induction with such substances both increases the expression of certain constituitive macrophage characteristics (see above), and encourages the expression of further macrophage characteristics such as substratum adherence and cessation of proliferation (Hass *et al.* 1990), thus giving the cell the morphological and functional characteristics of more differentiated monocyte-macrophages (Harris and Ralph, 1985).

5.2.2. Phorbol ester-induced U937 characteristics

When actively proliferating suspension cultures of U937 cells are treated with phorbol esters, including 4β-phorbol 12-myristate 13-acetate (PMA), cellular growth is inhibited and cells adhere to plastic surfaces (Nilsson *et al.* 1980; Ways *et al.* 1987; Hass *et al.* 1990), both characteristics of peripheral blood mononuclear cells. These adherent, phorbol ester-exposed, U937s express characteristics indicative of more differentiated cells than uninduced U937s (Elsas *et al.* 1990; William *et al.* 1990; Kemp *et al.* 1990). Such induced characteristics include (1) elevated expression of CR3 and FcR1 (Harris and Ralph 1985), (2) increased expression of: fluoride inhibitable esterase, alkaline and acid phosphatase, and β-glucuronidase activities (Harris *et al.* 1985), (3) monocyte-macrophage differentiation antigen expression, including CD14 (Pedrinaci *et al.* 1990) and 7C3 (Zuckerman *et al.* 1987), (4) a monocyte-like network of vimentin intermediate filaments (Taimi *et al.* 1990), (5) the elaboration of granulocyte-macrophage colony stimulating activity (GM-CSA), a glycoprotein capable of stimulating the growth of granulocyte and macrophage colonies from bone marrow cells - a macrophage characteristic (Ascensao and Mickman, 1984; Liu and Wu, 1992), (6) the capacity to generate superoxide anion (O_2^-) free radicals in response to appropriate stimuli (Balsinde and Mollinedo. 1988) a characteristic of activated macrophages (Johnston *et al.* 1978), (7) both peripheral blood monocytes (PBMs) and U937s secrete plasminogen activator (u-PA) and low levels of plasminogen activator inhibitor, secretion of the latter can be substantially increased, in both PBMs and U937s, by exposure to PMA (Gross and Sitrin, 1990). Interestingly, U937s have been observed to retrodifferentiate after removal of phorbol ester (Hass *et al.* 1990; Hass, 1992).

5.2.3. Growth factor synthesis by the U937

In addition to their role in tissue debridement wound macrophages are thought to elaborate various growth and regulatory factors, often grouped together as macrophage-derived growth factor (MDGF), which are thought to be critical for granulation tissue formation. MDGF is known incorporate the activities of: platelet-derived growth factor (PDGF), basic fibroblast growth factor (bFGF), transforming growth factor-β (TGF-β), insulin like growth factor-1 (IGF-1), tumour necrosis factor-α (TNF-α), the epidermal growth factor-related transforming growth factor-α (TGF-α) and interleukin-1 (IL-1) (Raines and Ross, 1989). Actively phagocytosing

peripheral blood monocyte-derived macrophages have also been shown to produce fibroblast activating factor (FAF) (Dohlman *et al.* 1984; Dohlman *et al.* 1985).

The U937 cell has been shown to elaborate the majority of these MDGF components. U937s express PDGF A chain mRNA, which increases with phorbol ester treatment (Alitalo *et al.* 1987; Makela *et al.* 1987). While immunoprecipitable levels of PDGF are clearly apparent in conditioned medium from phorbol ester induced U937s, little is apparent prior to induction (Makela *et al*, 1987). U937s also express mRNA for TGF-β which, like PDGF A chain mRNA, is upregulated by phorbol ester induction (Assoian *et al*, 1987; Wager and Assoian, 1990). Whether this upregulation in TGF-β mRNA is paralleled by secretion of active TGF-β into culture medium is as yet unknown. U937s exposed to the phorbol ester, PMA, release TNF-α into their culture medium; prior to induction they appear not to elaborate TNF-α. Peripheral blood monocytes have also been shown to synthesise TNF-α in response to PMA (Sabatini *et al.* 1990). Some reports suggest that U937s constitutively elaborate IL-1 (Palacios *et al.* 1982; Barak *et al.* 1986) while others question this, reporting that the elaboration of IL-1 requires the induction of differentiation by agents such as PMA (Wakasugi *et al.* 1984; Merluzzi *et al.* 1987). This confusion may partially be explained by the observation that U937s constitutively produce an IL-1 suppressor factor thought to mask IL-1 activity (Fujiwara and Ellner, 1986). The stimulation of U937s with PMA results in the appearance of both intracellular FAF and the secretion of FAF into the medium (Turck *et al.* 1988; Turck *et el.* 1989: Demeter *et al.* 1991). U937s at rest, prior to induction with PMA, transcribe the IGF-1 gene, express IGF-1 mRNA and release IGF-1 at a low level. Upon PMA exposure the rate of transcription increases, but there is a reduction in cytoplasmic IGF-1 mRNA. Despite this, exposure to PMA leads to a rapid release of IGF-1 from the cell, a process that occurs in the presence of protein synthesis blockers suggesting that it is a release of preformed IGF-1 (Nagoaka *et al.* 1990). The fact that U937 cells can rapidly release presynthesized IGF-1 is consistent with the role of mononuclear phagocytes in wound healing and tissue fibrosis. Thus, like the platelet that carries preformed growth factors such as PDGF, the macrophage may be primed to augment mesenchymal growth at the wound site.

5.2.4. Induction of differentiation/maturation by phorbol esters

Phorbol esters, a group of plant-derived compounds with diverse effects on cellular

function, are potent differentiation-inducing agents in several leukaemic cell lines (Nilsson *et al.* 1980). One mechanism through which they exert, at least, a portion of their effects, is by activating the Ca^{2+} phospholipid-dependent kinase, protein kinase C (Castagna *et al.* 1982). Phorbol esters activate protein kinase C by substituting for diacylglycerol (Castagna *et al.* 1982). Diacylglycerol, a product of the phosphatidyl inositol pathway, is an important cellular regulator of protein kinase C. Once activated, protein kinase C is able to phosphorylate serine or threonine residues on target proteins. Phorbol esters are thought, in part, to induce differentiation in U937s by activating protein kinase C to phosphorylate a 47 kD cytosolic protein termed pleckstrin (or P47) (Gailani *et al.* 1990).

5.2.5. Uses of the U937 cell line

The U937 cell is widely used as a model for monocyte-macrophages in many areas of biomedical investigation including research into the pathogenesis of HIV, cancer and pathogenic bacteria. Monocyte-macrophages are an important target for human immunodeficiency virus (HIV) infection; the U937 is widely used, and presumably widely accepted, as a model for studying HIV infection and therapy (Folks *et al.* 1988; Perno *et al.* 1990; Dubreuil *et al.* 1990; Kim *et al.* 1990; Vitkovic *et al.* 1990; Mann *et al.* 1990; Pauza and Singh, 1990; Gollapudi and Gupta, 1990; Mace and Gazzolo, 1991; Locardi *et al.* 1990). The U937 has also been employed as a macrophage model in other areas of virology including the study of herpes simplex type-1 pathogenesis (Tenney and Morahan, 1987). The U937 has been used in bacteriology research: as a model of bacteria-macrophage interaction in the cytopathology of *Legionella pneumophila*, which are thought multiply within alveolar macrophages (Pearlman *et al.* 1988; Cianciotto *et al.* 1990); as a model for the effect of bacterial leucotoxins on human monocytes (Simpson *et al.* 1988); and in the development of live oral vaccines of *Salmonella typhi* (Dragunsky *et al.* 1990). In its capacity as a leukaemia-derived cell line the U937 has been used in cancer research: as a target cell for attempts at leukaemia differentiation therapy (Nakaya *et al.* 1990; Peck and Bollag, 1991), to examine deficiencies in haemopoeitic organ homing of leukaemic cells (Hardy *et al.* 1990), and as an *in vitro* target cell to monitor the antitumour host defences of pulmonary macrophages from lung cancer patients (McDonald and Atkins, 1990).

5.2.6. Dissimilarity to cells of the monocyte-macrophage lineage

Some differences between the U937s induced to differentiate along the macrophage lineage and normal cells of the monocyte-macrophage lineage have been reported. These include: differences in the regulation and intracellular processing of cytokines e.g tumour necrosis factor-α (Hass *et al.* 1991); the expression of high levels of the CD4 surface antigen, a characteristic of T lymphocytes rather than monocyte/-macrophages (Teppler *et al.* 1990); and U937s, unlike peripheral blood monocytes, appear to be incapable of producing leukotrienes (Nolfo and Rankin, 1990).

5.2.7. The culture of U937s

U937s obtained from the European Collection of Animal Cell Cultures (Porton Down, UK.) were cultured in suspension in 80 cm^3 flasks in RPMI-1640 medium containing 10% v/v heat-inactivated fetal calf serum, 100 μg/ml of streptomycin, 100 units/ml penicillin and 25 mM Hepes buffer (pH 7.4). Flasks were seeded with U937s at a cell density of between 0.5 and 1 x 10^5 cells/ml. Population doubling time was observed to be approximately 40 hours. Cultures were split at a 1:5 ratio twice a week.

5.3. The methylene blue fibroblast proliferation bioassay

5.3.1. Introduction

The methylene blue bioassay was first described by Lagneau *et al.* (1977) as a technique for measuring cytotoxicity. It has since been modified and used as a proliferation assay for tumour cells (Martin *et al.* 1978), human and rat fibroblast cell lines and for epithelial cell lines (Oliver *et al.* 1989). The methylene blue bioassay was used in this work as the main method for quantitating fibroblast proliferation *in vitro*.

5.3.2. Overview of the methylene blue bioassay

This assay relies on (1) the ability of methylene blue to stain cells in monolayer, and (2) the ability to relate the amount of stain eluted from a monolayer to the number of cells within that monolayer. Methylene blue is a basic dye that is positively charged at pH 8.5. When added to cells in culture it forms salts with negatively charged tissue components. The main basophilic components of fibroblasts are the anionic

phosphate groups of DNA. During cell division, as the nucleic acid content of the monolayer increases, there is a proportional increase in the available binding sites for the dye. After methylene blue staining, the excess dye is removed leaving only the bound dye. The addition of acid-alcohol leads to the protonation of acidic groups which releases the previously bound dye into the eluent. The absorbance of the eluent is then determined using a spectrophotometer. This absorbance is related to the amount of bound dye, and therefore also to the amount of DNA present in the monolayer. By generating a standard curve of cell number versus absorbance, absorbance values obtained during experimentation, on the same cell line, can be converted into cell number (refer to page 152).

5.3.3. The binding of methylene blue.

The methylene blue dye used in this thesis (MB-1, Sigma Diagnostics, St. Louis, USA) not only binds to the basophilic anionic phosphate groups of DNA, but may also bind other basophilic cell components, including RNA and cytoplasmic proteins. Accordingly, if there is an increase in the synthetic activity of cells, in response to a given treatment, more methylene blue will bind per cell, thus over estimating cell number. Routine cell counts using a haemocytometer are necessary to control for such an outcome, and were carried out routinely in parallel with each methylene blue proliferation assay performed.

Methylene blue also appears to bind to components of the tissue culture medium, fetal calf serum supplement and biomaterials under test (e.g. components of platelet releasates and macrophage supernatants studied in this thesis). To control for this error a minimum of 12 wells on each 96-well plate were set aside as "medium blanks", cell-free wells which were plated with medium alone. Where various macrophage supernatants or platelet releasates were being compared on a single 96-well plate, medium blank wells were initially plated with fibroblast growth medium (Ham's F10 + 10% FCS), to control for fibroblast plating medium, then plated with the macrophage supernatant or platelet releasate, to control for the "substance under test". Average A_{650} values obtained from these "medium blank wells" were subtracted from the A_{650} values of cell-containing experimental wells prior to further analysis of fibroblast proliferation.

5.3.4. The relationship between absorbance (λ 650nm) and methylene blue dye concentration.

The relationship between absorbance (λ 650nm) and concentration of methylene blue has been investigated by Oliver *et al.* (1989). They demonstrated that when methylene blue was eluted from stained cells using acid-alcohol (ethanol : 0.1 M HCl) a positive linear relationship exists between methylene blue concentration (range 0 - 40 mgl^{-1}) absorbance at 650 nm. However, when eluted with an aqueous solution of lower pH this linear relationship was lost, due to dimer formation.

Oliver *et al.* (1989) also demonstrated that absorption spectra of methylene blue eluted from stained cells using acid-alcohol differed from that obtained by elution with an aqueous based solution of similar pH. Elution of methylene blue with acid alcohol resulted in a single, large, clearly defined, absorbance peak at 650 nm; compared with two, small, poorly defined peaks at 600 and 650 nm when aqueous elution was employed.

As a consequence of the observations made by Oliver *et al.* (1989), regarding both the linear relationship between methylene blue dye concentration and absorbance at 650 nm, and the absorption spectra generated by elution using acid alcohol, this was chosen as the method of dye elution throughout this thesis.

5.3.5. The relationship between absorbance and cell number.

The relationship between measured absorbance (λ 650 nm) and cell number is dependent upon a fixed mean nuclear:cytoplasmic ratio. It is theoretically possible that the nuclear:cytoplasmic ratio could vary with cell type, passage number, source species or in response to a given experimental condition. To overcome differences between cell type, passage number or source species a calibration curve (or standard plot) of absorbance at a wavelength (λ) of 650nm (i.e. A_{650}) versus cell number, was generated for each cell type. Thus facilitating the conversion of measured A_{650} into a cell number for each cell type under experimental investigation (see preparation of standard curve, p152).

A potential source of error in this assay is that under certain experimental conditions the mean nuclear:cytoplasmic ratio may change, thus altering A_{650}, which could be interpreted as a change in cell number, though without an actual change necessarily having taken place. The calibration curve, having been prepared prior to this hypothetical experimentally-induced change in nuclear:cytoplasmic ratio, can no

longer be used to accurately convert experimental absorbances into cell numbers. Oliver *et al.* (1989) examined a variety of cell lines, including Rat 1 (fetal rat lung fibroblasts); IMR90 (cloned human fetal lung fibroblasts); HFL (fetal lung fibroblast line) Chang cells (cloned liver epithelial cell line), and SIRC (rabbit corneal fibroblasts) under various culture conditions, which included studying the effects of platelet-derived growth factor (PDGF), prostaglandin E_2, and macrophage conditioned media, and found no change in nuclear:cytoplasmic ratio. However, this clearly does not preclude such a change taking place.

5.3.6. Preparation of a standard curve for the methylene blue bioassay

Introduction. Calibration curves of absorbance (λ 650 nm) versus fibroblast number were constructed (1) in order to confirm that there was a linear relationship between absorbance (λ 650 nm) and cell number, and (2) to facilitate the conversion of experimentally-obtained absorbances, generated using the methylene blue bioassay, into fibroblast number.

Method. The method employed here is based on the standard protocol for the "Methylene Blue Fibroblast Proliferation Assay" (Appendix 8, p342).
Briefly, adult forearm fibroblasts (p6) were resuspended in Ham's F10 medium supplemented with 10% fetal calf serum and 2% penicillin/streptomycin at a concentration of 1 x 10^5 cells/ml. This cell suspension was then serially diluted with culture medium to give cell suspensions containing 5 x 10^4, 2.5 x 10^4, 1.25 x 10^4 and 6.25 x 10^3 cells/ml. These cell suspensions were plated out, in 100μl volumes, into the wells of a 96-well flat bottomed tissue culture microtitre plate; such that for each cell concentration 16 duplicate wells were filled. The remaining wells were filled with culture medium only, to allow for later correction of absorbance due to culture medium. The 96 well plate was then sealed to guard against evaporation and placed in a 37°C incubator for a period of 12 hours to allow cells to attach to the tissue culture plastic. After 12 hours the culture medium was aspirated off, the fibroblasts (now in monolayer) were washed, fixed, stained, the stain eluted, and the absorbance (λ 650 nm) for each well measured.

Results. Average absorbance (λ 650 nm) values were calculated for each cell concentration, and the average absorbance (λ 650 nm) of medium-only wells subtracted from these values. These corrected average absorbance figures (table 5.1, p154) were plotted against cell concentration (figure 5.6A), and a linear regression analysis performed (figure 5.6B). Standard deviation and standard error of corrected absorbance was calculated, and plotted to display the distribution of absorbances from the average. It is apparent from figure 5.6B that there is a positive linear relationship between fibroblast number and absorbance (λ 650 nm). The regression analysis data can then be used to covert experimental absorbance figures into cell number as follows:

Linear regression data:	R^2	=	0.9996
	a	=	-0.001875
	b	=	0.040845

For a given experimental absorbance value X

$$Cell\ Number = \frac{X - a}{b}$$

Thus for this standard curve:

$$Cell\ Number = \frac{X + 0.001875}{0.040845}$$

Discussion. The observation that a linear relationship exists between cell number and absorbance (650 nm) up to a concentration of 1×10^4 cells per well (1×10^5 cells per ml) is consistent with the findings of Oliver *et al.* (1989). This observation indicates that as long as measured absorbances, obtained during experimentation, do not exceed the absorbance displayed by the 1×10^5 cells/ml suspension, they may be converted into cell number using this calibration curve. Several fibroblast calibration curves were carried out during the course of this work; for a given proliferation assay the calibration curve used will be indicated.

Table 5.1 Standard curve data. Change in absorbance (λ = 650 nm) with fibroblast seeding density.

Cell Number per well	625	1,250	2,500	5,000	10,000
Number of replicate wells	16	16	16	16	16
Mean absorbance (λ-650 nm)	0.02281	0.05025	0.09656	0.20694	0.40469
Standard deviation	0.00461	0.00475	0.00558	0.01934	0.01608
Standard error	0.00115	0.00119	0.00139	0.00484	0.00402

Figure 5.6

Standard plot of p6 human dermal fibroblast number against absorbance (λ 650 nm).

A. Prior to linear regression.

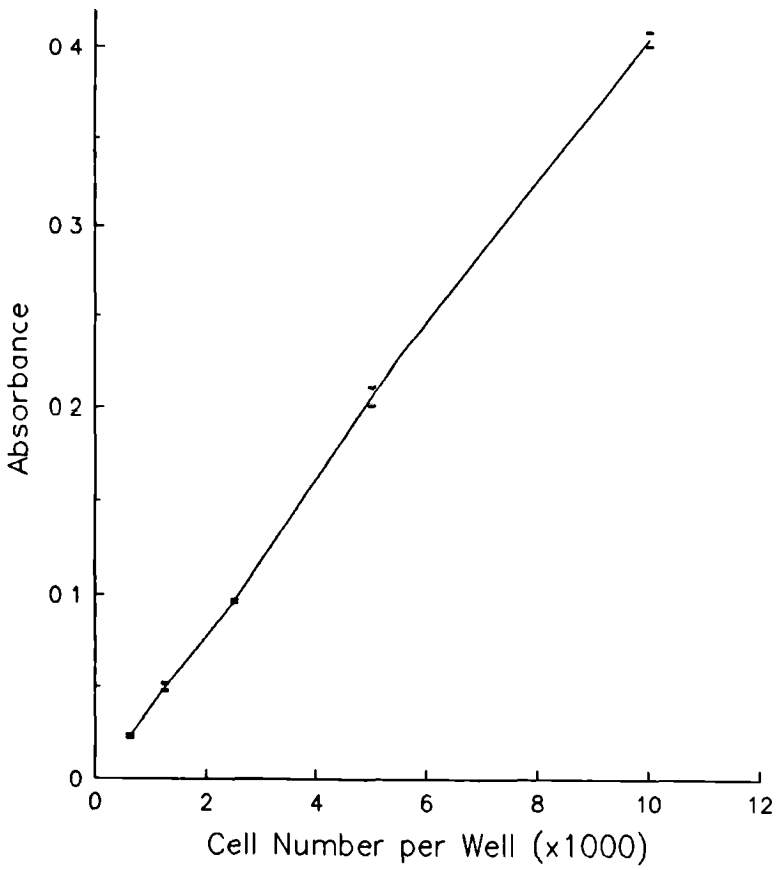

B. After linear regression.

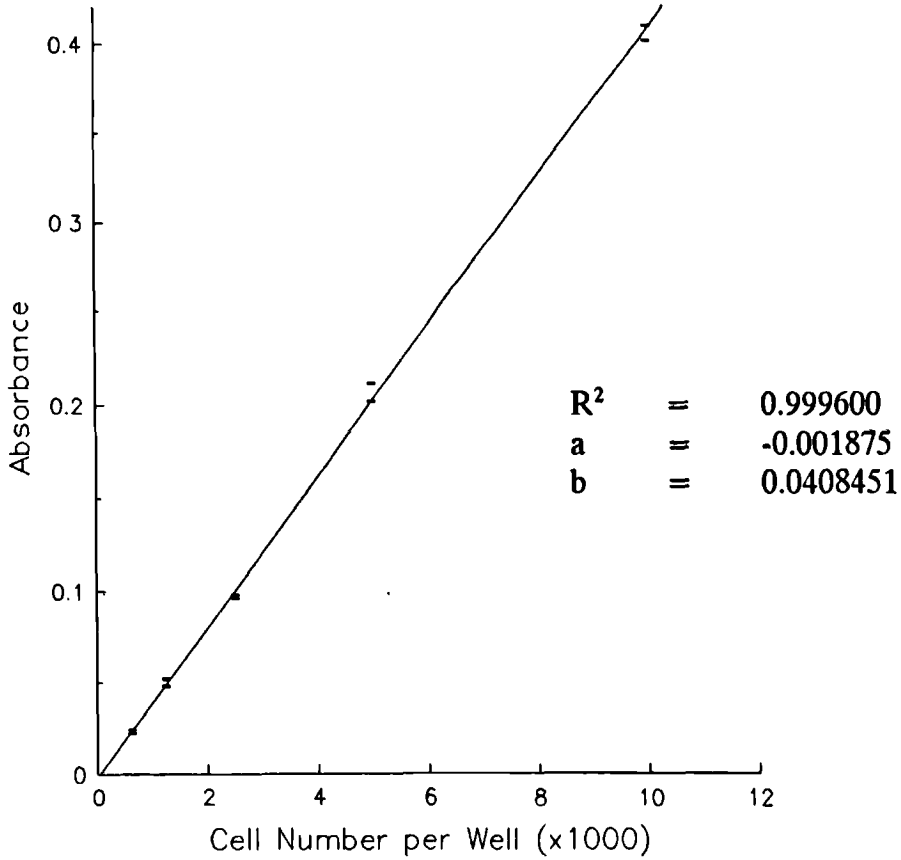

5.3.7. Examination of the sensitivity of the methylene blue fibroblast proliferation assay to exogenous stimulatory factors (fetal calf serum).

Introduction. Serum is known to contain varying quantities of several polypeptide growth factors capable of stimulating fibroblast proliferation *in vitro*. Serum growth factors mitogenic for fibroblasts *in vitro* include those released from platelet α-granules during clotting: platelet-derived growth factor, PDGF, (Ross *et al.* 1986); transforming growth factor-beta, TGF-β, (Moses *et al.* 1985); basic fibroblast growth factor, bFGF, (Gospodarowicz, 1974); and epidermal growth factor, EGF, (Davidson *et al.* 1988). The methylene blue proliferation assay was used to study the effect of fetal calf serum (FCS) concentration on the proliferation of p6 human dermal fibroblasts as a preliminary to investigating the effect of ultrasound.

This study was performed (1) to examine the ability of the p6 human dermal fibroblasts (used in this thesis) to respond to known mitogenic substances, and (2) to assess the ability of the methylene blue fibroblast proliferation assay to detect that proliferative response.

Method. A modified version of the standard methylene blue fibroblast proliferation assay protocol (Appendix 8, p342) was employed. Briefly, sub-confluent p6 human dermal fibroblasts were trypsinised (Appendix 4, p338) and resuspended in fibroblast growth medium (Appendix 2B, p335) to 3 x 10^4 cells/ml. 100 µl volumes of this suspension, containing 3000 cells, were dispensed into each well of rows B through G of a 96-well microtitre plate. Each well in rows A and H, of the same plate, received 100 µl of fibroblast growth medium (medium blank wells). The plate was then sealed to reduce desiccation and placed in a 37°C incubator for 12 hours to permit cell attachment. Four 96-well microtitre plates were set up in this way.

After 12 hours all four plates were removed from the incubator. One plate was "stopped" according to steps 6 through 8 of Appendix 8 (p342) and stored in a dust free environment. The three remaining plates were treated as follows:
Under sterile conditions, the sealing tape was removed and the medium in each well was carefully aspirated off without disturbing the fibroblast monolayer. 100 µl of fibroblast growth medium (Appendix 2B, p335), containing 0.5, 1.0, 2.5, 5.0, 10.0, or 20% FCS, was then added to each well such that 2 columns of wells on each plate, including medium blank wells, received a given FCS concentration. The three plates

set up in this manner were then sealed and returned to the 37°C incubator. Individual plates were removed from the incubator and "stopped" after 60, 108, or 156 hours. After the 156 hour plate had been "stopped", all 4 plates were stained with methylene blue, the stain eluted, and absorbance (A_{650}) values obtained for each well using a spectrophotometer. Average medium blank A_{650} readings were calculated and subtracted from the cell-containing wells. The resulting A_{650} values were converted into cell number using a standard curve (figure 5.6B, p155) for p6 human dermal fibroblast cell number versus A_{650}. Median fibroblast number was calculated for each of the FCS levels at each time point (Table 5.2) and displayed graphically along with their respective 95% confidence intervals (figure 5.7, p159). Non-parametric analysis (Mann Whitney U-test) was performed between each FCS concentration, at each time point, to ascertain the sensitivity of the methylene blue fibroblast proliferation assay to FCS (see Appendix 17, tables 1 through 4 (p353).

Results. From figure 5.7, showing cell number against FCS concentration at 12, 60, 108 and 156 hours post plating, it can be seen that as FCS concentration is increased there is a parallel increase in fibroblast number. The peak median fibroblast number is observed at the 108 hour time point in all FCS concentrations, with the exception of 20% FCS, where the cells continue to proliferate up until 156 hours. Fibroblast proliferation in response to 1.0% FCS is significantly faster than in response to 0.5% FCS at the 60, 108 and 156 hour time points ($p = 0.001815$, $p = 0.000036$ and $p = 0000137$ respectively). Similarly, when 2.5% FCS is compared with 1.0% FCS, or, 5.0% is compared with 2.5%, or, 10.0% is compared with 5.0%, or, 20% is compared with 10% at each of the 60, 108 or 156 hour time points, the higher FCS concentration always results in significantly more fibroblast proliferation (Appendix 17, tables 1 through 4, p353). No significant differences were observed between any of the columns in the 12 hour, pre-FCS, plate. A summary of the results of statistical analyses can be found in Appendix 17 (p353).

Discussion. The above data suggest that the p6 human dermal fibroblasts used in this thesis are capable of responding, in a dose dependent fashion, to known mitogenic substances. The data also indicates that the methylene blue assay used is capable of measuring that response. The observation that the assay reports a statistically significant difference in proliferation in response to 1.0% FCS compared with 0.5%

Table 5.2 The effect of fetal calf serum (FCS) concentration on the proliferation of human dermal fibroblasts.

Time post plating (hours)	12						60					
FCS concentration (%) applied to cells	0.5	1.0	2.5	5.0	10.0	20.0	0.5	1.0	2.5	5.0	10.0	20.0
Number of replicate wells	5	11	12	12	12	12	12	12	12	12	12	12
Median cell number ($\times 10^3$)	3.174	2.929	3.051	3.186	3.198	3.321	3.459	4.157	5.540	7 169	8.270	8 882
Minimum and maximum ($\times 10^3$)	2.915 to 3.286	2.586 to 3.369	2.243 to 3.492	2.562 to 3.492	2.757 to 3.516	2.757 to 3.639	2.994 to 6.006	3.704 to 4.806	4.904 to 6.422	6.520 to 7.744	7.695 to 9.213	8.062 to 9.433
95% Confidence interval ($\times 10^3$)	2.937 to 3.299	2.725 to 3.105	2.811 to 3.247	2.994 to 3.354	3.042 to 3.330	3.100 to 3.462	3.187 to 4.177	3.996 to 4.441	5.310 to 5.889	6.836 to 7.461	8.066 to 8.700	8.563 to 9.112

Time post-plating (hours)	108						156					
FCS concentration (%) applied to cells	0.5	1.0	2.5	5.0	10.0	20.0	0.5	1.0	2.5	5.0	10 0	20.0
Number of replicate wells	12	12	12	12	12	12	12	12	12	12	12	12
Median cell number ($\times 10^3$)	4.537	5.578	7.340	9.789	13.302	15.457	3.322	4.240	6.725	9.051	12.271	16.898
Minimum and maximum ($\times 10^3$)	4.354 to 4.941	5.113 to 6.459	6.386 to 8.271	8.663 to 12.310	10.180 to 14.416	13.975 to 16.693	2.710 to 4.203	3.934 to 5.060	5.941 to 7.435	8.268 to 9.492	11.695 to 13.360	15.221 to 17.571
95% Confidence interval ($\times 10^3$)	4.477 to 4.728	5.419 to 5.932	7.018 to 7.740	9.387 to 10.636	12.157 to 13.705	14.850 to 15.929	3.083 to 3.639	4.141 to 4.560	6.429 to 6.989	8.662 to 9.119	11.974 to 12.607	16.407 to 17.200

Figure 5.7. The effect of fetal calf serum on p6 human dermal fibroblast proliferation *in vitro* (95% confidence intervals are indicated).

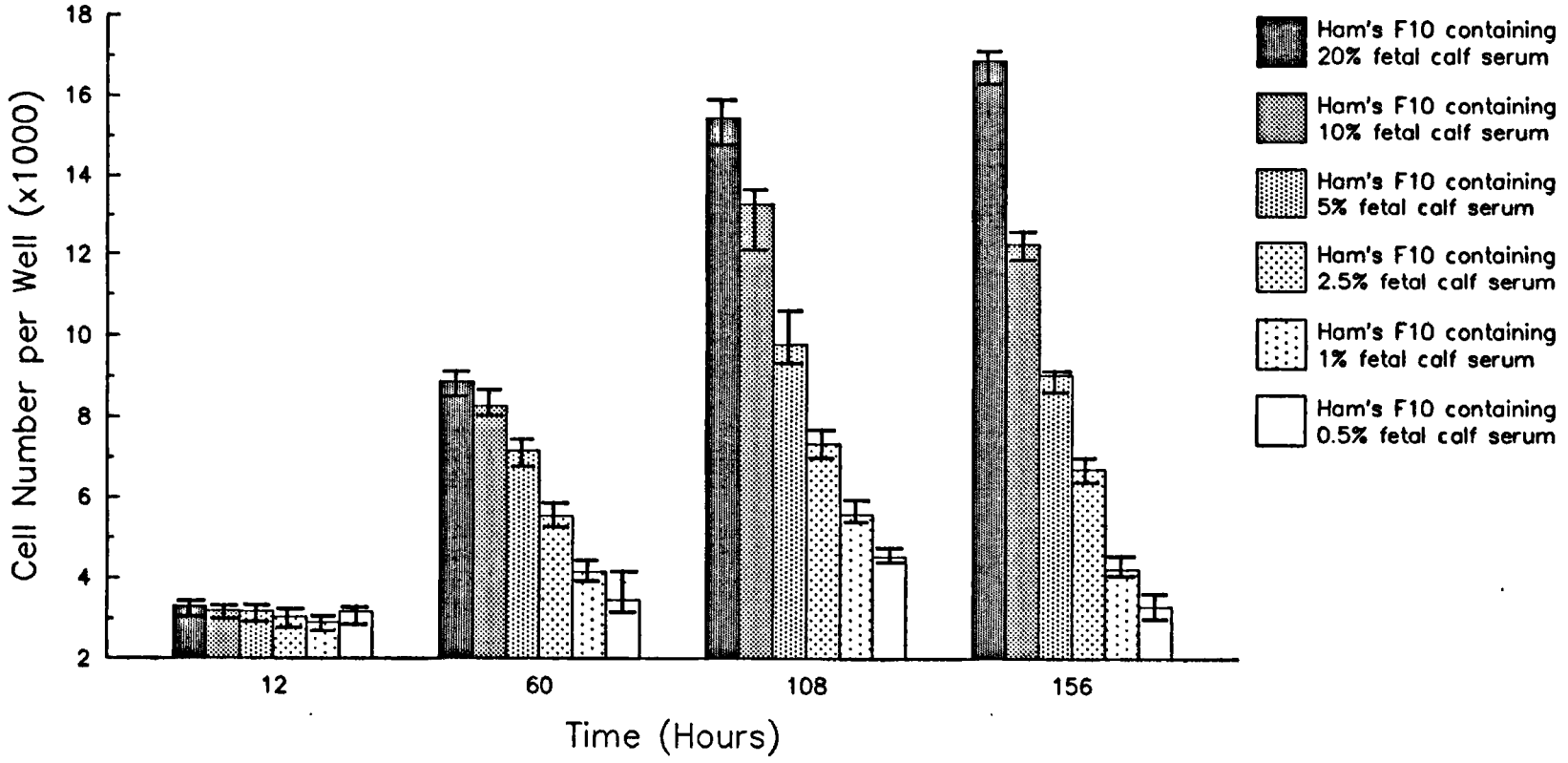

FCS suggests that this technique is a highly sensitive one; it also suggests that the assay may be able to detect even smaller differences in FCS concentration. The observation that peak median proliferation occurs at 108 hours post plating, in all but those wells receiving 20% FCS, is probably explained in terms of nutrient depletion.

Conclusions. In conclusion, p6 human dermal fibroblasts proliferate, in a dose dependent manner, to known mitogenic substances. The methylene blue assay, as employed above, is capable of detecting the response of fibroblasts to mitogenic agents.

5.4. The fibroblast-populated collagen lattice (FPCL) contraction assay

5.4.1. Introduction

In this section the use of the FPCL contraction assay as an *in vitro* model for wound contraction is considered. This model was used in experimental work to study the ability of therapeutic ultrasound to:

(1) interact directly with, and modulate the contractile capacity of, human dermal fibroblasts within collagen lattices.

(2) facilitate the release of substances from platelets capable of modulating the contractile ability of human dermal fibroblasts within collagen lattices.

(3) encourage the synthesis, and elaboration, of substances from macrophages (pro-monocyte U937) capable of modulating the contractile ability of human dermal fibroblasts within collagen lattices.

A brief overview of FPCL contraction, including the methodology involved in their manufacture, is given below. This is followed by a review of the evidence that supports the use of such three dimensional matrix-based *in vitro* techniques over planar culture techniques as a model for the role of the fibroblast *in vivo*. The literature regarding the suggested mechanisms by which fibroblasts mediate collagen lattice contraction will then be discussed. This section includes a literature-based review of fibroblast-collagen attachment and details the theories proposed to explain fibroblast-mediated lattice contraction. A description of some preliminary studies carried out prior to the examination of both the direct effect and indirect effects

(modulated via platelets or macrophages) of therapeutic ultrasound on FPCL contraction, then follows. These preliminary studies were carried out to determine the optimal concentrations of the various lattice components (collagen, cells and serum) and to determine the ability of fibroblast populated collagen lattices to respond to exogenous stimuli.

5.4.2. Overview of FPCL contraction

The contraction of hydrated collagen lattices seeded with human fibroblasts was initially observed by Elsdale and Bard (1972). They suggested that the diminution in lattice size, termed *gradual lattice collapse*, resulted from mechanical disturbance of the lattice as a consequence of cellular motility. Later Bell *et al.* (1979) described the possible use of fibroblast mediated collagen lattice contraction, both to produce an immunologically tolerated tissue-like wound dressing, and as a model for studying the role of the fibroblast in wound repair. Because fibroblast reorganisation of hydrated collagen lattices is an *in vitro* process that leads to the development of an *in vivo*-like tissue, there has also been considerable interest in this system as a model for fibrosis and connective tissue organisation (Guidry and Grinnell, 1987).

FPCLs are composed of a mixture of fibroblasts (in single cell suspensions after release from monolayer), culture medium and solubilised (monomeric) collagen. Once mixed, the fibroblast/medium/collagen combination is aliquoted into bacterial petri dishes, which are then placed in a 37°C environment. The collagen rapidly polymerises and traps the cells in a three dimensional matrix. After polymerisation the petri dish can be thought of as containing two phases, the solid phase being composed of polymerised collagen and cells, the liquid phase being composed of culture medium. Initially, and for some time after plating, fibroblasts have a spherical shape which, with time, becomes elongate. As the fibroblasts progressively elongate and spread within the matrix, a dynamic change occurs, termed *lattice contraction*, whereby the lattice undergoes a clearly visible reduction in size. Depending on whether lattices are freed from their attachment to the petri dish, termed rimming (Dodd *et al.* 1982), or left attached, this reduction in size is visualised as a decrease in lattice area (retaining the circular shape of the petri dish) or depth (Guidry and Grinnell, 1985), respectively. During lattice contraction the liquid phase is expressed from the FPCL as the collagen fibres are brought closer together. Initially, soon after plating, lattices are almost transparent, but as contraction proceeds they gradually

become opaque (Bell *et al.* 1979). Lattice contraction results in increased fibrillar density and a greater organisation of the collagen fibres (Bell *et al.* 1979; Ehrlich *et al.* 1983; Buttle and Ehrlich, 1983) The rate, and ultimate degree, of fibroblast mediated collagen lattice contraction, is dependent upon many variables, the most influential of which are serum concentration, cell number and collagen concentration. Lattice contraction does not occur in the absence of serum and is directly proportional to cell number and inversely proportional to collagen concentration (Buttle and Ehrlich, 1983; Ehrlich, 1988b).

5.4.3. Evidence to support the use of FPCL

The collagen lattice system allows a three dimensional (3d) interaction between fibroblasts and also between fibroblasts and the extracellular matrix. Several lines of evidence suggest that the study of cells within 3d tissue culture arrangements is physiologically more relevant to the *in vivo* situation than the more common planar arrangements. Monolayer culture imposes an abnormal dual environment and elicits responses not characteristic of cells *in vivo* (Nusgens *et al.* 1984). In monolayer, cells are subjected to two distinct environments: one, a solid substrate with which the ventral surfaces interact, and the other, a large volume of fluid that bathes the dorsal surfaces. In contrast fibroblasts of the dermis are embedded in a three dimensional matrix that provides similar conditions for all parts of the cell surface. Fibroblasts in monolayer grow to confluency, a condition not normally observed *in vivo*, but only when this abnormal state is attained are cells regulated *in vitro*. *In vivo*, on the other hand, in the dermis, for example, fibroblasts normally enter the G_0, i.e. leave the cell cycle even though separated by extracellular matrix. The FPCL is an *in vitro* system that can be used to examine the activities of effectively mitotically inactive cells (Bell *et al.* 1979; Sarber *et al.* 1981; Bell *et al.* 1983; Buttle and Ehrlich, 1983) similarly separated by matrix in a single relatively uniform environment (Nusgens *et al.* 1984).

As the loss of mitotic activity within FPCLs has been shown not to be due to exhaustion of the medium, cell-cell contact inhibition nor impermeability of the matrix to materials in the medium, and has been shown to be reversed by allowing cells to grow in monolayer (Sarber *et al.* 1981; Nusgens *et al.* 1984; Nishyama *et al.* 1989; Coustry *et al.* 1990); this lack of mitotic activity has been interpreted as being caused by a high level of cell-collagen fibril interactions or cell-matrix contact inhibition (Nishyama *et al*, 1989). Such proliferation control mechanisms are thought

to regulate connective tissue cells *in vivo*, and thus the effectively non-cycling cells in FPCLs are thus more representative of fibroblasts *in vivo* than monolayer cultures. Kono *et al.* (1990a) also observed the lack of mitotically active cells, demonstrating that only 4.3% of cells within a FPCL were in S phase the remainder being arrested in G_0/G_1. On the basis of such observations they considered the FPCL model to be analogous to the dermis with respect to cell growth and cell cycle phase composition.

Fibroblasts and other mesenchymal cells incorporated into three dimensional (3d) polymerised collagen lattices adopt stellate or elongate morphologies, depending on whether lattices are rimmed or are restricted by culture vessel attachment (Nakagawa *et al.* 1989). Such morphologies displayed in 3d lattices are more like those of cells *in vivo* than the flattened multi-pseudopodial or spindle shaped appearance of cells grown on two dimensional glass or plastic surfaces (Elsdale and Bard, 1972; Grinnell and Bennett, 1981; Tomasek *et al.* 1982; Tomasek and Hay, 1984). It has been suggested that this modulation in cell shape which occurs when cells are cultured within lattices may influence various cellular activities, including the selective regulation of gene transcription (Hatamochi *et al.* 1989; DiPersio *et al.* 1991) and the responsiveness to exogenous mitogenic stimuli including various peptide growth factors (Nakagawa *et al.* 1989). When attached FPCLs are freed from their restriction, a rapid contraction is observed over a period of a few minutes (Tomasek *et al.* 1992) indicating that while attached, a tension had developed within the lattice. This phenomenon termed "stress relaxation" of FPCLs (Mochitate *et al.* 1991), is associated with a change from the normal bipolar fibroblast morphology to a more rounded shape. Consequent with this change in shape after stress relaxation, an immediate reduction of 35% in DNA synthesis and 30% protein synthesis has been observed. The rapidity with which cell biosynthetic activity changes following stress relaxation provides direct evidence for a direct linkage between cell geometry and biosynthetic function (Mochitate *et al.* 1991).

There is also evidence that cells grown in collagen lattices retain more differentiated physiological functions than cells grown in monolayer (Reid and Rojkind, 1979). Nusgens *et al.* (1984) demonstrated that fibroblasts cultured within a lattice arrangement synthesised protein, in particular collagen, at a reduced level, approaching that of *in vivo* fibroblasts within normal skin, when compared to fibroblasts in monolayer. This observation was further substantiated by *in situ* hybridization studies demonstrating reduced amounts of collagen mRNA in

fibroblasts embedded in collagen lattices compared with monolayers (Mauch *et al.* 1988). Exogenous epidermal growth factor (EGF) is known to accelerate wound repair, stimulating the accumulation of mesenchymal cells and collagen synthesis (Buckley *et al.* 1985; Laato *et al.* 1986); however, when this growth factor is applied to planar cultures of fibroblasts, collagen synthesis is inhibited. Interestingly, collagen synthesis is upregulated following the addition of EGF to fibroblasts grown in a 3d collagen lattice. This would appear to indicate the retention of *in vivo* function and growth factor responsiveness by collagen lattice cultured fibroblasts (Colige *et al.* 1988). Greve *et al.* (1990), studying proteoglycan formation, similarly demonstrated that the synthesis of small dermatan sulphate proteoglycan II by human skin fibroblasts in a type 1 collagen lattice was down regulated when compared with that of monolayer culture; the synthesis of other proteoglycans, such as large chondroitin sulphate, dermatan sulphate and heparan sulphate, was unaffected by 3d culture. The synthesis of other, non-proteinaceous, extracellular components, for example glycosaminoglycans, appears to be unaffected by culture within 3d collagen lattices (Preistley, 1991). Coulomb *et al.* (1983) demonstrated that fibroblasts within lattices express a perinuclear peroxidase activity and exhibit permeability properties typical of cells *in vivo* rather than cells grown as monolayer cultures.

The apparent retention of the differentiated state, associated with culture on, or in, collagen lattices, has been demonstrated for cell types other than fibroblasts. Tateyama *et al.* (1990) studying the cell morphology and growth characteristics of normal canine mammary epithelial cells demonstrated that under planar culture conditions a monolayer of flattened polygonal cells was produced; however, when cultured within collagen lattices they grew into duct like structures of normal mammary tissues. Shabana *et al.* (1991) studying the culture of human oral epithelial cells, from hard palate/gingiva/alveolar mucosa found that a collagen based environment facilitated stratification and differentiation into basal cuboidal, polyhedral spinous cells and elongated superficial cells. Thus the collagenous environment not only encourages the retention of differentiated physiological functions, but, it also encourages further differentiation.

From the literature cited above, it would appear that the FPCL model facilitates the *in vitro* study of cells in a physiological environment, which appears to induce cellular phenotypes and functions more representative of the *in vivo* situation, than the more common monolayer *in vitro* culture techniques.

5.4.4. The mechanism of FPCL contraction

Collagen lattice contraction does not occur in the absence of cells or in the presence of cell conditioned media alone, the phenomenon requires that cells be trapped within a polymerising collagen lattice. As such, it is clear that the force for lattice contraction is generated by cells, rather than by some effect of self-aggregation of the collagen fibrils (Bell *et al.* 1979; Bellows *et al.* 1981; Ehrlich *et al.* 1989). However, the local secretion of "factors" by fibroblasts, present within a collagen lattice, has been suggested to complement this cell mediated physical reorganisation (Grinnell and Lamke, 1984).

For ease of description the process of FPCL contraction will be divided up into three phases: (1) attachment.

(2) contraction.

(3) stabilisation.

5.4.4.1. The Attachment Phase

After initial plating, lattice polymerisation and lattice detachment, there is a variable interval, prior to active contraction, during which minimal contraction occurs. This interval, termed the lag period by Nishyama *et al.* (1988), is thought to reflect the time taken for fibroblasts to attach and elongate along collagen fibrils. The way in which fibroblasts adhere to collagen fibrils, within a 3d collagen lattice, is the matter of some disagreement. It is widely accepted that fibroblasts bind to collagen fibrils to facilitate contraction, but whether it is a direct attachment or an indirect attachment, mediated by the adhesive glycoprotein fibronectin (Fn), is the centre of some debate.

Cellular adhesion to the extracellular matrix is brought about primarily by cell surface receptors called integrins, though non-integrin mediated adhesion has been reported (Klein *et al.* 1991; Schiro *et al.* 1991). The integrins are a family of at least 20 different transmembrane glycoproteins that interact with multiple matrix ligands in a divalent cation-dependent fashion. Integrins are heterodimers made up of an alpha (α) subunit non-covalently associated with a beta (β) subunit. Both α and β subunits have extracellular, transmembrane and cytoplasmic domains. The extracellular domains of both α and β subunits are thought to combine to form a ligand (matrix) binding head (Hynes, 1992). This binding head is connected by the α and β transmembrane domains to the two cytoplasmic domains which are thought

to interact with cytoskeletal proteins and perhaps with other cytoskeletal components (Burridge *et al.* 1988; Duband *et al.* 1986; Horwitz *et al.* 1986; Otey *et al.* 1990). There are presently 8 known β subunits (β_1...β_8) and 14 α subunits (α^1...α^8 and α^V, α^L, α^M, α^X, α^{IIb} and α^{IEL}). Although 8 β subunits and 14 α subunits could in theory associate to give more than 100 integrin heterodimers, the actual diversity appears to be much more restricted with only 20 integrin heterodimers known to date (Hynes, 1992). Individual integrins can often bind to more than one matrix ligand, for example the integrin $\alpha^3\beta_1$ has been shown to bind fibronectin, laminin and collagen. Equally, individual ligands are, more often than not, recognised by more than one integrin, for example fibronectin is recognised by the integrins $\alpha^3\beta_1$, $\alpha^4\beta_1$, $\alpha^5\beta_1$, $\alpha^V\beta_1$, $\alpha^V\beta_5$, $\alpha^V\beta_6$, $\alpha^V\beta_3$ and $\alpha^{IIb}\beta_3$. Considerable progress has been made in defining the integrin recognition sites on extracellular matrix ligands. The first binding site to be defined was the tripeptide sequence Arg-Gly-Asp (RGD) which is present in fibronectin, vitronectin and a variety of other adhesive proteins. This tripeptide sequence is recognised by several integrins ($\alpha^5\beta_1$, $\alpha^{IIb}\beta_3$, $\alpha^V\beta_1$, $\alpha^V\beta_5$, $\alpha^V\beta_6$ and $\alpha^V\beta_3$), but not by most of the other integrins. Other integrins recognise different amino acid sequences: $\alpha^2\beta_1$ binds Asp-Gly-Glu-Ala (DGEA) in type I collagen, $\alpha^4\beta_1$ binds Glu-Ile-Leu-Asp-Val (EILDV) in fibronectin, and $\alpha^X\beta_2$ binds Gly-Pro-Arg-Pro (GPRP) in fibrinogen. Other binding sites, for other known integrins, have yet to be defined (Hynes, 1992).

Evidence to support the view that fibronectin is involved in cell attachment to collagen fibrils prior to lattice contraction is limited. The majority of workers, with the exception of Gillery *et al.* (1986) have demonstrated that the absence of serum fibronectin (sFN), achieved by using precipitating antibodies or serum-free defined media in the preparation of collagen lattices, has no effect on the contraction of fibroblast populated collagen lattices (Grinnell and Lamke, 1984; Guidry and Grinnell, 1985; Guidry and Grinnell, 1987; Schafer *et al.* 1989; Gullberg *et al.* 1990a; Golubkov *et al.* 1990; Woodley *et al.* 1991). Asaga *et al.* (1991), similarly demonstrated that removal of sFN from serum, prior to the mixing and casting of FPCLs, had no effect on the rate of lattice contraction. They did, however, demonstrate that the application of an antibody to cellular fibronectin (cFN), which is produced by and deposited on fibroblasts within the lattice, clearly suppressed lattice contraction. They also demonstrated that in the presence of the anti-cfn antibody, fibroblasts were unable to elongate and spread, but rather remained

rounded up, thus demonstrating a functional difference between sFN and cFN and clearly implicating cFN in mediating fibroblast-collagen attachment and the subsequent contraction of collagen lattices. The work of Asaga *et al.* (1991) contradicts a similar experiment carried out by Schafer *et al.* (1989) which similarly employed antibodies against cFN and found no effect on lattice contraction. These contradictory observations may be explained by the observation that Asaga *et al.* (1991) employed anti-cFN antibodies at 1mg/ml, whereas Schafer *et al.* (1989) used similar antibodies at a concentration of 200μg/ml.

The proposal that cFN is required to facilitate the binding of fibroblasts to collagen fibres within 3d matrices may find some support in the observation that the application of certain retinoids, known to stimulate the synthesis of fibronectin (King, 1987) has been shown to facilitate more rapid fibroblast mediated lattice contraction (Adams and Preistley, 1988). Further, established and transformed fibroblasts, which secrete little cFN (Olden and Yamada, 1977; Rowe *et al.* 1978), are less able to contract collagen lattices than corresponding cells in primary culture, which secrete significantly more cFN (Steinberg *et al.* 1980; Buttle and Ehrlich, 1983; Kono *et al.* 1990b). However, cellular transformation has also been shown to affect integrin expression, including members of the β_1 family (Plantefaber and Hynes, 1989), which may be an alternative explanation for the reduced ability of transformed cells to contract collagen lattices.

Others have reported that fibroblasts interact directly with collagen fibres rather than using fibronectin as an intermediary. It has been proposed that the addition of synthetic peptides containing the RGD sequence would inhibit lattice contraction if mediated via Fn, by actively competing with one or more of the Fn RGD sequence receptor integrins (i.e. $\alpha^5\beta_1$, $\alpha^{IIb}\beta_3$, $\alpha^V\beta_1$, $\alpha^V\beta_5$, $\alpha^V\beta_6$ and $\alpha^V\beta_3$) on the fibroblast. As lattice contraction has been shown to be unaffected by the addition of such synthetic peptides (Grinnell *et al.* 1989; Gullberg *et al.* 1990a; Golubkov *et al.* 1990), it has been suggested that Fn does not mediate cellular attachment to collagen. This argument assumes that fibroblasts can only bind to fibronectin by integrin recognition of the RGD sequence. It has, however, been reported that cellular binding to fibronectin can occur via an interaction between the integrin receptor $\alpha^4\beta_1$ and the amino acid sequence Glu-Ile-Leu-Asp-Val (EILDV) (Hynes, 1992) i.e. non-RGD dependent adhesion via fibronectin which would not be blocked by the use of synthetic RGD peptides. It would nonetheless appear unlikely that $\alpha^4\beta_1$

is involved in the attachment of fibroblasts to collagen fibrils, via fibronectin, as it has been reported that fibroblasts: (1) are unable to recognise the EILDV sequence of fibronectin using the $\alpha^4\beta_1$ integrin (Dufour *et al.* 1988), (2) express only low levels of the α^4 subunit (Mould *et al.* 1990), and (3) expression of $\alpha^4\beta_1$ is down-regulated during lattice contraction (Klein *et al.* 1991), data which would suggest a lack of involvement of $\alpha^4\beta_1$ in the contraction process. Further, it has been suggested that $\alpha^4\beta_1$ expression is normally associated with the transient collagen adhesion that occurs during cell migration, rather than with the more stable collagen adhesion associated with lattice contraction (Chan *et al.* 1992).

It has been demonstrated, using function blocking antibodies and immuno-fluorescence microscopy, that lattice contraction depends upon the expression of one or more members of the β_1 integrin family (Gullberg *et al.* 1990a; Schiro *et al.* 1991; Klein *et al.* 1991; Mochitate *et al.* 1991). This, taken together with the fact that the addition of synthetic RGD peptides has no effect on contraction (Grinnell *et al.* 1989; Gullberg *et al.* 1990a), suggests that fibroblast attachment to collagen (type 1), within a lattice, is mediated either directly, or indirectly, by non-RGD-dependent β_1 integrin matrix receptors, as distinct from the RGD-dependent fibronectin integrin receptors described above. The observation that fibroblast-mediated lattice contraction was RGD independent was confirmed more recently by Schiro *et al.* (1991) who demonstrated that antibodies which block the classic RGD dependent fibronectin integrin receptor ($\alpha^5\beta_1$) had no effect on lattice contraction.

To discover which integrin of the β_1 integrin family was responsible for the adhesion of fibroblasts to collagen lattice fibrils, Schiro *et al.* (1991) monitored the ability of fibroblasts to contract collagen lattices in the presence of function blocking antibodies to various β_1 integrins. They found that anti-integrin $\alpha^2\beta_1$ was almost as effective at blocking contraction as a pan-specific anti-β_1 monoclonal antibody. Thus suggesting a major role for $\alpha^2\beta_1$ in fibroblast-mediated lattice contraction. The fact that anti-$\alpha^2\beta_1$ was not as effective as pan-specific anti-β_1, which prevents contraction, appears to suggest that another integrin of the β_1 family may be interacting with $\alpha^2\beta_1$ to facilitate lattice contraction. Schiro *et al.* (1991) was unable to demonstrate any inhibition of contraction following fibroblast incubation with antibodies directed against either $\alpha^3\beta_1$ or $\alpha^5\beta_1$ alone, or, any addition inhibition when incubated together with anti-$\alpha^2\beta_1$. The effect of blocking $\alpha^1\beta_1$, which may share the same collagen binding sequence (DGEA) as $\alpha^2\beta_1$ (Gullberg *et al.* 1990b), was not attempted due to

the lack of availability of an anti-$\alpha^1\beta_1$ monoclonal antibody. It would appear that no attempt was made to block $\alpha^4\beta_1$, the non-RGD dependent fibronectin integrin receptor, which, as a member of the β_1 integrin family would be blocked by the pan-specific anti-β_1 monoclonal antibody. However, as mentioned earlier, it would appear unlikely that the $\alpha^4\beta_1$ integrin is involved with fibroblast-fibronectin adhesion (Dufour *et al.* 1988; Mould *et al.* 1990; Klein *et al.* 1991; Chan *et al.* 1992).

Klein *et al.* (1991) also examined the effect of adding various combinations of integrin function blocking antibodies and demonstrated, in agreement with Schiro *et al.* (1991), that function blocking anti-α^2 in conjunction with anti-β_1 most efficiently inhibited fibroblast-mediated lattice contraction. Furthermore, Klein *et al.* (1991) studied the transcription and synthesis of members of the β_1 family and found that $\alpha^2\beta_1$, but not $\alpha^1\beta_1$ or $\alpha^3\beta_1$, is selectively upregulated when fibroblasts are seeded into collagen lattices. Time course experiments revealed that high synthetic levels of $\alpha^2\beta_1$ parallel the lattice contraction process and return to "baseline" levels after active contraction has subsided. Klein *et al.* (1991), like Schiro *et al.* (1991), reported the lack of availability of a function blocking antibody to $\alpha^1\beta_1$, but relying on observations regarding the synthesis and expression of the α^1 subunit during contraction suggested that the likelihood of a major role for α^1 in lattice contraction, was remote.

In contrast to the bulk of the literature, which suggests that fibroblasts adhere to collagen fibrils by recognition of the DGEA sequence (Asp-Gly-Glu-Ala) by the $\alpha^2\beta_1$ integrin, Grinnell *et al.* (1989) reported that lattice contraction could be inhibited by the introduction of synthetic peptides containing the RGE (Gly-Arg-Gly-Glu-Ser-Pro) sequence. The integrin receptor which recognises the RGE sequence has not, as yet, been identified.

From the evidence available, it would appear that the majority of integrin-mediated attachment, and consequently lattice contraction, results from the interaction of fibroblasts directly with collagen molecules via integrin $\alpha^2\beta_1$ recognising the DGEA sequence (Asp-Gly-Glu-Ala). RGD dependent adhesion, whether direct or mediated via fibronectin, would appear not to be involved in the attachment of fibroblasts to collagen fibrils in 3d lattices. There is, as yet, no evidence to suggest that fibroblasts within 3d lattices are able to interact indirectly with collagen, via cellular fibronectin, using the RGD-independent integrin $\alpha^4\beta_1$. However, cellular fibronectin may be involved in non-integrin mediated fibroblast-collagen interaction thus, perhaps, explaining the observations of Asaga *et al.* (1991).

The attachment of fibroblasts to collagen lattices is associated with a change in shape from the spherical (post-trypsinization) form to the elongate/stellate lattice attached form (Nishyama *et al*, 1988). In addition to this initial change in shape, fibroblasts within FPCL have been observed to form long cellular extensions which spread along and wrap around individual collagen fibrils (Bellows *et al*, 1981; Grinnell and Lamke, 1984). The ability of eukaryotic cells to adopt a variety of shapes and to carry out coordinated and directed movements depends on the cytoskeleton, a complex network of protein filaments that extends through the cytoplasm. The cytoskeleton is made up of three principle types of protein filaments: actin filaments (microfilaments), microtubules and intermediate filaments. Each type of filament is formed from a different protein monomer and can be built into a variety of structures according to its associated proteins. Some associated proteins link filaments to one another or to other cell components, such as the plasma membrane. Others control where and when microfilaments or microtubules are assembled in the cell by regulating the rate and extent of their polymerisation. Yet other associated proteins interact with filaments to produce movement, for example muscle contraction (microfilaments) and the beating of flagella (microtubules) (Alberts *et al.* 1989).

The role of the different cytoskeletal components in fibroblast activities associated with the lag phase of collagen lattice contraction has been examined using cyto-skeleton affecting drugs. Tomasek and Hay (1984) reported that either cytocholasin D or nocodazole, which affect microfilaments and microtubules respectively, inhibited the normal elongation of fibroblast within collagen lattices when applied at doses of more than 1μg/ml, thereby, it was suggested, demonstrating that both microfilaments and microtubules are required for processes of fibroblast elongation and spreading. It has also been reported that low doses of cytocholasins (less than 2 μg/ml cyto-cholasin B or 0.25 μg/ml cytocholasin D) applied to 3T3 fibroblasts in monolayer, allow elongation, whereas high doses cause cells to round up (Atlas and Lin, 1978). Nishyama *et al.* (1988) noted that when low doses of cytocholasin D (0.03 - 0.1 μg/ml) were applied to collagen lattice fibroblasts a reduction in the lag phase and more rapid fibroblast elongation was observed. It was suggested that this low dose of cytocholasin D in some way helped cytoskeleton dynamics by its influence on actin (Nishyama *et al.* 1988). Low doses (less than 0.03 μg/ml) of nocodazole or colcemid, both microtubule affecting agents, had no effect

on the lag phase. Such results led Nishyama *et al.* (1988) to suggest that the elongation and spreading of fibroblasts, and consequently lattice contraction, were primarily actin-dependent events.

The processes of cell attachment and spreading appear to be essential to lattice contraction. Cells that have an impaired spreading capacity, either because of cytoskeletal defects, such as of actin in transformed cell lines (Steinberg *et al.* 1980), or, due to the absence of serum within the culture medium (Guidry and Grinnell, 1985), have a decreased ability to contract collagen lattices. Interestingly, cells trapped within collagen lattices supplemented with certain factors, for example the growth factor PDGF, have an enhanced ability to spread along collagen fibres, which has been shown to shorten the lag phase and quicken the onset of rapid contraction (Clark *et al.* 1988). Coincident with cell spreading, collagen fibrils superficial to the area of attachment become more dense and aligned in the plane of cell spreading (Grinnell and Lamke, 1984). This is thought to represent the onset of lattice remodelling which is associated with lattice contraction.

The length of the lag phase, during which no discernable contraction occurs, has been shown to be dependent upon cell density and serum concentration, but independent of collagen concentration over the range 0.3 - 1.5 mg/ml. Increasing the cell density or serum concentration (up to a maximum of 10%), with all other lattice variables fixed, leads to a progressive reduction in the length of this phase (Nishyama *et al.* 1988).

5.4.4.2. The contraction phase

It is widely accepted that the contraction of FPCL is a cell-mediated event (Bell *et al.* 1979; Bellows *et al.* 1981; Ehrlich *et al.* 1989). Precisely how fibroblasts seeded within collagen lattices generate the force necessary for contraction is the centre of some disagreement. As FPCL contraction is widely used as a model of wound contraction (Ehrlich and Rajaratnam, 1990), this disagreement closely parallels, and sustains, the debate (p48) as to the way in which fibroblasts mediate wound contraction and scar contracture (Ehrlich 1988a; Ehrlich 1988b). Like wound contraction, two main theories have been proposed to explain the mechanism behind fibroblast-mediated collagen lattice contraction: the myofibroblast theory and the fibroblast theory. These two theories have been discussed previously (p48), and will only be described in brief here.

The myofibroblast theory

The myofibroblast theory of lattice contraction proposes that collagen lattices contract as a result of a coordinated multi-cellular contraction of myofibroblasts (see p49). According to this theory, myofibroblasts, cells morphologically similar to both fibroblasts and smooth muscle cells (Majno *et al.* 1971), which contain microfilament bundles and display many cell:cell and cell:matrix contacts, shorten as a multi-cellular unit, leading to a closer approximation of attached collagen fibrils. This theory was initially proposed to explain wound contraction (Gabbiani *et al.* 1971) it has since been accepted, by some workers, as a mechanism by which to explain contraction of fibroblast-populated collagen lattices *in vitro* (Dodd *et al.* 1982; Tomasek *et al.* 1989).

The fibroblast theory

The fibroblast theory (Stopak and Harris, 1982; Ehrlich, 1988a; Ehrlich and Rajaratnam, 1990) is primarily associated with cell traction. This theory proposes that fibroblasts neither shorten in length, nor do they act in a multi-cellular manner (as proposed by the myofibroblast theory), but that a composite force, made up of traction forces of many individual fibroblasts, is responsible for lattice contraction. Such traction forces are shearing forces tangential to the cell surface generated during cell elongation and spreading (Stopak and Harris, 1982). This traction force theory is based on the observation that as individual fibroblasts plated onto an elastic surface elongate and spread they cause that surface to wrinkle (Harris *et al.* 1981). This wrinkling is thought to represent a "gathering effect" of the fibroblast on the elastic surface. Fibroblasts within collagen lattices have also been observed to gather together collagen fibrils as they elongate and spread thus leading to compaction of the lattice (Bell *et al.* 1979).

Evidence given in support of the *myofibroblast theory* of lattice contraction invariably comes from FPCL studies carried out on fibroblast seeded lattices that remain attached to the plastic culture dish in which the lattice was polymerised. Such lattices are termed "attached lattices". No decrease in their surface area occurs due to the restriction imposed by petri dish attachment, though a limited reduction in lattice depth and thereby volume has been reported (Guidry and Grinnell, 1985). Fibroblasts within these restricted attached lattices have been observed to assume certain myofibroblastic characteristics including microfilament bundles and fibronexus-like structures (Farsi and Aubin, 1984; Unemori and Werb, 1986;

Mochitate *et al.* 1991; Tomasek *et al.* 1992). If these lattices are "rimmed" some time after polymerisation and the development of these myofibroblastic cells, they undergo a rapid and symmetrical contraction (Dodd *et al.* 1982; Unemori and Werb, 1986; Mochitate *et al.* 1991; Tomasek *et al.* 1992). Rapid contraction occurs within the first 10 minutes after release of the lattice from the substratum, with greater than 70% of this contraction occurring within the first 2 minutes (Tomasek *et al.* 1992). Rapid contraction results in a shortening of the elongate fibroblasts and a compaction of stress fibres with their subsequent disappearance from the cell (Dodd *et al.* 1982; Unemori and Werb, 1986; Mochitate *et al.* 1991; Tomasek *et al.* 1992). It has been suggested that this rapid lattice contraction, termed "recoil", results from the active contraction of these myofibroblastic cells, rather than from the release of cyto-tractile deformation of the matrix, as disruption of the actin cytoskeleton of the cell with cytocholasin D, just prior to release, inhibits this rapid contraction (Dodd *et al.* 1982; Tomasek *et al.* 1992). However, it is possible that this dissolution of the actin cytoskeleton may weaken integrin-mediated cell:matrix attachment and thereby release attached, deformed, matrix from the cell surface.

The majority of evidence in support of the *fibroblast theory* of collagen lattice contraction comes from studies using lattices that had been rimmed soon after polymerisation. These rimmed lattices float beneath the surface of exuded culture medium, and are termed free floating collagen lattices. The surface area, and volume, of such floating lattices diminishes with time (Bell *et al*, 1979). During the contraction of such free-floating lattices cells the majority of fibroblasts do not display the characteristic microfilament bundles (stress fibres), which are associated with the myofibroblastic phenotype (Bellows *et al.* 1982; Ehrlich, 1988a; Tomasek *et al.* 1992). Once active contraction has ceased, fibroblasts expressing myofibroblastic characteristics become more prevalent (Bellows *et al.* 1982; Ehrlich, 1988a), thus suggesting that the myofibroblast form is a consequence either the contraction process itself, or the inhibition of further contraction, rather than the cause.

Actively contracting free floating lattices are known to contain more myofibroblastic cells in the lattice periphery than in more central areas (Bellows *et al.* 1982; Stopak and Harris, 1982; Ehrlich, 1988a). Cells in the myofibroblast-rich periphery show many intercellular contacts, whereas, the cells of the fibroblast-rich interior show few if any intercellular contacts (Ehrlich 1988a). When the contraction of myofibroblast-rich portions of free floating lattices is compared with that of

fibroblast-rich areas, contraction is more rapid in the latter (Ehrlich, 1988a, Ehrlich and Rajaratnam, 1990), thus supporting the role of fibroblastic cells, acting individually, rather than myofibroblastic cells, acting as an intercommunicating group, in free floating lattice contraction. The myofibroblast theory suggests that lattice contraction is brought about by microfilament bundle contraction (Skalli and Gabbiani, 1988). It has been reported that when fibroblasts within collagen lattices are permeabilised with glycerol and their microfilaments induced to contract with ATP, neither cellular contraction, nor a stimulation in lattice contraction, is observed (Ehrlich and Rajaratnam, 1990), thus questioning the ability of cellular contraction to generate sufficient tension within the lattice matrix to facilitate contraction.

It is generally accepted that fibroblasts displaying certain myofibroblastic characteristics are present within both attached and free floating collagen lattices; their role, however, is in question. The appearance of such cells in lattices that are contraction-restricted, either by petri dish attachment or as a result of maximal lattice compaction, suggests that they may develop as a consequence of mechanical hindrance of contraction.

5.4.4.3. Stabilisation

It has been demonstrated that the removal of cells, by either trypsinization or detergent (Guidry and Grinnell, 1986), or the disruption of the cytoskeleton using cytocholasin D (Guidry and Grinnell, 1985) results in only a partial re-expansion of contracted collagen lattices. This partial re-expansion following the 'removal' of the cellular component of the lattice, suggests that cells are partially responsible for holding collagen fibrils of contracted lattices in position. The amount of re-expansion observed, when cells are removed, has been shown to be approximately equal to the amount of contraction that occurred during the 1 to 2 hours prior to removal of cells (Guidry and Grinnell, 1986). Thus suggesting that modifications in collagen fibril arrangement, brought about by cellular activity within the lattice, are. initially stabilised by mechanical activity of cells. This cellular stabilisation would appear to be superseded by collagen fibril stabilisation that is independent of the continued presence of cells, termed chemical stabilisation. As the amount of re-expansion is equivalent to 1 to 2 hours of contraction it would appear that period of time required for reorganised collagen fibrils to be chemically stabilised independent of cells is 1 to 2 hours.

Such chemical stabilisation may involve either covalent or non-covalent cross-linking of collagen fibrils. Comparing the rate of repolymerisation and electrophoretic mobility of resolubilised collagen from contracted lattices and control collagen, Guidry and Grinnell (1985) failed to reveal any permanent structural changes in collagen fibrils that could be attributed to the formation of covalent cross-links. Chemical stabilisation of collagen fibrils would thus appear to result from non-covalent cross-linking of juxtaposed collagen fibrils. It is possible that this non-covalent chemical stabilisation involves the cross-linking of collagen fibrils by extracellular matrix components secreted by cells (such as proteoglycans and glycoproteins). To investigate this possibility Guidry and Grinnell (1986), incubated contracted collagen lattices with trypsin/EDTA, chondroitinase or hyaluronidase, after the removal of cells using detergent. None of these treatments caused any further expansion of lattices beyond that observed with detergent alone, thus suggesting that cell-secreted products were not necessary for stabilisation of rearranged collagen fibrils and that chemical collagen fibril stabilisation results from the formation of direct interfibrillar noncovalent bonds between adjacent fibrils. This conclusion was supported by the observation that collagen fibrils could be reorganised and stabilised by the application of a non-cellular force to collagen lattices, i.e. centrifugation, in the absence of cells or cell products (Guidry and Grinnell 1986).

Collagen lattices reorganised (compacted) by centrifugation (693 x g), like those contracted by cells, demonstrate two mechanisms of stabilisation. When cell-free lattices are centrifuged compaction occurs. When centrifugation is stopped a partial expansion is observed. If lattice centrifugation is carried on for progressively longer periods, then stopped, a re-expansion, equivalent to the last 5 to 10 minutes of centrifugal (693 x g) 'contraction', occurs (Guidry and Grinnell, 1986). The discrepancy between the time taken for stable interfibrillar links to form in centrifuged lattices when compared with those in lattices contracted by fibroblasts is not surprising, as under the experimental conditions employed, centrifuged lattices were 50% 'contracted' in 20 minutes, while fibroblasts contracted lattices to 50% within 4 to 5 hours. Thus, initially, the centrifugal force, equivalent to the mechanical force of the cells, is required to hold the lattice fibrils together; but, with time, interfibrillar bonds develop which stabilise the compacted form, at which point lattices no longer re-expand when centrifugation is stopped.

In summary, during the contraction of collagen lattices by fibroblasts, collagen

fibrils, which have been rearranged by cellular activity, are stabilised in place by two different mechanisms. At first, fibrils are mechanically held in position by cells. Subsequently, the fibrils are stabilised by non-covalent chemical interactions that are independent of cells.

5.4.5. The effect of varying cell number and collagen concentration on fibroblast populated collagen lattice contraction.

Introduction. As the rate of lattice contraction has been reported to be directly proportional to cell number and inversely proportional to collagen concentration (Bell *et al.* 1979; Buttle and Ehrlich, 1983; Nishyama *et al.* 1988; Ehrlich 1988b), it was considered important to determine the most appropriate cell and collagen concentration for subsequent experimental work using this model. The most appropriate cell and collagen concentrations are those that allow contraction to proceed at a rate that is neither so fast nor so slow as to make photographic assessment of contraction difficult. Also very rapid contraction may preclude the manifestation of stimulatory activities; whereas, very slow contraction may preclude the manifestation of inhibitory activities. Other criteria for the most appropriate cell and collagen concentration include: (1) the most economical use of a limited number of p6 human dermal fibroblasts, (2) the most economical use of Vitrogen 100 bovine type I collagen, and (3) ease of lattice preparation.

Method. The standard protocol for the human dermal fibroblast collagen lattice contraction assay was employed (Appendix 10, p344) with some modifications.
Briefly, lattices were prepared at collagen concentrations of either 1.2 mg/ml or 1.6 mg/ml, with p6 human dermal fibroblast concentrations of either 1, 2 or 3 x 10^5 cells per ml, by combining the components, listed below, in various formulations. For formulations see Appendix 16 (p352). Three lattices were prepared for each cell/collagen concentration formulation. Eighteen lattices were prepared in all.
Lattice components:
1. Neutralised collagen (Appendix 10, p344) at 2.4 mg/ml.
2. Ham's F10 medium concentrate (x5)(Appendix 2D, p336).
3. Ham's F10 medium concentrate (x3)(Appendix 2D, p336).

4. p6 fibroblasts in fibroblast growth medium at concentrations of: 4, 6, 8, 12 and 18 x 10^5 cells/ml prepared according to (Appendix 6, p340).

Lattices mixtures were prepared (Appendix 16, p352), dispensed into 35 mm petri dishes, polymerised at 37°C, released (rimmed) and 1 ml of fibroblast growth medium (Appendix 2B, p335) added to each lattice. The lattices were then returned to the 37°C incubator in a humidified box. All eighteen lattices were photographed (Appendix 11A, p345) at 16, 21.4 and 37.8 hours after initial plating and the film developed according to Appendix 11B (p346). The area of each lattice, in mm^2, was then measured by computer-assisted planimetry (Appendix 12, p 347). Median area was calculated for each lattice formulation at each time point (table 5.3) and displayed graphically with minimum and maximum lattices areas (figures 5.8 a/b and 5.9 a/b/c).

Results. From figures 5.8a and 5.8b, showing lattice area (mm^2) versus time, the following points are apparent:

1. For a given collagen concentration, lattices prepared at a cell density of 3 x 10^5 cells/ml contract more rapidly than similar lattices prepared at a cell density of 2 x 10^5 cells/ml which in turn contract more rapidly than similar lattices seeded at a density of 1 x 10^5 cells/ml.
2. Lattices prepared with collagen at 1.2 mg/ml are more sensitive to variation in cell density than lattices prepared with collagen at 1.6 mg/ml, e.g. By 16 hours, lattices with a collagen concentration of 1.2 mg/ml seeded at 1, 2 and 3 x 10^5 cells/ml, contracted to 85, 63, and 40% of their original area respectively; whereas, those lattices with collagen at 1.6 mg/ml seeded at 1, 2 and 3 x 10^5 cells/ml contracted to 89, 83, and 73% of their original area.

From figures 5.9 a/b/c, showing lattice area (mm^2) versus time, the following points are apparent:

1. For a given cell density, lattices prepared at a collagen concentration of 1.2 mg/ml contract more rapidly than similar lattices prepared at a concentration of 1.6 mg/ml.
2. The slowest contraction observed was that of lattices prepared with collagen at 1.6 mg/ml and fibroblasts at a concentration of 1 x 10^5 cells/ml, which contracted to approximately 60% of their original size by 37.8 hours, whereas, the most rapid contraction observed was that of lattices prepared with collagen at 1.2 mg/ml and

fibroblasts at a concentration of 3 x 10^5 cells/ml, which contracted to approximately 15% of their original size.

Statistical analysis was not carried as statistical significance is inappropriate with such a low number of replicate lattices.

Discussion. The results are consistent with literature reports that increasing the cell density or decreasing the collagen concentration within collagen lattices increases the rate of lattice contraction (Bell *et al.* 1979; Buttle and Ehrlich, 1983; Nishyama *et al.* 1988; Ehrlich 1988b). Additionally, it was observed that decreasing collagen concentration amplifies the effect of changing cell number on the rate of contraction (collagen lattices prepared with 1.6 mg/ml of collagen are much less sensitive to increasing cell number than lattices prepared with collagen 1.2 mg/ml).
The formulation of 1.2 mg/ml collagen and 1 x 10^5 p6 human dermal fibroblasts per ml was chosen as the most appropriate cell and collagen combination for subsequent work. This combination is neither too rapid as to prevent photographic assessment or preclude the manifestation of added contraction stimulators, nor is it too slow as to preclude the manifestation of added contraction inhibitors. Of all six lattice formulations examined the 1.2 mg/ml collagen and 1 x 10^5 p6 fibroblast formulation uses the least Vitrogen 100 (bovine type I collagen) at 2.4 mg per lattice and the fewest fibroblasts at 2 x 10^5 cells per lattice.

Conclusions. This study confirmed the ability of cell number and collagen concentration to affect fibroblast populated collagen lattice contraction. It also indicated that at lower collagen concentrations lattice contraction is highly sensitive to cell density. This latter point prompted the generation of a standard protocol for the production of human dermal fibroblast-populated collagen lattices (Appendix 10, p 344), which was used to investigate both the direct effect, and indirect effects (via platelets and macrophages) of therapeutic ultrasound on fibroblast mediated contraction *in vitro*. According to this protocol all the collagen lattices are prepared from a single stock of lattice mixture, which is polymerised for a fixed period of time and then released. After polymerisation and release, lattices are randomly allocated

Table 5.3 The effect of varying both cell number and collagen concentration on the rate of fibroblast populated collagen lattice contraction.

Collagen Concentration (mg/ml)	1.2									1.6								
Fibroblast concentration (cells/ml)	1×10^5			2×10^5			3×10^5			1×10^5			2×10^5			3×10^5		
Time post plating (hours)	16.0	21.4	37.8	16.0	21.4	37.8	16.0	21.4	37.8	16.0	21.4	37.8	16.0	21.4	37.8	16.0	21.4	37.8
Number of lattices	3	3	3	3	3	3	3	3	3	3	3	3	3	3	3	3	3	3
Median lattice area (mm^2)	833.6	624.9	395.7	607.4	293.5	175.7	382.1	203.8	146.5	855.3	744.0	598.4	801.4	657.6	505.7	710.5	549.6	370.4
Minimum lattice area (mm^2)	784.1	617.8	354.6	595 5	276.2	164.9	366.7	200.5	144.8	853.5	738.6	546.0	782.7	516.8	328.9	655.0	366.7	272.3
Maximum lattice area (mm^2)	833.7	639.2	428.4	635.4	369.3	204.3	386.3	215.9	155.2	863.0	756.2	621.2	820.0	672.0	514.3	746.4	560.7	444.4

Figure 5.8. The effect of varying cell number at two different collagen concentrations on the rate of collagen lattice contraction (data range is indicated by bars).

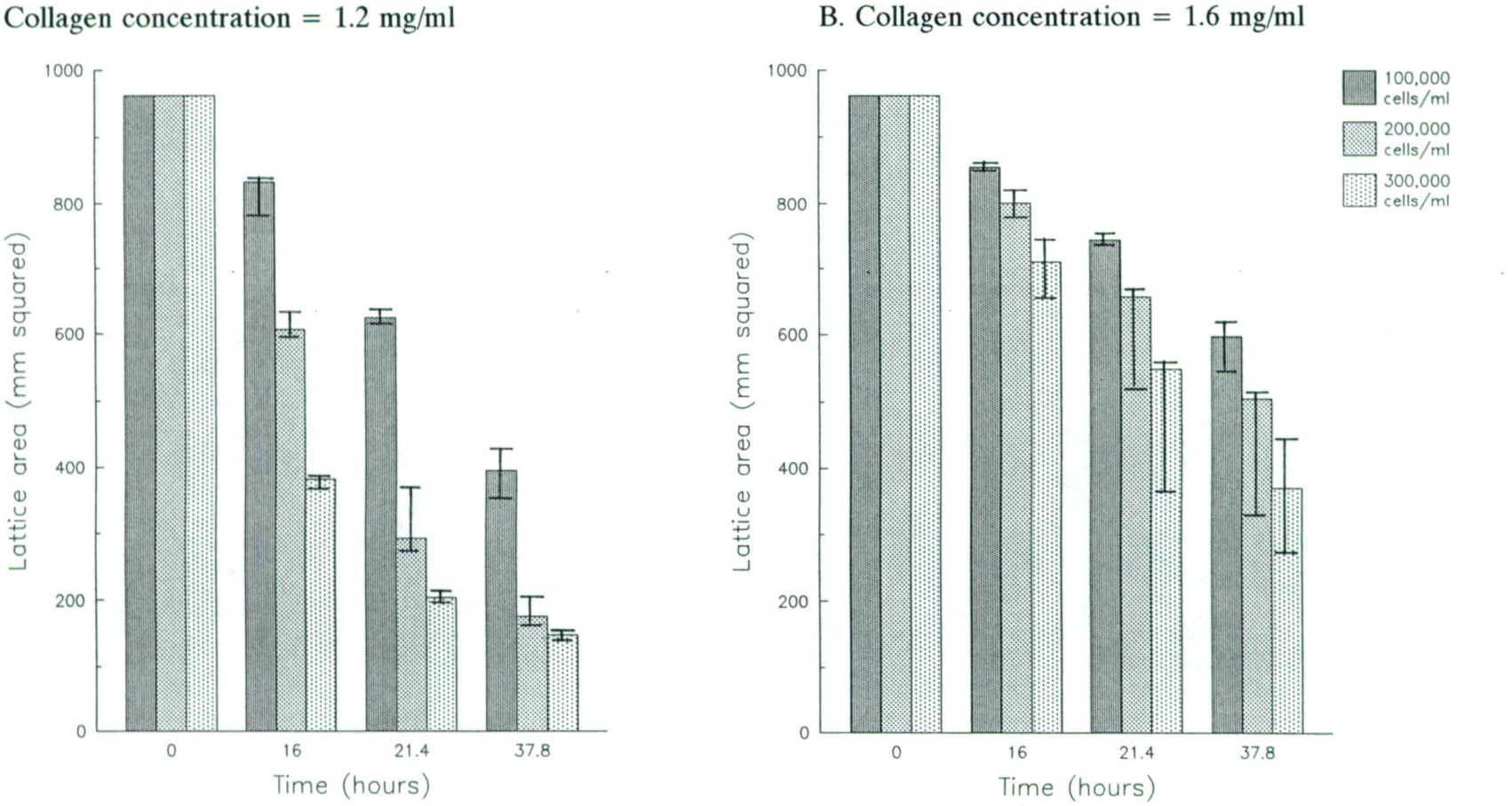

Figure 5.9.

The effect of varying collagen concentration at three cell densities on the rate of collagen lattice contraction (data range is indicated by bars).

A. Cell density = 100,000 cells/ml.

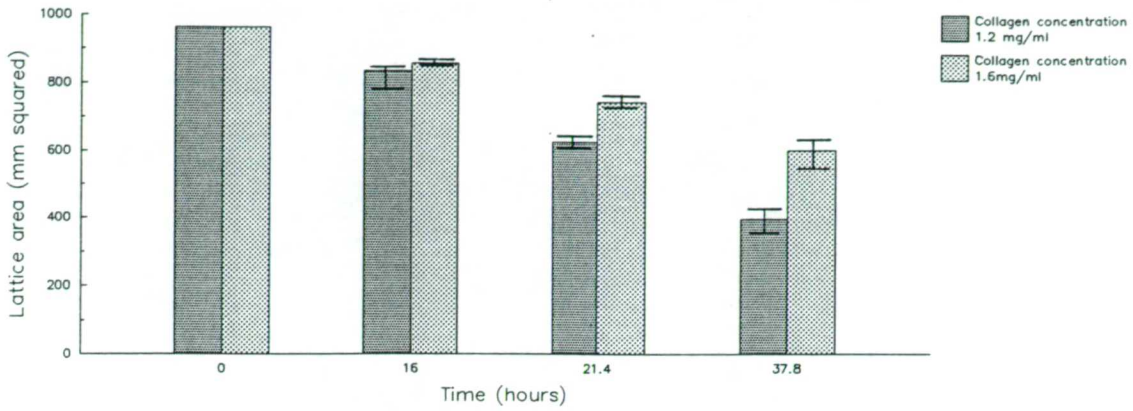

B. Cell density = 200,000 cells/ml.

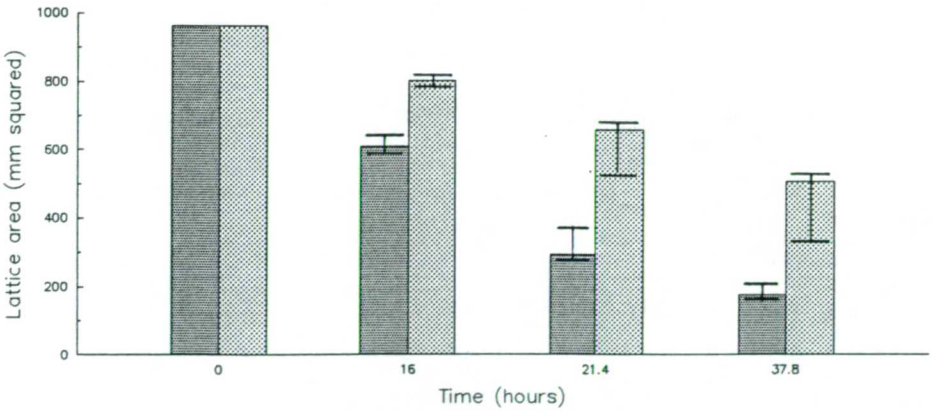

C. Cell density = 300,000 cells/ml

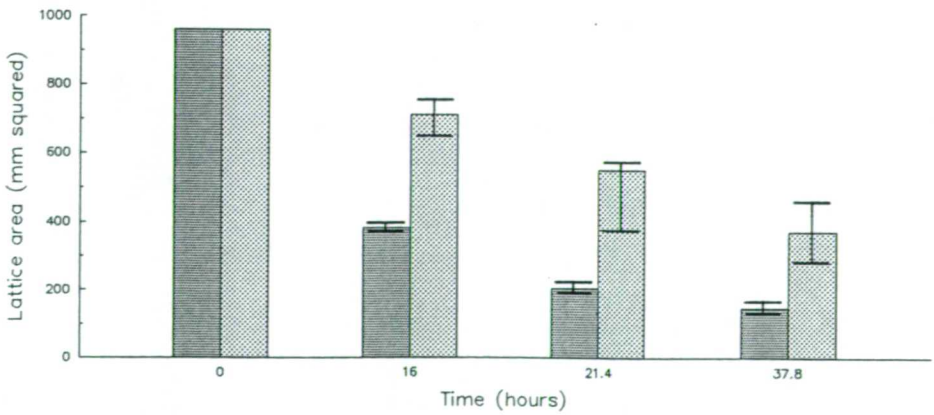

to groups and subsequently treated according to that allocation. Thus at the beginning of a given study, all lattices are the same (i.e. contain the same cell and collagen concentrations), and as such, would contract at the same rate without intervention (i.e. application of ultrasound, macrophage supernatant or platelet releasate). Consequently any change in the rate of lattice contraction observed following a given intervention, be it an increase or decrease, must be a result of that intervention. Lattices prepared at a collagen concentration of 1.2 mg/ml and a cell density of 1 x 10^5 cells/ml were found to be most suitable for further studies.

5.4.6. Examination of the effect of fetal calf serum on the contraction of human dermal fibroblast-populated collagen lattices.

Introduction. Fibroblast populated collagen lattice contraction is enhanced by increasing the serum concentration within the lattice (Steinberg *et al*, 1980; Montesano and Orci, 1988 Nishyama *et al.* 1988). The serum components responsible for stimulating contraction are the centre of some debate. However several polypeptide growth factors, known to be present in serum, have been shown to stimulate fibroblast mediated collagen lattice contraction *in vitro*. Such contraction stimulating growth factors include basic Fibroblast Growth Factor, bFGF, (Finesmith *et al.* 1990), transforming growth factor-β, TGF-β, (Montesano and Orci, 1988; Finesmith *et al.* 1990) and platelet-derived growth factor, PDGF, (Clark *et al.* 1989). The rate of lattice contraction in response to feeding standard collagen fibroblast populated collagen lattices with various concentrations of fetal calf serum (FCS) was examined. This study was performed (1) to confirm that elevating serum concentration increases p6 human dermal fibroblast populated collagen lattice contraction. (2) to examine the sensitivity of the assay to contraction stimulating substances or treatments.

Method. The standard protocol for the Human Dermal Fibroblast Collagen Lattice Contraction Assay (Appendix 10, p344) was employed - with some modifications. Briefly, 15 standard lattices, containing collagen at 1.2 mg/ml and p6 human dermal fibroblasts at a density of 1 x 10^5 cells/ml, were prepared according to steps 1 through 6 of Appendix 10 (p344). After polymerisation and detachment from the petri dish

sides, the 15 lattices were divided into 5 groups of 3. Ham's F10 growth media containing 0, 10, 20, 30 and 40 % FCS and supplemented with 2% penicillin/ streptomycin were prepared. The lattices in each group were fed with a 1 ml aliquot of one of the growth media described above.

The lattices were then returned to the 37°C incubator in a humidified box. All fifteen lattices were photographed (Appendix 11A, p345) at 6.5, 22.5 and 46.5 hours after initial plating and the film developed according to Appendix 11B (p346). The area of each lattice, in mm^2, was then measured by computer-assisted planimetry (Appendix 12, p347). Median area was calculated for each of the five groups at each time point (table 5.4) and displayed graphically with minimum and maximum lattice areas (figure 5.10).

Results From table 5.4 and figure 5.10 (p185) it is apparent that regardless of the FCS concentration all lattices contracted rapidly. At the 6.5 hour time point, the greatest contraction (i.e. 68%) was observed in those lattices fed with 40% FCS. The smallest contraction observed at this time point (i.e. 52%) was observed in those lattices fed with 0% FCS. The levels of contraction in response 30, 20 and 10% FCS were intermediate between these extremes. A similar pattern or contraction was observed for the 2 remaining time points of 22.5 and 46.5 hours.

Discussion. The effect of increasing FCS levels on the contraction of collagen lattices, seeded with p6 human dermal fibroblasts, was examined. At all three time points there was a positive dose dependent relationship between FCS concentration and the amount of contraction observed. Increasing FCS concentration fed to standard lattices enhances lattice contraction. Though statistical analysis of this data is inappropriate due to the small number of replicate lattices, it would appear from figure 5.10 which displays intra-group errors, that this assay is capable of detecting the presence, and discerning the relative concentration, of applied pro-contractile activities.

All lattices within this study contracted significantly faster than expected. If the rate of contraction of lattices fed with 10% FCS, from this study, is compared with the rate of supposedly identical lattices, from the previous validation study (i.e the 1.2 mg/ml collagen & 1 x 10^5 cells/ml lattices, fed with 1 ml of fibroblast growth medium p176), it is apparent that the former contract much more rapidly than the

Table 5.4 The effect on contraction of feeding standardised fibroblast populated collagen lattices with varying concentrations of fetal calf serum.

Time post plating (hours)	6.5					22.5					46.5				
Fetal calf serum concentration added to standard lattices (% FCS)	0	10	20	30	40	0	10	20	30	40	0	10	20	30	40
Number of lattices	3	3	3	3	3	3	3	3	3	3	3	3	3	3	3
Median lattice area (mm^2)	476.0	371.2	363.0	332.4	306.5	309.1	213.5	178.4	150.9	137.4	146.6	124.3	108.8	95.5	87.2
Minimum lattice area (mm^2)	404.8	370.9	343.3	317.9	306.4	284.3	212.1	167.6	147.3	136.7	138.7	123.1	103.9	92.7	86.3
Maximum lattice area (mm^2)	506.8	406.9	377.2	349.2	325.6	312.5	216.6	180.8	151.6	141.2	147.3	127.3	111.4	96.0	88.5

Figure 5.10. The effect of fetal calf serum on the contraction of fibroblast populated collagen lattices (data range is indicated on bars).

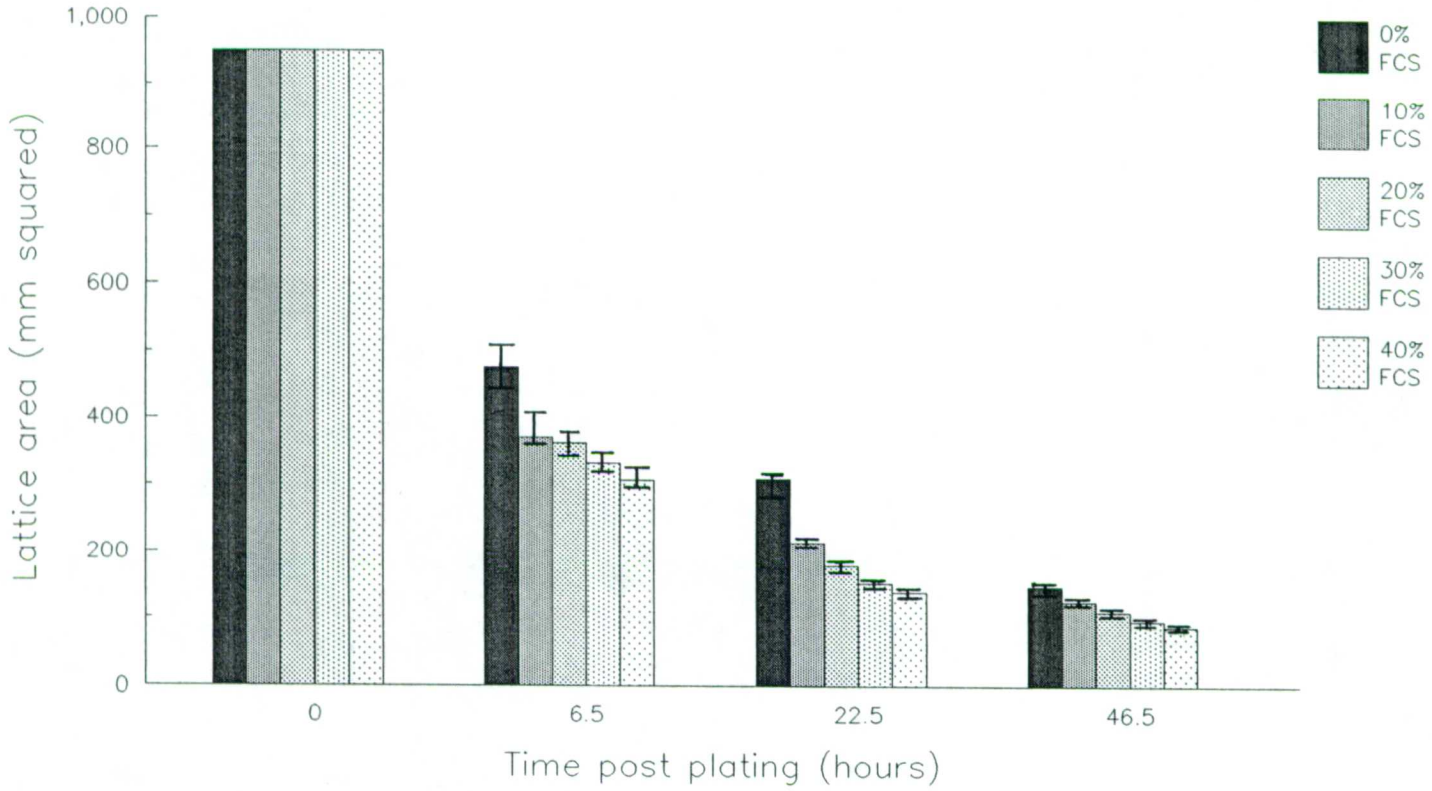

latter. This suggests that even though the preparation of lattices is highly standardised, significant differences can, and do, occur when lattices are prepared on different occasions. As a result of this observation, studies which were repeated on different occasions were only compared on the basis of statistical trends rather by direct comparison of lattice areas.

Conclusion. The contraction of collagen lattices by p6 human dermal fibroblasts responds, as previously observed (Steinberg *et al*, 1980; Montesano and Orci, 1988 Nishyama *et al.* 1988) in a dose dependent fashion to FCS concentration. The standardised human dermal fibroblast collagen lattice contraction assay (Appendix 10, p344) would appear to be a sensitive technique by which to assay for the presence of procontractile activities in a qualitative and quantitative manner.

Chapter 6. Ultrasonic dosimetry

Introduction

This chapter describes the methods used to characterise and standardise the ultrasonic exposure conditions to which animals and cells were exposed in studies carried out in completion of this thesis.

In a list of important parameters of irradiation that should be described when reporting the biological action of ultrasonic beams, Hill (1970) included the following:

1. The total acoustic energy flux across a region of interest (i.e. total acoustic power).
2. The spatial distribution of acoustic energy (i.e. the beam profile); this includes, in particular, the value of spatial peak intensity.
3. The time distribution of acoustic energy (i.e. the pulse shape, or modulation envelope).
4. Temperature change in a tissue consequent on irradiation.

In accordance with Hill (1970), this section will describe the ultrasonic output, as described in free field conditions, generated by an Enraf Nonius 434 therapeutic device, applied to both wound tissues *in vivo* and cell preparations *in vitro*. The dosimetric apparatus used and its application will be described; measurements and observations made will also be reported.

6.1. Total acoustic power

The most commonly used method used to measure the total acoustic power (also called total acoustic energy flux), being generated by a therapeutic ultrasound transducer, is one which relies upon the existence of a fundamental relationship between total acoustic power in a beam incident on a surface and the radiation force per unit area experienced by that surface when the beam is reflected by or absorbed within it (Rooney and Nyborg, 1972). The force exerted on a surface by any form of radiation energy, including ultrasound, corresponds to the rate of momentum transfer from the beam to the surface and, for a perfectly absorbing surface (or one causing 90° reflection of the beam) the radiation force F (newtons) along the beam axis is related to the power intercepted W (watts) by the relation:

$$W = FV$$

Where: V is the wave velocity (ms^{1})

Substituting into the above equation:

W = 1 watt

V = 1500 ms^{-1} (velocity of sound in water)

$$F = \frac{1}{1500}$$

$$F = 6.7 \times 10^{-4} \text{ N}$$

This force is equivalent to the force of gravity acting on a weight of 68.29 mg and as such can be measured on an appropriately modified balance.

i.e.

$$F_g = Mg$$

Where: F_g - is the gravitational force on a body (Newtons)

M - is the mass of a body (kg)

g - is the acceleration due to gravity on that body (9.81 ms^{-2})

hence:

$$M = \frac{F_g}{g}$$

substituting:

$$M = \frac{6.7 \times 10^{-4}}{9.81}$$

$$M = 6.829 \times 10^{-5} \text{ kg}$$

which is: $\underline{M = 68.29 \text{ mg}}$

Thus a total ultrasonic output of 1 watt from a ultrasonic transducer will give a balance deflection of 68.29 mg. This radiation force is independent of frequency.

1 watt total acoustic output = 68.29 mg

6.1.1. Force balance

The force balance used in this study (figure 6.1) was custom manufactured by Enraf Nonius Delft (Holland). In this balance a hollow aluminium wedge (the target), which is immersed in a water bath, is coupled to a standard laboratory digital top pan balance (Sartorius, Germany) by means of a 'U' shaped connecting rod. The aluminium wedge at the end of the connecting rod is orientated in such a way that the hypotenuse of the wedge makes an angle of 45° to the vertical (figure 6.2). The transducer whose beam is to be calibrated is mounted in a vertical orientation immediately above the wedge. The critical angle for acoustic reflection at a water/aluminium interface is 14°; the beam incident upon the wedge is thus totally reflected into a horizontal orientation and terminates in an absorbing structure consisting of a 'V' shaped rubber wedge.

In routine use it is found necessary to delay measurements for a period of 1 hour after setting up, in order to ensure temperature equilibration of the contents of the water bath.

Using this fundamental relationship between total acoustic power (watts) and radiation force (newtons), and knowing the effective radiating area (ERA) of the transducer under examination (section 6.2.5., p206), the average ultrasonic intensity generated for a given therapeutic device output can be measured using this balance. Average ultrasonic intensity, in the sense used above, is more correctly termed the spatial average intensity ($I^{(a)}$) and is usually expressed in terms of W/cm^2 (section 2.4, p84). For example, if a transducer with an ERA of 1 cm^2 is set to deliver continuous wave ultrasound and gives a force balance reading of 68.29 mg the spatial average intensity ($I^{(a)}$) generated is 1 W/cm^2.

If the same ultrasound generator is then set to give pulsed ultrasound (e.g. 2ms on : 8ms off), without any change in intensity, the force balance because of its speed of response would then read 13.66 mg. Having pulsed the ultrasonic output, the terminology used to describe the intensity of the field becomes more complicated (section 2.4, p84). The average intensity during the pulse (i.e. the "on" time) is termed the spatial average pulse average intensity ($I^{(SAPA)}$), whereas, the average intensity during one pulse repetition period (i.e. the "on" time plus "off" time) is termed the spatial average temporal average intensity ($I^{(SATA)}$). For the example above, the $I^{(SAPA)}$ and $I^{(SATA)}$ values are 1 W/cm^2 and 0.2 W/cm^2 respectively.

Figure 6.1. Total ultrasonic power is often measured using a force balance. This balance was custom made by Enraf Nonius Delft (Holland).

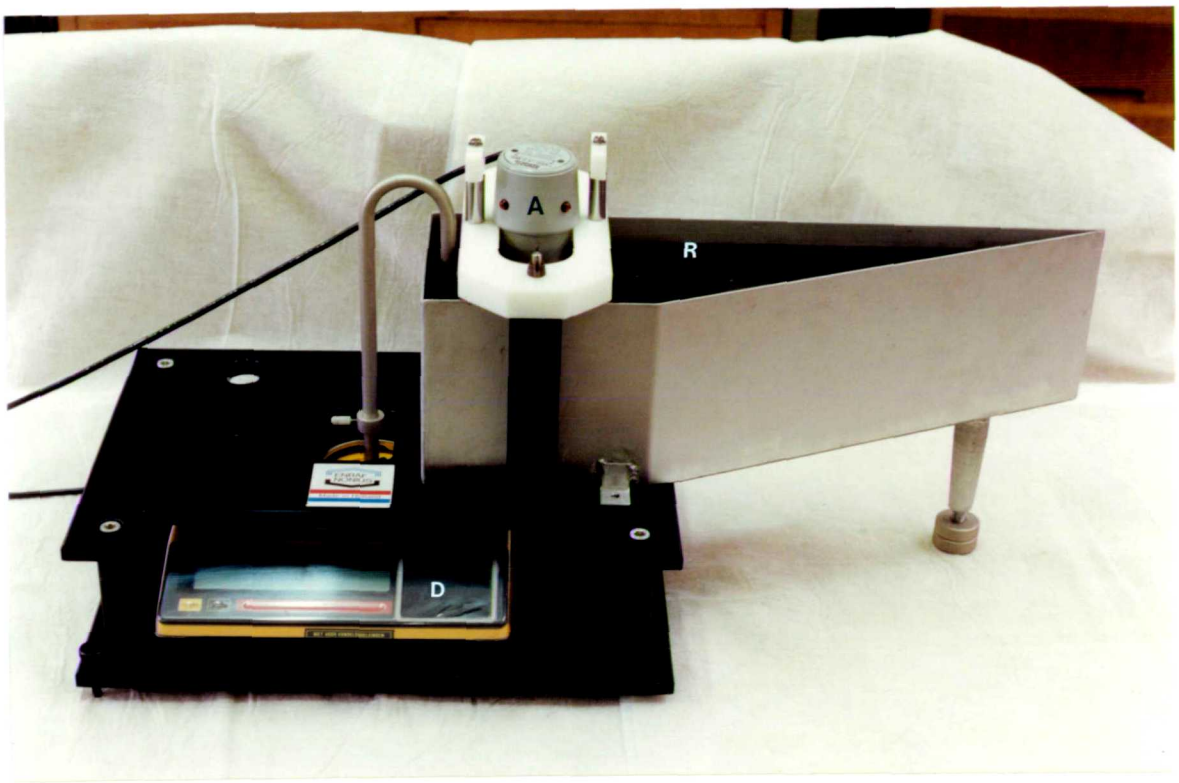

Key:

A = Applicator head

R = Absorbent rubber wedge

D = Digital top pan balance

Figure 6.2. Partially dismantled force balance showing the arrangement of the applicator head (containing the transducer), the 45° aluminium wedge (the target) and its connection via a 'U' shaped connecting rod to the top pan balance. The water bath was removed for photographic purposes.

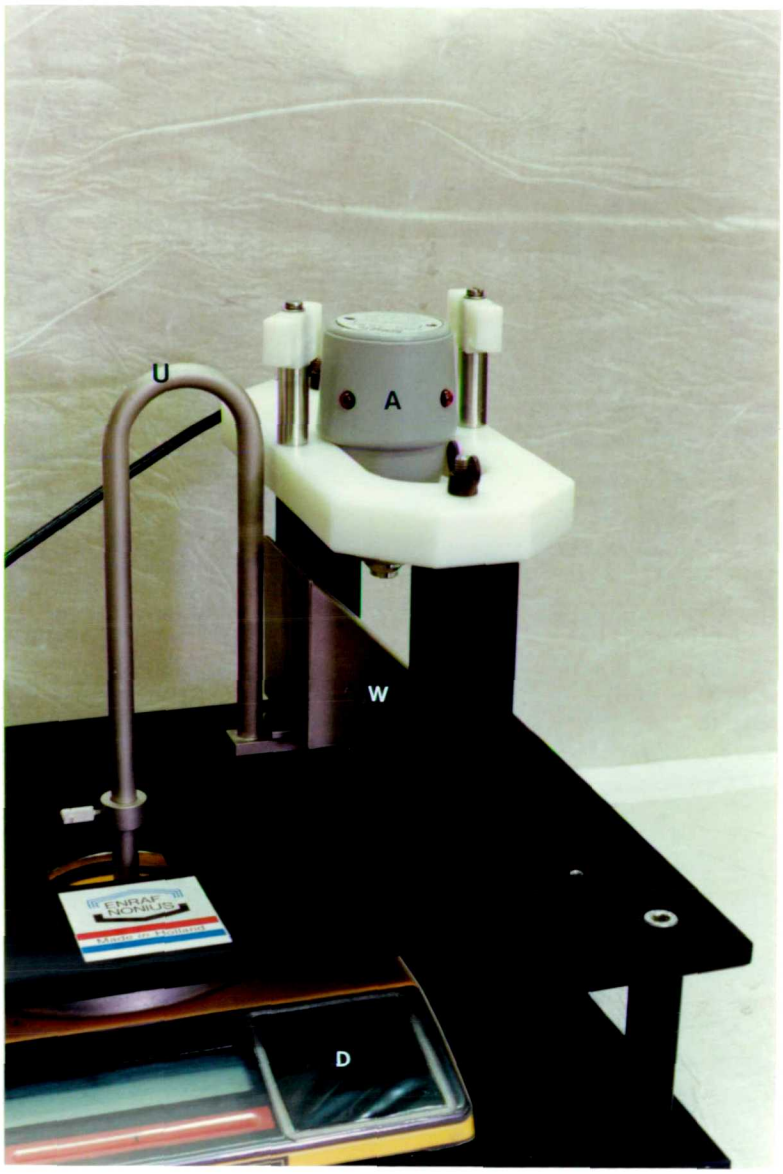

Key:

A = Applicator head

W = 45° Aluminium wedge

U = 'U' Shaped connecting rod

D = top pan digital balance

In setting, or resetting, the ultrasonic intensity level prior to, and during, experimental investigation, the balance reading (in mg) commensurate with the required $I^{(SAPA)}$, or $I^{(SATA)}$, value was calculated taking into account the effective radiating area (ERA calculation section 6.2.5. p206) of the transducer in use. The transducer was then positioned on the radiation force balance and the intensity increased until the calculated balance reading had been achieved.

For example, one experimental regime used in this thesis required pulsed (2ms on : 8 ms off) 3 MHz ultrasound at an intensity of 0.5 W/cm^2 $I^{(SATA)}$ (i.e. $I^{(SAPA)}$ of 2.5 W/cm^2). The ERA of the transducer was 0.5 cm^2. The calculated force balance setting required to obtain this intensity, for such a transducer in pulse mode (2ms on : 8 ms off), is 17.07 mg. This is calculated as follows:

The force balance setting for a 1cm^2 transducer delivering 0.5 W/cm^2 $I^{(SATA)}$ is 34.15 mg, which is half of that required for a 1cm^2 transducer delivering 1 W/cm^2 i.e. 68.29 mg. As the ERA of the transducer is 0.5cm^2, rather than 1cm^2, the former figure must be halved again to get the desired force balance setting of 17.07 mg. Table 6.1 shows the calculated balance settings for both of the ultrasound intensities used in this thesis.

Table 6.1. Calculated balance settings for intensities used throughout this thesis.

Required Intensity $I^{satp)}$ (W/cm^2)	Required Intensity $I^{(SATA)}$ (W/cm^2)	Effective Radiating Area (ERA) (cm^2)	Balance setting (mg)
2.5	0.5	0.48	16.39
0.5	0.1	0.48	3.28

6.2. The spatial distribution of acoustic energy

The volume into which energy passes from the transducer is known as the sound field. In this study, as with many clinical exposures, ultrasound was applied such that the tissue under treatment was within a few centimetres of the transducer face i.e. in the near field. As previously explained (section 2.3, p80) ultrasonic intensity within the near field can vary significantly from position to position. To examine this heterogeneous spatial distribution of acoustic energy, beam profile measurements

were carried out using piezoelectric hydrophones. Unlike the piezoelectric material in applicator head transducers, which convert electrical energy into ultrasonic energy, piezoelectric hydrophones convert the acoustic energy (pressure) of the sound field into electrical energy. When properly calibrated, the hydrophone output, measured in volts, can be precisely converted into pressure amplitude, measured in atmospheres, bars or mega pascals (MPa) (where 1 atmosphere ≡ 1 bar = 0.1 MPa) experienced within the field.

Hydrophone measurements of ultrasonic fields serve three main purposes: generation of beam profiles, assessment of peak pressure amplitude and assessment of effective radiating area.

1. Generation of beam profiles

This gives an overall impression of the distribution of energy within the sound field. Such profiles also supply information regarding the physical condition of the transducer element within the applicator. Fractured or poorly mounted transducers may have areas that are incapable of emitting sound. If the experimentalist, or clinician, is unaware of such a problem, and is simply using the nominal output of the generator to set the exposure intensity, the treatment area may be under exposed. Alternatively, if the intensity is set using a force balance, it is likely that peak ultrasonic intensities, of a possibly deleterious nature, will be required to compensate for the damage to the transducer.

2. Assessment of peak pressure amplitude

Once measured, the peak pressure amplitude can be used to calculate the spatial peak ultrasonic intensity (Ip) within the sound field. The involvement of cavitation, which is associated with Ip, in the therapeutic use of ultrasound is still open to question. As explained earlier (section 3.2.1.3. p99) the likelihood of cavitation occurring is dependent upon many factors. One major factor is thought to be the pressure change caused by the ultrasound wave (i.e. the variation in acoustic pressure amplitude). The threshold negative ultrasonic pressure required for the occurrence of cavitation is thought to be in the region of 0.1 MPa; the more the peak negative pressure amplitude exceeds this value then the greater the probability of generating cavitational activity within treated tissues (Williams, 1987). Thus by measuring the peak negative ultrasonic pressure in a sound field, it is possible to state the likelihood of the involvement of cavitation for a given observed bioeffect. It must be borne in

mind, however, that data on the sound field distribution within "loss less" media, such as water, is taken under effectively "ideal" conditions; and, as such, extrapolation to the sound field experienced by tissue under treatment, where significant attenuation is known to occur, is at best tenuous.

3. Assessment of effective radiating area (ERA)

This involves the generation of a beam profile by scanning the hydrophone across the face of the transducer. As previously mentioned, to set an ultrasonic transducer to accurately deliver the desired ultrasonic intensity, using a force balance (as described above), the ERA of the transducer must be known. The ERA is normally calculated from a pressure amplitude profile obtained by scanning some form of piezoelectric hydrophone across the applicator face during ultrasonic emission. The United States - Food and Drug Administration (US-FDA) definition of ERA is: the area consisting of all points of the effective radiating surface at which the intensity is 5% or more of the maximum intensity (I max) (Ferguson, 1985). Once the ERA is known, the force balance can be set and the desired spatial average intensity ($I^{(a)}$) generated. The US-FDA do not, however, state the distance in front of the transducer at which such measurements should be made. The effective radiating area measurements made in completion of this thesis were undertaken, following the directives of the US-FDA, at a distance of 0.5 cm from the transducer face. Such a distance was selected as it approximates to the position of the biological targets used experimentally.

6.2.1. The production of beam profiles

Lateral beam profiles, which are hydrophone scans across the sound field parallel to the transducer face, were carried out using the apparatus shown in figure 6.3 (drawn schematically in figure 6.4). The apparatus consists of a perspex tank, lined with an ultrasound absorbing material (dimpled rubber car matting) to reduce ultrasonic reverberations, and filled with degassed distilled water. The internal dimensions of the tank were 52 cm long, 22 cm wide and 25 cm deep. The treatment head (or applicator) containing the transducer to be examined was immersed in the tank and clamped firmly in position, directed along the long axis (z) of the tank in a horizontal fashion. The ultrasound detecting apparatus, a polyvinylidene difluoride (PVDF) piezo-electric membrane hydrophone (figure 6.5) with a 1.0 mm diameter sensitive element (Marconi, England), was clamped onto a mobile fixture within the tank. This fixture provided x, y and z movement throughout the tank. The hydrophone could

Figure 6.3 Arrangement of beam profiling apparatus
(Absorbent rubber matting removed for photograph)

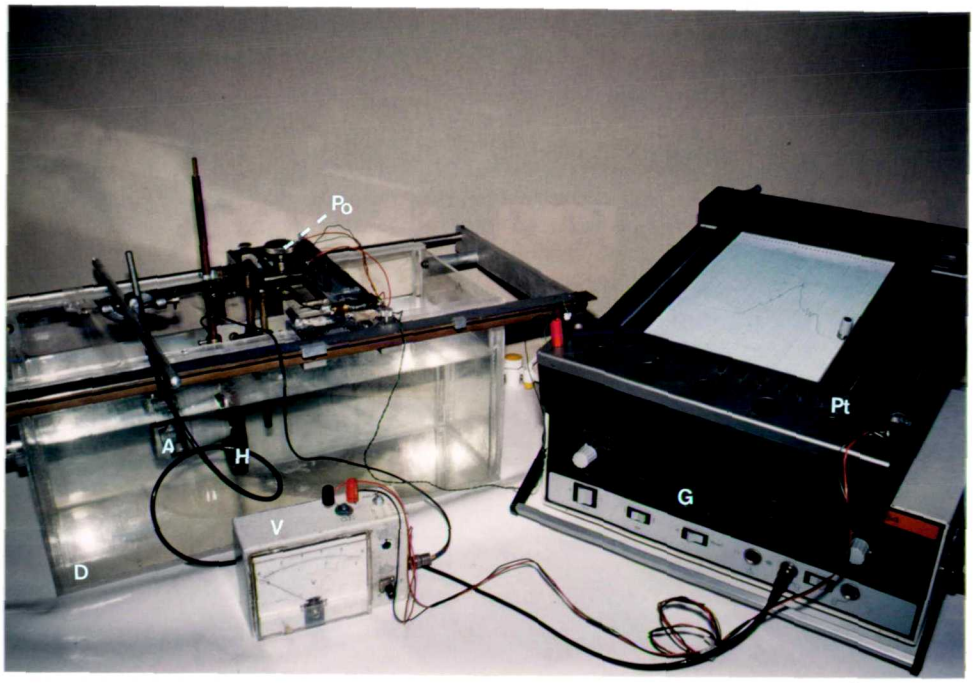

Key:

A = Applicator head

D = Degassed distilled water

H = PVDF membrane hydrophone (Marconi, UK)

Po = Linear potentiometer

Pt = X-Y Plotter

V = Variable gain video amplifier and diode bridge

G = Ultrasound generator

Figure 6.4 A schematic drawing of the beam profiling apparatus
(Absorbent rubber matting omitted)

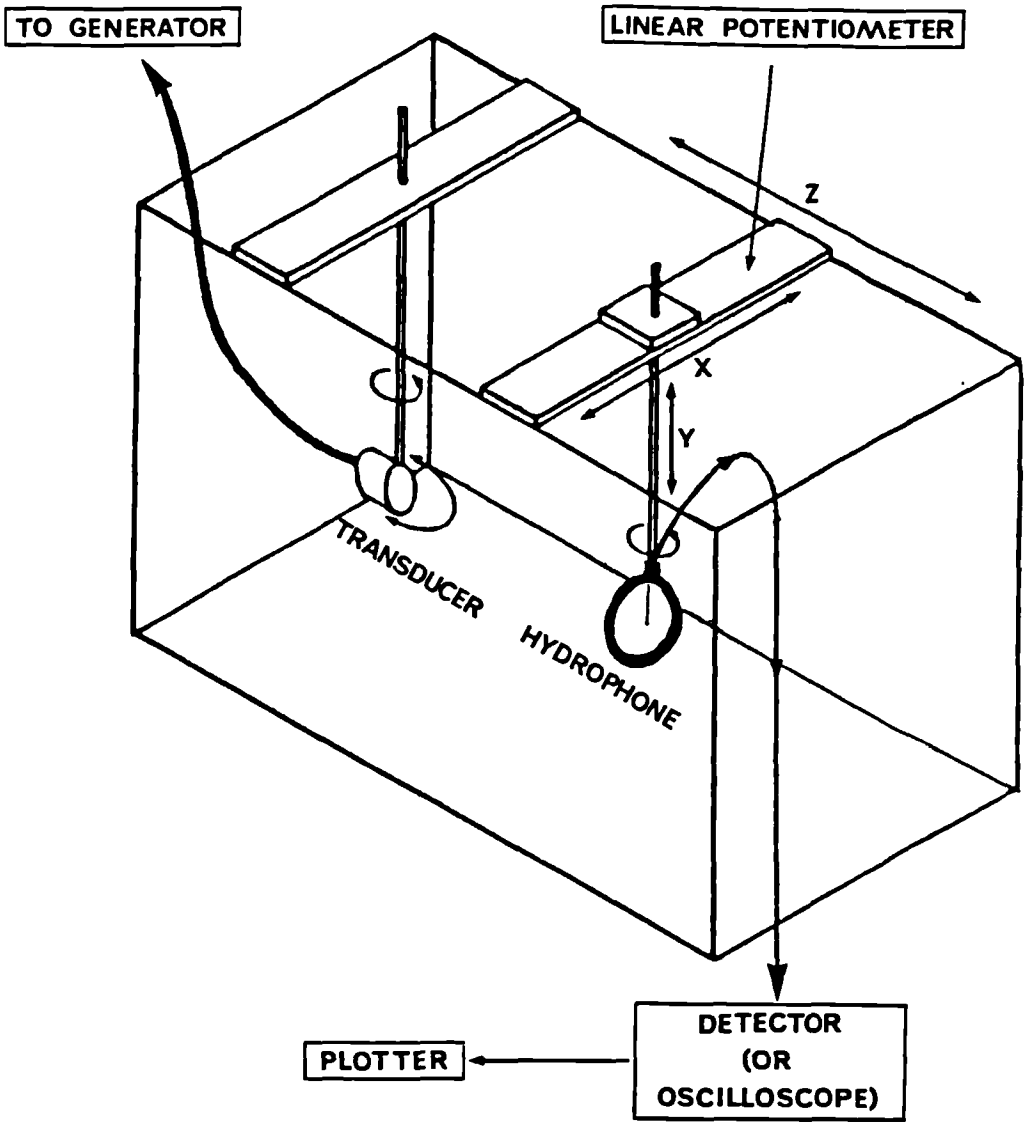

Figure 6.5 The Marconi polyvinylidene difluoride (PVDF) membrane hydrophone

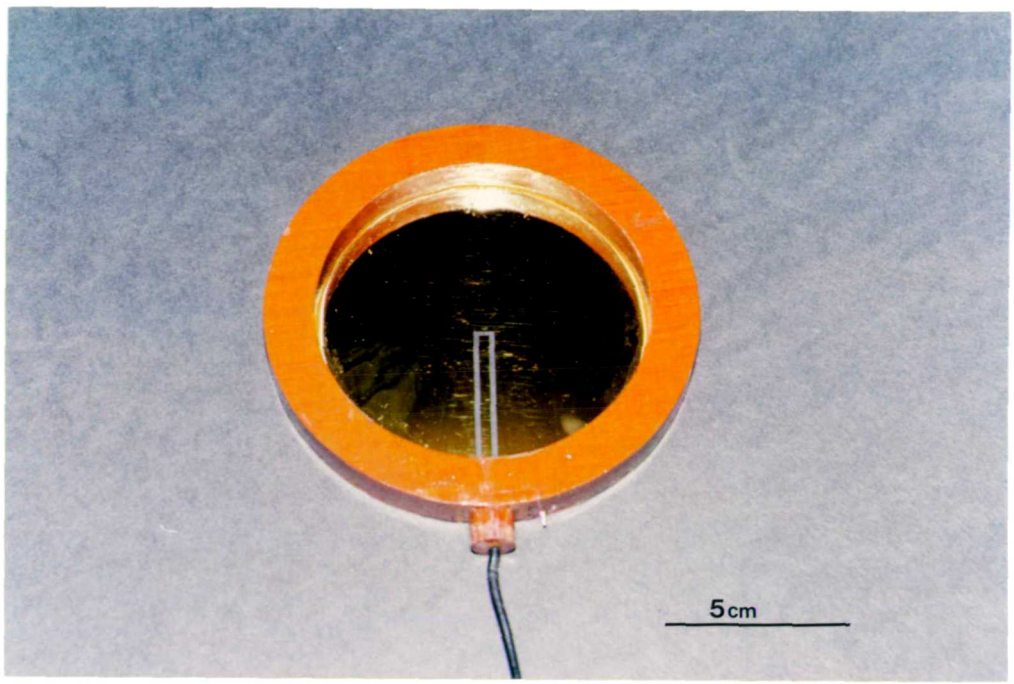

also be rotated about its vertical axis. For beam profile work in this thesis the hydrophone was positioned 0.5 cm in front of the treatment head, such that the detecting surface of the hydrophone was parallel to the emitting face of the treatment head.

The following semi-automated technique was used initially to obtain beam profiles for the calculation of transducer ERA at a nominal intensity, and subsequently to examine the spatial distribution of ultrasonic energy within the beam at the two calculated intensity settings used in this thesis (i.e. 0.5 W/cm^2 $I^{(SATA)}$ {2.5 W/cm^2 $I^{(SAPA)}$} and 0.1 W/cm^2 $I^{(SATA)}$ {0.5 W/cm^2 $I^{(SAPA)}$}). A detector was constructed using a variable gain video amplifier (NE592) linked to a diode bridge, and the gain was set so that as the hydrophone was scanned through the sound field, the amplified output remained within the linear region of the bridge. The result was a rectified voltage proportional to acoustic pressure which was used to drive axis Y of an X-Y plotter (JJ Instruments, model PL4). X of the plotter was fed from a linear potentiometer attached to the mobile hydrophone positioning device, which gave a fixed voltage for a given hydrophone location within the sound field. The arrangement was such that a curve of acoustic pressure versus linear displacement, across the transducer face, was produced immediately on sweeping the hydrophone through the sound field. All beam profiles were carried out at room temperature (19 - 22°C).

Beam profiles were made of the transducer under both free field and experimental conditions. Free field beam profiles, carried out in degassed water, in the absence of any biological tissue exposure apparatus (such as couplants or exposure chambers), were made at both the experimental ultrasonic intensities used. Similar profiles were made to show any modification of the sound field by the biological tissue exposure apparatus used in both *in vivo* and *in vitro* studies. Thus for both of the ultrasonic intensities, 0.5 W/cm^2 $I^{(SATA)}$ (2.5 W/cm^2 $I^{(SAPA)}$) and 0.1 W/cm^2 $I^{(SATA)}$ (0.5 W/cm^2 $I^{(SAPA)}$), the following beam profiles were carried out:

1. Free field profile (used to calculate ERA).
2. Field profile with transducer emitting through the wound dressing and ultrasound transmitting medium Geliperm (*in vivo* studies).
3. Field profile with transducer emitting through chamber window (*in vitro* studies).

The beam profiles generated in this way are shown in figures 6.6 and 6.7.

Figure 6.6 The spatial distribution of ultrasonic energy within the beam with the ultrasonic generator set to deliver 0.5 W/cm^2 $I^{(SATA)}$ (2.5 W/cm^2 $I^{(SAPA)}$).

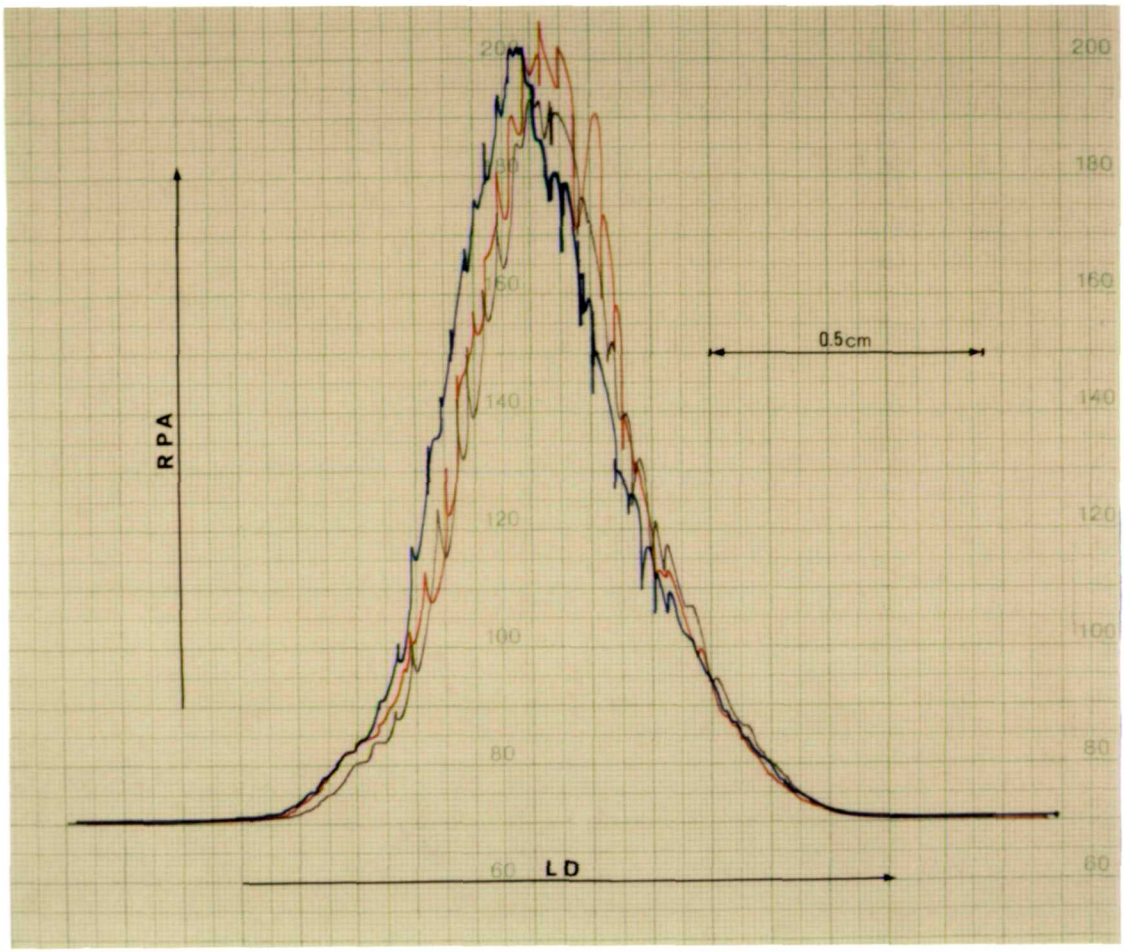

Key: RPA = Relative Pressure Amplitude

LD = Linear Displacement across transducer

Black trace = free field conditions

Blue trace = after introduction of *in vivo* exposimetry apparatus

Red Trace = after introduction of *in vitro* exposimetry apparatus

Figure 6.7 The spatial distribution of ultrasonic energy within the beam with the ultrasonic generator set to deliver 0.1 W/cm^2 $I^{(SATA)}$ (0.5 W/cm^2 $I^{(SAPA)}$).

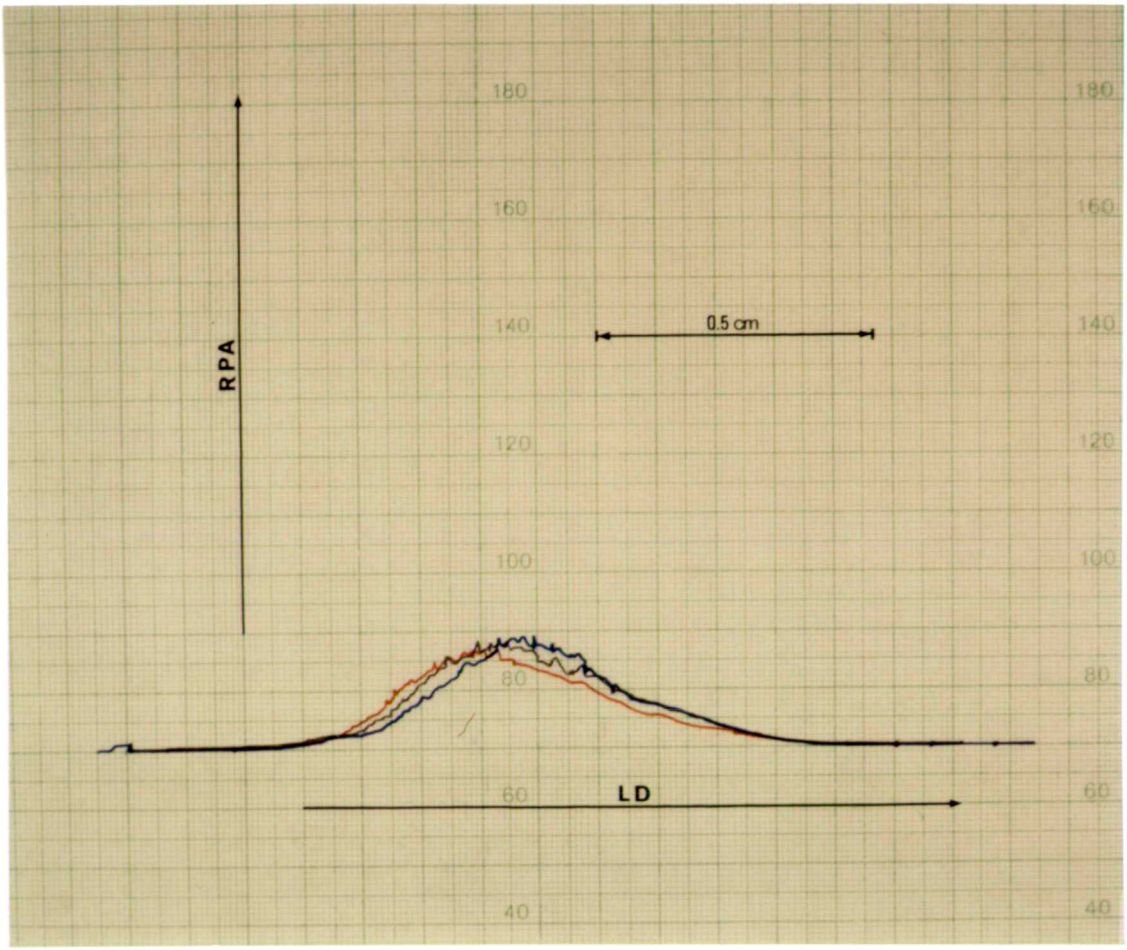

Key: RPA = Relative Pressure Amplitude

LD = Linear Displacement across transducer

Black trace = free field conditions

Blue trace = after introduction of *in vivo* exposimetry apparatus

Red Trace = after introduction of *in vitro* exposimetry apparatus

6.2.2. Interpretation of beam profiles

It can be seen from the beam profiles (figures 6.6 and 6.7), where the X axis represents linear distance across the transducer and the Y axis relative amplitude, that the applicator head is emitting ultrasound from all points along the diameter of the element which was scanned. The sound field produced under 'free field' conditions is characterised by a single pressure peak which approximates to the centre of the transducer. As the hydrophone scans towards the centre of the transducer the pressure amplitude increases in an apparently exponential manner. Such a pressure distribution is characteristic of 3 MHz therapeutic ultrasound transducer sound field profiles taken in the near field. Further, the beam profiles taken within the same sound field, following the introduction of either *in vivo* or *in vitro* exposimetry apparatus, appear not to have suffered any significant modification as a result, although, this, it may be argued, may result from a lack of sensitivity in the detection system.

Computer controlled hydrophone scanning systems have been developed to obtain an overall impression of the distribution of acoustic energy within a given plane perpendicular to the sound beam axis (parallel to the transducer face). They employ similar apparatus to that described here (for the generation of two dimensional beam profiles) to carry out sequential beam profiles across the transducer surface. Each scan through the field is separated by a short distance, as little as 0.25 mm, from the next. Computer controlled hydrophone measurements, within each scan, are taken in the order of one every 0.25 mm. This minute manipulation between, and within, scans is clearly beyond the limits of human dexterity and is consequently executed by very precise stepper motors; again under computer control. The three dimensional scans generated in this way are termed Raster scans. Such a scanning system was used to supply an overall impression of the sound field generated by the Enraf Nonius transducer used in this thesis (figure 6.8). Staff at the National Physical Laboratory (Teddington, UK) kindly performed this Raster scan on my behalf using a PVDF point hydrophone with a 0.6mm diameter sensitive element. From figure 6.8 the axial symmetry of the sound field can be appreciated. In confirmation of the single scan beam profiles, the Raster scan illustrates that ultrasound is being generated from all areas of the transducing surface, with the greatest pressure peak co-axial with the centre of the transducer. Unlike the single profiles, the Raster scan clearly detected additional pressure peaks

Figure 6.8 Raster scan of the sound field generated by the 3 MHz transducer used in these investigations.

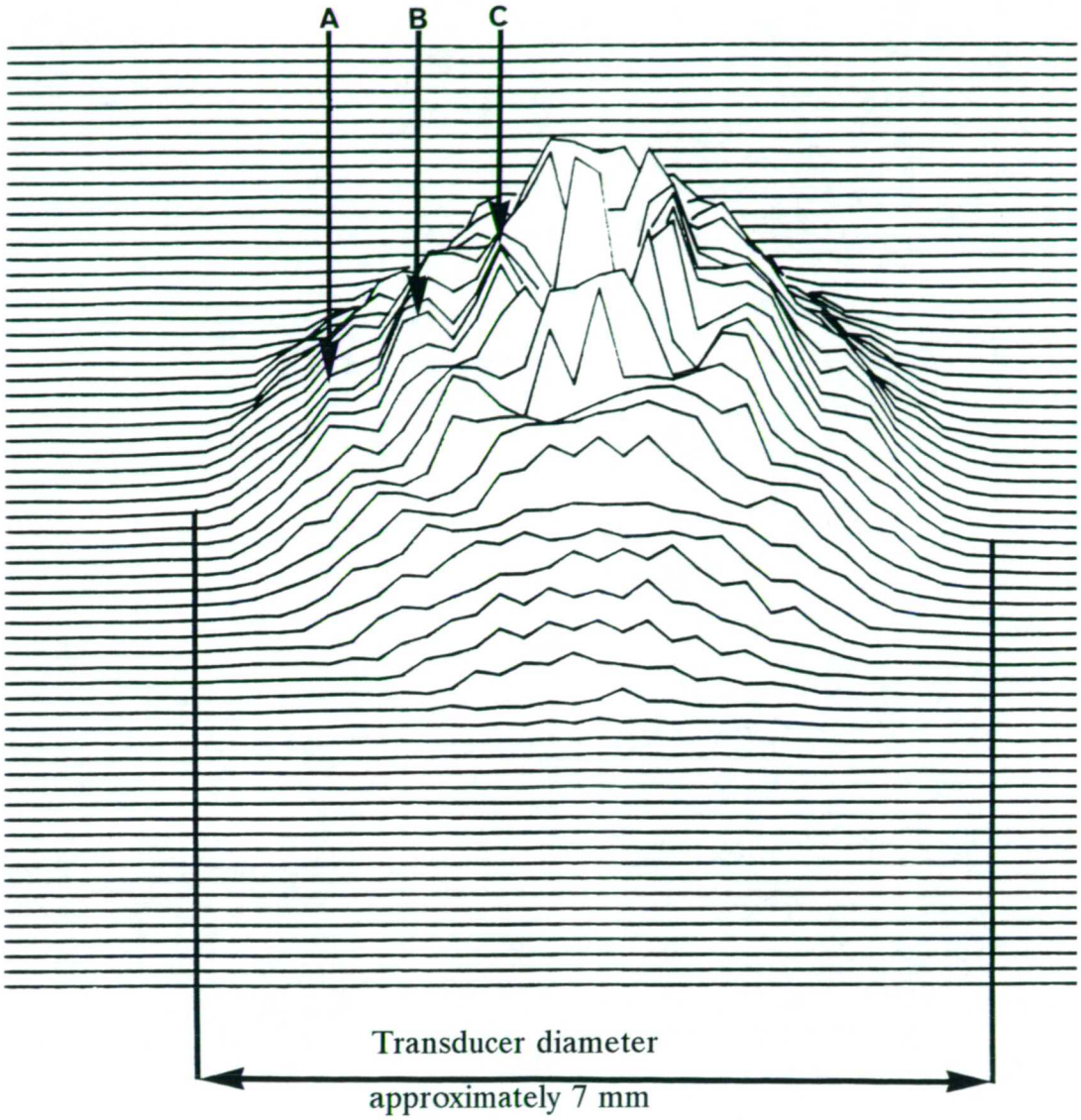

Raster Scan Information:

1. Enraf Nonius generator emitting 3 MHz continuous ultrasound
2. Nominal total power output 0.35 watts
3. Nominal spatial average power 0.7 W/cm^2
4. Scan separation 0.3 mm
5. Step size between measurements 0.5 mm
6. Area of scan 324 mm^2
7. Hydrophone measurement points on scan 3721
8. PVDF needle hydrophone used (0.6 mm diameter sensitive element)

concentric with the axial peak mentioned above (see A, B and C; figure 6.8). This probably results from the greater spatial resolution associated with the smaller point hydrophone used to generate the Raster scan (0.6 mm diameter sensitive element) as compared with the Marconi membrane hydrophone (1.0 mm diameter sensitive element) used for the single scan beam profiles.

6.2.3. Spatial Peak Pressure Amplitude (Spatial Peak Intensity (Isp))

Using the apparatus described earlier (p194) for the production of lateral beam plots, the spatial peak pressure amplitude, for a precalculated force balance setting, was initially located and measured using the PVDF membrane hydrophone (Marconi, U.K.). The hydrophone was directly connected to a calibrated Hitachi V-656 F measuring oscilloscope (figure 6.9) and the on-screen voltage observed while the hydrophone was swept through the sound field. Once located, the peak screen voltage was converted into peak pressure amplitude according to the calibrated sensitivity of the hydrophone for the ultrasonic frequency in use. The hydrophone used was calibrated by the National Physical Laboratory (NPL) (Teddington, U.K.) and was found to have a sensitivity of 0.185 μV/Pa at a frequency of 3 MHz. From this measure of peak pressure amplitude it is possible to calculate the spatial peak intensity (Isp) of the area of the sound field in which the scan was made. Such measurements and subsequent calculations were made initially from sound fields generated under free field conditions (i.e. in the absence of any *in vivo* or *in vitro* exposimetry equipment) at both the ultrasonic intensities studied. Any modification to the peak pressure, and hence Isp, within the sound field resulting from the introduction of either *in vivo* or *in vitro* exposimetry apparatus was then studied. Table 6.2 shows the peak voltages observed, and their corresponding spatial peak pressure amplitude and spatial peak intensity (Isp) values, for each of these calibration arrangements.

Figure 6.9 Arrangement of beam profiling apparatus for the measurement of spatial peak intensity (Isp).
(Absorbent rubber matting removed for photograph)

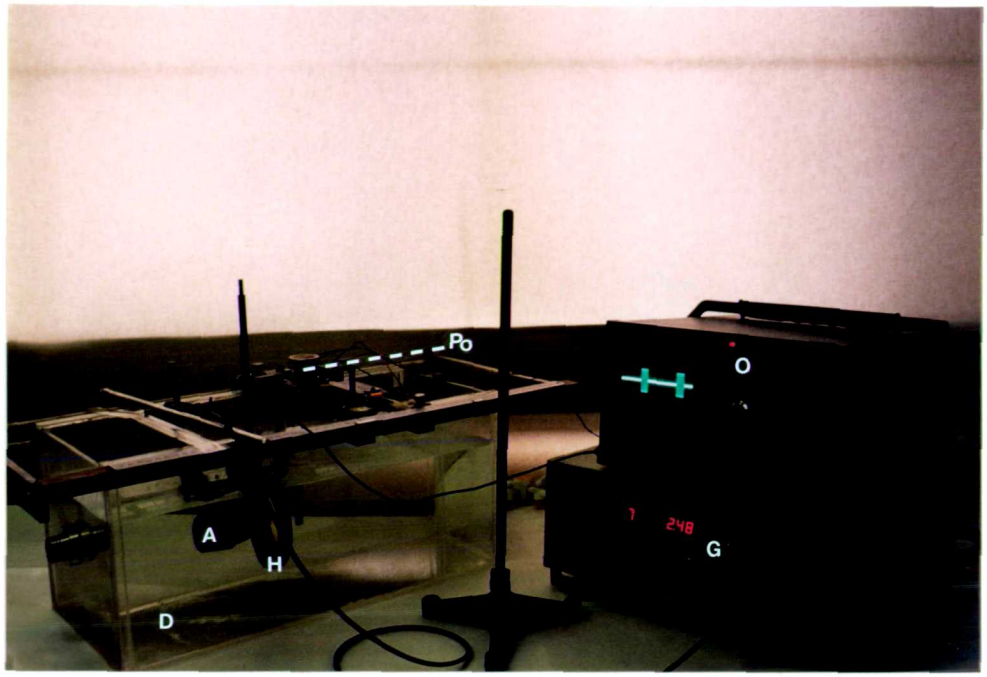

Key:

A = Applicator head
D = Degassed distilled water
H = PVDF membrane hydrophone (Marconi, UK)
O = Calibrated measuring oscilloscope (Hitachi V-656 F)
Po = Linear potentiometer
G = Ultrasound generator

6.2.4. Calculation of peak pressure amplitude and spatial peak intensity from oscilloscope output.

Peak Pressure Amplitude:

As stated above, the NPL-measured sensitivity of the hydrophone at a frequency of 3 MHz is 0.185 μV/Pa. As measurements taken from the oscilloscope screen are in mV this can be read as 1.85×10^{-4} mV/Pa. The screen voltage divided by 1.85×10^{-4} will give the peak pressure in pascals (Pa). This is divided by 1×10^{6} to give the more commonly quoted peak pressure amplitude in MegaPascals (MPa).

Spatial Peak Ultrasonic Intensity:

Peak intensity is related to the peak pressure (measured in bars) according to the following equation:

$$P_{bars\ (peak)} = \sqrt{3I}$$

P, the pressure in bars, can be calculated from the oscilloscope output voltage knowing the hydrophone sensitivity. As previously stated the hydrophone sensitivity = 0.185 μV/Pa; this is the same as 0.0185 V/bar as 1bar = 0.1 MPa.

$$I = \frac{P^2}{3}$$

so:

$$I = \frac{\left(\frac{volts}{0.0185}\right)^2}{3}$$

thus:

$$I = volts^2 \times 973.9469$$

Spatial peak intensity (Isp), in W cm^2, within the sound field is thus calculated by multiplying the square of the peak oscilloscope voltage, measured in volts, by 973.9469.

Table 6.2. Showing peak voltage, pressure amplitude and spatial peak intensity (Isp) for the spatially and temporally averaged ultrasonic intensities ($I^{(SATA)}$) used in this thesis.

Calibration arrangement	Average Intensity ($I^{(SATA)}$) (W/cm^2)	Peak scope voltage (mV)	Calculated peak pressure amplitude MPa	Calculated spatial peak intensity (Isp) (W/cm^2)
Free Field	0.5	56	0.30	3.06
	0.1	28	0.15	0.76
In vivo	0.5	56	0.30	3.06
	0.1	27	0.15	0.71
In vitro	0.5	56	0.30	3.06
	0.1	26	0.14	0.66

6.2.5. Calculation of effective radiating area

As previously stated the US-FDA definition of ERA is "*the area consisting of all points of the effective radiating surface at which the intensity is 5% or more of the maximum intensity (I max)*" at a given nominal intensity setting. Beam profiles, which are plots of relative pressure amplitude versus linear displacement across the transducer face, can be used to measure ERA provided that it is appreciated that:

$$Amplitude = \sqrt{Intensity}$$

and the definition modified accordingly.

According to this relationship the US-FDA value of 5% of I max is equivalent to 22.36% of the maximum amplitude value (A max) i.e.

$$I \text{ max} = 1.0 \text{ W/cm}^2$$

$$5\% \text{ of I max} = 0.05$$

$$A = \sqrt{I}$$

$$A = \sqrt{0.05}$$

$$A = 0.2236$$

Figure 6.10 Measurement of ERD. A beam profile showing the change in relative pressure amplitude with linear displacement across the transducer face The ultrasound generator was set to give a nominal ultrasonic output of 1.0 W/cm^2 $I^{(SATA)}$.

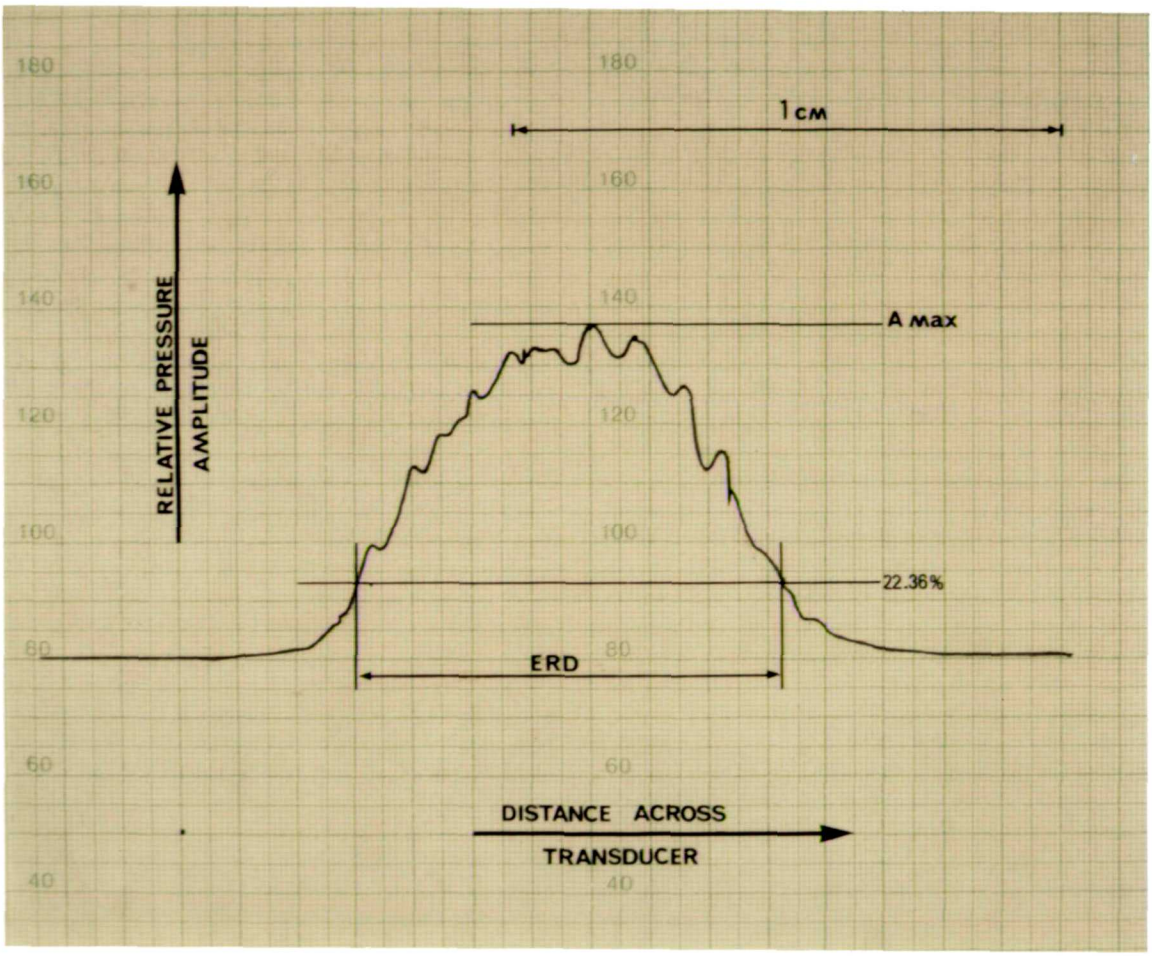

Key: ERD = Effective radiating diameter

A max = maximum relative pressure amplitude

Thus it is possible to reword the US-FDA definition in terms of relative amplitude to read *'the area consisting of all points of the effective radiating surface at which the relative pressure amplitude is 22.36% or more of the maximum relative pressure amplitude (A max)'* for a given nominal intensity setting. Figure 6.10 shows the free field profile, and measurements thereof, used to calculate the effective radiating area of the Enraf Nonius 3 MHz transducer used in this thesis. The nominal intensity setting used to produce this profile was 1.0 W/cm^2 (panel meter setting) with the generator set to deliver continuous wave ultrasound.
With reference to figure 6.10,

A max = 57

22.36% of A max = 12.75

The effective radiating diameter (ERD) of the transducer, consisting of all points at which the relative pressure amplitude is equal to or greater than 12.75, is measured directly from this trace and calibrated against the X axis sensitivity of the plotter. As a linear movement of 1 cm across the face of the transducer is equivalent to 9.3 cm on the trace. The ERD measured from the trace 7.25 cm is thus equal to a true linear displacement of 0.776 cm across the transducer face. The effective radiating radius is thus 0.390 cm and consequently the effective radiating area, assuming that the transducer is circular and symmetrical, is 0.48 cm^2. This correlates well with the manufacture's information on this transducer assembly, in which they state the ERA to be 0.5 cm^2. The ERA measurement is used to calculate the force balance setting required to accurately deliver a specified ultrasonic intensity to the biological target (see section 6.1).

6.3. The time distribution of acoustic energy

Hill (1970) stated the time distribution of ultrasound, applied to a given biological target, as a major irradiation parameter which should be reported in communicating ultrasonic bioeffects. To report properly on the time distribution of pulsed ultrasound it is necessary to examine two areas of possible variation.

1. The variation associated with the duration of the periods of ultrasonic emission and non-emission.
2. The variation associated with the distribution of ultrasonic energy within the pulse envelope.

6.3.1. Emission and non-emission

Nearly all therapeutic ultrasound generators can emit either a continuous beam of ultrasound, or chop this beam up into discrete bursts, or pulses, of ultrasound approximately 2 milliseconds in duration. The 'off', or inactive, time between bursts can normally be varied. *Mark: Space Ratio* is a term used, in pulsed ultrasound, to describe the time distribution of the ultrasonic energy supplied to a given biological target. It is the ratio of the pulse length (on time) to the gap length (off time), where time is expressed in milliseconds. The manufacturers of the generator used in this study, Enraf Nonius, indicate that it is capable of delivering pulsed ultrasound at the following mark:space ratios:- 2 ms : 8 ms, 2 ms : 18 ms and 2 ms : 38 ms.
As this study is primarily concerned with the biological effects of pulsed ultrasound at a mark:space ratio of 2ms: 8ms, the other mark: space ratios will be ignored.

The true mark: space ratio, for a given nominal mark: space ratio setting, is obtained by positioning a hydrophone within the generated sound field and displaying the output on an oscilloscope (as described earlier for beam profiling and the measurement of spatial peak pressure amplitude). When set to the correct time base, the oscilloscope will display the mark and space periods of the generated ultrasound in milliseconds. The oscilloscope was set such that each major grid line, dissecting the horizontal axis, corresponded to a time period of 2 ms.

The true mark: space ratio of the pulsed ultrasound emitted, when the ultrasound generator was set to supply a nominal mark: space ratio of 2ms: 8ms, was studied at both of the ultrasonic intensities used in this thesis. Black and white photographs, of the oscilloscope display, depicting the pulse modulation, were taken using a Shackman 7000 oscilloscope camera loaded with Polaroid 667 film (figure 6.11). It is apparent from these photographs that the manufacturer's mark: space ratio information is correct. It is similarly apparent that the mark: space ratio is unaffected by the ultrasonic intensity being generated.

6.3.2. Variation within the pulse envelope.

The shape of the ultrasonic pulses depends upon the electrical circuitry employed to modulate a continuous ultrasonic output into a pulsed output. Certain forms of electrical modulation, for example AC mains modulation, generate pulses in which the intensity varies throughout the pulse. During the first half of the pulse the

Figure 6.11 Polaroid oscilloscope photographs showing the temporal distribution of energy emitted when the ultrasound generator was set to deliver $I^{(SATA)}$ intensities of 0.5 and 0.1 W/cm^2.

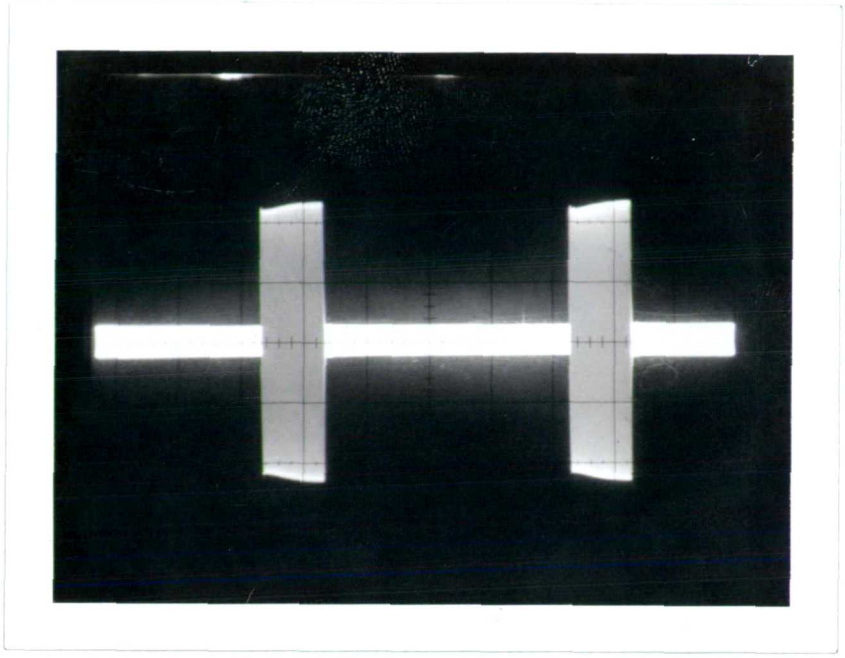

Intensity - 0.5 W/cm^2

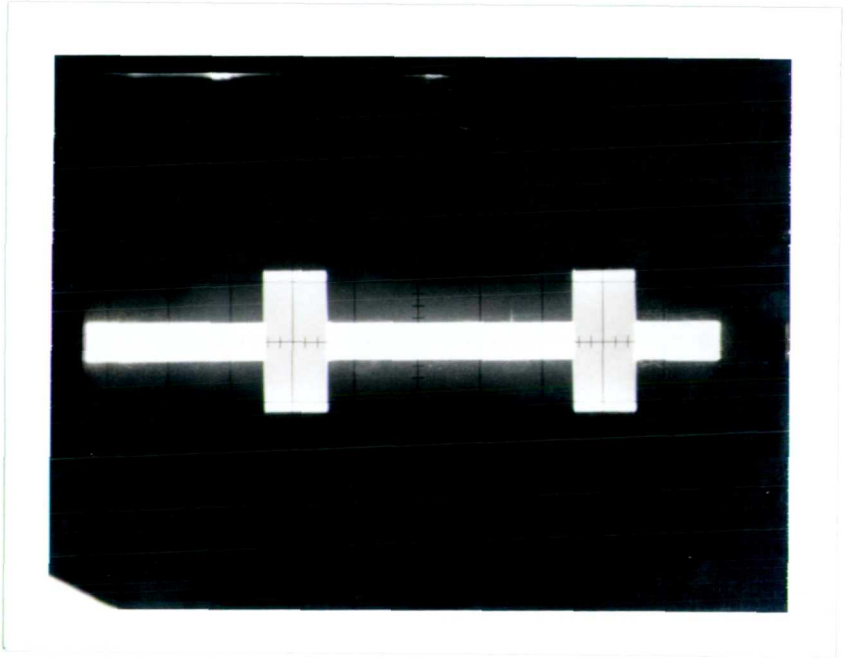

Intensity - 0.1 W/cm^2

intensity gradually rises, reaching a maximum mid way through the pulse; the intensity then falls off to zero during the latter half of the pulse. This regular rise and fall in 'in pulse' intensity often fails at high ultrasonic intensities; with the result that the pulse envelope tends to deform, leading to an even more complicated intensity distribution within the pulse. This lack of uniformity of intensity ($I^{(SAPA)}$) during the "on" period complicates the assessment of the temporal average intensity ($I^{(SATA)}$), for a given mark: space ratio. AC mains modulation also tends to suffer from the fact that as intensity is increased the actual mark:space ratio drifts from the manufacturer's quoted values (Allen and Battye, 1978).

Ideal pulse modulated outputs have a uniform ultrasonic intensity throughout the pulse period (rectangular pulse envelope), with mark: space ratios that are unaffected by the ultrasonic intensity being generated. Such pulse modulation allows ready assessment of the average intensity ($I^{(SATA)}$) being applied for a given mark: space ratio (Allen and Battye, 1978). Such ideal pulse modulation usually results from some form of precise electronic switching circuit, which is effectively set to generate ultrasound for a fixed number of wave cycles for a given pulse length. Thus for 3 MHz ultrasound (3×10^6 cycles per second), at mark: space ratio of 2ms: 8ms, the switching circuit allows the generator to emit ultrasound for 6000 wave cycles (pulse on) and then prevents it generating ultrasound for 24,000 cycles (pulse off).

The pulse shape generated by the therapy device used in the completion of this thesis had an 'ideal' appearance using the criteria of Allen and Battye (1978). From figure 6.11, it can be seen that the pulse envelope is perfectly rectangular at the lower ultrasonic intensity of 0.1 W/cm^2 $I^{(SATA)}$ used in this thesis, and at the higher intensity, of 0.5 W/cm^2 varies by less than 5%. This slight, and effectively insignificant, deviation from the 'ideal' perfectly rectangular pulse envelope, at the higher intensity, may result from an over compensation in power supplied to the transducer during ultrasonic discharge (Dr J B Pond - personal communication).

6.4. Temperature change in tissue consequent on irradiation

All tissues absorb a certain percentage of the ultrasound passing through them, and this absorbed energy appears as heat which raises the temperature of that tissue. It is possible to estimate the temperature rise, ΔT (°C) in skin, that may be expected after an irradiation at spatially and temporally averaged intensity $I^{(SATA)}$ (W/cm^2) after a time t (seconds) in the absence of any cooling mechanism, such as blood flow, from

the following equation:

$$\Delta T = \frac{2\alpha_a It}{\rho c_m}$$

Where:

α_a is the absorption coefficient of the skin (approximate)

ρ is the density of the tissue

c_m is the specific heat per unit mass of the tissue

Typical values for the above are $\rho \sim 1$ g/cm^3, c_m=4.2 joules/g. α_a is in the region of 0.03 Nepers/cm at a frequency of 1 MHz (Williams, 1983).

Thus the change in temperature (ΔT) is:

$$\Delta T = \frac{2 \times 0.03 \times 1 \times 1}{1 \times 4.2}$$

which is: $\underline{\Delta T = 0.0143\ ^\circ C/second}$

In this study 3 MHz ultrasound was employed at $I^{(SATA)}$ of 0.1 and 0.5 W/cm^2 . The expected increases in temperature rely heavily on the absorption coefficient which is a frequency dependent variable. i.e. α_a is in the region of 0.1 Nepers/cm at a frequency of 3 MHz.

Thus ΔT at an $I^{(SATA)}$ of 0.1 W/cm^2 is thus:

$$\Delta T = \frac{2 \times 0.1 \times 0.1 \times 1}{1 \times 4.2}$$

$\underline{\Delta T = 0.005\ ^\circ C/second}$

and ΔT at an $I^{SATA)}$ of 0.5 W/cm^2 is thus:

$$\Delta T = \frac{2 \times 0.1 \times 0.5 \times 1}{1 \times 4.2}$$

$\underline{\Delta T = 0.023\ ^\circ C/second}$

Bearing in mind that the insonation period used in this thesis was 5 minutes on all occasions, the expected temperature rises in the absence of any cooling mechanism (such as blood flow), within the skin (wound tissue) would be of the order of 1.43°C and 7.14°C, for $I^{(SATA)}$s of 0.1 and 0.5 W/cm^2 respectively.

The actual temperature rise consequent to 3 MHz insonation at the two intensities employed in this work was measured under both *in vivo* and *in vitro* exposure conditions. The temperature change during *in vivo* insonation was measured using a 1 mm K-type (Chrome Alumel) thermocouple (conforms with BS 4937/4) inserted under the skin in an otherwise uninjured but anaesthetized animal. The change in temperature monitored in this way, during 5 minute insonations at intensities of 0.1 and 0.5 W/cm^2 $I^{(SATA)}$ are shown in table 6.3 and graphically depicted in figure 6.12. The temperature values in table 6.3, which are displayed in figure 6.12, are average values calculated from triplicate measurements.

The temperature change during *in vitro* insonation was measured by inserting the above thermocouple into an exposure chamber via the loading port (Appendix 13, figure 13.1, p 349). Prior to inserting the thermocouple into the chamber, the latter was filled with a U937 cell suspension (1 x 10^6 cells per ml of RPMI 1640 culture medium). Once inserted the thermocouple was held in position using Blu-Tack (Bostik Ltd, UK) which also prevented the cell suspension from leaking out of the loading port. The change in temperature monitored in this way, during insonation periods of 5 minutes, at intensities of 0.1 and 0.5 W/cm^2 $I^{(SATA)}$ are shown in table 6.4 and graphically depicted in figure 6.13. The temperature values in table 6.4, which are displayed in figure 6.13, are average values calculated from triplicate measurements. It is apparent, from the measurements made above, that the observed temperature increases both *in vivo* and *in vitro* are significantly lower than those predicted by calculation at the beginning of this section.

The *in vivo* result may be explained by the fact that the calculation to predict temperature rise does not allow for the loss, or removal, of heat from the tissue. It thus assumes a linear relationship between the temperature of the tissue and the amount of ultrasound applied (which is a function of ultrasonic intensity and time). As can be seen from figure 6.12, showing the change in temperature as a consequence of insonation *in vivo*, the temperature rise within the tissue rises quite rapidly over the first minute or so; the rate of temperature increase then declines over the remainder of the exposure period. This loss of linearity is a consequence of

Table 6.3. The effect of insonation on temperature rise of biological target *in vivo*.

Intensity $I^{(SATA)}$ (W/cm^2)	Time (minutes)	Number of replicates	Average Temperature (°C)
0.1	0	3	21.7
	1	3	22.1
	3	3	22.5
	5	3	22.7
0.5	0	3	21.7
	1	3	22.8
	3	3	24.2
	5	3	25.0

Table 6.4. The effect of insonation on temperature rise of biological target *in vitro*.

Intensity $I^{(SATA)}$ (W/cm^2)	Time (minutes)	Number of replicates	Temperature (°C)
0.1	0	3	36.9
	1	3	37.0
	2	3	37.1
	3	3	37.1
	4	3	37.1
	5	3	37.1
0.5	0	3	36.9
	1	3	37.2
	2	3	37.3
	3	3	37.4
	4	3	37.4
	5	3	37.4

Figure 6.12 Temperature change during *in vivo* insonation at 0.1 and 0.5 W/cm^2 ($I^{(SATA)}$).

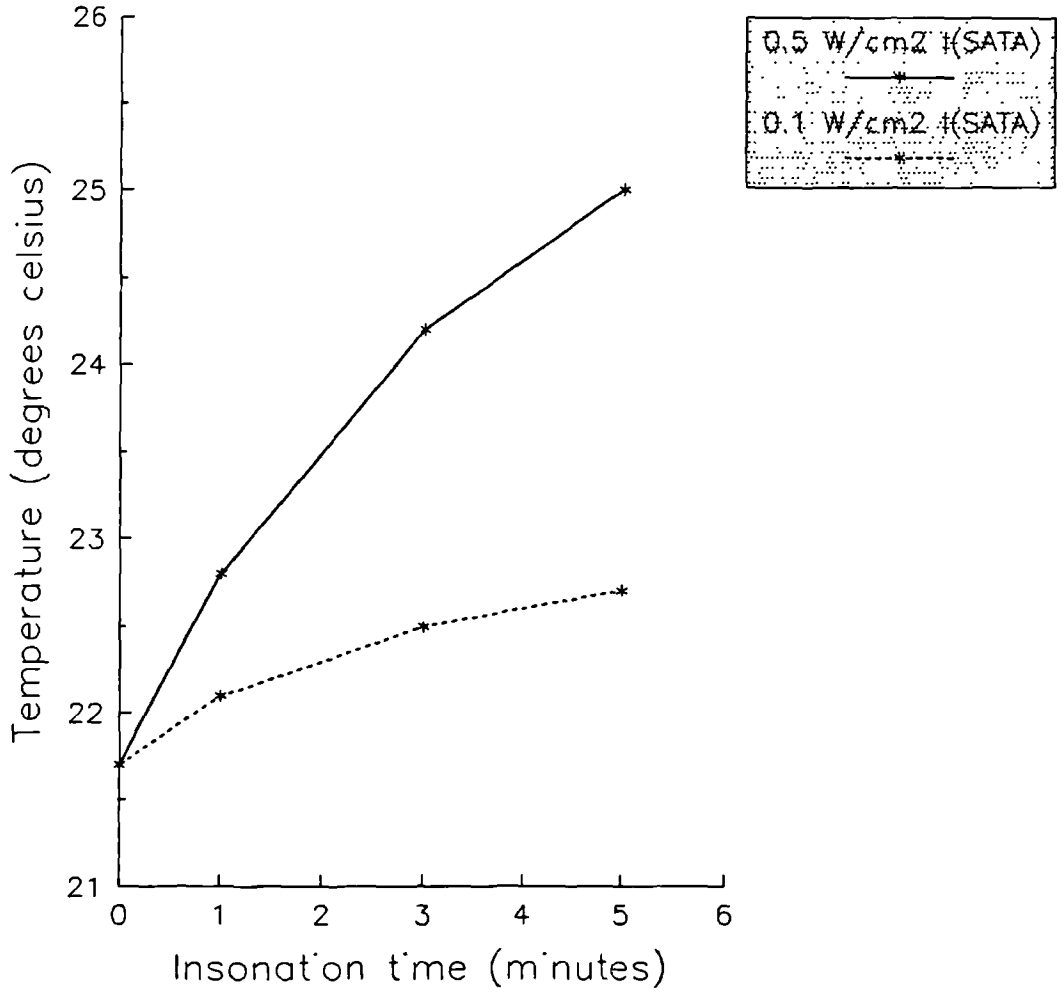

Figure 6.13 Temperature change during *in vitro* insonation at 0.1 and 0.5 W/cm^2 ($I^{(SATA)}$).

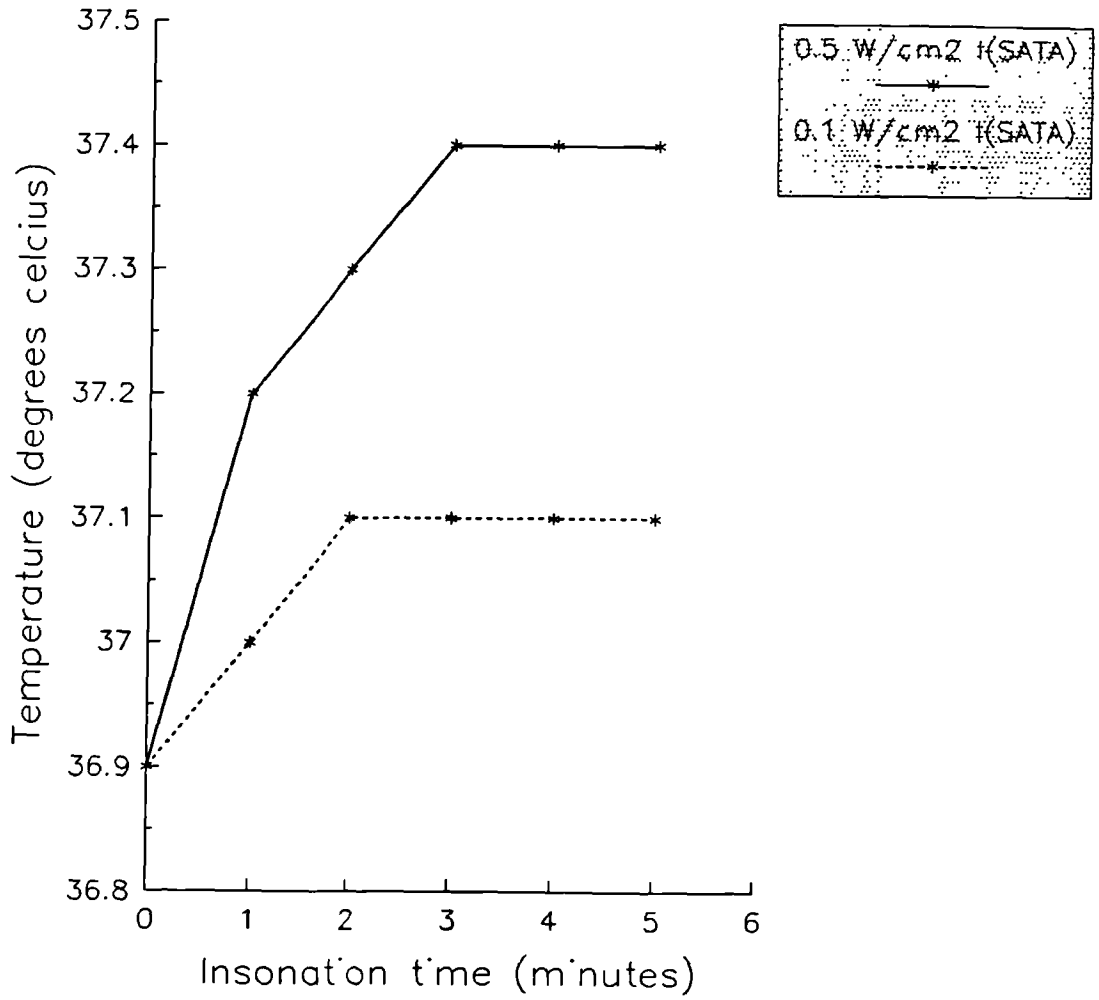

the action of cooling mechanisms.

Tissue cooling is effected by the transport of the ultrasonically generated heat to cooler regions. Part of the transport is accomplished by blood flow, that is, by perfusion (alternatively called convection), and the remainder is a result of heat conduction (alternatively called diffusion). In addition to the 'normal' loss of heat by perfusion, the elevation in tissue temperature, caused by the ultrasound, initiates physiological reflexes which result in the dilation of blood vessels and thus increased blood flow. This increased blood flow increases the rate at which heat is carried away from the area under exposure (Williams, 1983).

It is apparent from table 6.4, and figure 6.13, that the temperature rises experienced by the biological preparations exposed to ultrasound *in vitro* are much smaller than those temperature rises measured *in vivo* at both intensities studied. This is explained again in terms of cooling. Under the *in vitro* conditions used in this study, it is expected that any heat generated within the exposure chamber would be rapidly lost by conduction to the metal of the chamber and thence by conduction and convection to the circulating water within the exposure tank. Further, the absorption coefficient of the cell suspension would be expected to be far lower than that of skin, and as such, significantly less energy would be absorbed and hence significantly less heat generated under *in vitro* exposure conditions.

Chapter 7. The effect of pulsed 3MHz therapeutic ultrasound on wound contraction in the rat

7.1 Introduction

During the healing of a tissue defect, the edges of the wound are progressively brought together by the retraction of granulation tissue. The phenomenon, called wound contraction, is of great clinical importance in reducing the size of the wound. Therapeutic ultrasound has been shown to stimulate various aspects of wound healing under both clinical (Dyson *et al.* 1976; Roche and West, 1984; McDiarmid *et al.* 1985; Callam *et al.* 1987) and experimental conditions (Dyson and Pond, 1970; Webster *et al.* 1979; Young and Dyson, 1990a,c; Byl *et al.* 1992). Previous experimental studies, examining the interaction of therapeutic ultrasound with wound repair following mechanical trauma, have mainly focused on changes in wound cellularity while wound contraction has received little attention.

The aim of this study was to examine the effect of a clinically applicable ultrasound treatment regime on the progress, and ultimate extent, of wound contraction in Wistar rats following full-thickness excision of flank skin.

7.2 Materials and methods

This section describes the materials and methods employed to examine the effect of therapeutic ultrasound on wound contraction *in vivo*. Certain techniques have been covered elsewhere and are referenced accordingly.

7.2.1 Animal husbandry

Adult female Wistar rats (supplied by Tuck and Sons Ltd, London, U.K.) aged approximately 9 weeks and weighing between 180 and 220 grams were used in this study. Animals were housed in groups of three, in cages of dimensions 40 x 25 x 20 cm with sawdust bedding (changed twice weekly), in an environment maintained at an ambient temperature of 23°C with 12-hour light/dark cycles. They were provided with food (No. 1 maintenance diet, B.P.) and water *ad libitum*. Prior to experimentation animals were housed for seven days without disturbance, other than to refresh their bedding and to replenish their food and water provisions, in an attempt to accustom them to their new environment. All animal procedures were carried out under Home Office licence.

To reduce the likelihood of wound contamination and accidental self mutilation during the period of post-anaesthetic disorientation, animals were temporarily housed in recovery cages after anaesthesia. Further it is possible that returning a semi-conscious rat back into a shared cage, after surgery or treatment, could be a source of unnecessary stress for the fully conscious rats awaiting similar treatment. Recovery cages contained clean paper tissue, rather than wood chippings, to reduce the likelihood of wound contamination. Once the obvious effects of the anaesthetic had worn off, after approximately five minutes, they were returned to their original cages.

7.2.2 Creation of a standard wound

Animals were anaesthetized using inhalation of halothane (May & Baker Ltd, England) and air. One flank of each rat, chosen at random, was shaved and swabbed with a bactericide (Hibitane). Two concentric squares, of dimensions 2 cm by 2 cm and 1 cm by 1 cm, were marked onto the shaved skin using a flexible transparent plastic template (figure 7.1) and an indelible marker pen. The outer square, depicted by eight dots (one at each corner and one in the centre of each face) was then permanently tattooed into the skin using a 23 gauge sterile needle and millipore filtered (0.22 μm) TG 1 drawing ink (Faber-Castell, Nurnberg, Germany). A 1 cm by 1 cm full thickness excision was then made in this flank, using blunt nosed surgical scissors, of the tissue limited by the inner square. The excised tissue included the *panniculus carnosus* and hypodermis.

7.2.3 Experimental groups

Fifty four Wistar rats were randomly allocated into one of three treatment groups, namely:

1. Sham-insonation
2. Insonation with 3 MHz pulsed (2 ms on : 8 ms off) ultrasound at an intensity of 0.1 W/cm $I^{(SATA)}$ (i.e. 0.5 W/cm^2 $I^{(SAPA)}$).
3. Insonation with 3 MHz pulsed (2 ms on : 8 ms off) ultrasound at an intensity of 0.5 W/cm $I^{(SATA)}$ (i.e. 2.5 W/cm^2 $I^{(SAPA)}$).

7.2.4 Ultrasound application and photography of wounds

The therapeutic ultrasound source used in this study was a standard Enraf Nonius Delft 434 Sonopuls machine (figure 7.2) (Enraf Nonius Delft, Holland), which is

Figure 7.1 The Wound Template

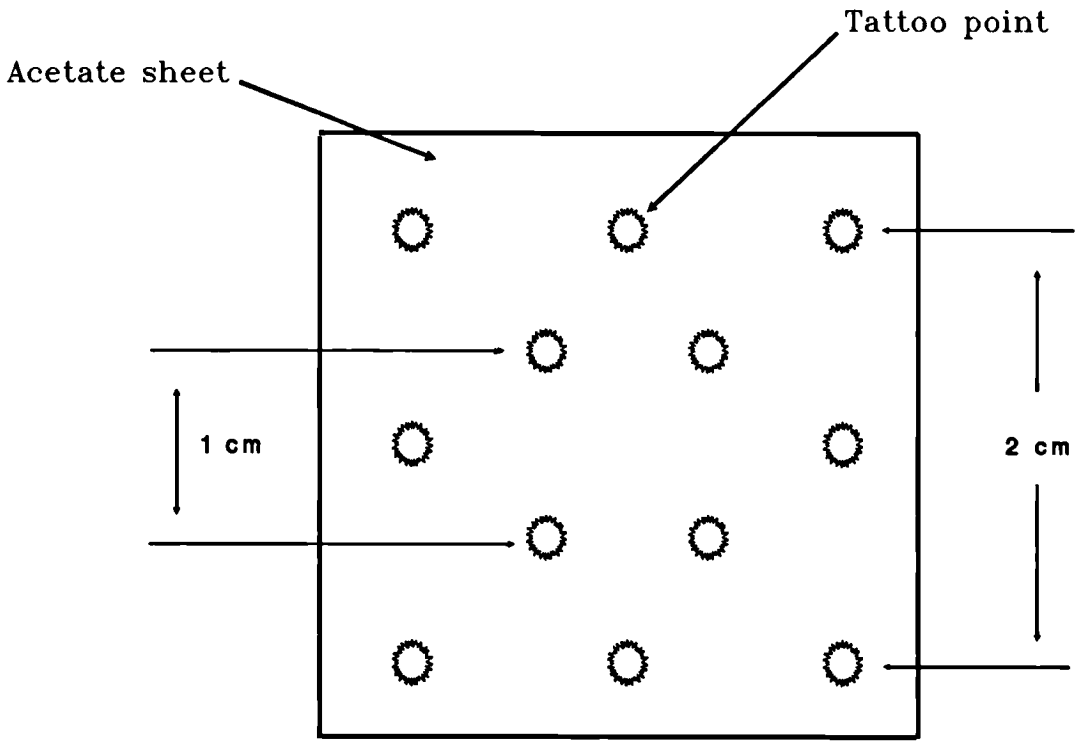

capable of generating either 1 or 3 MHz ultrasound by two separate applicator heads. Prior to each treatment session the ultrasonic output was checked using a custom engineered (Enraf Nonius Delft, Holland) sound balance (figure 6.1, p190).

Due to the delicate nature and sensitivity of fresh skin wounds it is necessary to protect them from further damage during treatment. Such damage is associated with the contact and movement of ultrasound applicator heads during therapy. This protection must shield the wound without significantly impeding the passage ultrasound. The wound dressing Geliperm Wet (Geistlich Pharmaceuticals, Switzerland) fulfils both of these requirements (figure 7.3). Geliperm Wet is a sterile, transparent polyacrylamide gel manufactured in 0.5 cm thick sheets. As it is 96-97% water, yet still quite rigid, it offers the required protection against frictional forces of the moving applicator and is responsible for little, or no, ultrasound beam impedance (figure 6.6, p 199).

After surgical excision of the 1 x 1 cm of flank skin, the post-surgical cavity thus formed was flooded with sterile physiological saline and carefully swabbed dry with sterile gauze to remove any tissue debris and blood. The wound was again filled with sterile physiological saline and then dressed with 4 x 4 cm square of Geliperm Wet (Geistlich, Switzerland). The wound cavity was filled with saline to ensure proper ultrasonic coupling from the applicator head, through the polyacrylamide dressing, and onto the wound bed. Any bubbles trapped beneath the Geliperm were released prior to exposure to insonation as ultrasound is reflected at air/water interfaces and as such, would not reach the wound, thereby confounding dosimetry. The ultrasound applicator was coupled to the dressing using the ultrasonic couplant Sonogel (Enraf Nonius Delft, Holland) see figures 7.2 and 7.4.

The applicator head was lowered into contact with the coupling gel. Contact was maintained throughout treatment by exerting a light pressure on the head. During treatment the applicator head was kept in continual motion. The practice of continually moving the ultrasound applicator is common to most clinical ultrasound treatment regimes, and was adopted to ensure that all areas of the underlying tissue received a similar, if not identical, ultrasonic exposure. As the ultrasonic fields generated by the majority of commercially available devices are non-uniform in nature this continual motion ensures that the applied ultrasound is not concentrated at any one location within the tissue receiving treatment (Forster and Palanstanga, 1981). It also reduces the likelihood of standing wave formation and subsequent

Figure 7.2 Apparatus for exposing rat skin wounds to therapeutic ultrasound

KEY: G - Ultrasound Generator

C - Coupling Gel

P - Polyacrylamide dressing

A - Applicator Head

Figure 7.3 An 8 day post-excision rat wound dressed with Geliperm (note tattoo points around wound)

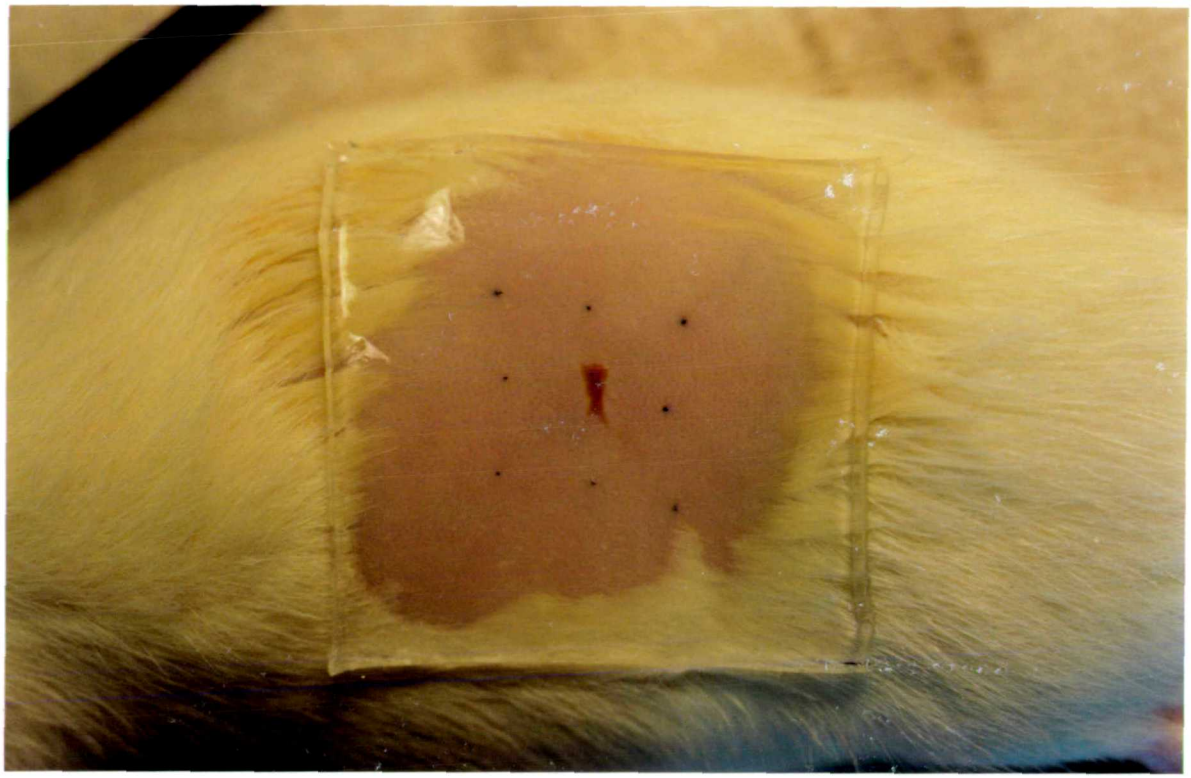

Figure 7.4 The application of ultrasound to a flank skin wound of an anaesthetized rat. The ultrasound is coupled to the wound via Sonogel, Geliperm and physiological saline.

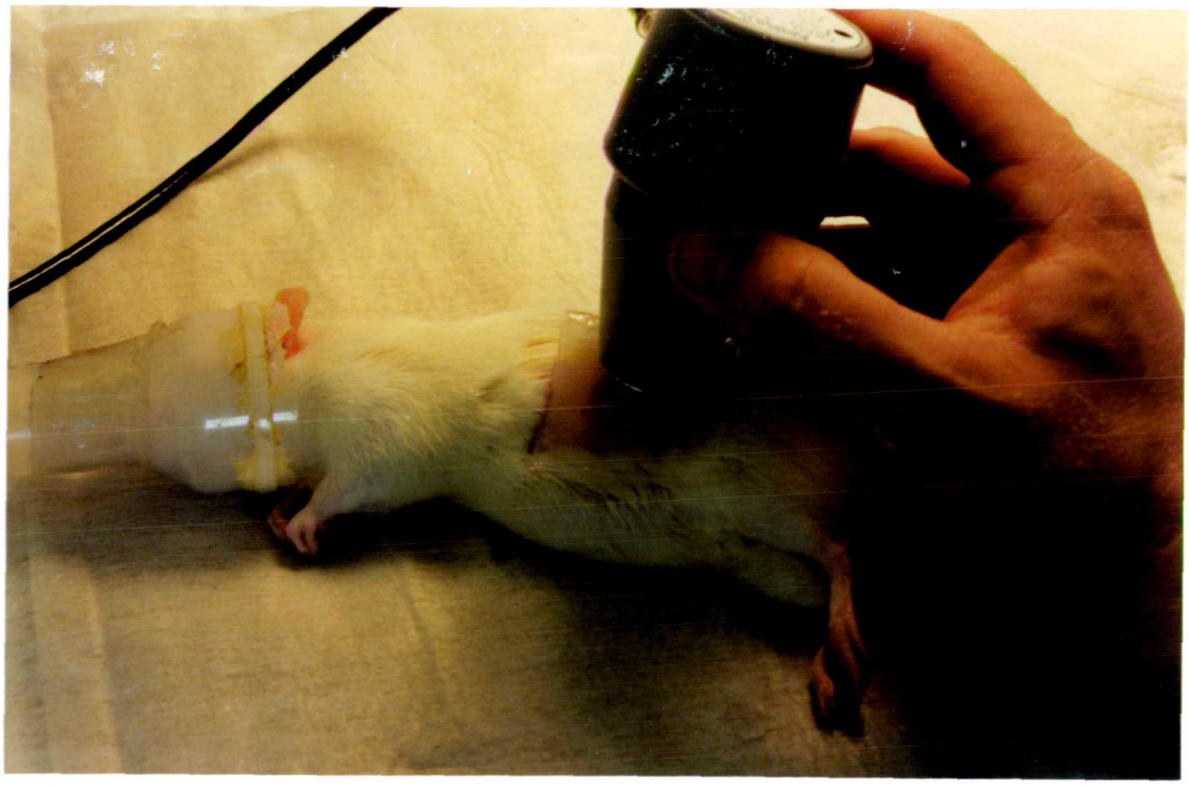

damage associated with cavitation (Dyson *et al.* 1974).

Each animal received a five minute insonation or sham insonation depending on the treatment group to which the animal belonged. Wounds were filled with saline, dressed with Geliperm and insonated in this way 24, 48, 72 and 96 hours after excision and initial insonation, having received a total of 5 insonations/sham insonations by the end of the treatment programme at 96 hours. While the animals were still under anaesthetic having just received their second ultrasound/sham exposure, at 24 hours post-excision, their wounds were photographed using a standard 35 mm camera (Pentax, Japan), fitted with a macro lens (50 mm) and loaded with FP4 125 ASA black and white film (Ilford, Cheshire). A plastic identity plate, carrying information on the animal, the time and date of photograph, and a centimetre rule (for standardisation) was placed in close proximity to the wound, and photographed along with the wound. Wounds were photographed in the same manner following treatment at 48, 72 and 96 hours post-excision. Daily photographs continued to be taken, after the ultrasound treatment program had ceased, up until the 11th post operative day. The film was processed as described in appendix 11B (p346). Animals were terminated painlessly on the 11th day of study by intraperitoneal injection of a lethal dose of 20% w/v sodium pentobarbitone (Lethobarb. Duphar Vet Ltd, UK).

7.2.5 Computerised Image Analysis

Computerised image analysis was used to measure wound area, as depicted by the eight tattoo points, on each of the photographic negatives. After developing, the negatives were transferred to a light box and digitised at 1280 by 1024 square pixels. The negatives were transilluminated on the light box and digitisation was then performed using a high resolution "charge couple device" CCD camera (Videk Megaplus, model K00792) fitted with a 55 mm Nikon Nikkor lens. The camera data was recorded using an IBM PC-AT compatible computer and a Univision UPX 1000 interface and the resulting image displayed using a Univision UDC2600 display controller. Optimas (Bioscan Inc, USA) software was used to capture and analyze the image of the transilluminated photo-negative.

Each wound image was analyzed with the help of an IBM PC-AT computer running Optimas software. Computer analysis, using the Optimas package, involved using the "mouse" to join the tattoo marks of the digitised wound image which had

been displayed on a large format high resolution monitor. The Optimas package then calculated the area depicted by the joined tattoo marks and expressed this information in terms of square pixels. Using the calibration facility within the Optimas program in conjunction with the centimetre scale, which was photographed with each wound, wound area was then expressed in terms of square centimetres.

7.2.6 Data Analysis

Wound contraction was expressed in terms of percentage wound area remaining with time. For a given wound, the wound area measured from the first photograph, taken at 24 hours after wound excision, was taken to be 100%. The median percentage wound area remaining and 95% confidence intervals were calculated for each of the three experimental groups at each time point (tables 7.1, 7.2 and 7.3) and displayed in the form of a histogram (figure 7.5). The data was analyzed, by non-parametric statistical analysis, using the Mann Whitney-U test. The rate of contraction observed in sham-insonated wounds was compared with that observed in both ultrasound-treated groups at each time point post-wounding (Appendix 18A, p357). Further analysis (Appendix 18B, p358) was carried out to compare the rate of wound contraction observed in response to ultrasound treatment at an intensity of 0.1 W/cm^2 ($I^{(SATA)}$) with that observed in response to the higher intensity of 0.5 W/cm^2 ($I^{(SATA)}$).

7.3 Results

Figure 7.5 displays the median % wound area remaining data from the three experimental groups over the 11 day experimental period, 95% confidence intervals are indicated to aid interpretation.

From figure 7.5, the results in tables 7.1 through 7.3, and statistical analysis (Appendix 18, p357) the following points are apparent:

1. Irrespective of treatment, the process of wound contraction appears to be biphasic. The first phase is characterised by rapid contraction, this subsequently gives way to the second phase of slower contraction. Differentially exposed wounds appear to remain in the first, rapid contraction phase, for differing periods of time. Sham-insonated wounds appear to remain in the rapid contraction phase for the shortest time, entering the slow contraction phase after day 6 post-wounding. Wounds exposed to 3 MHz ultrasound at an intensity of 0.5 W/cm^2 appear to continue rapid

contraction a little longer, entering the slow contraction phase after day 7. Ultrasonic exposure at the lower intensity, of 0.1 W/cm^2 $I^{(SATA)}$ results in wounds continuing to contract rapidly until day 8, entering the slow contraction phase at day 9.

2. Wounds exposed to ultrasound at an intensity of 0.1 W/cm^2 ($I^{(SATA)}$) were smaller, i.e. had contracted to a greater extent, than sham-insonated wounds at all time points. Though insonated wounds were physically smaller from day 2 onwards this observation did not prove statistically significant until 5 days post-wounding ($p < 0.002$). Insonated wounds were significantly smaller than sham-insonated wounds at all time points thereafter, i.e. at 6 ($p < 0.005$), 7 ($p < 0.000002$), 8 ($p < 0.00002$), 9 ($p < 0.00002$), 10 ($p < 0.0008$) and 11 ($p < 0.02$) days post wounding.

3. Wounds exposed to ultrasound at an intensity of 0.5 W/cm^2 $I^{(SATA)}$ were smaller, i.e. had contracted to a greater extent, than sham-insonated wounds at all time points. This difference proved to be statistically significant at all time points with the exception of days 4 and 5 post-wounding i.e. at 2 ($p < 0.006$), 3 ($p < 0.006$), 6 ($p = 0.040$), 7 ($p < 0.00003$), 8 ($p < 0.001$), 9 ($p < 0.0001$), 10 ($p = 0.014$) and 11 ($p < 0.003$) post wounding.

4. Wounds exposed to ultrasound at an intensity of 0.1 W/cm^2 were initially found to be larger than similar wounds exposed to an intensity of 0.5 W/cm^2, i.e at days 2, 3 and 4 post-wounding. This apparent difference did not prove to be statistically significant. From day 5 until the end of the study, wounds exposed to 0.1 W/cm^2 were found to be smaller than similar wounds exposed to 0.5 W/cm^2; this difference achieved significance at days 5 ($p = 0.046$), 8 ($p = 0.031$) and 9 ($p = 0.010$).

Table 7.1. The effect of sham-insonation on the contraction of 1 cm^2 rat flank skin wounds

	Days post-excision of 1 cm^2 rat flank skin										
	1	2	3	4	5	6	7	8	9	10	11
Median % wound area remaining	100	96.273	90.124	84.083	78.424	72.217	73.953	71.739	70.046	65.628	65.827
Sample size (n)	18	18	18	16	12	12	18	18	18	18	18
Minimum and Maximum (%)	N/A	80.979 to 105.483	80.867 to 93.906	70.369 to 89.528	71.016 to 94.727	66.655 to 87.264	66.522 to 84.286	61.684 to 80.452	52.391 to 74.158	54.173 to 73.445	56.636 to 79.781
95% Confidence interval (%)	N/A	92.491 to 98.518	86.503 to 90.990	79.997 to 85.510	74.414 to 83.442	70.690 to 79.672	70.934 to 76.399	68.242 to 74.070	66.381 to 71.579	63.331 to 67.786	64.095 to 70.186

Table 7.2. The effect of treatment with 3 MHz ultrasound at an intensity of 0.1 W/cm^2 (I^{SATA}) on the contraction of 1 cm^2 rat flank skin wounds.

	Days post-excision of 1 cm^2 rat flank skin										
	1	2	3	4	5	6	7	8	9	10	11
Median % wound area remaining	100	92.849	86.334	80.773	69.113	66.413	62.675	58.270	57.298	58.696	57.023
Sample size (n)	18	18	18	18	17	18	18	16	17	16	17
Minimum and Maximum (%)	N/A	63.350 to 108.776	70.899 to 110.146	68.314 to 91.619	61.377 to 79.028	59.392 to 75.168	54.690 to 69.134	50.064 to 68.108	49.784 to 67.226	51.550 to 70.261	46.304 to 95.781
95% Confidence interval (%)	N/A	84.927 to 96.336	81.593 to 92.546	77.239 to 84.687	69.300 to 72.943	63.554 to 69.197	60.597 to 64.329	56.284 to 62.006	60.597 to 64.329	56.499 to 61.927	53.194 to 66.544

Table 7.3. The effect of treatment with 3 MHz ultrasound at an intensity of 0.5 W/cm^2 (I^{SATA}) on the contraction of 1 cm^2 rat flank skin wounds.

	Days post-excision of 1 cm^2 rat flank skin										
	1	2	3	4	5	6	7	8	9	10	11
Median % wound area remaining	100	90.970	83.302	79.100	74.818	70.449	65.413	64.462	62.137	60.491	61.044
Sample size (n)	18	17	18	18	18	17	17	18	18	16	18
Minimum and Maximum (%)	N/A	81.485 to 98.053	71.559 to 93.806	68.836 to 88.396	62.818 to 82.994	59.635 to 76.388	56.784 to 71.278	54.298 to 73.579	51.569 to 69.040	51.457 to 71.755	54.297 to 70.164
95% Confidence interval (%)	N/A	87.679 to 92.686	80.470 to 86.372	76.843 to 82.459	71.191 to 77.203	66.285 to 71.709	61.778 to 66.263	61.113 to 66.563	59.691 to 64.029	57.493 to 63.887	59.201 to 63.500

Figure 7.5. The effect of pulsed 3 MHz therapeutic ultrasound on wound contraction in the rat (median wound area remaining and 95% confidence intervals are indicated).

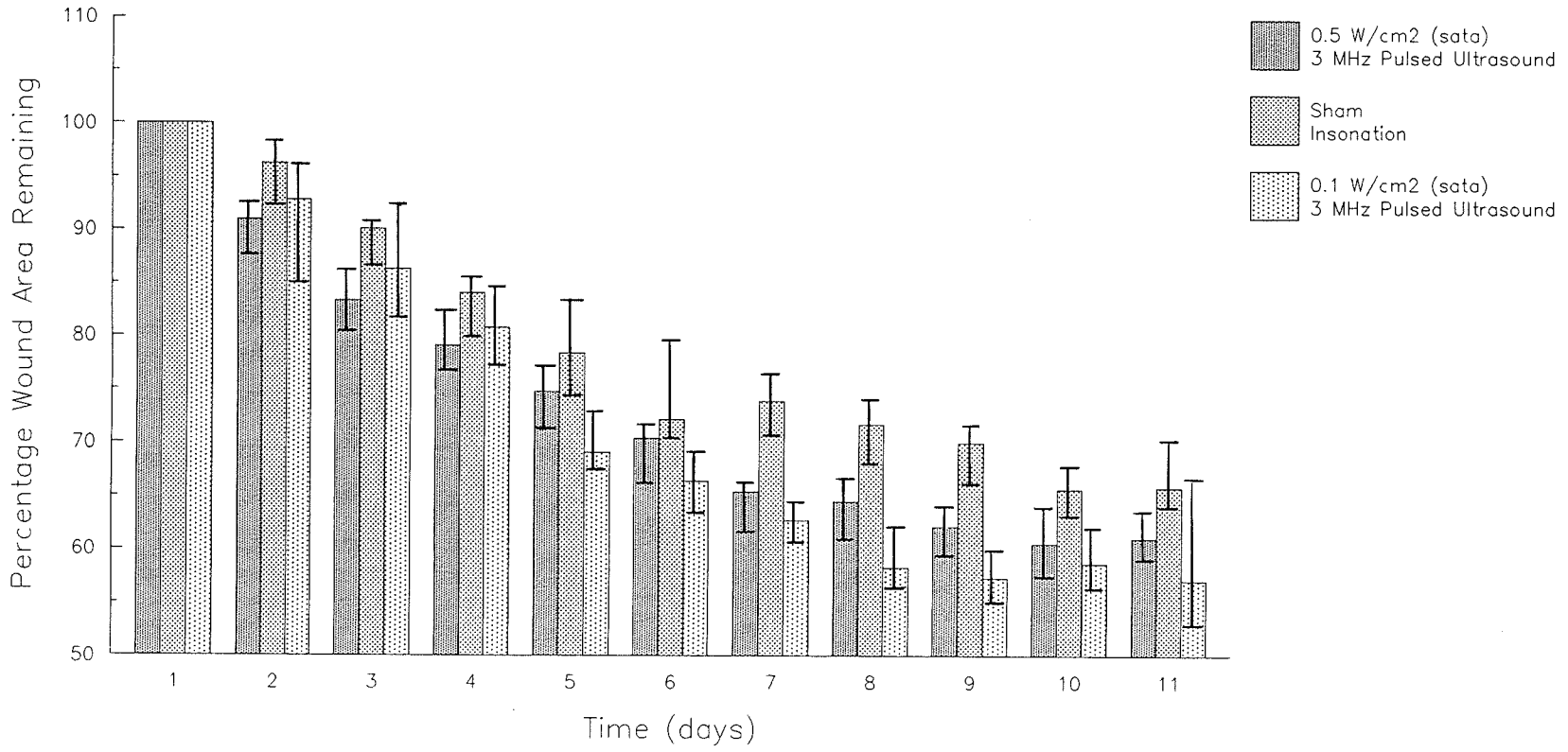

7.4 Discussion

The closure of full thickness wounds made in the flank skin of adult Wistar rats was used as a model of wound contraction. The model facilitated a quantitative and comparative assessment of the effect of therapeutic ultrasound on the process of contraction. The contraction of fully excised rat skin wounds treated with 3 MHz therapeutic ultrasound (at both intensities) was significantly more rapid than that of similar sham-treated control wounds. At the end of the experimental period ultrasound-exposed wound were significantly smaller than similar sham-exposed wounds. These observations suggests that the repair and more specifically the contraction of mechanical injuries can be accelerated by the application of therapeutic levels of ultrasound. Though significant differences were observed between insonated and sham-insonated wounds 2 days after injury, indicating an immediate effect of insonation, more apparent and statistically significant differences were observed several days after treatment had ceased. It is thus apparent that ultrasound exposure soon after injury can induce significant long term changes to the wound repair process.

It would appear from the results that the lower ultrasonic intensity (i.e. 0.1 W/cm^2, $I^{(SATA)}$) promoted wound contraction to a greater extent than the higher intensity (i.e. 0.5 W/cm^2, $I^{(SATA)}$). Temperature measurements made in uninjured dermis during treatment with ultrasound showed that the temperature rise over the 5 minute treatment period was 1°C at an intensity of 0.1 W/cm^2 and 3.3°C at an intensity of 0.5 W/cm^2 (table 6.3, p215). Such observations would appear to suggest that the mechanisms involved in the stimulation of wound contraction by ultrasound were not purely thermal.

The stimulation of wound contraction by ultrasound has been previously reported. Dyson and Smalley (1983), demonstrated that therapeutic intensities (0.1 W/cm^2, $I^{(SATA)}$) of 3 MHz pulsed ultrasound (2ms on, 8ms off) could stimulate the contraction of cryosurgical lesions made in the flank skin of rats. Freeze injuries are known to display both minimal inflammation and minimal contraction (Ehrlich, 1988) when compared with mechanical injuries. This study validates the report of Dyson and Smalley (1983) and further demonstrates that the stimulation of contraction by therapeutic ultrasound is not specific to cryosurgical injuries.

It has been suggested that therapeutic ultrasound acts by accelerating the rate at which wounds progress through the initial inflammatory phase of repair (Dyson,

1990), thereby encouraging a more rapid onset of the subsequent new tissue formation phase. This view is supported by the work of Young and Dyson (1990a) who observed that cells characteristic of the granulation tissue formation phase of repair (i.e fibroblasts and endothelial cells) were recruited more rapidly into insonated wounds than into similar sham-insonated wounds. The stimulated recruitment of fibroblasts into insonated wounds may explain the stimulation in contraction observed in this study, and in cryosurgical lesions by Dyson and Smalley (1983), as wound contraction is generally accepted to be a fibroblast-mediated process (Skalli and Gabbiani, 1988).

The recruitment of fibroblasts into cutaneous wounds is thought to involve both fibroblast migration and proliferation (p31 to 38). It is possible that ultrasound may stimulate this recruitment by interacting directly with fibroblasts to promote either their migration, as previously suggested by Mummery (1978), their proliferation, or both. Further studies later in this thesis address the direct effect of therapeutic ultrasound on fibroblast proliferation (chapter 8, p234).

During wound repair, fibroblast activities, including migration and proliferation, are thought to be directed by a variety of stimuli, including various regulatory peptides often referred to as growth factors (tables 1.2 & 1.3, p35 & 39). The source of these growth factors changes as the wound proceeds through the repair process; initially being released during platelet degranulation, they are subsequently synthesized and secreted by activated macrophages (Clark, 1990). In addition fibroblasts, endothelial cells and epithelial cells have also been shown to synthesize and release certain growth factors (Welch *et al.* 1990; Guidry *et al.* 1990; Nicolas *et al.* 1991). Thus it would appear that there is a continual capacity for the synthesis and release of growth factors throughout the healing process.

The majority of studies which report enhanced wound healing in response to therapeutic ultrasound, including this study, report the consequences of treatments carried out during the first few days after injury, i.e. during the inflammatory phase of repair (Dyson *et al.* 1970; Dyson and Pond, 1970; Webster *et al.* 1979; Dyson and Smalley, 1983; Young and Dyson 1990a,c; Byl *et al.* 1992). It is thus possible that ultrasound may interact with the wound via some component of the inflammatory phase, possibly modulating growth factor levels, and thereby regulate fibroblast function indirectly. *In vitro* studies designed to investigate the capacity of therapeutic ultrasound to interact with two major cellular components of the inflammatory phase

(i.e. platelets and macrophages) are described later in this thesis (Chapters 10, p253, and 11, p276). Future *in vivo* investigations comparing the effect of immediate treatment with delayed treatment (several days after initial injury) may help to define the ultrasound responsive target within cutaneous wounds.

It is possible that the early elevation in fibroblasts number in response to ultrasound, noted by Young and Dyson (1990), is the result of contraction rather than its cause. The process of wound contraction reduces granulation tissue volume, and thereby increases cellular density. It is possible that ultrasound may interact either directly or indirectly (mediated perhaps by platelets or macrophages) with fibroblasts in a manner that enhances the "contractile" capacity of individual cells, rather than by increasing the number of contractile cells within the wound. There are several lines of evidence that point to a direct effect of ultrasound on fibroblast-mediated wound contraction. Mummery (1978) reported that therapeutic levels of ultrasound could stimulate fibroblast migration *in vitro*; this observation may support a direct stimulation of fibroblast-mediated wound contraction by ultrasound, according to the cell traction theory of wound contraction (p52). The cell contraction, or myofibroblast, theory proposes that wound contraction is brought about by a muscle-like contraction of smooth muscle cell (SMC)-like fibroblasts, termed myofibroblasts. Smooth muscle contraction is caused by a transient flux of calcium ions activating actin-myosin sliding systems. As therapeutic levels of ultrasound have been shown to cause the contraction of guinea pig uterine SMC preparations *in vitro* (Talbert *et al.* 1975), increase the frequency of mouse uterine SMC contraction *in vivo* (ter Haar *et al.* 1978), and increase the uptake of calcium by fibroblasts *in vitro* (Mummery, 1978; Mortimer and Dyson, 1988), it is possible that ultrasound encourages wound contraction by stimulating myofibroblast contraction. *In vitro* studies, carried out using the fibroblast-populated collagen lattice wound contraction model, were performed to investigate the ability of ultrasound to stimulate fibroblast-mediated contraction both directly, and indirectly via platelets and macrophages (Chapters 9 (p244), 10 (p253) and 11 (p276) of this thesis).

In summary, this investigation demonstrates that clinical levels of therapeutic ultrasound can promote wound contraction in Wistar rats. If the observations made in this study can be extrapolated to the clinical situation, these results suggest that therapeutic ultrasound, applied at sites of tissue loss soon after injury, may encourage the process of wound contraction thereby reducing the size of the final scar.

Chapter 8. The direct effect of pulsed 3 MHz therapeutic ultrasound on the proliferation of human dermal fibroblasts *in vitro*.

8.1 Introduction.

The application of therapeutic ultrasound has been reported to stimulate the process of cutaneous repair both clinically and following experimental wounding in various experimental animals. Chapter 7 (p218) of this thesis, in which therapeutic ultrasound was shown to promote wound contraction in rat flank skin wounds, further sustains such reports. The mechanisms by which therapeutic ultrasound interacts with the process of wound repair, and more specifically the biological target with which it interacts to promote wound contraction are unknown. Wound contraction is thought to be a fibroblast-mediated event, and as such will clearly depend upon fibroblast density within the wound. *In vitro* reports suggest that ultrasound is capable of directly modulating certain fibroblast functions, including collagen synthesis (Harvey *et al.* 1975) and fibroblast migration (Mummery, 1978). It is possible that ultrasound may encourage wound contraction by directly stimulating the proliferation of fibroblasts, thereby endowing the wound with a greater capacity for contraction.

This investigation tests the hypothesis that ultrasound promotes wound contraction by stimulating fibroblast proliferation.

8.2 Methods

8.2.1 Insonation of human dermal fibroblasts - methodology

Primary cultures of human dermal fibroblasts were established and cultured according to Appendix 3 (p337). Sub-confluent human dermal fibroblast monolayers, passage 6, were trypsinized (Appendix 4, p338), washed in fibroblast growth medium (Appendix 2B, p335) and resuspended in the same, to make a fibroblast stock suspension that had a cell density of 1 x 10^6 viable cells/ml (Appendix 6, p340). 4 ml volumes of this fibroblast stock suspension were aliquoted into sterile, 15 ml centrifuge tubes, which were continually mixed on a rocking table and held at room temperature. The exposure chamber (Appendix 13, figure 13.1, p349) was then prepared and loaded, according to Appendix 13 (p348) with the first aliquot of fibroblasts. The exposure chamber was located in the exposure tank (figure 8.1, p 235) which was lined with ultrasound absorbent rubber (dimpled car matting) and filled with circulating degassed distilled water at 37°C. The exposure tank was 40cm

Figure 8.1. Experimental arrangement for the exposure of human dermal fibroblasts *in vitro*.

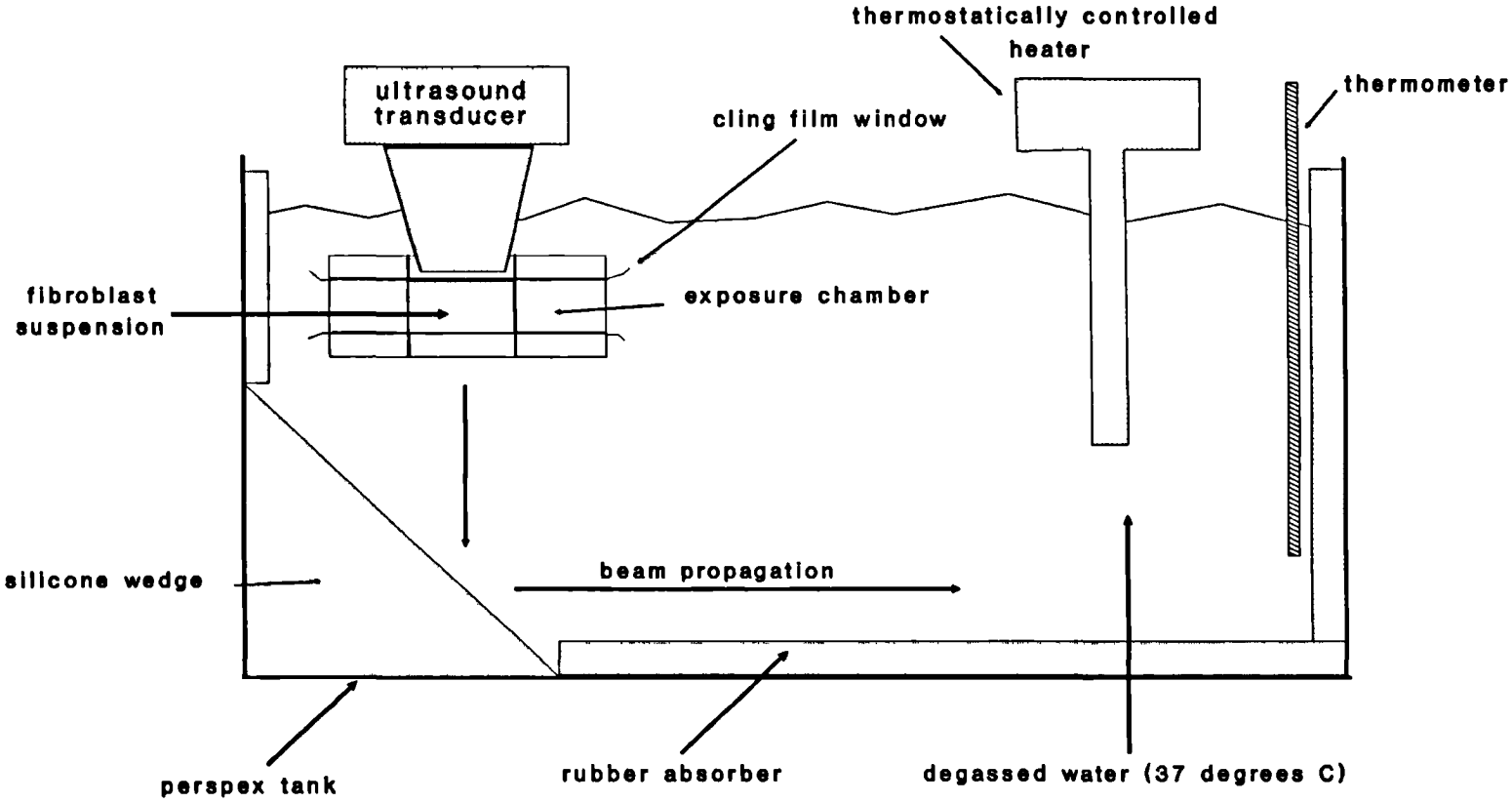

long 25cm wide and 25cm deep. The sample insonated or sham-insonated was placed in the exposure tank, as illustrated, for a period of 5 minutes. The ultrasound source used in this study was a standard Enraf Nonius Delft 434 Sonopuls machine (Enraf Nonius Delft, Holland), set to deliver 3 MHz ultrasound (figure 7.2, p222). Prior to fibroblast suspension exposure, ultrasonic output was calibrated and the generator set to deliver a fixed ultrasonic intensity - according to chapter 6 (p187).

Aliquots were allocated and exposed according to the following treatment groups:

1. Sham-insonation
2. 3 MHz pulsed (2ms:8ms) ultrasound, Intensity 0.1 W/cm^2 ($I^{(SATA)}$)
3. 3 MHz pulsed (2ms:8ms) ultrasound, Intensity 0.5 W/cm^2 ($I^{(SATA)}$)

After insonation, or sham-insonation, fibroblast suspensions were unloaded (Appendix 13, p348) from the exposure chamber into a sterile centrifuge tubes. The suspensions were continually mixed on a rocking table and held at room temperature until all insonations and sham-insonations had been completed. Once all insonations had been carried out the fibroblast suspensions were diluted from 1 x 10^6 cells per ml to 2 x 10^4 cells per ml, and kept in suspension on a rocking table. The methylene blue fibroblast proliferation assay (p149), a modification of the colorimetric assay described by Oliver *et al* (1989), was used to monitor the proliferation of insonated or sham-insonated fibroblasts.

8.2.2 Proliferation assay - methodology

The standard protocol for the "methylene blue fibroblast proliferation assay" (Appendix 8, p342), was employed as follows:

After dilution, to 2 x 10^4 cells per ml, the three fibroblast suspensions were plated-out on to 96 well flat-bottomed microtitre plates. On each plate, six replicate wells received a 100µl volume, representing 2000 cells, of each fibroblast suspension; thus filling eighteen wells. With reference to Appendix 9 (p343), the sham-insonated, 0.1 W/cm^2 insonated and 0.5 W/cm^2 insonated fibroblast suspensions were plated into the 6 central wells of columns 4, 6, and 8 respectively. Those outer wells of columns 4, 6 & 8 (i.e those in rows A and H) that did not receive a fibroblast suspension, and all wells in columns 3, 5, 7 & 9, were filled with fibroblast growth medium alone. Five replicate plates were set up in this manner. Plates were sealed and placed in an

incubator at 37°C.

Plates were removed from the incubator after 12, 36, 60, 84 and 108 hours. At each time point the plate sealing tape was removed and the plate "stopped", fixed and air dried, according to Appendix 8 steps 6 through 9 (p342). Plates stopped at 12, 36, 60 and 84 hours post fibroblast seeding were stored in a dust-free environment until the 108 hour plate had been stopped, fixed and air dried.

Fibroblast monolayers within the wells were then stained with methylene blue dye, washed with 0.01 M borate buffer and the dye eluted with acid-alcohol. The absorbance (A_{650}) of each well, on each plate, was then measured (Appendix 8, steps 10 through 12 p342). For each column of wells, and hence for each treatment group, the average A_{650} value of cell-free wells was subtracted from each of the A_{650} readings of cell containing wells. The fibroblast number within a given well was then calculated from this corrected absorbance reading using a standard plot of human dermal fibroblast number versus A_{650} (Appendix 30B, p398). This standard plot was prepared according to the method described on p152, using the same primary culture of fibroblasts, at the same passage (i.e. 6), as was used for the fibroblast proliferation assay described above.

Human dermal fibroblast proliferation in response to sham-insonation or insonation with pulsed therapeutic ultrasound at intensities of 0.1 or 0.5 W/cm^2 $I^{(SATA)}$ was compared at each of the five time points. The fibroblast proliferation data was tabulated (table 8.1) displayed graphically (figure 8.2) and analyzed using the non-parametric Mann Whitney-U test.

8.3 Results:

Figure 8.2 displays the change in median fibroblast number with time, in response to sham-insonation or insonation with pulsed 3 MHz therapeutic ultrasound at intensities of 0.1 or 0.5 W/cm^2 $I^{(SATA)}$. 95% confidence intervals are indicated to aid interpretation. A summary of the statistical analysis for this investigation can be found in Appendix 19 (p359).

From figure 8.2, and according to statistical analysis, the following points are apparent:

1. The rate of human dermal fibroblast proliferation in response to sham-insonation is not significantly different from that in response to insonation with 3 MHz pulsed ultrasound at intensities of either 0.1 or 0.5 W/cm^2.

Table 8.1. The direct effect of pulsed 3 MHz therapeutic ultrasound on the proliferation of human dermal fibroblasts *in vitro*.

Ultrasonic Exposure	Sham insonation					0.1 W/cm^2 (I^{SATA}) 3 MHz pulsed (2:8) ultrasound					0.5 W/cm^2 (I^{SATA}) 3 MHz pulsed (2:8) ultrasound				
Time post-plating (hours)	12	36	60	84	108	12	36	60	84	108	12	36	60	84	108
Number of replicate wells	6	6	6	6	6	6	6	6	6	6	6	6	6	6	6
Median cell number per well (x 10^3)	1.36	1.89	2.62	3.24	4.09	1.38	1.70	2.70	3.38	4.72	1.30	2.27	2.54	3.03	4.26
Minimum and Maximum (x 10^3)	1.22 to 1.82	1.48 to 2.52	2.29 to 3.11	2.92 to 3.74	3.60 to 4.69	1.22 to 1.55	1.32 to 3.66	2.51 to 2.95	3.08 to 3.73	4.04 to 4.96	1.22 to 1.71	1.97 to 2.46	2.24 to 2.84	2.97 to 3.08	4.03 to 5.29
95% confidence interval (x 10^3)	1.17 to 1.64	1.56 to 2.35	2.35 to 3.02	2.92 to 3.59	3.65 to 4.61	1.25 to 1.51	1.11 to 2.98	2.57 to 2.87	3.10 to 3.72	4.16 to 5.01	1.19 to 1.56	2.09 to 2.42	2.28 to 2.80	2.98 to 3.08	3.90 to 4.88

Figure 8.2. **The direct effect of pulsed 3 MHz therapeutic ultrasound on the proliferation of human dermal fibroblasts *in vitro* (median fibroblast numbers and 95% confidence intervals are indicated)**

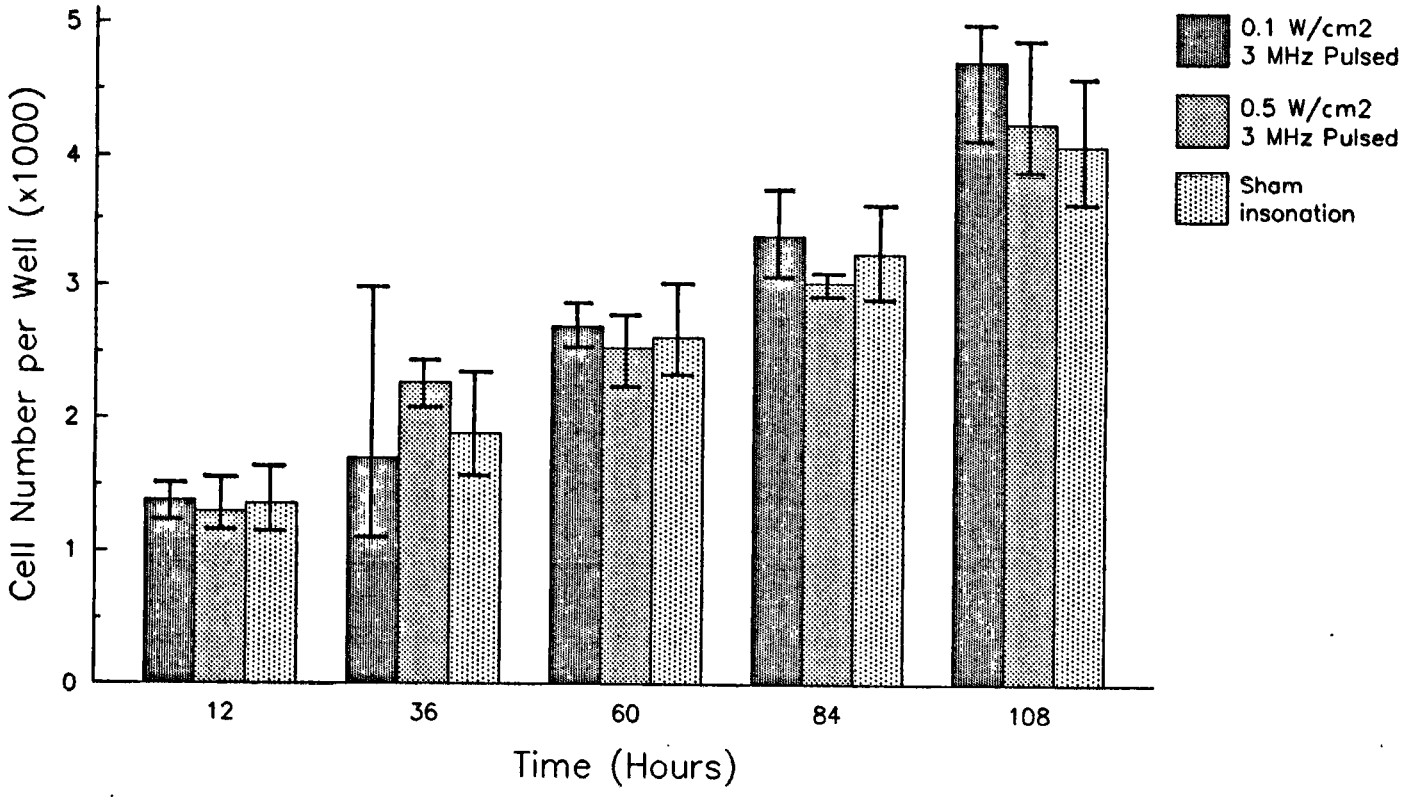

2. The rate of fibroblast proliferation in response to insonation at 0.1 W/cm^2 is not statistically different from that in response to insonation with 0.5 W/cm^2, with the exception of 84 hours post-insonation. At 84 hours post-seeding significantly more cells were observed in wells seeded with fibroblasts exposed to 0.1 W/cm^2 than in similar wells seeded with fibroblasts exposed to 0.5 W/cm^2. No such differences were observed at any other time point.

3. At termination of this study (108 hours) there would appear to be a trend indicating that exposure to ultrasound at 0.1 W/cm^2 encourage fibroblast proliferation to a greater extent than 0.5 W/cm^2, which, in turn encouraged fibroblast proliferation to a greater extent than sham exposure. However, this trend did not reach statistical significance.

8.4 Discussion

Under the experimental conditions employed in this study, it would appear that the direct application of therapeutic ultrasound to human dermal fibroblasts does not significantly effect the rate at which they proliferate. On the basis of statistical significance, this observation suggests that the mechanism by which therapeutic ultrasound promotes wound contraction in the rat (see chapter 7, p218) is unlikely to involve direct stimulation of wound fibroblast proliferation. This observation does not rule out the possibility that fibroblast density, within the wound site may increase in response to the application of therapeutic ultrasound, as has been reported in rat flank skin wounds, 5 days post wounding (Young and Dyson, 1990a). The recruitment of fibroblasts into the wound is thought to involve both fibroblast migration and proliferation; it is possible that ultrasound may interact directly with fibroblasts to promote their migration, as previously suggested by Mummery (1978), and thereby increase wound fibroblast numbers and promote contraction.

Alternatively, as the recruitment of fibroblasts is thought to depend on an array of mitogenic and migratory stimuli (tables 1.2 and 1.3, pages 35 and 39) generated during the inflammatory phase of repair; it is possible that therapeutic ultrasound may encourage the influx of fibroblasts into the wound site by modulating the generation of these mitogenic and migratory agents during inflammation. The increased elaboration of agents, mitogenic for fibroblasts and endothelial cells, may explain the enhanced rate of ^{3}H-thymidine incorporation in rabbit ear wounds exposed to 3 MHz ultrasound (Dyson *et al.* 1970). Investigations into the effect of

therapeutic ultrasound on the elaboration of mitogenic agents by platelets and macrophages, the principal sources of mitogenic and migratory substances for fibroblasts in wound repair, can be found in chapters 10 (p253) and 11 (p276).

There are several published reports of the effect of ultrasound on cellular growth *in vitro*, however, these studies appear to have been carried out either in response to safety concerns over possible hazards of exposure (i.e. loss of viability), or, to study the application of ultrasound to cancer therapy (selective cell killing), rather than in anticipation of a possibly therapeutic mitogenic effect. Consequently the ultrasonic parameters used in these studies, specifically ultrasonic intensity, are generally beyond the therapeutic range, and the experimental endpoints used are usually cell death or loss of proliferative capacity. There are no published reports describing the effect of therapeutic ultrasound at the precise parameters used in this thesis on cellular proliferation *in vitro*. The limited number of studies that have employed ultrasound at therapeutic levels have used frequencies of, or about, 1 MHz, in continuous wave mode. Such studies have been unable to detect a mitogenic effect in response to therapeutic levels of ultrasound. Rather, they have tended to indicate that mid intensity ultrasound (up 1 W/cm^2 $I^{(a)}$) has no effect on cellular growth (Kaufman *et al.* 1977; Ross *et al.* 1983; Decat and Leonard, 1984), whereas, at the upper end of the therapeutic range (approximately 3 W/cm^2 $I^{(a)}$) ultrasound leads to a loss of proliferative capacity (Kaufman *et al.* 1977; Ciaravino and Miller, 1978; Kaufman and Miller 1978; Fu *et al.* 1980). The loss of cellular proliferative capacity in response to insonation *in vitro* has been associated with cavitational damage as under non-cavitating conditions such losses are not observed (Armour and Corry, 1982; Ciaravino *et al.* 1981b; Coakley *et al.* 1971), even at intensities far in excess of the therapeutic range (Bleaney *et al.* 1972). The exposure tank employed in this thesis was designed to reduce standing wave formation and thereby reduce the likelihood of transient cavitation. A 45° silicone wedge, placed below the insonation chamber, was used to both (a) partially absorb, and, (b) partially reflect the ultrasonic beam into a rubber absorber lining the exposure tank. This, together with the use of a relatively higher frequency (3MHz) of ultrasound, at which cavitation is less likely (p101), may explain why a significant loss in fibroblast proliferative capacity was not observed in this study.

Studies examining the effect of ultrasound on DNA synthesis by cultured cells *in vitro* generally tend to contradict the cellular growth studies. Therapeutic

ultrasound has been shown to stimulate DNA synthesis, as measured by ^{3}H-thymidine incorporation, in cultured mouse tibial epiphyses (Elmer and Fleisher, 1974), concanavalin A stimulated lymphocytes (Repacholi *et al.* 1979) and mouse L cells (Kondo and Yoshii, 1985). ^{3}H-thymidine incorporation during DNA repair, following ultrasound-induced DNA damage, may explain the apparent contradiction in results between the proliferation studies and the DNA synthesis studies.

This investigation, like many other *in vitro* studies in the wound healing literature, makes the assumption that cultures of human dermal fibroblasts from normal forearm skin can respond to modulatory agents in a similar manner to that of fibroblasts within granulating wounds. In this study fibroblasts were cultured on plastic in monolayer, a two dimensional arrangement that affords cells a clearly different environment to the three dimensional arrangement of extracellular matrix found *in vivo* (Nusgens *et al.* 1984). The fibroblast-populated collagen lattice (p160), a three dimensional tissue culture system, may provide a more appropriate environment for the study of fibroblast function *in vitro*. This model was employed to investigate the direct and indirect effects (mediated by platelet and macrophages) of therapeutic ultrasound on the process of fibroblast-mediated collagen lattice remodelling in chapters 9, 10 and 11. Recently, it has become apparent that fibroblasts are capable of demonstrating both significant structural and functional heterogeneity (Sappino *et al.* 1990; Regan *et al.* 1991; Finesmith *et al.* 1990). For example, Regan *et al.* (1991) demonstrated that wound-harvested fibroblasts are less responsive to mitogenic stimuli, but have an increased capacity to synthesize collagen and have an increased capacity to contract collagen lattices, when compared with normal dermal fibroblasts. It is thus possible that the lack of effect observed here may not accurately represent the response of fibroblasts within granulating wounds. Further studies are necessary to investigate the capacity of wound-derived fibroblasts to respond to therapeutic ultrasound *in vitro*.

In summary, this investigation demonstrates that therapeutic ultrasound, at the parameters stated above, is not directly mitogenic for fibroblasts derived from normal human skin *in vitro*. This observation suggests that the numerous reports of ultrasound-stimulated wound healing (Dyson *et al.* 1970; Dyson *et al.* 1976;; Roche and West, 1984; McDiarmid *et al.* 1985; Young and Dyson, 1990a/c; Byl *et al.* 1992), including stimulated cryosurgical wound contraction (Dyson and Smalley, 1983) and mechanical wound contraction (reported in Chapter 7), is not due to a direct pro-

proliferative interaction of ultrasound with fibroblasts. However, care must be exercised in extrapolating the observations made in this study to other wound healing ultrasound bioeffects. This study examined the effect of applying a single frequency of pulsed ultrasound, at just two ultrasonic intensities, to fibroblasts cultured *in vitro*. Other studies have reported that ultrasound at clearly different parameters to those used in this study can modify various aspects of the repair process. It would be inappropriate to categorically state that all these effects are not a result of a direct pro-mitogenic ultrasonic effect on fibroblast populations.

Chapter 9. The direct effect of 3 MHz therapeutic ultrasound on the contraction of human dermal fibroblast-populated collagen lattices *in vitro*.

9.1 Introduction.

Ultrasound has been used as a therapeutic agent in physical medicine for over fifty years (Dyson and Suckling, 1978). A significant literature has developed during that time, included in this literature are many clinical, laboratory animal and *in vitro* model-based reports which suggest that, under appropriate conditions, ultrasound can stimulate the process of cutaneous repair (chapter 4, p107). Chapter 7 (p218) of this thesis, in which therapeutic ultrasound was shown to promote wound contraction in rat flank skin wounds, further sustains such reports. While various physical mechanisms by which ultrasound may interact with biological tissues have been described (p92), the responsive target that mediates the stimulation in cutaneous repair, and more specifically wound contraction, is as yet unknown.

Wound contraction is widely accepted as a fibroblast-mediated process. The way in which wound fibroblasts act to bring about wound contraction is, however, the centre of some debate (Ehrlich, 1988; Gabbiani *et al.* 1971). A widely accepted *in vitro* model for the process of wound contraction is the fibroblast-populated collagen lattice (FPCL) (p160). In this model, fibroblasts seeded within a three dimensional matrix of collagen progressively contract this matrix to a fraction of its original size.

Previous studies investigating the direct effect of therapeutic ultrasound on fibroblasts *in vitro* have demonstrated that ultrasound can stimulate fibroblast migration (Mummery, 1978) and collagen synthesis (Harvey *et al.* 1975). The FPCL model was employed in this study to examine the ability of ultrasound to directly modulate fibroblast-mediated contraction *in vitro*, with a view to explaining the stimulation of wound contraction observed *in vivo*.

This investigation tests the hypothesis that therapeutic ultrasound promotes wound contraction by directly stimulating fibroblast-mediated contraction.

9.2 Methods

Eighteen standard fibroblast-populated collagen lattices were prepared according to steps 1 through 6 of the human dermal fibroblast collagen lattice contraction assay - standard protocol (Appendix 10, p344). After polymerisation and lattice release, the 18 lattices were "fed" with 1.0 ml of fibroblast growth medium (Appendix 2B, p335)

Figure 9.1. Experimental arrangement for the insonation of fibroblast-populated collagen lattices.

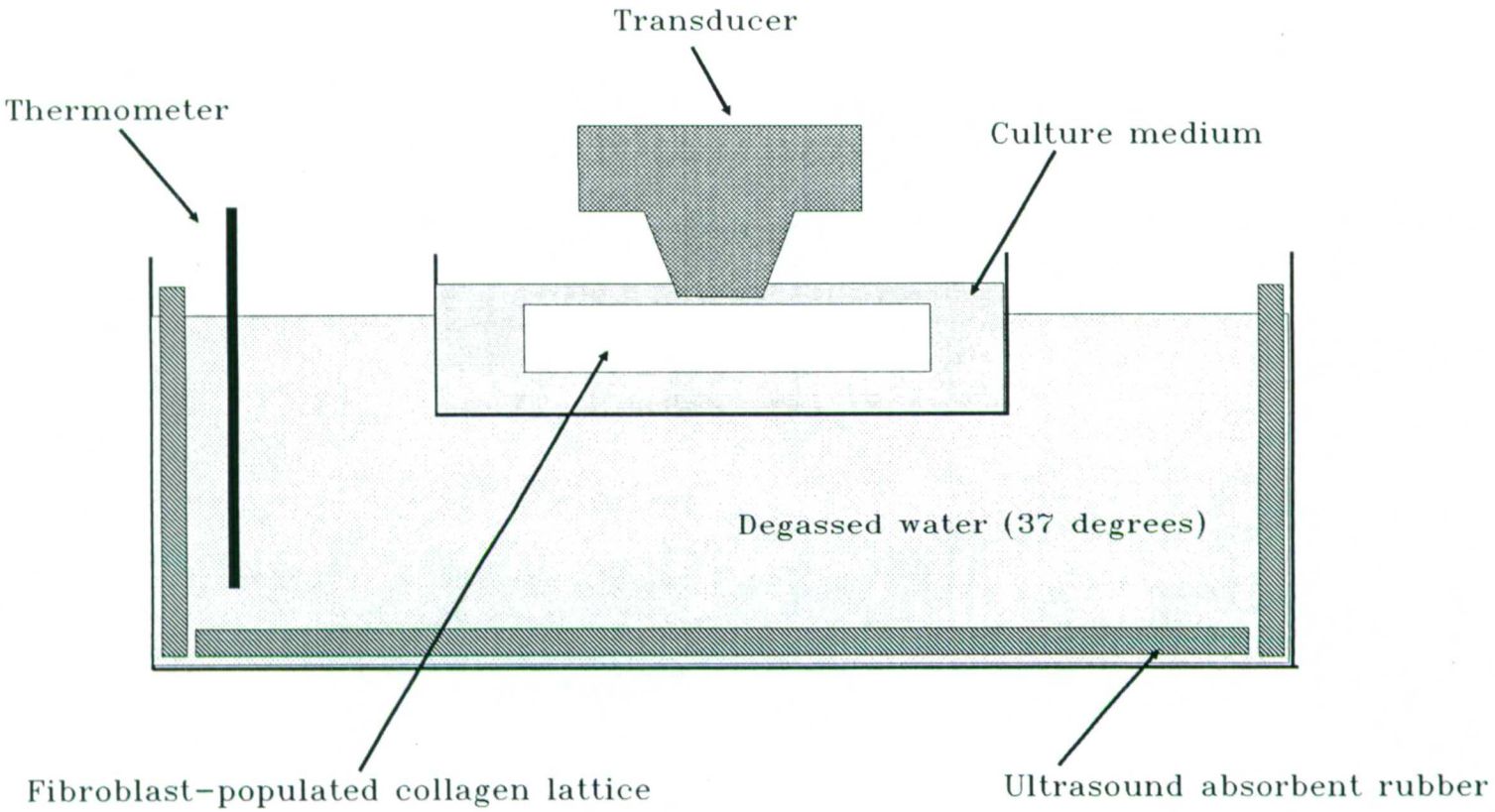

and randomly allocated into 3 experimental groups, each containing 6 lattices.

After polymerization and feeding, FPCLs received a single, 5 minute, insonation or sham-insonation of therapeutic ultrasound according to figure 9.1 (p245). Petri dishes, containing FPCLs, were floated on the surface of a heated (37°C) water tank of dimensions 15cm long, 15cm wide and 6cm deep. The ultrasound transducer, sterilised using 70% alcohol, was slowly lowered into place above the lattice in such a manner that the suspending medium of the lattice acted as an ultrasonic couplant. The lattice was then insonated or sham-insonated according to the experimental group to which it had been allocated. The water tank was lined with ultrasound absorbent rubber (dimpled car matting) and the petri dishes slowly moved to prevent standing wave formation and to ensure that all areas of the lattice were similarly insonated. The therapeutic ultrasound source used in this study was a standard Enraf Nonius Delft 434 Sonopuls machine (Enraf Nonius Delft, Holland), set to deliver 3 MHz ultrasound (figure 7.2, p222). Prior to lattice exposure, ultrasonic output was calibrated and the generator set to deliver a fixed ultrasonic intensity - according to chapter 6 (p187).

The three groups of lattices were treated as follows:

1. Sham-insonation
2. 3 MHz pulsed (2ms:8ms) ultrasound, Intensity 0.1 W/cm^2 ($I^{(SATA)}$)
3. 3 MHz pulsed (2ms:8ms) ultrasound, Intensity 0.5 W/cm^2 ($I^{(SATA)}$)

After insonation the lattices were placed in a humidified box and returned to the incubator. All eighteen lattices were photographed (Appendix 11A, p345) at 9, 21, 28, 50 and 58 hours after initial plating and the film developed according to Appendix 11B (p346). The area of each lattice, in mm^2, was then measured by computer-assisted planimetry (Appendix 12, p347). Median lattice area, minimum and maximum lattice area, and 95% confidence intervals were calculated for each group of lattices (i.e. in response to sham-insonation or insonation with 3 MHz therapeutic ultrasound at 0.1 or 0.5 W/cm^2 $I^{(SATA)}$) at each time point (table 9.1 p248) and the data was graphically displayed (figure 9.2, p248). Non-parametric statistical analyses (Mann Whitney-U tests) were performed to examine the modulation in the rate of lattice contraction in response to therapeutic ultrasound.

9.3 Results:

Figure 9.1 displays the change in median lattice area (mm^2) with time (hours), in

response to sham-insonation or insonation with pulsed therapeutic ultrasound at intensities of 0.1 or 0.5 W/cm^2. 95% confidence intervals are indicated to aid interpretation. A summary of the statistical analysis for this investigation can be found in Appendix 20 (p360).

From figure 9.2, and according to statistical analysis, the following points are apparent:

1. The rate of fibroblast-mediated lattice contraction in response to sham-insonation was not significantly different from that in response to insonation with 3 MHz pulsed ultrasound at an intensity of 0.1 W/cm^2.
2. The rate of fibroblast-mediated lattice contraction in response to sham-insonation was generally not significantly different to that observed in response to insonation with 3 MHz pulsed ultrasound at an intensity of 0.5 W/cm^2. At the first time point recorded, that of 9 hours after lattice polymerisation, FPCL insonated with an intensity of 0.5 W/cm^2 were significantly larger i.e. had contracted to a lesser extent than similar sham insonated FPCL ($p = 0.013$). After this time no significant differences were observed.
3. Lattice contraction in response to insonation at an ultrasonic intensity of 0.1 W/cm^2 was not statistically different from that observed in response to insonation at 0.5 W/cm^2.

9.4 Discussion

It is apparent from the results that a single insonation of pulsed 3 MHz therapeutic ultrasound has little effect on the rate of fibroblast-mediated collagen lattice contraction.

At the 9 hour sampling point, an ultrasound intensity-dependent trend in lattice area would appear to exist. According to this trend, maximal ultrasonic intensity is paralleled by minimal lattice contraction. At this time point, the first after insonation, sham-exposed FPCL were smaller (i.e had contracted more rapidly) than similar FPCL insonated at an intensity of 0.1 W/cm^2; which, in turn were smaller than lattices exposed to an intensity of 0.5 W/cm^2. Statistical significance was only observed between the sham-insonated lattices and the insonated lattices exposed to an intensity of 0.5 W/cm^2. This intensity dependent reduction in contraction may result from ultrasound-associated damage to fibroblasts. It is not clear whether this effect is thermal or non-thermal in nature. The heat generated as a consequence of

Table 9.1 The direct effect of therapeutic ultrasound on the contraction of human dermal fibroblast populated collagen lattices.

Ultrasonic exposure	Sham insonation					0.1 W/cm^2 (I^{SATA}) 3 MHz pulsed (2:8) ultrasound					0.5 W/cm^2 (I^{SATA}) 3 MHz pulsed (2:8) ultrasound				
Time post-plating (hours)	9	21	28	50	58	9	21	28	50	58	9	21	28	50	58
Number of replicate lattices	6	6	6	6	6	6	6	6	6	6	6	6	6	6	6
Median area of lattices (mm^2)	572.1	439.3	367.8	226.1	216.1	604.1	431.1	375.4	213.9	216.6	633.5	440.3	382.6	202.2	207.5
Minimum and Maximum (mm^2)	548.2 to 624.3	422.7 to 544.0	356.2 to 429.4	208.8 to 233.7	203.9 to 220.7	560.1 to 666.6	406.6 to 514.7	356.9 to 403.5	185.1 to 240.8	180.7 to 228.8	599.9 to 652.9	416.3 to 456.0	361.1 to 398.5	170.2 to 233.2	184.7 to 229.3
95% confidence interval (mm^2)	549.1 to 617.0	409.4 to 509.0	349.5 to 414.7	214.5 to 233.0	208.2 to 220.8	570.2 to 649.8	398.4 to 484.3	355.0 to 399.4	189.7 to 237.1	190.5 to 229.7	611.4 to 654.0	424.8 to 455.9	363.2 to 394.8	176.9 to 227.3	186.6 to 224.9

Figure 9.2 Graphical representation of the effect of 3 MHz therapeutic ultrasound on fibroblast-mediated collagen lattice contraction (median lattice areas and 95% confidence intervals are displayed).

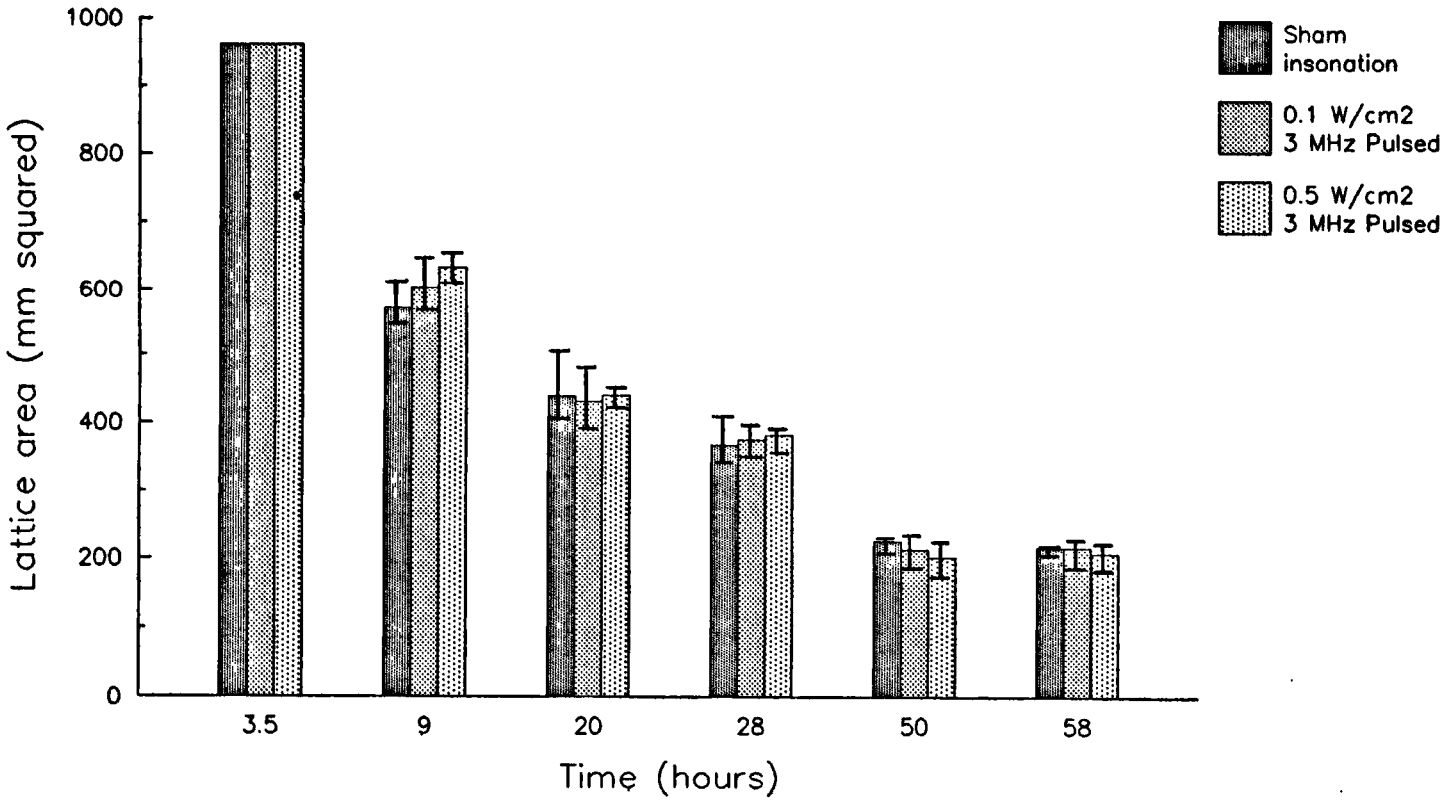

ultrasonic energy absorption by cells in suspension is quickly dissipated into the suspending medium, and as such, cells in suspension are less likely to be influenced by temperature rises than cells *in vivo* (Williams, 1985). However, the FPCL is a proteinaceous dermis-like matrix seeded with cells, which would be expected to absorb more energy and consequently generate more heat, than a simple suspension of cells. Heat dissipation is also probably less efficient due to a sponge-like restriction in fluid movement. Unlike the majority of *in vitro* cell insonation systems which both encourage non-thermal effects and mask thermal effects (Miller, 1985b; Williams, 1985), the dermis-like ultrasound attenuation characteristics of FPCLs makes them a more appropriate *in vitro* model for studying ultrasound bioeffects than cell suspensions. As the trend in lattice contraction inhibition was effectively restricted to the 9 hour sampling point it would appear that such damage, if damage was responsible, was of a limited and reversible nature.

This study would appear to suggest that therapeutic ultrasound lacks the capacity to interact directly with fibroblasts to promote fibroblast-mediated lattice contraction. As the FPCL is an *in vitro* system widely accepted as a model of the process of wound contraction *in vivo* (Ehrlich and Rajaratnam, 1990), such observations suggest that therapeutic ultrasound promotes wound contraction by means other than a direct stimulation of fibroblast activity.

Two theories have been proposed to explain how fibroblasts mediate both wound contraction *in vivo* and FPCL contraction *in vitro* (see chapters 1 (p18) and 5 (p132)). Briefly, the myofibroblast theory proposes that myofibroblasts, cells sharing phenotypic characteristics of fibroblasts and smooth muscle cells (SMC), undergo a muscle-like cellular contraction and thereby bring about wound or lattice contraction. The fibroblast theory proposes that fibroblasts gather extracellular matrix fibrils together by a cell migration-associated traction-like mechanism and in doing so facilitate wound or lattice contraction.

It has previously been reported that therapeutic levels of ultrasound can stimulate smooth muscle contraction both *in vitro* and *in vivo* (Talbert *et al.* 1975; ter Haar *et al.* 1978) and stimulate calcium uptake by fibroblasts (Mortimer and Dyson, 1988). According to the myofibroblast theory of smooth muscle-like cellular contraction, in which FPCL contraction is mediated by these SMC-like cells, therapeutic levels of ultrasound would be expected to promote lattice contraction. The lack of pro-contractile effects noted here may question the role of myofibroblasts

in lattice contraction. However, cells with myofibroblastic characteristics are slow to develop in collagen lattices, and would not have been present in significant numbers at the time lattices were insonated in this study. Consequently, it is impossible to rule out a direct ultrasonic effect on myofibroblast contraction as the mechanism responsible for the stimulated contraction of insonated rat wounds reported in chapter 7 (p218) and previously by Dyson and Smalley (1983).

Mummery (1978) reported that therapeutic levels of ultrasound could stimulate fibroblast motility *in vitro*, with insonated fibroblasts executing fewer changes in direction than similar non-insonated fibroblasts. According to the traction theory of contraction, in which FPCL contraction is mediated by a cell migration-associated traction-like mechanism, contraction may be expected to be more rapid if cellular migration was more rapid. The lack of a pro-contractile effect noted in this study may question the traction theory of lattice contraction. However, there are significant differences in experimental design between the work of Mummery (1978) and that reported here, including the cell culture environment under which fibroblasts were studied, which may invalidate any comparison between the two studies.

The lack of a pro-contractile effect in this study of the direct effect of ultrasound on fibroblast-mediated contraction does not rule out the possibility that therapeutic ultrasound acts to promote fibroblast activity in an indirect manner, possibly by encouraging the synthesis and/or elaboration of pro-contractile substances from other cell types involved in the wound repair process. As ultrasound exposure soon after injury, i.e during inflammation, has previously been reported to promote various aspects of the repair process, it is possible that ultrasound encourages the release of pro-contractile substances from inflammatory cells. Chapters 10 (p253) and 11 (p276) describe studies performed to investigate the ability of therapeutic ultrasound to encourage the elaboration of pro-contractile activities from platelets and macrophages, and thereby modulate fibroblast-mediated contraction indirectly.

Fibroblasts have been shown to be capable of significant morphological, structural and functional heterogeneity (Sappino *et al.* 1990; Regan *et al.* 1991; Finesmith *et al.* 1990). It has been proposed that the wound environment may induce, or select, specific fibroblast phenotypes that differ in their ability to respond to exogenous stimuli such as growth factors (Regan *et al.* 1991; Finesmith *et al.* 1990). It is possible therefore that the lack of response to therapeutic ultrasound observed

here results from the use of an inappropriate fibroblast phenotype. The extracellular matrix (ECM) component of the lattices used in this study is primarily type I collagen. The ECM experienced by granulation tissue fibroblasts is far more complex. Initially the ECM is rich in hyaluronic acid, fibronectin and collagen type III, but as repair proceeds this is gradually replaced by an ECM predominantly composed of type I collagen and sulphated proteoglycans. Further studies investigating the ability of therapeutic ultrasound to modulate fibroblast-mediated contraction of FPCLs, composed of granulation tissue-derived fibroblasts seeded into a more granulation tissue-like ECM are necessary to confirm the observations made in this study.

In summary, this investigation demonstrates that therapeutic ultrasound, at the parameters employed and with a type I collagen matrix, does not promote fibroblast-mediated collagen lattice contraction *in vitro*. If this *in vitro* observation can be extrapolated to the process of wound contraction *in vivo*, it would appear that ultrasound-stimulated wound contraction, reported in chapter 7 (p218) and by Dyson and Smalley (1983), is not due to a direct pro-contractile effect on fibroblasts.

Chapter 10. The effect of therapeutic ultrasound on the release from platelets of substances capable of modulating fibroblast activity *in vitro*.

10.1 Introduction

The inflammatory phase that occurs in response to tissue injury is essential to healing (Clark, 1990). Platelets respond directly to vascular insult by adhesion and activation of the blood coagulation system. Activated platelets also release a multitude of biologically active substances, some of which are thought to encourage the onset of later phases of repair. These active substances include various peptide growth factors which are thought to initiate cell migration, proliferation and matrix synthesis within the wound site (p32-46).

Therapeutic ultrasound has been shown to enhance several aspects of wound repair, in both the clinical and experimental arenas (chapter 4). However, its mechanism and site of action are not fully understood. As treatment with ultrasound has been shown to be particularly effective when applied during the inflammatory phase of repair, it has been suggested that ultrasound interacts with some component(s) of this phase.

The aim of this study was to examine the effect of therapeutic levels of pulsed ultrasound on the release from platelets of substances capable of modulating the proliferative and contractile capacity of human dermal fibroblasts *in vitro*.

The materials and methods employed in the exposure of platelets to ultrasound and the subsequent generation of platelet releasates is described first. An investigation into the effect of these ultrasonically generated platelet-releasates on fibroblast proliferation *in vitro* is then described, followed by a further investigation into the effect of similarly generated platelet releasates on fibroblast-mediated collagen lattice contraction.

10.2 Insonation of human platelets - methodology

A human platelet stock suspension containing 1 x 10^9 platelets per ml of platelet washing buffer (PWB) (Appendix 1C, p334) was prepared according to Appendix 7, (p341) and held on ice. (Note. One 450 ml transfusion bag full of freshly donated blood is sufficient to prepare 20 ml of platelet stock solution). 4 ml volumes of this platelet stock suspension were aliquoted into sterile, chilled, universal bottles, and held on ice. The exposure chamber (Appendix 13, figure 13.1, p349) was then

prepared and loaded, according to Appendix 13 (p 348) with the first aliquot. The exposure chamber was located in the exposure tank (figure 10.1, p255) which was lined with ultrasound-absorbent rubber (dimpled car matting) and filled with circulating degassed distilled water at 4°C. The exposure tank was 40cm long, 25cm wide and 25cm deep. The sample was insonated or sham-insonated for a period of 5 minutes. One aliquot, in each series, was neither insonated nor sham-insonated, but treated with 1 unit of sterile thrombin (Diagnostic Reagents Ltd, UK) per ml of platelet stock suspension at a temperature of 20°C for 5 minutes.

The therapeutic ultrasound source used in this study was a standard Enraf Nonius Delft 434 Sonopuls machine (Enraf Nonius Delft, Holland), set to deliver 3 MHz ultrasound (figure 7.2, p222). Prior to platelet exposure, ultrasonic output was calibrated and the generator set to deliver a fixed ultrasonic intensity as described in chapter 6 (p187).

Aliquots were allocated to the following treatment groups:

1. Sham-insonation
2. 3 MHz pulsed (2ms:8ms) ultrasound, Intensity 0.1 W/cm^2 ($I^{(SATA)}$)
3. 3 MHz pulsed (2ms:8ms) ultrasound, Intensity 0.5 W/cm^2 ($I^{(SATA)}$)
4. Thrombin - 1 unit per ml - incubated for 5 minutes

After insonation, sham-insonation, or thrombin exposure, platelet suspensions were unloaded from the exposure chamber into sterile centrifuge tubes. The platelet suspensions were then centrifuged at 950 x g to remove spent and remaining intact platelets, and platelet debris. The resulting supernatant was termed the platelet releasate for that treatment group. The releasates were then aliquoted into sterile cryo-tubes and stored at -70°C until required for bioassay assessment by either the methylene blue fibroblast proliferation assay (p149) or the human dermal fibroblast-populated collagen lattice contraction assay (p160).

Throughout the preparation of the platelet releasates, as described above, care was taken to minimise platelet perturbation associated with handling. Such care included the storage of platelet aliquots on ice throughout the procedure (with the exception of the thrombin releasate) and the gentle resuspension and transfer of platelet samples.

Figure 10.1. Experimental arrangement for the exposure of human platelets to pulsed 3 MHz therapeutic ultrasound *in vitro*.

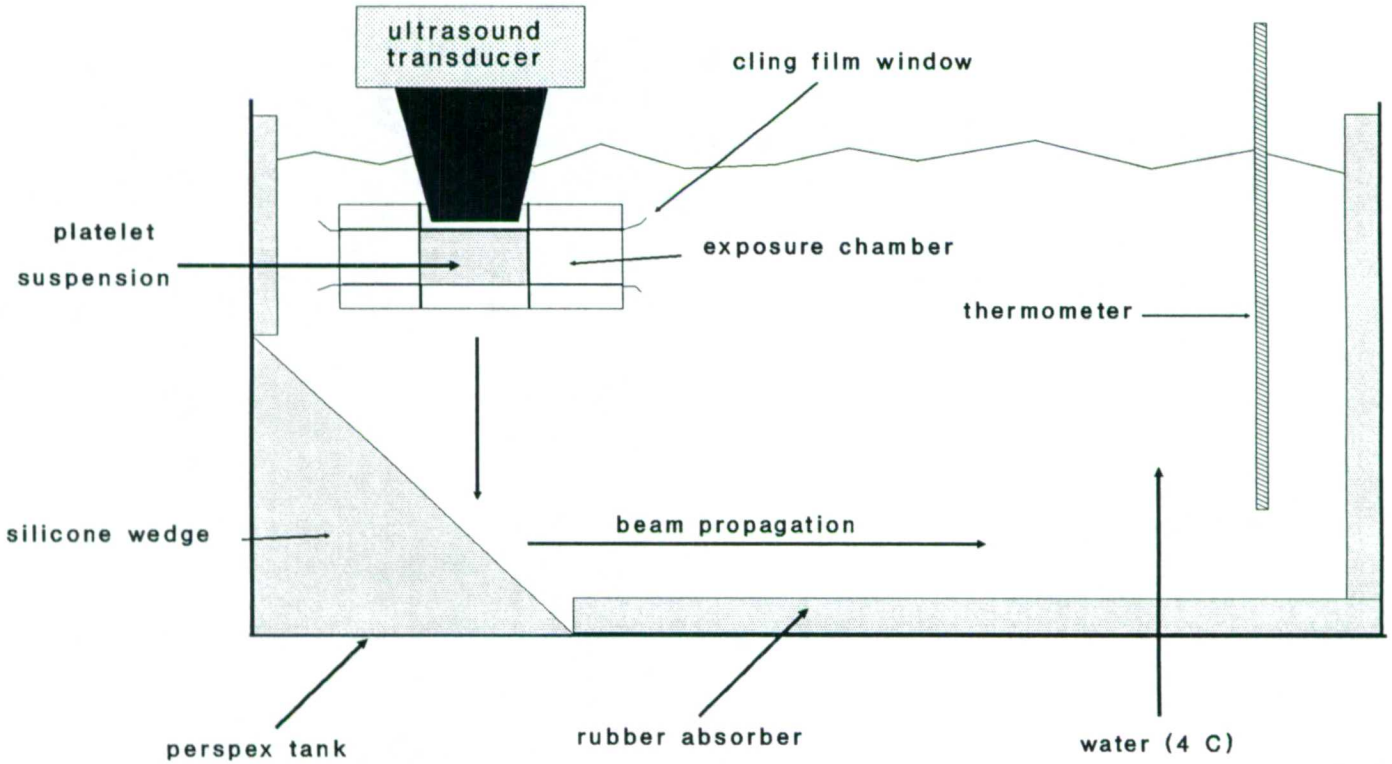

10.3 The effect of ultrasound on the release from platelets of substances capable of modulating fibroblast proliferation *in vitro*

10.3.1 Introduction

The methylene blue fibroblast proliferation assay (p149), a modification of the colorimetric assay described by Oliver *et al* (1989), was use to investigate the effect of ultrasonically generated human platelet releasates on the proliferation of human dermal fibroblasts *in vitro*.

10.3.2 Method

The standard protocol for the "methylene blue fibroblast proliferation assay" (Appendix 8, p342), was employed with the following modifications.

Sub-confluent human dermal fibroblast monolayers, passage 6, were trypsinised (Appendix 4, p338), washed in fibroblast growth medium (Appendix 2B, p335) and resuspended in the same, to a final concentration of 2 x 10^4 viable cells/ml (Appendix 6, p340). 100 µl volumes of this suspension, each containing 2000 cells, were aliquoted into 30 wells (i.e. filling all wells in columns 2, 3, 4, 5, and 6, with the exception of those wells in rows A and H) of a 96 well flat-bottomed microtitre plate (Appendix 9, p 343). 10 of the remaining wells (i.e. all wells in columns 2, 3, 4, 5, and 6 that did not receive the cell suspension) were filled with fibroblast growth medium alone. Four replicate plates were set up in this manner. The plates were sealed and placed in a 37°C incubator for 12 hours to allow for cell attachment.

After 12 hours, all 4 plates were removed from the incubator and the plate sealing tape removed. One of the four plates, subsequently termed the 12 hour plate, was "stopped" according to Appendix 8 steps 6 through 9 (p 342), and stored in a dust- free environment. On each of the three remaining plates, one of each of the 5 columns of wells was then designated to receive one of the four releasates or the vehicle, platelet washing buffer (PWB) (Appendix 1C, p334), alone. All 8 wells of a given column, including cell-free wells, received 100µl of a given releasate (or PWB). After thawing, platelet releasates were first sterilised with a 0.22 µm millipore filter and then diluted 1 in 10 with sterile phosphate buffered saline (Appendix 1A, p334) prior to use.

Once all wells had received either 100 µl of one of the four platelet releasates or PWB alone, the plates were resealed and returned to a 37°C incubator. Individual

plates were subsequently "stopped" at 60, 108 and 156 hours post initial seeding with fibroblasts, according to Appendix 8 steps 6 through 9 (p342). Plates stopped at 60 and 108 hours post fibroblast seeding were stored, with the 12 hour plate, in a dust free environment until the 156 hour plate had been stopped and air dried.

Fibroblast monolayers within the wells were then stained with methylene blue dye, washed with 0.01 M borate buffer and the dye eluted with acid-alcohol. The absorbance (A_{650}) of each well, on each plate, was then measured (Appendix 8, steps 10 through 12 p342). For each column of wells, and hence for each releasate under test, the average A_{650} value of cell-free wells was subtracted from each of the A_{650} readings of cell-containing wells. The fibroblast number within a given well was then calculated from this corrected absorbance reading using a standard plot of human dermal fibroblast number versus A_{650} (Appendix 30B, p398). This standard plot was prepared according to the method described on page 152, using the same primary culture of fibroblasts at the same passage (p6) as was used for the fibroblast proliferation assay described above.

Human dermal fibroblast proliferation in response to the application of each of the four platelet releasates (and platelet washing buffer - the vehicle) was compared at each of the four time points. The fibroblast proliferation data was tabulated (see tables 10.1 through 10.5), displayed graphically (figure 10.2) and analyzed using the non-parametric Mann Whitney-U test.

10.3.3 Results:

Figure 10.1 displays the change in median fibroblast number with time, in response to each of the four platelet releasates and PWB. 95% confidence intervals are indicated to aid interpretation. A summary of the statistical analysis for this investigation can be found in Appendix 21 (p361).

From figure 10.1, and according to statistical analysis, the following points are apparent.

1. Fibroblast proliferation measured over 156 hours is most rapid in the presence of the thrombin releasate (T-R) and slowest in the presence of the vehicle PWB at all time points after the addition of releasates (i.e. after 12 hours). After 60, 108 and 156 hours there are significantly more fibroblasts ($p < 0.005$) within T-R treated wells than in similar vehicle (PWB) treated wells.
2. The application of the sham-exposed platelet releasate (S-R) leads to more rapid

fibroblast proliferation than that observed in the presence of the vehicle, PWB, alone, with significantly more fibroblasts in S-R wells at 60 hours ($p = 0.012$), 108 hours ($p < 0.005$) and 156 hours ($p < 0.005$) post initial seeding.

3. Insonation of platelets with 3 MHz ultrasound at an intensity, $I^{(SATA)}$, of 0.1 W/cm^2 leads to the generation of a platelet releasate (0.1-R) with a greater stimulatory activity for the proliferation of fibroblasts than that of the platelet releasate generated by sham-insonation (S-R), with significantly more fibroblasts in 0.1-R wells at 108 ($p < 0.005$) and 156 hours ($p = 0.036$) post initial seeding. At the 60 hour time point, fibroblast number was not significantly different in those wells that received 0.1-R compared with those wells that received the sham-insonated platelet releasate, S-R.

4. Fibroblast proliferation is more rapid in the presence of the releasate (0.5-R) generated by the exposure of platelets to 3 MHz ultrasound at an intensity, $I^{(SATA)}$, of 0.5 W/cm^2 than in the presence of the sham-insonated platelet releasate, with significantly more fibroblasts in ultrasound-treated platelet releasate wells at 108 ($p = 0.036$) and 156 ($p < 0.005$) hours post initial seeding. In parallel with the comparison of the 0.1 W/cm^2 releasate with the sham-insonated releasate, fibroblast number was not significantly different in those wells that received 0.5-R compared with those wells that received S-R at 60 hours post seeding.

5. Though small differences are apparent from the data, there appear to be no significant differences in the rate of fibroblast proliferation observed in response to application of the 0.1 W/cm^2 ultrasound releasate compared with that observed in response to the application of the 0.5 W/cm^2 ultrasound releasate, at any time point.

6. Fibroblast proliferation was significantly more rapid in response to the thrombin platelet releasate than in response to the 0.1 W/cm^2 ultrasound platelet releasate, with significantly more fibroblasts present in the T-R wells at all time points ($p < 0.005$).

7. Fibroblast proliferation was more rapid in response to the thrombin platelet releasate than in response to the 0.5 W/cm^2 ultrasound platelet releasate, with significantly more fibroblasts present in T-R wells at the 108 ($p < 0.030$) and 156 ($p < 0.020$) hour time points. Though there were more fibroblasts in thrombin releasate wells than in 0.5 W/cm^2 releasate wells at the 60 hour time point, this difference did not reach statistical significance ($p = 0.065$).

Table 10.1 The effect of platelet washing buffer on the proliferation of p6 human dermal fibroblasts *in vitro*.

	Time post plating			
	12	60	108	156
Number of replicate wells	6	6	6	6
Median cell number per well (cells x 10^3)	1.206	1.642	2.102	1.970
Minimum and maximum (cells x 10^3)	1.152 to 1.806	1.533 to 1.861	1.939 to 2.375	1.779 to 2.051
95% confidence interval (cells x 10^3)	1.049 to 1.581	1.523 to 1.818	1.969 to 2.327	1.840 to 2.063

Table 10.2 The effect of thrombin platelet releasate, prepared by incubating a standard platelet suspension with thrombin at a concentration of 1.0 units ml, on the proliferation of p6 human dermal fibroblasts *in vitro*.

	Time post plating			
	12	60	108	156
Number of replicate wells	6	6	6	6
Median cell number per well (cells x 10^3)	1.261	2.678	4.038	3.878
Minimum and maximum (cells x 10^3)	1.043 to 1.752	2.460 to 3.006	3.520 to 4.610	3.578 to 4.723
95% confidence interval (cells x 10^3)	1.021 to 1.628	2.460 to 2.915	3.536 to 4.503	3.554 to 4.457

Table 10.3 The effect of the sham-insonated platelet releasate, prepared by sham-insonating a standard platelet suspension, on the proliferation of p6 human dermal fibroblasts *in vitro*.

	Time post plating			
	12	60	108	156
Number of replicate wells	6	6	6	6
Median cell number per well (cells x 10^3)	1.379	2.379	2.635	2.710
Minimum and maximum (cells x 10^3)	1.024 to 1.570	1.751 to 2.406	2.471 to 2.907	2.438 to 2.819
95% confidence interval (cells x 10^3)	1.085 to 1.528	1.897 to 2.514	2.501 to 2.805	2.491 to 2.802

Table 10.4 The effect of the 0.1 W/cm^2 insonated platelet releasate, prepared by insonating a standard platelet suspension with 3 MHz pulsed ultrasound at an intensity $I^{(SATA)}$ of 0.1 W/cm^2, on the proliferation of p6 human dermal fibroblasts *in vitro*.

	Time post plating			
	12	60	108	156
Number of replicate wells	6	6	6	6
Median cell number per well (cells x 10^3)	1.351	2.188	3.016	3.065
Minimum and maximum (cells x 10^3)	1.024 to 1.461	2.024 to 2.351	3.016 to 3.180	2.492 to 3.419
95% confidence interval (cells x 10^3)	1.164 to 1.485	2.036 to 2.303	2.983 to 3.122	2.762 to 3.355

Table 10.5 The effect of the 0.5 W/cm^2 insonated platelet releasate, prepared by insonating a standard platelet suspension with 3 MHz pulsed ultrasound at an intensity $I^{(SATA)}$ of 0.5 W/cm^2, on the proliferation of p6 human dermal fibroblasts *in vitro*.

	Time post plating			
	12	60	108	156
Number of replicate wells	6	6	6	6
Median cell number per well (cells x 10^3)	1.243	2.269	2.962	3.037
Minimum and maximum (cells x 10^3)	0.806 to 1.951	2.079 to 2.733	2.635 to 3.725	2.928 to 3.692
95% confidence interval (cells x 10^3)	0.859 to 1.773	2.044 to 2.659	2.631 to 3.566	2.852 to 3.586

Figure 10.2. The effect of therapeutic ultrasound on the release from platelets of substances capable of modulating fibroblast proliferation *in vitro*.

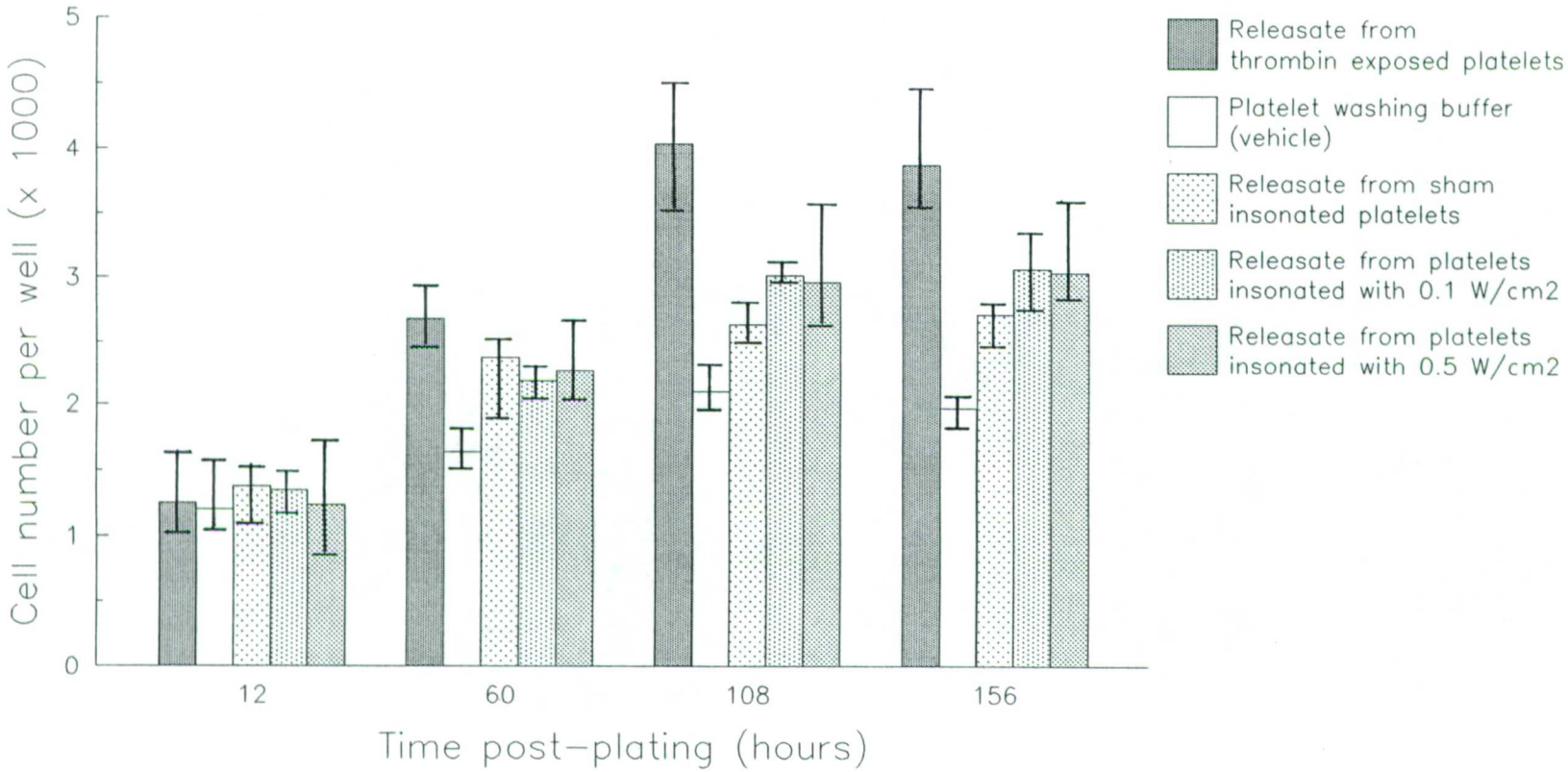

10.3.4. Discussion

From the results described above it would appear that therapeutic ultrasound, at the parameters used here, is capable of indirectly stimulating fibroblast proliferation *in vitro* by first interacting with platelets.

The fibroblast performs many essential functions during cutaneous repair. Early in the repair process fibroblasts elaborate a provisional matrix rich in fibronectin and hyaluronic acid, and supplemented with collagen types III and I; which provides a substrate on which macrophages (Ciano *et al.* 1986), new blood vessels (Madri and Pratt, 1988) and fibroblasts themselves (McCarthy *et al.* 1988) can migrate into the wound. Fibroblasts generate the forces necessary to facilitate the process of wound contraction (Ehrlich, 1988; Gabbiani *et al.* 1971), and are responsible for the process of matrix remodelling. During remodelling, the provisional fibroblast-generated matrix is gradually replaced, primarily by the activity of fibroblasts, by a mechanically superior matrix primarily composed of bundles of type I collagen (Clark, 1990).

The accumulation of fibroblasts into the wound site is thought to entail both fibroblast migration and proliferation. Fibroblast proliferation is thought to be under the control of a variety of stimuli including various peptide growth factors (table 1.3, p39). Many of these growth factors are present in the α-granules of platelets (Knighton *et al.* 1990) and are thought to be deposited within wounds following platelet degranulation. The platelet-derived growth factors reported to be mitogenic for fibroblasts include platelet-derived growth factor [PDGF] (Ross *et al.* 1986), transforming growth factor-beta [TGF-β] (Moses *et al.* 1985) which may not be directly mitogenic (Loef *et al.* 1986), transforming growth factor-alpha [TGF-α] (Delarco and Todaro, 1978), basic fibroblast growth factor [bFGF] (Raines and Ross, 1989), and platelet-derived endothelial cell growth factor [PD-ECGF] (Pierce *et al.* 1991; Miyazono and Heldin, 1989).

As platelet adhesion, degranulation and the concomitant elaboration of α-granule components are some of the earliest events in response to injury, and treatment with ultrasound soon after injury is conducive to a stimulation in repair (Dyson *et al.* 1970; Dyson and Pond, 1970; Webster *et al.* 1979; Dyson and Smalley, 1983; Young and Dyson 1990a,c; Byl *et al.* 1992) it is possible that platelets are one the responsive biological targets for ultrasound within the wound site.

An increase in the level of platelet-derived fibroblast mitogens following

treatment with ultrasound may explain several literature reports on ultrasound bioeffects, including the observations that: fibroblasts are recruited more rapidly into insonated rat skin wounds than into similar sham-insonated wounds (Young and Dyson 1990a); insonated rabbit ear wounds demonstrate a greater level of ^{3}H-thymidine labelling than sham-insonated wounds (Dyson *et al.* 1970); insonated cryosurgical rat skin lesions contract more rapidly than similar sham insonated lesions (Dyson and Smalley, 1983); the temporal scheme of matrix deposition advances more rapidly in insonated murine granulomata than in non-insonated granulomata (Pospisilova *et al.* 1971; Pospisilova and Rottova, 1977), and the collagen content of rat skin wounds 7 days after injury is greater in insonated than sham-insonated wounds (Webster *et al.* 1979).

In summary, this investigation demonstrates that clinical levels of therapeutic ultrasound promote the release of substances from platelets that are mitogenic for fibroblasts. If the observations made in this *in vitro* study can be extrapolated to the process of cutaneous repair *in vivo*, it is possible that the stimulation in wound contraction following treatment with ultrasound (reported in chapter 7), may be due to an increase in fibroblast recruitment into the wound site mediated by an elevated release of platelet-derived fibroblast mitogens.

10.4 The effect of ultrasound on the release from platelets of substances capable of modulating fibroblast-mediated collagen lattice contraction.

10.4.1 Introduction

The contraction of human dermal fibroblast populated collagen lattices, a widely accepted model of the process of wound contraction *in vitro* (Ehrlich and Rajaratnam, 1990), in response to the application of the different platelet releasates produced as described above (section 10.2, p253) was investigated.

10.4.2 Method

Thirty standard fibroblast populated collagen lattices were prepared according to steps 1 through 6 of the "human dermal fibroblast collagen lattice contraction assay - standard protocol (Appendix 10, p344). After polymerisation and lattice release, the 30 lattices were randomly allocated into 5 groups, each containing 6 lattices. All 6

lattices of each group received a 1 ml aliquot of one of the 4 different platelet releasates or PWB (Appendix 1C, p344), diluted 1:9 with sterile PBS (Appendix 1A, p 344). Once all 30 lattices had been "fed" in this manner they were placed in a humidified box and returned to the 37°C incubator. All thirty lattices were photographed (Appendix 11A, p345) at 4.00, 13.50, 26.00, 42.00 and 51.25 hours after initial plating and the film developed according to Appendix 11B (p346). The area of each lattice, in mm^2, was then measured by computer-assisted planimetry (Appendix 12, p347).

Median lattice area, minimum and maximum lattice area, and 95% confidence intervals were calculated for each group of lattices (i.e. in response to each platelet releasate or PWB) at each time point (tables 10.6 through 10.10 p 267-269) and the data was graphically displayed (figure 10.3, p270). Non-parametric statistical analysis was performed to examine the modulation in the rate of lattice contraction in response to different platelet releasates. Initially, a Kruskal Wallis test which was used to compare all 5 groups, at each time point, was carried out as an indicator for further statistical analysis. According to the Kruskall Wallace analysis, further two sample analyses were carried out between specific treatment groups using the Mann Whitney-U test.

10.4.3 Results

Figure 10.3 (p270) displays the change in lattice area (mm^2) with time (hours) in the form of a bar chart. For each time point there is a cluster of 5 bars, one for each platelet releasate and PWB. The maximum height of each bar represents the median area of the 6 lattices within the group. 95% confidence intervals are displayed (1) to show the distribution of points within each data group, and (2) to indicate the significance of apparent differences in median lattice areas between exposure groups. A summary of the statistical analyses carried out on this data can be found in (Appendix 22, p 365 - 368). Initial statistical analysis, using the Kruskal Wallace test, indicated that significant differences were present between the 5 experimental groups under study, at all time points (Appendix 22, table 1, p 365), thus indicating the requirement for further analysis between groups using the Mann Whitney-U test.

From figure 10.3 and according to statistical analysis the following points are apparent:

1. Fibroblast-mediated collagen lattice contraction occurs in response to the

application of all releasates and PWB. Those lattice that received the thrombin releasate (T-R) demonstrated the most rapid contraction; whereas those that received the vehicle (PWB) only, demonstrated the slowest contraction. Non-parametric analysis indicated that contraction was significantly more rapid in response to T-R than PWB, leading to significantly smaller lattices ($p < 0.05$) at all time points (Appendix 22, table 2, p365).

2. The rates of contraction of lattices in response to the two insonated platelet releasates (i.e. platelets insonated at ultrasonic intensities, $I^{(SATA)}$, of 0.1 W/cm^2 and 0.5 W/cm^2) and the sham-insonated platelet releasate, were found to be intermediate between those in response to T-R and PWB. An visible, though not always statistically significant, trend is apparent at all time points, whereby T-R results in the most rapid contraction, followed by the less rapid 0.1 W/cm^2 releasate, then the 0.5 W/cm^2 releasate, the sham releasate and finally the vehicle (PWB) alone.

3. When the rate of contraction in response to the sham-exposed platelet releasate (S-R) is compared to that of PWB, it would appear from figure 10.3 that the S-R leads to greater lattice contraction that PWB. This difference proved to be statistically significant at several time points, i.e. 4.00 hours ($p < 0.008$), 13.50 hours ($p < 0.005$) and 26.00 hours ($p < 0.020$), but not at 42.00 hours ($p < 0.093$) and 51.25 ($p < 0.298$) hours post plating (Appendix 22, table 3, p366).

4. Insonation of platelets with 3 MHz ultrasound at an intensity, $I^{(SATA)}$, of 0.1 W/cm^2 leads to the generation of a platelet releasate (0.1-R) with a greater stimulatory activity for fibroblast-mediated lattice contraction than that of S-R, the platelet releasate generated by sham-insonation, resulting in significantly smaller lattices in response to the 0.1-R than SR, at 4.00 ($p < 0.005$), 13.50 ($p = 0.031$), 26.00 ($p < 0.008$), 42.00 ($p < 0.008$) and 51.25 ($p < 0.008$) hours after initial plating (Appendix 22, table 4, p 366).

5. Fibroblast-mediated contraction in response to the platelet releasate 0.5-R, generated by insonation of platelets with 3 MHz ultrasound at an intensity, $I^{(SATA)}$, of 0.5 W/cm^2, is initially more rapid than that in response to the sham-insonated releasate (SR), resulting in significantly more contraction in response to 0.5-R than S-R by 4.00 hours ($p < 0.020$). The data in tables 10.8 and 10.10, represented in figure 10.3, indicates that the median lattice area values of 0.5-R are lower than S-R at all time points. However, after the 4.00 hour time point, these differences proved not to be statistically significant, with the exception of 42.00

Table 10.6 The effect of platelet washing buffer on the contraction of human dermal fibroblast-populated collagen lattices *in vitro*.

	Time post-plating (hours)				
	4.00	13.50	26.00	42.00	51.25
Number of replicate lattices	6	6	6	6	6
Median lattice area (mm^2)	759.6	587.2	375.8	301.4	236.7
Minimum and maximum (mm^2)	734.5 to 776.8	570.6 to 599.1	368.1 to 397.1	287.7 to 330.5	216.5 to 246.8
95% confidence interval (mm^2)	741.7 to 774.3	575.1 to 595.5	367.7 to 390.4	287.1 to 322.7	220.0 to 246.4

Table 10.7 The effect of adding the thrombin platelet releasate, prepared by incubating a standard platelet suspension with thrombin at a concentration of 1.0 units per ml, on the contraction of human dermal fibroblast-populated collagen lattices *in vitro*.

	Time post-plating (hours)				
	4.00	13.50	26.00	42.00	51.25
Number of replicate lattices	6	6	6	6	6
Median lattice area (mm^2)	617.3	499.9	288.3	220.6	177.6
Minimum and maximum (mm^2)	600.8 to 646.2	483.1 to 553.8	277.7 to 338.5	210.1 to 246.3	167.2 to 207.6
95% confidence interval (mm^2)	604.6 to 637.3	479.0 to 537.2	274.5 to 328.0	209.2 to 236.7	165.5 to 197.1

Table 10.8 The effect of adding the sham-insonated platelet releasate, prepared by sham-insonating a standard platelet suspension, on the contraction of human dermal fibroblast-populated collagen lattices *in vitro*.

	Time post-plating (hours)				
	4.00	13.50	26.00	42.00	52.25
Number of replicate lattices	6	6	6	6	6
Median lattice area (mm^2)	707.5	559.2	355.4	282.3	223.7
Minimum and maximum (mm^2)	676.3 to 741.8	535.7 to 570.4	323.4 to 372.2	269.3 to 314.9	203.9 to 236.8
95% confidence interval (mm^2)	681.2 to 735.0	539.5 to 571.1	331.2 to 371.2	270.3 to 305.2	211.2 to 233.7

Table 10.9 The effect of adding the 0.1 W/cm^2 insonated platelet releasate, prepared by insonating a standard platelet suspension with 3 MHz pulsed (2ms:8ms) ultrasound at an intensity $I^{(SATA)}$ of 0.1 W/cm^2, on the contraction of human dermal fibroblast-populated collagen lattices *in vitro*.

	Time post-plating (hours)				
	4.00	13.50	26.00	42.00	51.25
Number of replicate lattices	6	6	6	6	6
Median lattice area (mm^2)	639.8	524.0	308.0	238.5	197.6
Minimum and maximum (mm^2)	607.5 to 667.9	509.0 to 547.9	288.5 to 336.6	215.7 to 272.3	182.6 to 210.2
95% confidence interval (mm^2)	618.9 to 659.1	508.7 to 542.0	293.7 to 324.3	221.8 to 260.5	187.7 to 206.9

Table 10.10 The effect of adding the 0.5 W/cm^2 insonated platelet releasate, prepared by insonating a standard platelet suspension with 3 MHz pulsed (2ms:8ms) ultrasound at an intensity $I^{(SATA)}$ of 0.5 W/cm^2, on the contraction of human dermal fibroblast-populated collagen lattices *in vitro*.

	Time post-plating (hours)				
	4.00	13.50	26.00	42.00	51.25
Number of replicate lattices	6	6	6	6	6
Median lattice area (mm^2)	668.8	537.1	331.4	243.9	209.6
Minimum and maximum (mm^2)	648.0 to 696.3	504.0 to 554.1	304.2 to 381.3	220.9 to 283.1	192.2 to 233.9
95% confidence interval (mm^2)	652.9 to 686.5	508.0 to 552.3	307.9 to 363.2	226.0 to 269.1	196.4 to 225.6

Figure 10.3. The effect of therapeutic ultrasound on the release from platelets of substances capable of modulating fibroblast-mediated collagen lattice contraction *in vitro*.

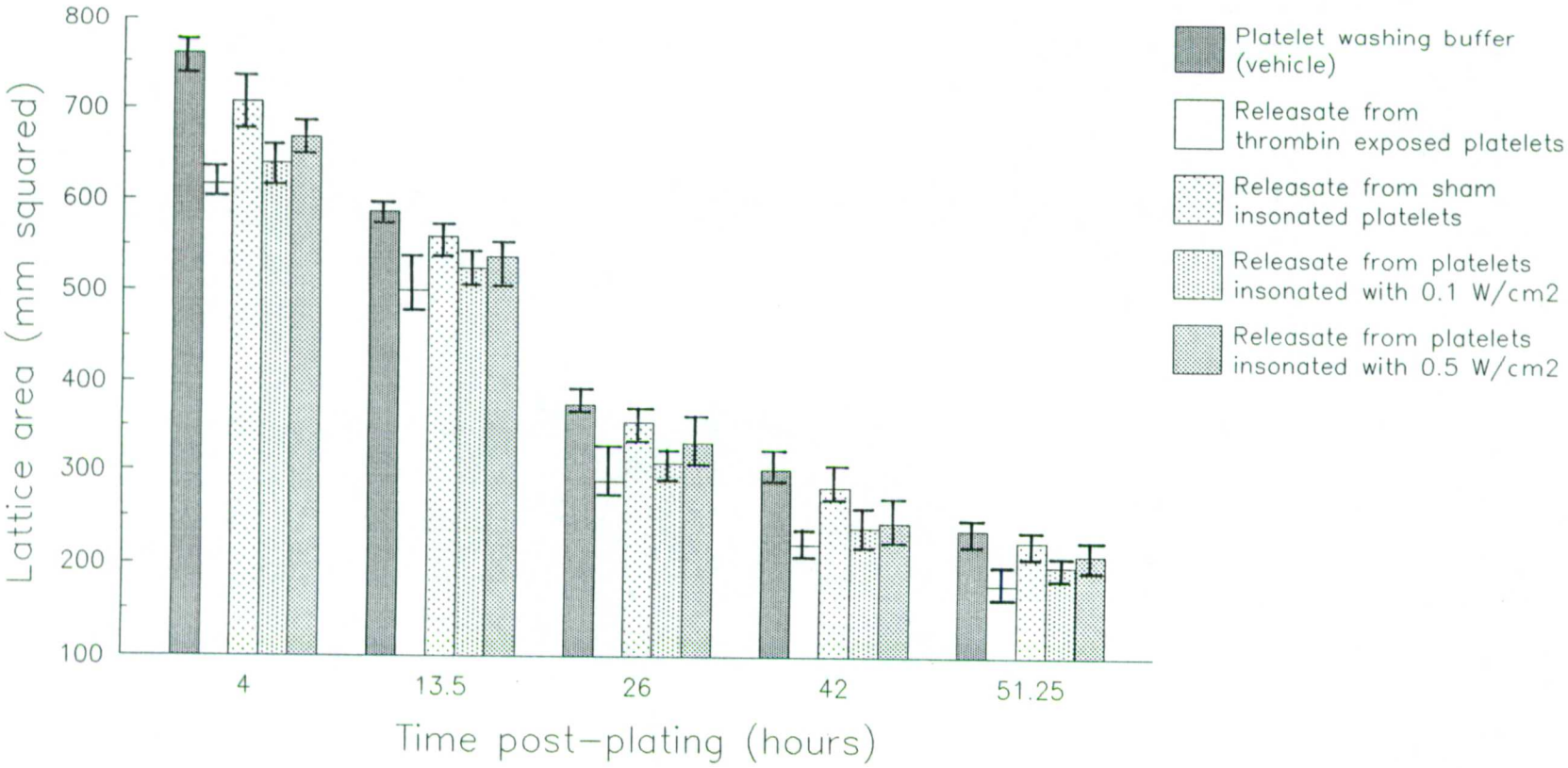

hours post plating ($p < 0.020$) (Appendix 22, table 5, p 367).

6. From the data in tables 10.9 (p268) and 10.10 (p269), and figure 10.3 (p270), the rate of fibroblast-mediated contraction in response to the 0.1-R is more rapid than that observed in response to the 0.5-R. At all time points studied, median lattice area values are consistently smaller in those lattices given 0.1-R than those given 0.5-R. However, with the exception of the 4.00 hour time point ($p < 0.020$), this response trend does not attain statistical significance (Appendix 22, table 8, p368).

7. From a comparison of the median data (tables 10.7 and 10.9, and figure 10.3) the rate of fibroblast-mediated contraction following the application of the thrombin releasate (T-R), to standard lattices is more rapid than the response to the 0.1-R. Non-parametric analysis was, however, unable to detect any statistically significant difference at any time point post-plating (Appendix 22, table 6, p 367).

8. When lattice contraction in response to the addition of the thrombin releasate (T-R) was compared with that in response to the addition of the ultrasonically generated 0.5-R platelet releasate, it became apparent that contraction in response to the T-R is more rapid than that in response to the 0.5-R. This observation is substantiated by statistical analysis at 4.00 ($p < 0.005$), 42.00 ($p < 0.045$) and 51.25 ($p < 0.020$) hours post plating. Statistical analysis failed to demonstrate any significance in this trend at 13.5 and 26.00 hours post plating (Appendix 22, table 7, p 368).

10.4.4 Discussion

From the results described above it would appear that therapeutic ultrasound, at the parameters used in this thesis, is capable of indirectly stimulating fibroblast-mediated collagen lattice contraction *in vitro* by first interacting with platelets.

FPCLs supplemented with the releasate from insonated platelets exposed to an intensity of 0.1 W/cm^2 contracted more rapidly than lattices supplemented with the releasate from 0.5 W/cm^2 insonated platelets, which in turn contracted more rapidly than those given the sham-insonated platelet releasate. While statistically significant differences were consistently observed between the 0.1 W/cm^2 and the sham releasate, few significant differences in pro-contractile activity were found between the 0.5 W/cm^2 and either the sham or the 0.1 W/cm^2 releasate. The thrombin platelet releasate, which was employed as a positive control for maximal platelet degranulation (see general discussion, section 10.5, p 273), was found to display the largest pro-contractile activity at all time points. The negative vehicle

control (i.e. PWB) was found to display the smallest pro-contractile activity at all time points. The observation that the sham-insonated releasate exhibited more pro-contractile activity than the vehicle control suggests that platelet degranulation had occurred within the former. Such degranulation may have been spontaneous or handling-induced.

As platelet α-granules are known to be stores of preformed growth factors, many of which have been shown to promote FPCL contraction, and supernatants of insonated platelets similarly promote FPCL contraction, it would appear that ultrasound acts to liberate these factors from α-granule storage. Platelet-derived factors previously reported to promote FPCL contraction *in vitro* include: TGF-β (Montesano and Orci, 1988; Finesmith *et al.* 1990); PDGF (Anderson *et al.* 1990; Clark *et al.* 1989) and bFGF (Finesmith *et al.* 1990). However, it has been suggested that TGF-β acts indirectly to promote lattice contraction by first inducing PDGF synthesis by fibroblasts, which then acts in an autocrine fashion to promote fibroblast-mediated contraction (Clark *et al.* 1989). Interestingly, basic fibroblast growth factor (bFGF) has been shown to promote contraction at low doses (0.1-1.0 ng/ml), but, inhibit contraction at high doses (>10ng/ml) (Finesmith *et al.* 1990). It is thought that certain growth factors, including IL-1β and TGF-β, promote lattice contraction by upregulating integrin expression on the surface of cells within the lattice (Heino and Massague, 1989; Milam *et al.* 1991).

While the growth factors described above are known to be mitogenic to fibroblasts in planar culture, similar mitogenic effects are not observed in free-floating collagen lattices (Nakagawa *et al.* 1989; Nishiyama *et al.* 1990; Rhudy and McPherson, 1988). One possible exception to this statement is PDGF which has been reported to be mitogenic to fibroblasts in fully contracted collagen lattices (Nishiyama *et al.* 1991), but without mitogenic effect during the contraction process (Clark *et al.* 1989). It has been suggested that human fibroblasts do not proliferate in FPCL (Paul Ehrlich - personal communication), however, the majority of evidence suggests that proliferation does occur albeit at a severely retarded rate (Rhudy and McPherson, 1988; Nishyama *et al.* 1989). It would appear from the literature that fibroblasts proliferate very poorly within collagen lattices and further that they are refractive to the mitogenic effects of growth factors. Consequently, the observations made in this study, whereby different platelet releasates differentially influence FPCL contraction, indicate that the different releasates are affecting lattice contraction by influencing

the ability of individual fibroblasts to contract the lattice, rather than influencing the number of fibroblasts within the lattice.

Ultrasound may indirectly enhance the capacity of individual fibroblasts to contract their extracellular matrix by first promoting the degranulation of platelets at the wound site. As it has previously been reported that therapeutic levels of ultrasound are unable to initiate the processes of platelet aggregation and degranulation during insonation of undamaged vasculature *in vivo* (Williams *et al.* 1981; Chater and Williams, 1982), it is possible that ultrasound may act in such a manner as to promote additional platelet degranulation once initiated by injury.

The elaboration of supplementary pro-contractile activity from platelets within cutaneous wounds as a consequence of exposure to therapeutic ultrasound may explain the observation that therapeutic ultrasound applied soon after injury promotes the process of contraction in both cryosurgical (Dyson and Smalley, 1983) and mechanical wounds (chapter 7 of this thesis, p218).

In summary, this investigation demonstrates that therapeutic ultrasound, at the parameters employed, promotes the release of substances from platelets that encourage the process of fibroblast-mediated collagen lattice contraction *in vitro*. If the observations made in this *in vitro* study can be extended to the process of cutaneous repair *in vivo*, it is possible that therapeutic ultrasound promotes wound contraction by encouraging the release of pro-contractile substances from platelets.

10.5 General discussion of the effects of platelet releasates

This section includes discussion points common to both the effect of platelet releasates on fibroblast proliferation and fibroblast-mediated lattice contraction.

1. Positive control

During this study, a thrombin releasate was used as a positive control for maximal platelet degranulation against which the effect of ultrasound-mediated degranulation could be measured. Platelets were treated with thrombin at a concentration of 1 unit/ml, a concentration that has previously been reported to cause maximal α-granule release (Assoian and Sporn, 1986). Of the various methods available to degranulate platelets thrombin was chosen as it has been identified as a physiological agonist for platelet degranulation at wound sites (Holmsen *et al.* 1981).

2. Mechanism of ultrasonic degranulation

Several studies examining the effect of ultrasound on platelet activity have been previously reported. Such studies were carried out due to concern over the hazards of inadvertently causing a haemostatic reaction during the clinical use of this modality, rather than in anticipation of a beneficial therapeutic interaction. Several *in vitro* studies have reported that ultrasound can promote platelet degranulation and aggregation. Williams *et al.* (1976a) was unable to demonstrate platelet damage using 1 MHz ultrasound at intensities as low as 0.065 W/cm^2 ($I^{(a)}$), but they reported that such an insonation could speed the clotting process of recalcified anticoagulated whole blood, an effect later attributed to limited damage of a small sub-population of platelets, rather than ultrasound-stimulated physiological degranulation, (Williams *et al.* 1976b). Further evidence to support ultrasound-induced platelet damage came from the work of Williams *et al.* (1978), who reported platelet degranulation following insonation even when the physiological platelet release mechanism had been chemically inhibited. As heat is rapidly dissipated from cells insonated *in vitro*, and in view of the observation that the magnitude of ultrasonic effects on platelets decreases with increasing ultrasonic frequency (Chater and Williams, 1977) cavitation has been implicated in platelet damage. While ultrasound has been shown to encourage platelet degranulation *in vitro*, the majority of evidence suggests that therapeutic levels of ultrasound cannot similarly damage platelets *in vivo* in the absence of previous injury even at ultrasonic intensities far in excess of the therapeutic range (Williams *et al.* 1981; Chater and Williams, 1982). *In vivo* studies to date have studied the effects of ultrasound on undamaged blood vessels. It is possible that the application of ultrasound to sites of damaged vessels may encourage additional platelet activity, possibly encouraging the repair process by promoting the release of growth factors and other stimulatory agents, rather than acting as an initiator of platelet adhesion and degranulation. However, as cavitation has yet to be conclusively demonstrated during exposure to therapeutic ultrasound *in vivo* (Watmough *et al.* 1991), it is possible that ultrasound-induced platelet degranulation is an event that is restricted to *in vitro* studies.

3. Platelet-derived wound healing formula

It has been reported that a platelet releasate preparation, termed platelet-derived wound healing formula (PDWHF), generated by incubating platelets with thrombin,

encourages the repair of chronic cutaneous wounds (Knighton *et al.* 1986; Knighton *et al.* 1990). Other studies have demonstrated that PDWHF is chemotactic to rabbit wound endothelial cells (Fiegel *et al.* 1990) and can promote neovascularisation in the rabbit cornea angiogenesis assay *in vivo* (Knighton *et al.* 1982). As therapeutic ultrasound has been shown to (1) degranulate platelets *in vitro*, generating platelet releasates with mitogenic and pro-contractile activities on a par with a thrombin releasate, (2) has previously been shown to promote the repair of chronic wounds including venous ulcers (Dyson *et al.* 1976; Callam *et al.* 1987) and pressure sores (McDiarmid *et al.* 1985), and, (3) has been reported to promote angiogenesis in the rat flank skin wounds (Young and Dyson, 1990c), it is tempting to link these observations and propose that one of the biological targets of therapeutic ultrasound during cutaneous repair is the platelet.

4. Ultrasonic intensity

It is apparent from the results described above that the use of the higher ultrasonic intensity of 0.5 W/cm^2 ($I^{(SATA)}$) had no additional effect on the release of pro-proliferative substances from platelets above that observed at an intensity of 0.1 W/cm^2, an observation that parallels the effect of ultrasonic intensity on wound contraction *in vivo* (chapter 7). Such an observation suggests that maximal platelet degranulation is achieved at the lower intensity. The observation that the thrombin releasate tended to promote proliferation and fibroblast-mediated lattice contraction to a greater level than insonated platelet releasates, may be a consequence of the activity of thrombin itself, as thrombin has been shown to be mitogenic for some fibroblast cell lines *in vitro* (Glenn and Cunningham, 1979; Seuwen and Pouyssegur, 1991).

Chapter 11. The effect of therapeutic ultrasound on the release from U937s (monocyte/macrophage-like cells) of substances capable of modulating fibroblast activity *in vitro*.

11.1 Introduction

It was initially thought that the primary function of the macrophage was the removal and degradation of injured tissue debris in anticipation of the repair process. However, in 1975, Leibovich and Ross demonstrated that the macrophage plays a key role in the orchestration and execution of both degradative and reparative phases of repair. They showed that the depletion of both circulating blood monocytes and tissue macrophages not only severely retarded tissue debridement but also impaired fibroblast proliferation and subsequent wound fibrosis.

Upon entering the wound tissue, monocytes undergo a rapid metamorphosis to macrophages in response to the wound environment (Riches, 1988). Macrophages not only phagocytose bacteria and scavenge tissue debris, but also generate chemotactic factors which recruit additional inflammatory cells and release enzymes which augment tissue degradation (Tsukamoto *et al.* 1981). In addition to their role in tissue debridement, macrophages are thought to release growth and regulatory factors critical for granulation tissue formation. Early studies by Leibovich and Ross (1976) reported that peritoneal macrophages cultured *in vitro* secreted growth factor activity called macrophage-derived growth factor (MDGF) which stimulated the proliferation of guinea pig wound fibroblasts. MDGF, secreted by activated macrophages, has also been shown to stimulate the proliferation of smooth muscle cells (Greenburg and Hunt 1978; Glenn and Ross, 1981; Martin *et al.* 1981), arterial endothelial cells (Greenburg and Hunt, 1978; Martin *et al.* 1981) and mouse keratinocytes (Ristow, 1986.) It has since been realised that MDGF activity is a combination of several well characterised growth factors (Raines and Ross, 1989).

The factors macrophages are known to secrete include platelet-derived growth factor (PDGF) (Shimokado *et al.* 1985; Martinet *et al.* 1986), basic fibroblast growth factor (bFGF) (Baird *et al.* 1985), transforming growth factor-β (TGF-β) (Assoian *et al.* 1987), insulin-like growth factor-1 (IGF-1) (Rom *et al.* 1989), tumour necrosis factor-α (TNF-α) (Kreigler *et al.* 1988), the epidermal growth factor-related transforming growth factor-α (TGF-α) (Madtes *et al.* 1988), interleukin-1 (IL-1) (Postlethwaite *et al.* 1983) and fibroblast-activating factor (FAF) (Dohlman *et al.*

1984). Further, macrophages within wounds have been shown to contain mRNA transcripts for TGF-α TGF-β, PDGF A-chain and insulin-like growth factor 1 (IGF-1) (Rappolee *et al.* 1988) These and possibly other, as yet uncharacterised, growth factors are thought to orchestrate the process of wound repair (refer to Chapter 1 for a discussion of growth factor activities within wound repair). Thus macrophages are able to play a pivotal role in the process of wound repair, elaborating substances (growth factors) that regulate fibroblast proliferation, migration, matrix synthesis and degradation, and the process of fibroblast-mediated contraction.

The U937 cell (Chapter 5, p145) is a widely accepted model for monocyte-macrophages in many areas of biomedical investigation (Mace and Gazzolo, 1991; Cianciotto *et al.* 1990; Dragunsky *et al.* 1990; Peck and Bollag, 1991; McDonald and Atkins, 1990). The U937 is a neoplastic cell of the monocytic lineage, sharing many morphological, histochemical and functional characteristics of immature monocyte-macrophages (Sundstrom and Nilsson, 1976; Harris and Ralph 1985; Lyons and Ashman, 1989). While the immature (uninduced) U937 is monoblastic, it can be induced to differentiate further along the monocyte-macrophage lineage by exposure to various inducing agents including phorbol esters (Lyons and Ashman, 1989). This induced differentiation involves phenotypic changes that resemble those during the terminal differentiation of normal monocytic cells (Pedrinaci *et al.* 1990). U937s have been shown to be capable of synthesizing many of the macrophage-derived growth factors thought to mediate the process of wound repair, including PDGF (Alitalo *et al.* 1987; Makela *et al.* 1987), TGF-β (Assoian *et al*, 1987; Wager and Assoian, 1990), FAF (Turck *et al.* 1988; Turck *et al.* 1989: Demeter *et al.* 1991), IGF-1 (Nagoaka *et al.* 1990), IL-1 (Palacios *et al.* 1982, Barak *et al.* 1986) and TNF-α (Sabatini *et al.* 1990) (Chapter 5, p146).

Therapeutic ultrasound has been shown to encourage various aspects of dermal repair (Chapter 4, p107), including wound contraction (Chapter 7, p218), and has previously been found to be most effective when applied during the inflammatory phase of repair, a time when macrophages are most numerous, and presumably most active. The studies described within this chapter were carried out in an attempt to examine the ability of therapeutic levels of ultrasound to modulate fibroblast activity indirectly by first interacting with macrophages. Previous *in vitro* studies within this thesis (p234 & 244) appear to indicate that fibroblasts are unable to respond directly to therapeutic ultrasound to bring about the stimulation in wound contraction

reported in chapter 7 (p218), and previously by Dyson and Smalley (1983).

The aim of this study was to examine the effect of therapeutic levels of pulsed 3 MHz ultrasound on the release from U937s of substances capable of modulating the proliferative and contractile capacity of human dermal fibroblasts *in vitro*.

Experimental overview

The macrophage-like cell line, U937, was employed in this study. Both uninduced and PMA-induced U937 cultures were either: insonated with 3 MHz pulsed therapeutic ultrasound (at intensities of 0.1 or 0.5 W/cm^2, $I^{(SATA)}$), sham-insonated or left uninsonated. After 24 hours, the media "bathing" these U937 cultures (i.e. conditioned medium) were removed and assayed for their ability to modulate both fibroblast proliferation and fibroblast-mediated collagen lattice contraction compared with non-conditioned medium.

After a description of how the various U937 conditioned media were generated (section 11.3, p279) a study carried out to examine the effect of U937 conditioned media on fibroblast proliferation *in vitro* is described (section 11.4, p284). Section 11.4 initially describes how fibroblast proliferation, in response to the various U937 conditioned media (from both uninduced and PMA-induced U937s), was studied (11.4.1. & 11.4.2., p284). The results obtained are then described and discussed. For the sake of clarity, fibroblast proliferation in response to the application of conditioned media from (1) uninduced U937s and (2) PMA-induced U937s is described, and discussed, separately. The effect of conditioned media from uninduced U937s is described in section 11.4.3 (p286) and discussed in section 11.4.4. (p291). The effect of conditioned media from PMA-induced U937s is described in section 11.4.5 (p297) and discussed in section 11.4.6. (p303).

Section 11.5 initially describes how FPCL contraction, in response to the various U937 conditioned media (from both uninduced and PMA-induced U937s), was studied (11.5.1. & 11.5.2, p307). The results obtained are then described and discussed. Like the proliferation studies described above, FPCL contraction in response to the application of conditioned media from (1) uninduced U937s and (2) PMA-induced U937s is described, and discussed, separately. The effect of conditioned media from uninduced U937s is described in section 11.5.3 (p308) and discussed in section 11.5.4. (p314). The effect of conditioned media from PMA-induced U937s is described in section 11.5.5 (p317) and discussed in section 11.5.6.

(p323). The chapter ends with a general summary of observations and conclusions (section 11.6, p324).

11.3 Insonation of U937s - generation of U937 conditioned media

U937 cells were cultured at 37°C in 80 cm^2 tissue culture flasks (Nunc, Denmark) in RPMI-1640 medium containing 10% (v/v) heat-inactivated fetal calf serum (FCS), 100 μg/ml streptomycin, 100 units/ml penicillin (macrophage growth medium, Appendix 2E, p336) according to Turck *et al* (1989). A U937 suspension was prepared at a concentration of 1 x 10^6 viable cells/ml in macrophage growth medium. This suspension was divided into two aliquots and then centrifuged for 5 minutes at 80 x g. The two cell pellets thus obtained were washed twice with serum-free growth medium and then resuspended to 1 x 10^6 viable cells/ml in either: A. Serum-free macrophage growth medium (Appendix 2G, p337), or, B. Serum-free macrophage growth medium containing 100 ng/ml of the phorbol ester 4β-phorbol 12-myristate 13-acetate (PMA) (Appendix 2H, p337), thus forming two U937 stock suspensions:

A. Non-PMA exposed U937s

B. PMA exposed U937s

4ml volumes of these two U937 stock suspensions were aliquoted into sterile, universal bottles, and held at approximately 20°C (room temperature). The exposure chamber (Appendix 13, figure 13.1, p 349) was then prepared and loaded, according to Appendix 13 (p348), with the first aliquot. The exposure chamber was located in the exposure tank (figure 11.1) which was lined with ultrasound absorbent rubber (dimpled car matting) and filled with circulating degassed distilled water at 37°C. The exposure tank was 40cm long, 25cm deep and 25cm wide. U937 samples were insonated with 3 MHz pulsed (2ms:8ms) ultrasound at intensities, $I^{(SATA)}$, of 0.1 W/cm^2 or 0.5 W/cm^2, or sham-insonated, for a period of 5 minutes. One aliquot of each U937 stock suspension, termed non-insonated was left untreated (i.e. neither insonated nor sham-insonated).

The therapeutic ultrasound source used in this study was a standard Enraf Nonious Delft 434 Sonopuls machine (Enraf Nonius Delft, Holland), set to deliver 3 MHz ultrasound (figure 7.2, p222). Prior to U937 exposure, ultrasonic output was calibrated and the generator set to deliver a fixed ultrasonic intensity - as described in chapter 6 (p187).

After treatment, U937 suspensions were unloaded from the exposure chamber

(or from the universal bottle in the case of the non-insonated aliquot) and decanted into sterile centrifuge tubes and centrifuged at 80 x g for 5 minutes. Supernatants were discarded and cell pellets resuspended to 1 x 10^6 cells per ml in serum-free growth medium with or without PMA according to which U937 stock suspension the treated sample originated from. U937 suspensions were then transferred to culture flasks and returned to a 37°C incubator, where they remained for a period of 24 hours. Cell-free flasks of serum-free macrophage growth medium, supplemented with PMA or otherwise, were also incubated at 37°C for a period of 24 hours. After 24 hours the post-treatment U937 cultures and cell-free RPMI-1640 media were removed from the incubator, transferred into centrifuge tubes and centrifuged at 80 x g for 5 minutes. Supernatants were collected, aliquoted into sterile cryotubes and stored at -20°C until required for bioassay. Conditioned media generation is summarised on page 283 in the form of a flow diagram. Table 11.1 describes the 10 different RPMI-1640 conditioned media generated in this way. The ability of these 10 different conditioned media to modulate fibroblast proliferation and fibroblast-mediated contraction was examined as described in sections 11.4 and 11.5.

Figure 11.1 Experimental arrangement for the exposure of U937s to pulsed 3 MHz therapeutic ultrasound *in vitro*.

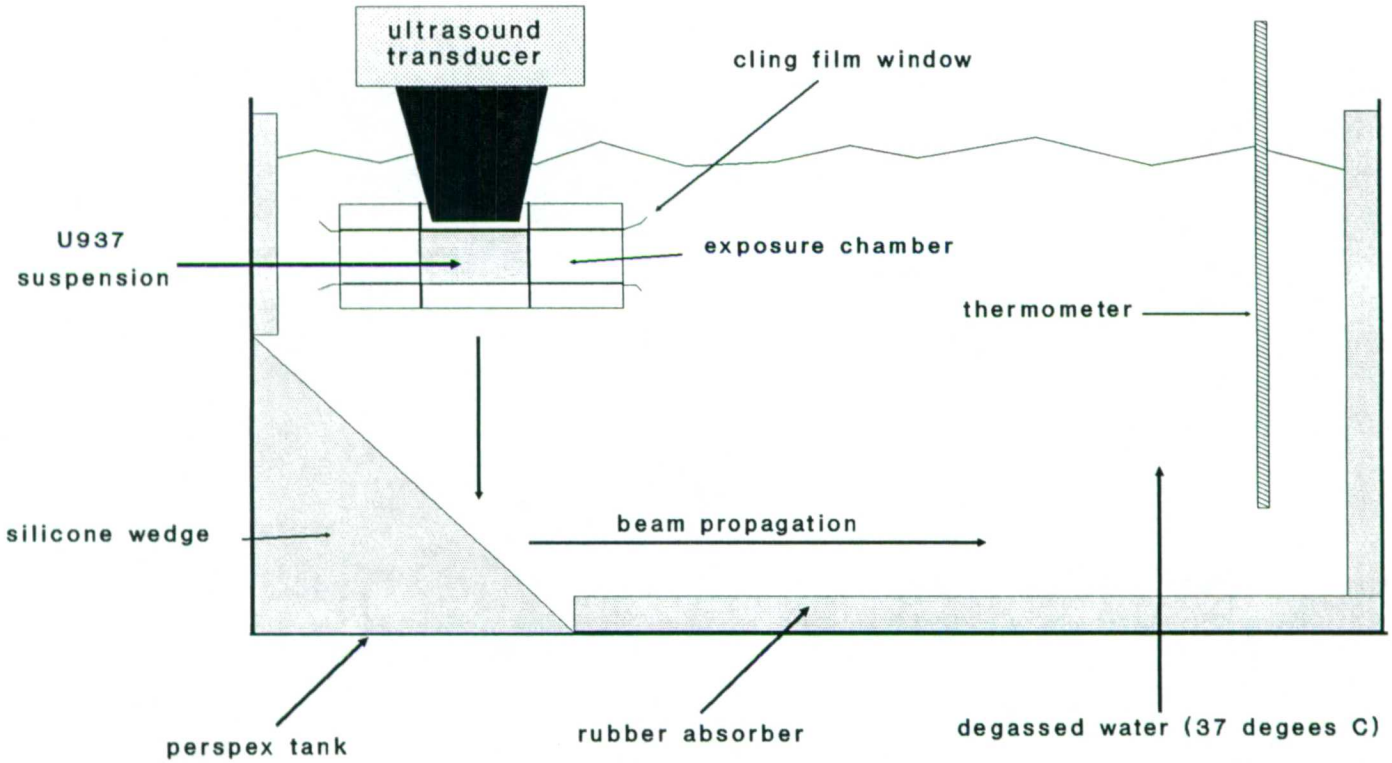

Table 11.1 RPMI-1640 "conditioned" media. Showing the treatment of U937 cultures from which the 10 conditioned media were derived.

	RPMI-1640 "conditioned" media	Name	Treatment of RPMI-1640 medium		
			U937	PMA	Cell insonation
1	*Non conditioned serum free* RPMI-1640	N-CM	-	-	No insonation
2	Conditioned medium from non insonated U937s	N-IM	+	-	No insonation
3	Conditioned medium from sham insonated U937s	S-IM	+	-	sham insonation
4	Conditioned RPMI 1640 medium from U937s insonated with 3 MHz ultrasound at an intensity of 0.1 W/cm^2	0.1 IM	+	-	0.1 W/cm^2 ($I^{(SATA)}$)
5	Conditioned RPMI 1640 medium from U937s insonated with 3 MHz ultrasound at an intensity of 0.5 W/cm^2	0.5 IM	+	-	0.5 W/cm^2 ($I^{(SATA)}$)
6	Non conditioned serum free RPMI 1640 supplemented with PMA	PMA N CM	-	+	No insonation
7	Conditioned RPMI 1640 from PMA induced, non-insonated U937	PMA N-IM	+	+	No insonation
8	Conditioned medium from PMA induced, sham insonated U937s	PMA S-IM	+	+	sham insonation
9	Conditioned RPMI 1640 medium from PMA induced U937s insonated with 3 MHz ultrasound at an intensity of 0.1 W/cm^2	PMA 0.1-IM	+	+	0.1 W/cm^2 ($I^{(SATA)}$)
10	Conditioned RPMI 1640 medium from PMA-induced U937s insonated with 3 MHz ultrasound at an intensity of 0.5 W/cm^2	PMA 0.5-IM	+	+	0.5 W/cm^2 ($I^{(SATA)}$)

Summary of the generation of U937 conditioned media

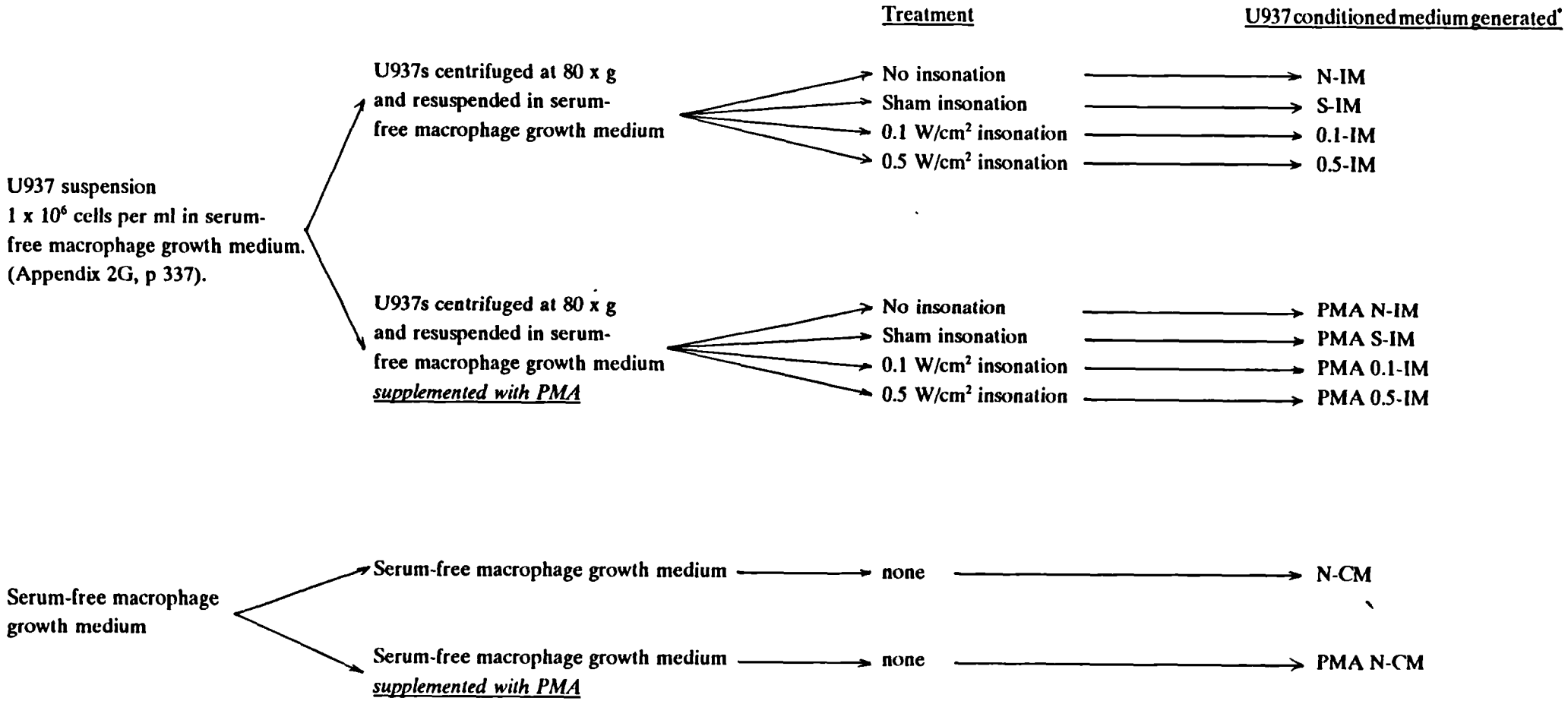

* *Conditioned media, from both uninduced and PMA-induced U937s, were assayed for their effects on fibroblast proliferation and fibroblast-mediated lattice contraction, see sections 11.4 (p284) and 11.5 (p307) respectively. Conditioned media abbreviations used in text.*

11.4 The effect of ultrasound on the release from the macrophage-like cell U937 of substances capable of modulating fibroblast proliferation *in vitro*.

11.4.1 Introduction

The methylene blue fibroblast proliferation assay (p149), a modification of the colorimetric assay described by Oliver *et al.* (1989), was used to investigate the effect of conditioned media, from ultrasound-exposed U937s, on human dermal fibroblast proliferation.

11.4.2 Method

The standard protocol for the Methylene Blue Fibroblast Proliferation Assay (Appendix 8, p342) was employed with the following modifications:

Briefly, sub-confluent human dermal fibroblast monolayers, passage 6, were trypsinized (Appendix 4, p338), washed in fibroblast growth medium (Appendix 2B, p335) and resuspended in the same to a final concentration of 2 x 10^4 viable cells/ml (Appendix 6, p340). 100 µl volumes of this cell suspension, containing 2000 cells, were aliquoted into 60 wells (i.e. filling all wells in columns 2 to 11, with the exception of those wells in rows A and H) of a 96 well flat-bottomed microtitre plate (Appendix 9, p343). 20 of the remaining wells (i.e. all wells in columns 2 to 11 that did not receive the cell suspension) were filled with fibroblast growth medium alone. Five replicate plates were set up in this manner. All plates were sealed and placed in a 37°C incubator for a period of 12 hours to allow for cell attachment.

After 12 hours all five plates were removed from the incubator and the plate sealing tape removed. One of the five plates, subsequently termed the 12 hour plate, was "stopped" according to Appendix 8 steps 6 through 9 (p342) and stored in a dust-free environment. On each of the four remaining plates, one of the ten columns of wells was designated to receive one of the 10 conditioned media (table 11.1, p282). All eight wells of a given column, including the cell-free wells, received 100 µl of a given conditioned medium. Conditioned media were thawed and sterilised with a 0.22 µm millipore filter before being applied to fibroblast cultures.

Once all wells had received 100 µl of one of the conditioned media the plates were resealed and returned to the 37°C incubator. Individual plates were "stopped" at 36, 60, 84 and 132 hours after initial fibroblast seeding, according to Appendix 8 steps 6 through 9 (p342). Plates "stopped" at 36, 60 and 84 hours were stored, with

the 12 hour plate, in a dust-free environment until the 132 hour plate had been stopped, fixed and air dried.

Fibroblast monolayers within the wells were then stained with methylene blue dye, washed with 0.01 M borate buffer, and the dye eluted with acid-alcohol. The absorbance (A_{650}) of each well, on each plate, was then measured (Appendix 8, steps 10 through 12, p342). For each column of wells, and hence for each conditioned medium under test, the average A_{650} value of cell-free wells was subtracted from each of the A_{650} readings of cell containing wells. The fibroblast number within a given well was then calculated from these corrected A_{650} values using a standard plot of human dermal fibroblast number versus A_{650} (Appendix 30B, p398). This standard plot was prepared according to the method described on page 152 using the same primary culture of fibroblasts, at the same passage (p6), as was used for the fibroblast proliferation assay above.

For each conditioned medium at each time point the median fibroblast number within the 6 wells was reported. Minimum and maximum fibroblast number and 95% confidence intervals were reported to indicate data distribution. The data was tabulated and graphically displayed. Non-parametric statistical analysis was employed to compare the ability of different conditioned media to differentially effect fibroblast proliferation. Statistical analysis took the form of Kruskal-Wallis and Mann Whitney U-tests.

This study contains two experiments:

I. The effect of ultrasound on the release of substances, from non-PMA-exposed U937s, capable of modulating fibroblast proliferation *in vitro*.

and II. The effect of ultrasound on the release of substances, from PMA-exposed U937s, capable of modulating fibroblast proliferation *in vitro*.

To aid understanding, the results and discussion of these two studies will be dealt with separately (see pages 286-296 and 297-306 respectively).

11.4.3 Results:

I. The effect of therapeutic ultrasound on the release from non-PMA exposed U937s of substances capable of modulating fibroblast proliferation *in vitro*.

Figure 11.2 displays the change in median fibroblast number with time in response to the application of the five non-PMA exposed conditioned media. 95% confidence intervals are displayed to indicate data distribution. A summary of the statistical analysis performed on this data can be found in Appendix 23, (p369). Figure 11.2, the data tables 11.2 through 11. 6 (pages 288 to 289), and statistical analysis of that data, demonstrate the following.

1. The effect of non-conditioned medium (N-CM) versus conditioned medium from non-insonated U937s (N-IM).

The conditioning of RPMI-1640 by U937s reduces its ability to support fibroblast proliferation. On the basis of the median data (tables 11.2 & 11.3) there are fewer fibroblasts in wells that received N-IM than received N-CM, at all time points studied. This observation proved statistically significant at the 60 and 132 hour time points ($p < 0.050$), with a clear trend towards significance at the 84 hour time point ($p = 0.064$).

2. The effect of conditioned medium from non-insonated U937s (N-IM) versus conditioned medium from sham-insonated U937s (S-IM).

Fibroblast proliferation in response to conditioned medium from sham-insonated U937s was not significantly different from that in response to conditioned medium from non-insonated U937s.

3. Conditioned medium from sham-insonated U937s (S-IM) versus conditioned medium from U937s insonated at an intensity, $I^{(SATA)}$, of 0.1 W/cm^2 (0.1-IM).

Fibroblast proliferation was more rapid in fibroblast cultures that received conditioned medium from U937s insonated with ultrasound at 0.1 W/cm^2,$I^{(SATA)}$, than similar fibroblast cultures that received conditioned medium from sham-insonated U937s. Significantly more fibroblasts were present at 84 ($p = 0.030$) and 132 ($p = 0.012$) hours post-plating in wells to which 0.1-IM was added than in wells in receipt of S-IM.

4. Conditioned medium from sham-insonated U937s (S-IM) versus conditioned medium from U937s insonated at an intensity, $I^{(SATA)}$, of 0.5 W/cm^2 (0.5-IM).

The application of conditioned medium from U937s insonated with 3 MHz therapeutic ultrasound, at an intensity of 0.5 W/cm^2, to fibroblasts in culture led to more rapid proliferation than was observed following the application of sham-insonated U937 conditioned medium. Significantly more fibroblasts were found in wells that received 0.5-IM at 84 ($p < 0.013$) and 132 ($p = 0.008$) than were found in wells in receipt of S-IM.

5. The effect of conditioned medium from U937s insonated at intensities of 0.1 W/cm^2 versus 0.5 W/cm^2.

The rate of fibroblast proliferation observed in response to the application of RPMI-1640 media conditioned by macrophages insonated with therapeutic ultrasound at an intensity of 0.1 W/cm^2 was not significantly different from that observed in response to conditioned media of U937s similarly insonated at an intensity of 0.5 W/cm^2.

6. The effect of conditioned media from ultrasonically insonated U937s (both intensities) versus non-conditioned medium.

Fibroblast proliferation observed in response to conditioned medium from U937s exposed to therapeutic ultrasound, at intensities of 0.1 and 0.5 W/cm^2, was not significantly different to that observed in response to the application of non-conditioned RPMI-1640 medium. No statistically significant differences were observed at any time point.

Table 11.2 **The effect of non-conditioned RPMI-1640 on the proliferation of human dermal fibroblasts *in vitro*.**

	Time post plating (hours)				
	12	36	60	84	132
Number of replicate wells	6	6	6	6	6
Median cell number per well (cells x 10^3)	1.933	1.699	2.188	2.392	2.978
Minimum and maximum (cells x 10^3)	1.524 to 2.560	1.181 to 2.054	1.561 to 2.379	2.147 to 2.910	2.542 to 3.851
95% confidence interval (cells x 10^3)	1.619 to 2.374	1.317 to 2.027	1.801 to 2.429	2.111 to 2.710	2.589 to 3.495

Table 11.3 **The effect of conditioning RPMI-1640 with non-insonated U937s on the proliferation of human dermal fibroblasts *in vitro*.**

	Time post plating (hours)				
	12	36	60	84	132
Number of replicate wells	6	6	6	6	6
Median cell number per well (cells x 10^3)	1.933	1.536	1.751	1.983	2.379
Minimum and maximum (cells x 10^3)	1.851 to 2.153	1.290 to 1.727	1.506 to 1.997	1.002 to 2.419	2.215 to 3.633
95% confidence interval (cells x 10^3)	1.823 to 2.153	1.383 to 1.688	1.555 to 1.929	1.398 to 2.478	2.003 to 3.117

Table 11.4 **The effect of conditioning RPMI-1640 with sham-insonated U937s on the proliferation of human dermal fibroblasts *in vitro*.**

	Time post plating (hours)				
	12	36	60	84	132
Number of replicate wells	6	6	6	6	6
Median cell number per well (cells x 10^3)	1.933	1.727	1.779	1.929	2.351
Minimum and maximum (cells x 10^3)	1.797 to 2 288	1.181 to 2 544	1.561 to 2.270	1.547 to 2.310	2.106 to 2.760
95% confidence interval (cells x 10^3)	1.810 to 2.202	1.274 to 2.234	1.535 to 2.168	1.634 to 2.260	2.149 to 2.626

Table 11.5 **The effect of conditioning RPMI-1640 with insonated U937s, exposed to pulsed 3 MHz ultrasound (2ms on : 8ms off) at an intensity of 0.1 W/cm^2, $I^{(SATA)}$, on the proliferation of human dermal fibroblasts *in vitro*.**

	Time post plating (hours)				
	12	36	60	84	132
Number of replicate wells	6	6	6	6	6
Median cell number per well (cells x 10^3)	1.961	1.754	2.106	2.474	2.787
Minimum and maximum (cells x 10^3)	1.797 to 2.233	1.399 to 2.381	1.888 to 2.706	1.983 to 3.019	2.651 to 2.924
95% confidence interval (cells x 10^3)	1.827 to 2.149	1.473 to 2.162	1.885 to 2.545	2.064 to 2.956	2.695 to 2.917

Table 11.6 **The effect of conditioning RPMI-1640 with insonated U937s, exposed to pulsed 3 MHz ultrasound (2ms on : 8ms off) at an intensity of 0.5 W/cm^2, $I^{(SATA)}$, on the proliferation of human dermal fibroblasts *in vitro*.**

	Time post plating (hours)				
	12	36	60	84	132
Number of replicate wells	6	6	6	6	6
Median cell number per well (cells x 10^3)	2.015	1.645	2.051	2.392	2.842
Minimum and maximum (cells x 10^3)	1.797 to 2.124	1.345 to 1.945	1.724 to 2.215	2.201 to 2.528	2.706 to 3.905
95% confidence interval (cells x 10^3)	1.879 to 2.115	1.423 to 1.849	1.805 to 2.225	2.273 to 2.511	2.572 to 3.512

Figure 11.2. The effect of therapeutic ultrasound on the release from uninduced U937s of substances capable of modulating fibroblast proliferation *in vitro*.

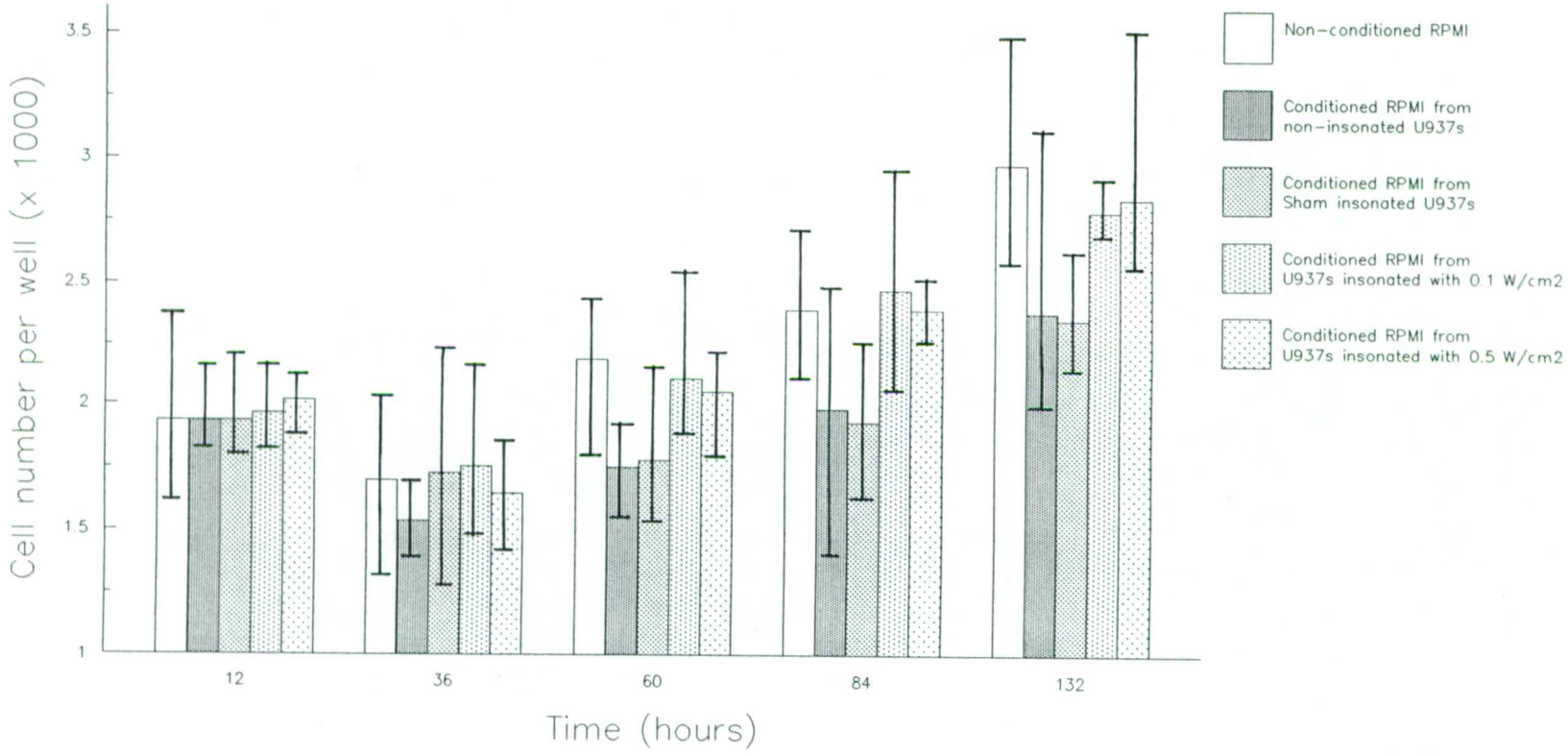

11.4.4 Discussion

Conditioned RPMI-1640 medium obtained after removal of non-insonated and sham-insonated U937s reduces the level of fibroblast proliferation when compared with non-conditioned RPMI-1640 medium. Insonation of U937s with 3 MHz therapeutic ultrasound at intensities of 0.1 or 0.5 W/cm^2 leads to the generation of U937 conditioned media that supports fibroblast proliferation at a level not dissimilar to that of RPMI-1640 medium prior to U937 conditioning.

Hypothetical explanations of these observations include the following:

1. During medium conditioning U937s deplete some component of RPMI-1640 medium essential for fibroblast proliferation. Insonation of U937s with therapeutic ultrasound prevents this depletion.
2. During medium conditioning U937s release an inhibitor of fibroblast proliferation. Insonation of U937s with therapeutic ultrasound prevents the elaboration of this inhibitor.
3. During medium conditioning U937s release an inhibitor for fibroblast proliferation. Insonation of U937s with ultrasound leads to the simultaneous elaboration of a substance that stimulates fibroblast proliferation.

Alternative 1.

The culture of U937s in RPMI-1640 medium leads to the depletion of some component(s) of that medium that is/are necessary for fibroblast proliferation. As (a) fibroblast proliferation is not significantly different in response to conditioned medium from non-insonated U937s compared with sham-insonated U937s, sham-insonation would appear not to effect this depletion, and (b) fibroblast proliferation is similar in wells that received ultrasonically-insonated U937 conditioned media and wells that received non-conditioned media, it is possible that ultrasound in some way prevents U937s from depleting RPMI-1640 of components necessary for fibroblast proliferation. The most effective way of ultrasound preventing U937s from depleting medium would be if it caused functional disruption, or death, of some of the U937s.

Alternative 2.

When U937s are cultured in RPMI-1640 medium they elaborate an inhibitor of

fibroblast proliferation. The elaboration of this fibroblast proliferation inhibitor by U937s is unaffected by sham-insonation, but significantly impaired by exposure to therapeutic ultrasound. By impairing, or completely preventing, the synthesis and/or elaboration of this inhibitor, ultrasound acts to promote fibroblast proliferation. This loss of inhibitory activity in conditioned medium of ultrasonically exposed U937s may be due either to a subtle change in the U937 function or, more dramatically, due to a complete loss of cell function, i.e. cell death.

Alternative 1 versus alternative 2

An experiment (Appendix 27, p385) was devised to investigate whether U937s (a) actively deplete RPMI-1640 of some component essential for fibroblast proliferation or (b) release a fibroblast proliferation inhibitor. The experiment examined fibroblast proliferation in response to progressive dilutions of U937 conditioned medium and unconditioned medium. If U937 conditioned RPMI-1640 medium was in some way deficient in a given component, compared with unconditioned RPMI-1640 medium, further dilution of this conditioned medium (with phosphate buffered saline, PBS) would enhance this deficiency; thus further reducing fibroblast proliferation. If, however, U937 conditioned RPMI-1640 medium contained an inhibitor for fibroblast proliferation, the same dilution of this medium would have the opposite effect and stimulate fibroblast proliferation. Fibroblast proliferation was found to be (1) more rapid following the application of diluted U937 conditioned medium, and (2) progressively less rapid following the application of progressively more dilute unconditioned medium. As such, under the tissue culture conditions used in this thesis, the macrophage-like cell line (U937) has been shown to release an inhibitor of fibroblast proliferation.

Alternative 3

The release of a fibroblast inhibitor having been proven, a further alternative exists to explain the experimental observations made above. When U937s are cultured in RPMI-1640 they release an inhibitor, a process unaffected by sham insonation. Ultrasonic insonation modulates the function of U937 encouraging them to produce a counteractive fibroblast proliferation promoting "factor", in addition to the fibroblast proliferation inhibitor. The production of functionally equal quantities of fibroblast proliferation stimulator and fibroblast proliferation inhibitor would be

necessary to explain the experimental results obtained. This third alternative is thought to be unlikely because (a) the simultaneous synthesis and release of directly counteractive substances, by the same cell, would appear physiologically uneconomical, unless they have other physiological effects, and (b) the generation of functionally balancing levels of directly counteractive substances would appear unlikely. Additionally, no reliable reports have been found within the literature to suggest that undifferentiated (uninduced) U937s are capable of elaborating factors mitogenic for fibroblasts.

As previously mentioned, exposure to therapeutic ultrasound appears to reduce, if not completely annul, the production of a fibroblast proliferation inhibitor by U937s. In order to investigate the mechanism by which ultrasound may prevent inhibitor production by U937s, a study was performed to investigate the effect of therapeutic ultrasound on U937 viability. U937 cultures were either sham-insonated, insonated with 3 MHz therapeutic ultrasound at intensities of 0.1 or 0.5 W/cm^2, or left untreated. Cell counts were performed 1 and 24 hours after treatment and cell viability measured (Appendix 28, p390). By comparing the number of viable U937s remaining after 1 and 24 hours in the four uninduced treatment groups it is apparent that ultrasound exposed U937 cultures contain significantly fewer viable cells than similar sham or non-insonated U937 cultures. This observation that ultrasound in some way depletes the number of viable U937s may partially explain the loss of inhibitory action in ultrasound-exposed U937 conditioned medium. The observation that a 50% fall in viable cell number is paralleled by a complete loss in fibroblast proliferation inhibitor activity, suggests that exposure to ultrasound *in vitro* may in some way selectively deplete U937s actively engaged in inhibitor production.

Although there are no literature reports regarding the release of specific fibroblast proliferation inhibitors by U937 cells, they have been shown to produce a lymphoid specific cytostatic factor (Wilkins and Warrington, 1984). However, other macrophage-derived substances are known be less specific in their anti-proliferative effects. Such macrophage-derived anti-proliferative substances include: (a) interleukin-1/prostaglandins, (b) thymidine, (c) hydrogen peroxide, (d) arginase, and (e) TGF-β.

(a). Interleukin-1/Prostaglandins. The inhibition of human fibroblast proliferation in response to human peripheral blood monocyte conditioned medium has been reported previously. For example, Korn *et al.* (1980) observed that

monocytes elaborated a factor that concomitantly inhibited proliferation and induced prostaglandin synthesis in fibroblast cultures. They showed, using indomethacin and exogenous prostaglandin, that the suppression of proliferation was due, in a large part, to the stimulation of prostaglandin synthesis by fibroblasts. The monocyte-derived factor responsible for stimulating prostaglandin synthesis by fibroblasts has since been identified as interleukin-1 (IL-1) (Sisson and Dinarello, 1989). Several research groups have demonstrated that U937s lack the capacity to produce IL-1 (Krane and Amento, 1983; Wakasugi *et al.* 1984; Knudsen *et al.* 1986; Demczuk *et al.* 1988) or prostaglandins (Schenkein, 1986; Roux-Lombard, 1986; Koehler *et al.* 1990) prior to exposure to a differentiating agent such as PMA. In disagreement with the majority of the literature, Palacios *et al.* 1982 and Barak *et al.* (1986), reported that U937s constitutively secreted IL-1.

(b). Thymidine. Thymidine is secreted by activated macrophages in culture and has been shown to contribute to the anti-proliferative nature of macrophage conditioned media (Stadecker *et al.* 1977). The thymidine within macrophage culture supernatants is thought to inhibit DNA synthesis by inhibiting the conversion of cytosine to deoxycytosine, thus causing a deficiency in one of the precursors of DNA (Stadecker *et al.* 1977). It is not known whether U937s, like activated macrophages, secrete thymidine into their culture medium.

(c). Hydrogen peroxide. Co-culture of activated macrophages and splenic lymphocytes leads to proliferation suppression in the latter; when catalase is added to this co-culture normal proliferation is reinitiated. This implicates hydrogen peroxide in this macrophage-associated suppression, as the only known physiological function of catalase is the reduction of hydrogen peroxide (Metzger *et al.* 1980). Hydrogen peroxide is an inducible characteristic of phorbol ester differentiated U937s, but it is not constitutively elaborated by U937 cultures (Harris *et al.* 1985) which suggests that it may not be involved in the inhibition of fibroblast proliferation noted here.

(d). Arginase. It has been demonstrated that activated macrophages produce arginase, an enzyme which thought to inhibit proliferation by depleting culture medium of the amino acid arginine (Currie, 1978). It is not known whether U937s, like activated macrophages, produce and secrete arginase into their culture medium.

(e). TGF-β. Transforming growth factor-β (TGF-β), while initially reported as a mitogen for rodent fibroblasts grown in soft agar (Moses *et al.* 1981; Roberts *et al.*

1981), was subsequently shown to inhibit anchorage dependent growth in rat kidney fibroblasts (Roberts *et al.* 1985) and bovine aortic smooth muscle cells (Assoian and Sporn, 1986). TGF-β has since been shown to be a potent, but reversible, inhibitor of the proliferation of many cell types *in vitro*, including epithelial cells, endothelial cells, most lymphoid cells and many myeloid cells (Graycar *et al.* 1989; Bascom *et al.* 1989). In addition to these *in vitro* observations, *in vivo* studies have reported that TGF-β inhibits the proliferation of epithelial cells, endothelial cells and fibroblasts in chorioallantoic membrane studies (Yang and Moses, 1990), and mammary epithelial cell proliferation in rodents (Siberstein and Daniel, 1987). It has been suggested that TGF-β is unlikely to be directly mitogenic to any cell type (Moses *et al.* 1991), and that mitogenic activities attributed to TGF-β are probably due to the induction of autocrine stimulation by endogenous growth factors such as PDGF (Loef *et al.* 1986). TGF-β is thought suppress proliferation by suppressing the transcription of a proto-oncogene, *c-myc*, which has been shown to be necessary for proliferation in a number of cells (Bascom *et al.* 1989). The U937 cell has been shown to express TGF-β mRNA and upregulate this expression in response to PMA induction (Assoian *et al.* 1987; Wager and Assoian, 1990). Whether this mRNA expression is paralleled by active secretion of TGF-β into culture is as yet unknown.

The identity of the U937-derived inhibitory factor for fibroblast proliferation observed in these studies is unknown. From literature reports it would appear there are several candidates for this inhibitory activity (see above). The majority, if not all, of these inhibitors are characteristically produced by differentiated, and usually activated, macrophages. The uninduced U937 is an immature promonocytic cell that is apparently unable to generate most of these inhibitors. Further work is necessary to characterise the inhibitor produced by uninduced U937s. In view of the observations of (1) Barak *et al.* (1986), who demonstrated that uninduced U937s constitutively produced IL-1, and, (2) Assoian *et al.* (1987) and Wager and Assoian (1990) who reported TGF-β mRNA expression in uninduced U937s, future work should include studies of the synthesis of IL-1 by uninduced U937s, the synthesis of E-series prostaglandins by fibroblasts in response to U937 conditioned media, and, the capacity of uninduced U937s to elaborate TGF-β.

Interestingly, it has previously been reported that therapeutic ultrasound, at the parameters used in this thesis, stimulates uninduced U937s to synthesize and release factors mitogenic to fibroblasts (Young and Dyson, 1990b). Such observations

appear to contradict the observations made in this study. On examination of the experimental protocol used by Young and Dyson (1990b) it is apparent that they did not employ an unconditioned medium control but restricted their comparisons to a medium conditioned by sham-insonated cells. They were thus unaware of either the presence of an inhibitory activity within their sham-insonated control, or the relief of this inhibition with exposure to ultrasound. They thus reported that U937 insonation appeared to lead to the generation of a pro-proliferative conditioned medium rather than a less inhibitive one.

In summary, it would appear that U937s, under the tissue culture conditions used in this work, produce an inhibitory factor for fibroblast proliferation - further studies are necessary to characterise this inhibitor of fibroblast proliferation. Therapeutic ultrasound exposure appears to reduce the level of this inhibitor in U937 culture supernatants. The observation that the reduction in inhibitory activity following ultrasound treatment is paralleled by a loss in viable cell number, suggests that ultrasound acts to reduce inhibitory activity by damaging inhibitor producing cells rather than encouraging the production of an antagonistic pro-proliferative factor.

11.4.5 Results:

II. The effect of therapeutic ultrasound on the release from PMA-exposed U937s of substances capable of modulating fibroblast proliferation *in vitro*

Figure 11.3 displays the change in median fibroblast number with time in response to the application of the four different conditioned media from PMA-exposed U937s and unconditioned RPMI-1640 supplemented with PMA. 95% confidence intervals are displayed to indicate the distribution of points about median values. A summary of the statistical analysis performed on this data can be found in Appendix 24, (p373). Figure 11.3, the data tables 11.7 through 11.11 (pages 300 to 301), and statistical analysis of that data, demonstrate the following.

1. The effect of non-conditioned medium containing PMA (PMA N-CM) versus conditioned medium from PMA-exposed non-insonated U937s (PMA N-IM).

U937 conditioning of RPMI-1640 medium (supplemented with PMA) reduces its ability to support fibroblast proliferation. From the median fibroblast number data (tables 11.7 & 11.8) there are fewer fibroblasts in wells that received PMA N-IM than received PMA N-CM, at all time points after the 60 hour time point, an observation which proved statistically significant at the 60 ($p < 0.016$), 84 ($p < 0.045$) and 132 ($p < 0.005$) hour time points.

2. The effect of conditioned medium from PMA-exposed non-insonated U937s (PMA N-IM) versus conditioned medium from PMA-exposed sham-insonated U937s (PMA S-IM).

Fibroblast proliferation in response to conditioned medium from PMA-exposed sham-insonated U937s was not significantly different from that of conditioned medium from PMA-exposed non-insonated U937s at any time point, with the exception of 60 hours post plating. At 60 hours fibroblast number was found to be significantly lower in those wells in receipt of PMA S-IM compared with those in receipt of PMA N-IM ($p = 0.030$).

3. The effect of conditioned medium from PMA-exposed sham-insonated U937s (PMA S-IM) versus conditioned medium from PMA-exposed U937s insonated with 3 MHz therapeutic ultrasound at an intensity, $I^{(SATA)}$, of 0.1 W/cm^2 (PMA 0.1-IM).

Fibroblast proliferation was more rapid in fibroblast cultures that received

conditioned medium from PMA-exposed U937s insonated with ultrasound at 0.1 W/cm^2, $I^{(SATA)}$, than similar fibroblast cultures that received conditioned medium from PMA-exposed sham-insonated U937s. Significantly more fibroblasts were present at 60 ($p = 0.008$), 84 ($p = 0.031$) and 132 ($p < 0.005$) hours post plating in wells in receipt of PMA 0.1-IM than in similar wells in receipt of PMA S-IM.

4. The effect of conditioned medium from PMA-exposed sham-insonated U937s (PMA S-IM) versus conditioned medium from PMA-exposed U937s insonated with 3 MHz therapeutic ultrasound at an intensity, $I^{(SATA)}$, of 0.5 W/cm^2 (PMA 0.5-IM).
The application of conditioned medium from PMA-exposed U937s insonated with 3 MHz therapeutic ultrasound, at an intensity of 0.5 W/cm^2, to fibroblasts in culture led to more rapid proliferation than was observed following the application of conditioned medium from sham-insonated PMA-exposed U937s. Significantly more fibroblasts were found in wells that received PMA 0.5-IM, at the 36 ($p = 0.045$), 60 ($p = 0.030$) and 132 ($p < 0.005$) hour time points, than were found in wells in receipt of PMA S-IM. No significant difference in fibroblast proliferation was observed in response to these conditioned media at 84 hours post initial fibroblast plating.

5. The effect of conditioned medium from PMA-exposed U937s insonated at intensities of 0.1 W/cm^2 versus 0.5 W/cm^2 (PMA 0.1-IM & PMA 0.5-IM).
The rate of fibroblast proliferation observed in response to the application of RPMI-1640 media conditioned by PMA-exposed macrophages insonated with therapeutic ultrasound at an intensity of 0.1 W/cm^2 was not significantly different from that observed in response to conditioned media of PMA-exposed U937s similarly insonated at an intensity of 0.5 W/cm^2.

6. The effect of conditioned media from PMA-exposed U937s insonated with therapeutic ultrasound at an intensity $I^{(SATA)}$, of 0.1 W/cm^2 (PMA 0.1-IM) versus non-conditioned medium containing PMA (PMA NC-M).
Fibroblast proliferation observed in response to conditioned medium from PMA-exposed U937s insonated with therapeutic ultrasound, at an intensity of 0.1 W/cm^2, was not significantly different to that observed in response to the application of non-conditioned RPMI-1640 medium until 132 hours post plating. At this time point

significantly more fibroblasts were observed in those wells that received PMA 0.1-IM than received PMA NC-M ($p = 0.013$).

7. The effect of conditioned media from PMA-exposed U937s insonated with therapeutic ultrasound at an intensity $I^{(SATA)}$, of 0.5 W/cm^2 (PMA 0.5-IM) versus non-conditioned medium containing PMA (PMA N-CM).

Proliferation in response to these two media was not significantly different when examined at the 36 and 84 hour time points. At 60 hours post initial fibroblast plating there were significantly fewer fibroblasts ($p < 0.013$) in wells given PMA 0.5-IM than in similar wells in receipt of the non-conditioned medium (PMA N-CM). However, at the final time point of 132 hours there were significantly more fibroblasts in those wells in receipt of ultrasonically-exposed U937 conditioned medium than in similar wells given non-conditioned medium ($p < 0.005$).

Table 11.7 **The effect of non-conditioned RPMI-1640 (containing PMA) on the proliferation of human dermal fibroblasts *in vitro*.**

	Time post plating (hours)				
	12	36	60	84	132
Number of replicate wells	6	6	6	6	6
Median cell number per well (cells x 10^3)	2.124	1.781	2.406	2.501	2.678
Minimum and maximum (cells x 10^3)	1.851 to 2.342	1.236 to 2.163	1.942 to 2.542	2.147 to 3.128	2.542 to 2.869
95% confidence interval (cells x 10^3)	1.933 to 2.316	1.408 to 2.082	2.066 to 2.564	2.154 to 2.976	2.564 to 2.829

Table 11.8 **The effect of conditioning RPMI-1640 (containing PMA) with non-insonated U937s on the proliferation of human dermal fibroblasts *in vitro*.**

	Time post plating (hours)				
	12	36	60	84	132
Number of replicate wells	6	6	6	6	6
Median cell number per well (cells x 10^3)	2.206	1.972	1.833	1.983	1.997
Minimum and maximum (cells x 10^3)	1.906 to 2.451	1.563 to 2.272	1.670 to 2.106	1.765 to 2.529	1.288 to 2.106
95% confidence interval (cells x 10^3)	1.929 to 2.371	1.677 to 2.176	1.666 to 2.055	1.788 to 2.361	1.560 to 2.216

Table 11.9 **The effect of conditioning RPMI-1640 (containing PMA) with sham-insonated U937s on the proliferation of human dermal fibroblasts *in vitro*.**

	Time post plating (hours)				
	12	36	60	84	132
Number of replicate wells	6	6	6	6	6
Median cell number per well (cells x 10^3)	2.151	2.108	1.615	2.256	1.778
Minimum and maximum (cells x 10^3)	2.015 to 2.397	1.563 to 2.926	1.506 to 1 833	1.765 to 2.801	1.561 to 1.888
95% confidence interval (cells x 10^3)	2.021 to 2.336	1.586 to 2.685	1.494 to 1.791	1.875 to 2.673	1.604 to 1.881

Table 11.10 **The effect of conditioning RPMI-1640 (containing PMA) with insonated U937s exposed to pulsed 3 MHz ultrasound (2ms on : 8ms off) at an intensity of 0.1 W/cm^2, $I^{(SATA)}$, on the proliferation of human dermal fibroblasts *in vitro*.**

	Time post plating (hours)				
	12	36	60	84	132
Number of replicate wells	6	6	6	6	6
Median cell number per well (cells x 10^3)	2.124	1.972	2.106	3.019	3.060
Minimum and maximum (cells x 10^3)	1.906 to 2.451	1.236 to 2.544	1.779 to 2.651	2.419 to 3.237	2.815 to 3.524
95% confidence interval (cells x 10^3)	1.903 to 2.327	1.459 to 2.540	1.767 to 2.554	2.533 to 3.269	2.822 to 3.426

Table 11.11 **The effect of conditioning RPMI-1640 (containing PMA) with insonated U937s exposed to pulsed 3 MHz ultrasound (2ms on : 8ms off) at an intensity of 0.5 W/cm^2, $I^{(SATA)}$, on the proliferation of human dermal fibroblasts *in vitro*.**

	Time post plating (hours)				
	12	36	60	84	132
Number of replicate wells	6	6	6	6	6
Median cell number per well (cells x 10^3)	2.124	1.427	1.861	2.692	3.251
Minimum and maximum (cells x 10^3)	1.961 to 2.288	1.236 to 2.217	1.724 to 2.051	2.256 to 3.128	3.033 to 3 360
95% confidence interval (cells x 10^3)	1.967 to 2.245	1.174 to 1.915	1.726 to 2.013	2.302 to 2.973	3.125 to 3.359

Figure 11.3. The effect of therapeutic ultrasound on the release from PMA-induced U937s of substances capable of modulating fibroblast proliferation *in vitro*.

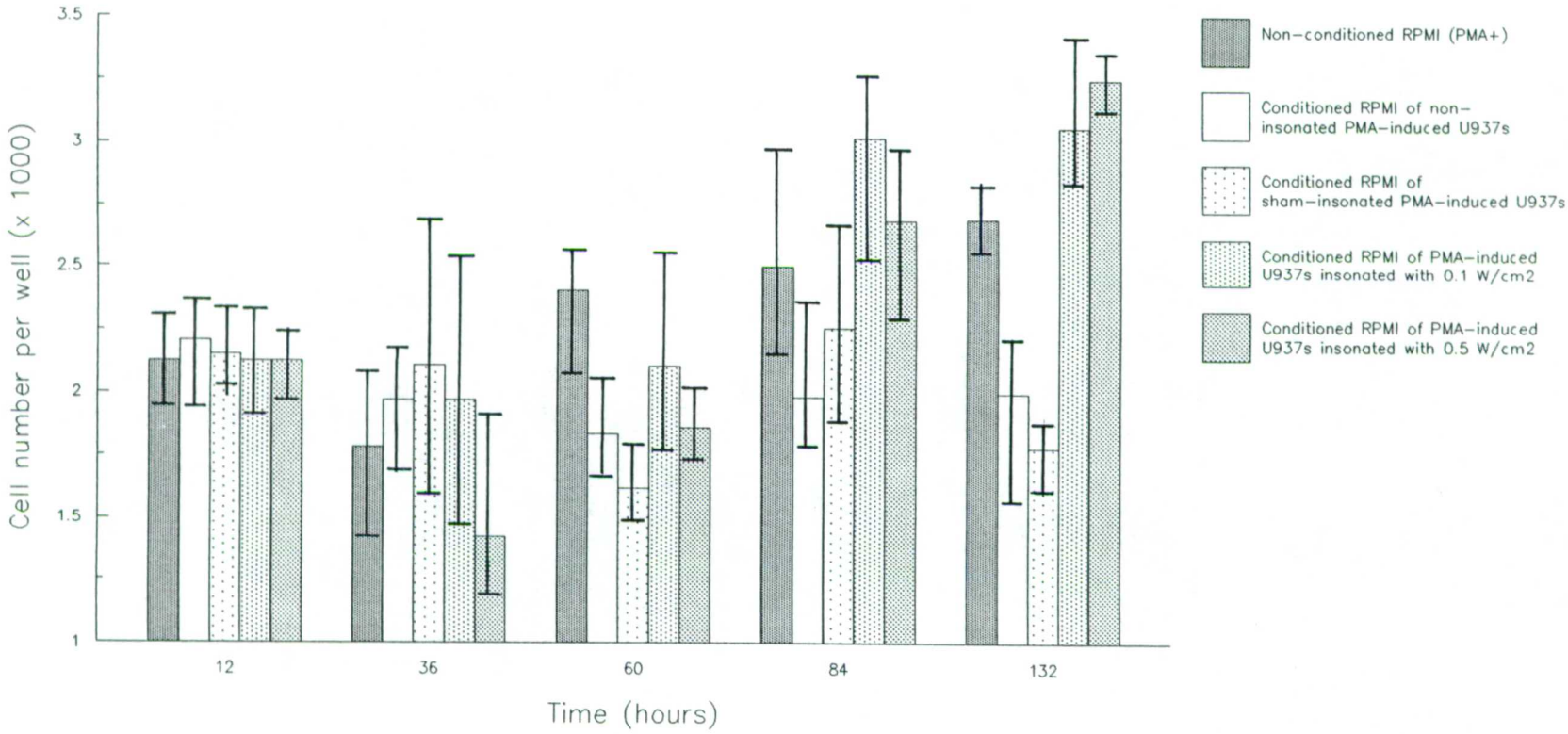

11.4.6 Discussion

To examine whether the lack of mitogenic agent release, reported in section 11.4.3, was due to the lack of U937 maturity, U937s were induced to differentiate using the phorbol ester 4β-phorbol 12-myristate 13 acetate, according to the method of Turk *et al.* (1989).

Conditioned RPMI-1640 medium obtained from non-insonated and sham-insonated PMA-exposed U937s reduces the level of fibroblast proliferation when compared with non-conditioned RPMI-1640 medium supplemented with PMA, an observation which can be explained on the basis of inhibitor generation by U937s (see Appendix 27, p385). Insonation of PMA-exposed U937s with 3 MHz therapeutic ultrasound at intensities of 0.1 or 0.5 W/cm^2 leads to the generation of U937 conditioned media that encourage fibroblast proliferation when compared to PMA-supplemented RPMI-1640 medium prior to U937 conditioning, thus suggesting that PMA-exposed U937s elaborate a substance which stimulates fibroblast proliferation after insonation with therapeutic ultrasound.

Hypothetical explanations of such observations include the following:

1. U937s may produce a fibroblast proliferation inhibitor (p292). The amount of which is reduced by exposure to ultrasound (section 11.4.4, p291) possibly because of damage to a subpopulation of U937s. PMA may modify a further sub-population so that they (a) are less responsive to the damaging effects of ultrasound, and (b) produce fibroblast proliferation promoters.
2. Ultrasound may predispose U937s to the effects of PMA. After insonation a previously resistant subpopulation of U937s become able to respond to PMA, which facilitates U937 maturation and the concomitant production of fibroblast proliferation promoters.

Alternative 1.

According to this hypothesis, in response to PMA pre-conditioning a fraction of U937s adopt novel characteristics that set them apart from the remainder of the culture. These U937s with novel characteristics, hereinafter termed modified U937s, are (a) no longer responsive to the damaging effects of ultrasound, and are (b) now able to produce substances capable of promoting fibroblast proliferation. Cells that retain the original U937 characteristics continue to elaborate the fibroblast inhibitor and are easily damaged by ultrasound. Conditioned medium from non-insonated or

sham-insonated PMA-exposed U937s is conditioned by both modified and original U937s. The inhibitory activity of the original (unmodified) U937s appears to outweigh the stimulatory activity of modified U937s, as demonstrated by the inhibitory action of conditioned media from non-insonated and sham-insonated PMA-exposed U937s on fibroblast proliferation. Insonation of a mixture population of modified and original U937s, with therapeutic ultrasound selectively depletes the latter, i.e. the ultrasound sensitive subpopulation. Fibroblast inhibitor production can be stopped by damaging U937s that produce the inhibitor, while the elaboration of the fibroblast proliferation promoter remains unaffected since this is from the modified, ultrasound resistant subpopulation. This would be expected to result in an elevation in proliferation in fibroblast cultures in receipt of conditioned medium from insonated PMA-exposed U937s. The observation that exposure of PMA-exposed U937s to ultrasound leads to a loss in the number of viable cells remaining in culture (Appendix 28, p390) supports the idea of selective damage of a sub-population of cells.

Alternative 1 is in agreement with the literature on U937 activity. U937s, which share many characteristics with promonocytes, have been shown to mature into macrophage-like cells following treatment with phorbol esters including PMA. These PMA-matured U937s have been shown to produce various factors mitogenic for fibroblasts (see Chapter 5, p146), including fibroblast activating factor (FAF) (Turck *et al.* 1988; Turck *et al.* 1989; Demeter *et al.* 1991), platelet-derived growth factor (PDGF) (Alitalo *et al.* 1987; Makela *et al.* 1987), transforming growth factor-beta (TGF-β) (Assoian *et al*, 1987; Wager and Assoian, 1990), tumour necrosis factor-alpha (TNF-α) (Sabatini *et al.* 1990), interleukin-1 (IL-1) (Palacios *et al.* 1982, Wakasugi *et al.* 1984) and insulin-like growth factor-1 (IGF-1) (Nagoaka *et al.* 1990). Additionally, several researchers have observed a distribution in U937 responsiveness to PMA within apparently homogenous cultures; some U937s undergo morphological and functional changes reminiscent of macrophage differentiation, while other U937s within the same culture appear unresponsive (Elsas *et al.* 1990; Hattori *et al.* 1983). Those responsive to PMA stop proliferating and tend to become adherent. These observations (1) support the idea that PMA may have acted by giving a selective advantage to a subpopulation of U937s within this study, and (2) point to a possible mechanism by which ultrasound may selectively deplete cells unresponsive to PMA i.e. ultrasound may preferentially damage actively dividing non-adherent cells.

Alternative 2

U937s were cultured in PMA supplemented RPMI-1640 medium both prior to, and after, exposure to ultrasound. According to this hypothesis, it is possible that ultrasound predisposes previously resistant U937s to the influence of PMA. i.e. some U937s may require insonation before they can mature into cells with the characteristics of macrophages in response to PMA. It is suggested that such mature U937s either produce less, or no longer produce any, fibroblast inhibitor, but rather produce a substance that encourages fibroblast proliferation. Sham-insonated and non-insonated U937s are not similarly predisposed and consequently cannot respond as readily to PMA; they thus continue to produce the fibroblast inhibitor characteristic of U937s not exposed to PMA. This hypothesis suggests that some U937s cannot respond directly to PMA, as the work of Elsas *et al.* (1990) and Hattori *et al.* (1983) suggests. However, the majority, if not all, of the pertinent U937 literature report that PMA is capable of acting directly on U937s to facilitate U937 maturation and growth factor production (Harris and Ralph, 1985; Turck *et al.* 1988; Alitalo *et al.* 1987; Makela *et al.* 1987; Assoian *et al,* 1987; Wager and Assoian, 1990; Sabatini *et al.* 1990; Nagoaka *et al.* 1990).

In summary, it would appear that conditioned medium from PMA-exposed U937s, like that of non-PMA exposed U937s, contains an inhibitor of fibroblast proliferation. Exposure of PMA-exposed U937s to therapeutic ultrasound results in the production of a conditioned medium that promotes fibroblast proliferation above that of non-conditioned PMA-supplemented medium. This gain in pro-proliferative activity is paralleled by a loss in viable U937s (Appendix 28, p390). This would appear to suggest that ultrasound selectively depletes inhibitor generating cells within the culture and in doing so enriches the culture with PMA-responsive, mitogen producing U937s.

Conditioned media from induced and non-induced U937s

The majority of the literature indicates that PMA-induced U937s produce factors that promote, rather than inhibit, fibroblast proliferation (Palacios *et al,* 1982; Sabatini *et al.* 1990; Assoian *et al.* 1987; Wager and Assoian, 1990; Makela *et al.* 1987 Turck *et al.* 1988; Turck *et al.* 1989; Demeter *et al.* 1991; Nagoaka *et al.* 1990). In this study conditioned media from non-insonated U937s, both uninduced and PMA-induced,

appears to contain a substance, or substances, that significantly inhibit fibroblast proliferation. The methods used to induce differentiation in U937s in this study were taken from the experimental methods of Turck *et al.* (1988), Turck *et al.* (1989) and Demeter *et al.* (1991) who reported the production of fibroblast proliferation promoters by U937s. One possible explanation for this disparity in results may involve genetic drift of the U937 line used here. It is known that monocytic cell lines can drift from their original characteristics, especially if repeatedly passaged (Lyons and Ashman, 1989). Further work using a fresh source of U937s, and involving a comparison of functional activities with the U937s presently in use, may help to explain the disparity described above.

11.5 The effect of ultrasound on the production by the macrophage-like cell line U937 of substances capable of modulating fibroblast-mediated collagen lattice (FPCL) contraction *in vitro*.

11.5.1 Introduction

The contraction of human dermal fibroblast-populated collagen lattices, a widely accepted model of the process of wound contraction *in vitro* (Ehrlich and Rajaratnam, 1990), was used to investigate the effect of conditioned media, from ultrasound-exposed U937s produced as described above (section 11.3, p297), on human dermal fibroblast-mediated collagen lattice contraction.

11.5.2 Method

Sixty standard fibroblast populated collagen lattices were prepared according to steps 1 through 6 of the Human dermal fibroblast collagen lattice contraction assay - Standard protocol (Appendix 10, p344). After polymerisation and lattice release, the 60 lattices were randomly allocated into 10 groups, each containing 6 lattices. All 6 lattices of each group received a 1 ml aliquot of one of the 10 different conditioned media (table 11.1, p282). Once all 60 lattices had been "fed" in this manner they were placed in a humidified box and returned to the 37°C incubator. All sixty lattices were photographed (Appendix 11A, p345) at 4.75, 21.25, 30.75, 45.75, 54.25 and 69.25 hours after initial plating and the film developed according to Appendix 11B (p346). The area of each lattice, in mm^2, was then measured by computer-assisted planimetry (Appendix 12, p347).

Median lattice area, minimum and maximum lattice area, and 95% confidence intervals were calculated for each group of lattices (i.e. in response to each conditioned medium) at each time point. The data was tabulated (tables 11.12 through 11.16) and displayed graphically (figure 11.4). Non-parametric statistical analysis was performed to examine the modulation in the rate of lattice contraction in response to different conditioned media. Kruskall Wallace tests were used to compare all groups, at each time point, as an indicator of any need for further statistical analysis. The Mann Whitney U-test was then applied between specific treatment groups where appropriate.

This study contains two studies:

I. An investigation of the effect of ultrasound on the production by non-PMA-

exposed U937s of substances capable of modulating fibroblast-mediated collagen lattice contraction *in vitro*.

and II. An investigation of the effect of ultrasound on the production by PMA-exposed U937s of substances capable of modulating fibroblast-mediated collagen lattice contraction *in vitro*.

In the interests of clarity the results and discussion of these two studies will be described separately (pages 308-316 and 317-323 respectively).

11.5.3 Results:

I. The effect of ultrasound on the production by non-PMA exposed U937s of substances capable of modulating FPCL contraction *in vitro*.

Figure 11.4 displays the change in median lattice area (mm^2) with time, in response to the application of the five non-PMA exposed conditioned media. 95% confidence intervals are displayed to indicate data distribution. A summary of the statistical analysis performed on this data can be found in Appendix 25, (p379). Figure 11.4, the data tables 11.12 through 11.16 (p311 to 312), and statistical analysis of that data, demonstrate the following.

1. Non-conditioned medium containing PMA (N-CM) versus conditioned medium from PMA-exposed non-insonated U937s (N-IM).

RPMI-1640 medium conditioned by non-insonated U937s stimulates fibroblast-mediated collagen lattice contraction. Fibroblast-populated collagen lattices (FPCL) that received N-IM were significantly smaller (i.e. had contracted faster) than those in receipt of N-CM at all time points studied ($p < 0.005$).

2. Conditioned medium from non-insonated U937s (N-IM) versus conditioned medium from sham-insonated U937s (S-IM).

FPCLs in receipt of conditioned RPMI-1640 medium conditioned by sham-insonated U937s (S-IM) contracted more slowly than those in receipt of conditioned medium from non-insonated U937s (N-IM). Based on the median lattice area data (tables 11.13 & 11.14, p311), FPCLs that received S-IM were always larger than those in receipt of N-IM at all time points studied. This observation reached statistical significance at 30.75 ($p = 0.013$), 54.25 ($p < 0.020$) and 69.25 ($p = 0.045$) hours post lattice polymerisation.

3. Conditioned medium from sham-insonated U937s (S-IM) versus conditioned medium from U937s insonated with 3 MHz therapeutic ultrasound at an intensity, $I^{(SATA)}$, of 0.1 W/cm^2 (0.1-IM).

Contraction appeared slower in FPCLs that received conditioned medium from U937s insonated with ultrasound at 0.1 W/cm^2, $I^{(SATA)}$, than in similar FPCLs that received conditioned medium from sham-insonated U937s. This observation was, however, not substantiated by statistical analysis. Lattices in receipt of 0.1-IM were found to be statistically larger (i.e. had contracted more slowly) only at 30.37 hours post lattice polymerisation ($p = 0.013$).

4. Conditioned medium from sham-insonated U937s (S-IM) versus conditioned medium from U937s insonated with 3 MHz therapeutic ultrasound at an intensity, $I^{(SATA)}$, of 0.5 W/cm^2 (0.5-IM).

Lattice contraction was observed to proceed more slowly in FPCLS that received conditioned medium from U937s insonated with ultrasound at 0.5 W/cm^2, $I^{(SATA)}$, than in similar FPCLs that received conditioned medium from sham-insonated U937s. This observation was substantiated by statistical analysis. Lattices in receipt of 0.5-IM were found to be statistically larger at 4.75 ($p = 0.020$), 54.25 ($p = 0.045$) and 69.25 ($p < 0.005$) hours post lattice polymerisation than those receiving S-IM.

5. Conditioned medium from U937s insonated with therapeutic ultrasound at intensities of 0.1 W/cm^2 (0.1-IM) versus 0.5 W/cm^2 (0.5-IM).

The rate of FPCL contraction observed in response to the application of RPMI-1640 medium conditioned by U937s insonated with therapeutic ultrasound at an intensity of 0.5 W/cm^2 was slower than that observed in response to conditioned RPMI-1640 medium from U937s insonated at an intensity of 0.1 W/cm^2. FPCL in receipt of 0.5-IM were found by non-parametric statistics to be significantly larger than those in receipt of 0.1-IM at 4.75 ($p = 0.020$), 21.25 ($p = 0.031$), 45.75 ($p = 0.031$) and 69.25 ($p < 0.005$) hours post lattice polymerisation.

6. Conditioned medium from U937s insonated at an intensity, $I^{(SATA)}$, of 0.1 W/cm^2 (0.1-IM) versus non-conditioned medium (N-CM).

The rate of FPCL contraction observed in response to conditioned medium from U937s insonated with therapeutic ultrasound, at an intensity of 0.1 W/cm^2, was more

rapid than that observed in response to the application of non-conditioned RPMI-1640 medium at all time points studied. FPCL supplemented with 0.1-IM were significantly smaller, and thus had contracted quicker, than FPCL supplemented with N-CM at all time points studied: 4.75 ($p = 0.31$), 21.25 ($p < 0.008$), 30.75 ($p < 0.008$), 45.75 ($p < 0.005$), 54.25 ($p < 0.005$), 69.25 ($p < 0.005$).

7. Conditioned media from U937s insonated with therapeutic ultrasound at an intensity, $I^{(SATA)}$, of 0.5 W/cm^2 (0.5-IM) versus non-conditioned medium (N-CM).

Contraction was observed to proceed more rapidly in FPCLS that received conditioned medium from U937s insonated at 0.5 W/cm^2, than in similar FPCLs that received non-conditioned medium. This observation was substantiated by statistical analysis. FPCLs given 0.5-IM were found to be statistically smaller than those given N-CM at 21.25 ($p = 0.031$), 30.75 ($p < 0.008$), 45.75 ($p < 0.013$) and 69.25 ($p < 0.005$) hours post lattice polymerisation.

Table 11.12 **The effect of non-conditioned RPMI-1640 on the contraction of human dermal fibroblast populated collagen lattices *in vitro*.**

	Time post plating (hours)					
	4.75	21.25	30.75	45.75	54.25	69 25
Number of replicate lattices	6	6	6	6	6	6
Median lattice area (mm^2)	603.3	370.3	290.6	242.1	207.0	203.3
Minimum and Maximum (mm^2)	574.3 to 668 7	341.0 to 419.5	271.9 to 324.7	219.0 to 252.7	193.7 to 215.8	195.3 to 215.3
95% Confidence interval (mm^2)	575.2 to 645.4	346.7 to 401.5	274.8 to 312.3	227.5 to 252.6	197.7 to 214.3	195.4 to 212.7

Table 11.13 **The effect of conditioning RPMI-1640 with non-insonated U937s on the contraction of human dermal fibroblast populated collagen lattices *in vitro*.**

	Time post plating (hours)					
	4.75	21.25	30.75	45.75	54.25	69.25
Number of replicate lattices	6	6	6	6	6	6
Median lattice area (mm^2)	554.8	319.1	267.0	205.0	174.0	162.4
Minimum and Maximum (mm^2)	514.0 to 580.3	315.1 to 327.1	254.9 to 274.6	188.7 to 209.1	168.7 to 181.6	156.8 to 164.9
95% Confidence interval (mm^2)	529.6 to 575.7	315.7 to 325.7	256.8 to 273.8	192.3 to 210.5	169.6 to 179.7	158.2 to 165.2

Table 11.14 **The effect of conditioning RPMI-1640 with sham insonated U937s on the contraction of human dermal fibroblast populated collagen lattices *in vitro*.**

	Time post plating (hours)					
	4.75	21.25	30.75	45.75	54.25	69.25
Number of replicate lattices	6	6	6	6	6	6
Median lattice area (mm^2)	568.7	336.2	279.8	206.3	180.9	167.2
Minimum and Maximum (mm^2)	491.9 to 608.6	314.3 to 348 6	272.6 to 284 9	201.7 to 217.2	179.1 to 212.3	162.2 to 173.5
95% Confidence interval (mm^2)	511.0 to 602.4	321.5 to 346.5	274.0 to 284.7	201.6 to 215.4	185.1 to 207.7	163.0 to 172.3

Table 11.15 **The effect of conditioning RPMI with insonated U937s, exposed to pulsed 3 MHz ultrasound (2ms on : 8ms off) at an intensity of 0.1 W cm^2, $I^{(SATA)}$, on the contraction of human dermal fibroblast populated collagen lattices *in vitro*.**

	Time post plating (hours)					
	4.75	21.25	30.75	45.75	54.25	69.25
Number of replicate lattices	6	6	6	6	6	6
Median lattice area (mm^2)	566.1	336.3	267.9	210.7	186.2	172.1
Minimum and Maximum (mm^2)	547.2 to 598.4	330.1 to 342.7	263.4 to 273 4	206.1 to 215.6	179.5 to 188.8	166.5 to 178.2
95% Confidence interval (mm^2)	552.1 to 587.8	331.3 to 340.7	264.7 to 271.4	206.9 to 214.6	181.1 to 189.1	168.1 to 176.1

Table 11.16 **The effect of conditioning RPMI with insonated U937s, exposed to pulsed 3 MHz ultrasound (2ms on : 8ms off) at an intensity of 0.5 W/cm^2, $I^{(SATA)}$, on the contraction of human dermal fibroblast populated collagen lattices *in vitro*.**

	Time post plating (hours)					
	4.75	21.25	30.75	45.75	54.25	69.25
Number of replicate lattices	6	6	6	6	6	6
Median lattice area (mm^2)	618.3	346.3	268.4	216.2	196.7	187.5
Minimum and Maximum (mm^2)	573.6 to 638.2	336.4 to 356.9	264.0 to 274.1	212.4 to 227.1	179.2 to 212.3	178.9 to 192.7
95% Confidence interval (mm^2)	587.1 to 635.5	338.6 to 354.8	265.1 to 272.4	212.2 to 224.0	185.1 to 207.7	181.4 to 192.4

Figure 11.4. The effect of therapeutic ultrasound on the production by uninduced U937s of substances capable of modulating fibroblast-mediated collagen lattice contraction *in vitro*.

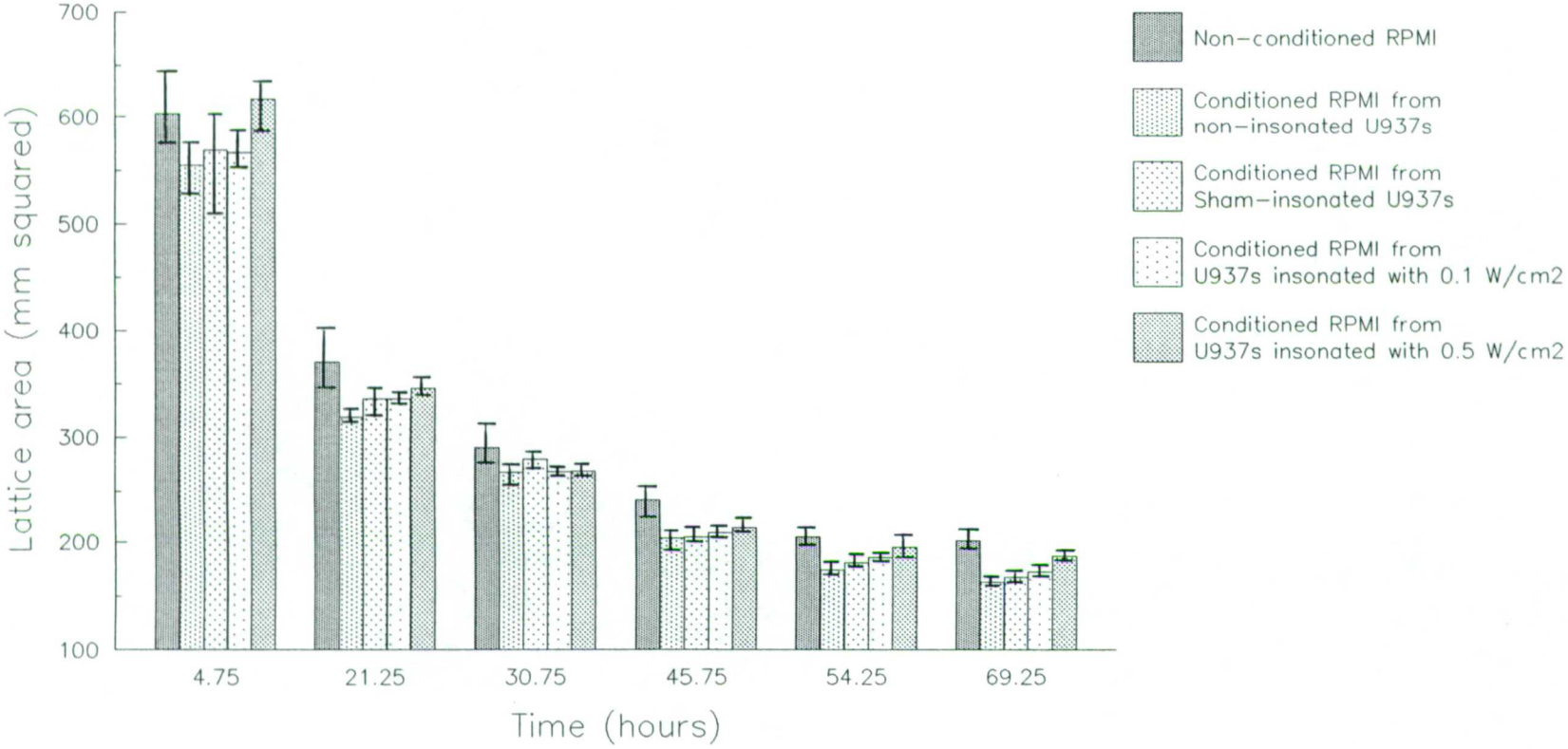

11.5.4 Discussion

The culture of U937s in RPMI-1640 medium leads to the generation of a conditioned medium that promotes the contraction of human fibroblast populated collagen lattices. FPCLs fed with U937 conditioned medium contracted more rapidly than similar FPCLs fed with unconditioned RPMI-1640 medium. Generally, when conditioned medium from sham-insonated U937s was applied to FPCLs, contraction was observed to proceed more rapidly than in those lattices supplemented with unconditioned medium; but, more slowly than in those lattices supplemented with conditioned medium from non-insonated U937s. FPCLs supplemented with conditioned medium from ultrasonically exposed U937s (at intensities of both 0.1 and 0.5 W/cm^2) tended to contract more slowly than similar lattices in receipt of sham-insonated U937 conditioned medium, and more rapidly than those lattices given non-conditioned RPMI-1640 medium.

As with the studies examining the effect of U937 conditioned media on fibroblast proliferation, several explanations exist to account for these observations, including the following:

1. U937s produce a substance, or substances, that act(s) to promote fibroblast-mediated collagen lattice contraction. Insonation, and to a certain degree sham-insonation, of U937s acts to reduce the production of such a substance(s).

2. Prior to insonation U937s produce a substance, or substances, that act(s) to promote fibroblast-mediated collagen lattice contraction. Insonation, and to a certain degree sham-insonation, with therapeutic ultrasound leads to the simultaneous production of an antagonistic substance(s) that inhibits fibroblast-mediated collagen lattice contraction.

Studies carried out to determine U937 viable cell density before and after exposure to therapeutic ultrasound (Appendix 28, p390) support the first of these alternatives. Such studies have demonstrated that U937 viable cell density falls after insonation *in vitro*. The concomitant loss of pro-contractile activity within U937 conditioned medium and fall in viable cell density of U937s conditioning that

medium, in response to ultrasonic exposure, suggests a causal relationship between the two, i.e. ultrasound depletes U937 cultures of pro-contractile activity-generating cells.

Such studies, while supporting the first alternative, also throws doubt on the second. Assuming that the generation of pro- and anti-contractile activities are active processes, the generation of an anti-contractile activity would depend on the retention of cell viability. The observation that a fall in cell viability apparently parallels an upregulation in the production of this anti-contractile activity, appears to confound this alternative. Such observations cannot preclude the concomitant elaboration of both stimulatory and inhibitory activities by ultrasound exposed U937s, as even after insonation, approximately 50% of the U937 culture remained viable (Appendix 28, p390). It is theoretically possible that ultrasound may act as an inducer of U937s, perhaps in a similar fashion to that of phorbol esters. Under such circumstances, exposure of U937s to therapeutic ultrasound may lead to the upregulation of factors such as IL-1 which have been shown to inhibit fibroblast-mediated collagen lattice contraction (Gillery *et al.* 1989). That FPCLs supplemented with insonated U937 conditioned medium contract less rapidly than similar FPCLs supplemented with non-insonated U937 conditioned medium is clear. However, it is not known whether insonation of U937s leads to a loss of pro-contractile activity, or a gain in anti-contractile activity, or a modulation of both pro- and anti-contractile activities.

The identity of this U937-derived pro-contractile activity is unknown. However, several substances, many of which are growth factors known to be produced by macrophages, have been shown to promote fibroblast-mediated collagen lattice contraction *in vitro* and are thought to involved with the process of wound contraction *in vivo*. Macrophage-derived factors which have been reported to stimulate fibroblast-mediated collagen lattice contraction include: FAF (Turck *et al.* 1989); TGF-β (Montesano and Orci, 1988; Finesmith *et al.* 1990); the AB and BB, but not the AA, isoforms of PDGF (Clark *et al.* 1989); aFGF (Turck *et al.* 1989); bFGF (Finesmith *et al.* 1990) and TGF-α (Finesmith *et al.* 1990). That one of these factors is involved in U937 conditioned medium stimulation of contraction can be questioned on the basis that (1) the uninduced U937 is not thought to produce biologically significant levels of any of these growth factors (see Chapter 5, p147), and (2) while many of these growth factors have been observed to stimulate

fibroblast proliferation *in vitro* (McGrath, 1990), U937 conditioned medium inhibits fibroblast proliferation (p291). One factor that has been shown to both stimulate fibroblast-mediated FPCL contraction (Montesano and Orci, 1988; Finesmith *et al.* 1990) and inhibit subconfluent monolayer proliferation of fibroblasts (Roberts *et al.* 1985) is TGF-β. Future work is planned to investigate the composition of U937 conditioned medium, specifically with respect to the presence of TGF-β.

In summary, it would appear that U937s, under the tissue culture conditions used in this work, produce a stimulatory factor for fibroblast-mediated FPCL contraction, further studies are necessary to characterise this stimulator. Therapeutic ultrasound exposure appears to reduce the level of this stimulator in U937 culture supernatants. The observation that the reduction in stimulatory activity following ultrasound treatment is paralled by a loss in viable cell number, suggests that ultrasound acts to reduce stimulatory activity by damaging the cells actively generating this stimulator.

11.5.5 Results:

II. The effect of ultrasound on the production by PMA-exposed U937s of substances capable of modulating FPCL contraction *in vitro*.

Figure 11.5 displays the change in median lattice area (mm^2) with time, in response to the application of the four different conditioned media from PMA-exposed U937s and unconditioned RPMI-1640 supplemented with PMA. 95% confidence intervals are displayed to indicate the distribution of points about median values. A summary of the statistical analysis performed on this data can be found in Appendix 26, (p381). Figure 11.5, the data tables 11.17 through 11.21 (p320 to 321), and statistical analysis of that data, demonstrate the following.

1. Non-conditioned medium containing PMA (PMA N-CM) versus conditioned medium from PMA-exposed non-insonated U937s (PMA N-IM).

U937 conditioning of RPMI-1640 medium (supplemented with PMA) increases its ability to support fibroblast-mediated collagen lattice contraction. FPCL that received PMA N-IM were significantly smaller (i.e had contracted more rapidly) than those in receipt of PMA N-CM at all time points studied ($p < 0.005$), with the exception of at 4.75 hours at which no significant difference was observed.

2. Conditioned medium from PMA-exposed non-insonated U937s (PMA N-IM) versus conditioned medium from PMA-exposed sham-insonated U937s (PMA S-IM).

Sham insonation of PMA-exposed U937s leads to the generation of a conditioned medium (PMA S-IM) that promotes FPCL contraction compared with conditioned medium (PMA N-IM) from non-insonated PMA-exposed U937s. FPCL in receipt of PMA S-IM demonstrated more rapid contraction at all time points studied ($p < 0.005$).

3. Conditioned medium from PMA-exposed sham-insonated U937s (PMA S-IM) versus conditioned medium from PMA-exposed U937s insonated with 3 MHz therapeutic ultrasound at an intensity, $I^{(SATA)}$, of 0.1 W/cm^2 (PMA 0.1-IM).

Fibroblast-mediated lattice contraction was slower in those lattices in receipt of conditioned medium from PMA-exposed U937s insonated with 0.1 W/cm^2 (PMA 0.1-IM) than in those lattices that were given conditioned medium from similarly exposed

U937s that were sham-insonated. FPCL in receipt of PMA 0.1-IM were consistently significantly larger than those in receipt of PMA S-IM at all time points studied ($P < 0.005$), with the exception of at the first time point of 4.75 hours.

4. Conditioned medium from PMA-exposed sham-insonated U937s (PMA S-IM) versus conditioned medium from PMA-exposed U937s insonated with 3 MHz therapeutic ultrasound at an intensity, $I^{(SATA)}$, of 0.5 W/cm^2 (PMA 0.5-IM).

FPCL supplemented with conditioned medium from PMA-exposed U937s insonated with 3 MHz therapeutic ultrasound at an intensity of 0.5 W/cm^2 contracted more slowly than similar FPCL supplemented with conditioned medium from PMA-exposed sham-insonated U937s. Those lattices given PMA 0.5-IM were found to be significantly larger than similar lattices given PMA S-IM at all time points studied (4.75 hrs, $p < 0.008$; 21.25 hrs, $p < 0.005$; 30.75 hrs, $p < 0.005$; 45.75 hrs, $p = 0.031$; 54.25 hrs, $p = 0.031$; 69.25 hrs, $p < 0.005$).

5. Conditioned medium from PMA-exposed, U937s insonated at intensities of 0.1 W/cm^2 (PMA 0.1-IM) versus 0.5 W/cm^2 (PMA 0.5-IM).

The rate of FPCL contraction observed in response to the application of RPMI-1640 medium conditioned by PMA-exposed U937s insonated with therapeutic ultrasound at an intensity of 0.5 W/cm^2 was similar to that observed in response to conditioned RPMI-1640 medium from PMA-exposed U937s similarly insonated at an intensity of 0.1 W/cm^2. FPCL in receipt of PMA 0.5-IM were found to have contracted at rates statistically indistinguishable from those in receipt of PMA 0.1-IM for the majority of the study. However, at the first time point, 4.75 hours, PMA 0.5-IM lattices were statistically larger (i.e had demonstrated less contraction) than PMA 0.1-IM lattices ($p < 0.005$); while at a later time point, 54.25 hours, PMA 0.5-IM lattices were statistically smaller (i.e had demonstrated more contraction) than PMA 0.1-IM lattices ($p < 0.005$).

6. Conditioned medium from PMA-exposed U937s insonated with therapeutic ultrasound at an intensity, $I^{(SATA)}$, of 0.1 W/cm^2 (PMA 0.1-IM) versus non-conditioned medium containing PMA (PMA N-CM).

The rate of FPCL contraction observed in response to conditioned medium from PMA- exposed U937s insonated with therapeutic ultrasound, at an intensity of 0.1

W/cm^2, was more rapid than that observed in response to the application of non-conditioned RPMI-1640 medium, supplemented with PMA, at all time points studied. FPCL supplemented with PMA 0.1-IM were significantly smaller than, and thus had contracted quicker, than FPCL supplemented with PMA N-CM at all time points studied ($p < 0.005$).

7. Conditioned media from PMA-exposed U937s insonated with therapeutic ultrasound at an intensity, $I^{(SATA)}$, of 0.5 W/cm^2 (PMA 0.5-IM) versus non-conditioned medium containing PMA (PMA N-CM).

Lattice contraction in response to conditioned medium from PMA-exposed U937s insonated with therapeutic ultrasound, at an intensity of 0.1 W/cm^2, was more rapid than that observed in response to the application of non-conditioned RPMI-1640 medium, supplemented with PMA, at all time points studied. FPCL supplemented with PMA 0.1-IM were significantly smaller, and thus had contracted quicker, than FPCL supplemented with PMA N-CM at all time points studied ($p < 0.005$).

11.5.6 Discussion

The culture of U937s in RPMI-1640 medium containing PMA leads to the generation of conditioned medium that promotes the contraction of human dermal fibroblast populated collagen lattices. FPCLs fed with PMA-exposed U937 conditioned medium contracted more rapidly than similar FPCLs fed with unconditioned RPMI-1640 medium supplemented with PMA. Sham-insonation of PMA-exposed U937s leads to the generation of a conditioned medium that stimulates FPCL contraction more than the conditioned medium generated by non-insonated PMA-exposed U937s. FPCLs supplemented with conditioned medium obtained from insonated PMA-exposed U937s (exposed to both 0.1 and 0.5 W/cm^2) contracted more slowly than similar lattices in receipt of conditioned medium from sham-insonated PMA-exposed U937s, but more rapidly than lattices given non-conditioned medium supplemented with PMA.

The majority of observations regarding the effect of PMA-exposed U937 conditioned media on FPCL contraction follow the general scheme observed for non-PMA-exposed U937 conditioned media on FPCL contraction. During conditioning of RPMI-1640, be it by uninduced or PMA-induced U937s, an activity is acquired that promotes FPCL contraction; ultrasonic exposure leads to the generation of

Table 11.17 The effect of non-conditioned RPMI-1640, containing PMA, on the contraction of human dermal fibroblast populated collagen lattices (FPCL) *in vitro*.

	Time post plating (hours)					
	4.75	21.25	30.75	45.75	54.25	69.25
Number of replicate lattices	6	6	6	6	6	6
Median lattice area (mm^2)	677.7	425.4	331.4	253.5	240.8	211.6
Minimum and Maximum (mm^2)	615.5 to 749.5	389.0 to 519.8	304.9 to 396.4	244.9 to 281.2	235.5 to 246.3	207.1 to 216.7
95% Confidence interval (mm^2)	631.0 to 727.5	382.1 to 483.8	300.5 to 377.7	243.4 to 272.6	237.1 to 244.5	208.3 to 215.3

Table 11.18 The effect of conditioned RPMI-1640 (conditioned with non-insonated, PMA exposed, U937s) on the contraction of human dermal FPCL *in vitro*.

	Time post plating (hours)					
	4.75	21.25	30.75	45.75	54.25	69.25
Number of replicate lattices	6	6	6	6	6	6
Median lattice area (mm^2)	621.3	356.4	293.2	221.1	200.4	178.9
Minimum and Maximum (mm^2)	601.3 to 668.0	341.6 to 379.5	279.6 to 303.3	203.5 to 242.8	197.1 to 204.6	169.9 to 184.8
95% Confidence interval (mm^2)	601.1 to 655.6	344.7 to 372.4	282.1 to 302.3	208.7 to 235.1	197.9 to 203.2	171.5 to 185.4

Table 11.19 The effect of conditioned RPMI-1640 (conditioned with sham-insonated, PMA-exposed, U937s) on the contraction of human dermal FPCL *in vitro*.

	Time post plating (hours)					
	4.75	21.25	30.75	45.75	54.25	69.25
Number of replicate lattices	6	6	6	6	6	6
Median lattice area (mm^2)	552.3	303.7	233.8	188.0	173.1	163.1
Minimum and Maximum (mm^2)	505.7 to 598.3	285.5 to 333.5	221.8 to 250.1	179.9 to 196.7	168.3 to 182.9	158.2 to 169.3
95% Confidence interval (mm^2)	520.4 to 584.1	288.4 to 327.5	224.2 to 245.8	180.5 to 195.5	168.7 to 180.1	159.5 to 167.6

Table 11.20 **The effect of conditioned RPMI-1640 (conditioned with PMA-exposed U937s *insonated with pulsed 3 MHz ultrasound {2ms on : 8ms off} at an intensity of 0.1* W/cm², I($^{(SATA)}$) on the contraction of human dermal FPCL *in vitro*.**

	Time post plating (hours)					
	4 75	21.25	30.75	45.75	54.25	69.25
Number of replicate lattices	6	6	6	6	6	6
Median lattice area (mm^2)	562.4	348.3	291.1	217.4	202.1	178.1
Minimum and Maximum (mm^2)	542.0 to 591.4	341.4 to 357.1	280.0 to 303.6	195.5 to 226.8	193.2 to 210.6	173.2 to 187.1
95% Confidence interval (mm^2)	545.4 to 587.4	342.4 to 355.7	282.5 to 300.5	202.4 to 226.5	194.1 to 209.7	173.7 to 184.6

Table 11.21 **The effect of conditioned RPMI-1640 (conditioned with PMA-exposed U937s insonated with pulsed 3 MHz ultrasound {2ms on : 8ms off} at an intensity of 0.5 W/cm², I($^{(SATA)}$) on the contraction of human dermal FPCL *in vitro*.**

	Time post plating (hours)					
	4.75	21.25	30.75	45.75	54.25	69.25
Number of replicate lattices	6	6	6	6	6	6
Median lattice area (mm^2)	604.2	340.5	275.6	212.6	182.4	175.5
Minimum and Maximum (mm^2)	593.5 to 633.5	334.9 to 378.1	254.8 to 304.0	181.2 to 226.4	178.5 to 189.4	159.2 to 184.5
95% Confidence interval (mm^2)	593 2 to 625.3	340.5 to 375.3	258.1 to 297.6	193.2 to2 227.3	178.8 to 188.1	163.7 to 183.3

Figure 11.5. The effect of 3 MHz therapeutic ultrasound on the production by PMA-induced U937s of substances capable of modulating fibroblast-mediated collagen lattice contraction *in vitro*.

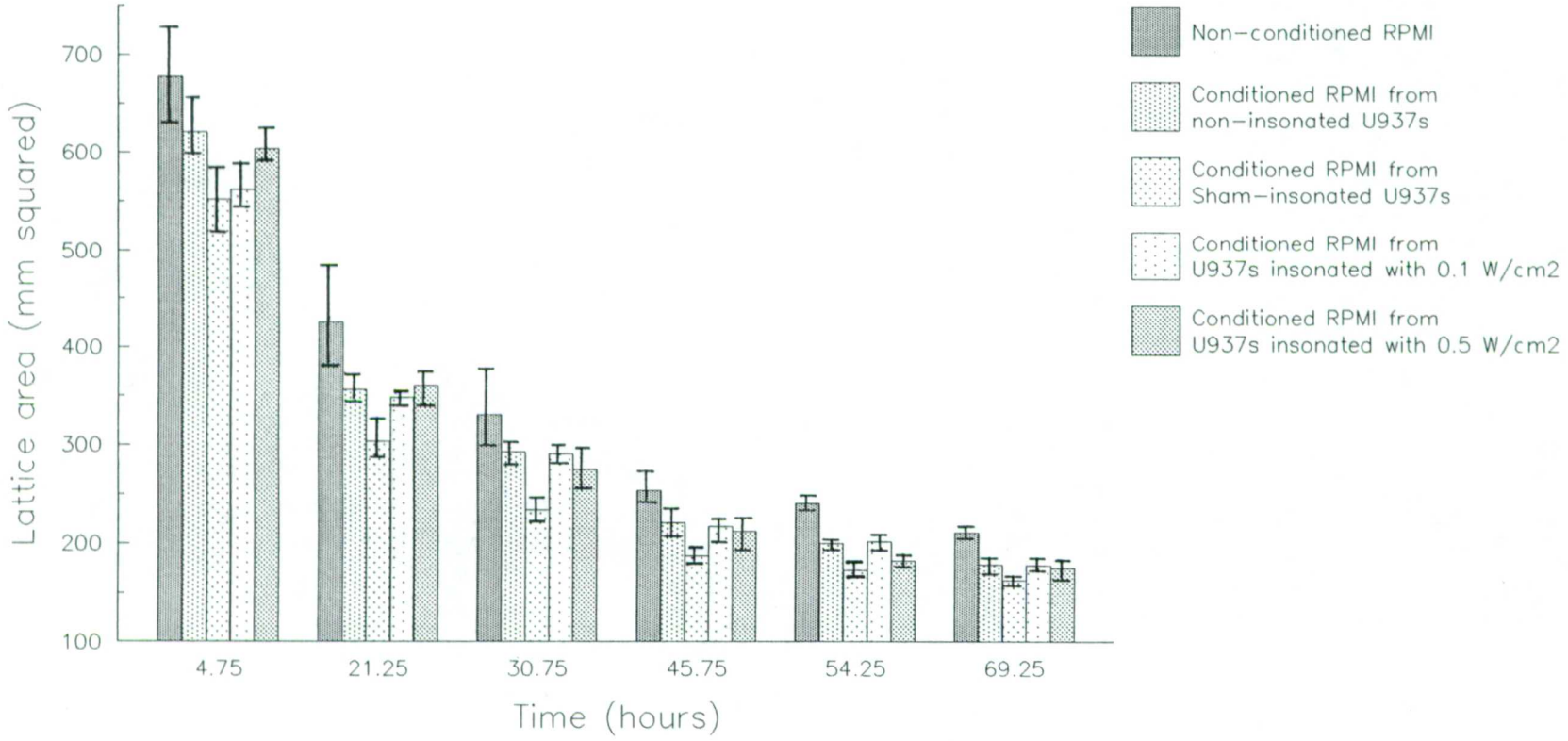

conditioned media that have a reduced capacity to encourage FPCL contraction. Two theoretical explanations to explain these observations have been previously described. Briefly, ultrasound could cause the loss of this contraction promoting activity by either (1) depleting U937 cultures of those cells elaborating this activity, or, (2) encouraging the production of a substance(s) with anti-contractile activities, or (3) modulating the production of both pro- and anti-contractile activities (for a discussion of these two theoretical explanations refer to page 314).

The FPCL contraction data from PMA-exposed U937s does differ from that of non-induced U937s in one respect. Using non-PMA-exposed U937s, FPCL contraction was more rapid in response to medium from non-insonated cells than that in response to medium from sham-insonated cells. However, using PMA-exposed U937s, FPCL contraction in response to medium from sham-insonated cells displayed significantly more pro-contractile activity than medium from non-insonated cells. As PMA treatment was the only manner in which the two sham-insonated cell populations differed, this effect can be assumed to be a direct effect of PMA exposure. One possible explanation for this observation may be that PMA exposure primes the U937 into a state that is responsive to mechanical disturbance. The physical processes of pipetting the PMA-primed U937 culture into and out of the exposure chamber may in some way encourage the elaboration of pro-contractile activities by these primed cells. Future work to test this hypothesis should include PMA induction of U937s which should be followed by variable levels of agitation (repeated aspiration). The pro-contractile capacity of conditioned medium from differentially agitated cultures should then be assessed using the fibroblast-populated collagen lattice contraction assay.

In summary, it is apparent that PMA-exposed U937s, cultured as described above, produce a stimulatory factor for fibroblast-mediated collagen lattice contraction; further studies are necessary to characterise this stimulator. Therapeutic ultrasound exposure appears to reduce the level of this stimulator in U937 culture supernatants. The observation that the reduction in stimulatory activity following ultrasound treatment is paralled by a loss in viable cell number, suggests that ultrasound acts to reduce stimulatory activity by damaging the cells actively generating this stimulator. PMA exposure would appear to have little effect on the generation of pro-contractile substances by U937s.

11.6 General summary of chapter 11.

The effect of therapeutic ultrasound on the release from macrophage-like U937 cells of substances capable of stimulating fibroblast proliferation and fibroblast-mediated collagen lattice contraction *in vitro* was examined. Therapeutic ultrasound was applied to both differentiation-induced and uninduced U937 suspensions. It was found that both types of U937s, cultured without ultrasonic intervention, produced conditioned media which demonstrated inhibitory activity for fibroblast proliferation and stimulatory activity for fibroblast-mediated collagen lattice contraction.

The conditioned medium taken from ultrasound-treated uninduced U937s was found not to inhibit fibroblast proliferation like similar non-insonated and sham-insonated culture supernatants, but was similar in effect to the application of unconditioned U937 medium. When applied to fibroblast-populated collagen lattices ultrasound-treated uninduced U937 conditioned medium encouraged lattice contraction when compared with unconditioned medium, but delayed contraction when compared with conditioned media from non-insonated or sham-insonated U937s. Ultrasound treatment of uninduced U937 cultures leads to the loss of both fibroblast growth inhibition activity and lattice contraction stimulation activity. As the losses in both these activities were paralleled by a reduction in viable U937 cells after insonation, ultrasound-associated damage may be responsible for these effects.

When differentiation-induced U937 cultures were treated with ultrasound the conditioned medium so generated was found promote fibroblast proliferation above that observed in response to non-conditioned U937 growth medium. When applied to fibroblast-populated collagen lattices, ultrasound-treated differentiation-induced U937 conditioned media modulated lattice contraction in a similar fashion to ultrasound-treated uninduced U937 conditioned media, i.e. encouraged lattice contraction when compared with unconditioned medium, but delayed contraction when compared with conditioned media from non-insonated or sham-insonated U937s. This gain in mitogenic activity and loss in stimulatory activity for lattice contraction, in response to treatment with ultrasound, was paralleled by a reduction in U937 viable cell density. It is suggested that ultrasound acts to selectively deplete U937 cultures of PMA-unresponsive cells, which elaborate an inhibitory activity for fibroblast growth and a stimulatory activity for lattice contraction, and in doing so positively selects for PMA-responsive cells, which elaborate a fibroblast growth promoting agent(s).

Chapter 12. Summary of experimental findings

1. p6 human dermal fibroblasts

Human dermal fibroblasts were cultured from a small elliptical skin biopsy, taken from the forearm of a 35 year old healthy male volunteer, by the primary explant technique. By passage 2, cell cultures were morphologically homogenous, being multipolar in disperse culture and forming whorls of bipolar cells at near-confluency both characteristic of fibroblasts in culture. Passage 6 cultures, which retained the morphological characteristics of passage 2 cultures, were further characterised by immunohistochemistry. They were found to be vimentin positive, Factor VIII and cytokeratin LE1 and LP34 negative. These morphological and immunohistochemical observations confirm p6 human dermal fibroblast cultures to be of the fibroblastic lineage.

2. Sensitivity of the methylene blue fibroblast proliferation assay

The proliferation of p6 human dermal fibroblasts cultured under different concentrations of fetal calf serum (FCS) was studied. Fibroblast proliferation was found to increase as FCS concentration increased, thus indicating that the p6 human dermal fibroblasts were capable of responding, in a dose dependent fashion, to known mitogenic substances. The data also indicated that the methylene blue assay was capable of measuring that response. The observation that the assay could detect a statistically significant difference in proliferation between 1.0% FCS and 0.5% FCS suggests that this technique is a highly sensitive one; it also suggests that the assay may be able to detect even smaller differences in FCS concentration. These observations supported the use of the methylene blue proliferation assay to monitor changes in fibroblast proliferation.

3. FPCL formulation and its effect on lattice contraction

The rate of lattice contraction has previously been reported to be dependent on lattice formulation, being directly proportional to fibroblast number and inversely proportional to collagen concentration. A study was performed (1) to examine the effect of varying fibroblast density and collagen concentration on the rate of lattice contraction, and (2) to determine the most appropriate fibroblast number and collagen concentration for subsequent experimental work with this model. Lattice contraction was found to be more rapid with increasing cell density and decreasing collagen concentration. The data also indicated that lattices prepared at low collagen concentrations are more sensitive to changes in cell density than lattices prepared at

higher collagen concentrations. The lattice formulation of 1.2 mg/ml collagen and 1 x 10^5 cells/ml was found to be the most appropriate choice for further studies on FPCL contraction. Lattices formulated in this way represent the most economic use of both collagen and cells and yet contract at a rate that does not preclude the manifestation of stimulatory or inhibitory activities.

4. Sensitivity of the fibroblast-populated collagen lattice contraction assay

Fibroblast-populated collagen lattice contraction has previously been reported to be more rapid with increasing serum concentration. A pilot study was performed (1) to confirm this report, and (2) examine the sensitivity of the FPCL contraction assay to pro-contractile substances. FPCL contraction was found to increase in a dose-dependent fashion with increasing fetal calf serum (FCS) concentration. Though the number of replicate lattices at each FCS concentration made statistical analysis inappropriate, the data indicated that the FPCL contraction assay was a sensitive technique capable of detecting pro-contractile activity.

5. Temperature changes consequent on exposure to therapeutic ultrasound

The temperature rise consequent to 3 MHz insonation at the two intensities employed in this thesis was measured under both *in vivo* and *in vitro* exposure conditions. Under *in vivo* exposure conditions a 5 minute insonation at an intensity of 0.1 W/cm^2, $I^{(SATA)}$, led to a mean temperature rise of 1.0°C, whereas a similar insonation at an intensity of 0.5 W/cm^2, $I^{(SATA)}$, led to a mean temperature rise of 3.3°C. Under *in vitro* exposure conditions a 5 minute insonation at an intensity of 0.1 W/cm^2, $I^{(SATA)}$, led to a mean temperature rise of 0.2°C, whereas a similar insonation at an intensity of 0.5 W/cm^2, $I^{(SATA)}$, led to a mean temperature rise of 0.5°C.

6. The effect of pulsed 3 MHz therapeutic ultrasound on wound contraction in the rat.

The closure of full thickness wounds made in the flank skin of adult Wistar rats was used as a model of wound contraction. The model facilitated a quantitative assessment of the effect of therapeutic ultrasound on the process of contraction. The contraction of fully-excised rat skin wounds treated with 3 MHz therapeutic ultrasound (at both intensities) was significantly more rapid than that of similar sham-treated control wounds. At the end of the experimental period ultrasound-exposed wounds were significantly smaller than similar sham-exposed wounds. Wounds insonated at an intensity of 0.1 W/cm^2 ($I^{(SATA)}$) displayed a tendency to contract more rapidly, and were ultimately smaller, than similar wounds insonated

at an intensity of 0.5 W/cm^2 ($I^{(SATA)}$).

7. The direct effect of pulsed 3 MHz therapeutic ultrasound on the proliferation of human dermal fibroblasts *in vitro*.

The methylene blue proliferation assay was employed to investigate the direct effect of therapeutic ultrasound on the proliferation of p6 human dermal fibroblasts *in vitro*. Under the experimental conditions employed in this study, the direct application of therapeutic ultrasound did not significantly effect the rate of fibroblast proliferation.

8. The direct effect of pulsed 3 MHz therapeutic ultrasound on the contraction of human dermal fibroblast-populated collagen lattices *in vitro*.

The fibroblast-populated collagen lattice contraction assay, a widely accepted *in vitro* model for the process of wound contraction, was employed to investigate the direct effect of therapeutic ultrasound on fibroblast-mediated contraction. Under the experimental conditions employed in this study, the direct application of 3 MHz pulsed therapeutic ultrasound to fibroblast-populated collagen lattices did not significantly effect lattice contraction.

9. The effect of pulsed 3 MHz therapeutic ultrasound on the release from platelets of substances capable of modulating fibroblast activity *in vitro*.

To investigate the effect of therapeutic ultrasound on platelet degranulation, suspensions of human platelets were either sham-insonated, insonated with 3 MHz pulsed therapeutic ultrasound (at intensities, $I^{(SATA)}$, of either 0.1 or 0.5 W/cm^2) or treated with thrombin (physiological release). The platelet releasates, generated by centrifugation of platelet suspensions after exposure, were then studied for their ability to modulate fibroblast proliferation and fibroblast-mediated collagen lattice contraction. Releasates generated from platelet suspensions exposed to therapeutic ultrasound were found to promote both fibroblast proliferation and fibroblast-mediated collagen contraction when compared with similar releasates generated from sham-insonated platelet suspensions. Fibroblast proliferation in response to the releasate generated by insonating platelets at an intensity of 0.1 W/cm^2 did not differ from that generated by insonating platelets at 0.5 W/cm^2. Lattice contraction was more rapid in response to the 0.1 W/cm^2 releasate than in response to the 0.5 W/cm^2 releasate. Platelet releasates generated by exposing platelet suspensions to thrombin were generally found to promote fibroblast proliferation and fibroblast-mediated collagen lattice contraction when compared with releasates generated from insonated platelet suspensions.

10. The effect of pulsed 3 MHz therapeutic ultrasound on the release from U937s (monocyte/macrophage-like cells) of substances capable of modulating fibroblast activity *in vitro*.

The effect of 3 MHz therapeutic ultrasound (at intensities of 0.1 and 0.5 W/cm^2 $I^{(SATA)}$) on the release from U937s of substances capable of modulating fibroblast proliferation and fibroblast-mediated collagen contraction *in vitro* was examined. Studies were carried out on both differentiation-induced and uninduced U937 suspensions. Both types of U937s, cultured without ultrasonic intervention, produced conditioned media which demonstrated inhibitory activity for fibroblast proliferation and stimulatory activity for fibroblast-mediated collagen lattice contraction.

Ultrasound treatment of uninduced U937 cultures led to the generation of conditioned media that displayed a loss of both fibroblast proliferation inhibition activity and lattice contraction stimulation activity relative to non-insonated U937 conditioned medium, losses which were paralleled by a reduction in U937 viability. Fibroblast proliferation in response to conditioned medium taken from uninduced U937s insonated at an intensity of 0.1 W/cm^2 did not differ from that in response to conditioned medium taken from uninduced U937s insonated at an intensity of 0.5 W/cm^2. Lattice contraction was more rapid in response to conditioned medium from uninduced U937s insonated at an intensity of 0.1 W/cm^2 than that in response to conditioned medium from uninduced U937s insonated at an intensity of 0.5 W/cm^2.

Ultrasound treatment of differentiation-induced U937 cultures led to the generation of conditioned media that promoted fibroblast proliferation and exhibited a loss of lattice contraction stimulation activity. The gain in pro-proliferative activity and loss of pro-contractile activity was paralleled by a loss in U937 viability. The conditioned media generated by differentiation-induced U937s insonated at an intensity of 0.1 W/cm^2 was similar, with regard to its effects on both fibroblast proliferation and FPCL contraction, to that generated by differentiation-induced U937s insonated at an intensity of 0.5 W/cm^2.

Chapter 13. Conclusions

This thesis describes studies carried out to examine the effect of therapeutic levels of ultrasound on certain aspects of mammalian cutaneous repair. From these studies it is possible to draw the following conclusions:

1. Ultrasound at therapeutic levels, when applied soon after injury, can interact with and promote the process of mammalian wound contraction at sites of tissue loss (Chapter 7, p218), suggesting that treatment with therapeutic ultrasound soon after injury is clinically advisable.

2. *In vitro* results suggest that this promotion in wound contraction is unlikely to be due to a direct stimulation of fibroblast proliferation (Chapter 8, p234) or fibroblast-mediated contraction (Chapter 9, p244).

3. Since therapeutic ultrasound, at levels used to stimulate wound contraction in the rat, has been shown to encourage the release of pro-proliferative and pro-contractile substances from platelets *in vitro* (Chapter 10, p253) it is suggested that therapeutic ultrasound may promote the process of cutaneous repair by elevating the release of platelet-derived pro-proliferative and pro-contractile substances within the wound site. As several platelet-derived substances are known to be attractants for both monocytes and fibroblasts, it is possible that ultrasound may act to promote wound repair, and more specifically wound contraction, by encouraging the release of these cellular attractants.

4. The conditioned medium of differentiation-induced U937 cells (which are morphologically, histochemically and functionally more macrophage-like than uninduced U937s) while displaying reduced levels of pro-contractile activity, acquire an activity which is mitogenic for fibroblasts when treated with therapeutic ultrasound *in vitro* (Chapter 11. p276). If similar behaviour occurs in activated macrophages at the wound site, this could lead to an increase in fibroblast number, which may, in part, explain the ability of therapeutic ultrasound to stimulate fibroblast-mediated wound contraction.

5. Therapeutic ultrasound at an intensity of 0.1 W/cm^2 ($I^{(SATA)}$) was found to promote the process of wound contraction to a greater extent than when applied at an intensity of at 0.5 W/cm^2 ($I^{SATA)}$) (Chapter 7, p218). Temperature measurements

made in uninjured dermis during treatment with ultrasound showed that the temperature rise over the 5 minute treatment period was 1°C at an intensity of 0.1 W/cm^2 and 3.3°C at an intensity of 0.5 W/cm^2 (table 6.3, p215). Such observations would appear to suggest that the mechanisms involved in the stimulation of wound contraction by ultrasound were not purely thermal. These observations question the benefit of using high intensity ultrasound and support the use of low intensity therapeutic ultrasound in clinical practice.

Chapter 14. Future work

In completion of this thesis various lines of future work have revealed themselves. Possible avenues of future work include:

1. Similar investigations to those performed on healthy young Wistar rats, on rats which are known to be impaired with respect to their capacity to repair. Studies may include investigations into the effect of ultrasound on genetically obese diabetic mice, strain C57BL/KsJ-db/db, or on elderly rats, both known to displayed impaired healing (Sprugel *et al.* 1990; Broadley *et al.* 1990).

2. Fibroblasts have been shown to be capable of significant morphological, structural and functional heterogeneity. Additionally, it has been proposed that the wound environment may induce, or select, specific fibroblast phenotypes that differ in their ability to respond to exogenous stimuli such as growth factors. The observation that therapeutic ultrasound cannot directly modulate fibroblast proliferation or fibroblast-mediated lattice contraction may result from the use of an inappropriate fibroblast phenotype. Further studies to test this possibility may include comparative studies into the effect of therapeutic ultrasound on fibroblasts derived from normal skin and wound tissue.

3. The extracellular matrix (ECM) component of the lattices used in this thesis is primarily type I collagen. The ECM experienced by granulation tissue fibroblasts is far more complex. Initially the ECM is rich in hyaluronic acid, fibronectin and collagen type III, but as repair proceeds this is gradually replaced by an ECM predominantly composed of type I collagen and sulphated proteoglycans. Further studies investigating the ability of therapeutic ultrasound to modulate fibroblast-mediated contraction may include the use of lattices formulated in a more granulation tissue-like fashion.

4. The mechanisms of fibroblast-mediated collagen lattice contraction are not clear. It is known that culture medium must contain serum for contraction to occur. This requirement for serum has complicated studies utilising various biological mediators. A serum-free model for cell-mediated contraction of collagen lattices is necessary to define the role of serum components in lattice contraction. Anderson *et al.* (1990) described a serum-free FPCL contraction assay using human foreskin fibroblasts and studied the effects of various agents including growth factors. It may

be more appropriate to employ such a model in further investigations into detecting ultrasound-induced release of substances from both platelets and macrophages capable of modulating fibroblast-mediated contraction.

5. It has been demonstrated that therapeutic ultrasound, at the parameters employed in this thesis, can promote the release of substances from platelets that stimulate fibroblast proliferation and fibroblast-mediated collagen lattice contraction. Platelet α-granules are known to contain various growth factors, many of which have been shown to promote either fibroblast proliferation or fibroblast-mediated lattice contraction, or both. In order to investigate which platelet-derived substance(s) is/are primarily responsible for stimulating fibroblast proliferation or fibroblast-mediated lattice contraction, future studies may involve the use of neutralising (or precipitating) antibodies to selectively deplete platelet releasates of one or more α-granule components.

6. It has been demonstrated that the application of a murine antibody MA 710F to PMA-treated U937s further encourages differentiation of U937s into cells with the morphological appearance of macrophages. Therapeutic ultrasound applied to wounds would interact with both monocytes (blood borne) and macrophages (extravascular), the latter being thought to orchestrate repair. Further studies on MA 719F treated, PMA-exposed U937s may prove beneficial in understanding the effect of therapeutic ultrasound on wound repair (Koyama *et al-* see U937 search 89/90 in FW folder).

7. U937s are monoblastic cells that must be induced to differentiate in order to develop some properties peculiar to mature monocytes (Koren *et al.* 1979), such as antibody-dependent cell-mediated cytotoxicity, phagocytosis and expression of the My4-defined antigen (Hermann *et al.* 1985). Even after induction, U937s have been shown not to express various antigenic markers (such as 63D3, M42, Mo2, LeuM3 and U1HM1) known to be expressed by peripheral blood monocytes (Zeigler-Heitbrock *et al.* 1988). Another cell line, Mono Mac 6, has been established from the peripheral blood of a patient with monoblastic leukemia. This cell line has the morphological appearance of monocytes (under both light and electron microscopy) and constitutively expresses certain phenotypic and functional features of mature monocytes. Including the expression of significant levels of various peripheral blood monocyte markers and the ability to phagocytose antibody-coated erythrocytes (Zeigler-Heitbrock *et al.* 1988). Such observations suggest that Mono Mac 6 is a more

appropriate *in vitro* model of mature monocytes. Future studies are planned to compare the effect of therapeutic ultrasound on PMA-induced U937s and the Mono Mac 6 cell line. Conditioned media from these two cell lines will be assayed for its ability to promote fibroblast proliferation, FPCL contraction and, additionally, fibroblast migration.

8. One theoretical explanation for the loss of fibroblast growth inhibitory activity in conditioned medium after U937 insonation, is that ultrasound damages U937s which leads to less U937-derived inhibitor being released into the medium they condition, and consequently more proliferation when that conditioned medium is applied to fibroblasts in culture. Future work to test this theory may include studying the effect of cellular damage on the release of fibroblast proliferation inhibitors by U937s.

9. Sham-insonated differentiation-induced U937s tend to produce more pro-contractile activity than non-insonated differentiation-induced cells. It is possible that the physical process of pipetting the PMA-induced U937s into and out of the exposure chamber in some way encourages the release of pro-contractile activities from these cells. Future work may include a study into the effect of variable levels of agitation (repeated aspiration) on the release of pro-contractile activities by PMA-induced U937s.

APPENDIX 1

Appendix 1A. Phosphate Buffered Saline (PBS) pH 7.3

Prepared by dissolving 1 PBS tablet (Oxoid, Unipath Ltd, Basingstoke, UK) in 100 ml distilled water, thus making Dulbecco phosphate buffered saline (solution "A").

Components:		
	KCl	0.2 grams/litre
	KH_2PO_4	0.2 grams/litre
	NaCl	8.0 grams/litre
	$Na_2HPO_4.7H_2O$	2.16 grams/litre

To sterilise, autoclave or filter with 0.22 μm filter.

Appendix 1B. 0.01 M Borate Buffer pH 8.6

Prepared according to the method of Clark and Lub, (1917).

Solution A: 0.1 M boric acid in 0.1 M potassium chloride
= 6.2 g H_2BO_4 + 7.46 g KCl per litre

Solution B: 0.1 N sodium hydroxide
= 4.0 g NaOH per litre

Add 12 ml of B to 50 ml of A and make up to 100 ml with distilled water to give 0.1 M borate buffer. Dilute this by the addition of a further 900 ml of distilled water to make 0.01 M borate buffer.

Appendix 1C. Platelet Washing Buffer (PWB)

Prepared according to the method of Knighton *et al.* (1986).

Components to make 250 ml PWB:

1 M HEPES Buffer solution (Gibco BRL, Scotland)	12.000 ml
Dextrose (AnalaR, BDH)	1.350 g
KCl (AnalaR, BDH)	0.075 g
NaCl (AnalaR)	2.045 g
Crystallised Bovine Albumin (BDH)	0.875 g

Method:

1. Dissolve the above components in 100 ml distilled water.
2. Add more distilled water to final volume of 250 ml.
3. Check pH, which should be 7.4, correct if necessary.
4. Sterilise by passing through a 0.22 μm millipore filter.
5. Store at 20°C, and use within 5 days of preparation.

Appendix 1D. 4% Paraformaldehyde (fixative)

To prepare 2.5 litres of stock:

1. Dissolve 100 g paraformaldehyde (Solmedia, Essex, UK) in 2 litres of stirring distilled water at 60-70°C adding a maximum of 4 drops/l of 10 M NaOH in a fume cupboard.
2. When cool, filter if necessary (Whatman 113).
3. Add PBS salts (Oxoid, UK) 1 tablet per 100 ml and make up to 2.5 l.

APPENDIX 2

Culture Media

Appendix 2A. Primary Culture Wash

Components to make 100 ml wash:	
Ham's F10 (Gibco BRL, Scotland)	97.0 ml
Gentamycin (Gibco BRL, Scotland)	1.0 ml
Penicillin/Streptomycin (Gibco BRL, Scotland)	2.0 ml

Appendix 2B. Fibroblast Growth Medium

Components to make 100 ml medium:	
Ham's F10 (Gibco BRL, Scotland)	88.0 ml
Fetal calf serum (Gibco BRL, Scotland)	10.0 ml
Penicillin/streptomycin (Gibco BRL, Scotland)	2.0 ml

Appendix 2C. Fibroblast Freeze Medium

Components to make 100 ml medium:	
Ham's F10 (Gibco BRL, Scotland)	68.0 ml
Fetal calf serum (Gibco BRL, Scotland)	10.0 ml
Penicillin/streptomycin (Gibco BRL, Scotland)	2.0 ml
Tissue culture grade dimethyl sulfoxide [DMSO] (Sigma, UK)	10.0 ml

Notes applying to Appendix 2A, 2B and 2C:

Penicillin/Streptomycin is supplied as a solution containing 5000 units/ml and 5000 μg/ml respectively. Gentamycin is supplied as a solution containing 10 mg/ml. The final concentrations of antibiotics within the medium are: gentamycin 100 μg/ml, penicillin 100 units/ml and streptomycin 100 μg/ml.

Appendix 2D. Concentrated Fibroblast Growth Medium.

Growth Medium x 3

Components to make 100 ml concentrated medium:

7.5% Sodium bicarbonate (Flow Laboratories, Scotland)	4.8 ml
1 M HEPES Buffer solution (Gibco BRL, Scotland)	6.0 ml
Penicillin/Streptomycin (Gibco BRL, Scotland)	3.0 ml
Fetal Calf Serum (Gibco BRL, Scotland)	30.0 ml
Ham's F10 (x3) (Gibco BRL, Scotland)	56.2 ml

Growth Medium x 5

Components to make 100 ml concentrated medium:

7.5% Sodium bicarbonate (Flow Labs, Scotland)	8.0 ml
1 M HEPES buffer solution (Gibco BRL, Scotland)	10.0 ml
Penicillin/Streptomycin (Gibco BRL, Scotland)	5.0 ml
Fetal Calf Serum (Gibco BRL, Scotland)	50.0 ml
Ham's F10 (x5) (Gibco BRL, Scotland)	27.0 ml

Note: 1. Ham's F10 x3 & x5 is prepared by diluting Ham's F10 (x10) medium concentrate with sterile distilled water.

2. Ham's F10 (x10) concentrate is supplied sodium bicarbonate free, hence the requirement for supplementation with 7.5% sodium bicarbonate.

3. The final concentrations of antibiotics within the medium are: penicillin 150 units/ml and streptomycin 150 μg/ml.

Appendix 2E. Macrophage Growth Medium

Components to make 100 ml medium:

RPMI 1640 (Gibco BRL, Scotland)	88.0 ml
Heat-inactivated fetal calf serum (Gibco BRL, Scotland)	10.0 ml
Penicillin/streptomycin (Gibco BRL, Scotland)	2.0 ml

Appendix 2F. Macrophage Freeze Medium

Components to make 100 ml medium:

RPMI 1640 (Gibco BRL, Scotland)	68.0 ml
Heat-inactivated fetal calf serum (Gibco BRL, Scotland)	10.0 ml
Penicillin/streptomycin (Gibco BRL, Scotland)	2.0 ml
Tissue culture grade dimethyl sulfoxide	10.0 ml

Appendix 2G. Serum-free macrophage growth medium

Components to make 100 ml medium:	
RPMI 1640 (Gibco BRL, Scotland)	98.0 ml
Penicillin/streptomycin (Gibco BRL, Scotland)	2.0 ml

Appendix 2H. PMA supplemented serum-free macrophage growth medium

Components to make 100 ml medium:

PMA/acetone (100μg/ml)	0.1 ml
Serum-free macrophage growth medium (Appendix 2G)	99.9 ml

Notes applying to appendix 2E & 2F:

1. Fetal calf serum employed has complement activity removed by heat-inactivation.

2. The final concentrations of Penicillin/Streptomycin are as Appendix 2A.

APPENDIX 3

Protocol for the Explant Technique for the Primary Culture of Human Biopsy Material - Adult Human Forearm Fibroblast Primary Culture.

1. Obtain biopsies under sterile operating conditions, and place then directly into a sterile universal containing primary culture wash (Appendix 2A). Hold in wash for 1 hour at 37°C.
2. Wash the biopsy material with sterile PBS (Appendix 1A) and transfer to a sterile petri dish.
3. Using 2 sterile scalpel blades, chop the tissue into pieces of less than 0.1 mm^3. Transfer these pieces of tissue to the "normal culture surface", (i.e. the upper surface) of an inverted 50 cm^3 tissue culture flask using a sterile Pasteur pipette.
4. Aliquot 1 ml of fibroblast growth medium (Appendix 2B) into the base of the inverted flask and place the flask, still in its inverted orientation, in a 37°C incubator for 24 hours. During incubation this fibroblast growth medium provides a humid environment for the pieces of tissue thus preventing desiccation.
5. After 24 hours gently turn the flask the correct way round, such that the pieces of tissue are now bathed in fibroblast growth medium. Carefully add

an additional 1 ml of growth medium to the flask. The pieces of tissue should attach to the culture surface during this initial incubation, and should not move when this additional growth medium is added.

6. Examine the pieces of tissue for cellular outgrowth, on a regular basis, using an inverted microscope. Outgrowth normally starts to become visible from day 5 onwards.
7. As soon as outgrowth is established renew the growth medium. Renew growth medium every 2 to 3 days.
8. When the outgrowth appears near-confluent use short trypsinisation (Appendix 4) to remove the fibroblasts without removing the generally more adherent keratinocytes. Fibroblast cultures are maintained by feeding on a twice weekly basis, and are passaged upon near confluency with a subcultivation ratio of 1:3. *Protocol adapted from Freshney (1987)*

APPENDIX 4

Fibroblast Trypsinisation Protocol

1. Discard used culture medium into waste receptacle, and rinse near-confluent fibroblast monolayer with sterile PBS (Appendix 1A).
2. Add sufficient Trypsin-EDTA (Gibco BRL, UK) to cover the base of the flask (3 ml to a 260 ml flask; 1 ml to a 50 ml flask).
3. Return flask to 37°C incubator for 10 minutes (5 minutes for short trypsinisation).
4. Remove flask from incubator and examine under inverted microscope for detachment of cells. If detachment is not complete either swirl trypsin over the monolayer until the majority of cells go into suspension or incubate for a further 5 minutes.
5. Decant fibroblast/trypsin suspension into a sterile centrifuge tube and add an equivalent volume of fibroblast growth medium (Appendix 2B). Serum containing growth medium not only dilutes the trypsin but also actively reduces further proteolytic attack of cells by supplying an alternative substrate for the enzyme.
6. Centrifuge for 5 minutes at 80 x g to form a cell pellet and supernatant. Discard the supernatant and resuspend the cell pellet in fibroblast growth medium (Appendix 2B).

APPENDIX 5

Cell storage and recovery

Appendix 5A. Freezing-down of cells (adapted from that of Freshney, 1987)

1. Perform standardised trypsinisation (Appendix 4) and resuspend in fibroblast freeze medium (Appendix 2C) at an approximate concentration of 5 x 10^6 fibroblasts per ml.
2. Dispense 1.0 ml aliquots of this cell suspension into each 1.8 ml cryo-ampule (Nunc, Inter Med, Denmark), place in polystyrene box and transport immediately to -70°C freezer. Hold at -70°C for between 2 and 3 hours. This permits the cell suspension to freeze at the recommended rate of 1°C per minute (Leibo and Mazur, 1971; Harris and Griffiths, 1977).
3. After -70°C cooling and holding, quickly transfer to liquid nitrogen (-196°C) for storage.

Appendix 5B. Recovering cells from cryo-store (adapted from that of Freshney, 1987)

1. Remove cryo-ampule from nitrogen store and place immediately in 37°C water.
2. Once thawed, swab the ampule with 70% alcohol and open. Pour the contents of the ampule into a 15 ml sterile centrifuge tube and slowly add 5 ml of fibroblast growth medium. Medium should be added slowly to reduce the likelihood of osmotic damage as the DMSO within the freeze medium (Appendix 2C), is diluted.
3. Centrifuge the suspension for 3 minutes at 80 g, discard the supernatant, gently resuspend the pellet in 5 ml of fresh growth medium and decant into a 50 ml tissue culture flask.
4. Place in 37°C incubator. Feed with fibroblast growth medium (Appendix 2B) on a twice weekly basis.

Note: The techniques for cry-storage and recovery for the pro-monocyte cell line U937 are essentially those described above. However, as anchorage independent cells they do not require trypsinisation, and are routinely cultured in macrophage growth medium (Appendix 2E). The basic techniques described above were employed substituting macrophage freeze medium (Appendix 2F) for fibroblast freeze medium and macrophage growth medium (Appendix 2E) for fibroblast growth medium.

APPENDIX 6

Haemocytometer Cell Counting

Percentage viability and the concentration of viable cells per ml.

1. Trypsinise cells according to Appendix 4 and resuspend in 2 ml of fibroblast growth medium per 260 ml flask trypsinised. Ensure that the pellet is thoroughly resuspended such that cells are in single cell suspension.
2. Remove a 300 µl sample of this suspension and place in a 15 ml centrifuge tube, and add 300 µl of 0.4% trypan blue solution (Sigma T-8154) and mix thoroughly.
3. Dispense approximately 20 µl of this mixture into the cell counting chamber of a correctly assembled modified Neubaur haemocytometer.
4. Place the haemocytometer on the stage of a light microscope and focus on the chamber grid. The Improved Neubaur haemocytometer slide is basically a 3 x 3 arrangement of 9, 1.0 mm^2, large squares. These large squares are divided up into 25 small squares each of which is further divided up into 16 smaller squares.
5. Count the number of cells within each of the 9 large squares, noting for each large square counted:
   (a) the total number of clear and blue cells (i.e viable and non-viable cells)
   (b) the number of blue cells (non-viable).

Then calculate:

(i). The average number of non-viable cells/large square, defined as B.

(ii). The average number of both viable and non-viable/large square, defined here as T.

A. Percentage viability:

$$\% \text{ viability} = 1 - (B/T) \times 100$$

B. The concentration of viable cells per ml:

(i). Calculate the average number of viable cells per large square, defined as N.

$$N = T - B$$

(ii). Calculate the volume, V, of cell suspension over one large square.

Knowing the area of a large square to be 1 mm^2 and the depth to be 0.1mm;

$$V = 1 \times 1 \times 0.1 \text{ mm}^3$$
$$= 0.1 \text{ mm}^3$$
$$= 0.0001 \text{ cm}^3$$
$$= 1 \times 10^{-4} \text{ ml}$$

(iii). Calculate C, the concentration of cells per ml in suspension under study.

$$C = N/V$$
$$= N \times 10^4 \text{ cells per ml}$$

APPENDIX 7

The preparation of the platelet stock suspension

1. Perform venepuncture and fill a 450 ml blood transfusion bag containing anticoagulant (Travenol)*, with freshly donated human blood. During collection place the transfusion bag on ice.
2. Aliquot the contents of the transfusion bag into 50 ml sterile centrifuge tubes and hold on ice. Complete the following steps (3 to 8) within 1 hour.
3. Centrifuge aliquots at 150 x g for 15 minutes at 4°C to form a platelet rich plasma supernatant (PRP). The erythrocytes and leucocytes form the pellet.
4. Aspirate off the PRP taking care not to disturb the underlying cell pellet and perform a platelet count, using a Coulter counter, on the PRP.
5. Centrifuge the PRP at 1500 x g for 20 minutes at 4°C to form a platelet pellet and a platelet poor plasma (PPP) supernatant. Perform a platelet count on the PPP using a coulter counter.
6. Using the PRP and PPP platelets counts, and taking into consideration the total volume of PRP, calculate the number of platelets in the pellet.
7. Resuspend the platelet pellet in platelet washing buffer (Appendix 1C) to give a concentration of 1 x 10^9 platelets per ml - thus making the platelet stock suspension. The platelet stock suspension is held on ice.

* The transfusion bag (Travenol) is a 450 ml blood transfusion bag containing 63 ml citrate phosphate dextrose adenine formula 1 (CPD-adenine 1). Each 100 ml of CPD-adenine 1 contained sodium citrate 2.63 g, anhydrous glucose 2.90 g, citric acid monohydrate 327.00 mg, phosphate 251.00 mg and adenine 27.50 mg.

APPENDIX 8

Methylene Blue Fibroblast Proliferation Assay - Standard Protocol

1. Trypsinise sub-confluent monolayers of passage 6 (p6) human dermal fibroblasts and generate cell pellets according to the *Fibroblasts Trypsinisation Protocol* (Appendix 4).
2. Resuspend cell pellet in Ham's F10 medium, supplemented with 10% fetal calf serum and 2% penicillin/streptomycin, to make a cell suspension of 2 x 10^4 viable cells/ml (Appendix 6).
3. Aliquot 100 µl volumes of this cell suspension (i.e. 2000 cells) into each well in rows B through G (Appendix 9) of a sterile 96-well flat bottomed cell culture microtitre plate (Linbro, Flow Laboratories, Scotland).
4. Plate out 100 µl aliquots of Ham's F10, supplemented with 10% fetal calf serum and 2% penicillin/streptomycin, into each well in rows A and H of the same plate. These wells are medium blank wells as discussed earlier (p152).

Note. The number of plates prepared in this way depends upon the number of intended time points at which proliferation is going to be studied.

5. Once all wells of each plate have received their 100µl aliquot of the cell suspension or growth medium alone, seal the plates with plate sealing tape (Titertek, Flow Laboratories, Scotland) and place in a 37°C incubator.
6. At predetermined times remove plates from the incubator, remove the plate sealing tape, and discard the medium within the wells by inverting the plate over a sink.
7. Carefully wash each plate by immersing in 5 changes of PBS (pH 7.6) and gently tap on tissue paper to remove excess PBS.
8. Aliquot 100µl of methanol (AnalaR, BDH) into each well and allow to fix for 10 minutes. After fixation discard the methanol by inverting the plate over an alcohol waste tank, place the plate upside down and allow to air dry.
9. Once dry, plates are stored in a dust free environment until the plate of the final time point, of a given investigation, has been fixed and dried. All plates from a given study are then stained, as a batch, with methylene blue.
10. 100 µl of 1% methylene blue in 0.01 M borate buffer (Appendix 1B) is added to each well, of each plate in the study, and left to stain for 30 minutes. Excess stain is then discarded and the plates washed by carefully immersing

in 5 changes of 0.01 M borate buffer and then tapped onto tissue paper to remove excess buffer. Plates are then placed upside down to air dry.

11. Once dry, 100µl of acid-alcohol (50% 0.1 M HCl : 50% absolute ethyl-alcohol) is then added to each well to elute the methylene blue.
12. The absorbance (λ 650 nm) of each well is then measured using a microplate photometer (Anthos Labtech Instrument type 10 500, Austria), after ensuring the eluted dye is thoroughly mixed with the elution solvent. This is accomplished by programming the photometer to shake the plate for 60 seconds prior to taking A_{650} readings.

APPENDIX 9

96-well microtitre plate.

The diagram below shows the well vectors of the 96 well flat bottomed tissue culture microtitre plate used in the methylene blue fibroblast proliferation assay.

Column

Row	1	2	3	4	5	6	7	8	9	10	11	12
A												
B												
C												
D												
E												
F												
G												
H												

APPENDIX 10

Human Dermal Fibroblast Collagen Lattice Contraction Assay - Standard Protocol

This protocol uses Vitrogen 100 purified, pepsin solubilised bovine dermal collagen (Celtrix Laboratories, Palo Alto, California, USA)

1. Prepare a cell suspension containing 4 x 10^5 viable (p6) human dermal fibroblasts per ml of fibroblast growth medium (Appendix 6) by following the trypsinisation protocol (Appendix 4).
2. Prepare concentrated fibroblast growth medium (Appendix 2D).
3. Prepare neutralised collagen solution as follows:

   Materials:

   (i) Vitrogen 100 Collagen, chilled to a temperature of 4 - 6°C.

   (ii) Sterile PBS (Appendix 1A) at 10 times normal concentration.

   (iii) 0.1 M HCl.

   (iv) 0.1 M NaOH.

   (v) pH indicator strips (Sigma, UK).

   Preparation:

   (i) Mix 8 ml of chilled Vitrogen with 1 ml of PBS (10X). Add 1 ml of 0.1 M NaOH and mix thoroughly.

   (ii) Check pH and adjust if necessary to pH 7.2 ± 0.2 by the addition of a few drops of 0.1 M HCl or 0.1 M NaOH.

   (iii) One neutralised the collagen solution can be stored at 4°C for several hours prior to use.

Note. Vitrogen 100 is supplied at 3.0 mg/ml in 0.012 N HCl, once neutralised the collagen concentration falls to 2.4 mg/ml.

4. Thoroughly mix the neutralised collagen with the concentrated growth medium and then add the cell suspension, followed by further thorough mixing, in the following proportions to produce the *lattice mixture.*

   (i) Neutralised collagen 3.0 ml

   (ii) Concentrated fibroblast growth medium 1.5 ml

   (iii) Fibroblast suspension (4 x 10^5 cells/ml) 1.5 ml

Note. Once combined in this way the concentrations of collagen and fibroblasts are 1.2 mg/ml and 1 x 10^5 cells/ml respectively. Upon mixing 3 ml of neutralised collagen with 1.5 ml of concentrated growth medium the medium component of the lattice mixture returns to that of normal fibroblast growth medium (Appendix 2B).

5. Carefully dispense the *lattice mixture*, in 2 ml aliquots, into 35 mm diameter bacteriological petri dishes (Falcon, Becton Dickinson, UK); ensuring that there are no bubbles. Place the lattice mixture containing petri dishes in a 37°C humidified incubator and leave undisturbed to polymerise for 1 hour.
6. After 1 hour remove the polymerised lattices from the incubator and release them from their attachment to the sides of the petri dish by "rimming". This is performed by first tilting the petri dish, then gently tapping around the circumference of the inclined dish as it is rotated.
7. Add either 1 ml of fibroblast growth medium, of 1 ml of the substance under test to the petri dish. The lattices should then float freely within the petri dish.
8. Place lattices in a sealed humidified box and place in a 37°C incubator.
9. Examine lattices at 30 minute intervals for the onset of lattice contraction.
10. Photograph lattices at regular time points (Appendix 11) and develop films according to Appendix 12.
11. Measure lattice area by computer-assisted planimetry as described in Appendix 13 .

APPENDIX 11A

Lattice photography

Requirements:

Light box

Clear plastic ruler with millimetre graduations

Pentax ME super single lens reflex camera loaded with FP4 black and white film (Ilford, Cheshire, UK) and fitted with macro lens

Camera gantry

Method:

1. Load camera and attach to camera gantry. The gantry arrangement is such that it: (i) provides rigid support for the camera, thus reducing camera shake, and (ii) holds the camera at a fixed distance from lattice, thus ensuring a fixed photographic magnification of the lattice.
2. For each film, prepare an acetate sheet of the experimental information. This should include the time and date at which the photographs were taken and indicate of the investigation being monitored. This acetate should be the first

photograph taken.

3. Carefully remove the fibroblast populated lattices from the incubator and place them on the light box in preparation for photography. Remove the lids of the petri dishes to reduce distortion of the final photographic image. Prepare an acetate strip name tag for each lattice and label appropriately. Place these name tags in close proximity to the petri dish within the photographic field of view. Similarly, locate a clear plastic rule within the photographic field of view, then photograph the whole assembly. The image of the ruler is used as a standard during subsequent planimetric quantitation of lattice areas. As petri dish lids are removed for photography all photographs are taken within the sterile confines of a laminar flow cabinet.
4. Films are developed according to the procedure described in appendix 12.

APPENDIX 11B

Black and white film (Ilford FP4) processing.

Requirements:

Hand held developing tank

ID11 developer (Ilford, Cheshire, UK) at 20°C

Hypam-Rapid-fix fixative (Ilford, Cheshire, UK) at 20°C

Running tap-water at 20°C

Distilled water

Timer

Method:

Under dark room conditions:

1. Open film cartridge, detach film from cartridge spindle and cut off film tongue.
2. Wind film onto developing spool and place the loaded spool in the light-proof developing tank.
3. Pour sufficient ID11 developer (20°C) into the developing tank to cover the loaded spool. Start timer.
4. Develop film for a total of 6.5 minutes, with 20 seconds agitation per minute.
5. Discard developer and wash in running 20°C tap water for 30 seconds.
6. Discard tap water and add sufficient Hypam-Rapid-Fix fixative to cover loaded

spool. Start timer.

7. Fix film for a total of 5 minutes, with 30 seconds of agitation at the beginning and end of this period.
8. Discard fixative and wash in running tap water for 30 minutes.
9. Rinse with distilled water and hang weighted film to dry in drying cabinet.

APPENDIX 12

Computer-assisted planimetry

1. Lattices are photographed using standard black and white photography (Appendix 11), and the films developed according to Appendix 12.
2. After developing, transfer the photographic negatives to a light box and digitise at 1280 by 1024 square pixels. The negatives are transilluminated on the light box and digitisation is then performed using a high resolution "charge couple device" CCD camera (Videk Megaplus, model K00792) fitted with a 55 mm Nikon Nikkor lens. The camera data is recorded using an IBM PC-AT compatible computer and the Univision UPX 1000 interface and the resulting image displayed using a Univision UDC2600 display controller. Optimas (Bioscan Inc, USA) software is used to capture and analyze the image of the transilluminated photo-negative.
3. With the aid of an IBM PC-AT computer running Optimas software analyze each image of each black and white lattice negative. Using the "mouse" draw round the perimeter of each of the digitised lattice images, which are displayed on a large format high resolution monitor. The lattice images displayed on this large format high resolution monitor are magnified by a factor of 10 (a 3.5 cm diameter petri dish measuring 35 cm on the monitor). Once the perimeter of the lattice has been defined the Optimas software package calculates lattice area and expresses this information in terms of square pixels. Using the calibration facility within the Optimas program in conjunction with the scale on the millimetre rule, photographed with each lattice, lattice area is then expressed by the computer in terms of square millimetres.

APPENDIX 13

The cell exposure chamber

1. Loosen the 6 end plate retaining nuts and disassemble the exposure chamber (figure 13.1).
2. Thoroughly wash all components in 5% aqueous solution of RBS 25 detergent (Solmedia, Essex, UK) at a temperature of 50°C and rinse well with distilled water. Dry components in a 60°C oven.
3. Assemble components loosely, place in an autoclave bag and autoclave at 100 kPa at a temperature of 120°C for 20 minutes.
4. Once the chamber assembly is sterile, ultrasound-transparent cling film windows are then fitted. Stretch cling film over a wooden embroidery frame, sterilise the cling film by rinsing with 70% ethanol, and leave to dry in a laminar flow cabinet.
5. On one side of chamber, loosen end plate retaining nuts, and remove the end plate assembly. Lay stretched cling film sheet over centre plate such that the side washed with 70% ethanol is innermost. Replace end plate and end plate retaining nuts. Firmly tighten all three nuts, thus trapping and sealing the cling film in position against the rubber "O" ring of the centre plate. Repeat procedure for other side of chamber.
6. After constructing the cling film windows at each end of the chamber, remove the loading port bolt and load 2 ml of sterile PBS with a sterile glass pasteur pipette. Replace the loading port bolt and swirl the PBS over all inner surfaces of the chamber; this practice wets the inner surfaces of the chamber and thus reduces the likelihood of bubble formation within the chamber during loading of cell suspensions. After wetting, remove PBS with a sterile glass pippete.
7. The chamber is now ready to be loaded with a given cell suspension.
8. Loading is accomplished using a sterile long shaft pasteur pipette. After filling the pipette with the cell suspension, the tip of the pipette is gently inserted into the loading port and lowered until it touches the inner wall of the chamber. The contents are then slowly dispensed into the chamber ensuring that bubble formation is avoided. The loading port bolt is then replaced, the loaded chamber transported to the exposimentry apparatus and exposed appropriately.

Appendix 13 - continued

9. After treatment the chamber is first rinsed in 70% alcohol to sterilise, the loading port bolt removed and the cell suspension extracted.

10. Before the chamber is used again it is rinsed with three changes of sterile PBS.

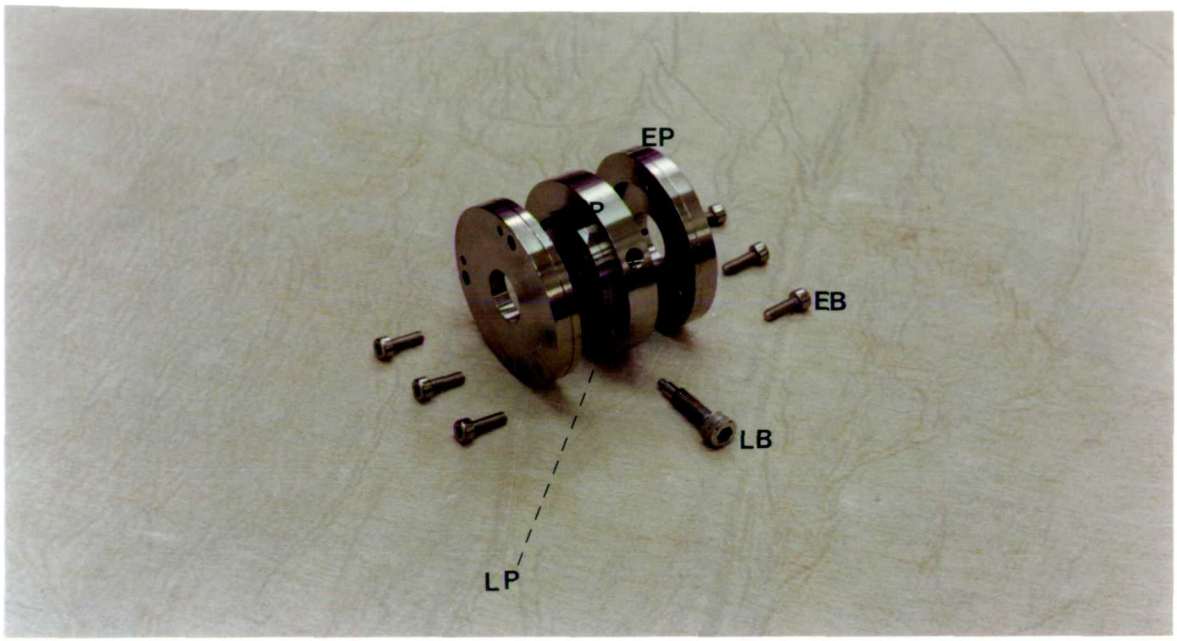

KEY: CP - Centre plate
EB - End plate retaining bolt
EP - End plate
LB - Loading port bolt
LP - Loading port

Figure 13.1 The cell exposure chamber

APPENDIX 14

Lattice formulations used in the study of the effect of cell number and collagen concentration on fibroblast populated collagen lattice contraction (p176).

1. *Lattices with 1.2 mg/ml collagen & 1 x 10^5 fibroblasts per ml.*
   3 ml neutralised collagen (Appendix 10)
   1.5 ml Ham' F10 (x3) (Appendix 2D)
   1.5 ml of 4 x 10^5 cells/ml fibroblast suspension (Appendix 6)
2. *Lattices with 1.2 mg/ml collagen & 2 x 10^5 fibroblasts per ml*
   3 ml neutralised collagen
   1.5 ml Ham' F10 (x3)
   1.5 ml of 8 x 10^5 cells/ml fibroblast suspension
3. *Lattices with 1.2 mg/ml collagen & 3 x 10^5 fibroblasts per ml*
   3 ml neutralised collagen
   1.5 ml Ham' F10 (x3)
   1.5 ml of 12 x 10^5 cells/ml fibroblast suspension
4. *Lattices with 1.6 mg/ml collagen & 1 x 10^5 fibroblasts per ml*
   4 ml neutralised collagen
   1.0 ml Ham' F10 (x5) (Appendix 2D)
   1.0 ml of 6 x 10^5 cells/ml fibroblast suspension
5. *Lattices with 1.6 mg/ml collagen & 2 x 10^5 fibroblasts per ml*
   4 ml neutralised collagen
   1.0 ml Ham' F10 (x5)
   1.0 ml of 12 x 10^5 cells/ml fibroblast suspension
6. *Lattices with 1.6 mg/ml collagen & 3 x 10^5 fibroblasts per ml*
   4 ml neutralised collagen
   1.0 ml Ham' F10 (x5)
   1.0 ml of 18 x 10^5 cells/ml fibroblast suspension

Note. The above represent the components mixed to prepare three 2 ml lattices of each formulation.

APPENDIX 15

Immunohistochemical characterisation of p6 human dermal fibroblasts

Antibodies employed, sources and dilutions.

Primary antibody	Source & product	Concentration*1	Secondary antibody	Source	Concentration*1
Anti-vimentin	DAKO - M725	1 in 200	anti-mouse-FITC*2	Sigma - F-6257	1 in 100
Anti-cytokeratin LP34	Gift from London Hospital	neat	anti-mouse-FITC	Sigma - F-6257	1 in 100
Anti cytokeratin LP1	Gift from London Hospital	neat	anti-mouse-FITC	Sigma - F-6257	1 in 100
Anti-factor-VIII	DAKO - A082	1 in 200	anti-rabbit-TRITC*3	Sigma - T-5268	1 in 100

*1 - dilutions made in 1% w/v bovine serum albumin (Sigma A-7030) in PBS (Appendix 1A)

*2 - FITC = fluorescein isothiocyanate

*3 - TRITC = teramethylrhodamine isothiocyanate

APPENDIX 16

Indirect immunofluorescence method used to characterise p6 human dermal fibroblasts

1. Prepare sterile coverslips:
    a. Immerse coverslips in 70% alcohol and flame to sterilise.
    b. Place coverslips in the bottom of 60 mm petri dishes.
2. Plate out p6 human dermal fibroblasts, p31 SVK14 transformed keratinocytes and p7 bovine aortic endothelial cells onto coverslips in different petri dishes.
    a. Trypsinize cell monolayers (Appendix 4).
    b. Resuspend cells to a concentration of 1 x 10^6 cells per ml.
    c. Place 2 ml of cell suspension into each 60 mm petri dish.
    d. Place seeded petri dishes in a 37°C humidified incubator until cells are confluent.
3. Once confluent monolayers are achieved fix the coverslips.
    a. Wash coverslips twice in PBS (Appendix 1A).
    b. Fix cells with 4% paraformaldehyde (Appendix 1D).
    c. Wash twice more in PBS.
4. Label with antibody.
    a. Permeabilize cells with 0.1% v/v triton X-100 detergent diluted in PBS for 15 minutes.
    b. Wash twice in PBS to remove detergent.
    c. Apply appropriately diluted primary antibody to coverslip (sufficient to completely cover the coverslip).
    d. Incubate for 1 hour at room temperature in a humidified box.
    e. Tap off the antibody onto absorbent paper, wash the coverslip 3 times in PBS and tap off excess PBS.
    f. Apply appropriately diluted secondary antibody to coverslip, return to the humidified box and incubate for 1 hour.
    g. Repeat step e.
    h. Wash in distilled water.
    i. Mount the coverslip onto a microscope slide with the water based anti-quenching mountant Citifluor.
    j. Seal the coverslip to the microscope slide with nail varnish.
    k. View under Olympus BH2 fluorescence microscope fitted with appropriate excitation filters to fluorochrome (FITC or TRITC) in use, and photograph.

APPENDIX 17

Table 1. Summary of the non-parametric analysis (Mann Whitney U-test), showing probability values, carried out to compare the effect of varying the fetal calf serum concentration on the proliferation of passage 6 human dermal fibroblasts *in vitro*.

12 hours after seeding.

		Fetal calf Serum Concentration (%)					
		0.5	1.0	2.5	5.0	10.0	20.0
Fetal Calf Serum Concentration (%)	20.0	0.154223	0.080398	0.056370	0.285056	0.235767	
	10.0	0.428910	0.526528	0.259509	0.930817		
	5.0	0.492710	0.336204	0.311794			
	2.5	0.635046	0.254401				
	1	0.173684					
	0.5						

Where present **bold** indicates a statistically significant difference between groups (i.e. $p < 0.05$)

APPENDIX 17 - continued

Table 2. Summary of the non-parametric analysis (Mann Whitney U-test), showing probability values, carried out to compare the effect of varying the fetal calf serum concentration on the proliferation of passage 6 human dermal fibroblasts *in vitro*.

60 hours after seeding.

		Fetal calf Serum Concentration (%)					
		0.5	1.0	2.5	5.0	10.0	20.0
Fetal Calf Serum Concentration (%)	20.0	**0.000037**	**0.000037**	**0.000037**	**0.000037**	**0.049498**	
	10.0	**0.000036**	**0.000036**	**0.000036**	**0.000154**		
	5.0	**0.000036**	**0.000037**	**0.000036**			
	2.5	**0.000306**	**0.000037**				
	1	**0.001815**					
	0.5						

Where present **bold** indicates a statistically significant difference between groups (i.e. $p < 0.05$)

APPENDIX 17 - continued

Table 3. Summary of the non-parametric analysis (Mann Whitney U-test), showing probability values, carried out to compare the effect of varying the fetal calf serum concentration on the proliferation of passage 6 human dermal fibroblasts *in vitro*.

108 hours after seeding.

		Fetal calf Serum Concentration (%)					
		0.5	1.0	2.5	5.0	10.0	20.0
Fetal Calf Serum Concentration (%)	20.0	**0.000037**	**0.000037**	**0.000037**	**0.000037**	**0.000097**	
	10.0	**0.000037**	**0.000037**	**0.000037**	**0.000196**		
	5.0	**0.000037**	**0.000037**	**0.000037**			
	2.5	**0.000036**	**0.000047**				
	1	**0.000036**					
	0.5						

Where present **bold** indicates a statistically significant difference between groups (i.e. $p < 0.05$)

APPENDIX 17 - continued

Table 4. Summary of the non-parametric analysis (Mann Whitney U-test), showing probability values, carried out to compare the effect of varying the fetal calf serum concentration on the proliferation of passage 6 human dermal fibroblasts *in vitro*.

156 hours after seeding.

		Fetal calf Serum Concentration (%)					
		0.5	1.0	2.5	5.0	10.0	20.0
Fetal Calf Serum Concentration (%)	20.0	**0.000037**	**0.000036**	**0.000036**	**0.000037**	**0.000037**	
	10.0	**0.000037**	**0.000036**	**0.000036**	**0.000037**		
	5.0	**0.000037**	**0.000036**	**0.000037**			
	2.5	**0.000037**	**0.000036**				
	1	**0.000137**					
	0.5						

Where present **bold** indicates a statistically significant difference between groups (i.e. $p < 0.05$)

APPENDIX 18A

Summary of non-parametric statistical analysis (Mann Whitney-U test). A comparison of "percentage wound area remaining" data. Both experimental groups, insonated with intensities of 0.1 or 0.5 W/cm^2 (3 MHz ultrasound), are compared with the sham-insonated control group at each time point. The statistical significance and p value is stated for each comparison.

Experimental Insonation		Sham Insonation	Probability (p value)
Day 2	0.1 W/cm^2	Not Significant	0.304
	0.5 W/cm^2	Significant	5.853×10^{-3}
Day 3	0.1 W/cm^2	Not Significant	0.275
	0.5 W/cm^2	Significant	5.634×10^{-3}
Day 4	0.1 W/cm^2	Not Significant	0.593
	0.5 W/cm^2	Not Significant	0.094
Day 5	0.1 W/cm^2	Significant	1.326×10^{-3}
	0.5 W/cm^2	Not Significant	0.144
Day 6	0.1 W/cm^2	Significant	4.875×10^{-3}
	0.5 W/cm^2	Significant	0.040
Day 7	0.1 W/cm^2	Significant	1.196×10^{-6}
	0.5 W/cm^2	Significant	2.225×10^{-5}
Day 8	0.1 W/cm^2	Significant	2.035×10^{-5}
	0.5 W/cm^2	Significant	9.457×10^{-4}
Day 9	0.1 W/cm^2	Significant	1.655×10^{-5}
	0.5 W cm^2	Significant	6.276×10^{-5}
Day 10	0.1 W/cm^2	Significant	7.68×10^{-4}
	0.5 W cm^2	Significant	0.014
Day 11	0.1 W/cm^2	Significant	0.011
	0.5 W cm^2	Significant	2.26×10^{-3}

APPENDIX 18B

Summary of non-parametric statistical analysis (Mann Whitney-U test). A comparison of the effect of ultrasonic intensity on wound contraction. The effect of exposing rat skin wounds to pulsed (2ms on : 8 ms off) 3 MHz therapeutic ultrasound at intensities of either 0.1 Wcm^2 ($I^{(SATA)}$) or 0.5 Wcm^2 ($I^{(SATA)}$). The statistical significance and p value are stated for each comparison.

	The effect of 3 MHz ultrasound at an intensity of 0.1 W/cm^2 *versus* the effect of 0.5 W/cm^2 on rat flank skin wound contraction									
Time post-wounding (Days)	2	3	4	5	6	7	8	9	10	11
Statistically significant difference (Yes/No)	N	N	N	Y	N	N	Y	Y	N	N
Probability (p)	0.542	0.319	0.496	0.046	0.216	0.314	0.031	0.010	0.720	0.117

APPENDIX 19

Table 1. The effect of therapeutic ultrasound on fibroblast proliferation *in vitro*. Summary of non-parametric statistical analysis (Mann Whitney-U test). Both experimental groups, insonated with intensities of 0.1 or 0.5 W/cm^2 (3 MHz pulsed [2:8] ultrasound), are compared with the sham-insonated control group at each time point. The statistical significance and p value are stated for each comparison.

Experimental Insonation		Sham Insonation	Probability (p value)
12 hours	0.1 W/cm^2	Not significant	0.808
	0.5 W/cm^2	Not significant	0.935
36 hours	0.1 W/cm^2	Not significant	0.575
	0.5 W/cm^2	Not significant	0.145
60 hours	0.1 W/cm^2	Not significant	0.687
	0.5 W/cm^2	Not significant	0.470
84 hours	0.1 W/cm^2	Not significant	0.467
	0.5 W/cm^2	Not significant	0.375
108 hours	0.1 W/cm^2	Not significant	0.093
	0.5 W/cm^2	Not significant	0.521

Table 2. The effect of therapeutic ultrasound on fibroblast proliferation *in vitro*. Summary of non-parametric statistical analysis (Mann Whitney-U test). Human fibroblast proliferation in response to insonation with 3 MHz therapeutic ultrasound at an intensity of 0.1 W/cm^2 compared with 0.5 W/cm^2. The statistical difference and p value are stated for each comparison (i.e at each time point).

Time (hours)	12	36	60	84	108
Statistically different	No	No	No	Yes	No
Probability (p value)	0.746	0.334	0.261	0.008	0.470

APPENDIX 20

Table 1. The effect of therapeutic ultrasound on the contraction of fibroblast-populated collagen lattices *in vitro*. Summary of non-parametric statistical analysis (Mann Whitney-U test). Both experimental groups, insonated with intensities of 0.1 or 0.5 W/cm^2 (3 MHz pulsed [2:8] ultrasound), are compared with the sham-insonated control group at each time point. The statistical significance and p value are stated for each comparison.

Experimental Insonation		Sham Insonation	Probability (p value)
9 hours	0.1 W/cm^2	Not significant	0.230
	0.5 W/cm^2	Significant	0.013
21 hours	0.1 W/cm^2	Not significant	0.471
	0.5 W/cm^2	Not significant	0.936
28 hours	0.1 W/cm^2	Not significant	0.810
	0.5 W/cm^2	Not significant	0.810
50 hours	0.1 W/cm^2	Not significant	0.575
	0.5 W/cm^2	Not significant	0.093
58 hours	0.1 W/cm^2	Not significant	0.936
	0.5 W/cm^2	Not significant	0.471

Table 2. The effect of therapeutic ultrasound on the contraction of fibroblast-populated collagen lattices *in vitro*. Summary of non-parametric statistical analysis (Mann Whitney-U test). FPCL contraction in response to insonation with 3 MHz therapeutic ultrasound at an intensity of 0.1 W/cm^2 is compared with 0.5 W/cm^2. The statistical difference and p value are stated for each comparison (i.e at each time point).

Time (hours)	9	21	28	50	58
Statistically different	No	No	No	No	No
Probability (p value)	0.298	0.575	0.810	0.379	0.810

APPENDIX 21

The effect of ultrasound on the release from platelets of substances capable of modulating fibroblast proliferation *in vitro*.

1. The effect of the thrombin platelet releasate compared with the effect of the vehicle, PWB on human dermal fibroblast proliferation. A summary of the non-parametric statistical analysis (Mann Whitney U-test).

	Platelet releasate produced by exposure of platelet suspension to thrombin *versus* Platelet washing buffer (vehicle)			
Time post-plating (hours)	12	60	108	156
Statistically significant difference (Y/N)	N	Y	Y	Y
Probability (p) value	0.687	0.005	0.005	0.005

2. The effect of the sham-insonated platelet releasate compared with the effect of the vehicle, PWB on human dermal fibroblast proliferation. A summary of the non-parametric statistical analysis (Mann Whitney U-test).

	Platelet releasate produced by sham exposure of platelet suspension to ultrasound *versus* Platelet washing buffer (vehicle)			
Time post-plating (hours)	12	60	108	156
Statistically significant difference (Y/N)	N	Y	Y	Y
Probability (p) value	0.936	0.012	0.005	0.005

APPENDIX 21 - continued

3. The effect of the sham-insonated platelet releasate compared with the effect of the 0.1 W/cm^2 insonated platelet releasate on human dermal fibroblast proliferation. A summary of the non-parametric statistical analysis (Mann Whitney U-test).

	Platelet releasate produced by sham exposure of platelet suspension to ultrasound *versus* Platelet releasate produced by exposure of platelet suspension to 0.1 W/cm^2 3 MHz pulsed ultrasound			
Time post plating (hours)	12	60	108	156
Statistically significant difference (Y/N)	N	N	Y	Y
Probability (p) value	0.934	0.418	0.005	0.036

4. The effect of the sham-insonated platelet releasate compared with the effect of the 0.5 W/cm^2 insonated platelet releasate on human dermal fibroblast proliferation. A summary of the non-parametric statistical analysis (Mann Whitney U-test).

	Platelet releasate produced by sham exposure of platelet suspension to ultrasound *versus* Platelet releasate produced by exposure of platelet suspension to 0.5 W/cm^2 3 MHz pulsed ultrasound			
Time post-plating (hours)	12	60	108	156
Statistically significant difference (Y/N)	N	N	Y	Y
Probability (p) value	0.936	0.746	0.036	0.005

5. The effect of the 0.1 W/cm^2 insonated platelet releasate compared with the effect of the thrombin platelet releasate on human dermal fibroblast proliferation. A summary of the non-parametric statistical analysis (Mann Whitney U-test).

	Platelet releasate produced by exposure of platelet suspension to 0.1 W/cm^2 3 MHz pulsed ultrasound *versus* Platelet releasate produced by exposure of platelet suspension to thrombin			
Time post-plating (hours)	12	60	108	156
Statistically significant difference (Y/N)	N	Y	Y	Y
Probability (p) value	0.809	0.005	0.005	0.005

6. The effect of the 0.5 W/cm^2 insonated platelet releasate compared with the effect of the thrombin platelet releasate on human dermal fibroblast proliferation. A summary of the non-parametric statistical analysis (Mann Whitney-U test).

	Platelet releasate produced by exposure of platelet suspension to 0.5 W/cm^2 3 MHz pulsed ultrasound *versus* Platelet releasate produced by exposure of platelet suspension to thrombin			
Time post-plating (hours)	12	60	108	156
Statistically significant difference (Y/N)	N	N	Y	Y
Probability (p) value	0.936	0.065	0.030	0.020

APPENDIX 21 - continued

7. The effect of the 0.1 W/cm^2 insonated platelet releasate compared with the effect of the 0.5 W/cm^2 platelet releasate on human dermal fibroblast proliferation. A summary of the non-parametric statistical analysis (Mann Whitney U-test).

	Platelet releasate produced by exposure of platelet suspension to 0.1 W/cm^2 3 MHz pulsed ultrasound *versus* Platelet releasate produced by exposure of platelet suspension to 0.5 W/cm^2 3 MHz pulsed ultrasound			
Time post-plating (hours)	12	60	108	156
Statistically significant difference (Y/N)	N	N	N	N
Probability (p) value	0.936	0.331	0.514	0.687

APPENDIX 22

Summary of non-parametric statistical analysis of the effect of ultrasound on the release from platelets of substances capable of modulating fibroblast-mediated collagen lattice contraction *in vitro*.

1. A comparison of all groups at each time point. Carried out prior to two sample analysis by Mann Whitney-U test.

	Kruskal Wallis comparison of all groups				
Time post-plating (hours)	4.00	13.50	26.00	42.00	51.25
Statistically significant difference (Y/N)	Y	Y	Y	Y	Y
Probability (p) value	0.00004	0.00048	0.00074	0.00016	0.00031

2. Thrombin platelet releasate versus the vehicle, PWB on fibroblast-mediated collagen lattice contraction.

Mann Whitney U-test	Platelet releasate produced by exposure of platelet suspension to thrombin *versus* Platelet washing buffer (vehicle)				
Time post-plating (hours)	4.00	13.50	26.00	42.00	51.25
Statistically significant difference (Y/N)	Y	Y	Y	Y	Y
Probability (p) value	0.005	0.005	0.005	0.005	0.005

APPENDIX 22 - continued

3. Sham-insonated platelet releasate versus the vehicle, PWB, on fibroblast-mediated collagen lattice contraction.

Mann Whitney U-test	Platelet releasate produced by sham exposure of platelet suspension to ultrasound *versus* Platelet washing buffer (vehicle)				
Time post-plating (hours)	4.00	13.50	26.00	42.00	51.25
Statistically significant difference (Y/N)	Y	Y	Y	N	N
Probability (p) value	0.008	0.005	0.020	0.093	0.298

4. Sham-insonated platelet releasate versus the 0.1 W/cm^2 insonated platelet releasate on fibroblast-mediated collagen lattice contraction.

Mann Whitney U-test	Platelet releasate produced by sham exposure of platelet suspension to ultrasound *versus* Platelet releasate produced by exposure of platelet suspension to 0.1 W/cm^2 3 MHz pulsed ultrasound				
Time post-plating (hours)	4.00	13.50	26.00	42.00	51.25
Statistically significant difference (Y/N)	Y	Y	Y	Y	Y
Probability (p) value	0.005	0.031	0.008	0.008	0.008

APPENDIX 22 - continued

5. Sham-insonated platelet releasate versus the 0.5 W/cm^2 insonated platelet releasate on fibroblast-mediated collagen lattice contraction.

Mann Whitney U-test	Platelet releasate produced by sham exposure of platelet suspension to ultrasound *versus* Platelet releasate produced by exposure of platelet suspension to 0.5 W/cm^2 3 MHz pulsed ultrasound				
Time post-plating (hours)	4.00	13.50	26.00	42.00	51.25
Statistically significant difference (Y/N)	Y	N	N	Y	N
Probability (p) value	0.020	0.066	0.298	0.020	0.173

6. The 0.1 W/cm^2 insonated platelet releasate versus the thrombin platelet releasate on fibroblast-mediated collagen lattice contraction.

Mann Whitney U-test	Platelet releasate produced by exposure of platelet suspension to 0.1 W/cm^2 3 MHz pulsed ultrasound *versus* Platelet releasate produced by exposure of platelet suspension to thrombin				
Time post-plating (hours)	4.00	13.50	26.00	42.00	51.25
Statistically significant difference (Y/N)	N	N	N	N	N
Probability (p) value	0.173	0.298	0.378	0.093	0.066

APPENDIX 22 - continued

7. The 0.5 W/cm^2 insonated platelet releasate versus the thrombin platelet releasate on fibroblast-mediated collagen lattice contraction.

Mann Whitney U-test	Platelet releasate produced by exposure of platelet suspension to 0.5 W/cm^2 3 MHz pulsed ultrasound *versus* Platelet releasate produced by exposure of platelet suspension to thrombin				
Time post-plating (hours)	4.00	13.50	26.00	42.00	51.25
Statistically significant difference (Y/N)	Y	N	N	Y	Y
Probability (p) value	0.005	0.173	0.093	0.045	0.020

8. The 0.1 W/cm^2 insonated platelet releasate versus the 0.5 W/cm^2 platelet releasate on fibroblast-mediated collagen lattice contraction.

Mann Whitney-U test	Platelet releasate produced by exposure of platelet suspension to 0.1 W/cm^2 3 MHz pulsed ultrasound *versus* Platelet releasate produced by exposure of platelet suspension to 0.5 W/cm^2 3 MHz pulsed ultrasound				
Time post-plating (hours)	4.00	13.25	26.00	42.00	51.25
Statistically significant difference (Y/N)	Y	N	N	N	N
Probability (p) value	0.020	0.810	0.093	0.298	0.093

APPENDIX 23

Statistical analysis of the effect of therapeutic ultrasound on the release of substances, from non-PMA-exposed U937s, capable of modulating fibroblast proliferation *in vitro*.

1. Overview analysis - Kruskal-Wallis test ($p < 0.05$ is significant)

	Kruskal-Wallis (non-parametric) analysis of all groups				
Time post-plating (hours)	12	36	60	84	132
Statistically significant difference (Y/N)	N	N	Y	Y	Y
Probability (p) value	0.981	0.489	0.047	0.020	0.004

2. A comparison of non-conditioned RPMI-1640 medium with non-insonated U937 conditioned RPMI-1640 medium on fibroblast proliferation *in vitro* ($p < 0.05$ is significant).

Mann Whitney U-test	Non-conditioned RPMI medium *versus* Conditioned medium from non-insonated U937s				
Time post-plating (hours)	12	36	60	84	132
Statistically significant difference (Y/N)	Not done	Not done	Y	N	Y
Probability (p) value	Not done	Not done	0.045	0.064	0.044

APPENDIX 23 - continued

3. A comparison of sham-insonated U937 conditioned RPMI-1640 medium with non-insonated U937 conditioned RPMI-1640 medium on fibroblast proliferation *in vitro* ($p < 0.05$ is significant)

Mann Whitney U-test	Conditioned RPMI medium from non-insonated U937s *versus* Conditioned medium from sham-insonated U937s				
Time post-plating (hours)	12	36	60	84	132
Statistically significant difference (Y/N)	Not done	Not done	N	N	N
Probability (p) value	Not done	Not done	0.686	0.809	0.872

4. A comparison of conditioned RPMI-1640 medium from U937s insonated with 3 MHz ultrasound at an intensity of 0.1 W/cm^2 ($I^{(SATA)}$) with sham-insonated U937 conditioned RPMI-1640 medium on fibroblast proliferation *in vitro* ($p < 0.05$ is significant).

Mann Whitney U-test	Conditioned RPMI medium from sham-insonated U937s *versus* Conditioned medium from U937s insonated with 0.1 W/cm^2 3 MHz pulsed ultrasound				
Time post-plating (hours)	12	36	60	84	132
Statistically significant difference (Y/N)	Not done	Not done	N	Y	Y
Probability (p) value	Not done	Not done	0.127	0.030	0.012

APPENDIX 23 - continued

5. A comparison of conditioned RPMI-1640 medium from U937s insonated with 3 MHz ultrasound at an intensity of 0.5 W/cm^2 ($I^{(SATA)}$) with sham-insonated U937 conditioned RPMI-1640 medium on fibroblast proliferation *in vitro* ($p < 0.05$ is significant).

Mann Whitney U-test	Conditioned RPMI medium from sham-insonated U937s *versus* Conditioned medium from U937s insonated with 0.5 W/cm^2 3 MHz pulsed ultrasound				
Time post plating (hours)	12	36	60	84	132
Statistically significant difference (Y/N)	Not done	Not done	N	Y	Y
Probability (p) value	Not done	Not done	0.374	0.013	0.008

6. A comparison of conditioned RPMI-1640 medium from U937s insonated with 3 MHz ultrasound at an intensities of 0.1 W/cm^2 ($I^{(SATA)}$) versus 0.5 W/cm^2 ($I^{(SATA)}$) on fibroblast proliferation *in vitro* ($p < 0.05$ is significant)

Mann Whitney U-test	Conditioned medium from U937s insonated with 0.1 W/cm^2 3 MHz pulsed ultrasound *versus* Conditioned medium from U937s insonated with 0.5 W/cm^2 3 MHz pulsed ultrasound				
Time post-plating (hours)	12	36	60	84	132
Statistically significant difference (Y/N)	Not done	Not done	N	N	N
Probability (p) value	Not done	Not done	0.376	0.809	0.373

APPENDIX 23 - continued

7. A comparison of conditioned RPMI-1640 medium from U937s insonated with 3 MHz ultrasound at an intensity of 0.1 W/cm^2 ($I^{(SATA)}$) with non-conditioned RPMI-1640 medium on fibroblast proliferation *in vitro* ($p < 0.05$ is significant).

Mann Whitney U-test	Non-conditioned RPMI medium *versus* Conditioned medium from U937s insonated with 0.1 W/cm^2 3 MHz pulsed ultrasound				
Time post plating (hours)	12	36	60	84	132
Statistically significant difference (Y/N)	Not done	Not done	N	N	N
Probability (p) value	Not done	Not done	0.936	0.686	0.090

8. A comparison of conditioned RPMI 1640 medium from U937s insonated with 3 MHz ultrasound at an intensity of 0.5 W/cm^2 ($I^{(SATA)}$) with non conditioned RPMI 1640 medium on fibroblast proliferation *in vitro* ($p < 0.05$ is significant).

Mann Whitney U-test	Non-conditioned RPMI medium *versus* Conditioned medium from U937s insonated with 0.5 W/cm^2 3 MHz pulsed ultrasound				
Time post-plating (hours)	12	36	60	84	132
Statistical significant difference (Y/N)	Not done	Not done	N	N	N
Probability (p) value	Not done	Not done	0.294	0.808	0.686

APPENDIX 24

Statistical analysis of the effect of therapeutic ultrasound on the release of substances, from PMA-exposed U937s, capable of modulating fibroblast proliferation *in vitro*.

1. Overview analysis - Kruskal-Wallis test ($p < 0.05$ is significant)

	Kruskal-Wallis (non-parametric) analysis of all groups				
Time post plating (hours)	12	36	60	84	132
Statistically significant difference (Y/N)	N	Y/N	Y	Y	Y
Probability (p) value	0.93981	0.16212	0.00247	0.01120	0.00005

2. A comparison of non-conditioned RPMI-1640 medium containing PMA with non-insonated PMA-exposed U937 conditioned RPMI-1640 medium on fibroblast proliferation *in vitro* ($p < 0.05$ is significant).

Mann Whitney U-test	Non-conditioned RPMI medium containing PMA *versus* Conditioned medium from non-insonated PMA exposed U937s				
Time post-plating (hours)	12	36	60	84	132
Statistically significant difference (Y/N)	Not done	N	Y	Y	Y
Probability (p) value	Not done	0.295	0.016	0.045	0.005

APPENDIX 24 - continued

3. A comparison of sham-insonated PMA-exposed U937 conditioned RPMI-1640 medium with non-insonated PMA-exposed U937 conditioned RPMI-1640 medium on fibroblast proliferation *in vitro* ($p < 0.05$ is significant)

Mann Whitney U-test	Conditioned RPMI medium from non-insonated PMA exposed U937s *versus* Conditioned medium from sham-insonated PMA exposed U937s				
Time post-plating (hours)	12	36	60	84	132
Statistically significant difference (Y/N)	Not done	N	Y	N	N
Probability (p) value	Not done	0.518	0.030	0.332	0.125

4. A comparison of conditioned RPMI-1640 medium from PMA-exposed U937s insonated with 3 MHz ultrasound at an intensity of 0.1 W/cm^2 ($I^{(SATA)}$) with sham-insonated PMA-exposed U937 conditioned RPMI-1640 medium on fibroblast proliferation *in vitro* ($p < 0.05$ is significant).

Mann Whitney U-test	Conditioned RPMI medium from sham-insonated PMA exposed U937s *versus* Conditioned medium from PMA exposed U937s insonated with 0.1 W/cm^2 3 MHz pulsed ultrasound				
Time post-plating (hours)	12	36	60	84	132
Statistically significant difference (Y/N)	Not done	N	Y	Y	Y
Probability (p) value	Not done	0.936	0.008	0.031	0.005

APPENDIX 24 - continued

5. A comparison of conditioned RPMI-1640 medium from PMA-exposed U937s insonated with 3 MHz ultrasound at an intensity of 0.5 W/cm^2 ($I^{(SATA)}$) with sham-insonated PMA-exposed U937 conditioned RPMI-1640 medium on fibroblast proliferation *in vitro* ($p < 0.05$ is significant).

Mann Whitney U-test	Conditioned RPMI medium from sham-insonated PMA exposed U937s *versus* Conditioned medium from PMA exposed U937s insonated with 0.5 W/cm^2 3 MHz pulsed ultrasound				
Time post-plating (hours)	12	36	60	84	132
Statistically significant difference (Y/N)	Not done	Y	Y	N	Y
Probability (p) value	Not done	0.045	0.030	0.148	0.005

6. A comparison of conditioned RPMI-1640 medium from PMA-exposed U937s insonated with 3 MHz ultrasound at an intensities of 0.1 W/cm^2 ($I^{(SATA)}$) versus 0.5 W/cm^2 ($I^{(SATA)}$) on fibroblast proliferation *in vitro* ($p < 0.05$ is significant)

Mann Whitney U-test	Conditioned medium from PMA exposed U937s insonated with 0.1 W/cm^2 3 MHz pulsed ultrasound *versus* Conditioned medium from PMA exposed U937s insonated with 0.5 W/cm^2 3 MHz pulsed ultrasound				
Time post-plating (hours)	12	36	60	84	132
Statistically significant difference (Y/N)	Not done	N	N	N	N
Probability (p) value	Not done	0.336	0.227	0.199	0.518

APPENDIX 24 - continued

7. A comparison of conditioned RPMI-1640 medium from PMA-exposed U937s insonated with 3 MHz ultrasound at an intensity of 0.1 W/cm^2 ($I^{(SATA)}$) with non-conditioned RPMI-1640 medium containing PMA on fibroblast proliferation *in vitro* ($p < 0.05$ is significant).

Mann Whitney U-test	Non-conditioned RPMI medium containing PMA *versus* Conditioned medium from PMA exposed U937s insonated with 0.1 W/cm^2 3 MHz pulsed ultrasound				
Time post-plating (hours)	12	36	60	84	132
Statistically significant difference (Y/N)	Not done	N	N	N	Y
Probability (p) value	Not done	0.420	0.423	0.147	0.013

8. A comparison of conditioned RPMI-1640 medium from PMA-exposed U937s insonated with 3 MHz ultrasound at an intensity of 0.5 W/cm^2 ($I^{(SATA)}$) with non-conditioned RPMI-1640 medium containing PMA on fibroblast proliferation *in vitro* ($p < 0.05$ is significant).

Mann Whitney U-test	Non-conditioned RPMI medium containing PMA *versus* Conditioned medium from PMA exposed U937s insonated with 0.5 W/cm^2 3 MHz pulsed ultrasound				
Time post-plating (hours)	12	36	60	84	132
Statistically significant difference (Y/N)	Not done	N	Y	N	Y
Probability (p) value	Not done	0.336	0.013	0.630	0.005

APPENDIX 25

Statistical analysis of the effect of therapeutic ultrasound on the release from non-PMA-exposed U937s of substances capable of modulating fibroblast-mediated collagen lattice contraction *in vitro*.

1. Overview analysis - Kruskal-Wallis test ($p < 0.05$ is significant)

	Kruskal-Wallis (non-parametric) analysis of all groups					
Time post-plating (hours)	4.75	21.25	30.75	45.75	54.25	69.25
Statistically significant difference (Y/N)	Y	Y	Y	Y	Y	Y
Probability (p) value	0.0030	0.0003	0.0008	0.0004	0.0002	0.00003

2. A comparison of non-conditioned RPMI-1640 medium with non-insonated U937 conditioned RPMI-1640 medium on fibroblast-mediated collagen lattice contraction *in vitro* ($p < 0.05$ is significant).

Mann Whitney U-test	Non-conditioned RPMI medium *versus* Conditioned RPMI medium from non-insonated U937s					
Time post-plating (hours)	4.75	21.25	30.75	45.75	54.25	69.25
Statistically significant difference (Y/N)	Y	Y	Y	Y	Y	Y
Probability (p) value	0.008	0.005	0.008	0.005	0.005	0.005

APPENDIX 25 - continued

3. A comparison of sham-insonated U937 conditioned RPMI-1640 medium with non-insonated U937 conditioned RPMI-1640 medium on fibroblast-mediated collagen lattice contraction *in vitro* ($p < 0.05$ is significant).

Mann Whitney U-test	Conditioned RPMI medium from non-insonated U937s *versus* Conditioned medium from sham-insonated U937s					
Time post-plating (hours)	4.75	21.25	30.75	45.75	54.25	69.25
Statistically significant difference (Y/N)	N	N	Y	N	Y	Y
Probability (p) value	0.471	0.065	0.013	0.336	0.020	0.045

4. A comparison of conditioned RPMI-1640 medium from U937s insonated with 3 MHz ultrasound at an intensity of 0.1 W/cm^2 ($I^{(SATA)}$) with sham-insonated U937 conditioned RPMI 1640 medium on fibroblast-mediated collagen lattice contraction *in vitro* ($p < 0.05$ is significant).

Mann Whitney U-test	Conditioned RPMI medium from sham-insonated U937s *versus* Conditioned medium from U937s insonated with 0.1 W/cm^2 3 MHz pulsed ultrasound					
Time post-plating (hours)	4.75	21.25	30.75	45.75	54.25	69.25
Statistically significant difference (Y/N)	N	N	Y	N	N	N
Probability (p) value	0.936	1.000	0.008	0.575	0.336	0.229

APPENDIX 25 - continued

5. A comparison of conditioned RPMI-1640 medium from U937s insonated with 3 MHz ultrasound at an intensity of 0.5 W/cm^2 ($I^{(SATA)}$) with sham-insonated U937 conditioned RPMI-1640 medium on fibroblast-mediated collagen lattice contraction *in vitro* ($p < 0.05$ is significant).

Mann Whitney U-test	Conditioned RPMI medium from sham-insonated U937s *versus* Conditioned medium from U937s insonated with 0.5 W/cm^2 3 MHz pulsed ultrasound					
Time post-plating (hours)	4.75	21.25	30.75	45.75	54.25	69.25
Statistically significant difference (Y/N)	Y	N	N	N	Y	Y
Probability (p) value	0.020	0.093	0.008	0.066	0.045	0.005

6. A comparison of conditioned RPMI-1640 medium from U937s insonated with 3 MHz ultrasound at an intensities of 0.1 W/cm^2 ($I^{(SATA)}$) versus 0.5 W/cm^2 ($I^{(SATA)}$) on fibroblast-mediated collagen lattice contraction *in vitro* ($p < 0.05$ is significant)

Mann Whitney U-test	Conditioned medium from U937s insonated with 0.1 W/cm^2 3 MHz pulsed ultrasound *versus* Conditioned medium from U937s insonated with 0.5 W/cm^2 3 MHz pulsed ultrasound					
Time post-plating (hours)	4.75	21.25	30.75	45.75	54.25	69.25
Statisticallyu significant difference (Y/N)	Y	Y	N	Y	N	Y
Probability (p) value	0.020	0.031	0.575	0.031	0.066	0.005

APPENDIX 25 - continued

7. A comparison of conditioned RPMI-1640 medium from U937s insonated with 3 MHz ultrasound at an intensity of 0.1 W/cm^2 ($I^{(SATA)}$) with non-conditioned RPMI 1640 medium on fibroblast-mediated collagen lattice contraction *in vitro* ($p < 0.05$ is significant).

Mann Whitney U-test	Non-conditioned RPMI medium *versus* Conditioned medium from U937s insonated with 0.1 W/cm^2 3 MHz pulsed ultrasound					
Time post-plating (hours)	4.75	21.25	30.75	45.75	54.25	69.25
Statistically significant difference (Y/N)	Y	Y	Y	Y	Y	Y
Probability (p) value	0.031	0.008	0.008	0.005	0.005	0.005

8. A comparison of conditioned RPMI-1640 medium from U937s insonated with 3 MHz ultrasound at an intensity of 0.5 W/cm^2 ($I^{(SATA)}$) with non-conditioned RPMI-1640 medium on fibroblast-mediated collagen lattice contraction *in vitro* ($p < 0.05$ is significant).

Mann Whitney U-test	Non-conditioned RPMI medium *versus* Conditioned medium from U937s insonated with 0.5 W/cm^2 3 MHz pulsed ultrasound					
Time post-plating (hours)	4.75	21.25	30.75	45.75	54.25	69.25
Statistically significant difference (Y/N)	N	Y	Y	Y	N	Y
Probability (p) value	0.936	0.031	0.008	0.013	0.128	0.005

APPENDIX 26

Statistical analysis of the effect of therapeutic ultrasound on the release of substances, from PMA-exposed U937s, capable of modulating fibroblast-mediated collagen lattice contraction *in vitro*.

1. Overview analysis - Kruskal-Wallis test ($p < 0.05$ is significant)

	Kruskal-Wallis (non-parametric) analysis of all groups					
Time post-plating (hours)	4.75	21.25	30.75	45.75	54.25	69.25
Statistically significant difference (Y/N)	Y	Y	Y	Y	Y	Y
Probability (p) value	0.00008	0.00012	0.00012	0.00026	0.00003	0.00032

2. A comparison of non-conditioned RPMI-1640 medium containing PMA with non-insonated PMA-exposed U937 conditioned RPMI-1640 medium on fibroblast-mediated collagen lattice contraction *in vitro* ($p < 0.05$ is significant).

Mann Whitney U-test	Non-conditioned RPMI medium *versus* Conditioned RPMI medium from non-insonated U937s					
Time post-plating (hours)	4.75	21.25	30.75	45.75	54.25	69.25
Statistically significant difference (Y/N)	Y	Y	Y	Y	Y	Y
Probability (p) value	0.066	0.005	0.005	0.005	0.005	0.005

APPENDIX 26 - continued

3. A comparison of sham-insonated PMA-exposed U937 conditioned RPMI-1640 medium with non-insonated PMA-exposed U937 conditioned RPMI-1640 medium on fibroblast-mediated collagen lattice contraction *in vitro* ($p < 0.05$ is significant).

Mann Whitney U-test	Conditioned RPMI medium from non-insonated U937s *versus* Conditioned medium from sham-insonated U937s					
Time post-plating (hours)	4.75	21.25	30.75	45.75	54.25	69.25
Statistically significant difference (Y/N)	Y	Y	Y	Y	Y	Y
Probability (p) value	0.005	0.005	0.005	0.005	0.005	0.005

4. A comparison of conditioned RPMI-1640 medium from PMA-exposed U937s insonated with 3 MHz ultrasound at an intensity of 0.1 W/cm^2 ($I^{(SATA)}$) with sham-insonated PMA-exposed U937 conditioned RPMI-1640 medium on fibroblast-mediated collagen lattice contraction *in vitro* ($p < 0.05$ is significant).

Mann Whitney U-test	Conditioned RPMI medium from sham-insonated U937s *versus* Conditioned medium from U937s insonated with 0.1 W/cm^2 3 MHz pulsed ultrasound					
Time post-plating (hours)	4.75	21.25	30.75	45.75	54.25	69.25
Statistically significant difference (Y/N)	N	Y	Y	Y	Y	Y
Probability (p) value	0.379	0.005	0.005	0.008	0.005	0.005

APPENDIX 26 - continued

5. A comparison of conditioned RPMI-1640 medium from PMA-exposed U937s insonated with 3 MHz ultrasound at an intensity of 0.5 W/cm^2 ($I^{(SATA)}$) with sham-insonated PMA-exposed U937 conditioned RPMI-1640 medium on fibroblast-mediated collagen lattice contraction *in vitro* ($p < 0.05$ is significant).

Mann Whitney U-test	Conditioned RPMI medium from sham-insonated U937s *versus* Conditioned medium from U937s insonated with 0.5 W/cm^2 3 MHz pulsed ultrasound					
Time post-plating (hours)	4.75	21.25	30.75	45.75	54.25	69.25
Statistically significant difference (Y/N)	Y	Y	Y	Y	Y	Y
Probability (p) value	0.008	0.005	0.005	0.031	0.031	0.005

6. A comparison of conditioned RPMI-1640 medium from PMA-exposed U937s insonated with 3 MHz ultrasound at an intensities of 0.1 W/cm^2 ($I^{(SATA)}$) versus 0.5 W/cm^2 ($I^{(SATA)}$) on fibroblast-mediated collagen lattice contraction *in vitro* ($p < 0.05$ is significant).

Mann Whitney U-test	Conditioned medium from U937s insonated with 0.1 W/cm^2 3 MHz pulsed ultrasound *versus* Conditioned medium from U937s insonated with 0.5 W/cm^2 3 MHz pulsed ultrasound					
Time post-plating (hours)	4.75	21.25	30.75	45.75	54.25	69.25
Statistically significant difference (Y/N)	Y	N	N	N	Y	N
Probability (p) value	0.005	0.298	0.230	0.810	0.005	0.378

7. A comparison of conditioned RPMI-1640 medium from PMA-exposed U937s insonated with 3 MHz ultrasound at an intensity of 0.1 W/cm^2 ($I^{(SATA)}$) with non-conditioned RPMI-1640 medium containing PMA on fibroblast-mediated collagen lattice contraction *in vitro* ($p < 0.05$ is significant).

Mann Whitney U-test	Non-conditioned RPMI medium *versus* Conditioned medium from U937s insonated with 0.1 W/cm^2 3 MHz pulsed ultrasound					
Time post-plating (hours)	4.75	21.25	30.75	45.75	54.25	69.25
Statistically significant difference (Y/N)	Y	Y	Y	Y	Y	Y
Probability (p) value	0.005	0.005	0.005	0.005	0.005	0.005

8. A comparison of conditioned RPMI-1640 medium from PMA-exposed U937s insonated with 3 MHz ultrasound at an intensity of 0.5 W/cm^2 ($I^{(SATA)}$) with non-conditioned RPMI 1640 medium containing PMA on fibroblast-mediated collagen lattice contraction *in vitro* ($p < 0.05$ is significant).

Mann Whitney U-test	Non-conditioned RPMI medium *versus* Conditioned medium from U937s insonated with 0.5 W/cm^2 3 MHz pulsed ultrasound					
Time post-plating (hours)	4.75	21.25	30.75	45.75	54.25	69.25
Statistically significant difference (Y/N)	Y	Y	Y	Y	Y	Y
Probability (p) value	0.013	0.005	0.005	0.005	0.005	0.005

APPENDIX 27

The effect of progressive dilutions of both U937 conditioned medium and unconditioned RPMI-1640 on fibroblast proliferation *in vitro*.

Introduction

When U937 conditioned RPMI-1640 medium is applied to fibroblasts in culture fibroblast proliferation is inhibited. Unconditioned RPMI-1640 does not similarly suppress fibroblast proliferation. Inhibition may be brought about by a number of mechanisms, including (1) the depletion of a nutrient component of RPMI-1640 by U937s, which is essential for fibroblast proliferation, and (2) the elaboration by U937s of a "factor" that inhibits fibroblast proliferation. In order to explain the inhibitory nature of U937 conditioned medium on fibroblast growth, serial dilutions of both conditioned and unconditioned macrophage medium (RPMI-1640) were applied to fibroblast cultures. If U937 conditioned medium is in some way deficient, compared with unconditioned RPMI-1640 medium, further dilution of this conditioned medium would further enhance this deficiency, thus further reducing fibroblast growth. If, however, U937 conditioned medium contained an inhibitor for fibroblast growth, dilution of this medium would have the opposite effect and stimulate fibroblast growth.

The methylene blue fibroblast proliferation assay (p149), a modification of the colorimetric assay described by Oliver *et al.* (1989), was used to investigate the effect of adding various dilutions of both U937 conditioned and unconditioned RPMI-1640 on human dermal fibroblast proliferation.

Method

The standard protocol for the Methylene Blue Fibroblast Proliferation Assay (Appendix 8) was employed with the following additions/modifications.

Briefly, sub-confluent human dermal fibroblast monolayers, passage 6, were trypsinised (Appendix 4), washed in fibroblast growth medium (Appendix 2B) and resuspended in the same to a final concentration of 2×10^4 viable cells ml (Appendix 6). 100 µl volumes of this cell suspension, containing 2000 cells, were aliquoted into 72 wells (i e. filling all wells in columns 1 to 12, with the exception of those wells in rows A and H) of a 96 well flat-bottomed microtitre plate (Appendix 9). The 24 remaining wells (i.e. all wells in columns 1 to 12 that did not receive the cell suspension) were filled with fibroblast growth medium alone. The plate was sealed and placed in a 37°C incubator for a period of 12 hours to allow for cell attachment. U937 conditioned medium (RPMI-1640 "conditioned" media

number 2, table 11.1, p282) was removed from -20°C storage, thawed and sterilised with a 0.22 μm millipore filter. After sterilisation the conditioned medium was serially diluted to 80, 60, 40 and 20% of its original concentration using sterile PBS. Unconditioned RPMI-1640 was similarly diluted using PBS.

After 12 hours the plate was removed from the incubator and the plate sealing tape removed. One of the twelve columns of wells was designated to receive one of the five U937 conditioned RPMI-1640 dilutions (100%, 80%, 60%, 40% or 20%) or one of the five unconditioned RPMI-1640 dilutions. The two remaining columns were designated to receive the diluent, PBS, alone. All eight wells of a given column, including the cell free wells, received 100 μl of a given RPMI-1640 dilution or PBS. Once all wells had received 100 μl of media, or PBS, the plate was resealed and returned to the 37°C incubator. 108 hours after initial seeding with fibroblasts the plate was stopped according to Appendix 8 steps 6 through 9).

Fibroblast monolayers within the wells were then stained with methylene blue dye, washed with 0.01 M borate buffer, and the dye eluted with acid-alcohol. The absorbance (A_{650}) of each well was then measured (Appendix 8, steps 10 through 12). For each column of wells, and hence for each medium dilution under test, the average A_{650} value of cell-free wells was subtracted from each of the A_{650} readings of cell containing wells. The fibroblast number within a given well was then calculated from these corrected A_{650} values using a standard plot of human dermal fibroblast number versus A_{650} (Appendix 29B). This standard plot was prepared according to the method described in chapter 5 (p152) using the same primary culture of fibroblasts, at the same passage (p6), as was used for the fibroblast proliferation assay above.

For each medium dilution and PBS the median fibroblast number within the 6 wells (or 12 wells in the case of PBS) was reported. Minimum and maximum fibroblast number and 95% confidence intervals were reported to indicate data distribution (table 27.1).

Results and discussion:

Figure 27.1 displays the variation in median fibroblast number in response to the application of the five U937 conditioned medium dilutions, the five unconditioned medium dilutions and PBS. 95% confidence intervals are displayed to indicate data distribution.

From figure 27.1, the data table 27.1, the following points are apparent.

1. The application of progressive serial dilutions of normal unconditioned serum-free RPMI-1640 to fibroblast cultures results in a progressive reduction in fibroblast proliferation. By 108 hours there are more fibroblasts within wells supplemented with 100% unconditioned RPMI-1640 medium than in similar wells supplemented with 80% unconditioned

Table 27.1. The effect on proliferation of applying progressively diluted unconditioned and U937-conditioned RPMI-1640 to fibroblast monolayers.

	Unconditioned RPMI-1640 medium					PBS	U937 conditioned RPMI-1640 medium				
	100%	80%	60%	40%	20%	100%	100%	80%	60%	40%	20%
Number of replicate wells	6	6	6	6	6	12	6	6	6	6	6
Median cell number per well (cells x 10^3)	2.601	2.086	1.774	1.524	1.352	1.225	1.509	1.774	1.384	1.384	1.274
Minimum and Maximum (cells x 10^3)	2.225 to 3.101	1.727 to 2.445	1.633 to 2.008	1.102 to 1.789	1.290 to 1.602	0.915 to 1.446	1.165 to 2.008	1.509 to 1.946	1.103 to 1.571	1.290 to 1.571	1.071 to 1.446
95% confidence interval (cells x 10^3)	2.306 to 2.990	1.733 to 2.400	1.635 to 1.936	1.242 to 1.744	1.263 to 1.546	1.150 to 1.352	1.204 to 1.906	1.592 to 1.904	1.142 to 1.521	1.290 to 1.550	1.132 to 1.438

Figure 27.1 The effect on proliferation of applying progressively diluted unconditioned and U937-conditioned RPMI-1640 to fibroblast monolayers (95% confidence intervals are indicated).

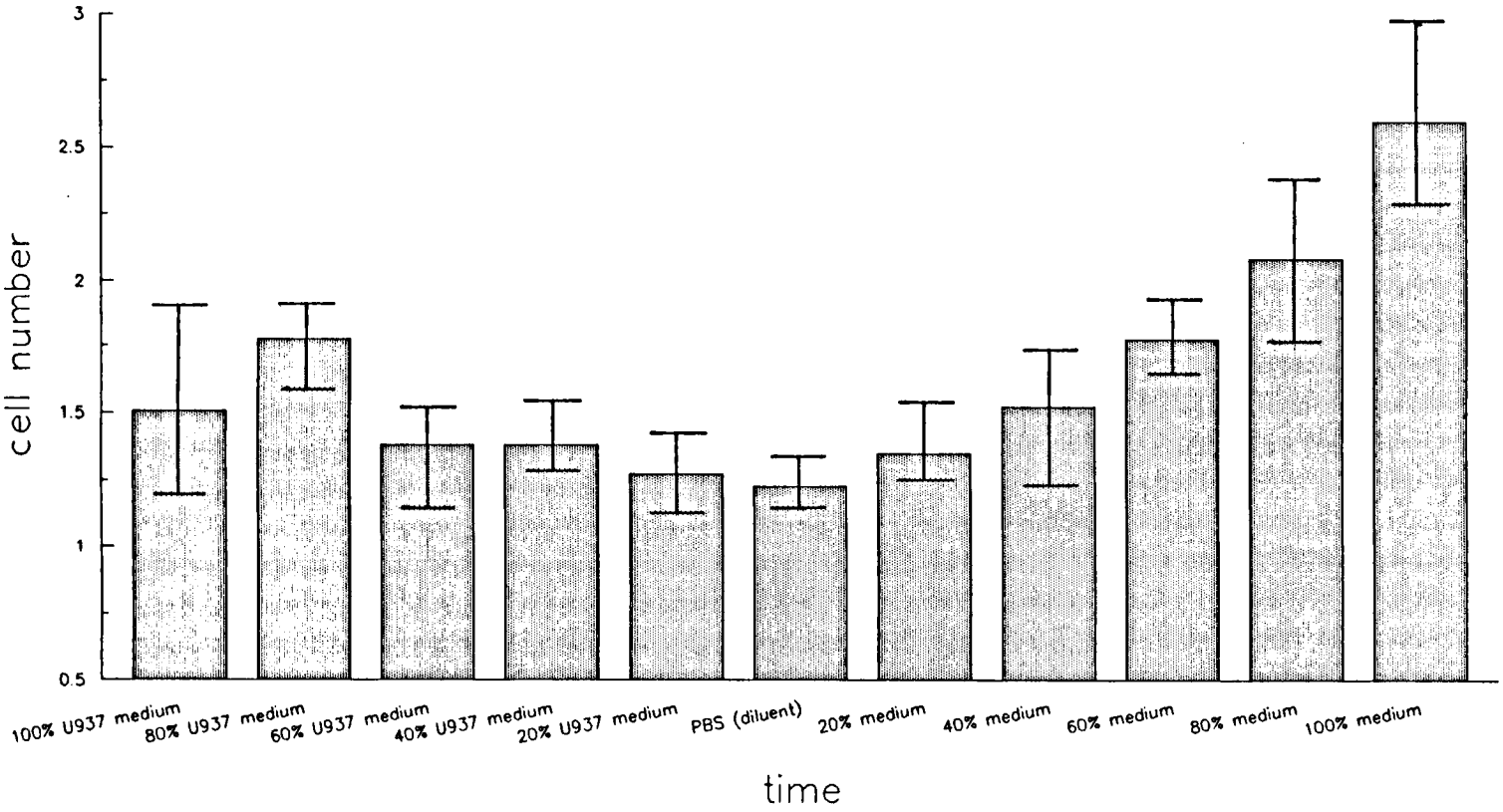

medium; the latter, in turn contain more fibroblasts than those wells supplemented with 60% unconditioned medium. This trend is continued with progressive dilution, with the fewest fibroblasts found in wells supplemented with the diluent, PBS alone.

2. The application of progressive serial dilutions of U937 conditioned medium to fibroblast cultures does not result in a progressive reduction in fibroblast proliferation. By 108 hours there are fewer fibroblasts within wells supplemented with 100% unconditioned than in similar wells supplemented with 80% unconditioned medium. Serial dilution of U937 conditioned medium from 80% to 20% appears to follow a trend similar to that of unconditioned medium, in that progressive dilutions of U937 conditioned medium appear to result in progressively fewer fibroblasts within wells.

The progressive reduction in fibroblast growth in response to the application of progressively more dilute unconditioned RPMI-1640 to fibroblast cultures indicates that fibroblasts can respond to growth medium deficiencies. Thus, if nutrient depletion was primarily involved in the U937 conditioned medium inhibition of fibroblast growth, further depletion of U937 conditioned medium, by dilution, should result in further fibroblast growth inhibition. However, the observation that fibroblast proliferation was found to be more rapid in response to 80% U937 conditioned medium than 100% U937 conditioned medium suggests that U937 conditioned medium contains some form of inhibitor for fibroblast growth. With subsequent progressive dilutions of conditioned medium fibroblast growth was inhibited, it is therefore suggested that this reduction in fibroblast growth, which parallels medium dilution, may be associated with nutrient depletion.

In summary, under the tissue culture conditions used in this thesis, the macrophage-like cell line (U937) has been shown to elaborate an inhibitor of fibroblast growth. (A discussion relating to the possible identity of this fibroblast growth inhibitor can be found on page 293).

APPENDIX 28

The effect of therapeutic ultrasound on U937 viability

Under the culture conditions employed in this thesis U937s (both uninduced and PMA-induced) appear to elaborate an inhibitor of fibroblast growth. Exposure of U937s to therapeutic ultrasound appears to reduce, if not completely annul, the production of a fibroblast growth inhibitor by U937s (chapter 11, p276). In order to investigate the mechanism by which therapeutic ultrasound may prevent inhibitor production by U937s, a study was performed to investigate the effect of therapeutic ultrasound on U937 viability. A loss in viability of fibroblast growth inhibitor-producing cells would be expected to lead to a reduction in the level of inhibitor within medium conditioned by those cells.

Insonation of U937s and cell counting

U937 cells were cultured at 37°C in 80 cm^2 tissue culture flasks (Nunc, Denmark) in RPMI-1640 medium containing 10% (v/v) heat inactivated fetal calf serum (FCS), 100 μg/ml streptomycin, 100 units/ml penicillin (macrophage growth medium, Appendix 2E, p336) according to Turck *et al* (1989). A U937 suspension was prepared at a concentration of 1 x 10^6 viable cells/ml in macrophage growth medium. This suspension was divided into two aliquots and then centrifuged for 5 minutes at 80 x g. The two cell pellets thus obtained were washed twice with serum-free growth medium and then resuspended to 1 x 10^6 viable cells/ml in either: A. Serum-free macrophage growth medium (Appendix 2G, p337), or, B. Serum-free macrophage growth medium containing 100 ng/ml 4β-phorbol 12-myristate 13-acetate (PMA) (Appendix 2H, p337).

Thus forming two U937 stock suspensions:

A. Non-PMA exposed U937s

B. PMA exposed U937s

4ml volumes of these two U937 stock suspensions were aliquoted into sterile, universal bottles, and held at 20°C (room temperature). The exposure chamber (Appendix 13, figure 13.1, p349) was then prepared and loaded, according to Appendix 13 (p348), with the first aliquot. The exposure chamber was located in the exposure tank (figure 11.1, p281) which was lined with ultrasound absorbent rubber (dimpled car matting) and filled with circulating degassed distilled water at 37°C.

U937 samples were insonated with 3 MHz pulsed (1:4) ultrasound at intensities, $I^{(SATA)}$, of 0.1 W/cm^2 or 0.5 W/cm^2, or sham-insonated, for a period of 5 minutes. One aliquot of each U937 stock suspension, termed non-insonated, was neither insonated nor sham-insonated, but, rather left untreated. The therapeutic ultrasound source used in this study was a standard Enraf Nonius Delft 434 Sonopuls machine (Enraf Nonius Delft, Holland), set to deliver 3 MHz ultrasound (figure 7.2, p222). Prior to U937 exposure, ultrasonic output was calibrated and the generator set to deliver a fixed ultrasonic intensity - according to chapter 6 (p187).

After treatment U937 suspensions were unloaded from the exposure chamber (or from the universal bottle in the case of the non-insonated aliquot) into sterile centrifuge tubes and centrifuged at 80 x g for 5 minutes. Supernatants were discarded and cell pellets resuspended in serum-free growth medium with or without PMA according to which U937 stock suspension the treated sample originated. The volume of medium used to resuspend the different cell pellets depended upon the cell suspension volume previously centrifuged. U937 suspensions were then transferred to culture flasks and returned to a 37°C incubator.

One hour post-exposure the U937 cultures were removed from the incubator, gently mixed to homogeneity, samples removed and viable cell counts performed on these samples using a haemocytometer. Cell counts were performed according to Appendix 6 (p340) employing trypan blue to assess cell viability. Counts were performed in triplicate. After sampling the different U937 cultures were returned to a 37°C incubator. Viable cell counts were similarly performed twenty four hours after exposure. Average viable cell counts were tabulated (table 28.1).

Results: Non-PMA-exposed U937s

1. By studying the number of viable cells present after 1 hour the following points are apparent:

   (a) There was a loss in viable cell number, relative to the initial seeding density of 0.97 x 10^6 cells/ml, in all treatment groups.

   (b) Sham-insonated U937 cultures appeared to experience a slightly greater loss in viable cell number than similar non-insonated cultures.

   (c) Ultrasound-exposed U937 cultures experienced a significantly greater loss in viable cell number than similar non-insonated or sham-insonated U937 cultures.

2. By studying the number of viable cells present after 24 hours the following points are apparent:

(a) There were further losses in viable cell number, above that observed at 1 hour, in all treatment groups.

(b) Non-insonated U937 cultures experienced the smallest "further loss" in viability (viability fell by 12.5%). The remaining U937 cultures experienced more extensive further losses in viability, with viability falls of 24.1% for the sham-, 26.1% for the 0.1 W/cm^2, and 26.0% for the 0.5 W/cm^2-insonated cultures .

Results: PMA-exposed U937s

1. By studying the number of viable cells present after 1 hour the following points are apparent:

(a) As with the non-PMA-exposed U937 cultures, there was a loss in viable cell number, relative to the initial seeding density of 0.97 x 10^6 cells/ml, in all treatment groups.

(b) Sham-insonated U937 cultures appeared to experience a similar loss in viable cell number to non-insonated cultures.

(c) In a similar fashion to non-PMA-exposed cultures, ultrasound-treated PMA-exposed U937 cultures experienced a significantly greater loss in viable cell number than similar non-insonated or sham-insonated U937 cultures.

2. By studying the number of viable cells present after 24 hours the following points are apparent:

(a) As with the non-PMA-exposed U937 cultures, there were further losses in viable cell number, above that observed at 1 hour, in all treatment groups.

(b) The extent of this further loss in viability was dependent upon treatment. In parallel with the results observed in non-PMA-exposed U937s, non-insonated PMA-exposed U937 cultures experienced the smallest further loss in viability (viability fell by 20.7%). The remaining U937 cultures experienced more extensive further losses in viability, with viability falls of 29.0% for the sham-, 55.0% for the 0.1 W/cm^2, and 52.0% for the 0.5 W/cm^2-insonated cultures.

Table 28.1 U937 viable cell counts in response to PMA induction and ultrasonic exposure.

		Uninduced U937s				PMA-induced U937s			
		NI	S	0.1	0.5	NI	S	0.1	0.5
Number of viable cells remaining ($x10^6$ cells per ml)	1 hour after exposure	0.88	0.83	0.65	0.67	0.82	0.81	0.53	0.50
	24 hours after exposure	0.77	0.63	0.48	0.50	0.65	0.58	0.24	0.24

Key:
- NI = Non-insonated U937s
- S = Sham-insonated U937s
- 0.1 = U937s insonated with 3 MHz therapeutic ultrasound at an intensity of 0.1 W/cm^2
- 0.5 = U937s insonated with 3 MHz therapeutic ultrasound at an intensity of 0.5 W/cm^2

Note:
1. Initial cell density from which all U937s were derived = 0.97 x 10^6 U937s per ml.
2. U937 conditioned medium examined in chapter 12 was removed from cultures after 24 hours.
3. All viable cell counts represent average values of triplicate counts.

Discussion

U937s exposed to therapeutic ultrasound experience a significant loss in cell viability. It is apparent that ultrasound-exposed U937 cultures, both non-PMA-exposed and PMA-exposed, contain significantly fewer viable cells than similar sham or non-insonated U937 cultures when studied 1 hour after exposure. This observation suggests ultrasound-mediated cell killing. This killing occurs during ultrasound exposure, or soon thereafter. It is also apparent that in addition to this exposure-associated cell killing a further population of cells are irreversibly damaged, to such an extent that cell death occurs some time after exposure. The results indicate PMA-exposed U937s are less resistant to the damaging effects of ultrasound. It is possible that PMA-exposure prior and during ultrasonic exposure predisposes U937 cultures, or subpopulations thereof, to the damaging effects of ultrasound.

APPENDIX 29A.

Table 29.1 Data for standard plot of human dermal fibroblast number versus Absorbance (A_{650})

Cell Number per well	625	1,250	2,500	5,000	10,000
Number of replicate wells	16	16	16	16	16
Absorbance (λ-650 nm)	0.02200	0.04263	0.08781	0.15869	0.32431
Standard deviation	0.00717	0.00783	0.00665	0.00891	0.01344
Standard error	0.00196	0.00179	0.00166	0.00223	0.00336

APPENDIX 29B.

Standard plot of human dermal fibroblast number versus Absorbance (A_{650})

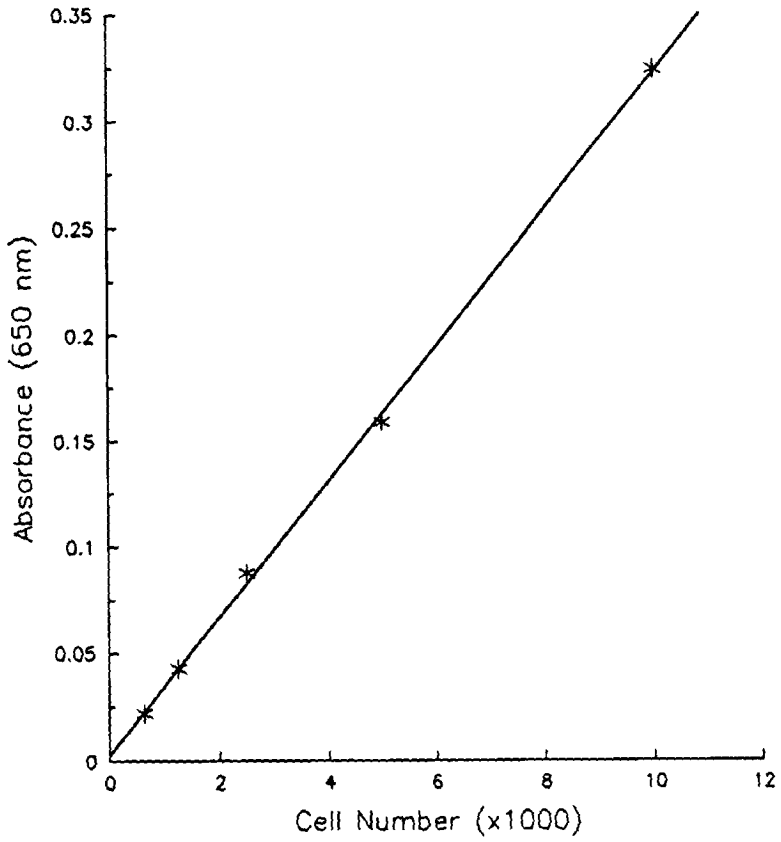

Regression analysis data:

R^2	=	0.9992523
b	=	0.0320138
a	=	0.0030337

To convert an absorbance reading into a cell number:

$$Cell\ Number = \frac{Absorbance - 0.0320138}{0.0030337}$$

APPENDIX 30A.

Table 30.1 Data for standard plot of human dermal fibroblast number versus Absorbance (A_{650})

Cell Number per well	625	1,250	2,500	5,000	10,000
Number of replicate wells	16	16	16	16	16
Absorbance (λ-650 nm)	0.00250	0.01369	0.03306	0.07675	0.17456
Standard deviation	0.00374	0.00671	0.00599	0.00576	0.01902
Standard error	0.00093	0.00168	0.00150	0.00144	0.00297

APPENDIX 30B.

Standard plot of human dermal fibroblast number versus Absorbance (A_{650})

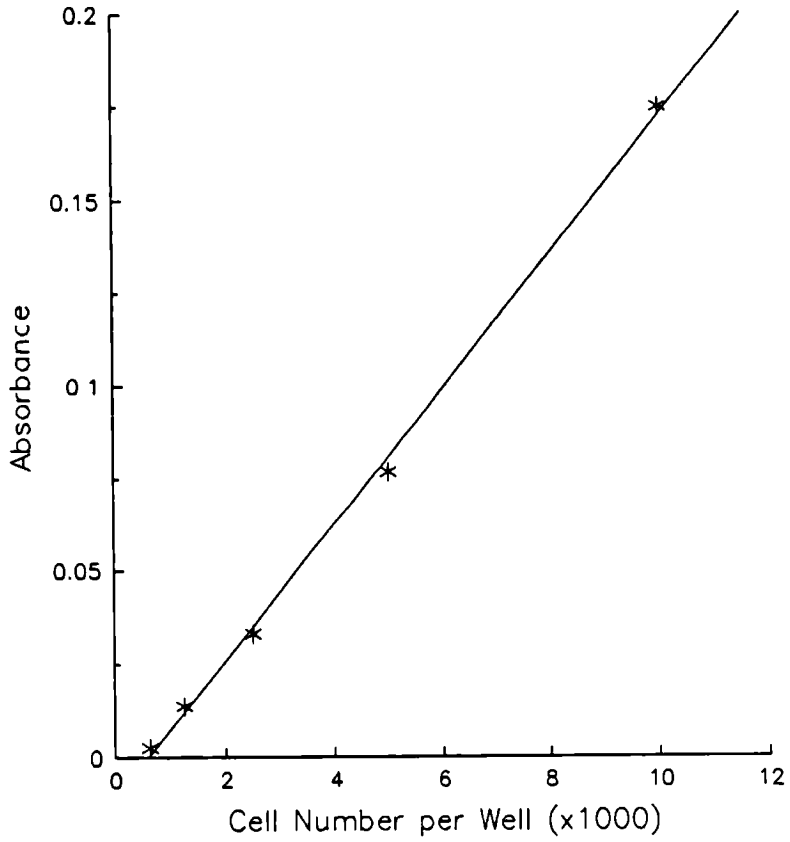

Regression analysis data:

R^2	=	0.9984312
b	=	0.0183401
a	=	-0.010955

To convert an absorbance reading into a cell number:

$$Cell\ Number = \frac{Absorbance - -0.010955}{0.0183401}$$

References:

Abercrombie, M., Flint, M.H. and James, D W. (1954) Collagen formation and wound contraction during repair of small excised wounds in the skin of rats. J. Embryol. Exp. Morph. 2:264-274.

Abercrombie, M., Flint, M.H. and James, D.W. (1956). Wound contraction in relation to collagen formation in scorbutic guinea pigs. J. Embryol. Exp. Morph. 4:167-175.

Abercrombie, M., James, D.W. and Newcombe, J.F.(1960) Wound contraction in rabbit skin. J. Anat. Lond. 94:170-182.

Abramson, D., Burnet, C., Bell, Y., Turk, S., Rejal, J. and Fleisher, J. (1960) Changes in blood flow, oxygen uptake and tissue temperatures produced by therapeutic physical agents. I. Effects of ultrasound. Am. J. Phys. Med. 39:51-62.

Adams, L.W. and Preistley, G.C. (1988) Contraction of collagen lattices by skin fibroblasts: drug induced changes. Arch. Dermatol. Res. 280:114-118

Agelli, M., Sobel, M.E. and Wahl, S.M. (1987) Cytokine modulation of fibroblast collagen production. Fed. Proc. 46:924.

Alberts, B., Bray, D., Lewis, J., Raff, M., Roberts, K., Watson, J.D. (1989) Molecular biology of the cell. Second edition. Garland Publishing. New York & London.

Alitalo, R., Andersson, L.C., Betsholtz, C., Nilsson, K., Westermark, B. Heldin, C.H. and Alitalo, K. (1987) Induction of platelet-derived growth factor gene expression during megakaryoblastic and monocytic differentiation of human leukemia cell lines. EMBO. J. 6:1213-8.

Allen, K.G.R. and Battye, C.K. (1978) Performance of ultrasonic therapy instruments. Physiotherapy. 64:174-179.

Anderson, C.L. (1982) Isolation of the receptor for IgG from a human monocyte cell line U937 and from human peripheral blood monocytes. J. Exp. Med. 156:1794-1806.

Anderson, S.N., Ruben, Z. and Fuller, G.C. (1990) Cell-mediated contraction of collagen lattices in serum-free medium: effect of serum and non-serum factors. *In vitro* Cellular and Developmental Biology 26:61-66.

Anseth, A. (1961) Glycosaminoglycans in corneal regeneration. Exp. Eye Res. 1:122-127.

Armitage, P.M. and Chapman, J.A. (1971) New fibrous long spacing form of collagen. Nature (London). 229:151-152.

Armour, E.P. and Corry, P.M. (1982) Cytotoxic effects of ultrasound in vitro dependence on gas content, frequency, radical scavengers, and attachment. Radiation Res. 89:369-380.

Asaga, H. Kikuchi, S. and Yoshizato, K. (1991) Collagen gel contraction by fibroblasts requires cellular fibronectin but not plasma fibronectin. Exp. Cell. Res. 193:167-174.

Ascensao, J.L. and Mickman, J.K. (1984) Differentiation of human leukemic cell lines (HL60, U937) toward macrophages is accompanied by production of colony-stimulating activity (CSA). Exp. Hematol. 12:177-82.

Assoian, R.K. (1988) Chapter 12. The role of growth factors in tissue repair IV: Type β-transforming growth factor and stimulation of fibrosis. In "The molecular and cellular biology of wound repair". (Ed. Clark, R.A.F and Henson, P.M.). Plenum Press. New York and London. p 273-280.

Assoian, R.K. and Sporn, M.B. (1986) Type β transforming growth factor in human platelets: Release during platelet degranulation and action on vascular smooth muscle cells. J. Cell Biol. 102:1217-1223.

Assoian, R.K., Fleurdelys, B.E., Stevenson, H.C., Miller, P.J., Madtes, D.K., Raines, E.W., Ross, R. and Sporn, M.B. (1987) Expression and secretion of type beta transforming growth factor by activated human macrophages. Proc. Natl. Acad. Sci. (U.S.A.). 84:6020-4.

Atlas, S.J. and Lin, S. (1978) Dihydrocytocholasin B. Biological effects and binding to 3t3 cells. J. Cell Biol. 76:360-370.

Ausprunk, D.H. and Folkman, J. (1977) Migration and proliferation of endothelial cells in preformed and newly formed vessels during tumour angiogenesis. Microvascular. Res. 14:53-65.

Ausprunk, D.H., Falterman, K. and Folkman, J. (1978) The sequence of events in the regression of corneal capillaries. Lab. Invest. 38:284-294.

Ausprunk, D.H., Boudreau, C.L. and Nelson, D.A. (1981) Proteoglycans in the microvasculature. II. Histochemical localization in proliferating capillaries of the rabbit cornea. Am. J Pathol. 103:367-75.

Azizkhan, R.G., Azizkhan, J.C., Zetter, B.R. and Folkman, J. (1980) Mast cell heparin stimulates migration of capillary endothelial cells *in vitro*. J. Exp. Med. 152.931-944.

Bailey, A.J., Bazin, S., Sims, T.J., LeLeus, M., Nicholetis, C. and Delaunay, A. (1975) Characterization of the collagen of human

hypertrophic and normal scars. Biochim. Biophys. Acta **405**:412-421.

Baird, A. and Ling, N. (1987) Fibroblast growth factors are present in the extracellular matrix produced by endothelial cells *in vitro*: implications for a role of heparinase-like enzymes in the neovascular response. Biochem. Biophys. Res. Commun. **142**:428-35

Baird, A., Mormede, P. and Bohlen, P. (1985) Immunoreactive fibroblast growth factor in cells of peritoneal exudate suggests its identity with macrophage-derived growth factor. Biochem. Biophys. Res. Commun. **126**:358-364.

Balazs, A. and Holmgren, H. J. (1950) The basic dye-uptake and the presence of growth inhibiting substance in the healing tissue of skin wounds. Exp. Cell. Res. **1**:206-216.

Balsinde, J. and Mollinedo, F. (1988) Specific activation by concanavalin A of the superoxide anion generation capacity during U937 differentiation. Biochem. Biophys. Res. Commun. **151**:802-8.

Banks, A.R. (1988) Chapter 10. The role of growth factors in tissue repair II: Epidermal growth factor. In "The molecular and cellular biology of wound repair". (Ed. Clark, R.A.F and Henson, P.M.). Plenum Press. New York and London.

Barak, V., Yamin, M., Braun, S., Halperin, M., Biran, S., Milner, Y. and Treves, A.J.(1986) Detection of different interleukin-1 activities in human monocytes and monocytic cell lines. J. Biol. Response. Mod. **5**:362-75.

Barbul, A. (1988). Role of the T cell-dependent immune system in wound healing. In "Growth factors and other aspects of wound healing: Biological and clinical implications". (A. Barbul, E. Pines, M. Caldwell and T.K. Hunt Eds). Alan R Liss. New York. pp 161-175.

Bar-Shavit, R., Kahn, A., Fenton, J.W. and Wilner, G.D. (1983) Chemotactic response of monocytes to thrombin. J. Cell Biol. **96**:282-285.

Bascom, C.C., Sipes, N.J., Coffey, R.J. and Moses, H.L. (1989) Regulation of epithelial cell proliferation by transforming growth factors. J. Cell Biochem. **39**:25-32.

Bauer, E.A., Cooper, T.W., Huang, J.S., Altman, J. and Deuel, T F. (1985) Stimulation of *in vitro* human skin collagenase expression by platelet-derived growth factor. Proc. Natl. Acad. Sci. USA. **82**:4132-4135.

Belewa-Staikowa, R. and Kraschkowa, A. M. (1967) Effects of biophysical factors on the redox process and biological oxidation. Rad. Biol. Ther. **8**:655-662.

Bell, E., Ivarsson, B. and Merril, C. (1979) Production of a tissue-like structure by contraction of collagen lattices by human fibroblasts of different proliferative potential *in vitro*. Proc. Natl. Acad. Sci. USA. **76**:1274-1278.

Bell, E., Sher, S., Hull, B., Merril, C., Rosen, S., Chamson, A., Asselineau, D., Dubertret, L., Coulomb, B., Lapiere, C., Nusgens, B. and Neveux, Y. (1983) The reconstitution of living skin. J. Invest. Dermatol. **81**:2s-10s.

Beller, D.I., Springer, T.A. and Schreiber, R.D. (1982) Anti-Mac-1 selectively inhibits the mouse and human type three complement receptor. J. Exp. Med. **156**:1000-1009

Bellows, C.G., Melcher, A.H. and Aubin, J.E. (1981) Contraction and organisation of collagen gels by cells cultured from peridontal ligament, gingiva and bone suggest functional differences between cell types. J. Cell Sci. **50** 299-314.

Bellows, C.G., Melcher, A.H., Bhargava, U. and Aubin, J.E. (1982) Fibroblasts contracting three dimensional collagen gels exhibit ultrastructure consistent with either contraction or protein secretion. J. Ultrastructure Res. **78**:178-192.

Bently, J.P. (1967) Rate of chondroitin sulfate formation in wound healing. Ann. Surg. **165**:186-191.

Beutler, B.A. and Cerami, A. (1986) Cachectin and tumor necrosis factor as two sides of the same biological coin. Nature **320**:584-588.

Billingham R.E. and Russell P.S. (1956). Studies on wound healing, with special reference to the phenomenon of contracture in experimental wounds in rabbits' skin. Ann. Surg. **144**:961-981.

Binder, A., Hodge, G., Greenwood, A.M., Hazleman, B.L. and Thomas, D.P P. (1985) Is therapeutic ultrasound effective in treating soft tissue lesions? Br. Med. J. **290**:512-524.

Bleaney, B.I., Blackbourn, P. and Kirkley, J. (1972) Resistance of CHLF hamster cells to ultrasonic radiation of 1.5 MHz frequency. Br. J. Radiol. **45**.354-357.

Bouissou, H., Pieraggi, M., Julian, M., Uhart, D. and Kokolo, J. (1988). Fibroblasts in dermal tissue repair. Electron microscope and immunohistochemical study. Int. J. Dermatol.**27**:564-570.

Bowersox, J C. and Sorgente, N. (1982) Chemotaxis of aortic endothelial cells in response to fibronectin. Cancer Res. **42**:2547-2551.

Brennan, M.J., Oldberg, A., Hayman, E.G. and Ruoslahti, E. (1983) Effect of proteoglycan produced by rat tumour cells on their adhesion to fibronectin-collagen substrata. Cancer Res. **43**:4302-4307.

Broadley, K.N., Aquino, A M., Hicks, B., Ditessheim, J.A. Demetriou, A.A., Woodward. and Davidson J.M. (1990) Effect of age on wound healing: Differential response to basic fibroblast growth factor and transforming growth factor β. Proceedings of the 3rd International symposium on tissue repair. Clinical and experimental approaches to dermal and epidermal repair: Normal and Chronic wounds. January 10 - 14, 1990. Miami, Florida, USA. Cited from abstract.

Brown, E.J. (1986) The role of extracellular matrix proteins in the control of phagocytosis. J. Leuk. Biol. **39**:579-591

Bryant, W.M. (1977) Wound healing. CIBA Clin. Symp. **29**:1-36.

Buckley, A., Davidson, J., Kamerath, C., Wolt, T. and Woodward, S. (1985) Sustained release of epidermal growth factor accelerates wound repair. Proc. Natl. Acad. Sci. USA. **82**:7340-7344.

Buckley-Sturrock, A., Woodward, S.C., Senior, R.M., Griffin, G.L., Klagsburn, M. and Davidson, J.M. (1989). Differential stimulation of collagenase and chemotactic activity in fibroblasts derived from rat wound tissue and human skin by growth factors. J. Cell Physiol. **138**:70-78.

Burger, P.C. and Klintworth, G.K. (1981) Autoradiographic study of corneal neovascularisation induced by chemical cautery. Lab. Invest. **45**:328-335.

Burridge, K., Fath, K., Kelly, T., Nuckolls, G., and Turner, C. (1988) Focal adhesions: transmembrane junctions between the extracellular matrix and the cytoskeleton. Ann Rev. Cell. Biol. **4**:487-525.

Buttle, D.J. and Ehrlich, H.P. (1983) Comparative studies of collagen lattice contraction utilising a normal and transformed cell line. J. Cell. Physiol. **116**:159-166.

Byers, H.R., White, G.E., and Fujiwara, K. (1983) Organisation of stress fibres *in vitro* and *in situ*: A review. In: Cell and muscle motility. J. W. Shaw, ed. Plenum Press, New York, Vol 5, pp 83-132.

Byl, N.N., McKenzie, A.L., West, J.M., Whitney, J.D., Hunt, T.K. and Heinz, A.S. (1992) Low dose ultrasound effect on wound healing: A controlled study with Yucatan pigs. Arch. Phys. Med. Rehabil. 73:656-664.

Cady, W.G. (1964) Piezoelectricity. Dover Press. New York.

Callam, M.J., Harper, D.R., Dale, J.J., Ruckley, C.V. and Prescott, R.J. (1987) A controlled rial of weekly ultrasound therapy in chronic leg ulceration. The Lancet. **2**:204-206.

Castagna, M., Takai, Y., Kaibachi, K., Sano, K. Kiddawa, Y. and Nishizuka, Y. (1982) Direct activation of calcium-activated, phospholipid-dependent protein kinase by tumor-promoting phorbol esters. J. Biol. Chem. **257**:7847-7851.

Chan, B.M.C., Kassner, P.D., Schiro, J.A., Byers, H.R., Kupper, T.S. and Hemler, M.E. (1992) Distinct Cellular functions mediated by different VLA integrin α subunit cytoplasmic domains. Cell. **68**:1051-1060.

Charlton, C.A.C., Higton, D.I.R., James, D. W., Nicol, A.R. and Stewart, J.O. (1961) Experimental surgery; wound contraction in the guinea pig. Brit. J. Surg., 1961, 49:96-102.

Chater, B.V. and Williams, A.R. (1977) Platelet aggregation *in vitro* by therapeutic ultrasound. Thrombosis and Haemostasis. **38**:640-651.

Chater, B.V. and Williams, A.R. (1982) Absence of platelet damage *in vivo* following the exposure of non-turbulent blood to therapeutic ultrasound. U.M.B. **8**:85-87.

Chen. L.B., Gudor, R.C., Sun, T.T., Chen, A.B. and Mosesson, M. (1977) Control of a cell surface major glycoprotein by epidermal growth factor. Science **197**:776-778.

Chiang, C.-P., and Nilsen-Hamilton, M. (1986). Opposite and selective effects of epidermal growth factor and human platelet transforming growth factor-beta on the production of secreted proteins by murine 3T3 cells and human fibroblasts. J. Biol. Chem. **261**:10478-10481.

Chua C.C., Geisman D E., Keller G.H., Ladda R.L. (1985). Induction of collagenase secretion in human fibroblast cultures by growth promoting factors. J. Biol. Chem. **260**:5213-5216 .

Chvapil, M. and Koopman, C.F. (1984) Scar formation: Physiology and pathological states. Otolaryngol. Clin. North. Am. **17**:265-272.

Cianciotto, N P., Eisenstein, B.I., Mody, C.H. and Engleberg, N.C. (1990) A mutation in the mip gene results in an attenuation of *Legionella pneumophila* virulence. J Infect. Dis **162**:121-6.

Ciano, P.S., Colvin, R.B., Dvorak, A.M., McDonagh, J. and Dvorak, H. F. (1986) Macrophage migration in fibrin gel matrices. Lab. Invest. **54**:62-79.

Ciaravino, V. and Miller, M.W. (1978) The effect of 1 MHz ultrasound on synchronised mammalian cell proliferation. Radiation Res. 74:583-584.

Ciaravino, V., Miller, M.W. and Carstensen, E.L. (1981) Pressure mediated reduction of ultrasonically induced cell lysis. Radiation Res. 88.209-213.

Clark and Lub (1917) J. Bact. 2:1 (Cited in Giegy Scientific Tables 1984. Physical chemistry of Blood, Hemotology and Somatometric data (C. Lentner. Ed.) Vol 3 pp 59-60)

Clark, R.A.F. (1988a) Potential roles of fibronectin in cutaneous wound repair. Arch. Dermatol. 124:201-206.

Clark, R.A.F. (1988b) Chapter 1. Overview and general considerations of wound repair. In "The molecular and cellular biology of wound repair". (Ed. Clark, R.A.F and Henson, P.M.). Plenum Press. New York and London.

Clark, R.A.F. (1990) Cutaneous wound repair. In "Biochemistry and Physiology of the skin". (Ed. L E Goldsmith). Oxford University Press, Oxford. pp 576-601.

Clark, R.A.F., Winn, H.J., Dvorak, H.F. and Colvin, R.B. (1983) Fibronectin beneath reepithelialization epidermis *in vivo*. Sources and significance. J Invest. Dermatol (Suppl.) 80:26s-30s.

Clark, R.A.F., Wikner, N.E., Doherty, D.E. and Norris, D.A. (1988) Cryptic chemotactic activity of fibronectin for human monocytes resides in the 120kDa fibroblastic cell-binding fragment. J. Biol. Chem. 263:12115-12123.

Clark, R.A.F., Folkvord, J.M., Hart, C.E., Murrey, M.J. and McPherson, J.M. (1989) Platelet isoforms of platelet-derived growth factor stimulate fibroblasts to contract collagen matrices. J. Clin. Invest. 84:1036-1040.

Clark, P.R. and Hill, C.R. (1969) Biological action of ultrasound in relation to the cell cycle. Exptl. Cell. Res. 58:443-444.

Clarke, G.R. and Stenner, L. (1976) Use of therapeutic ultrasound. Physiotherapy. 62:185-190.

Clore, J.N., Cohen, I.K. and Diegelmann, R.F. (1979) Quantitation of collagen types I and III during wound healing in rat skin. Proc. Soc. Exp. Biol. Med. 161:337-340.

Coakley, W.T., Hampton, D. and Dunn, F. (1971) Quantitative relationships between ultrasonic cavitation and effects upon amoebae at 1 MHz. J. Acoust. Soc. Am. 50:649-653.

Coakley, W.T. and Nyborg, W.L. (1978) Cavitation: Dynamics of gas bubbles; applications. Chapter 4. In "Ultrasound: Its Applications in Medicine and Biology" (Ed F.J.Fry). Elsevier, Amsterdam.

Coffey, R.J., Derynck, R., Wilcox, J.N., Brigham, T.S., Goustin, A.S., Moses, H.L. and Pittelkow, M. R. (1987) Production and autoinduction of transforming growth factor-alpha in human keratinocytes. Nature (London) 328:817-820.

Cohnheim, J. (1867). Ueber entzundung und eiterung. Virchows Arch. [A] 40:1-79. Cited from Skalli and Gabbiani (1988).

Colige, A., Nusgens, B. and Lapiere, C.M. (1988) Effect of EGF on human skin fibroblasts is modulated by the extracellular matrix. Arch. dermatol. Res. 280: S42-S46.

Conover, C.A., Hintz, R.L. and Rosenfeld, R. G. (1985) Comparative effects of somatomedin C and Insulin on the metabolism and growth of cultured fibroblast. J. Cell. Physiology 122:133-141.

Conover, C.A., Rosenfeld, R. G. and Hintz, R.L. (1986) Hormonal control of the replication of human fetal fibroblasts: Role of Somatomedin C/Insulin-like growth factor 1. J. Cell. Physiology 128:47-54.

Couchman, J.R. and Rees, D.A. (1979) The behaviour of fibroblasts migrating from chick heart explants: Changes in adhesion, locomotion and growth, and the distribution of actomyosin and fibronectin. J. Cell Sci. 39: 149-165.

Coulomb, B., Dubertret, L., Bell, E., Merrill, C., Fosse, M., Breton-Gorius, Prost, C. and Touraine, R. (1983) Endogenous peroxidases in normal human dermis: a marker of fibroblast function. J. Invest. Dermatol. 81:75-78.

Coustry, F., Gillery, P., Maquart, F X., and Borel, J.P. (1990) Effect of transforming growth factor β on fibroblasts in three dimensional lattice cultures. FEBS Letters, 262:339-341.

Crocker, D.J., Murad, T.M. and Geer, J.C. (1970) Role of the pericyte in wound healing. An ultrastructural study. Exp. Mol. Pathol. 13:51-65.

Crum, L.A. (1984) Rectified diffusion. Ultrasonics. 22.215-223.

Crum, L.A, Walton, A.J., Mortimer, A. Dyson, M., Crawford, D C. and Gaitan, D.F (1987) Free radical production in amniotic fluid and blood plasma by medical ultrasound. J. Ultrasonics. Med. 6 643-647.

Culp, L.A., Murray, B.A. and Rollins, B.J. (1979) Fibronectin and proteoglycans as determinants of cell substratum adhesion. J. Supramol. Struct. 11:401-427.

Currie, G.A. (1978) Activate macrophages kill tumour cells by releasing arginase. Nature **273**:758-759.

Cuthbertson, A.M. (1959) Contraction of full thickness skin wounds in the rat. Surg. Gyn. Obst. **108**:421-432.

Darby, I., Skalli, O. and Gabbiani, G. (1990). α-smooth muscle actin is transiently expressed by myofibroblasts during experimental wound healing. Lab. Invest. **63**:21-29.

Davidson, J., Buckley, A., Woodward, S., Nichols, W, McGee, G. and Demetriou, A. (1988). Mechanisms of accelerated wound repair using epidermal growth factor and basic fibroblast growth factor. In "Growth Factors and Other Aspects of Wound Healing. Biological and Clinical Implications" (Ed. A Barbul, E Pines, M Caldwell and T K Hunt). Alan R Liss Inc. N.Y. p63.

Dayer, J.M., Beutler, B. and Cerami, A. (1985) Cachetin/tumour necrosis factor stimulates collagenase and prostaglandin E2 production by human synovial cells and dermal fibroblasts. J. Exp. Med. **162**:2163-2168.

Decat, G., and Leonard, A. (1984) [In vitro study of the cytogenetic effects produced by ultrasound used in medical therapy and administered alone or in combination with X rays]. C. R. Soc. Biol. **178**:224-229.

Delarco, J.E. and Todaro, G.J. (1978) Growth factors from murine sarcoma virus transformed cells. Proc. Natl. Acad. Sci. USA **75**:4001-4005.

Del-Duca, M., Yeager, E., Davies, M.O. and Hovorka, F.H. (1958) Isotopic techniques in the study of the sonochemical formation of hydrogen peroxide. J. Acoust. Soc. Am. **30**:301-307.

Demczuk, S., Baumberger, C., Mach, B. and Dayer, J.M. (1988) Differential effects of in vitro mycoplasma infection on interleukin-1 alpha and beta mRNA expression in U937 and A431 cells. J. Biol. Chem. **263**:13039-45.

de Prada, M., Richards, J.G. and Kettler, R., (1981) Amine storage organelles in platelets. In "Platelets in Biology and Pathology". Vol 2. (Ed J.L. Gordon). Elsevier/North-Holland, Amsterdam. pp 107-146

Demeter, J., Medzihradszky, D., Kha, H., Goetzl, E.J. and Turck, C.W. (1991) Isolation and partial characterization of the structures of fibroblast activating factor-related proteins from by U937 cells. Immunology. **72**:350-354.

de Reggi, A.S., Roth, S.C., Kenny, J.M., Edelman, S. and Harris, G.R. (1981). Piezoelectric polymer probe for ultrasonic applications. J. Acoust. Soc. Am. **69**:853-858.

Deuel, T.F. and Huang, J.S. (1984) Platelet-derived growth factor: Structure, function and roles in normal and transformed cells. J. Clin. Invest. **74**:669-676.

Deuel, T.F., Senior, R.M., Chuang, D., Griffin, G.L. and Heinrikson, R.L. (1981). Platelet factor 4 is chemotactic for neutrophils and monocytes. Proc. Natl. Acad. Sci. USA. **74**:4584-4587.

Deuel, T.F., Senior, R.M., Huang, J.S. and Griffin, G.L. (1982). Chemotaxis of monocytes and neutrophils to platelet-derived growth factor. J. Clin. Invest. **69**:1047-1049.

Desai, B.P., Sosolik, R.C., Ciaravino, V. and Teale, J.M. (1989) Effect of fetal exposure to ultrasound on B cell development in BALB/c mice. U.M.B. **15**:567-573.

Dipersio, C.M., Jackson, D.A. and Zaret, K.S. (1991) The extracellular matrix coordinately modulates liver transcription factors and hepatocyte morphology. Molecular and Cellular Biology. **11**:4405-4414.

Docherty, A.J.P., Lyons, A., Smith, B.J., Wright, E.M., Stephens, P.E., and Hams, T.J.R. (1985). Sequence of human tissue inhibitor of metalloproteinases and its identity to erythroid-potentiating activity. Nature (Lond.). **318**:66-69.

Dodd, N.J.F., Schor, S.L. and Rushton, G. (1982) The effects of a collagenous extracellular matrix on fibroblast membrane organisation. Exp. Cell Res. **141**:421-431.

Dohlman, J.G., Payan, D.G. and Goetzl, E.J. (1984) Generation of a unique fibroblast-activating factor by human monocytes. Immunology **52**:577-584.

Dohlman, J.G., Cooke, M P., Payan, D.G. and Goetzl, E.J. (1985) Structural diversity of the fibroblast activating factors generated by human blood monocytes and U937 cells. J. Immunol. **134**:3185-3192.

Dooley, D.A., Child, S.Z., Carstensen, E.L. and Miller, M.E. (1983) The effects of continuous wave and pulsed ultrasound on rat thymocytes *in vitro*. U.M.B **9**:379-384.

Dorner, R. W. (1967) Glycosaminoglycans of regenerating tendon. Arth. Rheum. **10**:275-276.

Dragunsky, E.M., Rivera, E., Hochstein, H.D. and Levenbook, I.S. (1990) *In vitro* characterization of *Salmonella typhi* mutant strains for live oral vaccines. Vaccine. 8.263-8.

Dubreuil, M., Sportza, L., D'Addario, M., Lacoste, J., Rooke, R., Wainberg, M A. and Hiscott, J. (1990) Inhibition of HIV-1 transmission by interferon and 3'azido-3'deoxythymidine during de novo infection of promonocytic cells Virology **179**:388-94.

Duband, J.L., Rocher, S., Chen, W.T., Yamada, K.M. and Thiery, J.P. (1986) Cell adhesion and migration in the early vertebrate embryo: location and possible role of putative fibronectin receptor complex. J. Cell Biol. **102**:160-178.

Duck, F.D. and Whish, W.D. (1986) Intracellular DNA breakage: an investigation of thresholds. Proc. Inst. Acoust. **8**:159-161.

Dufour, S., Duband, J.L., Humphries, M.J., Obara, M., Yamada, K.M. and Thiery, J.P. (1988) Attachment, spreading and locomotion of avian neural crest cells are mediated by multiple adhesion sites on fibronectin molecules. EMBO J. **7**:2661-2671.

Duncan, M.R. and Berman, B. (1985) Gamma interferon is the lymphokine and beta interferon is the monokine responsible for inhibition of fibroblast collagen production and late but not early fibroblast proliferation. J. Exp. Med. **162**:516-527.

Dvorak, H.F., Kaplan, A.P., and Clark, R. A.F. (1988) Potential functions of the clotting system in wound repair. In "Molecular and Cellular Biology of Wound Repair"(eds. R.A. F. Clark and P.M. Henson). Plenum Press, New York. pp. 57-85.

Dyson, M. (1981) Chapter 17. Stimulation of tissue repair by therapeutic ultrasound. In "The Surgical Wound" (Eds P Dineen and G Hildick-Smith). Lea and Faber, Philadelphia.

Dyson, M. (1985) Chapter 11. Therapeutic Applications of Ultrasound. In " Clinics in Diagnostic Ultrasound Vol 16 - Biological effects of Ultrasound" (Eds W L Nyborg and M C Ziskin). Churchill Livingstone. New York, Edinburgh, London, Melbourne. pp 121-133.

Dyson, M, (1990) Chapter 13. Role of ultrasound in wound healing. In "Wound healing: Alternatives in management" (Eds L C Kloth, J M McCulloch, J A Feedar). F A Davis, Philadelphia.

Dyson, M., Pond, J.B., Joseph, J. and Warwick, R. (1968) The stimulation of tissue regeneration by means of ultrasound. Clin. Sci. **35**:273-285.

Dyson, M., Pond, J.B., Joseph, J. and Warwick, R. (1970) Stimulation of tissue repair by pulsed wave ultrasound. I.E.E.E. Transactions on Sonics and Ultrasonics **SU-17**:133-140.

Dyson, M., Pond, J.B., Woodward, B. and Broadbent, J. (1974) The production of blood cell stasis and endothelial damage in the blood vessels of chick embryos treated with ultrasound in a stationary wave field. U.M.B. **1**:133-148.

Dyson, M., Franks, C. and Suckling, J. (1976) Stimulation of healing of varicose ulcers by ultrasound. Ultrasonics. **14**:232-236.

Dyson, M. and Brookes, M. (1983) Stimulation of bone repair by ultrasound. In " Ultrasound 82, Proceedings of the 3rd Meeting of the World federation of Ultrasound in Medicine and Biology" (Eds R.A. Lerski and P. Morley). Permagon Press, Oxford.

Dyson, M and Smalley, D.S. (1983) Effects of ultrasound on wound contraction. In: Ultrasound interactions in medicine and biology (Eds Millner, R., Rosenfeld, E., Cobet, U.). Plenum Publishing Corporation. pp 151-158.

Eddy, R.J., Petro, J.A. and Tomasek, J.J. (1988) Evidence for the non-muscle nature of the myo-fibroblast of granulation tissue and hypertrophic scar. An Immunofluorescence study. Am. J. Pathol. **130**:252-260.

Edmonds, P.D. and Ross, P. (1988) Protein synthesis by neuroblastoma cells is enhanced by exposure to burst-mode ultrasound cavitation. U.M.B. **14**:219-223.

Ehrlich, H. P. (1984) The connective tissue matrix control of cell mediated wound contraction and scar contracture. J. Trauma **24**:s35-39.

Ehrlich, H. P. (1988a) Wound closure: Evidence of cooperation between fibroblasts and collagen matrix. Eye **2**:149-157.

Ehrlich, H. P. (1988b) The role of connective tissue matrix in wound healing. In: Growth factors and other aspects of wound healing -Biological and clinical implications. Progress in clinical and biological research. Vol 266. (Barbul, A., Pines, E., Caldwell, M., Hunt, T.K. Eds) Alan R. Liss, Inc. New York. pp 243-258.

Ehrlich, H.P. (1992) Personal communication. Therapeutic advances in wound healing. 29th - 30th June 1992. National Heart and Lung Institute, London.

Ehrlich, H.P. and White, B.S. (1981) The identification of αA and αB collagen chains in hypertrophic scars. Exp. Mol. Pathol. **34**:1-8.

Ehrlich, H.P. and White, M.E. (1983) Effects of increased concentrations of prostaglandin E levels with Epidermolysis Bullosa Dystrophica recessive fibroblasts within a populated collagen lattice. J. Invest. Derm. **81**:572-575.

Ehrlich, H.P. and Hembry, R.M. (1984) A comparative study of fibroblasts in healing freeze and burn injuries in rats. Am J. Path. **117**:288-294.

Ehrlich, H.P. and Rajaratnam, J.B.M. (1990) Cell locomotion forces versus cell contraction forces for collagen lattice contraction: An *in vitro* model of wound contraction. Tissue and Cell **22**:407-417.

Ehrlich, H.P., Buttle, D.J., Trelstad, R.L. and Hayashi, K. (1983) Epidermolysis bullosa dystrophica recessive fibroblasts altered

behaviour within a collagen matrix. J. Invest. Dermatol. 80:56-60.

Ehrlich, H.P., Buttle, D.J. and Bernanke D.H. (1989) Physiological variables affecting collagen lattice contraction by human dermal fibroblasts. Exp. Molec. Pathol. 50:220-229.

EL-Hag, M., Coghlan, K., Christmas, P., Harvey, W. and Harris, M. (1985) The anti-inflammatory effects of dexamethasone and therapeutic ultrasound in oral surgery. Brit. J. Oral. Maxillofacial. Surg. 23:17-23.

Elmer, W.A. and Fleisher, A.C. (1974) Mitotic reduction in rat liver exposed to ultrasound. J. Clin. Ultrasound. 2:123-126.

Elsas, M.I., Dessein, A.J. and Elsas, P.X. (1990) Selection of U937 histiocytic lymphoma cells highly responsive to phorbol ester-induced differentiation using monoclonal antibody to the eosinophil cytotoxicity-enhancing factor. Blood. 75:2427-33.

Elsdale, T. and Bard, J. (1972) Collagen substrata for studies on cell behaviour. J. Cell Biol. 54:626-637.

Epstein, E.H., Jr., (1974) [α1(III)]$_3$ human skin collagen. Release by pepsin digestion and preponderance in fetal life. J. Biol. Chem. 249:3225-3231.

Esposito, C.J., Veal, S.J. and Farman, A.G. (1984) Alleviation of myofascial pain with ultrasonic therapy. J. Prosthet. Dent. 51:106-108.

Farsi, J.M.A., and Aubin, J.E. (1984) Microfilament rearrangements during fibroblast induced contraction of three dimensional hydrated collagen gels. Cell Motility 4:29-40

Ferguson, B. (1985) A practitioners guide to ultrasonic therapy equipment standard. Rockville, MD: Center for Devices and Radiological Health, Office of Training and Assistance; HHS Publication FDA 85-8240.

Ferguson, H. N. (1981) Ultrasound in the treatment of surgical wounds. Physiotherapy. 67.43

Findlay, J.K. (1986) Angiogenesis in reproductive tissues. J. Endochr. 111:357-366.

Finesmith, T.H., Broadley, K.N. and Davidson J. M. (1990) Fibroblasts from wounds of different stages of repair vary in their ability to contract a collagen gel in response to growth factors. J. Cell. Physiology. 144:99-107

Flax, H.J. (1964) Ultrasound treatment of peritendinitis calcarea of the shoulder. Am. J. Phys. Med. 43:117-124.

Flynn, H.G. (1964) Cavitation. In "Physical Acoustics" (Ed W.P. Mason) Vol. 1B. Academic Press, New York.

Folkman, J. (1982) Angiogenesis: initiation and control. Ann. N. Y. Acad. Sci. 401:212-227.

Folkman, J. and Klagsbrun, M. (1987) Angiogenic factors. Science 235:442-447.

Folks, T.M., Justement, J., Kinter, A., Schnittman, S., Orenstein, J., Poli, G. and Fauci, A.S. (1988) Characterization of a promonocyte clone chronically infected with HIV and inducible by 13-phorbol-12-myristate acetate. J. Immunol. 140:1117-22.

Ford, W.L., Sedgley, M., Sparshott, S.M. and Smith, M.E. (1976) The migration of lymphocytes across specialised vascular endothelium. II the contrasting consequences of treating lymphocytes with trypsin or neuraminidase. Cell Tissue Kinet. 9:351-361.

Ford-Hutchinson, A.W., Bray, M.A., Doig, M.V., Shipley, M.E. and Smith, M.J. (1980) Leukotriene B, a potent chemokinetic and aggregating substance released from polymorphonuclear leukocytes. Nature (London) 286:264-265.

Form, D.M. and Auerbach, R. (1983) PGE_2 and angiogenesis. Proc. Soc. Exp. Biol. Met. 172:214-18.

Forster, A. and Palanstanga, N. (1981) In "Clayton's Electrotherapy. Theory and Practice (8th edition). Bailliere Tindal. Toronto, Canada. pg 52.

Fox, G.M. (1988) Chapter 11. The role of growth factors in tissue repair III: Fibroblast growth factor. In "The molecular and cellular biology of wound repair". (Ed. Clark, R.A.F and Henson, P.M.). Plenum Press. New York and London.

Frater-Schroder, M.F., Risau, W., Hallmann, R., Gautschi, P. and Bohlen, P. (1987) Tumor necrosis factor type α, a potent inhibitor of endothelial cell growth *in vitro*, is angiogenic *in vivo*. Proc. Natl. Acad. Sci. 84:5277-81.

Freer, R.J., Day, A.R., Radding, J.A., Schiffmann, E., Aswanikumar, S., Showell, H.J. and Becker, E.L. (1980) Further studies on the structural requirement for synthetic peptide chemoattractants. Biochemistry 19:2404-2410.

Freshney, R.I. (1987) Culture of animal cells: A manual of basic technique. 2nd Edition 1987. Alan R Liss. Inc. New York.

Frizzell, L.A., Lees, C.S., Aschenback, P D., Borrelli, M.J., Morimoto, R.S. and Dunn. F. (1983) Involvement of ultrasonically induced cavitation in the production of hind limb paralysis of the mouse neonate. J. Acoust. Soc. Am. 74:1062-1065.

Froesch, E.R., Schmid, C., Schwander, J. and Zapf, J. (1985) Actions of insulin-like growth factors. Annu. Rev. Physiol.

47 443-67

Fry, F.J. (1979) Biological effects of ultrasound - a review. Proc. I.E.E.E. 67:604-619.

Fu, Y.K., Miller, M.W., Lange, C.S. and Griffiths, T.D. (1980) Ultrasound lethality to synchronous and asynchronous chinese hamster V-79 cells. U.M.B. 6:39-46.

Fujikawa, L.S., Foster, S., Harrist, T.J., Lanigan, J.M. and Colvin, R.B. (1981) Fibronectin in healing rabbit corneal wounds. Lab. Invest. 45:120-129.

Fujiwara, H. and Ellner, J.J. (1986) Spontaneous production of a suppressor factor by the human macrophage-like cell line U937. 1. Suppression of Interleukin 1, Interleukin 2 and mitogen-induced blastogenesis in mouse thymocytes. J. Immunol. 136:181-185.

Fulton, J.F. (1951) "Decompression sickness: Caisson Sickness, Diver's and Flier's Bends and Related Syndromes". W.B. Saunders, Philadelphia.

Fung, H., Cheung, K., Lyons, E.A. and Kay, N.E. (1978) The effect of low dose ultrasound on human peripheral lymphocyte function *in vitro*. In: Ultrasound in Medicine. Vol 4. (D. White & E.A. Lyons Eds). Plenum Press, New York & London. pp 583-586.

Furcht, L.T. (1986) Critical factors controlling angiogenesis: Cell products, cell matrix, and growth factors. Lab. Invest. 55:505-509.

Fyfe, M.C. and Chahl, L.A. (1984) Mast cell degranulation and increased vascular permeability induced by 'therapeutic' ultrasound in the rat ankle joint. Br. J. Exp. Path. 65:671-676.

Fyfe, M.C. and Chahl, L.A. (1985) The effect of single or repeated applications of "therapeutic" ultrasound on plasma extravasation during silver nitrate induced inflammation of the rat hindpaw ankle joint *in vivo*. U.M.B. 11:273-283.

Gabbiani, G., Ryan, G.B. and Majno, G. (1971). Presence of modified fibroblasts in granulation tissue and their possible role in wound contraction. Experientia. 27:549-551.

Gabbiani, G., Hirsh, B.J., Ryan, G.B., Statkov, P.R. and Majno, G. (1972) Granulation tissue as a contractile organ. A study of structure and function. J. Exp. Med. 135:719-734.

Gabbiani, G., Chapponnier, C. and Huttner, I. (1978) Cytoplasmic filaments and gap junctions in epithelial cells and myofibroblasts during wound healing. J. Cell Biol. 76:561-568.

Gabbiani, G. Schmid, E., Winter, S., Chaponnier, C., de Chastonay, C., Vanderkerckhove, J., Weber, K. and Franke, W.W. (1981) Vascular smooth muscle cells differ from other smooth muscle cells: Predominance of vimentin filaments and a specific α-type actin. Proc. Natl. Acad. Sci. USA. 78:298-302.

Gailani, D., Fisher, T.C., Mills, D.C. and Macfarlane, D.E. (1990) P47 phosphoprotein of blood platelets (pleckstrin) is a major target for phorbol ester-induced protein phosphorylation in intact platelets, granulocytes, lymphocytes, monocytes and cultured leukaemic cells: absence of P47 in non-haematopoietic cells. Br. J. Haematol. 74:192-202.

Gallin, J.I.and Kaplan, A.P. (1974) Mononuclear cell chemotactic activity of kallikrein and plasminogen activator and its inhibition by C1 inhibitor and α_2 macroglobulin. J. Immunol. 113:1928-1934.

Garcia-Valdecasas, J.C., Garcia-Valdecasas, F. and Pera, C. (1981). Pharmacological reactivity of granulation tissue. J. Pharm. Pharmacol. 33:650-654.

Gay, S., Vijanto, J., Raekallio, J. and Penttinen, R. (1978) Collagen types in early phases of wound healing in children. Acta Chir. Scand. 144:205-211.

Ghebrehiwet, B., Silverberg, M., and Kaplan, A.P. (1981) Activation of classic pathway of complement by Hageman factor fragment. J. Exp. Med. 153:665-676.

Gillery, P , Maquart, F.X., Borel, J P. (1986) Fibronectin dependence of the contraction of collagen lattices by human skin fibroblasts. Exp. Cell Res. 167:29-37.

Gillery, P., Coustry, F., Pujol, J.-P. and Borel, J.-P. (1989) Inhibition of collagen synthesis by interleukin-1 in three dimensional collagen lattice cultures of fibroblasts. Experientia. 45:98-101.

Gnatz, S.M. (1989) Increased radicular pain due to therapeutic ultrasound applied to the back. Arch. Phys. Med & Rehabil. 70:493-494.

Golublov, S.P., Belkin, V.M., Rudneva, S.V , Terskikh, V V. (1990) Blood plasma fibronectin does not influence fibroblast-induced collagen gel contraction. Tsitologiia 32.499-503. English abstract only.

Goddard, D.H., Revell, P.A., Cason, J., Gallagher, S. and Currey, H.L.F (1983) Ultrasound has no anti-inflammatory effect.

Ann. Rheum. Dis. **42**:582-584.

Goetzl, E.J. (1981) Oxygenation products of arachidonic acid and mediators of hypersensitivity and inflammation. Med. Clin. North Am. **65**:809-828.

Goetzl, E.J. and Gorman, R.R. (1978) Chemotactic and chemokinetic stimulation of human eosinophil and neutrophil polymorphonuclear leukocytes by HHT. J.Immunol. **120**:526-531.

Gollapudi, S. and Gupta, S. (1990) Human immunodeficiency virus I-induced expression of P-glycoprotein. Biochem. Biophys. Res. Commun. **171**:1002-7.

Gospodarowicz, D. (1974) Localisation of a fibroblast growth factor and its effects alone and with hydrocortisone on 3T3 cell growth. Nature (London)**249**:123-127.

Gospodarowicz, D., Ferrara, N., Schweigerer, L. and Neufeld, G. (1987). Structural characterization and biological functions of fibroblast growth factor. Endocrine Reviews. **8**:95-113.

Graycar, J.L., Miller, D.A., Arrick, B.A. Lyons, R.M., Moses, H.L. and Derynck, R. (1989) Human transforming growth factor-β3: recombinant expression, purification and biological activities in comparison with transforming growth factors-β1 and-β2. Mol. Endocrinol. **3**:1977-1986.

Greve, H., Blumberg, P., Schmidt, G., Schlumberger, W., Rauterberg, J and Kresse, H. (1990) Influence of collagen lattice on the metabolism of small proteoglycan II by cultured fibroblasts. Biochem. J. **269**:149-155.

Gramiak, R. and Shah, P.M. (1971) detection of intracardiac blood flow by pulsed echo-ranging ultrasound. Radiology. **100**:415-418.

Griffin, J.E. (1966) Physiological effects of ultrasonic energy as it is used clinically. Phys. Ther. **46**.18-26.

Grillo, H. C., Watts, G.T. and Gross, J. (1958) Studies in wound healing - I, contraction and the wound contents. Ann. Surg. **148**:145-152.

Grinnell, F. and Bennett, M.H. (1981) Fibroblast adhesion to collagen substrata in the presence and absence of plasma fibronectin. J. Cell. Sci. **48**: 19-34.

Grinnell, F. and Lamke, C.R. (1984) Reorganisation of hydrated collagen lattices by human skin fibroblasts. J. Cell Sci. **66**:51-63.

Grinnell, F., Feld, M., & Minter, D. (1980) Fibroblast adhesion to fibrinogen and fibrin substrata: Requirement for cold-insoluble globulin (plasma fibronectin). Cell **19**:517-525.

Grinnell, F., Nakagawa, S. and Ho, C.H. (1989) The collagen recognition sequence for fibroblasts depends on collagen topography. Exp. Cell Res. **182**:668-672.

Gross, J.L., Moscatelli, D. and Rifkin, D.B. (1983) Increased capillary endothelial cell protease activity in response to angiogenic stimuli *in vitro*. Proc. Natl. Acad. Sci. **80**:2623-27.

Gross, T.J. and Sitrin, R.G., (1990) The THP-1 cell line is a urokinase-secreting mononuclear phagocyte with a novel defect in the production of plasminogen activator inhibitor-2. J. Immunol. **144**:1873-9

Grotendorst, G.R., Martin, G.R. Pencev, D., Sodek, J. and Harvey, A.K. (1985) Stimulation of granulation tissue formation by platelet derived growth factor in normal and diabetic rats. J. Clin. Invest. **76**:2323-2329.

Grotendorst, G.R., Grotendorst C.A. and Gilman, T. (1988). Production of growth factors (PDGF and TGF-B) at the site of tissue repair. In "Growth Factors and Other Aspects of Wound Healing: Biological and Clinical Implications". (Eds. A Barbul, E Pines, M. Caldwell, T K Hunt). Alan. R. Liss, Inc. N.Y. p47.

Guidry, C. and Grinnell, F. (1985) Studies on the mechanism of hydrated collagen gel reorganisation by human skin fibroblasts. J. Cell Sci. **79**:67-81.

Guidry, C. and Grinnell, F. (1986) Contraction of hydrated collagen gels by fibroblasts: Evidence for two mechanisms by which collagen fibrils are stabilized. Collagen Rel. Res. **6**:515-529.

Guidry, C. and Grinnell, F. (1987) Heparin modulates the organisation of hydrated collagen gels and inhibits contraction by fibroblasts. J. Cell Biol. **104**.1097-1103.

Gullberg, D., Tingstrom, A., Thuresson, A.C., Olsson, L., Terracio, L., Borg, T.K. and Rubin, K. 1990a) β_1 Integrin-mediated collagen gel contraction is stimulated by PDGF Exp Cell Res. 186, 264-272.

Gullberg, D., Turner, D.C., Borg, T K , Terracio, L. and Rubin, K. (1990b) Different β-integrin collagen receptors on rat hepatocytes and cardiac fibroblasts. Exp. Cell Res. **190**:254-264.

Halle, J S., Scoville, C.R. and Greathouse, D.G (1981) Ultrasound's effect on the conduction latency of the superficial radial

nerve in man. Phys. Ther. **61**:345-350.

Halliwell, B. (1987) Oxidants and human disease: some new concepts. FASEB J. 1:358-364.

Hanahan, D.J. (1986) Platelet activating factor: a biologically active phosphoglyceride. Ann. Rev. Biochem. **55**:483-509.

Hansson, G.K., Hellstrand, M., Rymo, L. Rubbia, L. and Gabbiani, G. (1989) γ interferon inhibits both proliferation and the expression of differentiation-specific α-smooth muscle actin in arterial smooth muscle cells. J. Exp. Med. **170**:1595-608.

Hardy, C.L., Omoto, E. and Tavassoli, M. (1990) Measurement of homing receptors on the surface of leukemic and nonleukemic cell lines. Pathobiology. **58**:179-84.

Harris, E D. and Krane, S.M. (1974) Collagenases. N. Engl. J. Med. **291**:652-661.

Harris, L.W. and Griffiths, J.B. (1977) Relative effects of cooling and warming rates on mammalian cells during the freeze thaw cycle. Cryobiology. **14**:662-669.

Harris, P. and Ralph, P. (1985) Human leukemic models of myelomonocytic development: a review of the HL-60 and U937 cell lines. J. Leukoc. Biol. **37**:407-22.

Harris, A.K., Stopak, D. and Wild, P. (1981) Fibroblast traction as a mechanism for collagen morphogenesis. Nature. **290**:249-251.

Harris, P.E., Ralph, P., Litcofsky, P., Moore, M.A.S. (1985) Distinct activities of interferon-gamma, lymphokine and cytokine differentiation-inducing factors acting on the human monoblastic leukemia cell line U937. Cancer Res. **45**:9-13.

Harrison, R.G. (1907) Observations on the living developing nerve fiber. Proc. Soc. Exp. Biol. Med. **4**:140-143.

Harvey, E.N. (1951) Physical factors in bubble formation. In "Decompression Sickness" (Ed J.F. Fulton), Chapter 4. pp 90-114. W. B. Saunders, Philadelphia.

Harvey, W., Dyson, M., Pond, J.B. and Grahame, R. (1975) The stimulation of protein synthesis in human fibroblasts by therapeutic ultrasound. Rheum & Rehabil. **14**:237.

Hascall, V.C., & Hascall, G.K. (1981) Proteoglycans. In "Cell Biology of Extracellular Matrix (ed. E. B. Hay), pp. 39-63. Plenum Press, New York.

Hashimoto, H. and Prewitt, R.L. (1987) Microvascular changes during wound healing. Int. J. Microcirc: Clin. Exp. **5**:303-310.

Hashish, I. (1986) The effects of ultrasound therapy on post-operative inflammation. Ph.D thesis. University of London.

Hashish, I., Harvey, W. and Harris, M. (1986) Anti-inflammatory effects of ultrasound therapy: Evidence for a major placebo effect. Brit. J. Rheumatol. **25**:77-81.

Hashish, I., Hai, H.K., Harvey, W., Feinmann, C. and Harris, M. (1988) Reduction in post-operative pain and swelling by ultrasound treatment: a placebo effect. Pain. **33**:303-311.

Haslett, C. and Henson, P. M. (1988) Resolution of inflammation. In "Molecular and Cellular Biology of Wound Repair" (eds. R.A.F. Clark and P.M. Henson). Plenum Press, New York. pp. 185-211.

Hass, R. (1992) Retrodifferentiation - an alternative biological pathway in human leukemia cells. Eur. J. Cell. Biol. **58**:1-11.

Hass, R., Giese, G., Meyer, G., Hartmann, A., Dork, T., Kohler, L., Resch, K., Traub, P. and Goppelt-Strube, M. (1990) Differentiation and retrodifferentiation of U937 cells: reversible induction and suppression of intermediate filament protein synthesis. Eur. J. Cell. Biol. **51**:265-71.

Hass, R., Lonnemann, G. Mannel, D. Topley, N, Hartmenn, A., Kohler, L., Resch, K. and Goppelt-Strube, M. (1991) Regulation of TNF-alpha, IL-1 and IL-6 in differentiating human monoblastoid leukemic cells Leuk. Res. **15**:327-39.

Hatamochi, A., Aumailley, M., Mauch, C., Chu, M L., Timpl, R. and Kreig, T (1989) Regulation of collagen VI expression in fibroblasts. Effects of cell density, cell-matrix interactions, and chemical transformation. J. Biol. Chem. **264**:3494-3499.

Hattori, T., Pack, M., Bougnoux, P., Chang, Z.L., Hoffman, T. (1983) Interferon-induced differentiation of U937 cells. Comparison with other agents that promote differentiation of human myeloid or monocyte-like cell lines. J. Clin. Invest. **72**:237-44.

Heimark, R. L. and Schwartz, S. M. (1988) The role of cell-cell interaction in the regulation of endothelial cell growth. In "Molecular and Cellular Biology of Wound Repair" (eds. R.A.F. Clark and P.M. Henson). Plenum Press, New York. pp 359-371.

Heino, J. and Massague, J. (1989) Transforming growth factor-beta switches the pattern of integrins expressed in MG-63 human osteosarcoma cells and causes a selective loss of cell adhesion to laminin. J. Biol. Chem. **264**.21806-21811

Hembry, R. M., Bernanke, D.H., Hayakashi, K., Trelstad, R.L. and Ehrlich, H.P. (1986) Morphologic examination of mesenchymal cells in healing wounds of normal and tight skin mice. Am. J. Pathol. **125**:81-89.

Hennings, H., Michael, D., Cheng, D., Steinert, P., Holbrook, K. and Yuspa, S.H. (1980) Calcium regulation of growth and differentiation of mouse epidermal cells in culture. Cell **19**:245 254.

Herman, I.M., Crisona, N.J. and Pollard, T.D. (1981) Relation between cell activity and the distribution of cytoplasmic actin and myosin. J. Cell Biol. **90**:84-91.

Hering, T.M., Marchant, R.E. and Anderson, J. M. (1983) Type V collagen during granulation tissue development. Exp. Mol. Pathol. **39**:219-229.

Heughan, C. and Hunt, T.K. (1975) Some aspects of wound healing research: A Review. Can. J. Surg. **18**:118-126.

Hibbs, M.S., Hasty, K.A., Seyer, J.M., Kang, A.H. and Mainardi, C.L. (1985a) Biochemical and immunological characterization of the secreted forms of human neutrophil gelatinase. J. Biol. Chem. **260**:2493-2501.

Hibbs, M.S., Hoidal, J.R. and Kang, A.H. (1985b) Secretion of a metalloproteinase by human alveolar macrophages which degrades gelatin and native type V collagen. J. Cell. Biol. **101**:216 (abstract).

Hill, C.R. (1970) Calibration of ultrasonic beams for bio-medical applications. Phys. Med. Biol. **15**:241-248.

Hill, C.R. (1972) Ultrasonic exposure thresholds for changes in cells and tissues. J. Acoust. Soc. Am. **52**.667-672.

Ho, Y-S., Lee, W.M.F. and Snyderman, R. (1987) Chemoattractant-induced activation of c-fos gene expression in human monocytes. J. Exp. Med. **165**:1524-1538.

Hockel, M., Sasse, J. and Wissler, J.H. (1987) Purified monocyte-derived angiogenic substance (angiotrophin) stimulates migration, phenotypic changes, and tube formation but not proliferation of capillary cells *in vitro*. J. Cell. Physiol. **133**: 1-13.

Hogan, R.D.B., Burke, K.M. and Franklin, T.D. (1982) The effect of ultrasound on the microvascular haemodynamics in skeletal muscle: effects during ischemia. Microvascular Research. **23**:370

Holland, P.W.H., Harper, S.J., McVey, J.H. and Hogan, B.L.M. (1987) *In vivo* expression of mRNA for the Ca^{++}-binding protein SPARC (osteonectin) revealed by *in situ* hybridization. J. Cell Biol. **105**:473-482.

Holund, B., Clemmensen, I., Junker, P. and Lyon, H. (1982) Fibronectin in experimental granulation tissue. Acta Pathol. Microbiol. Immunol. Scand. **90**:159-165.

Horwitz, A., Duggan, E., Buck, C., Berkerle, M.C. and Burridge, K. (1986) Interaction of plasma fibronectin membrane receptor with talin - a transmembrane linkage. Nature **320**:531-533.

Hosein, B., Mosessen, M.W. and Bianco, C. (1985) Monocyte receptors for fibronectin. In "Mononuclear phagocytes: Characteristic, Physiology, and Function (Ed. R. van Furth). Martinus Nijhoff, Dordrecht, Holland. pp 723-730.

Huang, J.S., Olsen, T.J. and Huang, S.S. (1988) Platelet-derived growth factor. In "Molecular and Cellular Biology of Wound Repair" (eds. R A F Clark & P M Henson). Plenum Press, New York.pp. 243-251.

Hugli, T.E. and Morgan, E.L. (1984) Mechanisms of leukocyte regulation by complement-derived factors. Contemp. Topics Immunobiol. **14**:109-53.

Humes, J.L., Bonney, R.J., Pelus, L., Dahlgren, M E., Saelowski, S.J., Kuehl, F.A., Jr. and Davies. P. (1977) Macrophages synthesize and release prostaglandins in response to inflammatory stimuli. Nature (London) **269**:149-151.

Hunt, T.K. (1987) Prospective: A retrospective perspective on the nature of wounds. In Growth Factors and Other Aspects of Wound Healing (eds. A. Barbul, E. Pines, M. Caldwell, and T. K. Hunt), pp. xiii-xx. Liss, New York.

Hustler, J.E., Zarod, A.P. and Williams, A.R. (1978) Ultrasonic modification of experimental bruising in the guinea pig pinna. Ultrasonics. **Sept**:223-228.

Huybrechts-Godin, G., Peiters-Joris, C. and Vaes, G (1985) Partial characterisation of the macrophage factor that stimulates fibroblasts to produce collagenase and to degrade collagen. Biochim-Biophys. Acta **846**.51-54.

Hynes, R.O. (1992) Integrins: Versatility, modulation, and signalling in cell adhesion. Cell **69**:11-25.

Iernetti, G. (1971) Cavitation threshold dependence on volume. Acustica. **24**:191-196.

Ignotz, R. A. and Massague, J. (1986) Transforming growth factor-β stimulates the expression of fibronectin and collagen and their incorporation into extracellular matrix. J. Biol. Chem. **261**:4337-4340.

Ignotz, R.A., Endo, T. and Massague, J. (1987) Regulation of fibronectin and type I collagen mRNA levels by transforming growth factor-β. J. Biol. Chem. **262**:6443-6446.

Imig, C. J., Randall, B. F. and Hines, H. M. (1954) Effect of ultrasonic energy on blood flow. Am. J. Phys. Med. 33:100-102.

Inaba, M.K. and Piorkowski, M. (1972) Ultrasound in the treatment of painful shoulders in patients with hemiplegia. Phys. Ther. 52:737-741.

Isenberg, G., Rathke, P.C., Hulsmann, N., Franke W.W. and Wohlfahrt-Bottermann K.E. (1976). Cytoplasmic actomyosin fibrils in tissue culture cells. Direct proof of contractility by visualisation of ATP-induced contraction in fibrils isolated by laser microbeam dissection. Cell Tissue Res. 166.427-433.

Ishikawa, F., Miyazono, K. Hellman, U., Drexler, H., Wernstedt, C., Hagiwara, K., Usuki, K., Takaku, F., Risau, W. and Heldin, C.H. (1989) Identification of angiogenic activity and the cloning and expression of platelet-derived endothelial cell growth factor. Nature 338:557-562.

Issekutz, A.C. (1981) Vascular responses during acute neutropolic inflammation. Their relationship to *in vivo* neutrophil emigration. Lab. Invest. 45:435-441.

Izzard, C.S. and Lochner, L.R. (1980) Formation of cell-to-substrate contacts during fibroblast motility: An interference-reflexion study. J. Cell. Sci. 42:81-116.

Jackson, B.A., Schwane, J.A. and Starcher, B.C. (1991) Effect of ultrasound therapy on the repair of achilles tendon injuries in rats. Medicine. Science. Sports. Exercise. 23:171-176.

Jaffe, B., Roth, R.S. and Marzullo, S. (1955) Properties of piezoelectric ceramics in solid-solution series lead titanate-lead zirconate-lead oxide; tin oxide and lead titanate-lead hafnate. J. Res. Natn. Bur. Stand. 55:239-254.

Janoff, A. (1985) Elastase in tissue injury. Ann. Rev. Med. 36:207-216.

Jiminez, S.A., Freundlich, B. and Rosenbloom, J. (1984) Selective inhibition of human diploid fibroblast collagen synthesis by interferons. J. Clin. Invest. 74:1112-1116

Johnson, R.B., Godzik, C.A. and Cohen, Z.A. (1978) Increased superoxide anion production by immunologically activated and chemically-elicited macrophages. J. Exp. Med. 148:115-127.
Jones, R. J. (1984) Treatment of acute herpes zoster using ultrasonic therapy, Physiotherapy, 70:94-95.

Johnson-Wint, B. (1980) Regulation of stromal cell collagenase production in adult rabbit cornea: *In vitro* stimulation and inhibition by epithelial cell products. Proc. Natl. Acad. Sci. USA. 77:5331-5335.

Kaplan, D.R., Chao, F.C., Stiles, C.D., Antoniades, H.N. and Scher, C.D. (1979). Platelet α-granules contain a growth factor for fibroblasts. Blood. 53:1043-1052

Kaufman, G.E., Miller, M.W., Griffiths, T.D., Ciaravino, V. and Carstenson, E.L. (1977) Lysis and viability of cultured mammalian cells exposed to 1MHz ultrasound. U.M.B. 3:21-25.

Kaufman, G.E. and Miller, M.W. (1978) Growth retardation in chinese hamster V-79 cells exposed to 1MHz ultrasound. U.M.B. 4:139-144.

Kehrl, J.H., Wakefield, L.M., Roberts, A.B., Jakowlew, S., Alvarez-Mon, M., Derynck, R., Sporn, M.B. and Fauci, A.S. (1986). Production of transforming growth factor-beta by human T lymphocytes and its potential role in the regulation of T cell growth. J. Exp. Med. 163:1037-1050.

Kemp, L.M., Estridge, J.K., Brennan, A., Katz, D.R. and Latchman, D.S. (1990) Mononuclear phagocytes and HSV-1 infection: increased permissivity in differentiated U937 cells is mediated by post-transcriptional regulation of viral immediate-early gene expression. J. Leukoc. Biol. 47:483-9.

King, I.A. (1987) All-trans retinoic acid (ATRA) and arotinoid ethyl ester (Ro 13-6298) increase fibronectin synthesis in human keratinocyte cultures. Br. J. Dermatol. 116:422-423 (abstract)

Kim, S., Ikeuchi, K., Groopman, J. and Baltimore, D. (1990) Factors affecting cellular tropism of human immunodeficiency virus. J. Virol. 64:5600-4.

Kitchen, S S. and Partridge, C.J. (1990) A review of therapeutic ultrasound. Part 2: The efficacy of ultrasound. Physiotherapy 76:593-595.

Kischer, C.W. and Shetlar, M.R. (1974) Collagen and mucopolysaccharides in the hypertrophic scar. Connect. Tissue Res. 2:205-213.

Klagsbrun, M. and Shing, Y. (1985) Heparin affinity of anionic and cationic growth factors: Analysis of hypothalamus-derived growth factors and fibroblast growth factors Proc. Natl. Acad. Sci. U.S.A. 82:805-809.

Klein, C, E., Dressel, D., Steinmayer, T., Mauch, C., Eckes, B., Kreig, T., Bankert, R.B. and Weber, L. (1991) Integrin $\alpha^2\beta_1$ is upregulated in fibroblasts and highly aggressive melanoma cells in three dimensional collagen lattices and mediates the reorganisation of collagen I fibrils. J. Cell. Biol. 115:1427-1436.

Klemp, P., Staberg, B., Korsgard, J., Nielsen, H. V. and Crone, P. (1982) Reduced blood flow in fibromyotic muscles during ultrasound therapy. Scan. J. Rehabil. Med. **15**:21-23

Knighton, D R., Hunt, T.K., Scheuenstuhl, H. and Halliday, B.J. (1983) Oxygen tension regulates the expression of angiogenesis factor by macrophages. Science. **221**:1283-85.

Knighton, D.R., Fiegel, V.D., Austin, L.L. and Ciresi, K.F (1986) Classification and treatment of chronic non-healing wounds. Ann. Surg. **204**:322-330.

Knighton, D R., Ciresi, K.F, Fiegel, V.D., Butler, E. and Cerra, F. (1990) Stimulation of repair in chronic, non-healing, cutaneous ulcers using platelet-derived wound healing formula. Surg. Gyn & Obstet. **170**:56-60

Knudsen, P.J., Dinarello, C.A. and Strom ,T.B. (1986) Prostaglandins post-transcriptionally inhibit monocyte expression of interleukin 1 activity by increasing intracellular cyclic adenosine monophosphate. J. Immunol. **137**:3189-94.

Koehler, L., Hass, R., Wessel, K., DeWitt, D.L., Kaever, V., Resch, K. and Goppelt-Struebe, M. (1990) Altered arachidonic acid metabolism during differentiation of the human monoblastoid cell line U937. Biochim. Biophys. Acta. **1042**:395-403.

Kolega, J. Shure, M.S., Chen, W-T. and Young, N.D. (1982) Rapid cellular translocation is related to close contacts formed between various cells and their substrata. J. Cell. Sci. **54**:23-34.

Kondo, T. and Yoshii, G. (1985) Effect of intensity of 1.2 MHz ultrasound on change in DNA synthesis of irradiated mouse L cells. U.M.B. **11**:113-119.

Kono, T., Tanii, T., Furukawa, M., Mizuno, N., Ishii, M., Hamada, T., Yoshizato, K. 1990(a) Cell cycle analysis of human dermal fibroblasts cultured on or in hydrated type I collagen lattices. Arch. Dermatol. Res. **282**:258-262

Kono, T., Tanii, T., Furukawa, M., Mizuno, N., Taniguchi, S., Ishii, M., Hamada, T.,Yoshizato, K. (1990b) Correlation of contractility and proliferative potential with the extent of differentiation in mouse fibroblastic cell lines cultured in collagen lattices. J. Derm. **17**:149-154.

Korn, J.H., Halushka, P.V. and LeRoy, E.C. (1980) Mononuclear cell modulation of connective tissue function. J. Clin. Invest. **65**:543-554.

Koyama, Y. Yamanoha, B. and Yoshida, T. (1990) A novel monoclonal antibody induces the differentaiation of monocyte leukemic cells. Biochem. Biophys. Res. Commun. **168**:898-904.

Kraemer, P.M. and Tobey, R.A. (1972) Cell-cycle dependent desquamation of heparan sulfate from the cell surface. J. Cell Biol. **55**:713-717.

Kramer, J.F. (1984) Ultrasound: Evaluation of its mechanical and thermal effects. Arch. Phys. Med and Rehabil. **65**:223-227.

Krane, S.M. and Amento, E.P. (1983) Cellular interactions and control of collagenase secretion in the synovium. J. Rheumatol. Suppl. **11**:7-12.

Krane, S.M., Dayer, J.M., Simon, L.S. and Byrne, L.S. (1985) Mononuclear cell-conditioned medium containing mononuclear cell factor (MCF), homologous with interleukin-1, stimulates collagen and fibronectin synthesis by adherent rheumatoid synovial cells: effects of prostaglandin E2 and indomethacin. Coll. Relat. Res. **5**:99-117.

Krawczyk, W.S. and Wilgram, G.F. (1973) Hemidesmosome and desmosome morphogenesis during epidermal wound healing. J. Ultrastruct. Res. **45** 93-101.

Kreigler, M., Perez, C., Defay, K., Albert, I. and Lu, S D A. (1988) A novel form of TNF/Cachectin is a cell surface cytotoxic transmembrane protein: ramifications for the complex physiology of TNF. Cell **53**:45-53.

Kreis T.E. and Birchmeier W. (1980). Stress fiber sarcomeres of fibroblasts are contractile. Cell. **22**:555-561

Kremkau, F.W. and Wilcofski, R.L. (1974) Mitotic reduction in rat liver exposed to ultrasound. J Clin Ultrasound. **2**:123-126.

Kumar, S., West, D.C. and Ager, A. (1987) Heterogeneity in endothelial cells from large vessels and microvessels. Differentiation **36**:57-70.

Kurkinen, M., Vaheri, A., Roberts, D.J. and Stenman, S. (1980) Sequential appearance of fibronectin and collagen in experimental granulation tissue. Lab. Invest. **43** 47-51.

Laato, M., Kahari, V.M., Nunikoski, J. and Vuorio, E. (1986) Epidermal growth factor increases collagen production in granulation tissue by stimulation of fibroblast proliferation and not by activation of procollagen genes. Biochem. J **247**:385-388.

Laiho, M., Sakesela, O., Andreasen, P.A. and Keski-Oja, J. (1986). Enhanced production and extracellular deposition of the endothelial-type plasminogen activator inhibitor in cultured human lung fibroblasts by transforming growth factor-beta. J. Cell Biol. **103**:2403-2410.

Lane, E.B., Bartek, J., Purkis, P.E. and Leigh, I. (1985) Keratin antigens in differentiating skin. Ann. N.Y. Acad Sci. **455**:241-258.

Lark, M.W., Laterra, J. and Culp, L.A. (1985) Close and focal contact adhesions of fibroblasts to a fibronectin-containing matrix. Fed. Proc **44**:394-403.

Lawrence, W.T., Norton, J.A., Sporn, M.B., Gorschboth, C. Grotendorst, G R. (1986) The reversal of an adriamycin induced impairment with chemoattractants and growth factors. Ann. Surg. **203**:142-147.

Lee, C.S and Frizzell, L.A. (1988) Exposure levels for ultrasonic cavitation in the mouse neonate. U.M.B. **14**.735-742.

Lehman, J.F., Brunner, G.D. and Stow, R.W. (1958) Pain threshold measurements after therapeutic application of ultrasound, microwaves and infrared. Arch. Phys. Med & Rehabil. **39** 560-565.

Lehman, J.F. and Guy, A.W. (1972) Ultrasound therapy. In "Interaction of ultrasound with biological tissues" (Eds J.M. Reid and M.T. Sikov), pp 141-152. DHEW Publication (FDA) 73-8008.

Lehman, J.F. and de Lateur, B.J. (1982) Therapeutic heat. In "Therapeutic heat and cold - Third edition". Williams and Wilkins, Baltimore.

Leibo, S.P. and Mazur, P. (1971) The role of cooling rate in low temperature preservation. Cryobiology. **8**:447-452.

Leibovich, S.J. and Ross, R. (1975) The role of the macrophage in wound repair - A study with hydrocortisone and antimacrophage serum. Am. J. Pathol. **78**:71-100.

Leibovich, S.I., Polverini, P.J., Shepard, H.M. Wiseman, D.M., Shively, V. and Nuseir, N. (1987) Macrophage-induced angiogenesis is mediated by tumour necrosis factor alpha. Nature **329**:630-32.

Lele, P.P. (1978) Cavitation and its effects on organised mammalian tissues- a summary. Appendix I. In "Ultrasound: Its Applications in Medicine and Biology" (Ed F.J. Fry), pp. 737-741. Elsevier, Holland.

Lembach, K. J. (1976) Enhanced synthesis and extracellular accumulation of hyaluronic acid during stimulation of quiescent human fibroblasts by mouse epidermal growth factor. J. Cell. Physiol. **89**:277-288.

Letourneau, P.C., Ray, P.N., & Bernfield, M.R. (1980) The regulation of cell behaviour by cell adhesion. In Biological Regulation and Development **Vol 2** (ed. R. Goldberger), pp. 339-376. Plenum Press, New York.

Levenson, S.M., Geever, E.F., Growley, L.V., Oates, J. F. III Berard, C.W., and Rosen, H. (1965) The healing of rat skin wounds, Ann. Surg. **161**: 293-308.

Li, A.K.C., Ehrlich, H.P. Trelstad, R.L. (1980) Differences in healing of skin wounds caused by burn and freeze injuries. Ann. Surg. **191**:244-248.

Libby, P. Wyler, D.J., Janicka, M.W. and Dinarello, C.A. (1985) Differential effects of human interleukin 1 on the growth of human fibroblasts and vascular smooth muscle cells. Atherosclerosis **5**:186-191.

Liu, M.Y. and Wu, M.C. (1992) Induction of human monocyte cell line differentiation and CSF-1 production by phorbol ester. Exp. Hematol. **20**:974-979.

Locardi, C., Petrini, C., Boccoli, G., Testa, U., Dieffenbach, C., Butto, S. and Belardelli, F. (1990) Increased human immunodeficiency virus (HIV) expression in chronically infected U937 cells upon in vitro differentiation by hydroxyvitamin D3: roles of interferon and tumor necrosis factor in regulation of HIV production. J. Virol. **64**:5874-82.

Loch, E.G., Fisher, A.B. and Kuwert, E., (1971) Effect of diagnostic and therapeutic intensities of ultrasonics on normal and malignant human cells *in vitro*. Am. J. Obst Gyn. **110**:457-460.

Loef, E.B., Proper, J.A., Goustin, A.S., Shipley, G.D., DiCorleto, P.E. and Moses, H.L. (1986) Induction of c-sis mRNA and activity similar to platelet derived growth factor by transforming growth factor-β: a proposed model for indirect mitogenesis involving autocrine activity. Proc. Natl. Acad. Sci. USA **83**.2453-2457.

Lundberg, C. and Gerdin, B. (1984) The inflammatory reaction in an experimental model of open wounds in the rat. The effect of arachidonic acid metabolites. Euro. J. Pharmacol. **97**:229-238.

Lundeberg, T., Nordstrom, F., Brodda-Jansen, G., Eriksson, S.V., Kjartansson, J. and Samuelson, U.E. (1990) Pulsed ultrasound does not improve healing of venous ulcers. Scand. J. Rehab. Med. **22** 195-197.

Lyons, A.B. and Ashman, L K. (1989) Monocyte cell lines. In " Human Monocytes" (Eds: M. Zembala and G L. Asherson). Academic Press. London. pp 59-69.

Mace, K. and Gazzolo, L. (1991) Interferon-regulated viral replication in chronically HIV1-infected promonocytic U937 cells. Res. Virol. **142**:213-20

Madri, J.A. and Pratt, B.M. (1988) Angiogenesis. In "Molecular and Cellular Biology of Wound Repair" (eds. R.A.F. Clark and P.M. Henson), pp. 337-358. Plenum Press, New York.

Madtes, D.K., Raines, E.W., Sakariassen, K.S., Assoian, R.K., Sporn, M.B., Bell, G.I. and Ross, R. (1988) Induction of transforming growth factor-β in activated human alveolar macrophages. Cell **53**:285-293.

Majno, G., Gabbiani, G., Hirshel, B.J. and Ryan, G.B. (1971) Contraction of granulation tissue *in vitro*: Similarity to smooth muscle. Science **173**.548-550.

Makela, T.P., Alitalo, R., Paulsson, Y., Westermark, B., Heldin, C.H. and Alitalo, K. (1987) Regulation of platelet-derived growth factor gene expression by transforming growth factor beta and phorbol ester in human leukemia cell lines. Mol. Cell. Biol. **7**:3656-62.

Manjo, G., Gabbiani, G., Hirschel, B.J. and Ryan, G.B. (1971) Contraction of granulation tissue *in vitro*: similarity to smooth muscle. Science **173**:548-550.

Mann, D.L., Gartner, S., LeSane, F., Blattner, W.A. and Popovic, M. (1990) Cell surface antigens and function of monocytes and a monocyte-like cell line before and after infection with HIV. Clin. Immunol. Immunopathol. **54**:174-83.

Mansbridge, J.N. and Knapp, A.M. (1987) Changes in keratinocyte maturation during wound healing. J. Invest. Dermatol. **89**:253-263.

Marder, S.R., Chenoweth, D.E., Goldstein, I.M., and Perez, H.D. (1985) Chemotactic responses of human peripheral monocytes to the complement-derived peptides C5a and C5a des Arg. J.Immunol. **134**:3325-3331.

Markham, D.E. and Wood, M.R. (1980) Ultrasound for Dupuytren's contracture, Physiotherapy. **66**:55-58.

Martin, C.J., Gregory, D.W. and Hodgkiss, M. (1981) The effects of ultrasound *in vivo* on mouse liver in contact with an aqueous coupling medium. U.M.B. **7**:235-265.

Martinet, Y., Bitterman, P.B., Mornex, J., Grotendorst, G. R., Martin, G. R. and Crystal, R. G. (1986) Activated human monocytes express the c-sis proto-oncogene and release a mediator showing PDGF-like activity. Nature (London) **319**:158-160.

Matrisian, L.M., Leroy, P., Ruhlmann, C., Gesnel, M.-C. and Breathnach, R. (1986). Isolation of the oncogene and epidermal growth factor induced transin gene: complex control in rat fibroblasts. Mol. Cell Biol. **6**:1679-1686.

Mauch, C., Hatamochi, A., Scharffetter, K. and Kreig, T. (1988) Regulation of collagen synthesis in fibroblasts within a three dimensional collagen gel. Exp. Cell Res. **178**:493-503.

McDiarmid, T., Burns, P.N., Lewith, G.T. and Machin, D. (1985) Ultrasound and the treatment of pressure sores. Physiotherapy. **71**:66-70.

McDiarmid, T. and Burns, P.N. (1987) Clinical applications of therapeutic ultrasound. Physiotherapy. **73**:155-162.

McDonald, C.F. and Atkins, R.C. (1990) Defective cytostatic activity of pulmonary alveolar macrophages in primary lung cancer. Chest. **98**:881-5.

McDonald, J.A., Kelly, D.G., Broekelmann, T.J. (1982) Role of fibronectin in collagen deposition. Fab, to the gelatin-binding domain of fibronectin inhibits both fibronectin and collagen organisation in fibroblast extracellular matrix. J. Cell. Biol. **92**:485-92.

McCarthy, J.B., Basara, M.L., Palm, S.L., Sas, D.F. and Furcht, L.T. (1985) The role of cell adhesion proteins - laminin and fibronectin - in the movement of malignant and metastatic cells. Cancer Met. Rev. **4**:125-152.

McCarthy, J.B., Hagen, S.T. and Furcht, L.T. (1986) Human fibronectin contains distinct adhesion- and motility-promoting domains for metastatic melanoma cells. J. Cell. Biol. **102**:179-188.

McCarthy, J B., Sas, D.F. and Furcht, L.T. (1988) Mechanisms of parenchymal cell migration into wounds In "Molecular and Cellular Biology of Wound Repair" (eds. R. A. F. Clark & P. M. Henson), pp. 281-319. Plenum Press, New York.

McGrath, M H. and Hundahl, S.A. (1982). The spatial and temporal quantification of myofibroblasts. Plast. Reconst. Surg. **69**.975-985.

McKenzie, R., Pepper, D.S. and Kay, A.B. (1975) The generation of chemotactic activity for human leukocytes by the action of plasmin on human fibrinogen. Thromb. Res. **6**.1-8.

McPherson, J.M. and Piez, K.A. (1988) Collagen in dermal wound repair In "Molecular and Cellular Biology of Wound Repair (eds. R A F Clark & P M Henson), pp. 471-496. Plenum Press, New York.

Merluzzi, V.J., Faanes, R.B., Czajkowski, M , Last-Barney, K., Harrison, P.C., Kahn, J. and Rothlein, R (1987) Membrane-associated interleukin 1 activity on human U937 tumor cells:stimulation of PGE2 production by human chondrosarcoma cells J. Immunol. **139**:166-168

Metzger, Z., Hoffeld, J.T. and Oppenheim, J.J. (1980) Macrophage mediated suppression. 1. Evidence for participation of both hydrogen peroxide and prostaglandins in suppression of murine lymphocyte proliferation. J. Immunol. **124**:983-988.

Mignatti, P., Welgus, H., and Rifkin, D.B. (1988) Role of degradative enzymes in wound healing. In Molecular and Cellular Biology of Wound Repair (eds. R.A.F. Clark and P M. Henson), Plenum Press, New York pp. 497-523.

Milam, S.B., Magnuson, V.L., Steffensen, B., Chen, D. and Klebe, R.J. (1991) IL-1β and Prostaglandins Regulate Integrin mRNA expression. J. Cell. Physiology. **149**:173-183.

Miller, E.J. (1976) Biochemical characteristics and biological significance of genetically distinct collagens. Mollec. Cell. Biochem. **13**:165-189.

Miller, M.W. (1985a) Does ultrasound induce sister chromatid exchanges? U.M.B. **11**:561-570

Miller, D.L., Nyborg, W.L. and Whitcomb, C.C. (1978) *In vitro* clumping of platelets exposed to low intensity ultrasound. In "Ultrasound in Medicine" Vol. 4 (Eds D. White and E.A. Lyons), pp 545-553. Plenum, New York.

Miller, D.L., Nyborg, W.L. and Whitcomb, C.C. (1979a) Platelet aggregation induced by ultrasound under specialised conditions *in vitro*. Science. **205**:505-507.

Miller, D.L., Williams, A.R. and Nyborg, W.L. (1979b) Photochemical detection of platelet damage induced by low intensity ultrasound. Proc. 24th annual meeting of American Institute Ultrasound in Medicine, Oaklahoma City.

Miller, M.W. (1985b) Chapter 4. In vitro cell Studies: Cells and Multicell Spheroids. In " Clinics in Diagnostic Ultrasound Vol 16 - Biological effects of Ultrasound" (Eds W L Nyborg and M C Ziskin). Churchill Livingstone. New York, Edinburgh, London, Melbourne. pp 35-48.

Miller, M.W., Church, C.C. and Cox, C. (1988) Lack of effect of continuous wave ultrasound exposure on in vivo Chinese hamster cheek pouch epithelial mitotic index. Ultrasonics. **26**:277-279.

Miller, M.W., Azadniv, M., Cox, C. and Miller, WM. (1991) Lack of induced sister chromatid exchanges in human lymphocytes exposed to *in vivo* therapeutic ultrasound. U.M.B. **17**:81-83.

Ming, W.J., Bersani, L. and Mantovani, A. (1987) Tumor necrosis factor is chemotactic for monocytes and polymorphonuclear leukocytes. J. Immunol. **138**:469-74.

Miyazono, K. and Heldin, C.H. (1989) High-yield purification of platelet-derived endothelial cell growth factor: structural characterization and establishment of a specific antiserum. Biochemistry **28**:1704-10.

Mochitate, K., Pawelek, P. and Grinnell, F. (1991) Stress relaxation of contracted collagen gels: disruption of actin filament bundles, release of cell surface fibronectin, and down regulation of DNA and protein synthesis. Exp. Cell Res. **193**:198-207.

Montesano, R. and Orci, L. (1988) Transforming growth factor B stimulates collagen-matrix contraction by fibroblasts: Implications for wound healing. Proc. Natl. Acad. Sci. USA.**85**:4894-4897.

Moses, H.L., Branum, E.B., Proper, J.A. and Robinson, R.A. (1981) Transforming growth factor production by chemically transformed cells. Cancer Res. **41**:2842-2848.

Moses H.L., Tucker, R.F., Leof, E.B., Coffry, R.J., Halper, J. and Shipley, G.D. (1985) Type-β transforming growth factor is a growth stimulator and a growth inhibitor. Cold Spring Harbor Conf. Cancer Cells. **3**:65-71

Moses, H.L., Yang, E, Y. and Pietenpol, J.A. (1991) Regulation of epithelial proliferation by TGF-β. In "Clinical applications of TGF-β". Ciba foundation Symposium 157. John Wiley & Sons. Chichester, England.pp 66-74.

Mortimer, A.J. (1981) Effects of ultrasound on membrane electrophysiology. In "International Symposium on therapeutic ultrasound" Canadian Physiology Association. pp 67-92.

Mortimer, A.J., Forester, G.V. and Roy, O.Z. (1984) Action of ultrasound on the functioning myocardium: Physical and physiological mechanics. Proc. 29th Annual Meeting of the American Institute of Ultrasound in Medicine., p28.

Mortimer, A.J., Forester, G.V., Trollope, B.J., Villeneuve, E.J. and Roy, O.Z. (1986) Improved performance of the paced cat heart *in situ* with therapeutic ultrasound. IEEE Trans. Ultrasonics, Ferroelect. Freq. Control. UFFC. **33** 210-217

Mortimer, A.J. and Dyson, M. (1988) The effect of therapeutic ultrasound on calcium uptake in fibroblasts. U M B. **14**.499-506.

Mould, A.P., Wheldon, L.A., Komoriya, A., Wayner, E.A., Yamada, K M and Humphries, M.J. (1990) Affinity chromatographic isolation of the melanoma adhesion receptor for the IIICS region of fibronectin and its identification as the integrin $\alpha^4\beta_1$ J. Biol. Chem. **265** 4020-4024.

Mueller, E.E., Mead,.S., Schultz, B.F. and Vaden, M R. (1954) A placebo-controlled study of ultrasound treatment for periarthritis. Am. J. Phys. Med. **33**.31-35.

Mummery, C.L. (1978) The effect of ultrasound on fibroblasts 'in vitro'. P.hD thesis. University of London.

Murphy, K.G. and Daniel, J C. (1987) Human periodontal ligament *in vitro*: cell culture passage effect on collagen gel contraction. J. Periodont. Res. **22**:342-347.

Nagoaka, I., Trapnell, B.C. and Crystal, R.G. (1990) Regulation of insulin-like growth factor 1 gene expression in the human macrophage-like line U937. J. Clin. Invest. **85**:448-455.

Nakagawa, S., Pawelek, P. and Grinnel, F. (1989) Extracellular matrix organisation modulates fibroblast growth and growth factor responsiveness. Exp. Cell Res. **182**:572-582.

Nakaya, K., Chou, S., Deguchi, Y. and Nakamura, Y. (1990) Induction of differentiation of human leukemia cells by various combinations of cytokines and low-molecular-weight inducers. Chem-Pharm-Bull-(Tokyo). **38**:966-70.

Narayanan, A.S. and Page, R.C. (1983) Biosynthesis and regulation of type V collagen in diploid human fibroblasts. J. Biol. Chem. **258**:11694-11699.

Neilson, E.G., Phillips, S.M., Jimenez, S. (1982). Lymphokine modulation of fibroblast proliferation. J. Immunol. **128**:1484-1486

Newman, D. and Marcone, J. (1991). Mitogenic response of different fibroblasts to platelet releasates and combinations of purified growth factors. Cited from abstract. 1st European Tissue Repair Society Meeting. Oxford.

Newman, S.L., Henson, J.E. and Henson, P.M. (1982) Phagocytosis of senescent neutrophils by human monocyte derived macrophages and rabbit inflammatory macrophages. J. Exp. Med. **156**:430-442.

Ngai, J., Coleman, T.R. and Lazarides, E. (1990) Localisation of newly synthesized vimentin subunits reveals a novel mechanism of intermediate filament assembly. Cell. **60**:415-427.

Nickoloff, B.J., Mitra, R.S., Riser, B.L., Dixit, V. M., & Varani, J. (1988) Modulation of keratinocyte motility. Correlation with production of extracellular matrix molecules in response to growth promoting and antiproliferative factors. Am. J. Path. **132**:543-551.

Nicolas, J.F., Gaucherand, M., Delaporte, E., Hartman, D., Richard, M. Groute, F. and Thivolet, J. (1991) Wound healing: A result of coordinate keratinocyte-fibroblast interactions. The role of keratinocyte cytokines. In " Wound Healing". (eds. H Janssen, R Rooman, JIS Robertson). Wrightson Biomedical Publishing Ltd, Petersfield, UK. pp 71-80.

Nilsson, K. Andersson, L.C. and Gahmberg, C.G. (1980) Cell surface characteristics of human histiocytic lymphoma lines. I. Surface glycoprotein patterns. Leukemia Res. **4**:271-277.

Nishyama, T., Tominaga, N., Nakajima, K. and Hayashi, T. (1988) Quantitative evaluation of the factors affecting the process of fibroblast-mediated collagen gel contraction by separating the process into three phases. Collagen Rel. Res. **8**:259-273.

Nishyama, T., Tsunenaga, M., Nakayama, Y., Adachi, E. and Hayashi, T. (1989) Growth rate of human fibroblasts is repressed by the culture within reconstituted collagen matrix but not by the culture on the matrix. Matrix **9**:193-199.

Nolfo, R. Rankin, J.A. (1990) U937 and THP-1 cells do not release LTB4, LTC4, or LTD4 in response to A23187. Prostaglandins. **39**:157-65.

Noltingk, B.E. and Neppiras, E.A. (1950) Cavitation produced by ultrasonics. Proc. Phys. Soc. (Lond) **B63**:674-685.

Nusgens, B., merrill, C., Lapiere, C. and Bell, E. (1984) Collagen biosynthesis by cells in a tissue equivalent matrix *in vitro*. Collagen Rel. Res. **4**:351-364.

Nwuga, V.C.B. (1983) Ultrasound in the treatment of back pain resulting from prolapsed intervertebral disc. Arch. Phys. Med & Rehabil. **64**:78-83.

Nyborg, W.L. (1965) Acoustic streaming. In "Physical Acoustics" (Ed W.P. Mason) Vol. 2B. Academic Press, New York.

Nyborg, W.L. (1977) Physical mechanisms for biological effects of ultrasound. HEW Publication (FDA) 78-8062.

Oakley, E.M. (1982) Evidence for effectiveness of ultrasound treatment in physical medicine. Brit. J Cancer. **45** 233-237.

Odland, G. and Ross, R. (1968) Human wound repair I. Epidermal regeneration. J. Cell. Biol. **39**:135-151.

Olden, K. and Yamada, K.M. (1977) Mechanism of the decrease in the major cell surface protein of chick embryo fibroblasts after transformation. Cell **11**:957-969.

Oosta, G.M., Favreau, L.V., Beeler, D.L. and Rosenberg, R.D. (1982) Purification and properties of human platelet heparitinase. J. Biol. Chem. **257**:11249-55

Orlidge, A. and D'Amore P A. (1987) Inhibition of capillary endothelial cell growth by pericytes and smooth muscle cells J. Cell. Biol. **105**:1455-62.

Otey, C.A., Pavalko, F.M. and Burridge, K. (1990) An interaction between α-actinin and the β_1 integrin subunit *in vitro*. J Cell Biol. **111**:721-729.

Owens, R.B., Smith, H.S. and Hackett, A.J. (1974) Epithelial cell culture from normal glandular tissue in mice. Mouse epithelial cultures enriched by selective trypsinisation. J. Natl. Cancer Inst. **53**:261-269.

Palacios, R., Ivhed, I., Sideras, P., Nilsson, K. Sugawara, I. and Fernandez, C. (1982) Accessory function of human tumor cell lines. 1. Production of Interleukin-1 by the histiocytic lymphoma cell line U937. Eur. J. Immunol. **12**:895-899.

Paul, B.J., La Fratta, C.W., Dawson, A.R., Baab, E. and Bullock, F. (1960) Use of ultrasound in the treatment of pressure sores in patients with spinal cord injury. Arch. Phys. Med. Rehabil. **41**:438-440.

Paulsson, E., Hammachet, A., Heldin, C-H. and Westermark, B. (1987). Possible autocrine feedback in the prereplicative phase of human fibroblasts. Nature. **328**:715-717.

Pauza, C.D. and Singh, M.K. (1990) Extrachromosomal HIV-1 DNA in persistently infected U937 cells. AIDS Res. Hum. Retroviruses. **6**:1027-30.

Peacock, E.E. (1984) Contraction. In "Wound Repair". 3rd Edition. (Ed. E E Peacock). W B Saunders & Company. pp 39-55.

Pearlman, E., Jiwa, A.H., Engleberg, N.C. and Eisenstein, B.I. (1988) Growth of *Legionella pneumophila* in a human macrophage-like (U937) cell line. Microb. Pathog. **5**:87-95

Peck, R. and Bollag, W. (1991) Potentiation of retinoid induced differentiation of HL-60 and U937 cell lines by cytokines. Eur. J. Cancer. **27**:53-57.

Pedrinaci, S., Ruiz-Cabello, F., Gomez, O., Collado, A. and Garrido, F. (1990) Protein kinase C-mediated regulation of the expression of CD14 and CD11/CD18 in U937 cells. Int. J. Cancer. **45**:294-8.

Perno, C.F., Cooney, D.A., Currens, M.J., Rocchi, G., Johns, D.G., Broder, S. and Yarchoan, R. (1990) Ability of anti-HIV agents to inhibit HIV replication in monocyte/-macrophages or U937 monocytoid cells under conditions of enhancement by GM-CSF or anti-HIV antibody. AIDS-Res. Hum. Retroviruses. **6**:1051-5.

Pierce, G.F., Yanagihara, D., Costigan, V., Tarpley, J., Hockman, H., Boone, T., Song, S-Z., Germain, L., Klopchin, K., Altrock, B.W. and Thomason, A. (1991). Platelet-derived endothelial cell growth factor (PD-ECGF) in angiogenesis and wound healing. Cited from abstract. 1st European Tissue Repair Society Meeting. Oxford, U.K.

Plantefaber, L.C. and Hynes, R.O. (1989) Changes in integrin receptors on oncogenically transformed cells. Cell **56**:281-290.

Pledger, W.J., Stiles, C.D., Antonides, H.N. and Scher, C.D. (1977) Induction of DNA synthesis in BALB/c 3T3 cells by serum components: Reevaluation of the commitment process. Proc Natl. Acad. Sci. USA.**74**:4481-4485.

Polverini, P.J., Cotran, R.S., Gimbrone, M.A., Jr. and Unanue, E.R. (1977) Activated macrophages induce vascular proliferation. Nature (London) **269**:804-806.

Pospisilova, J. (1976) Effect of ultrasound on collagen synthesis and deposition in experimental granuloma tissue. Possibilities of clinical uses of ultrasound in healing disorders. Acta. Chir. Plast. **18**:176-183.

Pospisilova, J. Pospisil, M. and Rottova, A. (1971) The influence of ultrasound on the early developmental stage of experimental granuloma in mice. Scripta. medica. **44**:441-449.

Pospisilova, J. Brazdova, K. and Velecky, R. (1974) Effect of ultrasound multiplied by non-pathologic infection on the collagen tissue formation. Specialia. **15**:755-757.

Pospisilova, J. and Rottova, A. (1977) Ultrasonic effect on collagen synthesis and deposition in differently localised experimental granulomas. Acta. Chir. Plast. **19**:148-157.

Postlethwaite, A.E. and Kang, A.H. (1976) Collagen and collagen peptide-induced chemotaxis of human blood monocytes. J. Exp. Med. **143**:1299-1307.

Postlethwaite, A.E. and Kang, A.H. (1988) Fibroblasts. In: Inflammation. basic principles and clinical correlates (Eds Gallin J I, Goldstein I M, Snyderman R). Raven, New York, pp 577-597.

Postlethwaite, A.E., Synderman, R., Kang, A.H. (1976). The chemotactic attraction of human fibroblasts to a lymphocyte-derived factor. J. Exp. Med. **144**:1188-1203.

Postlethwaite, A.E., Snyderman, R. and Kang, A.H. (1979) Generation of a fibroblast chemotactic factor in serum by activation of complement. J Clin. Invest. **64**:1379-1385.

Postlethwaite, A., Keski-Oja, J., Balian, G. and Kang, A.H. (1981). Induction of fibroblast chemotaxis by fibronectin Localization of the chemotactic region to a 140,000 molecular weight non gelatin-binding fragment. J. Exp. Med. **153**:494-499.

Postlethwaite, A.E., Lachman, L.B., Mainardi, C.L., and Kang, A.H. (1983) Interleukin-1 stimulation of collagenase production by cultured fibroblasts. J. Exp. Med. **157**:801-806.

Postlethwaite, A.E., Keski-Oja, J., Moses, H.L. and Kang, A.H. (1987). Stimulation of the chemotactic migration of human fibroblasts by transforming growth factor-β. J. Exp. Med. **165**:251-256.

Preistley, G.C. (1991) Production of glycosaminoglycans by human skin fibroblasts growing in a collagen lattice. Cell Biology International Reports **15**:459-466.

Proud, D. and Kaplan, A.P. (1988) Kinin formation: Mechanisms and role in inflammatory disorders. Ann. Rev. Immunol. **6**:49-83.

Raines, E.W. and Ross, R. (1985) Platelet-derived growth Factor: High yield purification and evidence for multiple forms. J Biol. Chem. **257**:5154-5160.

Raines, E.W. and Ross, R. (1989) Macrphage-derived growth factors. In " Human Monocytes" (Eds: M. Zembala and G.L. Asherson). Academic Press. London. pp 247 -259.

Ralph, P., Moore, M.A.S. and Nilsson, K. (1976) Lysozyme synthesis by established human and murine histiocytic cell lines. J.Exp. Medl. **143**:1528-1533.

Rappersberger, K., Binder, M., Zonzits, E., Hornick, U. and Wolff, K. (1990) Immunogold staining of intermediate-sized filaments of the vimentin type in human skin: a postembedding immunoelectron microscope study. J. Invest. Dermatol. **94**:700-705.

Rappolee, D.A., Mark, D., Banda, M.J. and Werb, Z. (1988) Wound macrophages express TFG-β and other growth factors in vivo: Analysis by mRNA phenotyping. Science **241**:708-712.

Regan, M.C., Kirk, S.J., Wasserkrug, H.L. and Barbul, A. (1991) The wound environment as a regulator of fibroblast phenotype. J. Surg. Res. **50**:442-448.

Reich, E. Rifkin, D.B. and Shaw, E. [eds] (1976) Proteases and biological control, Cold Spring Harbour Conference on Cell Proliferation.

Reid, L.M. and Rojkind, M. (1979) New techniques for culturing differentiated cells: reconstituted basement membrane rafts. Methods in Enzymology **58**:263-278

Repacholi, M.H. (1970) Electrophoretic mobility of tumor cells exposed to ultrasound and ionising radiation. Nature. **227**:166-167.

Repacholi, M.H., Woodcock, J.P., Newman, D.L. and Taylor, K.J.W. (1971) Interaction of low intensity ultrasound and ionising radiation with the tumor cell surface. Phys. Med. Biol. **16**:221-227.

Repacholi, M.H., Kaplan, J.G. and Little, J, (1979) The effect of therapeutic ultrasound on the DNA of human lymphocytes. In: The molecular basis of immune cell function, (J.G. Kaplan Ed). Elsevier/North Holland Biomedical Press. Amsterdam. pp 443-446.

Repacholi, M.H. (1981) Ultrasound: Characteristic and biological action. National Research Council of Canada report No 19244.

Repesh, L.A., Fitzgerald, T.J. and Furcht, L.T. (1982) Fibronectin involvement in granulation tissue and wound healing in rabbits. J. Histochem. Cytochem. **30**:351-358.

Riches, D.W.H. (1988) The multiple roles of the macrophage in wound healing. In "The Molecular and Cellular Biology of Wound Repair" (Eds. R.A.F Clark and P M. Henson). Plenum Press, New York. pp 213-239.

Roberts, A.B., Anzano, M.A., Lamb, L.C., Smith, J M. and Sporn, M.B. (1981) New class of transforming growth factors potentiated by epidermal growth factor: isolation from non-neoplastic tissues. Proc. Natl. Acad. Sci. USA **78**:5339-5343.

Roberts, A B., Anzano, M A., Wakefield, L.M., Roche, N S., Stern, D F. and Sporn, M.B. (1985) Type β transforming growth factor: a bifunctional regulator of cellular growth. Proc. Natl. Acad. Sci. USA **82**.119-123.

Roberts, A.B., Sporn, M B , Assoian, R K., Smith, J.M., Roche, M.S., Heine, U.F., Liotta, L., Falanga, V., Kehrl, J H., & Fauci, A.S. (1986) Transforming growth factor beta: Rapid induction of fibrosis and angiogenesis *in vivo* and stimulation of collagen formation. Proc. Natl. Acad. Sci. U.S.A. **83** 4167-4171.

Roche, C. and West, J. (1984) A controlled trial investigating the effect of ultrasound on venous ulcers referred from general practitioners. Physiotherapy. **70**:475-477

Rola-Pleszczynski, M., Lieu, H., Hamel, J. and Lemaire, I. (1982). Stimulated human lymphocytes produce a soluble factor which inhibits fibroblast migration Cell Immunol **74**:104-110.

Rollins, B.J. and Culp, L.A. (1979) Glycosaminoglycans in the substrate adhesion sites of normal and virus-transformed murine cells. Biochemistry **18**:141-148.

Rom, W.N., Basset, P., Fells, G.A., Nukiwa, T., Trapnell, B.C. and Crystal, R.G, (1988) Alveolar macrophages release an insulin-like growth factor I-type molecule. J. Clin. Invest. **82**:1685-93.

Roman, M P. (1960) A clinical evaluation of ultrasound by the use of a placebo technic. Phys. Ther. Rev. **40**.649-652.

Rooney, J A. and Nyborg, W.L. (1972) Acoustic radiation pressure in a travelling plane wave. Am. J. Phys. **40**:1825-1830.

Ross, P., Yamawaki, R.M., Rimer, V.G. and Edmonds, P.D. (1983) Effect of ultrasound on metabolism of neuroblastoma cells in culture. AIUM Annual Meeting. New York.

Ross, R., Raines, E.W. and Bowen-Pope, D.F. (1986) The biology of platelet-derived-growth-factor. Cell **46**:155-169

Roux-Lombard, P., Cruchaud, A. and Dayer, J.M. Effect of interferon-gamma and 1 alpha,25-dihydroxyvitamin D3 on superoxide anion, prostaglandins E2, and mononuclear cell factor production by U937 cells. Cell. Immunol. **97**:286-96.

Rouzer, C.A., Scott, W.A., Hamill, A.L., Liu, F.T., Katz, D.H. and Cohn, Z.A. (1982) Secretion of leukotriene C and other arachidonic acid metabolites by macrophages challenged with immunoglobulin E immune complexes. J. Exp. Med. **156**:1077-1086.

Rowe, D.W., Moen, R.C., Davidson, J.M., Byers, P.H. Bornstein, P. and Palmiter, R.D. (1978) Correlation of procollagen mRNA levels in normal and transformed chick embryo fibroblasts with different rates of procollagen synthesis. Biochemistry **17**:1581-1590.

Rudolph, R. (1979). Inhibition of myofibroblasts by skin grafts. Plast. Reconstr. Surg. **63**:473-480.

Rudolph, R. (1980). Contraction and the control of contraction. World J. Surg. **4**:279-287.

Rudolph, R., Guber, S., Suzuki, M. and Woodward, M. (1977). The life cycle of the myofibroblast. Surg. Gyn. Obstet. **145**:389-394.

Ruggiero, S.L., Bertolami, C.N., Bronson, R.E. and Damiani, P.J. (1987) Hyaluronidase activity of rabbit skin wound granulation tissue fibroblasts. J. Dent. Res. **66**:1283-1287.

Rungger-Brandle, E. and Gabbiani, G. (1983) The role of cytoskeletal and cytocontractile elements in pathologic processes. Am. J. Path. **110**: 361-391.

Saad, A.H. and Williams, A.R. (1982) Effects of therapeutic ultrasound on clearance rate of blood borne colloidal particles *in vivo*. Br. J. Cancer. **45** (supp V):202-205.

Saad, A.H. and Williams, A.R. (1986) Effects of therapeutic ultrasound on the activity of the mononuclear phagocyte system *in vivo*. U.M.B. **12**:145-150.

Saba, T.M. and Jaffe, E. (1980). Plasma fibronectin (opsonic glycoprotein): Its synthesis by vascular endothelial cells and role in cardiopulmonary integrity after trauma as related to reticuloendothelial function. Am.J.Med. **68**:577-594.

Sabatini, M., Chavez, J., Mundy, G.R. and Bonewald, L.F. (1990) Stimulation of tumor necrosis factor release from monocytic cells by the A375 human melanoma via granulocyte-macrophage colony-stimulating factor. Cancer. Res. **50**:2673-8.

Sacks, P.G., Miller, M.W. and Sutherland, R.M. (1981) Influences of growth conditions and cell-cell contact on responses of tumour cells to ultrasound. Radiation Res. **87**:175-186.

Sappino, A.P., Schurch, W. and Gabbiani, G. (1990) Biology of disease. Differentiation repertoire of fibroblastic cells: Expression of cytoskeletal proteins as a marker of phenotypic modulation Lab. Invest. **63**:144-161.

Sarber, R., Hull, B., Merrill, C., Soranno, T. and Bell, E. (1981) Regulation of proliferation of low and high population doubling levels grown in collagen lattices. Mech. Aging. Develop. **17**:107-117.

Sas, D.F., Herbst, T.J. and Furcht, L.T (1985) Cell locomotion and formation of fibronectin substrate fibrils (unpublished, cited by McCarthy *et al.* 1988).

Sasaki, M S. and Matsubara, S. (1972) free radical scavenging in protection of human lymphocytes against chromosome abberation formation by gamma radiation. Int. J. Radiat. Biol. **32**:439-445.

Schafer, I.A., Shapiro, A, Kovach, M, Lang, C. and Fratianne, R.B. (1989) The interaction of human papillary and reticular fibroblasts and human keratinocytes in the contraction of three dimensional floating collagen lattices. Exp. Cell Res. **183**:112-125.

Schenkein, H.A. (1986) LPS-stimulated release of prostaglandin E and thromboxane B2 from the U937 cell line. Cell Immunol. **102**:307-14.

Scher, C.D., Shepard, R.C., Antoniades, H.N. and Stiles, C.D. (1979) Platelet-derived growth factor and the regulation of the mammalian fibroblast cell cycle. Biochem. Byophys. Acta **560**:217-241.

Schiffman, E. and Gallin, J.I. (1979) Biochemistry of phagocyte chemotaxis. Curr. Top. Cell. Regulat. 15:203-261.

Schiro, J.A., Chan, B.M.C., Roswit, W.T., Kassner, P D., Pentland, A.P., Hemler, M E, Eisen, A.Z. and Kupper, T S. (1991) Integrin $\alpha^2\beta_1$ (VLA-2) mediates reorganisation and contraction of collagen matrices by human cells. Cell **67**:403-410

Schmidt, J.A., Mizel, S.B., Cohen, D. and Green, I (1982) Interleukin 1, a potential regulator of fibroblast proliferation. J. Immunol. **128**:2177-2182.

Schultz, R.J. and Tomasek, J.J. (1990) cellular structure and interconnections. In: Dupuytren's Disease. R.M. McFarlane, D.A. McGrouther, and M.H. Flint, eds. Churchill Livingstone, Edinburgh, pp 86-98.

Schurch, W., Seemayer, T.A., Lagace, R. and Gabbiani, G. (1984) The intermediate filament cytoskeleton of myofibroblasts An immunofluorescence and ultrastructural study. Virchows Arch. [A] **403**:323-336.

Schwartz, M.A. and Juliano, R.L. (1985) Two distinct mechanisms for the interaction of cells with fibronectin substrata. J. Cell. Physiol. **124**:113-119.

Schwartz, S.M., Gajdusek, C.M. and Owens, G.K. (1982) Vessel wall growth control. In Nossel, H.L., Vogel, H.J. (eds). Pathobiology of the endothelial cell. New York. Academic Press, Inc., pp. 63-78.

Semich, R. and Robenek, H. (1990) Organisation of the cytoskeleton and focal contacts of bovine aortic endothelial cells cultured on type I and III collagen. J. Histochem. Cytochem. **38**:159-67.

Senior, R.M., Griffin, G.L. and Mecham, R.P. (1980) Chemotactic activity of elastin-derived peptides. J. Clin. Invest. 66:859-862.

Senior, R.M., Griffin, G.L., Huang, J.S., Walz, D.A. and Deuel, T.F. (1983) Chemotactic activity of platelet α-granule proteins for fibroblasts. J. Cell. Biol. **96**:382-385.

Senior, R.M., Skogen, W.F. and Griffin, G.I. (1986) Effects of fibrinogen derivatives upon the inflammatory response. J. Clin. Invest. **77**:1014-1019.

Seppa, H., Grotendorst, G., Seppa, S., Schiffmann, E. and Martin, G.R. (1982). Platelet-derived growth factor is chemotactic for fibroblasts. J. Cell. Biol. **92**:584-588.

Shabana, A.H., Ouhayoun, J.P., Sawaf, M.H. and Forest, N (1991) Cytokeratin patterns of human oral mucosae in histiotypic culture. Arch. Oral. Biol. **36**:747-758.

Shetlar, M.R., Shetlar, C.L., Chien, S.-F., Linares, H.A., Dobrokovsky, M. and Larson, D.L. (1972) The hypertrophic scar. Hexosamine containing components of burn scars. Proc. Soc. Exp. Biol. Med. **139**:544-547.

Shimokado, K., Raines, E. W., Madtes, D. K., Barrett, T. B., Benditt, E. P. and Ross, R. (1985) A significant part of macrophage-derived growth factor consists of two forms of PDGF. Cell **43**:277-286.

Shipley, G.D., Pittelkow, M.R., Wille, J.J., Scott, R E. and Moses, H.L. (1986) Reversible inhibition of normal human prokeratinocyte proliferation by type transforming growth factor-growth inhibitor in serum free medium. Cancer Res. **46**:2068-2071.

Shoshan, S., (1981) Wound healing. In "International review of connective tissue research". Vol 9. (Eds. D.A. Hall and D.S. Jackson). Academic Press. New York.

Silberstein, G.B. and Daniel, C.W. (1987) Reversible inhibition of mammary gland growth by transforming growth factor-β. Science (Wash DC) **237**:291-293.

Simpson, D M. and Ross, R. (1972) The neutrophillic leukocyte in wound repair. A study with antineutrophil serum. J. Clin. Invest. **51**:2009-2023.

Simpson, D L., Berthold, P. and Taichman, N S (1988) Killing of human myelomonocytic leukemia and lymphocytic cell lines by *Actinobacillus actinomycetemcomitans* leukotoxin. Infect. Immun. **56**:1162-6

Singer, I.I. (1979) The fibronexus: A transmembrane association of fibronectin-containing fibres of 5nm microfilaments in hamster and human fibroblasts. Cell **16**:675-685.

Singer, I.I , Kawka, D.W., Kazazis, D.M. and Clark, R.A.F. (1984) In vivo codistribution of fibronectin and actin fibres in granulation tissue: Immunofluorescence and electron microscope studies of fibronexus at the myofibroblast surface. J Cell Biol. **98**.2091-2106.

Sisson, S.D. and Dinarello, C A. (1989) Interleukin-1 In " Human Monocytes" (Eds: M Zembala and G.L. Asherson). Academic Press. London. pp 183-194.

Skalli, O. and Gabbiani, G. (1988) The biology of the myofibroblast relationship to wound contraction and fibrocontractive diseases. In: Molecular and Cellular Biology of Wound Repair. R.A F. Clark, and P.M. Henson, eds. Plenum press, New York. pp. 373-402.

Skalli, O., Ropraz, P., Trzeciak, A., Benzonana, G., Gillesson, D. and Gabbiani, G. (1986) A monoclonal antibody against α-smooth muscle actin: a new probe for smooth muscle differentiation. J. Cell Biol. **103**:2787-96.

Sluiter, W., Elzenga-Claasen, I., Hulsing-Hesselink, E. and van Furth, R. (1982) Properties of the factor increasing monopoiesis (FIM) in rabbit peripheral blood. Adv. Exp. Med. Biol. **155**:189-193.

Snow, C.J. and Johnson, K.J. (1988) Effect of therapeutic ultrasound on acute inflammation. Physiotherapy Canada. **40**:162-167.

Snowden J.M., Kennedy D.F. and Cliff W.J. (1984) The contractile properties of wound granulation tissue. J. Surg. Res. **36**:108-114.

Snowden, J.M. and Cliff, W.J. (1985). Wound contraction. Correlations between the tension generated by granulation tissue, cellular content and rate of contraction. Quart. Jour. Exp. Physiol. **70**:539-548.

Snyderman, R., Phillips, J., and Mergenhagen, S.E., (1970) Polymorphonuclear leukocyte chemotactic activity in rabbit serum and guinea pig serum treated with immune complexes: evidence for C5a as the major chemotactic factor. Infect. Immun. **1**:521-525.

Sommer, G.F. and Pounds, D. (1982) Transient cavitation in tissues during ultrasonically induced hyperthermia. Med Phys. **9**:1-3.

Speigel, S., Schlessinger, J. and Fishman, P.H. (1984) Incorporation of fluorescent gangliosides into human fibroblasts: Mobility, fate and interaction with fibronectin. J. Cell. Biol. **99**:699-704.

Sporn, M.B., Roberts, A.B. Wakefield, L. and de Crombrugghe, B. (1987) Some recent advances in the chemistry and biology of transforming growth factor-beta. J. Cell Biology. **105**:1039-1045.

Sprugel, K., Greenhalgh, D., Murray, M. and Ross, R. (1990) PDGF and impaired wound healing. Proceedings of the 3rd International symposium on tissue repair. Clinical and experimental approaches to dermal and epidermal repair: Normal and Chronic wounds. January 10 - 14, 1990. Miami, Florida, USA. Cited from abstract.

Stadecker, M.J., Calderon, J., Karnovsky, M.L. and Unanue, A. (1977) Synthesis and release of thymidine by macrophages. J. Immunol. **119**:1738-1743.

Stenn, K.S. and Depalma, L. (1988) Re-epithelialization. In "Molecular and Cellular Biology of Wound Repair" (eds. R.A.F. Clark and P.M. Henson). Plenum Press, New York. pp 321-335.

Stern, D.M., Handley, D., and Nawroth, P.P. (1988) Endothelial cell regulation of coagulation. In "Molecular and Cellular Biology of Wound Repair" (eds. R.A.F. Clark and P.M. Henson). Plenum Press, New York. pp. 87-114.

Stevenson, J.H., Pang, C.Y., Lindsay, W.K. and Zuker, R.M. (1986) Functional, mechanical, and biochemical assessment of ultrasonic therapy on tendon healing in the chicken toe. Plast. Reconst. Surg. **77**:965-972.

Staburzynski, G. (1964) The influence of ultrasounds on the histamine content of blood and tissues. Poznan. Towarz. Przyjaciol Nauk, Wydzial Lekar., Prace Komisji Med. Dosiwadczalnej **29**:269-288.

Steinberg, B.M., Smith, K., Colozzo, M. and Pollack, R. (1980) Establishment and transformation diminish the ability of fibroblasts to contract a native collagen gel. J. Cell Biol. **87**:304-308.

Stopak, D. and Harris, A.K. (1982) Connective tissue morphogenesis by fibroblast traction. 1. Tissue culture observations. Developmental Biology **90**:383-398.

Sugarman, B.J., Aggarwal, B.B., Hass, P.E., Figari, I.S., Palladino M.A. Jr. and Shepard, H.M. (1985) Recombinant human tumor necrosis factor-alpha: effects on proliferation of normal and transformed cells in vitro. Science **230**:943-945.

Summer, W. and Patrick, M.K. (1964) "Ultrasonic Therapy - A Textbook for Physiotherapists". Elsevier, London.

Sundstrom, C. and Nilsson, K. (1976) Establishment and characterisation of a human histiocytic cell line (U937). Int. J. Cancer. **17**:565-577.

Taimi, M., Chateau, M.T., Marti, J. and Pacaud, M. (1990) Induction of differentiation of human histiocytic lymphoma cell line U937 in the absence of vimentin expression. Differentiation. **45**.55-60.

Takase, S. Leo, M.A., Nouchi, T. and Lieber, C.S (1988) Desmin distinguishes cultured fat storing cells from myofibroblasts, smooth muscle cells and fibroblasts in the rat. J Hepatol. **6**.267-276.

Tateyama, S., Furukawa, H., Yamaguchi, R., Nosaka, D. and Kondo, F. (1990) Plate and collagen-gel cultures of normal canine mammary epithelial cells. Res. Vet. Sci. **49**.14-19.

Taylor, K.J.W. and Newman, D.L. (1972) Electrophoretic mobility of Ehrlich cell suspensions exposed to ultrasound of varying parameters. Phys. Med. Biol. **17**:270-276.

Taylor-Papadimitrou, J. Purkis, P.E., Lane, E.B., McKay, I.A. and Chang, S.E. (1982) Effects of SV40 transformation on the cytoskeleton and behaviour properties of human keratinocytes. Cell Differentiation. **11**.169-180.

Tenney, D.J. and Morahan, P.S. (1987) Effects of differentiation of human macrophage-like U937 cells on intrinsic resistance to herpes simplex virus type 1. J-Immunol. **139**:3076-83.

Teppler, H., Lee, S.H., Rieber, E.P. and Gordon, S. (1990) Murine immunoglobulin G anti-CD4 monoclonal antibodies bind to primary human monocytes and macrophages through Fc receptors as well as authentic CD4. AIDS. **4**:627-32.

ter Haar, G., Dyson, M. and Talbert, D. (1978) Ultrasonically induced contractions in mouse smooth muscle *in vivo*. Ultrasonics. **16**:275-276

ter Haar, G.R., Dyson, M. and Smith, S.P. (1979) Ultrastructural changes in the mouse uterus brought about by ultrasonic irradiation at therapeutic intensities in standing wave fields. U.M.B. **5**:167-179.

ter Haar, G.R. and Daniels, S. (1981) Evidence for ultrasonically induced cavitation *in vivo*. Phys. Med. Biol. **26**:1145-1149.

ter Haar, G. and Hopewell, J.W. (1982) Ultrasonic heating of mammalian tissues in vivo. Brit. J. Cancer. **45**:65-67.

ter Haar, G.R., Daniels, S., Eastaugh, K.C. and Hill, C.R. (1982) Ultrasonically induced cavitation *in vivo*. Brit. J. Cancer. **45**:151-155.

Terkeltaub, R.A. and Ginsberg, M. H. (1988) Platelets and response to injury. In "Molecular and Cellular Biology of Wound Repair" (eds. R.A.F. Clark and P. M. Henson). Plenum Press, New York. pp. 35-55.

Terragno, N.A., Lonigro, A.J., Malik, K.U. and McGiff, J.C. (1972) The relationship of the renal vasodilator action of bradykinin to the release of prostaglandin E-like substances. Experientia **28**:437-439.

Toda, K.-I., Tuan, T-L., Brown, P.J. and Grinnell, F. (1987) Fibronectin receptors of human keratinocytes and their expression during cell culture. J. Cell Biol. **105**:3097-3104.

Tomasek, J.J., Hay, E.D. and Fujiwara, K. (1982) collagen modulates cell shape and cytoskeleton of embryonic corneal and fibroma fibroblasts: Distribution of actin, α-actinin, and myosin. Dev. Biol., **92**:107-122.

Tomasek, J.J., and Hay, E.D. (1984) Analysis of the role of microfilaments and microtubules in acquisition of bipolarity and elongation of fibroblasts in hydrated collagen gels. J. Cell Biol. **99**:536-549.

Tomasek, J.J., Schultz, R.J. and Haaksma, C.J. (1987) Extracellular matrix-cytoskeletal connections at the surface of the specialized contractile fibroblast
(myofibroblast) in Dupuytren's disease. J. Bone Joint Surg. **69A**:1400-1407

Tomasek, J.J., Haaksma, C.J. and Eddy, R.J. (1989) Rapid contraction of collagen lattices by myofibroblasts is dependent upon organised actin microfilaments. J. Cell Biol. **107**:602a

Tomasek, J.J. and Haaksma, C.J. (1991) Fibronectin filaments and actin micro-filaments are organised into a fibronexus in Dupuytren's diseased tissue. Anat. Rec. **230**:175-182.

Tomasek, J.J., Haaksma, C.J., Eddy, R.J. and Vaughan, M.B. (1992) Fibroblast contraction occurs on release of tension in attached collagen lattices: Dependency on an organised cytoskeleton and serum Ana. Rec. **232**:359-368.

Tomida, M., Koyama, H. and Ono, T. (1974) Hyaluronic acid synthetase in cultured mammalian cells producing hyaluronic acid. Oscillatory change during the growth phase and suppression by 5-bromodeoxyuridine. Biochim. Biophys. Acta **338**:352-363.

Tonnesen, M.G., Worthen, G.S.and Johnston, R.B. Jr. (1988) Neutrophil emigration. activation, and tissue damage. In "Molecular and Cellular Biology of Wound Repair" (eds. R A F. Clark and P M. Henson). Plenum Press, New York. pp. 149-183.

Toole, B. P. (1972) Hyaluronate turnover during chondrogenesis in the developing chick limb and axial skeleton. Dev. Biol. **29**. 321-329.

Toole, B.P. (1981) Glycosaminoglycans in morphogenesis, in " Cell biology of the extracellular matrix" (E.D. Hay, ed), pp. 259-294, Plenum, New York.

Toole, B.P. and Trelstad, R.L. (1971) Hyaluronate production and removal during corneal development in the chick. Dev. Biol. **26**:28-35.

Trelstad, R. L., & Silver, F. H. (1981) Matrix assembly In "Cell Biology of Extracellular Matrix" (ed E. B. Hay), Plenum Press, New York. pp. 179-215.

Tsukamoto, Y., Helsel, W.E. and Wahl, S.M. (1981) Macrophage production of fibronectin, a chemoattractant for fibroblasts. J. Immunol. **127**:673-678.

Turck, C.W., Tom, J.W., Kennedy, P.W. and Goetzl, E.J. (1988) Isolation and partial characterization of a fibroblast activating factor generated by U937 human monocytic leukocytes. J. Immunol. **141**:1225-1230.

Turck, C.W., Kennedy, P.W., Schiogolev, S I and Goetzl, E.J. (1989) Diverse responses of human fibroblasts to a highly purified fibroblast activating factor from the U937 line of human monocytes. Immunology. **68** 410-415.

Turk, J.L., Heather. C.J. and Diengdoh, J V. (1976) A histochemical analysis of mononuclear cell infiltrates of the skin with particular reference to delayed hyper-sensitivity in the guinea pig. Int. Arch. Allergy Appl. Immunol. **29**:278-289.

Turley, H., Pulford, K.A. Gatter, G.C. and Mason D.Y. (1988) Biochemical evidence that cytokeratins are present in smooth muscle. Br. J. Expo. Pathol. **63**:433-440.

Unemori, E.N. and Werb, Z. (1986) Reorganisation of Polymerised actin: A possible trigger for the induction of procollagenase in fibroblasts cultured in and on collagen gels. J. Cell Biol. **103**:1021-1031.

Underhill, C.B. and Keller, J.M. (1976) Density-dependent changes in the amount of sulfated glycos-aminoglycans associated with mouse 3T3 cells. J. Cell. Physiol. **89**:53-63 .

van Furth, R., Diesselhoff-den Dulk, M.M.C., and Mattie, H. (1973) Quantitative study of the production and kinetics of mononuclear phagocytes during an acute inflammatory reaction. J. Exp. Med. **138**:1314-1330.

van Waarde, D., Hulsing-Hesselink, E. and van Furth, R. (1976) A serum facted by newborn calf serum. Cell Tissue Kin. **9**:51-63.

van Waarde, D., Hulsing-Hesselink, E. and van Furth, R. (1978) Humoral control of monocytopoiesis by an activator and an inhibitor. Agents Action. **8**:423-437.

Van Winkle, W. (1967). Wound contraction. Surg. Obstet. Gyn. **116**:131-142.

Vetter, U., Zapf, J., Heit, W., Helbin, G., Heinze, E., Froesch, E.R. and Teller, W.M. (1986) Human fetal and adult chondrocytes. Effect of insulin-like growth factors I and II, insulin, and growth hormone on clonal growth. J. Clin. Invest. **77**:1903-8.

Vilcek, J., Polombella, V.J., Zhang Y Liu, J.X., Feinman, R., Reis, L.F.L. and Le, J. (1988) Mechanisms and significance of the mitogenic and antiviral actions of TNF. Ann. Inst. Pasteur/Immunol. **139**:309-311.

Viljanto, J., Penttinen, R. and Raekallio, J (1981) Fibronectin in early phases of wound healing in children. Acta Chir. Scand. **147**:7-13.

Vitkovic, L., Kalebic, T., de Cunha, A. and Fauci, A.S. (1990) Astrocyte-conditioned medium stimulates HIV-1 expression in a chronically infected promonocyte clone. J. Neuroimmunol. **30**:153-60.

Vlodavsky, I., Folkman, J., Sullivan R, Fridman, R., Ishai-Michaeli, R., Sasse, J. and Klagsbrun, M. (1987) Endothelial cell-derived basic fibroblast growth factor synthesis and deposition into subendothelial extracellular matrix. Proc. Natl. Acad. Sci. USA. **84**:2292-96.

Wager, R.E. and Assoian, R.K. (1990) A phorbol ester-regulated ribonuclease system controlling transforming growth factor beta 1 gene expression in hematopoietic cells. Mol. Cell. Biol. **10**:5983-90.

Wahl, S.M. (1985). Host immune factors regulating fibrosis. In Fibrosis. Ed. D. Evered and J. Whelan. Pitman. (Ciba Foundation Symposium 114) p 175.

Wahl, S.M. (1989) Acute and chronic inflammation. In "Human monocytes" (Eds M. Zembala and G.L. Asherson). Academic Press. London. pp 361-371.

Wahl, S.M., Hunt, D.A., Wakefield, L.M., McCartney-Francis, N., Wahl, L.M., Roberts, A.B. and Sporn, M B. (1987). Transforming growth factor type-β induces monocyte chemotaxis and growth factor production. Proc. Natl. Acad. Sci. USA. **84**:5788-5792.

Wakasugi, H., Harel, A., Dokhelar, M C., Fradelizi, D and Tursz, T. (1984) Accessory function and interleukin 1 production by human leukemic cell lines. J. Immunol. **132**:2939-47.

Walter, J.B. and Israel, M.S. (1987). General Pathology. 6th edition. Churchill Livingstone.

Ward, J.F. (1981) Some biochemical consequences of the spatial distribution of ionising radiation-produced free radicals. Radiat. Res. **86**:185-195

Ward, J.F., Blakely, W F. and Joner, E.I (1985) Mammalian cells are not killed by DNA single strand breaks caused by hydroxyl radicals from hydrogen peroxide. Radiat. Res. **103**:383-392.

Watmough, D.J., Davies, H.M., Quan, K.M., Wytch, R. and Williams, A.R. (1991) Imaging microbubbles and tissues using a linear focussed scanner operating at 20 MHz: possible implications for the detection of cavitation thresholds. Ultrasonics. **29**:312-318.

Watts, G T. Grillo, H.C. and Gross, J (1958) Studies in wound healing - II, the role of granulation tissue in contraction Ann. Surg. **148**:153-160.

Ways, D.K., Dodd, R.C., Bennett, T.E., Gray, T.K. and Earp, H.S. (1987) 1,25-Dihydroxyvitamin D3 enhances phorbol ester-stimulated differentiation and protein kinase C-dependent substrate phosphorylation activity in the U937 human monoblastoid cell. Endocrinology. **121**:1654-61.

Webster, D.F. (1980) The effect of ultrasound on wound healing. Ph.D thesis. University of London.

Webster, D.F, Pond, J.B., Dyson, M. and Harvey, W. (1978) The role of cavitation in the *in vitro* stimulation of protein synthesis in human fibroblasts by ultrasound. U.M.B. **4**:343-351.

Webster, D.F, Dyson, M., and Harvey, W. (1979) Ultrasonically induced stimulation of collagen synthesis *in vivo*. In Proc. 4th Ultrasound in Biol. and Med. Symp Vol 1. Edited by P. Greguss. Visegrad, Hungary, pp 135-140.

Wedmore, C.V., and Williams, T.J. (1981a) Platelet-activating factor (PAF), a secretory product of polymorphonuclear leukocytes, increases vascular permeability in rabbit skin. BR. J. Pharmacol. **74**:916-917.

Wedmore, C.V., and Williams, T.J. (1981b) Control of vascular permeability by polymorphonuclear leukocytes in inflammation. Nature (Lond). **289**:646-650.

Weksler, B.B., and Goldstein, I.M. (1980) Prostaglandins: Interactions with platelets and polymorphonuclear leukocytes in hemostasis and inflammation. Am. J. Med. **68**:419-428.

Welch, M.P. Odland, G.F. and Clark, R.A.F. (1990) Temporal relationships of F-actin bundle formation, collagen and fibronectin assembly and fibronectin receptor expression. J. Cell Biol. **110**:133-145

Wells, P.N.T. (1969) Physical principles of ultrasonic diagnosis. Academic Press. London and New York.

Wells, P.N.T. (1977) Biomedical Ultrasonics. Academic Press, London, New York, San Francisco.

Werb, Z. and Gordon, S. (1975a) Secretion of a specific collagenase by stimulated macrophages. J. Exp. Med. **142**:346-360.

Werb, Z. and Gordon, S. (1975b) Elastase secretion by stimulated macrophages. *J. Exp. Med.* **142**:361-377.

Whiteside,T.L., Wonall, J.G., Prince, R.K. Buckingham, R.B. Rodnan, G.P. (1986) Soluble mediators from mononuclear cells increase the synthesis of glycosaminoglycans by dermal fibroblast cultures derived from normal subjects and progressive systemic sclerosis patients. Arthritis Rheum. **28**:188-197.

Wilkins, J.A. and Warrington, R.J. (1984) The production of immunoregulatory factors by human macrophage-like cell line. III. The relation ship between the lymphoid-specific inhibitor of DNA synthesis and γ-interferon. Cellular Immunol. **86**:354-361.

Wilkner, N.E., Perischitte, K.A., Baskin, J.B., Nielsen, L.D. and Clark, R.A.F. (1988) Transforming growth factor-β stimulates the expression of fibronectin by human keratinocytes. J. Invest. Dermatol. **91**:207-212.

William, F., Wagner, F., Karin, M. and Kraft, A.S. (1990) Multiple doses of diacylglycerol and calcium ionophore are necessary to activate AP-1 enhancer activity and induce markers of macrophage differentiation. J. Biol. Chem. **265**:18166-71.

Williams, A.R. (1972) Disorganisation and disruption of mammalian and amoeboid cells by acoustic microstreaming. J. Acoust. Soc. Am. **52**:688-693.

Williams, A.R. (1981) Interactions of ultrasound with platelets and the blood coagulation system. Proc Ultrasound Interactions in Medicine and Biology. Symposium, Reinhardsbrunn, East Germany, Nov. 10 - 14.

Williams, A.R. (1982) Absence of meaningful thresholds for bioeffect studies on cells in suspension *in vitro*. Brit. J. Cancer. **45** 192-195.

Williams, A.R. (1983) Ultrasound: Biological effects and potential hazards. Academic Press. London, New York, Paris.

Williams, A.R. (1985) Chapter 5. Effects of Ultrasound on Blood and the Circulation. In " Clinics in Diagnostic Ultrasound Vol 16 - Biological effects of Ultrasound" (Eds W L Nyborg and M C Ziskin). Churchill Livingstone. New York, Edinburgh, London, Melbourne. pp 49-66.

Williams, A.R. (1987) Production and transmission of ultrasound. Physiotherapy. **73**.113-116.

Williams, T.J. (1988) Factors that affect vessel reactivity and leukocyte emigration. In "Molecular and Cellular Biology of Wound Repair"(eds. R.A. F. Clark and P M Henson). Plenum Press, New York. pp. 115-183.

Williams, A.R., O'Brien, W.D. and Coller, B.S. (1976a) Exposure to ultrasound decreases the recalcification time of platelet rich plasma. U.M.B. **2**:113-118.

Williams, A R., Sykes, S.M. and O'Brien, W D. (1976b) Ultrasonic exposure modifies platelet morphology and function *in vitro*. U M B. **2**:311 317.

Williams, A R., Chater, B.V., Allen, K.A., Sherwood, M.R. and Sanderson, J.H. (1978) Release of ß-thromboglobulin from human platelets by therapeutic intensities of ultrasound. Brit. J. Haemotol. **40**.133-142.

Williams, A.R. and Miller, D.L. (1980) Photometric detection of ATP release from human erythrocytes exposed to ultrasonically activated gas filled pores. U.M.B. **6**:251-256.

Williams, A.R., Chater, B.V., Allen, K.A. and Sanderson, J.H. (1981) The use of ß-thromboglobulin to detect platelet damage by therapeutic ultrasound *in vivo*. J. Clin. Ultrasound. **9**:145-151.

Williams, A.R., Miller, D.L. and Gross, D.R. (1986) Haemolysis in vivo by therapeutic intensities of ultrasound. U.M.B. **12** 501-509.

Williams, T.J. (1988) Chapter 5. Factors that affect vessel reactivity and leukocyte emigration. In "The molecular and cellular biology of wound repair". (Ed. Clark, R.A.F and Henson, P.M.). Plenum Press. New York and London.

Willingham, M.C., Yamada, K.M., Yamada, S.S. Pouyssegur, J., Pastan, I. (1977) Microfilament bundles and cell shape are related to adhesiveness to substratum and are dissociable from growth control in fibroblasts. Cell **10**:375-380.

Wittenzeller, R. (1976) Tissue damaging effects of ultrasound. Ultrasonics. **14**: 281-282.

Winter, G.D. (1972) Epidermal regeneration studied in the domestic pig. In "Epidermal Wound Healing" (eds. H.I. Maibach and D T. Rovee). Yearbook Medical Pub., Chicago. pp. 71-112.

Wong, G.H.W and Goeddel, D.V.. (1989) Tumor necrosis factor. In "Human monocytes" (Eds M. Zembala and G.L. Asherson). Academic Press. London. pp 195-215.

Wong, H.L and Wahl, S.M. (1989) Tissue repair and fibrosis. In "Human monocytes" (Eds M. Zembala and G.L. Asherson). Academic Press. London. pp 383-394.

Wong, H.L and Wahl, S.M. (1991) Inflammation and Repair. In "Peptides growth factors and their receptors II".(Eds. M B Sporn and A B Roberts). Springer-Verlag, New York. pp 509-537.

Wong, Y.S and Watmough, D.J. (1981) Haemolysis of red blood cells in vitro and in vivo caused by therapeutic ultrasound at 0.75 MHz. Proc. Ultrasound Interactions in Medicine and Biology Symposium, Reinhardsbrunn, East Germany, Nov 10 - 14.

Wood, G.G. (1960) The formation of fibrils from collagen solutions. Effect of chondroitin sulfate and other naturally occurring polyanions on the rate of formation. Biochem. J. **75**:605-612.

Woodley, D.T. and Briggaman, R.A. (1988) Reformation of the dermal-epidermal junction during wound healing. In "Molecular and Cellular Biology of Wound Repair" (eds. R.A.F. Clark and P.M. Henson). Plenum Press, New York. pp. 559-586.

Woodley, D.T., O'Keefe, E.J. and Prunieras, M. (1985) Cutaneous wound healing: A model for cell-matrix interactions J. Am. Acad. Dermatol. **12**:420-433.

Woodley, D.T., Yamauchi, M., Wynn, K.C., Mechanic, G. and Briggaman, R.A. (1991) Collagen telopeptides (cross-linking sites) play a role in collagen gel lattice contraction. J. Invest. Derm. **97**:580-585.

Woost, P.G., Brightwell, J., Eiferman, R.A. and Schultz, G.S. (1985) Effect of growth factors with dexamethazone on healing of rabbit corneal stromal incisions. Exp. Eye Res **40**:47-60.

Yamada, K.M. and Kennedy, D.W. (1984) Dualistic nature of adhesive protein function: Fibronectin and its biologically active peptide fragments can autoinhibit fibronectin function. J. Cell. Biol. **99**:29-36.

Yang, E.Y. and Moses, H.L. (1990) Transforming growth factor β1-induced changes in cell migration, proliferation, and angiogenesis in the chick chorioallantoic membrane. J. Cell Biol.**111**:731-742.

Young, S R. (1988) The effect of therapeutic ultrasound on the biological mechanisms involved in dermal repair. Ph D thesis. University of London.

Young, S R. and Dyson, M. (1990a) Effect of therapeutic ultrasound on the healing of full-thickness excised skin lesions. Ultrasonics. **28** 175-180.

Young, S R. and Dyson, M. (1990b) Macrophage responsiveness to therapeutic ultrasound. U M B. **16**.809-816

Young, S R. and Dyson, M. (1990c) Effect of therapeutic ultrasound on angiogenesis. U M.B. **16**:261-269.

Yurt, R.W. (1981) Chapter 4. Role of the mast cell in traumas. In " The Surgical Wound" (Eds P. Dineen and G. Hildick-Smith). Lea and Fabiger, Philadelphia. pp 37-62.

Zarod, A.P. and Williams, A.R. (1977) Platelet aggregation in vivo by therapeutic ultrasound. Lancet. 1:1266.

Zetter, B.R. (1988) Angiogenesis. State of the art. Chest 93:159S-166S.

Zeitz, M., Ruiz-Torres, A., and Merker, H.J. (1978) Collagen metabolism in granulating wounds of rat skin. Arch. Dermatol. Res. 263:207-214.

Zeigler-Heotbrock, H.W.L., Thiel, E., Futterer, A., Herzog, V., Wirtz, A. and Reithmuller, G. (1988) Establishment of a human cell line (Mono Mac 6) with characteristics of mature monocytes. Int. J. Cancer. 41: 456-461.

Ziche, M., Jones, J. and Gullino, P. (1982) Role of prostaglandin E1 and copper in angiogenesis. J. Natl. Cancer. Inst. 69:475-82.

Zuckerman, S.H. Tang, J., Gitter, B.D. and Scheetz, M.E. (1987) 7C3, a marker for the differentiation of human macrophage cell lines. J. Leukoc. Biol. 42:491-7.